Abstract
The 35th Commemorative Fullerene-Nanotubes General Symposium

第35回記念フラーレン・ナノチューブ総合シンポジウム

講演要旨集

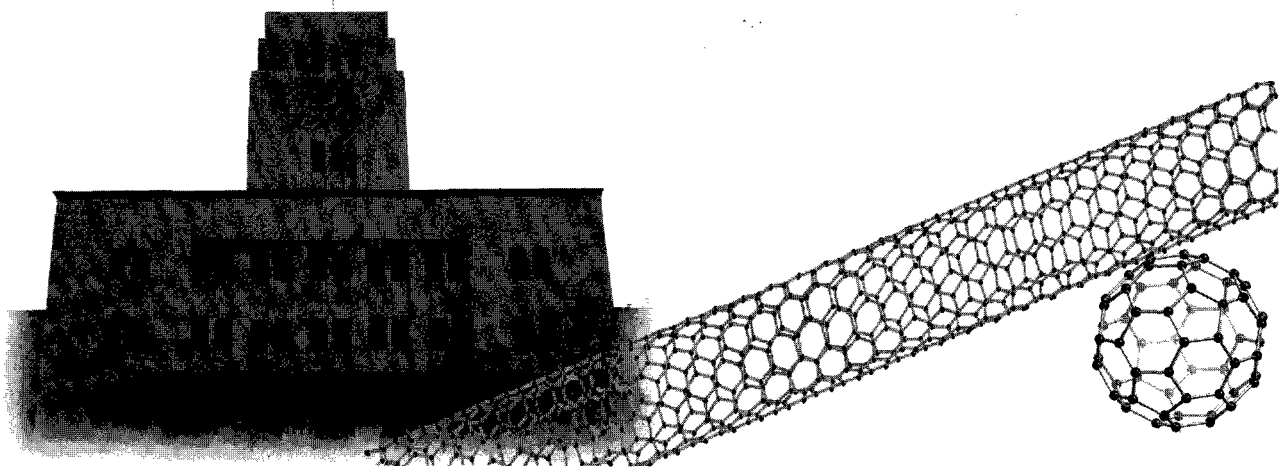

August 27-29, 2008, Oh-okayama, Tokyo
平成20年8月27日ー29日　東京工業大学

The Fullerenes and Nanotubes Research Society
フラーレン・ナノチューブ学会

燃料電池用 新素材を開発

http://www.atr-atr.co.jp

製品一覧

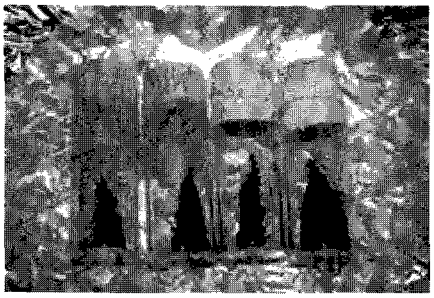

左からホスホン酸化フラーレン / スルホン酸化フラーレン
共存型フラーレン誘導体 / イミダゾール化フラーレン

ホスホン酸化フラーレン
$C60\text{-}PO(OC_2H_5)_2$

スルホン酸化フラーレン
$C60\text{-}SO_3K$

共存型フラーレン誘導体
$C60\text{-}SO_3K\text{-}PO(OC_2H_5)_2$

仕様　特許 第 3984280 号

製品名	結合数	溶解性	熱安定性	H 型の EW
ホスホン酸化フラーレン $C60\text{-}PO(OC_2H_5)_2$	3–4	有機溶媒可溶性	350℃程度	160–130
スルホン酸化フラーレン $C60\text{-}SO_3K$	4–5	水溶性	300℃程度	260–224
共存型フラーレン誘導体 $C60\text{-}SO_3K\text{-}PO(OC_2H_5)_2$	4–5 2	有機溶媒可溶性	300℃程度	150–142

$PO(OC_2H_5)_2 \rightarrow PO(OH)_2$ への変換

トリメチルシリルブロマイド $(CH_3)_3SiBr$ でエステル交換をして水に作用させます。
塩酸中で加熱して加水分解します。
$PO(OC_2H_5)_2$ は、空気中や溶媒中で 180-200℃に加熱すると $PO(OH)_2$ に変わります。

OH ラジカルの作用に対しては、フラレノール構造で安定化すると考えられます。

$X\text{-}C\text{-}CH+ \cdot OH \rightarrow X\text{-}C\text{-}C \cdot + H_2O$

$X\text{-}C\text{-}C \cdot + \cdot OH \rightarrow X\text{-}C\text{-}C\text{-}OH$

イオン交換基型の変換など、特注品の合成もご相談に応じます。
結合数も最大 12 個まで特注品で応じられます。

応用例

イオン交換基導入剤としての利用

EW1 と EW2 の二成分を混合した時の EW の計算式は次の通りです。
EW=1/(w1/EW1+w2/EW2):w1,w2 は各成分の重量分率 EW1=200 のフラーレン誘導体をイオン交換基を持たないマトリックスポリマーに 20%添加した場合、EW2= 無限大なので混合物は EW1000 と成ります。

Ce イオン架橋ホスホン酸化フラーレンの耐酸化剤としての利用

水、有機溶媒に不溶の粉末状であり、熱安定性は 350℃程度です。
膜や電極触媒層に添加すると、Ce イオンにより OH ラジカルが不活性化します。
Ce イオン架橋は、膜ポリマーや触媒インクへの添加前または添加後に行います。

この他、PCBM フラーレン、SWNT、MWNT、水溶性ナノチューブ、アミノ酸フラーレン誘導体
アミノカプロン酸フラーレン、金属内包フラーレン、酸化物微粒子群、非酸化ナノ化合物
金ナノ微粒子等、販売しております。お気軽にお問い合わせ下さい。

株式会社 ATR
〒270-0021 千葉県松戸市小金原 7-10-25
TEL：047-394-2112　FAX：047-394-2100
Mail：sales@atr-atr.co.jp　担当：前田・川野
Advanced Technology Research

Abstract
The 35th Commemorative Fullerene-Nanotubes General Symposium
第 35 回記念フラーレン・ナノチューブ総合シンポジウム

講演要旨集

The Fullerenes and Nanotubes Research Society

The Chemical Society of Japan
Research Center for Nanometer-Scale Quantum Physics, Tokyo TECH
The Physical Society of Japan
The Japan Society of Applied Physics
The Society of Polymer Science, Japan
The Electrochemical Society of Japan

主催：フラーレン・ナノチューブ学会

共催：日本化学会・
東京工業大学量子ナノ物理学研究センター
協賛：日本物理学会・応用物理学会・
高分子学会・電気化学会

Date: August 27th(Wed)－29th(Fri), 2008
Place: Tokyo Institute of Technology
2-12-1 Oh-okayama, Meguro-ku, Tokyo 152-8551
TEL: 03-5734-3712
Presentation: Plenary Lecture (40 min presentation, 5min discussion)
Special Lecture (25 min presentation, 5min discussion)
General Lecture (10 min presentation, 5min discussion)
Poster Preview (1 min presentation, no discussion)

日時：平成 20 年 8 月 27 日(水)～29 日(金)
場所：東京工業大学
〒152-8551　東京都目黒区大岡山 2-12-1
TEL：03-5734-3712
発表時間：基調講演　(発表　40 分・質疑応答　5 分)
特別講演　(発表　25 分・質疑応答　5 分)
一般講演　(発表　10 分・質疑応答　5 分)
ポスタープレビュー　(発表　1 分・質疑応答　なし)

展示団体御芳名（五十音順、敬称略）

IOP英国物理学会出版局

（株）アド・サイエンス

（株）インタフェース

大塚電子（株）

コスモ・バイオ（株）

サイバネットシステム（株）

（株）サーモ理工

（株）島津製作所

（株）セントラル科学貿易

（株）タロウ

ナカライテスク（株）

日立工機（株）

（株）堀場製作所

（株）名城ナノカーボン

広告掲載団体御芳名（五十音順、敬称略）

（株）アド・サイエンス
（株）インタフェース
（株）ATR
エクセルソフト（株）
大塚電子（株）
（株）岡村製作所
（株）カーク
（株）サイエンスラボラトリーズ
サイバネットシステム（株）
（株）サーモ理工
（株）産業タイムズ社
シグマ アルドリッチ ジャパン（株）
（株）島津製作所
（株）十合
スペクトラ・フィジックス（株）
住友商事（株）
（株）セントラル科学貿易
東洋炭素（株）
東レ（株）
ナカライテスク（株）
ナノファクトリー・インストルメンツ・ジャパン（株）
日本電子（株）
日本分析工業（株）
フロンティアカーボン（株）
（株）フロンティア出版
ブルカー・ダルトニクス（株）
（株）堀場製作所
（株）マシナックス
（株）マツボー
（株）名城ナノカーボン
（株）ユニソク

Contents

Time Table 1
Chairperson 3
Program Japanese 4
English 16
Abstracts Plenary lecture・Special lecture 29
General lecture 35
Poster preview 75
Author Index 229

目次

早見表 1
座長一覧 3
プログラム 和文 4
英文 16
講演予稿 基調講演・特別講演 29
一般講演 35
ポスター発表 75
発表索引 229

プログラム早見表

各項目敬称略

8月27日(水)		8月28日(木)		8月29日(金)	
	受付(8：30～)		受付(8：30～)		受付(8：30～)
9:30	基調講演 (遠藤守信)	9:30	基調講演 (Matthew Rosseinsky)	9:30	特別講演 (阿知波洋次)
10:15	一般講演3件 (ナノチューブの応用)	10:15	一般講演2件 大澤賞受賞対象者講演	10:00	一般講演4件 (ナノチューブの生成と精製・物性)
11:00	休憩	10:55	休憩	11:00	休憩
11:15	一般講演5件 (ナノチューブの物性)	11:10	一般講演4件 飯島賞受賞対象者講演	11:15	一般講演5件 (内包ナノチューブ・Siフラーレン)
12:30	昼食	12:30	昼食	12:30	昼食
13:30	特別講演 (水谷孝)	13:30	総会	13:30	特別講演 (塚越一仁)
14:00	一般講演4件 (ナノチューブの応用・ナノホーン)	13:45	特別講演 (角谷均)	14:00	一般講演4件 (グラフェン、フラーレンの化学・金属内包フラーレン)
15:00	休憩	14:15	一般講演3件 (フラーレン固体)	15:00	ポスタープレビュー
15:15	一般講演3件 (フラーレン固体)	15:00	休憩	16:00	ポスターセッション
16:00	ポスタープレビュー	15:15	一般講演3件 (ナノチューブの生成と精製)	17:30	
17:00	ポスターセッション	16:00	ポスタープレビュー		
18:30		17:00	ポスターセッション		
		18:30	懇親会		

Time Table

Wed. August 27		Thur. August 28		Fri. August 29	
	Registration (from 8:30)		Registration (from 8:30)		Registraion (from 8:30)
9:30	Plenary Lecture (M. Endo)	9:30	Plenary Lecture (M. Rosseinsky)	9:30	Special Lecture (Y. Achiba)
10:15	General Lectures [3] (Applications of Nanotubes)	10:15	Lectures by Candidates for the Osawa Award [2]	10:00	General Lectures [4] (Formation, Purification and Properties of Nanotubes)
11:00	Break	10:55	Break	11:00	Break
11:15	General Lectures [5] (Properties of Nanotubes)	11:10	Lectures by Candidates for the Iijima Award [4]	11:15	General Lectures [5] (Endohedral Nanotubes, Si Fullerene)
12:30	Lunch	12:30	Lunch	12:30	Lunch
13:30	Special Lecture (T. Mizutani)	13:30	Meeting	13:30	Special Lecture (K. Tsukagoshi)
14:00	General Lectures [4] (Applications of Nanotubes, Nanohorns)	13:45	Special Lecture (H. Sumiya)	14:00	General Lectures [4] (Graphene, Chemistry of Fullerene, Metallofullerenes)
15:00	Break	14:15	General Lectures [3] (Fullerene Solids, Network Solids)	15:00	Poster Preview
15:15	General Lectures [3] (Fullerene Solids)	15:00	Break	16:00	Poster Session
16:00	Poster Preview	15:15	General Lectures [3] (Formation and Purification of Nanotubes)	17:30	
17:00	Poster Session	16:00	Poster Preview		
18:30		17:00	Poster Session		
		18:30	Banquet		

座長一覧

8月27日(水)　　(敬称略)

	時間	座長
基調講演(遠藤) 一般講演	9:30 ～ 11:00	斎藤 晋
一般講演	11:15 ～ 12:30	市田 正夫
特別講演(水谷)	13:30 ～ 14:00	藤原 明比古
一般講演	14:00 ～ 15:00	湯田坂 雅子
一般講演	15:15 ～ 16:00	久保園 芳博
ポスタープレビュー	16:00 ～ 17:00	若林 知成 柳 和宏
ポスターセッション	17:00 ～ 18:30	

8月28日(木)

	時間	座長
基調講演(Rosseinsky)	9:30 ～ 10:15	谷垣 勝己
大澤賞対象者講演	10:15 ～ 10:55	加藤 立久
飯島賞対象者講演	11:10 ～ 12:30	宮本 良之
特別講演(角谷)	13:45 ～ 14:15	斎藤 晋
一般講演	14:15 ～ 15:00	緒方 啓典
一般講演	15:15 ～ 16:00	片浦 弘道
ポスタープレビュー	16:00 ～ 17:00	神戸 高志 斎藤 毅
ポスターセッション	17:00 ～ 18:30	

8月29日(金)

	時間	座長
特別講演(阿知波)	9:30 ～ 10:00	丸山 茂夫
一般講演	10:00 ～ 11:00	坂東 俊治
一般講演	11:15 ～ 12:30	岡田 晋
特別講演(塚越) 一般講演	13:30 ～ 14:30	粟野 祐二
一般講演	14:30 ～ 15:00	小林 本忠
ポスタープレビュー	15:00 ～ 16:00	菅井 俊樹 中西 毅
ポスターセッション	16:00 ～ 17:30	

8月27日 (水)

基調講演	発表40分・質疑応答5分
特別講演	発表25分・質疑応答5分
一般講演	発表10分・質疑応答5分
ポスタープレビュー	発表1分・質疑応答なし

基調講演 (9:30-10:15)

1S-1 ＣＣＶＤ法によるカーボンナノチューブ ～量産、応用　そして成功に向けての安全性～ 29
遠藤守信、林卓哉、Y.A. Kim、竹内健司、村松寛之、小山省三

一般講演 (10:15-11:00)
ナノチューブの応用

1-1 電子線照射による C_{60} 分子構造変化を用いたカーボンナノチューブ固定 35
○千賀 亮典、円山 拓行、平原 佳織、中山 喜萬

1-2 単層カーボンナノチューブ/ポリ (N-イソプロピルアクリルアミド) 複合ゲルの可逆的な近赤外光誘起相転移 36
○森本達郎、藤ヶ谷剛彦、新留康郎、中嶋直敏

1-3 化学修飾 CNT-FET の可視発光特性 37
○熊代 良太郎、小松 直也、赤阪 健、前田 優、谷垣 勝己

☆☆☆☆☆☆☆ 休憩 (11:00-11:15) ☆☆☆☆☆☆☆

一般講演 (11:15-12:30)
ナノチューブの物性

1-4 光吸収分光による直径制御合成 SWCNT の電子状態考察 38
○斎藤 毅、大森滋和、ビカウシュクラ、湯村守雄、飯島澄男

1-5 原子間力顕微鏡と高分解能透過型電子顕微鏡を用いた同一 CNT 観察 39
○桑原彰太、菅井俊樹、篠原久典

1-6 単層カーボンナノチューブにおける励起子の輻射寿命とサイズ 40
○宮内雄平, 広理英基, 松田一成, 金光義彦

1-7 Fabrication of suspended single-walled carbon nanotubes with a tweezers tip for the optical property study 41
○ Huaping Liu, Shohei Chiashi, Masafumi Ishiguro and Yoshikazu Homma

1-8 単層ナノチューブにおけるフォノンの振動数変化の螺旋度依存性 42
○佐々木健一、齋藤理一郎、G. Dresselhaus, M.S. Dresselhaus, H. Farhat, J. Kong

☆☆☆☆☆☆☆ 昼食 (12:30-13:30) ☆☆☆☆☆☆☆

特別講演 (13:30-14:00)

1S-2 カーボンナノチューブ FET の作製と評価 30
水谷 孝、大野雄高、岸本 茂

一般講演 (14:00-15:00)
ナノチューブの応用・ナノホーン

1-9 Photoinduced electrical transport properties of azafullerene peapod field-effect transistors 43
○ Yongfeng Li, Toshiro Kaneko, and Rikizo Hatakeyama

1-10 半導体電極上への複合ナノカーボン薄膜の作製とその光電気化学特性 44
○梅山有和、手塚記庸、俣野善博、今堀 博

1-11 カーボンナノチューブで擦ることによるカーボンナノチューブの回転運動 45
○高木祥光、大野隆央、岡田晋

1-12 カーボンナノホーン表面における分子立体配座変換の画像化 46
○原野幸治，越野雅至，田中隆嗣，新見佳子，中村優希，磯部寛之，中村栄一

☆☆☆☆☆☆☆ 休憩 (15:00-15:15) ☆☆☆☆☆☆☆

8月27日 (水)

一般講演 (15:15-16:00)

フラーレン固体

1-13 フラーレンを用いた超高感度ガスセンサーの開発 47
○才田守彦、表研次、大泉春菜、相模寛之、溝渕裕三、笠間泰彦、横尾邦義、小野昭一、溝上員章、古川猛夫

1-14 電子構造に対するフラーレン誘導体の置換基の効果：PCBM 48
○赤池幸紀、金井要、吉田弘幸、堤潤也、西寿朗、佐藤直樹、大内幸雄、関一彦

1-15 Preparation of Fullerene (C_{60}) Nanosheets by Liquid-liquid Interfacial Precipitation Method 49
○ M. Sathish, K. Miyazawa and T. Wakahara

ポスタープレビュー (16:00-17:00)

ポスターセッション (17:00-18:30)

フラーレンの化学

1P-1 単純なアミドによる C_{60} のアジリジン化とアジリジノフラーレンのアザフレロイドへの触媒的転位 75
崔岡亮治、○長町俊希、南方聖司

1P-2 メカノケミカル法によるフラーレン C_{60} の固相酸素酸化の生成に対する添加物の効果 76
○石山雄一、田島右副、仙名保、渡辺洋人

1P-3 インドリノフラーレン誘導体の電気化学特性に関する研究 77
○沼田陽平，川嶋淳一，田島右副

1P-4 [60] フラーレンエポキシドを用いたベンゾ [b] フラノ [60] フラーレンの合成 78
○川嶋淳一、沼田陽平、田島右副

金属内包フラーレン

1P-5 フラーレン固体中における $La@C_{82}$ の電子スピンの振る舞い 79
○伊藤 靖浩, Jamie H. Warner, Mujtaba Zaka, 青野 貴行, 泉 乃里子, 沖本 治哉, John J. L. Morton, 篠原 久典, G. Andrew D. Briggs

1P-6 $M_2@C_{80}$ (M=La, Ce, Lu, LuC) の紫外光電子分光 80
○宮崎隆文、青木雄祐、徳本頌治、隅井良平、沖本治哉、梅本 久、赤池祐彦、伊藤靖浩、篠原久典、日野照純

1P-7 Sc_2C_{82} カルベン誘導体の合成とキャラクタリゼーション 81
○栗原広樹, 山崎裕子, 生沼みどり, 土屋敬広, 赤阪健, 溝呂木直美, 永瀬茂

1P-8 金属内包フラーレン誘導体：$La@C_{82}(C_6H_3Cl_2)$ 82
○久我秀徳、二川秀史、土屋敬広、生沼みどり、Zdenek Slanina、赤阪 健、溝呂木直美、永瀬 茂

1P-9 $Sc@C_{82}$ カルベン誘導体の合成とそのキャラクタリゼーション 83
○蜂屋誠、山崎裕子、生沼みどり、土屋敬広、赤阪健、溝呂木直美、永瀬茂

1P-10 $La_2@C_{80}$ とシラシクロプロパンとの熱反応 84
○美野輪まり、山田道夫、加固昌寛、土屋敬広、生沼（石塚）みどり、赤阪健

フラーレン固体

1P-11 導電性ポリマー電極を使った C_{60} 薄膜電界効果トランジスタの作製と特性評価 85
加地由美子，川崎菜穂子，○久保園芳博，藤原明比古

1P-12 電子線照射フラーレン薄膜の振動分光 86
○西井 俊明，高嶋 明人，龍崎 奏，甲斐 敏浩，尾上 順

1P-13 垂直配向フラーレンマイクロチューブの走査型電子顕微鏡観察 87
○戸板翔、宮澤薫一、橘勝

1P-14 酸素に暴露した C_{60} 薄膜表面の原子スケール物性計測 88
志村匡史、加藤恵介、才田守彦、大泉春菜、表研次、横尾邦義、山本恵彦、○佐々木正洋

1P-15 Cu(111) 上 C_{60} 単分子層の局所仕事関数分布 89
○加藤恵介、志村匡史、才田守彦、表研次、横尾邦義、佐々木正洋

1P-16 電界効果トランジスタのための有機溶液からの C_{60} 結晶の成長 90
○栗原浩平、飯尾靖也、野苅家亮、松山史彦、岩田展幸、山本寛

1P-17 薄膜蒸着中自由電子レーザ照射による C_{60} ポリマーサイズの拡張 91
○野苅家 亮、蜂谷 真司、飯尾 靖也、岩田 展幸、山本 寛

炭素ナノ粒子

1P-18 ラットの肺に気管注入したフラーレンナノ粒子の電子顕微鏡観察 92
○山本和弘、牧野雅、小林恵美子、大神明、森本泰夫

1P-19 遠心分離による粉末状ナノダイヤモンドのサイズ分離 93
○小松直樹、森田陽一、瀧本竜哉、山中博、粂川勝美、森野静香、青沼秀児、木村隆英

1P-20 ストロンチウムナノカーボン化合物の作製と磁化率 94
○平郡 諭, 木全 希, 小林 本忠

ナノチューブの物性

1P-21 Global Spectral Analysis Method for Simulating Excitation-Emission Maps of Semiconducting Single-Walled Carbon Nanotubes 95
○ Adam M. Gilmore

1P-22 カーボンナノチューブ内部の電場変調 96
○宮本良之

1P-23 ボロンドープカーボンナノチューブ集合体における超伝導 97
○松平将治、中村仁、村田尚義、春山純志、J.Reppert、A.M.Rao、是常隆、斎藤晋、八木優子

1P-24 二層カーボンナノチューブに形成された層間 pn 接合 98
○清水台生, 春山純志, 野澤響子, 菅井俊樹, 篠原久典

1P-25 半導体単層カーボンナノチューブにおける3次非線形光学応答と位相緩和時間 99
○市田正夫、齋藤伸吾、宮田耕充、片浦弘道、安藤弘明

1P-26 有機分子内包単層カーボンナノチューブの Li 貯蔵特性 100
○廣瀬 雅一、川崎 晋司、岩井 勇樹

1P-27 高速液体クロマトグラフィーによる単層カーボンナノチューブの長さ分離および分光測定による評価 101
○浅田有紀、菅井俊樹、北浦良、篠原久典

1P-28 カーボンナノチューブの化学修飾におけるカルベン誘導体の立体効果 102
○湯村尚史、Miklos Kertesz

1P-29 二層カーボンナノチューブにおける圧力誘起構造相転移と新炭素ナノ物質の電子状態 103
○櫻井誠大、斎藤晋

1P-30 垂直配向カーボンナノチューブの偏光ラマン分光 104
○張正宜、村上陽一、エリック エイナルソン、宮内雄平、丸山茂夫

1P-31 金属単層ナノチューブにおけるラマン G バンドのレーザー誘起欠陥の影響 105
○姜 東哲、加藤 健一、小島 謙一、橘 勝

ナノチューブの応用

1P-32 SWCNT エミッタ1次元配列のマイクロカソード内への瞬間実装 106
○野田優, 古市考次, 白鳥洋介, 辻佳子, 杉目恒志

1P-33 半導体カーボンナノチューブを用いたトランジスタ 107
○イザル ニコラ、カザウィ サイ、南 信次

1P-34 SiC 表面分解法により作製したカーボンナノチューブの放熱応用 108
○乗松航、河合千尋、楠美智子

1P-35 直接成長法によるカーボンナノチューブトランジスタの作製と輸送特性 109
○藤原明比古、井波暢人、モハメドモハマドアンブリ、仕幸英治

1P-36 高純度半導体単層カーボンナノチューブを用いた電界効果トランジスタの作製と評価 110
○藤井俊治郎, 宮田耕充, 柳和宏, 田中丈士, 西出大亮, 片浦弘道

1P-37 光で駆動するカーボンナノチューブ-マイクロデバイス 111
○都 英次郎、長田 英也、平野 研、廣津 孝弘

ナノチューブの生成と精製

1P-38 Genomic DNA-Mediated Solubilization and Separation of Single Wall Carbon Nanotubes 112
○ Sang Nyon Kim, Kristi M. Singh, Fahima Ounchen, James G. Grote and Rajesh R. Naik

1P-39 An Experimental Investigation of Active Roles of sp^2 Carbon Precursors in SWCNT Growth 113
○ B. Shukla, T. Saito, M. Yumura, S. Iijima

1P-40 Optical and (n, m) Enrichments of (7,5)-SWNTs through Extraction with Chiral Monoporphyrin 114
○ Xiaobin Peng, Naoki Komatsu, Takahide Kimura, Atsuhiro Osuka

1P-41 1 2相交流アーク放電法によるシングルウォールカーボンナノチューブの生成 115
○松浦次雄、近藤幸江、真木教雄

1P-42 超遠心分離法によるカーボンナノチューブと金属不純物の高効率分離 116
○西出大亮, 宮田耕充, 柳和宏, 田中丈士, 片浦弘道

1P-43 単層カーボンナノチューブの一方向成長 117
○石神直樹、吾郷浩樹、西徹志、池田賢一、辻正治、生田竜也、高橋厚史

1P-44 外層を部分的に剥離したDWNTの創製 118
○福井信志, 今津直樹, 小林慶太, 吉田宏道, 桑原彰太, 菅井俊樹, 橋詰富博, 篠原久典

1P-45 FT-IRによるACCVDのガス分析(2) 119
○島津智寛、鈴木義信、大島久純、丸山茂夫

1P-46 ガス透過性基板を用いたＣＮＴ成長 120
○向中野 信一、桶結 憲二、大島 久純、丸山 茂夫

1P-47 スーパーグロース：大量生産に向けたSWNTsの大面積成長 121
○保田諭、二葉ドン、湯村守雄、飯島澄男、畠賢治

内包ナノチューブ

1P-48 Rotating fullerene chains in carbon nanopeapods 122
○ Jamie H. Warner, Yasuhiro Ito, Mujtaba Zaka, Ling Ge, Takao Akachi, Haruya Okimoto, Kyriakos Porfyrakis, Andrew A. R. Watt, Hisanori Shinohara, G. Andrew D. Briggs

1P-49 金属1、2、3原子内包フラーレン・金属カーバイドフラーレンピーポッドを用いた、ナノテンプレート反応による金属ナノワイヤー内包カーボンナノチューブの創製 123
○今津直樹、北浦良、小林慶太、沖本治哉、伊藤靖浩、斎藤毅、篠原久典

1P-50 ナノチューブ内に閉じ込められたDNA運動の電子顕微鏡観察 124
○荘田真幸、丸山有成、坂東俊治、飯島澄男

1P-51 細孔内流体の相挙動と界面張力 125
○濱田嘉信、甲賀研一郎、田中秀樹

1P-52 銅ナノロッド内包カーボンナノチューブの電気・物質移動の研究 126
○木村文隆、安坂幸師、中原仁、小海文夫、齋藤弥八

8月28日 (木)

基調講演	発表 40 分・質疑応答 5 分
特別講演	発表 25 分・質疑応答 5 分
大澤賞飯島賞対象者講演	発表 10 分・質疑応答 10 分
一般講演	発表 10 分・質疑応答 5 分
ポスタープレビュー	発表 1 分・質疑応答なし

基調講演 (9:30-10:15)

2S-1 Superconductivity in expanded fullerides 31
Matthew J. Rosseinsky

大澤賞対象者講演 (10:15-10:55)

2-1 未知なるフラーレン世界への旅 50
○二川秀史、菊池隆、山田智也、久我秀徳、伊藤剛、Slanina Zdenek、赤阪健、溝呂木直美、永瀬茂

2-2 分子サイズの車、ナノカーの開発 51
○白井康裕、Andrew J. Osgood、Jean-Francois Morin、佐々木崇、Yuming Zhao、Jason M. Guerrero、Kevin F. Kelly、James M. Tour

☆☆☆☆☆☆☆ 休憩 (10:55-11:10) ☆☆☆☆☆☆☆

飯島賞対象者講演 (11:10-12:30)

2-3 炭化鉄微粒子からのカーボンナノチューブ核形成・成長の直接観察 52
○吉田秀人、内山徹也、河野日出夫、竹田精治、本間芳和

2-4 簡単なカーボンナノチューブの金属・半導体分離 53
○田中 丈士, 金 赫華, 宮田 耕充, 藤井 俊治郎, 菅 洋志, 内藤 泰久, 片浦 弘道

2-5 インクジェット法を用いた高性能 SWNT 薄膜トランジスタの作製 54
○沖本治哉、竹延大志、柳和宏、宮田耕充、片浦弘道、浅野武志、岩佐義宏

2-6 カーボンナノチューブ基板を用いた集積 3 次元 MEMS デバイスの創製 55
○早水裕平, 山田健郎, 水野耕平, ロバート・デービス, 二葉ドン, 湯村守雄, 畠賢治

☆☆☆☆☆☆☆ 昼食 (12:30-13:30) ☆☆☆☆☆☆☆

総会 (13:30-13:45)

特別講演 (13:45-14:15)

2S-2 直接変換によるナノ多結晶ダイヤモンドの高圧合成と特性 32
角谷均

一般講演 (14:15-15:00)
フラーレン固体・ネットワーク固体

2-7 走査トンネル顕微鏡による C_{70} 最密充填表面の研究 56
○太田 洋平, 三橋 了爾, 久保園 芳博

2-8 電子線照射フラーレン薄膜の電子的・光学的性質 57
○尾上 順、伊藤孝寛、木村真一、戸田泰則、龍崎 奏、大野かおる、T.A. Beu

2-9 フラーレンやナノチューブにより構成される規則性ネットワーク構造の鋳型合成 58
○西原洋知, 今井克明, 侯鵬翔, Juan I. Paredes, Amelia Martnez-Alonso, Juan M.D. Tascn, 京谷隆

☆☆☆☆☆☆☆ 休憩 (15:00-15:15) ☆☆☆☆☆☆☆

一般講演 (15:15-16:00)
ナノチューブの生成と精製

2-10 ACCVD 法による垂直配向 SWNT 膜の直径制御 59
○項栄、張正宜、エリック エイナルソン、大川潤、村上陽一、丸山茂夫

2-11 表面修飾したシリコン基板上での単層ナノチューブの水平配向成長 60
○吉原直記、吾郷浩樹、今本健太、辻正治、生田竜也、高橋厚史

2-12 直径 5 nm の単層カーボンナノチューブと CVD 時の触媒粒径増大 61
○長谷川 馨、野田 優

8月28日 (木)

ポスタープレビュー (16:00-17:00)

ポスターセッション (17:00-18:30)

フラーレンの化学

2P-1 カチオン性フラーレン誘導体による HL-60 細胞のアポトーシス誘導 127
○横尾祥子、西澤千穂、高橋恭子、中村成夫、増野匡彦

2P-2 発光性環状ベンゼノイドをコアとするカルバゾールフェニルのフラーレン十重付加体 128
○張 小涌・松尾 豊・中村栄一

2P-3 ダブルデッカーバッキーフェロセンにおける電子ドナー・アクセプター相互作用 129
○松尾敬子, 松尾 豊, Dirk M. Guldi, 中村栄一

2P-4 5 重付加フラーレン部位を有するメタクリル酸エステルの合成 130
○大山裕美, 松尾豊, 中村栄一

金属内包フラーレン

2P-5 単核及び複核ツリウム内包フラーレンからの近赤外蛍光観測 131
○泉乃里子、赤地祐彦、伊藤靖浩、岡崎俊也、北浦良、菅井俊樹、篠原久典

2P-6 Non-IPR 構造を有する La@C_{72} の二付加体の合成 132
○伊藤剛、二川秀史、赤阪健、生沼みどり、土屋敬広、ズデネクスラニナ、溝呂木直美、永瀬茂

2P-7 金属内包フラーレン配位子の合成とその性質 133
○横澤裕也、土屋敬広、赤阪健

2P-8 金属内包フラーレン／拡張π電子系ホスト分子による包接錯体の形成と性質 134
○佐藤 亜由美、土屋敬広、赤阪 健、ナザリオ マーチン

2P-9 La@C_{82} と 1,2,3,4,5-ペンタメチルシクロペンタジエンの位置選択的可逆付加反応 135
○佐藤悟、前田優、稲田浩司、山田道夫、土屋敬広、石塚みどり、長谷川正、赤阪健、加藤立久、溝呂木直美、Zdenek Slanina、永瀬茂

フラーレン固体

2P-10 フラーレン・亜鉛ポルフィリン積層膜の外部量子効率 136
○龍崎 奏, 甲斐 敏浩, 西井 俊明, 尾上 順

2P-11 PMA 誘導した THP-1 細胞と FNWs の相互作用の研究 137
○ぬで島真一, 宮澤薫一, 奥田順子, 谷口彰良

2P-12 1次元ピーナッツ型 C_{60} ポリマーの第一原理電子状態計算 138
○高嶋 明人、西井 俊明、尾上 順

2P-13 ダブルデッカーバッキーフェロセンの電気伝導特性の第一原理計算による解析 139
○大島良久

2P-14 有機及び分子結晶薄膜の非接触膜厚モニター 140
○大泉春菜、才田守彦、相模寛之、表研次、溝渕裕三、笠間泰彦、横尾邦義、小野昭一、田所利康

2P-15 フラーレンナノチューブの高温熱処理 141
○加藤 良栄, 宮澤 薫一, 西村 聡之, 王 正明

フラーレン生成・高次フラーレン

2P-16 原子状炭素挿入反応による環状炭素鎖の最も簡単な成長 142
○尾形照彦、紫尾雄岳、畳谷仁男

ナノチューブの物性

2P-17 3ω法による垂直配向単層カーボンナノチューブ膜の熱伝導率の特性評価 143
○石川 桂, 田中 三郎, 宮崎 康次, 塩見 淳一郎, 丸山 茂夫

2P-18 Si02 上に吸着された半導体ナノチューブの電子状態とエネルギー論 144
○岡田晋

2P-19 ポリフルオレンによって選択的に分散された半導体単層カーボンナノチューブの吸光係数の決定 145
○二見能資、カザウィサイ、南信次

2P-20 熱によって誘起されたサファイアから配向ナノチューブへの電荷移動 146
○吾郷浩樹、田中伊豆美、辻正治、池田賢一、水野清義

2P-21 アームチェアナノチューブの詳細構造 147
○加藤幸一郎、斎藤晋

2P-22 超遠心分離サンプルを用いた単層カーボンナノチューブの吸光係数決定 148
○桑原彰太、浅田有紀、菅井俊樹、篠原久典

2P-23 2 STM 端子間のカーボンナノチューブ伝導度における干渉効果 149
○中西 毅, 安藤 恒也

2P-24 つぶれた単層カーボンナノチューブの電子構造変化：アームチェア・チューブ 150
○長谷川正之、西館数芽

2P-25 アニールによるカーボンナノコイルの機械的特性への影響 151
○佐藤峻、 荒木義昭、 金田亮、 中山喜萬、 秋田成司

2P-26 単層カーボンナノチューブの高温赤外分光 152
○ムフタール・エフェンディ、横井裕之、黒田規敬

ナノチューブの応用

2P-27 イオン液体を用いたカーボンナノチューブ原子間力顕微鏡探針の作製と評価 153
○上薗裕也、邱建超、吉村雅満、上田一之、浅田有紀、桑原彰太、北浦良、菅井俊樹、篠原久典

2P-28 カーボンナノチューブネットワークを用いたガスセンサー特性の最適化 154
○佐々木 功、南 信次

2P-29 ＣＮＴをベースとしたフォース・トランスデューサーを用いたラット消化管の収縮運動測定 155
○平田孝道、谷中崇嗣、坂原聖士、小池加奈子、筒井千尋、坂井貴文、秋谷昌宏

2P-30 マイクロ波照射下でのカーボンナノチューブのバイオハザード 156
○堀口拓一、佐野正人

2P-31 カーボンナノチューブ電界クロマトグラフィの分離条件の検討 157
○折之内祐樹、橋本紅良、鈴木康志、渡邉康之、佐野正人

2P-32 理想的な界面構造を有する燃料電池電極触媒用 MWNT/Polybenzimidazole/Pt の作製 158
○岡本稔、藤ヶ谷剛彦、中嶋直敏

2P-33 電子顕微鏡用カーボンナノチューブ電界放出エミッタの電子光学的評価 159
○草野賢和, 安坂幸師, 中原仁, 齋藤弥八

ナノチューブの生成と精製

2P-34 FEL 照射による半導体 SWNT のカイラリティ制御 160
○石塚大祐, 境恵二郎, 内田勝美, 岩田展幸, 矢島博文, 山本寛

2P-35 OPO パルスレーザーを用いた金属性、半導体性単層カーボンナノチューブの選択的分離 161
○田島勇, 内田勝美, 石井忠浩, 矢島博文

2P-36 アルコールガスソース法によるカーボンナノチューブ低温成長への酸化アルミニウムバッファ層の適用 162
○丸山隆浩、佐藤一徳、白岩倫行、成塚重弥

2P-37 糖類を密度勾配剤として用いた金属型・半導体型単層カーボンナノチューブの分離 163
○柳和宏、飯塚敏江、藤井俊次郎、片浦弘道

2P-38 熱処理したステンレス基板を用いた高配向カーボンナノチューブの液相合成 164
○山際清史、山口吉弘、喜々津智郁、山下俊介、竹内恒晴、齋藤守弘、桑野潤

2P-39 吸収スペクトル測定による単層カーボンナノチューブの直径分布の温度依存性 165
○中山崇、井上亮人、横井一馬、鶴岡泰広、兒玉健、阿知波洋次

2P-40 極めて細い単層カーボンナノチューブの分光 166
○高水直子、大西侑気、浦田圭輔、鈴木信三、長澤浩、阿知波洋次

2P-41 Co を用いた触媒 CVD 法における単層カーボンナノチューブ垂直配向成長の前駆体 167
○杉目恒志、野田優

2P-42 キャリアガスによるカーボンナノチューブの層数制御 168
○横山大輔, 岩崎孝之, 石丸研太郎, 飯塚正知, 佐藤信太郎, 二瓶瑞久, 粟野祐二, 川原田洋

2P-43 拡散プラズマ CVD におけるガス圧力と単層カーボンナノチューブ直径分布の相関関係 169
○黒田 峻介, 加藤 俊顕, 金子 俊郎, 畠山 力三

2P-44 Co/Sn 触媒を使用した触媒 CVD によるヘリカルカーボンナノファイバの成長 170
○篠原 雄一郎, 横田 真志, 須田 義行, 桶 真一郎, 滝川 浩史, 藤村 洋平, 山浦 辰雄, 伊藤 茂生, 三浦 光治, 盛興 昌勝

8月28日 (木)

内包ナノチューブ

2P-45 フラーレン内包による単層カーボンナノチューブの直径に依存したバンドギャップ変化 171
○岡崎俊也、大窪清吾、岸直希、中西毅、岡田晋、飯島澄男

2P-46 カーボンナノチューブ・ピーポッド中の C_{60} フラーレンの融合過程 172
○山上雄一郎、斎藤晋

2P-47 カルシウム内包単層カーボンナノチューブの作製と特性評価 173
○清水哲弘, 加藤俊顕, 大原渡, 畠山力三

2P-48 Nano Scale Separation of the Different Cage Size Empty Fullerene by Nanopeapod Synthesis 174
○ Teguh Endah Saraswati,Naoki Imazu and Hisanori Shinohara

ナノホーン

2P-49 スーパーキャパシタ電極材料用のアークスートへの超音波を用いたコロイド法による酸化ルテニウムの担持 175
○宇留野光, 山本真伸, 和泉勇毅, 桶真一郎, 須田善行, 滝川浩史, 伊藤茂生, 山浦辰雄, 三浦光治, 大川隆, 青柳伸宜

2P-50 PEG-ペプチド複合体によるカーボンナノホーンの分散化効果と肺への蓄積 176
○松村幸子、佐藤重男、湯田坂雅子、冨田章弘、鶴尾隆、飯島澄男、芝清隆

2P-51 シスプラティン内包ナノホーンの抗癌効果 177
○湯田坂 雅子

2P-52 ナノホーンの熱閉孔現象におよぼす化学官能基の影響 178
○入江 路子、范 晶、飯島 澄男、宮脇 仁、弓削 亮太、河合 孝純、湯田坂 雅子

8月29日 (金)

特別講演　　発表25分・質疑応答5分
一般講演　　発表10分・質疑応答5分
ポスタープレビュー　発表1分・質疑応答なし

特別講演 (9:30-10:00)

3S-1 カーボンナノチューブの成長機構とカイラル制御 33
阿知波 洋次

一般講演 (10:00-11:00)
ナノチューブの生成と精製・物性

3-1 シリカライト-1 ゼオライト結晶面からの単層カーボンナノチューブ成長と顕微蛍光分光 62
○村上 陽一，茂木 堯彦，チャイキッティスィン ワッチャロップ，宮内 雄平，野田 優，大久保 達也，丸山 茂夫

3-2 多層グラフェンと配向カーボンナノチューブから形成された新規炭素構造体の硬X線光電子分光による研究 63
○近藤 大雄，佐藤 信太郎，二瓶 瑞久，池永 英司，小畠 雅明，金 正鎮，小林 啓介，粟野 祐二

3-3 単層カーボンナノチューブの超強磁場分光 64
○横井裕之、ムフタール・エフェンディ、南信次、小嶋映二、嶽山正二郎

3-4 ボロンドープカーボンナノチューブ薄膜におけるマイスナー効果 65
村田尚義、○春山純志、J. Reppert、A. M. Rao、是常隆、斎藤晋

☆☆☆☆☆☆☆ 休憩 (11:00-11:15) ☆☆☆☆☆☆☆

一般講演 (11:15-12:30)
内包ナノチューブ・Si フラーレン

3-5 準一次元系における水の構造と相挙動 66
○高岩大輔、甲賀研一郎、田中秀樹

3-6 単層カーボンナノチューブのブリージングモードに対するフラーレン内包の影響 67
○鄭淳吉、岡崎俊也、岸直希、中西毅、岡田晋、坂東俊治、飯島澄男

3-7 カーボンナノチューブテンプレートを用いた細い金属ナノワイヤの合成とキャラクタリゼーション 68
○北浦良、中西亮、斎藤毅、吉川浩史、阿波賀邦夫、篠原久典

3-8 ナノワイヤー完全内包カーボンナノチューブのレーザー蒸発による簡単な形成 69
○小海文夫、島津智行、足立一磨、高橋裕、小塩明

3-9 分子動力学シミュレーションによるSiフラーレンの自己組織化 70
○西尾憲吾、尾崎泰助、森下徹也、三上益弘

☆☆☆☆☆☆☆ 昼食 (12:30-13:30) ☆☆☆☆☆☆☆

特別講演 (13:30-14:00)

3S-2 グラフェン電気伝導のゲート電界制御 34
塚越一仁、宮崎久生、小高隼介、佐藤崇、田中翔、 神田晶申、大塚洋一、青柳克信

一般講演 (14:00-15:00)
グラフェン

3-10 グラフェン系スピンバルブにおけるスピン注入・スピン操作とスピン偏極率評価 71
○白石誠司・大石恵・野内亮・野崎隆行・新庄輝也・鈴木義茂

3-11 グラフェンシート引き裂きのMDシミュレーション：端の原子構造 72
○河合孝純、岡田晋、宮本良之、日浦英文

フラーレンの化学・金属内包フラーレン

3-12 液晶性十重付加型[60]フラーレンの合成，光物性と規則的な超分子構造 73
○李 昌治、松尾 豊、中村 栄一

3-13 常磁性金属内包フラーレン $La@C_{82}$ におけるラジカルカップリング反応 74
○高野勇太、蓬田知行、二川秀史、若原孝次、土屋敬広、生沼みどり、前田優、赤阪健、加藤立久、ズデネク・スラニナ、溝呂木直美、永瀬茂

8月29日 (金)

ポスタープレビュー (15:00-16:00)

ポスターセッション (16:00-17:30)

フラーレンの化学

3P-1 五重付加型 [60] フラーレンおよびその鉄・ルテニウム錯体の有機光電変換デバイス 179
○松尾 豊，新実高明，橋口昌彦，佐藤佳晴，中村栄一

3P-2 Fullerenes C_{32} and $X@C_{32}^{n}$ (X= He, Ne and Ar; n= 0, 2) 180
○ Weiwei Wang, Xiang Zhao

3P-3 [70] フラーレン二核ルテニウム錯体の合成と電気化学的性質 181
○藤田健志，松尾豊，中村栄一

3P-4 精密金属触媒によるフラーレンの化学修飾 182
○森進、南保正和、伊丹健一郎

金属内包フラーレン

3P-5 金属内包フラーレン $M@C_{82}(C_{2v})$ の放射光 X 線回折を用いた系統的な結晶構造研究 183
○青野貴行、西堀英治、北浦良、青柳忍、高田昌樹、坂田誠、澤博、篠原久典

3P-6 $N@C_{60}$ / C_{60} ナノウィスカーの ESR 測定 184
○加藤立久、長田良一、枝松徹、Michael Scheloske、Wolfgang Harneit、若原孝次、宮澤薫一

3P-7 内包フラーレン製造のためのイオン注入装置の開発 185
○片渕 竜也、福田 一志、長谷川 純、小栗 慶之、渡辺 智

3P-8 $N@C_{60}$ の生成および ESR 検出 186
○若林知成、黒田孝義

3P-9 non-IPR フラーレンの化学修飾：$La_2@C_{72}$ 二付加体の合成と構造 187
○廬 興、二川秀史、石塚みどり、土屋敬広、前田 優、赤阪 健、スラニナズデネク、溝呂木直美、永瀬 茂

フラーレン固体

3P-10 超伝導相ナトリウム添加フラーレン化合物 $Na_{8.2}C_{60}$ の ESR 測定 188
○木全 希、平郡 諭、小林 本忠

3P-11 $Eu_{2.75}C_{60}$ 及び $Sm_{2.75}C_{60}$ における電子相転移 189
○神戸高志，山成悠介，川崎菜穂子，太田洋平，今井久美子，久保園芳博

3P-12 $NaxHyC_{60}$ 化合物の結晶構造と電子物性 190
○緒方啓典，大波英幸

3P-13 Cs_3C_{60} の電子構造 191
○斎藤 晋

3P-14 Cs_3C_{60} における Tc の圧力依存性 192
○高野 琢，竹下 直，A. Y. Ganin，高林 康裕，M. J. Rosseinsky，K. Prassides，高木 英典，十倉 好紀，岩佐 義宏

3P-15 放射光による単結晶 $H_2@C_{60}$ の精密構造解析 193
○土岐睦、澤博、若林祐助、西堀英治、村田清次郎、小松紘一、二川秀史、赤阪健、谷垣勝巳

フラーレン生成・高次フラーレン

3P-16 原子状炭素挿入反応による直線型炭素鎖の最も簡単な成長 194
○尾形照彦、畳谷仁男

ナノチューブの物性

3P-17 単層カーボンナノチューブ pn 接合特性におけるドーパントコンビネーション効果 195
○加藤 俊顕, 宍戸 淳, 大原 渡, 畠山 力三, 田路 和幸

3P-18 DNA により分散された単層カーボンナノチューブの偏光蛍光励起分光 196
○ Erik Einarsson, Yoichi Murakami, Ming Zheng, Slava V. Rotkin, Yuhei Miyauchi, Shigeo Maruyama

3P-19 周囲物質による SWNT 熱伝導の低下 197
○塩見淳一郎，丸山茂夫

3P-20 分散剤を用いた単層カーボンナノチューブの溶媒への再分散 198
○酒井歩、内田勝美、石井忠浩、矢島博文

3P-21 熱フィラメント CVD 法により合成したホウ素ドープ MWNT 199
○石井聡，渡邊徹，津田俊輔，山口尚秀，高野義彦

3P-22 金属単層カーボンナノチューブ薄膜のシート抵抗 200
○宮田耕充、柳和宏、真庭豊、片浦弘道

3P-23 Electric Double Layer Transistor of Graphene 201
○ J. T. Ye, H. Shimotani, M. F. Craciun, A. F. Murpurgo, and Y. Iwasa

3P-24 不純物ドープしたカーボンナノチューブの電子状態 202
○是常隆、斎藤晋

3P-25 酸処理によるカーボンナノコイルの重量減少とその温度と時間による依存 203
○横田 真志, 篠原 雄一郎, 須田 善行, 桶 真一郎, 滝川 浩史, 藤村 洋平, 山浦 辰雄, 伊藤 茂生, 三浦 光治, 盛興 昌勝

3P-26 in vivo によるラット軟組織に対する脱フッ素化法による多層カーボンナノチューブブロックの組織反応 204
○佐藤義倫、横山敦郎、笠井孝夫、橋口慎二、本宮憲一、バラチャンドラン ジャヤデワン、田路和幸

ナノチューブの応用

3P-27 単層カーボンナノチューブ/UV 硬化性樹脂ナノコンポジットの熱拡散率 205
○福丸貴弘、藤ヶ谷剛彦、中嶋直敏

3P-28 垂直配向 SWNT 膜成長過程の特性評価と色素増感型太陽電池への応用 206
○大川 潤, 塩見 淳一郎, 丸山 茂夫

3P-29 可溶性 S W N T による ITO 基板への安定な電気化学的活性な薄膜形成 207
○王 奇観、森山広思

3P-30 電子レンジを用いた単層カーボンナノチューブの効率的化学官能基化 208
○黒木希、近藤真理子、菅井俊樹、森山広思

3P-31 Single Wall Carbon Nanohorn for Controlled Release 209
○ Xu Jianxun, Yudasaka Masako, Iijima Sumio

3P-32 Comparative Study of Carbon and BN Nanographenes: Ground Electronic States and Energy gap Engineering 210
○ Xingfa Gao, Zhongfang Chen and Shigeru Nagase

ナノチューブの生成と精製

3P-33 金触媒からの単層カーボンナノチューブ CVD 成長における水素ガス効果 211
○ゾーレ ゴラネビス, 加藤 俊顕, 金子 俊郎, 畠山 力三

3P-34 密度勾配電気泳動法を用いた単層カーボンナノチューブのカイラリティー分離 212
○上之薗 佳也、 内田 勝美、 石井 忠浩、 矢島 博文

3P-35 (Fe,Co)Pt 触媒によるカーボンナノチューブの化学気相成長 213
○園村拓也、岩田展幸、山本寛

3P-36 その場 FTIR 測定と数値計算によるカーボンナノチューブ成長中の原料ガス分解量の解析 214
○佐藤信太郎、野末竜弘、川端章夫、村上智、近藤大雄、二瓶瑞久、粟野祐二

3P-37 高真空 CVD 法による単層カーボンナノチューブの合成制御 215
○山本 洋平, 岡部 寛人, 丸山 茂夫

3P-38 光学測定による金属および半導体単層カーボンナノチューブの比率評価 216
○宮田耕充、柳和宏、真庭豊、片浦弘道

3P-39 窒素雰囲気中アーク放電法で作製した単層カーボンナノチューブの分散 217
○水澤崇志、鈴木信三、阿知波洋次

3P-40 急速昇温法を用いた ACCVD 法による単層カーボンナノチューブの合成 218
○庄司真雄, 緒方啓典

3P-41 e-DIPS 法における SWCNT 直径の反応温度依存性 219
○斎藤 毅、ビカウシュクラ、岡崎俊也、湯村守雄、飯島澄男

3P-42 メゾ及びマイクロ多孔質内部からの触媒担持化学的気相成長法による単層カーボンナノチューブ成長 220
○小林慶太, 北浦良, 熊井葉子, 後藤康友, 稲垣伸二, 篠原久典

内包ナノチューブ

3P-43 カーボンナノチューブ内部での触媒金属による単層カーボンナノチューブ生成 221
○伊豆 好史, 塩見 淳一郎, 丸山 茂夫

3P-44 C_{60} ピーポッドの ^{13}C NMR 222
○松田和之、片浦弘道、真庭豊

3P-45 単層カーボンナノチューブ内部の水の相転移 223
客野遥、三上史記、今泉利美、○松田和之、斎藤毅、大島哲、湯村守雄、飯島澄男、宮田耕充、片浦弘道、真庭豊

3P-46 ナノチューブ内分子リニアモーターにおける温度依存性の分子動力学計算 224
○上野 吉範、 杣田 博史、 平原 佳織、 中山 喜萬、 秋田 成司

3P-47 単層カーボンナノチューブ内包ユーロピウムナノワイヤの合成、構造および磁気物性 225
○中西亮、北浦良、斎藤毅、吉川浩史、阿波賀邦夫、篠原久典

3P-48 二層カーボンナノチューブへの直鎖ポリイン分子の内包 226
○趙晨、西出大亮、北浦良、篠原久典

3P-49 Fabrication and Characterization of Room Temperature Ionic Liquids inside SWNTs 227
○ Shimou Chen, Chen Zhao, Keita Kobayashi, Naoki Imazu, Ryo Kitaura, Hisanori Shinohara

グラフェン

3P-50 Co電極を持つグラフェン電界効果トランジスタの異常な伝達特性 228
○野内亮、白石誠司、鈴木義茂

August 27th, Wed.

Plenary Lecture:	40 min (Presentation) + 5 min (Discussion)
Special Lecture:	25 min (Presentation) + 5 min (Discussion)
General Lecture:	10 min (Presentation) + 5 min (Discussion)
Poster Preview:	1 min (Presentation), No Discussion

Plenary Lecture (9:30-10:15)

1S-1 Carbon Nanotubes by CCVD Process ~Mass production, Applications and Safety for Success~ 29
M. Endo, T. Hayashi, Y.A. Kim, K. Takeuchi, H. Muramatu, S. Koyama

General Lecture (10:15-11:00)
Applications of Nanotubes

1-1 Attachment of Carbon Nanotubes using Structural Changes in C_{60} Molecules by Electron Irradiation 35
○ Ryosuke Senga, Hiroyuki Maruyama, Kaori Hirahara, Yoshikazu Nakayama

1-2 Near-IR laser-driven reversible volume phase transition of single-walled carbon nanotubes / poly (N-isopropylacrylamide) composite gels 36
○ Tatsuro Morimoto, Tsuyohiko Fujigaya, Yasuro Niidome, Naotoshi Nakashima

1-3 Properties of Visible-Light-Emission in Chemically-Modified CNT-FET 37
○ Ryotaro Kumashiro, Naoya Komatsu, Takeshi Akasaka, Yutaka Maeda, Katsumi Tanigaki

☆☆☆☆☆☆☆ Coffee Break (11:00-11:15) ☆☆☆☆☆☆☆

General Lecture (11:15-12:30)
Properties of Nanotubes

1-4 Studies on Electronic Structures of Single-Walled Carbon Nanotubes Synthesized Controlling the Diameter by Optical Absorption Spectroscopy 38
○ Takeshi Saito, Shigekazu Ohmori, Bikau Shukla, Motoo Yumura, Sumio Iijima

1-5 AFM-HRTEM Combined Technique for Probing Electronic Transition of Isolated Carbon Nanotubes 39
○ Shota Kuwahara, Toshiki Sugai, Hisanori Shinohara

1-6 Radiative lifetimes of excitons and their sizes in single-walled carbon nanotubes 40
○ Yuhei Miyauchi, Hideki Hirori, Kazunari Matsuda,Yoshihiko Kanemitsu

1-7 Fabrication of suspended single-walled carbon nanotubes with a tweezers tip for the optical property study 41
○ Huaping Liu, Shohei Chiashi, Masafumi Ishiguro and Yoshikazu Homma

1-8 Chirality dependent phonon frequency shift of carbon nanotubes 42
○ K. Sasaki, R. Saito, G. Dresselhaus, M.S. Dresselhaus, H. Farhat, J. Kong

☆☆☆☆☆☆☆ Lunch Time (12:30-13:30) ☆☆☆☆☆☆☆

Special Lecture (13:30-14:00)

1S-2 Fabrication and Characterization of Carbon Nanotube FETs 30
Takashi Mizutani, Yutaka Ohno and Shigeru Kishimoto

General Lecture (14:00-15:00)
Applications of Nanotubes • Nanohorns

1-9 Photoinduced electrical transport properties of azafullerene peapod field-effect transistors 43
○ Yongfeng Li, Toshiro Kaneko, and Rikizo Hatakeyama

1-10 Preparation and Photoelectrochemical Properties of Nanocarbon Composite Films on Semiconductor Electrodes 44
○ Tomokazu Umeyama, Noriyasu Tezuka, Yoshihiro Matano, Hiroshi Imahori

1-11 Rotational Motion of Carbon Nanotube Induced by Rubbing with Carbon Nanotube 45
○ Yoshiteru Takagi, Takahisa Ohno, Susumu Okada

1-12 Imaging of Conformational Changes of Triamide Molecules Covalently Bonded to a Carbon Nanohorn Surface 46
○ Koji Harano, Masanori Koshino, Takatsugu Tanaka, Yoshiko Niimi, Yuki Nakamura, Hiroyuki Isobe, Eiichi Nakamura

☆☆☆☆☆☆☆ Coffee Break (15:00-15:15) ☆☆☆☆☆☆☆

August 27th, Wed.

General Lecture (15:15-16:00)

Fullerene Solids

1-13 Development of ultra-sensitive gas sensor utilizing fullerenes 47
○ Morihiko Saida, Kenji Omote, Haruna Oizumi, Hiroyuki Sagami, Yuzo Mizobuchi, Yasuhiko Kasama, Kuniyoshi Yokoo, Shoichi Ono, Kazuaki Mizokami, Takeo Furukawa

1-14 Affect of the Substituent of C_{60}-derivatives on Electronic Structure: [6,6]-Phenyl-C61-Butyric Acid Methyl Ester (PCBM) 48
○ Kouki Akaike, Kaname Kanai, Hiroyuki Yoshida, Jun'ya Tsutsumi, Toshio Nishi, Naoki Sato, Yukio Ouchi and Kazuhiko Seki

1-15 Preparation of Fullerene (C_{60}) Nanosheets by Liquid-liquid Interfacial Precipitation Method 49
○ M. Sathish, K. Miyazawa and T. Wakahara

Poster Preview (16:00-17:00)

Poster Session (17:00-18:30)

Chemistry of Fullerenes

1P-1 Aziridination of C_{60} with Simple Amides and Catalytic Rearrangement of the Aziridinofullerenes to Azafulleroids 75
Ryouji Tsuruoka, ○ Toshiki Nagamachi, Satoshi Minakata

1P-2 Effects of various additives on reaction products of solid-state oxygenation of fullerene C_{60} via mechanochemical route 76
○ Yuichi Ishiyama, Yusuke Tajima, Mamoru Senna, Hiroto Watanabe

1P-3 Electrochemical Properties of Indolino[2',3':1,2][60]fullernens 77
○ Youhei Numata, Jun-ichi Kawashima, Yusuke Tajima

1P-4 Formation of *Benzo*[b]*furano*[60]fullerene from [60]Fullerene Monoepoxide 78
○ Junichi Kawashima, Youhei Numata, Yusuke Tajima

Metallofullerenes

1P-5 Electron Spin Properties for La@C_{82} in Solid Empty Fullerene Matrices 79
○ Yasuhiro Ito, Jamie H. Warner, Mujtaba Zaka, Takayuki Aono, Noriko Izumi, Haruya Okimoto, John J. L. Morton, Hisanori Shinohara, G. Andrew D. Briggs

1P-6 Ultraviolet Photoelectron Spectroscopy of M_2@C_{80} (M=La, Ce, Lu, LuC) 80
Takafumi Miyazaki, Yuusuke Aoki, Youji Tokumoto, Ryohei Sumii, Haruya Okimoto,

1P-7 Synthesis and Characterization of a Carbene Derivative of Sc_2C_{82} 81
○ Hiroki Kurihara, Yuko Yamazaki, Midori O. Ishitsuka, Takahiro Tsuchiya,Takeshi Akasaka, Naomi Mizorogi and Shigeru Nagase

1P-8 Endohedral Metallofullerene Derivative: La@C_{82}($C_6H_3Cl_2$) 82
○ Hidenori Kuga, Hidefumi Nikawa, Takahiro Tsuchiya, Midori O. Ishitsuka, Zdenek Slanina, Takeshi Akasaka, Naomi Mizorogi, Shigeru Nagase

1P-9 Preparation and Characterization of A Carbene Derivative of Sc@C_{82} 83
○ Makoto Hachiya, Yuko Yamazaki, Midori O. Ishitsuka, Takahiro Tsuchiya, Takeshi Akasaka, Naomi Mizorogi, Shigeru Nagase

1P-10 Thermal reaction of La_2@C_{80} with silacyclopropane 84
○ Minowa Mari, Yamada Michio, Kako Masahiro, Tsuchiya Takahiro, Ishitsuka O. midori, Akasaka Takeshi

Fullerene Solids

1P-11 Fabrication and characteristics of C_{60} thin film FETs with conducting polymer electrodes 85
Yumiko Kaji, Naoko Kawasaki, ○ Yoshihiro Kubozono, Akihiko Fujiwara

1P-12 Vibrational Spectroscopy of an Electron-beam-irradiated C_{60} Film 86
○ Toshiaki Nishii, Akito Takashima, Sou Ryuzaki, Toshihiro Kai, and Jun Onoe

1P-13 SEM Observation of Vertically-Aligned Fullerene Microtubes 87
○ Sho Toita, Kun'ichi Miyazawa and Masaru Tachibana

1P-14 Atomistic observations of O_2 exposed C_{60} thin films 88
Masashi Shimura, Keisuke Kato, Morihiko Saida, Haruna Oizumi, Kenji Omote, Kuniyoshi Yokoo, Shigehiko Yamamoto, ○ Masahiro Sasaki

1P-15 Local work function of C_{60} monolayer on Cu(111) observed with scanning tunneling microscopy 89
○ Keisuke Kato, Masashi Shimura, Morihiko Saida, Kenji Omote, Kuniyoshi Yokoo, Masahiro Sasaki

1P-16 C_{60} crystal growth from organic solution for the field effect transistor 90
○ Kurihara Kouhei, Yasunari Iio, Ryo Nokariya, Humihiko Matsuyama, Nobuyuki Iwata, Hirosi Yamamoto

1P-17 Extending the Polymerized C_{60} Size by Irradiating the Free Electron Laser during the Film Deposition 91
○ Ryo Nokariya, Shinji Hachiya, Yasunari Iio, Nobuyuki Iwata, Hiroshi Yamamoto

Carbon Nanoparticles

1P-18 TEM observation of fullerenes intratracheally instilled in the rat lung 92
○ Kazuhiro Yamamoto, Miyabi Makino, Emiko Kobayashi, Akira Ogami, Yasuo Morimoto

1P-19 A Facile and Scalable Process for Size-Controllable Separation of Nanodiamond as Small as 4 nm in Size 93
○ Naoki Komatsu, Yoichi Morita, Tatsuya Takimoto, Hiroshi Yamanaka, Katsumi Kumekawa, Shizuka Morino, Shuji Aonuma, Takahide Kimura

1P-20 Synthesis and Magnetic Properties of Strontium Carbon Compound 94
○ Satoshi Heguri, Nozomu Kimata, Mototada Kobayashi

Properties of Nanotubes

1P-21 Global Spectral Analysis Method for Simulating Excitation-Emission Maps of Semiconducting Single-Walled Carbon Nanotubes 95
○ Adam M. Gilmore

1P-22 Electric-field modulation in Carbon nanotubes 96
○ Yoshiyuki Miyamoto

1P-23 Superconductivity in ensemble of boron-doped carbon nanotubes 97
○ M.Matsudaira, J.Nakamura, N.Murata, J.Haruyama, J.Reppert, A.M.Rao, T.Koretsune, S.Saito, Y.Yagi

1P-24 Interlayer nano p-n junctions formed in double-walled carbon nanotubes 98
○ T.Shimizu, J.Haruyama, K.Nozawa, T.Sugai, H.Shinohara

1P-25 Third-order nonlinear optical properties and phase relaxation time in semiconducting single-walled carbon nanotubes 99
○ M. Ichida, S. Saito, Y. Miyata, H. Kataura, and H. Ando

1P-26 Li ion storage properties of organic molecules encapsulated single-walled carbon nanotubes 100
○ M. Hirose, S. Kawasaki, Y. Iwai

1P-27 High-Performance Liquid Chromatographic Separation and Characterization of DNA-Wrapped Single-Wall Carbon Nanotubes 101
○ Yuki Asada, Toshiki Sugai, Ryo Kitaura, Hisanori Shinohara

1P-28 Roles of Conformational Restrictions of Carbene-derivatives in the Interactions with a Carbon Nanotube 102
○ Takashi Yumura, Miklos Kertesz

1P-29 Pressure-Induced Structural Phase Transition of Double-walled Carbon Nanotube and Electronic Structure of Carbon Nano-structured Materials 103
○ Masahiro Sakurai and Susumu Saito

1P-30 Polarized Raman spectroscopy of Vertically Aligned Single-walled Carbon Nanotubes 104
○ Zhengyi Zhang, Yoichi Murakami, Erik Einarsson,Yuhei Miyauchi, Shigeo Maruyama

1P-31 The effect of laser-induce defects on the Raman G band in metallic SWNTs 105
○ Dongchul Kang, Kenichi Kato, Kenichi Kojima, Masaru Tachibana

Applications of Nanotubes

1P-32 1D-array of SWCNT emitters instantly mounted in micro-cathodes 106
○ Suguru Noda, Koji Furuichi, Yosuke Shiratori, Yoshiko Tsuji, Hisashi Sugime

1P-33 Semiconducting single wall carbon nanotubes network for field effect transistors devices 107
○ Nicolas Izard, Said Kazaoui, Nobutsugu Minami

1P-34 Application for heat-release devices of carbon nanotube films made by surface decomposition of SiC 108
○ Wataru Norimatsu, Chihiro Kawai, Michiko Kusunoki

1P-35 Fabrication and Transport Properties of Carbon Nanotube Transistors by Direct Growth Method 109
○ A. Fujiwara, N. Inami, M. A. Mohamed, E. Shikoh

1P-36 Fabrication and characterization of field effect transistors by using high-purity semiconducting single-wall carbon nanotubes 110
○ Shunjiro Fujii, Yasumitsu Miyata, Kazuhiro Yanagi, Takeshi Tanaka, Daisuke Nishide, Hiromichi Kataura

1P-37 Light-driven Carbon Nanotube-Microdevice 111
○ Eijiro Miyako, Hideya Nagata, Ken Hirano, Takahiro Hirotsu

Formation and Purification of Nanotubes

1P-38 Genomic DNA-Mediated Solubilization and Separation of Single Wall Carbon Nanotubes 112
○ Sang Nyon Kim, Kristi M. Singh, Fahima Ounchen, James G. Grote and Rajesh R. Naik

1P-39 An Experimental Investigation of Active Roles of sp^2 Carbon Precursors in SWCNT Growth 113
○ B. Shukla, T. Saito, M. Yumura, S. Iijima

1P-40 Optical and (n, m) Enrichments of (7,5)-SWNTs through Extraction with Chiral Monoporphyrin 114
○ Xiaobin Peng, Naoki Komatsu, Takahide Kimura, Atsuhiro Osuka

1P-41 Synthesis of single-walled carbon nanotubes by arc plasma reactor with twelve-phase alternating current discharge 115
○ Tsugio. Matsuura, Yukie. Kondo, Norio. Maki

1P-42 Effective Separation of Carbon Nanotubes and Metal Particles from Pristine Raw Soot by Ultracentrifugation 116
○ Daisuke Nishide, Yasumitsu Miyata, Kazuhiro Yanagi, Takeshi Tanaka, Hiromichi Kataura

1P-43 Unidirectional Growth of Single-Walled Carbon Nanotubes 117
○ Naoki Ishigami, Hiroki Ago, Tetsushi Nishi, Ken-ichi Ikeda, Masaharu Tsuji Tatsuya Ikuta, Koji Takahashi

1P-44 Fabrication and Characterization of Telescope type Double Walled Carbon Nanotubes 118
○ Nobuyuki Fukui, Naoki Imazu, Keita Kobayashi, Hiromichi Yoshida, Shota Kuwahara, Toshiki Sugai, Tomihiro Hahisuzme, Hisanori Shinohara

1P-45 FT-IR Analysis in Alcohol Catalytic Chemical Vapor Deposition (2) 119
○ Tomohiro Shimazu, Yoshinobu Suzuki, Hisayoshi Oshima and Shigeo Maruyama

1P-46 CNT growth on gas permeable substrates 120
○ Shinichi Mukainakano, Kenji Okeyui, Hisayoshi Oshima, and Shigeo Maruyama

1P-47 Super-Growth: Large Area Synthesis of SWNTs, -Toward Industrial-scale Production- 121
○ Satoshi Yasuda, Don N. Futaba, Motoo Yumura, Sumio Iijima, and Kenji Hata

Endohedral Nanotubes

1P-48 Rotating fullerene chains in carbon nanopeapods 122
○ Jamie H. Warner, Yasuhiro Ito, Mujtaba Zaka, Ling Ge, Takao Akachi, Haruya Okimoto, Kyriakos Porfyrakis, Andrew A. R. Watt, Hisanori Shinohara, G. Andrew D. Briggs

1P-49 Fabrication of Metal-Nanowire in Carbon Nanotube via Nano-Template Reaction Using Various Mono-, Di-,Tri-Metallofullerenes and Metal-Carbide Fullerenes Peapods 123
○ Naoki Imazu, Ryo Kitaura, Keita Kobayashi, Haruya Okimoto, Yasuhiro Ito,Takeshi Saito and Hisanori Shinohara

1P-50 Motion of ssDNA inside the single-wall nanotube studied by electron microscopy 124
○ Masayuki Shoda, Yusei Maruyama, Shunji Bandow, Sumio Iijima

1P-51 Phase behavior and fluid-wall interfacial tension of confined fluids 125
○ Yoshinobu Hamada, Kenichiro Koga, and Hideki Tanaka

1P-52 Investigation of Electric and Mass Transport of a Copper Nano-Rod Encapsulated in a Carbon Nanotube 126
○ Fumitaka Kimura, Koji Asaka, Hitoshi Nakahara, Fumio Kokai, Yahachi Saito

August 28th, Thu.

Plenary Lecture:	40 min (Presentation) + 5 min (Discussion)
Special Lecture:	25 min (Presentation) + 5 min (Discussion)
General Lecture by Candidates for the Osawa or Iijima Award:	10 min (Presentation) + 10 min (Discussion)
General Lecture:	10 min (Presentation) + 5 min (Discussion)
Poster Preview:	1 min (Presentation), No Discussion

Plenary Lecture (9:30-10:15)

2S-1 Superconductivity in expanded fullerides 31
Matthew J. Rosseinsky

General Lecture by Candidates for the Osawa Award (10:15-10:55)

2-1 Visit to the Missing Fullerene World 50
○ Hidefumi Nikawa, Takashi Kikuchi, Tomoya Yamada, Hidenori Kuga, Tsuyoshi Ito, Slanina Zdenek, Takeshi Akasaka, Naomi Mizorogi, and Shigeru Nagase

2-2 Design, Synthesis, and Testing of Fullerene-wheeled Nanocars 51
○ Yasuhiro Shirai、Andrew J. Osgood、Jean-Francois Morin、Takashi Sasaki、Yuming Zhao、Jason M. Guerrero、Kevin F. Kelly、James M. Tour

☆☆☆☆☆☆☆ Coffee Break (10:55-11:10) ☆☆☆☆☆☆☆

General Lecture by Candidates for the Iijima Award (11:10-12:30)

2-3 Direct observation of nucleation and growth of carbon nanotubes from iron carbide nanoparticles 52
○ Hideto Yoshida, Tetsuya Uchiyama, Hideo Kohno, Seiji Takeda, and Yoshikazu Homma

2-4 Simple Separation of Metallic and Semiconducting Carbon Nanotubes 53
○ Takeshi Tanaka, Hehua Jin, Yasumitsu Miyata, Shunjirou Fujii, Hiroshi Suga, Yasuhisa Naitoh and Hiromichi Kataura

2-5 Ink-jet Printing of High-Performance SWNT Film Transistors 54
○ Haruya Okimoto, Taishi Takenobu, Kazuhiro Yanagi, Yasumitsu Miyata, Hiromichi Kataura, Takeshi Asano, Yoshihiro Iwasa

2-6 Integrated Three-Dimensional Microelectromechanical Devices from Processable Carbon Nanotube Wafers 55
○ Yuhei Hayamizu, Takeo Yamada, Kohei Mizuno, Robert C. Davis, Don N. Futaba, Motoo Yumura, Kenji Hata

☆☆☆☆☆☆☆ Lunch Time (12:30-13:30) ☆☆☆☆☆☆☆

General Meeting (13:30-13:45)

Special Lecture (13:45-14:15)

2S-2 High pressure synthesis of nano-polycrystalline diamonds by direct conversion from various carbon materials and their characterization 32
Hitoshi Sumiya

General Lecture (14:15-15:00)
Fullerene Solids • Network Solids

2-7 STM study on C_{70} close-packed layers 56
○ Yohei Ohta, Ryoji Mitsuhashi, Yoshihiro Kubozono

2-8 Electronic and optical properties of electron-beam-irradiated C_{60} films 57
○ J. Onoe, T. Ito, S. Kimura, Y. Toda, S. Ryuzaki, K. Ohno, and T.A. Beu

2-9 Template Synthesis of Ordered Network Structure of Fullerene- or Nanotube-like Molecules 58
○ Hirotomo Nishihara, Katsuaki Imai, Peng-Xiang Hou, Juan I. Paredes, Amelia Martnez-Alonso, Juan M.D. Tascn, and Takashi Kyotani

☆☆☆☆☆☆☆ Coffee Break (15:00-15:15) ☆☆☆☆☆☆☆

August 28th, Thu.

General Lecture (15:15-16:00)

Formation and Purification of Nanotubes

2-10 Diameter Control of Vertically Aligned SWNT Arrays from ACCVD 59
○ Rong Xiang, Zhengyi Zhang, Erik Einarsson, Jun Okawa, Yoichi Murakami, Shigeo Maruyama

2-11 Growth of Horizontally-Aligned Single-Walled Carbon Nanotubes on Surface Modified Silicon Substrate 60
○ Naoki Yoshihara, Hiroki Ago, Kenta Imamoto, Masaharu Tsuji, Tatsuya Ikuta, Koji Takahashi

2-12 5-nm-thick SWCNTs originated from catalyst particles with increasing diameters 61
○ Kei Hasegawa and Suguru Noda

Poster Preview (16:00-17:00)

Poster Session (17:00-18:30)

Chemistry of Fullerenes

2P-1 Apoptosis Induction on HL-60 Cell by Cationic Fullerene Derivatives 127
○ Sachiko Yokoo, Chiho Nishizawa, Kyoko Takahashi, Shigeo Nakamura, Tadahiko Mashino

2P-2 A Light-Emitting Cyclic Benzenoid as a Dendritic Core —Deca(carbazolylphenyl)[60]fullerene— 128
○ Xiaoyong Zhang, Yutaka Matsuo, and Eiichi Nakamura

2P-3 Electron Donor-Acceptor Interactions in Uniquely Shaped Double-Decker Buckyferrocenes 129
○ Keiko Matsuo, Yutaka Matsuo, Dirk M. Guldi, and Eiichi Nakamura

2P-4 Synthesis of Penta(organo)[60]fullerenes Methacrylates 130
○ Hiromi Oyama, Yutaka Matsuo, Eiichi Nakamura

Metallofullerenes

2P-5 Enhanced *Photoluminescence* from Mono- and Di- Thulium Metallofullerenes 131
○ Noriko Izumi, Masahiro Akachi, Yasuhiro Ito, Toshiya Okazaki, Ryo Kitaura, Toshiki Sugai and Hisanori Shinohara

2P-6 Bis-adduct of Non-IPR La@C_{72} 132
○ Tsuyoshi Ito, Hidefumi Nikawa, Takeshi Akasaka, Midori O. Ishitsuka, Takahiro Tsutiya, Zdenek Slanina, Naomi Mizorogi, Shigeru Nagase

2P-7 Synthesis and Properties of Endohedral Metallofullerene Ligands 133
○ Yuya Yokosawa, Takahiro Tsuchiya, Takeshi Akasaka

2P-8 Formation and Behavior of Supramolecular Complex based on Endhedral Metallofullerene 134
○ Sato Ayumi, Takahiro Tsuchiya, Takeshi Akasaka, Nazario Martin

2P-9 Reversible and Regioselective Reaction of La@C_{82} with 1,2,3,4,5-Pentamethylcyclopentadiene 135
○ Satoru Sato, Yutaka Maeda, Koji Inada, Michio Yamada, Takahiro Tsuchiya, Midori O. Ishitsuka, Tadashi Hasegawa, Takeshi Akasaka, Tatsuhisa Kato,Naomi Mizorogi, Zdenek Slanina, Shigeru Nagase

Fullerene Solids

2P-10 The external quantum efficiency of C_{60}/Zinc-porphyrin layered films 136
○ Sou Ryuzaki, Toshihiro Kai, Toshiaki Nishii, and Jun Onoe

2P-11 Study of the Interaction between PMA-treated THP-1 Cells and FNWs 137
○ Shin-ichi Nudejima, Kun'ichi Miyazawa, Junko Okuda-Shimazaki and Akiyoshi Taniguchi

2P-12 First-principle calculations of the thorough electron states of one-dimensional peanut-shaped C_{60} polymers 138
○ Akito Takashima, Nishii Toshiaki, Jun Onoe

2P-13 First principles study of electron transport properties of Double-Decker Buckyferrocene 139
○ Yoshihisa Ohshima

2P-14 Noncontact Thickness Monitor of Organic and Molecular Films 140
○ Haruna Oizumi, Morihiko Saida, Hiroyuki Sagami, Kenji Omote, Yuzo Mizobuchi, Yasuhiko Kasama, Kuniyoshi Yokoo, Shoichi Ono, Toshiyasu Tadokoro

2P-15 High Temperature Heat-treatment of C_{60} Nanotubes 141
○ Ryoei Kato, Kun ' ichi Miyazawa, Toshiyuki Nishimura and Zheng-ming Wang

Formation of Fullerenes, Higher Fullerenes

2P-16 The simplest cyclic-carbon-chain growth by atomic-carbon-insertion reactions 142
○ Teruhiko Ogata, Yutaka Shibi and Yoshio Tatamitani

Properties of Nanotubes

2P-17 Thermal conductivity characterization of vertically-aligned single-walled carbon nanotube films by three-omega method 143
○ Kei Ishikawa, Saburo Tanaka, Koji Miyazaki, Junichiro Shiomi, Shigeo Maruyama

2P-18 Electronic Structure and Energetics of Semiconducting Nanotubes adsorbed on SiO_2 (0001) Surfaces 144
○ Susumu Okada

2P-19 Determination of the absorption coefficient of semiconducting single-wall carbon nanotubes selectively dispersed with polyfluorene 145
○ Yoshisuke Futami, Said Kazaoui, Nobutsugu Minami

2P-20 Heat-Induced Charge Transfer from Sapphire to Aligned Carbon Nanotubes 146
○ Hiroki Ago, Izumi Tanaka, Masaharu Tsuji, Ken-ichi Ikeda, Seigi Mizuno

2P-21 Geometries, Electronic Properties and Energetics of Single-Walled Armchair Carbon Nanotubes 147
○ Koichiro Kato and Susumu Saito

2P-22 Diameter Dependence on Absorption Coefficients of Single-Wall Carbon Nanotubes 148
○ Shota Kuwahara, Yuki Asada, Toshiki Sugai, Hisanori Shinohara

2P-23 Interference Effects on Conductance between Two STM Probes in Carbon Nanotubes 149
○ Takeshi Nakanishi and Tsuneya Ando

2P-24 Electronic-Structure Modifications of Collapsed Single-Walled Carbon Nanotubes: The case of Armchair Tubes 150
○ Masayuki Hasegawa, Kazume Nishidate

2P-25 Annealing effect on mechanical properties of carbon nanocoils 151
○ Shun Sato, Yoshiaki Araki, Ryo Kanada, Yoshikazu Nakayama and Seiji Akita

2P-26 High Temperature Infrared Optical Spectroscopy of Single-Walled Carbon Nanotubes 152
○ Mukhtar Effendi, Hiroyuki Yokoi, Noritaka Kuroda

Applications of Nanotubes

2P-27 Fabrication of Carbon Nanotube Atomic Force Microscope Tip by Using Ionic Liquid and Its Characterization 153
○ Yuya Kamizono, Chien-Chao Chiu, Masamichi Yoshimura, Kazuyuki Ueda, Yuki Asada, Shota Kuwahara, Ryo Kitaura, Toshiki Sugai, and Hisanori Shinohara

2P-28 Optimization of gas sensing characteristics using networked SWNTs 154
○ Isao Sasaki, Nobutsugu Minami

2P-29 Contractile activity measurement of rat's digestive organ by CNT-based force transducer 155
○ Takamichi Hirata, Takatsugu Yanaka, Satoshi Sakahara, Kanako Koike, Chihiro Tsutsui, Takafumi Sakai, Masahiro Akiya

2P-30 Bio-Hazardous Effects of Carbon Nanotubes under Microwave Radiation 156
○ Hirokazu Horiguchi, Masahito Sano

2P-31 Field Effect Chromatography for Separating Chiral Carbon Nanotubes 157
○ Yuki Orinouchi, Akara Hashimoto, Yasushi Suzuki, Yasuyuki Watanabe and Masahito Sano

2P-32 Ideal interfacial structure constructed by the two-step assembly of Polybenzimidazole with Multi-walled Carbon Nanotubes and Pt nanoparticles for fuel cell catalyst 158
○ Minoru Okamoto, Tsuyohiko Fujigaya, Naotoshi Nakashima

2P-33 Electron Optical Evaluation of a Carbon Nanotube Field Emitter for Electron Microscopes 159
○ Yoshikazu Kusano Kouji Asaka Hitoshi Nakahara Yahachi Saitou

Formation and Purification of Nanotubes

2P-34 The Attempt of Chirality Control of Semiconducting Single-Walled Carbon Nanotubes by the Free Electron Laser Irradiation 160
○ Daisuke Ishizuka, Keijiro Sakai, Katsumi Uchida, Nobuyuki Iwata, Hirofumi Yajima and Hiroshi Yamamoto

2P-35 Selective Separation Methods for Metallic and Semiconducting Single-walled Carbon Nanotube in Aqueous Solution with High-fluence Pulsed OPO Laser 161
○ Isamu Tajima, Katsumi Uchida, Tadahiro Ishii, and Hirofumi Yajima

2P-36 Enhancement of Carbon Nanotube Growth at Low Temperature using Al2Ox Buffer Layer in Alcohol Gas Source Method 162
○ Takahiro Maruyama, Kuninori Sato, Tomoyuki Shiraiwa, Shigeya Naritsuka

2P-37 Separation of metallic and semiconducting single-wall carbon nanotubes by using sucrose as a gradient medium 163
○ Kazuhiro Yanagi, Iitsuka Toshie, Shunjiro Fujii, Hiromich Kataura

2P-38 Liquid-phase Synthesis of Highly Aligned Carbon Nanotubes with Heat-treated Stainless Steel Substrates 164
○ Kiyofumi Yamagiwa, Yoshihiro Yamaguchi, Tomoka Kikitsu, Shunsuke Yamashita, Tsuneharu Takeuchi, Morihiro Saito, Jun Kuwano

2P-39 Temperature dependence in the diameter distributions of SWNTs revealed by optical absorption measurements in solution 165
○ Takashi Nakayama, Akihito Inoue, Kazuma Yokoi, Yasuhiro Tsuruoka, Takeshi Kodama, Yohji Achiba

2P-40 Optical properties of SWNTs with very small diameter 166
○ N.Takamizu,Y.Ohnishi,K.Urata,S.Suzuki,H.Nagasawa,Y.Achiba

2P-41 Precursors in Co catalyzed CVD for vertically aligned SWCNT 167
○ Hisashi Sugime and Suguru Noda

2P-42 Controlling the wall number of carbon nanotubes by changing the carrier gases 168
○ Daisuke Yokoyama, Takayuki Iwasaki, Kentaro Ishimaru, Masatomo Iizuka, Shintaro Sato, Mizuhisa Nihei, Yuji Awano, Hiroshi Kawarada

2P-43 Correlations between gas pressure and diameter distribution of single-walled carbon nanotubes in diffusion plasma CVD 169
○ Shunsuke Kuroda, Toshiaki Kato, Toshiro Kaneko, and Rikizo Hatakeyama

2P-44 Growth of Helical Carbon Nanofiber by Catalytic Chemical Vapor Deposition Using Co/Sn Catalyst 170
○ Yuichiro Shinohara, Masashi Yokota, Yoshiyuki Suda, Shinichiro Oke, Hirofumi Takikawa, Youhei Fujimura, Tatsuo Yamaura, Shigeo Itoh, Kouji Miura, Masakatsu Morioki

Endohedral Nanotubes

2P-45 Diameter-Dependent Band Gap Modification of Single-Walled Carbon Nanotubes by Encapsulated Fullerenes 171
○ Toshiya Okazaki, Shingo Okubo, Naoki Kishi, Takeshi Nakanishi, Susumu Okada, Sumio Iijima

2P-46 Fusion Process of C_{60} fullerenes in Carbon-Nanotube Peapod 172
○ Yuichiro Yamagami, Susumu Saito

2P-47 Fabrication and Property Evaluation of Calcium Encapsulated Single-Walled Carbon Nanotubes 173
○ Tetsuhiro Shimizu, Toshiaki Kato, Wataru Oohara, Rikizo Hatakeyama

2P-48 Nano Scale Separation of the Different Cage Size Empty Fullerene by Nanopeapod Synthesis 174
○ Teguh Endah Saraswati,Naoki Imazu and Hisanori Shinohara

Nanohorns

2P-49 Supporting RuO_2 on Arc-Soot by Colloidal Method using Ultrasonic Sonication for Electrode Material of Supercapacitors 175
○ H. Uruno, M. Yamamoto, Y. Izumi, S. Oke, Y. Suda, H. Takikawa, S. Itoh, T. Yamaura, K. Miura, T. Okawa, N. Aoyagi

2P-50 Effect of Polyethylene Glycol-Peptide Conjugates on Dispersing Carbon Nanohorns and Their Accumulation in Lung 176
○ Sachiko Matsumura, Shigeo Sato, Masako Yudasaka, Akihiro Tomida, Takashi Tsuruo, Sumio Iijima, Kiyotaka Shiba

2P-51 Anticancer Effect of Cisplatin Incorporated Inside Single-Walled Carbon Nanohorns 177
○ Masako Yudasaka

2P-52 Thermal Hole closing of Single-Wall Carbon Nanohorns 178
○ Michiko Irie, Jing Fan, Sumio Iijima, Jin Miyawaki, Ryota Yuge, Takazumi Kawai, and Masako Yudasaka

August 29th, Fri.

Special Lecture:	25 min (Presentation) + 5 min (Discussion)
General Lecture:	10 min (Presentation) + 5 min (Discussion)
Poster Preview:	1 min (Presentation), No Discussion

Special Lecture (9:30-10:00)

3S-1 Chairality control; possible or not possible 33
Yohji Achiba

General Lecture (10:00-11:00)
Formation, Purification and Properties of Nanotubes

3-1 Synthesis of Single-Walled Carbon Nanotubes from Defined Surface of Silicalite-1 Zeolite and their Photoluminescence Characterizations 62
○ Yoichi Murakami, Takahiko Moteki, Watcharop Chaikittisilp, Yuhei Miyauchi, Suguru Noda, Tatsuya Okubo, Shigeo Maruyama

3-2 Hard x-ray photoelectron spectroscopy analyses of novel carbon structure consisting of graphene multi-layers and aligned carbon nanotubes 63
○ Daiyu Kondo, Shintaro Sato, Mizuhisa Nihei, Eiji Ikenaga, Masaaki Kobata, Jung Jin Kim, Keisuke Kobayashi and Yuji Awano

3-3 Megagauss Spectroscopy of Single-Walled Carbon Nanotubes 64
○ Hiroyuki Yokoi, Mukhtar Effendi, Nobutsugu Minami, Eiji Kojima, Shojiro Takeyama

3-4 Meissner effect in thin films of boron-doped carbon nanotubes 65
N. Murata, ○ J. Haruyama, J. Reppert, A. M. Rao, T. Koretsune, S. Saito

☆☆☆☆☆☆☆ Coffee Break (11:00-11:15) ☆☆☆☆☆☆☆

General Lecture (11:15-12:30)
Endohedral Nanotubes • Si Fullerene

3-5 Structures and Phase behavior of quasi-one-dimensional water 66
○ Daisuke Takaiwa, Kenichiro Koga, and Hideki Tanaka

3-6 Fullerene Encapsulation Effects on Radial Breathing Mode Frequencies of Single-Walled Carbon Nanotubes 67
○ Soon-Kil Joung, Toshiya Okazaki, Naoki Kishi, Takeshi Nakanishi, Susumu Okada, Shunji Bandow and Sumio Iijima

3-7 Fabrication and Characterization of Thin Metal Nanowires using Carbon Nanotube Template 68
○ R. Kitaura, R. Nakanishi, T. Saito, H. Yoshikawa, K. Awaga and H. Shinohara

3-8 A Simple Formation of Carbon Nanotubes Filled Perfectly with Nanowires by Laser Vaporization 69
○ Fumio Kokai, Tomoyuki Shimazu, Kazuma Adachi, Yutaka Takahashi, Akira Koshio

3-9 Formation of Si fullerenes: A molecular dynamics study 70
○ kengo nishio, taisuke ozaki, tetsuya morishita, masuhiro mikami

☆☆☆☆☆☆☆ Lunch Time (12:30-13:30) ☆☆☆☆☆☆☆

Special Lecture (13:30-14:00)

3S-2 Conduction control of graphene by gate-electric field 34
K.Tsukagoshi, H.Miyazaki, S.Odaka, T.Sato, S.Tanaka, H.Goto, A.Kanda, Y.Ootuka, and Y.Aoyagi

General Lecture (14:00-15:00)
Graphene

3-10 Spin injection, spin coherence and robust spin polarization in graphene-based spin valves at room temperature 71
○ M. Shiraishi, M. Ohishi, R. Nouchi, T. Nokzai, T. Shinjo and Y. Suzuki

3-11 MD Simulations for Mechanical Tearing of Graphene Sheets: Identification of Atomic Edge Configuration 72
○ Takazumi Kawai, Susumu Okada, Yoshiyuki Miyamoto, Hidefumi Hiura

Chemistry of Fullerenes • Metallofullerenes

3-12 Synthesis, Photophysical Properties, and Ordered Supramolecular Structures of Liquid Crystalline Deca(organo)[60]Fullerenes 73
○ Chang-Zhi Li, Yutaka Matsuo, Eiichi Nakamura

3-13 Radical Coupling Reaction of Paramagnetic Endohedral Metallofullerene La@C_{82} 74
○ Yuta Takano, Akinori Yomogida, Hidefumi Nikawa, Takatsugu Wakahara, Takahiro Tsuchiya, Midori O. Ishitsuka, Yutaka Maeda, Takeshi Akasaka, Tatsuhisa Kato, Zdenek Slanina, Naomi Mizorogi, Shigeru Nagase

Poster Preview (15:00-16:00)

Poster Session (16:00-17:30)

Chemistry of Fullerenes

3P-1 Organic Photovoltaic Devices of Penta(organo)[60]fullerenes and Their Iron and Ruthenium Complexes 179
○ Yutaka Matsuo, Takaaki Niinomi, Masahiko Hashiguchi, Yoshiharu Sato, and Eiichi Nakamura

3P-2 Fullerenes C_{32} and $X@C_{32}^{n}$ (X= He, Ne and Ar; n= 0, 2) 180
○ Weiwei Wang, Xiang Zhao

3P-3 Syntheses and Electrochemical Properties of Di-ruthenium [70]Fullerene Complexes 181
○ Takeshi Fujita, Yutaka Matsuo, Eiichi Nakamura

3P-4 Well-Defined Metal Catalysts for Fullerene Functionalization 182
○ Susumu Mori, Masakazu Nambo, and Kenichiro Itami

Metallofullerenes

3P-5 Systematic X-Ray Diffraction Studies on Crystal Structure of Mono-metallofullerene M@C_{82} (C_{2v}) 183
○ Takayuki Aono, Eiji Nishibori, Ryo Kitaura, Shinobu Aoyagi, Masaki Tanaka, Makoto Sakata, Hiroshi Sawa and Hisanori Shinohara

3P-6 Characterization of N@C_{60} / C_{60} Nano-whisker by ESR 184
○ Tatsuhisa Kato, Ryouichi Osada, Tohru Edamatsu, Michael Scheloske, Wolfgang Harneit, Takatsugu Wakahara, Kunich Miyazawa

3P-7 Ion Implantation System for Production of Endohedral Fullerenes 185
○ Tatsuya Katabuchi, Hitoshi Fukuda, Jun Hasegawa, Yoshiyuki Oguri, Satoshi Watanabe

3P-8 Production and ESR detection of N@C_{60} 186
○ Tomonari Wakabayashi and Takayoshi Kuroda

3P-9 Bis-carbene derivatives of a non-IPR metallofullerene: $La_2@C_{72}$ 187
○ Xing Lu, Hidefumi Nikawa, Midori O. Ishitsuka, Takahiro Tsuchiya, Yutaka Maeda, Takeshi Akasaka, Zdenek Slanina, Naomi Mizorogi, Shigeru Nagase

Fullerene Solids

3P-10 ESR spectra of superconducting sodium fulleride $Na_{8.2}C_{60}$ 188
○ Nozomu Kimata, Satoshi Heguri, and Mototada Kobayashi

3P-11 Electric phase transitions of $Eu_{2.75}C_{60}$ and $Sm_{2.75}C_{60}$ 189
○ Takashi Kambe, Yusuke Yamanari, Naoko Kawasaki, Yohei Ohta, Kumiko Imai, Yoshihiro Kubozono,

3P-12 Structure and Electronic Properties of $NaxHyC_{60}$ Ternary Compounds 190
○ Hironori Ogata and hideyuki Oonami

3P-13 Electronic Structure of Cs_3C_{60} 191
○ Susumu Saito

3P-14 Pressure dependence of Tc in Cs_3C_{60} 192
○ T. Takano, N. Takeshita, A. Y. Ganin, Y. Takabayashi, M. J.Rosseinsky, K. Prassides, H. Takagi, Y. Tokura, Y. Iwasa

3P-15 precise structural study of a single crystal $H_2@C_{60}$ using synchrotron X-ray diffraction 193
○ Makoto Toki,Hiroshi. Sawa, Yusuke Wakabayashi, Eiji Nishibori, Yasujiro Murata, Koichi Komatsu, Hidefumi Nikawa , Takeshi Akasaka, Katsumi Tanigaki

Formation of Fullerenes, Higher Fullerenes

3P-16 The simplest linear-carbon-chain growth by atomic-carbon-insertion reactions. 194
○ Teruhiko Ogata and Yoshio Tatamitani

Properties of Nanotubes

3P-17 Effect of dopant combinations on the single-walled carbon nanotube pn junction features 195
○ T. Kato, J. Shishido, W. Oohara, R. Hatakeyama, and K. Tohji*

3P-18 Polarized photoluminescence excitation spectroscopy of DNA-wrapped single-walled carbon nanotubes 196
○ Erik Einarsson, Yoichi Murakami, Ming Zheng, Slava V. Rotkin, Yuhei Miyauchi, Shigeo Maruyama

3P-19 Reduction of SWNT heat conduction by surrounding materials 197
○ Junichiro Shiomi, Shigeo Maruyama

3P-20 Recovering and Redispersion of Composite of Single-Walled Carbon Nanotubes and Dispersing Agent 198
○ Ayumu Sakai, Katsumi Uchida, Tadahiro Ishii, Hirofumi Yajima

3P-21 Boron-doped MWNTs synthesized by hot-filament CVD 199
○ Satoshi Ishii, Tohru Watanabe, Shunsuke Tsuda, Takahide Yamaguchi, Yoshihiko Takano

3P-22 Sheet resistance of metallic single-wall carbon nanotube thin films 200
○ Yasumitsu Miyata, Kazuhiro Yanagi, Yutaka Maniwa, Hiromichi Kataura

3P-23 Electric Double Layer Transistor of Graphene 201
○ J. T. Ye, H. Shimotani, M. F. Craciun, A. F. Murpurgo, and Y. Iwasa

3P-24 Electronic structures of impurity doped carbon nanotubes 202
○ Takashi Koretsune, Susumu Saito

3P-25 Decrease in Weight of Carbon Nanocoil by Acid Treatment and Its Dependence on Temperature and Time 203
○ Masashi Yokota, Yuichiro Shinohara, Yoshiyuki Suda, Shinichiro Oke, Hirofumi Takikawa, Youhei Fujimura, Tatsuo Yamaura, Shigeo Itoh, Kouji Miura, Masakatsu Morioki

3P-26 Tissue response of multi-walled carbon nanotube blocks cross-linked by de-fluorination against subcutaneous tissue of rats in vivo 204
○ Yoshinori Sato, Atsuro Yokoyama, Takao Kasai, Shinji Hashiguchi, Kenichi Motomiya, Balachandran Jeyadevan, Kazuyuki Tohji

Applications of Nanotubes

3P-27 Thermal diffusivity of single walled carbon nanotube/UV-curable resin nanocomposites 205
○ Takahiro Fukumaru, Tsuyohiko Fujigaya, and Naotoshi Nakashima

3P-28 Characterization of growth process of VA-SWNT films and their applications for Dye-Seneitized Solar Cell 206
○ Jun Okawa, Junichiro Shiomi, Shigeo Maruyama

3P-29 A Stable Electroactive Monolayer Composed of Soluble Single-Walled Carbon Nanotube on ITO 207
○ Qiguan Wang, Hiroshi Moriyama

3P-30 Effective Chemical Functionalization of SWNT with microwave oven 208
○ Nozomi Kuroki, Mariko Kondo, Toshiki Sugai, Hiroshi Moriyama

3P-31 Single Wall Carbon Nanohorn for Controlled Release 209
○ Xu Jianxun, Yudasaka Masako, Iijima Sumio

3P-32 Comparative Study of Carbon and BN Nanographenes: Ground Electronic States and Energy gap Engineering 210
○ Xingfa Gao, Zhongfang Chen and Shigeru Nagase

Formation and Purification of Nanotubes

3P-33 Effect of hydrogen gas on single walled carbon nanotubes growth over gold catalyst using chemical vapor deposition 211
○ Z. Ghorannevis, T. Kato, T. Kaneko and R. Hatakeyama

3P-34 Chirality Separation for Single-walled Carbon Nanotube with Density Gradient Electrophoresis 212
○ Yoshiya Kaminosono, Katsumi Uchida, Tadahiro Ishii, Hirofumi Yajima

3P-35 Carbon nanotube growth with (Fe,Co)Pt catalysts by a chemical vapor deposition method 213
○ Takuya Sonomura, Nobuyuki Iwata and Hiroshi Yamamoto

3P-36 Analyses of Source Gas Consumption during Carbon Nanotube Growth using In-situ FTIR Measurements and Numerical Simulations 214
○ Shintaro Sato, Tatsuhiro Nozue, Akio Kawabata, Tomo Murakami, Daiyu Kondo, Mizuhisa Nihei, Yuji Awano

3P-37 Growth Control of Single-Walled Carbon Nanotubes by High Vacuum CVD Method 215
○ Yohei Yamamoto, Hiroto Okabe, Shigeo Maruyama

3P-38 Evaluation of the ratio of metallic to semiconducting single-wall carbon nanotubes by optical measurement 216
○ Yasumitsu Miyata, Kazuhiro Yanagi, Yutaka Maniwa, Hiromichi Kataura

3P-39 Dispersion of single-walled carbon nanotubes made by using arc-burning technique in nitrogen atmosphere 217
○ Takashi Mizusawa, Shinzo Suzuki, Yohji Achiba

3P-40 Synthesis of Single-Walled Carbon Nanotube by using Rapid Temperature Alteration Alcohol CCVD Method 218
○ Mao Shoji and Hironori Ogata

3P-41 Reaction Temperatures Dependence of SWCNT Diameters in e-DIPS Process 219
○ Takeshi Saito, Bikau Shukla, Toshiya Okazaki, Motoo Yumura, Sumio Iijima

3P-42 Growth of Single-Wall Carbon Nanotube within the Pores of Meso-, and Micro-Porous Materials by Catalyst-Supported Chemical Vapor Deposition 220
○ Keita Kobayashi, Ryo Kitaura, Yoko Kumai, Yasutomo Goto, Shinji Inagaki, Hisanori Shinohara

Endohedral Nanotubes

3P-43 Nucleation of an SWNT from a catalytic metal cluster inside a carbon nanotube 221
○ Yoshifumi Izu, Junichiro Shiomi and Shigeo Maruyama

3P-44 ^{13}C NMR Study of C_{60}-Peapods 222
○ Kazuyuki Matsuda, Yutaka Maniwa, and Hiromichi Kataura

3P-45 Phase transition of water inside SWCNTs 223
Haruka Kyakuno, Fuminori Mikami, Toshimi Imaizumi, ○ Kazuyuki Matsuda, Takeshi Saito, Satoshi Ohshima, Motoo Yumura, Sumio Iijima, Yasumitsu Miyata, Hiromichi Kataura, Yutaka Maniwa

3P-46 Molecular dynamics simulations for temperature dependence of molecular-linear-motor inside nanotube 224
○ Y. Ueno, H. Somada, K. Hirahara, Y. Nakayama, and S. Akita

3P-47 Synthesis, Characterization, and Magnetic properties of Europium-Nanowires Fully Encapsulated into Single Wall Carbon Nanotubes. 225
○ R. Nakanishi, R. Kitaura, T. Saito, H. Yoshikawa, K. Awage and H. Shinohara

3P-48 Encapsulation of Linear-Polyynes inside Thin Double-Wall 226
○ Chen Zhao, Daisuke Nishide, Ryo Kitaura and Hisanori Shinohara

3P-49 Fabrication and Characterization of Room Temperature Ionic Liquids inside SWNTs 227
○ Shimou Chen, Chen Zhao, Keita Kobayashi, Naoki Imazu, Ryo Kitaura, Hisanori Shinohara

Graphene

3P-50 Anomalous Transfer Characteristics of Graphene Field-Effect Transistors with Co Contacts 228
○ Ryo Nouchi, Masashi Shiraishi and Yoshishige Suzuki

基調講演
Plenary Lecture

特別講演
Special Lecture

1S – 1 ～ 1S – 2
2S – 1 ～ 2S – 2
3S – 1 ～ 3S – 2

Carbon Nanotubes by CCVD Process ~Mass production, Applications and Safety for Success~

M. Endo, T. Hayashi, Y.A. Kim, K. Takeuchi, H. Muramatu, S. Koyama+

Faculty of Engineering, Shinshu University, 4-17-1 Wakasato, Nagano-shi 380-8553, Japan
+School of Medicine, Shinshu University, 3-1-1 Asahi, Matsumoto 390-8621, Japan

Abstract

Nanotechnology as innovation for tomorrow's world is the ability to understand and design complex things on nanoscale, and will change our way of life soon. The most distinguished nanotechnology related nonmaterial is "one-dimensional carbon nanotubes" which have attracted a particular interest from academy and industry, and thereby their related science and technology have developed at an emerging speed. Carbon nanotubes, consisting of rolled graphene layer built from sp^2 units, have attracted the imagination of scientists as ideal macromolecules [1] and their unusual growth process, physical and chemical properties make them useful in the fabrication of nanocomposites, nano-electronic devices and sensors etc. By selecting transient metal, support materials and synthetic conditions (temperature, duration) judiciously, we are able to synthesize different types of carbon nanotubes such as multi-[2], double-[3] and single-walled carbon nanotubes, respectively. At present, a large quantity of multi-walled carbon nanotubes (up to several hundred ton/year) is available, because highly ordered and pure carbon nanotubes are industrially produced in a semi-continuous system through the right combination of the catalytic chemical vapor deposition method and the subsequent high-temperature thermal treatment in argon [1, 2]. In this talk, by reviewing the catalytic synthesis of carbon nanotubes known as CCVD process, the controlled growth of double walled CNT with their specific structural properties is demonstrated. And current applications from the industrial point of view are shown.

Among the recent applications of carbon nanotubes, their high potential toward nanocomposites as multi-functional filler and their bio-medical applications [4] will be discussed with a strong emphasis on the recent hot issue "toxicity and safety of carbon nanotubes" [5]. To achieve the success story of carbon nanotubes, the most important "safety" issue has to be clarified based on long-term and systematic biological studies. Suitable and scientific evaluation process and metrology on the safety of structured CNT should be developed, and now such a wide range of toxicity study has been developing, on which recent results will be shown from view point of *"safety for success"*.

References

1. A. Oberlin, M. Endo, T. Koyama, J. Crys. Grow, 32, 335-349 (1976).
2. M. Endo, Chem. Tech. 568-576 (1988).
3. M. Endo *et al.*, Nature 433, 476 (2005).
4. M. Endo *et al.*, Nano Lett. 5, 101-106 (2005).
5. S. Koyama and M. Endo *et al.* Carbon 44, 1079-1092 (2006).

Corresponding Author: E-mail: endo@endomoribu.shinshu-u.ac.jp; Tel & Fax: +81-26-269-5201 & +81-26-269-5208

Fabrication and Characterization of Carbon Nanotube FETs

○Takashi Mizutani, Yutaka Ohno and Shigeru Kishimoto

Department of Quantum Engineering, Nagoya University
Furo-cho, chikusa-ku, Nagoya 464-8603, Japan

Carbon nanotube FETs are attracting much attention because of their excellent electrical properties such as high carrier mobility and a large current driving capability, and are expected to be key devices for next generation electronics. In this talk, we present our recent results on the transport at the contacts and also on the CNTFETs with multichannel.

The conduction type of the CNTFETs was dependent on the work function of the contact metal, which suggests that Fermi level pinning at the metal/nanotube interface is not strong [1]. Based on the two-probe and four-probe resistance measurements, it was shown that the carrier transport at the contact is explained by the edge contact model even in the diffusive regime [2]. The chemical doping using F_4TCNQ was effective to reduce not only the channel resistance but also the contact resistance [3]. The effect was more pronounced in decreasing the contact resistance than in the channel resistance. This has been explained by the dipole formation at the contact/nanotube interface resulting in a decrease of the effective Schottky barrier height.

Multichannel CNTFETs with a high-k top-gate structure are fabricated using horizontally-aligned nanotubes grown on a quarts substrate [4]. The devices show normally-on and n-type conduction property without any impurity doping with a relatively-high ON current of 13 mA/mm. CNTFETs with a CNT random network as a channel have also been fabricated using CNT networks grown directly on a SiO_2/Si substrate by plasma-enhanced CVD [5]. The ON/OFF ratio of the devices was $10\sim10^4$ depending on the growth condition and the device structure. The maximum field-effect mobility was as high as 20 cm^2/Vs with a large drain current of 6 mA/mm. Drain current uniformity for 10 devices was very good with a small fluctuation of $\pm$ 12%.

This work is partially supported by Grant-in-Aid for Scientific Research on Priority Area of MEXT, Innovation Research Project on Nanoelectronics Materials and Structures of METI, Promotion of Science and Strategic Information and Communications R&D Promotion Program of MIC.

References

[1] Y. Nosho et al., Nanotechnology, 17 (2006) 3412.
[2] Y. Nosho et al., Jpn. J. Appl. Phys., 46 (2007) L474.
[3] Y. Nosho et al., Nanotechnology, 18 (2007) 415202.
[4] D. Phokharatkul et al., Appl Phys. Lett. (submitted)
[5] T. Mizutani et al., NT08 (2008) D42.

Corresponding Author: Takashi Mizutani
E-mail: tmizu@nuee.nagoya-u.ac.jp, Tel: +81-52-789-5230, Fax: +81-52-789-5232

Superconductivity in expanded fullerides

Alexey Y. Ganin[1], Yasuhiro Takabayashi[2], ○Matthew J. Rosseinsky[1] & Kosmas Prassides[2]

[1]*Department of Chemistry, University of Liverpool, Liverpool L69 7ZD, UK*

[2]*Department of Chemistry, University of Durham, Durham DH1 3LE, UK*

The fullerene based A_3C_{60} solids have the highest superconducting transition temperatures for molecular materials. A key structure-property-composition relationship is that the supercoducting transition temperature T_c increases monotonically with the separation between the C_{60}^{3-} anions within the fcc structure adopted by the superconducting materials.
This presentation describes approaches to probe the limiting behaviour accessible when the largest possible cations are used to expand the separation between the C_{60}^{3-} anions. The methylamine (MA) molecule can bind to intercalated potassium cations to access lower symmetry fcc-related $(MA)K_3C_{60}$[1] which is non-superconducting but has unconventional behaviour of the magnetic ordering temperature[2]. When used as a solvent, methylamine gives access to two polymorphs of Cs_3C_{60}[3,4] with fcc and bcc related packings. The bcc-related polymorph is not superconducting at ambient pressure but upon application of pressures above 3 kbar becomes superconducting with a maximum T_c of 38K.[5] The resulting behaviour of electroncu properties upon the fulleride packing density reveals that the previous views of fulleride superconductivity are over-simplified.

(1) Ganin, A. Y.; Takabayashi, Y.; Bridges, C. A.; Khimyak, Y. Z.; Margadonna, S.; Prassides, K.; Rosseinsky, M. J. *J. Am. Chem. Soc.* **2006**, *128*, 14784-14785.

(2) Takabayashi, Y.; Ganin, A. Y.; Rosseinsky, M. J.; Prassides, K. *Chemical Communications* **2007**, 870-872.

(3) Palstra, T. T. M.; Zhou, O.; Iwasa, Y.; Sulewski, P. E.; Fleming, R. M.; Zegarski, B. R. *Solid State Communications* **1995**, *93*, 327-330.

(4) Saito, S.; Umemoto, K.; Louie, S. G.; Cohen, M. L. *Solid State Communications* **2004**, *130*, 335-339.

(5) Ganin, A. Y.; Takabayashi, Y.; Khimyak, Y. Z.; Margadonna, S.; Tamai, A.; Rosseinsky, M. J.; Prassides, K. *Nature Materials* **2008**, *7*, 367-371.

High pressure synthesis of nano-polycrystalline diamonds by direct conversion from various carbon materials and their characterization

H. Sumiya

Electronics & Materials R&D Lab., Sumitomo Electric Industries,Itami 664-0016, Japan

The authors have successfully synthesized single-phase nano-polycrystalline diamond (NPD) through direct conversion from high-purity graphite under static high pressures of ≧ 15 GPa and a strictly controlled temperature of 2300 °C [1, 2]. Although the size of the NPD in the initial development was about 1 mm, recently much larger specimens of 4 or 5 millimeter in diameter were successfully obtained [3]. The NPD is transparent, having a light brownish color. The NPD consists of fine diamond particles of several tens nanometers tightly bound each other and containing no secondary phases [4]. The NPD has extremely high hardness, which is equivalent to or even higher than those of single-crystal diamonds [5]. At high temperatures (>800 °C) the hardness of the NPD is about 2 times higher than those of single-crystal diamonds. The extremely high hardness is believed to be due to the blocking effect of dislocation movement (development of plastic deformation) at grain boundaries. In addition, the NPD has no anisotropy of hardness and no cleavage features, because each grain orients in a random direction. The NPD also has excellent thermal stability and resistance to crack propagation [6]. These salient characteristics permit us to apply the NPD to a wide field of industrial and scientific applications such as high-precision cutting tools, abrasion-resistant materials, optical windows, high-pressure anvils.

We also showed that NPD consists of much smaller particles of 5-10 nm in size can be obtained from non-graphitic carbons such as carbon black, glassy carbon, C_{60} and CNTs at 1600-2000 °C under ≧15 GPa [7]. However, the hardness of the NPD from non-graphitic carbons is significantly lower than that of NPD from graphite. Microstructure investigation beneath the indentation [6] revealed that the decrease in hardness of the NPD consisting of the very fine grains (10 nm or less) is not caused by grain boundary sliding (the inverse Hall-Petch effect [8]), but rather by the marked occurrence of intercrystalline cracks induced by insufficient grain boundary cohesion.

The research on synthesis of the NPD was performed in collaboration with Professor Irifune of Geodynamics Research Center of Ehime University.

References:

[1] T. Irifune, A. Kurio, S. Sakamoto, T. Inoue, H. Sumiya, Nature, 421 (2003) 599.
[2] H. Sumiya, T. Irifune, SEI Technical Review, 59 (2005) 52.
[3] H. Sumiya, T. Irifune, SEI Technical Review, 66 (2008) 85.
[4] H. Sumiya, T. Irifune, A. Kurio, S. Sakamoto, T. Inoue, J. Mater. Sci., 39 (2004) 445.
[5] H. Sumiya, T. Irifune, Diamond and Related Materials, 13 (2004) 1771.
[6] H. Sumiya, T. Irifune, J. Mater. Res., 22 (2007) 2345.
[7] H. Sumiya, H. Yusa, T. Inoue, H. Ofuji, T. Irifune, High Press. Res., 26 (2006) 63.
[8] S. Yip, Nature, 391 (1998) 532.

Corresponding Author: H. Sumiya
E-mail: sumiya@sei.co.jp, Tel: +81-72-772-4804, Fax: +81-72-770-6727

Chiral control; possible or not possible?
-Towards a selective production of SWNT with a single chirality-

Yohji Achiba

Department of Chemistry, Tokyo Metropolitan University, Minami-Ohsawa 1-1 Hachioji, Tokyo 192-0037, Japan

Controlling the chirality and/or the selective production of single wall carbon nanotube (SWNT) with a single chirality must be one of the most interesting and important issues among many potential capabilities of SWNTs for both scientific interests as well as industrial applications for such as nano-electronic devices and nano-biotechnology. However, it has been seemed to be the consensus that even the fact whether there is a sort of preferentiality in the chiral distributions of SWNTs in the growth process or not is still obscure. Therefore, a lot of efforts has been placed on the developing separation methods by which a particular SWNT with a particular chiral and/or structural property could be separated from an ensemble of the SWNTs with a huge numbers of chirality distributed tubes.

On the contrary, however, generally speaking, the formation of nano carbon structures are seemed to be controlled by a sort of propensity rule which sometimes clearly appears as a distinct experimental evidence. For example, we know very well the evidence of a significant yield of C_{60} among many other potentially possible fullerene structures. Favorite structure of C2vC82 or IhC80 cage for metallofullerenes might be another example.

In the present paper, we will demonstrate some experimental results which might be strongly related with the propensity of the growth process in the formation of single wall carbon nanotubes. On the basis of experimental results revealed by both laser vaporization and CVD preparation methods, we will show how a significant difference is seen in the distributions of the size and chirality of SWNTs by changing the experimental condition such as temperature, pressure and metal particles..

Corresponding Author: Yohji Achiba
Tel: 042-677-2534, E-mail: achiba-yohji@tmu.ac.jp

Conduction control of graphene by gate-electric field

○K. Tsukagoshi,[125] H. Miyazaki,[125] S. Odaka,[123], T. Sato,[4] S.Tanaka[4], H. Goto,[45]
A. Kanda,[45] Y. Ootuka,[4] and Y. Aoyagi[235]

[1]*AIST, Tsukuba 305-8562, Japan*

[2]*RIKEN, Wako 351-0198, Japan*

[3]*Department of Information Processing, Tokyo Institute of Technology, Yokohama 226-8502, Japan*

[4]*Institute of Physics and TIMS, University of Tsukuba, Tsukuba 305-8571, Japan*

[5]*CREST, JST, Kawaguchi, Saitama 332-0012, Japan*

We present fundamental researches on thin graphite film, with the goal of realizing future nanometer scale electronic applications. Because thin graphite films are by nature nanometer scale materials with remarkable electrical conductions, they are expected to be an important element in nano-carbon electronics. For a control of the conduction of the thin graphite channel, gating effect must be fully clarified. Here, we established an effective gate-structure on graphene channel, and realized energy-gap control in gate-electric field modulation.

Our starting materials are thin layers (thickness 1-10 nm) of graphite films pealed off from bulk graphite on SiO_2/doped-Si substrate. The thin film is connected to two or multiple metallic electrodes. In general, conduction of the graphite can be changed in gate voltage applied to the doped-Si substrate. In this configuration, the gate electric field can be applied from the substrate side (back-gate configuration). Observed resistance in the gate-voltage change shows ambipolar behavior based on clear carrier polarity change.

We also attached a front gate, which was directly formed on the surface of the graphite film. We deposit an Al electrode on the graphite film (Fig. 1). The graphite channel and the Al electrode are naturally insulated by exposed in air. Then the Al electrode can be used as a front gate. The front gate also changes the conduction of the thin graphite film. A scan of the top gate voltage (V_{tg}) generates a resistance peak in the ambiploar response. The back gate voltage (V_{bg}) shifts the ambipolar peak depending on the graphite thickness. The shift is larger in thinner film. The thickness-dependent peak shift is clarified in terms of the inter-layer screening length λ to the electric field in the dual-gated graphite film. We assume that the gate-induced carriers decay exponentially from both surfaces, and that the conductivity in each layer increases proportionally to the induced carrier density. Then the condition for the ambipolar resistance peak in V_{tg} scan is obtained as a function of V_{bg}, λ, and the graphite film thickness d. Applying this model to the thickness-dependence, we estimated a screening length of 1.2 nm.

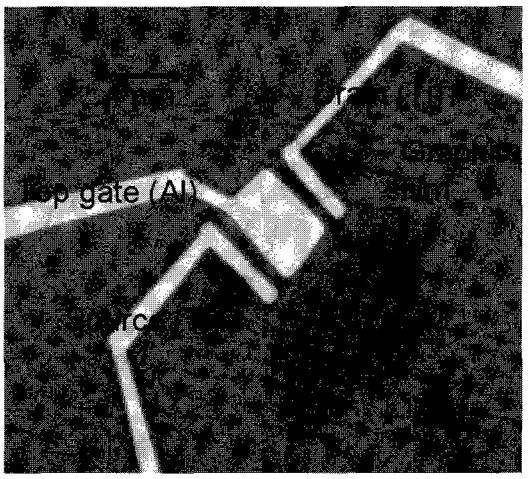

Fig.1 Optical microscope image of a thin graphite film with source-drain electrodes and a Al top gate on SiO_2/Si substrate.

一般講演
General Lecture

1－1 ～ 1－15
2－1 ～ 2－12
3－1 ～ 3－13

Attachment of Carbon Nanotubes using Structural Changes in C_{60} Molecules by Electron Irradiation

○Ryosuke Senga[1,2], Hiroyuki Maruyama[1,2], Kaori Hirahara[1,2,3], Yoshikazu Nakayama[1,2]

[1]*Department of Mechanical Engineering, School of Engineering, Osaka University, 2-1 Yamadaoka, Suita, Osaka 565-0871, Japan*
[2]*CREST, Japan Science and Technology Agency, Japan*
[3]*Frontier Research Base for Young Researchers, School of Engineering, Osaka University, Japan*

Carbon nanotubes (CNTs) have been applied to functional devices such as probes for scanning probe microscopy. In fabrication process of CNT devices, it is essential to manipulate and attach an isolated CNT onto a specific site of a substrate with electric conduction. In this study, we propose a new method for attaching CNTs in transmission electron microscope (TEM); The workspace of TEM is generally too clean to deposit amorphous carbon as the adhesive as it has been done in a scanning electron microscope [1], so that we utilized C_{60} molecules and their structural changes caused by electron irradiation.

First, we deposited a few layers of C_{60} molecules on a platinum coated silicon (Pt/Si) substrate. A CNT was placed at the edge of the substrate in TEM. Then, an electron beam converged by 15nm diameter was irradiated to the C_{60} molecules around the interface between the CNT and substrate. During the irradiation, C_{60} molecules continuously gathered to a central part of the irradiation area. By 2×10^8 electrons/nm^2 irradiation, features of C_{60} molecules changed to amorphous-like structures. After 3×10^8 electrons/nm^2 irradiation, lamellar structures were reconstructed at the same region (Fig.1(c)). The interlayer distance measured was 0.35~0.4nm, which corresponds to that of graphite. In addition, the measurement of electric conductance between CNTs and Pt/Si substrate indicated that the conductance improved by electron irradiation. It suggests that structural change in C_{60} molecules to graphite results in not only attaching CNTs to the substrate but also improvement of the conductance.

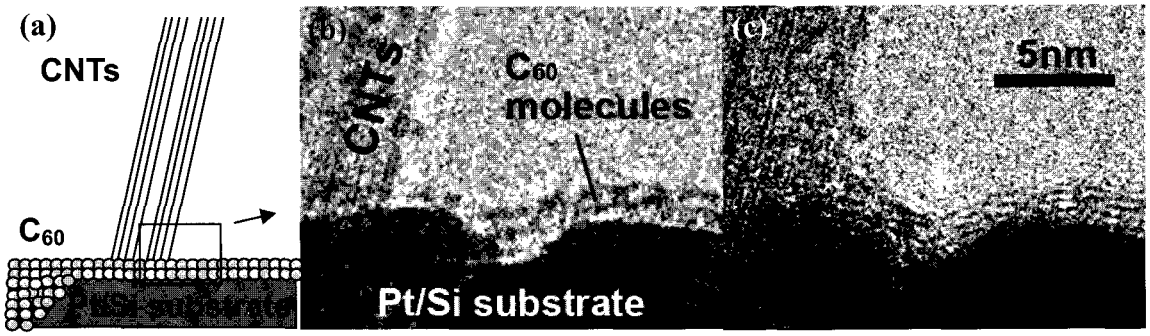

Fig.1 (a) Schematic of C_{60} molecules deposited between CNTs and substrates, and TEM images (b) before and (c) after electron irradiation with 3×10^8 electrons/nm^2 .

[1] H.Nishijima, S.Kamo, S.Akita, and Y.Nakayama, *Appl. Phys. Lett.* **74**, 26 (1999)

Corresponding Author: Yoshikazu Nakayama
TEL: +81-6-6879-7815, FAX: +81-6-6879-7815, E-mail: senga@ne.mech.eng.osaka-u.ac.jp

Near-IR laser-driven reversible volume phase transition of single-walled carbon nanotubes / poly (N-isopropylacrylamide) composite gels

○Tatsuro Morimoto, Tsuyohiko Fujigaya, Yasuro Niidome, and Naotoshi Nakashima

Department of Applied Chemistry, Graduate School of Engineering, Kyushu University, 744 Motooka, Fukuoka 819-0395, Japan

Single-walled carbon nanotubes (SWNTs) are nanomaterials possessing remarkable electrical, mechanical and thermal properties and show characteristic absorption bands in the near-IR (NIR) region [1]. On the other hand, polymer gel, in particular, poly (N-isopropylacrylamide) (PNIPAM) gel is of interest in wide area of science and technology from the aspects of both fundamentals and applications, because it shows volume phase transition [2]. The aim of this study is the development of a gel which responses to NIR light, conjugating SWNTs and PNIPAM gel.

In this study, we show the utilization of SWNTs as a photon antenna that serves as an effective "molecular heater" around the NIR region [3]. We prepared SWNTs-embedded PNIPAM gel by synthesizing PNIPAM gel in aqueous solution of acid treated SWNTs. The columnar composite gel was irradiated from NIR laser in water. Fig.1 illustrates the behavior of the gel. It showed a reversible volume phase transition via ON/OFF switching of NIR laser light irradiation. The interesting feature of the composite gel was its repetitive durability (more than 1200 cycles). That could be derived from rigid structure of SWNTs. The composite gel has great potential for various applications including biological field, because it has the character to responses to NIR light.

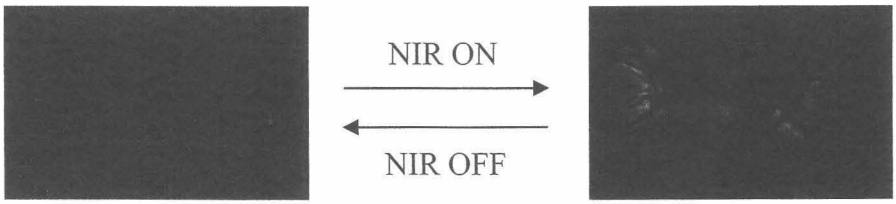

Fig.1 The behavior of the composite gel when it is irradiated from NIR laser.

[1] M. J. O'Connell et al., *Science* **2002**, *297*, 593.

[2] T. Tanaka et al., *Phys. Rev. Lett.* **1985**, *55*, 2455.

[3] T. Fujigaya et al., *Adv. Mater.* in press.

Corresponding Author: Naotoshi Nakashima

TEL & FAX: +81-92-802-284, E-mail: nakashima-tcm@mail.cstm.kyushu-u.ac.jp

Properties of Visible-Light-Emission in Chemically-Modified CNT-FET

○Ryotaro Kumashiro[1], Naoya Komatsu[1], Takeshi Akasaka[2], Yutaka Maeda[3,4] and Katsumi Tanigaki[1,5]

[1] *Department of Physics, Graduate School of Science, Tohoku University, Sendai, Japan*
[2] *Center for Tsukuba, Advanced Research Alliance, University of Tsukuba, Tsukuba, Japan*
[3] *Department of Chemistry, Tokyo Gakugei University, Tokyo, Japan*
[4] *PRESTO, Japan Science and Technology Agency, Saitama, Japan*
[5] *World Premier International Research Center, Tohoku University, Sendai, Japan*

Abstract: Semiconducting carbon nanotubes (CNT) have shown promising applications as electronic materials for nano-scale devices in the future. It is well known that the field effect transistors (FET) fabricated by CNT show high performance. Semiconducting CNT have hole- and electron-carrier type, therefore, CNT-FET usually exhibit ambipolar charge transport. In recent years, the FET structure has attracted intense research interest as a light emitting device, and the research related to organic light-emitting FET are of fundamental and practical significance. In this study, we will report the light emission properties of CNT-FET with organic light emitter. 1,3,6,8-tetraphenylpyrene (TPPy) was used as a light-emitting organic-material. TPPy/CNT-FET devices were fabricated by drop-cast method on SiO_2/Si substrate. From the experimental results, it was shown that the light emission in visible-light region can be observed in FET operation (Fig.1A) and the state of light emission is changed by V_G (Fig.1B,C). The mechanism of light emission in TPPy/CNT-FET will also be discussed.

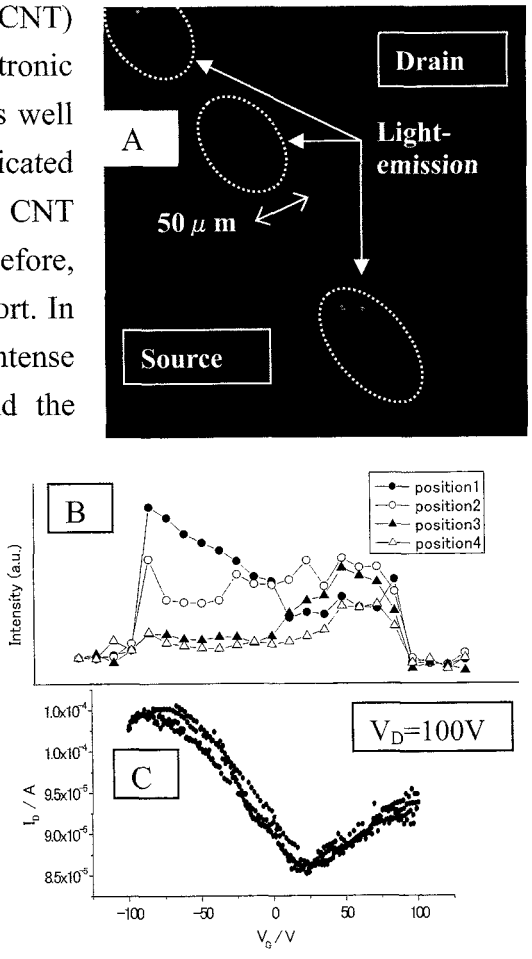

Figure 1. (A) Optical image of light emission in TPPy/CNT-FET. (B) Emission intensity vs. V_G plots. (C) I-V_G plot of TPPy/CNT-FET

Corresponding Author: Ryotaro Kumashiro
E-mail:rkuma@sspns.phys.tohoku.ac.jp Tel&Fax:+81-22-795-6468(tel),+81-22-795-6470(fax)

Studies on Electronic Structures of Single-Walled Carbon Nanotubes Synthesized Controlling the Diameter by Optical Absorption Spectroscopy

○Takeshi Saito[1,2], Shigekazu Ohmori[1], Bikau Shukla[1], Motoo Yumura[1] and Sumio Iijima[1]

[1] *Nanotube Research Center, AIST, Tsukuba 305-8565, Japan*
[2] *PRESTO, Japan Science and Technology Agency, Kawaguchi 332-0012, Japan*

Development of controlled synthesis of SWCNTs in terms of their structural characteristics, i.e., diameter, length, number of defects and so forth, is an enabling step for realization of their many potential applications and fundamental studies requiring defined structures and properties. Above all, the controllability of the tube diameter would be the key and possibly become the starting point for the chirality separation. Although pulsed-laser and dc-arc vaporization methods are known to be good synthesis methods with controllability of the tube diameter, the controllable diameter range is limited. In addition, these methods are not efficient for industrial scale synthesis. Recently, for the purpose of this diameter-controlled large-scale synthesis of SWCNTs, we have developed novel gas phase CVD growth that is designated as the enhanced direct injection pyrolytic synthesis (e-DIPS) method [1]. The e-DIPS method needs two kinds of hydrocarbons as carbon sources and control of these carbon sources enabled us to tune the mean diameter of produced SWCNTs to any point in the range of ca. 1 nm to 2 nm.

Here, we report the characterization of our various diameter-controlled SWCNTs by optical absorption spectroscopy as one of the basic properties, which shows the electronic structures near Fermi level of SWCNTs. Characteristic diameter dependences have been observed not only in the interband transition peaks but also in the pi plasmon peaks. Details of this dependence will be discussed at the presentation.

Reference

[1] T. Saito, S. Ohshima, T. Okazaki, S. Ohmori, M. Yumura and S. Iijima, *Journal of Nanoscience and Nanotechnology*, in press.

Corresponding Author: Takeshi Saito
E-mail: takeshi-saito@aist.go.jp
Tel / Fax: 029-861-4863 / 029-861-4413

AFM-HRTEM Combined Technique for Probing Electronic Transition of Isolated Carbon Nanotubes

○Shota Kuwahara, Toshiki Sugai*, Hisanori Shinohara

Department of Chemistry & Institute for Advanced Research, Nagoya University, Nagoya 464-8602, Japan

High-resolution transm ission electron m icroscope (HR TEM) is a very powerful technique to characterize a structure of carbon nanotubes (CNTs), which provides us not only the detailed atom ic structure of CNT s but also internal structure of CNT s such as the number of layers and stru cture of encapsulated species. However, HRTEM cannot be applicable to CNT s supported on substrat es, therefore, the m ethods is incom patible with probe microscopy (AFM and STM) and device performance measurements such as field ef fect tran sistors. If we can com bine HR TEM and AFM, we can ev aluate correlation between detailed st ructure of CNT s and their optical, transport and device properties, which lead to be tter understanding of properties of CNT s and a design of high-performance devices.

The experim ental procedures are the followi ngs: (i) TEM struc tural c haracterization of isolated CNT s supported on carbon m embrane grids, (ii) transfer printing of the CNTs with the c arbon m embranes onto s ilicon oxide subs trates, (iii) position ing the TEM characterized CNTs by AFM observati ons, (iv) removal of the carbon m embranes by air-oxidation at 300 °C and (v) evaluation of the transfer -printed CNTs with other microscopic or spectroscopic m ethods. In th is work, electrostatic force m icroscopy (EFM) has been used for a detailed study on the electr ic properties of structure-determined CNT s. HiPco DWNT s (consists of 60 % DWNT s, 20 % single-walled CNTs and 20 % m ultiwalled CNTs; Carbon Nanotechnologies Inc.) were used for this purpose.

Figure 1 shows HR TEM, AFM and EFM im ages of CNT s observ ed at ex actly the same region obtained by the present AF M-TEM combined m ethod. HR TEM observation revealed that the CNT highlighted by a black arrow is a single-wall carbon nanotube with a diameter of 2.13 nm, which is about 16 % larger than those obtained by AFM observations. We are also going to discus s the correlation betw een electric forces and the d iameter of CNT s (in the case of DWNTs, both of inner and outer , and the interlayer distance).

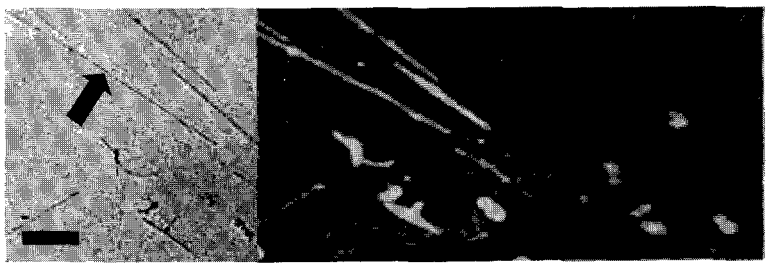

Figure 1: TEM image (left), AFM topographic image (middle) and EFM image (right) of the same observation region. Scale bar is 200 nm.

*Present Address: Dept. of Chemistry, Toho Univ.

Corresponding Author:
Hisanori Shinohara
E-mail:
noris@cc.nagoya-u.ac.jp
TEL: +81-52-789-2482,
FAX: +81-52-747-6442

Radiative lifetimes of excitons and their sizes in single-walled carbon nanotubes

○Yuhei Miyauchi[1], Hideki Hirori[2], Kazunari Matsuda[1], and Yoshihiko Kanemitsu[1]

[1]*Institute for Chemical Research, Kyoto University, Uji, Kyoto 611-0011, Japan*
[2]*Institute for Integrated Cell-Material Sciences, Kyoto University, Sakyo-ku, Kyoto 606-8502, Japan*

Single-walled carbon nanotubes (SWNTs) are attracting much interest as a novel material for various potential applications in future optoelectronic devices. Since performances of light-emitting materials depend on their luminescence quantum efficiencies and radiative/nonradiative decay rates, it is very important to determine the absolute values of the efficiencies and rates and to understand the luminescence mechanism in SWNTs. In this paper, we have investigated radiative lifetimes of excitons in SWNTs synthesized with various methods such as alcohol CCVD, HiPco and CoMoCAT. SWNTs were dispersed in D_2O with sodium dodecyl benzene sulfonate (SDBS) and the micelle-suspended SWNTs were used for the optical measurements. Radiative lifetimes τ_{rad} can be obtained from quantum efficiencies η and photoluminescence (PL) lifetimes τ_{PL} as $\tau_{rad} = \tau_{PL} / \eta$. We measured PL lifetimes using a femtosecond excitation correlation (FEC) method [1] and PL quantum efficiencies were estimated by comparing the absorbance and PL intensities of SWNTs with those of the reference dye (Styryl 13) [2]. Figure 1 shows PL lifetimes of SWNTs as a function of tube diameter. We found that the PL lifetimes are 30-50 ps and their values mainly depend on the synthesis method, while the diameter and chirality dependence is not clear. The PL quantum efficiencies also depend on the SWNT fabrication method. From the PL lifetimes shown in Fig. 1 and the measured quantum efficiencies, the radiative lifetimes on the order of 1 ns were obtained. The effect of the dark exciton bands on the radiative lifetimes and the exciton size in SWNTs deduced from the radiative lifetime will be discussed.

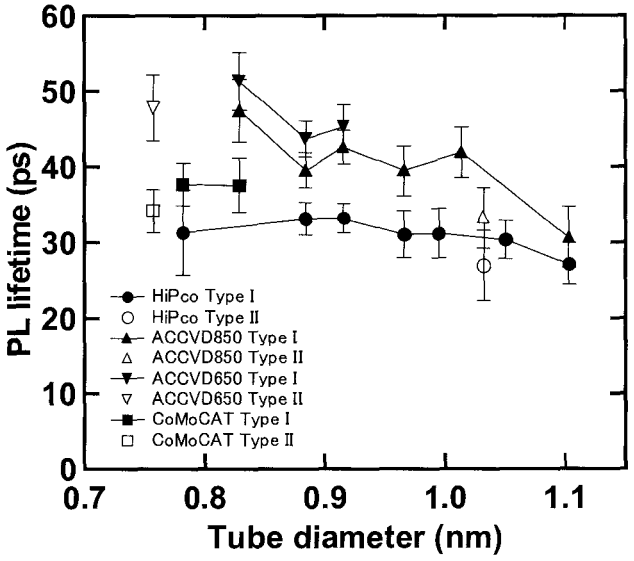

Fig. 1 PL lifetimes of various SWNTs samples.

[1] H. Hirori, K. Matsuda, Y. Miyauchi, S. Maruyama, and Y. Kanemitsu, Phys. Rev. Lett. **97**, 257401 (2006).

[2] J. R. Lakowicz, *Principles of Fluorescence Spectroscopy, 3rd ed.* (Springer, New York 2006).

Corresponding Author: Yuhei Miyauchi
TEL: +81-774-38-4513,
FAX: +81-774-38-4511
E-mail: y.miyauchi@at7.ecs.kyoto-u.ac.jp

Fabrication of suspended single-walled carbon nanotubes with a tweezers tip for the optical property study

○Huaping Liu, Shohei Chiashi, Masafumi Ishiguro and Yoshikazu Homma

Department of Physics, Tokyo University of Science, Kagurazaka, Shinjuku-ku, Tokyo 162-8601, Japan

Because of their unique mechanical and electronic properties, single-walled carbon nanotubes (SWCNTs) are promising for the fabrication of nano-electronic devices. However, the ability to assemble them in a controllable and predictable manner still remains a challenge in nanotechnology. Here, we developed a simple and efficient method to manipulate SWCNT films and individual SWCNTs (or bundles) with a tweezers tip on the substrates where they are grown. We can align, bend and cut SWCNTs using a tweezers tip. With this manipulation technique, we are able to control the position, direction, and length of SWCNTs and even fabricate multi-terminal net-work structures and other complex circuits. More importantly, we can directly fabricate suspended and aligned SWCNTs on a bare trench-contained substrate (figure 1a). It is well known that suspended SWCNTs can exhibit intense Raman signals as well as PL signals. Since the aligned nanotubes in our experiment are perfectly isolated from catalysts and other nanotubes, it is easy to investigate their electronic properties by measuring the Raman and PL spectra of their suspended segments. Figure 1b shows that almost no D-band peaks are observed in the high-intensity Raman spectra obtained from different suspended segments in the same aligned nanotube, suggesting that the nanotube manipulated with a tweezers tip was not damaged seriously. We can also observe a high-intensity PL signal from a suspended segment of an aligned nanotube (figure 1c), which definitely demonstrates that the suspended nanoutbes manipulated with a tweezers tip is optically active and useful for PL studies. These findings would be very useful for the property study on nanotubes and the fabrication of nano-electronic devices.

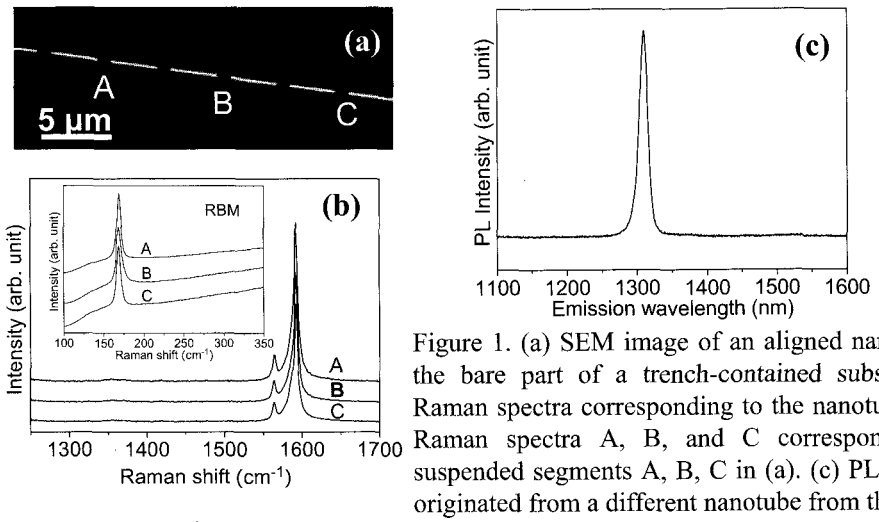

Figure 1. (a) SEM image of an aligned nanotube on the bare part of a trench-contained substrate, (b) Raman spectra corresponding to the nanotube in (a). Raman spectra A, B, and C correspond to the suspended segments A, B, C in (a). (c) PL spectrum originated from a different nanotube from that in (a).

This work was partially supported by Japan Science and Technology Agency.

Corresponding author: Huaping Liu, E-mail: hliu@rs.kagu.tus.ac.jp Tel : +81-3-5228-8244

Chirality dependent phonon frequency shift of carbon nanotubes

K. Sasaki[1]○, R. Saito[1], G. Dresselhaus[2], M.S. Dresselhaus[3], H. Farhat[4], and J. Kong[5]

[1]*Department of Physics, Tohoku University, Sendai, Japan*

[2]*Francis Bitter Magnet Laboratory, MIT, Cambridge, MA, USA*

[3]*Dept. of Physics, Dept. of Electrical Engineering and Computer Science, MIT, Cambridge, MA, USA*

[4]*Department of Materials Science and Engineering, MIT, Cambridge, MA, USA*

[5]*Department of Electrical Engineering and Computer Science, MIT, Cambridge, MA, USA*

In metallic single wall carbon nanotubes (SWNTs), frequency of the in-plane longitudinal optical (LO) phonon mode consisting of the G band in Raman spectroscopy becomes soft, which is understood by Kohn anomaly effect for phonon by the free electrons (for example, see[1]). In the last year, Farhat *et al.*, reported in the SWNTs Raman spectroscopy with changing the Fermi energy position by the electro-chemical doping that not only the LO phonon mode but also the transverse optical (TO) phonon mode frequencies are sensitive to the Fermi energy positions[2].

We have investigated the phonon frequency shifts of both the LO and TO phonon modes by calculating the phonon self-energy in the presence of the electron-phonon interactions for electrons near the Dirac point. We found that the phonon frequency shift is strongly chirality dependent. In particular, there is no self-energy correction to the TO mode (G^+ band) for arm chair SWNTs while phonon frequency hardening for the TO phonon mode occurs for metallic zigzag SWNTs, which is understood by the curvature effect on the electron-phonon interaction. This chirality dependence of phonon frequency shift for the TO and LO modes is opposite to the chirality dependence of the relative intensity of Raman G^+ and G^- bands, which can be understood in terms of a special symmetry of π electron's wave function and the trigonal warping effect. The calculated results are directly compared with the SWNTs Raman spectroscopy for a variety of chiralities and with analytical expression of the effective-mass theory with use of a gauge theory, whose agreement is very well. Our results will provide another tool to observe chiral angle in the Raman spectroscopy which is important for sample characterization and evaluation. We will plan to report the phonon frequency shift for other phonon modes.

[1] Piscanec *et al.*, Phys. Rev. Lett. **93**, 185503 (2004).

[2] Farhat *et al.*, Phys. Rev. Lett. **99**, 145506 (2007).

[3] K. Sasaki *et al.*, Phys. Rev. B **77**, 245441 (2008).

Corresponding Author: Ken-ichi Sasaki, E-mail: sasaken@flex.phys.tohoku.ac.jp

1-9

Photoinduced electrical transport properties of azafullerene peapod field-effect transistors

○Y. F. Li, T. Kaneko, and R. Hatakeyama

Department of Electronic Engineering, Tohoku University, Sendai 980-8579, Japan

Nanomaterials have great potentials for applications in opto-electronics. In particular, carbon nanotube field-effect transistors (FETs) have a high potential as light sensors as they combine exceptional electrical performance with intrinsic nanoscale feature size and original optical properties. In this work, we have studied the photoinduced electrical transport properties of azafullerene $C_{59}N$ encapsulated single-walled carbon nanotubes ($C_{59}N$@SWNTs) by fabricating them as the channels of FETs. The synthesis of $C_{59}N$ fullerenes is realized by a nitrogen-plasma irradiation method, and their encapsulation inside SWNTs is prepared by either a vapor reaction method or a plasma irradiation method, which is confirmed in detail by a transmission electron microscope (TEM, Hitachi HF-2000). The transport properties of $C_{59}N$@SWNTs are studied both in dark and upon light illumination. As a result, an *n*-type characteristic of the $C_{59}N$@SWNTs is observed [1], as seen in Fig. 1(a), which is significantly different from a *p*-type characteristic of the C_{60} peapod. Interestingly, the conduction of *n*-type $C_{59}N$@SWNTs is found to be extremely sensitive to light. The sharp decrease of current is significantly observed in the I_{DS}-V_G (I_{DS}: source-drain current, V_G: gate voltage of FET) transport characteristics of an azafullerene peapod when incident light falls on the FET device, as shown in Fig. 1(b). Moreover, the light sensitivity of azafullerene peapod devices has proven to be dependent strongly on the wavelength of light.

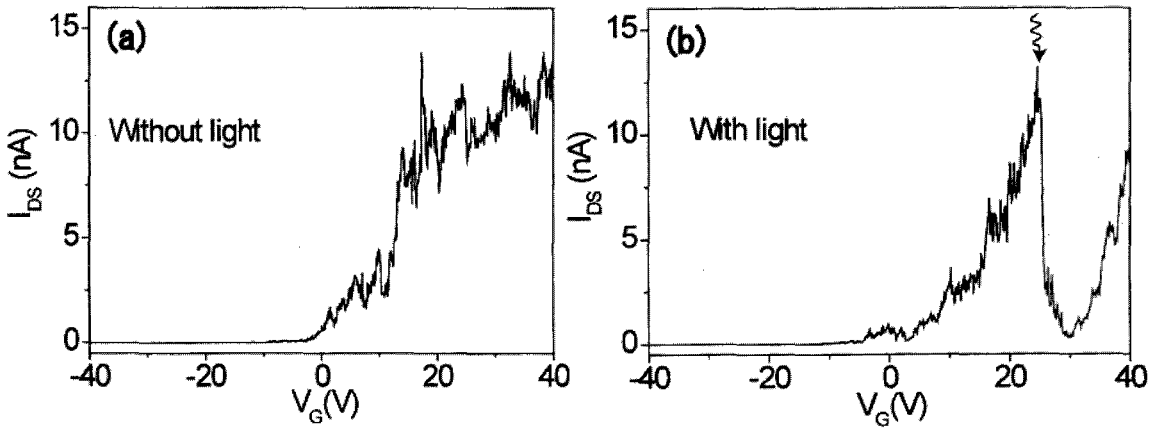

Fig.1 Characteristics of I_{DS}-V_G for a C_{59}@SWNT FET without (a) and with light illumination (b)

[1] T. Kaneko, Y.F. Li, S. Nishigaki, and R. Hatakeyama, *J. Am. Chem. Soc.* **130**, 2714 (2008).

Corresponding Author: Yongfeng Li

Tel : 81-22-795-7046, FAX: 81-22-263-9225, E-mail: yfli@plasma.ecei.tohoku.ac.jp

Preparation and Photoelectrochemical Properties of Nanocarbon Composite Films on Semiconductor Electrodes

○Tomokazu Umeyama[1], Noriyasu Tezuka[1], Yoshihiro Matano[1] and Hiroshi Imahori[1,2]

[1]*Graduate School of Engineering, Kyoto University, Kyoto 615-8510, Japan*
[2]*Institute for Integrated Cell-Material Sciences, Kyoto University, Kyoto 615-8510, Japan*

Both single-walled carbon nanotubes (SWNTs) and fullerenes have been considered as promising nanocarbon materials because of their unique mechanical and electrical properties. Thus, a combination of SWNTs and fullerenes is expected to act as excellent optical and electronic materials in various applications. Examples of such nanocarbon composites, however, have been limited to fullerene encapsulated SWNT (bucky-peapods). As such, few nanocarbon composites utilizing π–π interaction of fullerene with the outside of SWNT sidewalls have been investigated.

Here we report on a novel strategy for the arrangement of C_{60} molecules on the external surface of SWNT.[1,2] First, acid treatment cuts pristine SWNT (denoted as p-SWNT) to yield shortened SWNT (denoted as s-SWNT) with carboxylic groups at the open ends and defect sites (Scheme 1, Step 1). Then, s-SWNT is functionalized with sterically hindered amine (i.e., swallow-tailed secondary amine) to yield soluble, functionalized SWNT (denoted as f-SWNT) in organic solvents (Step 2). Finally, poor solvent (i.e., acetonitrile) is rapidly injected into a mixture of C_{60} and f-SWNT in good solvent (*o*-dichlorobenzene (ODCB)), resulting in formation of the composite clusters of C_{60} and f-SWNT (denoted as $(C_{60}$+f-SWNT$)_m$, Step 3). Measurements of scanning electron microscopy for cast samples revealed that the composites are categorized into three groups; i) f-SWNT bundles covered with layers of C_{60} molecules, ii) round, large C_{60} clusters (sizes of 500 – 1000 nm) containing f-SWNT, and iii) typical, round C_{60} clusters (sizes of 150 – 250 nm). The electrophoretic deposition of the composites onto a nanostructured SnO_2 electrode yielded the hierarchical film with gradient composition depending on the difference in the mobilities of C_{60} and f-SWNT during the electrophoretic process. The composite film exhibited an incident photon-to-photocurrent efficiency as high as 18% at 400 nm under an applied potential of 0.05 V vs. SCE. The highly aligned structure of C_{60} molecules on f-SWNT rationalizes the efficient photocurrent generation.

Scheme 1

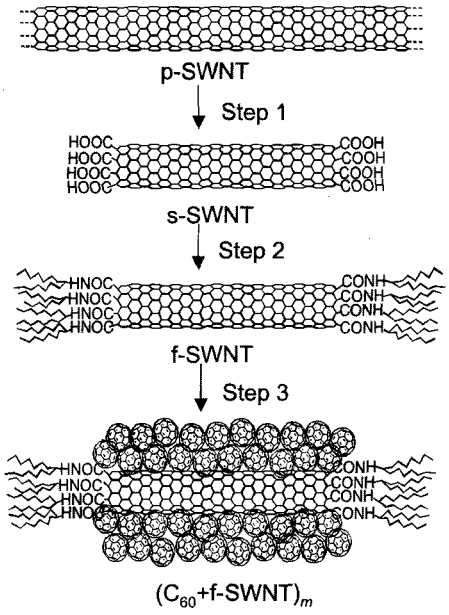

[1] Umeyama, T.; Tezuka, N.; Fujita, M.; Hayashi, S.; Kadota, N.; Matano, Y.; Imahori, H. *Chem. Eur. J.* **2008**, *14*, 4875-4885.

[2] Umeyama, T.; Imahori, H. *Energy Environ. Sci.* in press.

Corresponding Author: Tomokazu Umeyama
TEL: +81-75-383-2568, FAX: +81-75-383-2571, E-mail: umeyama@scl.kyoto-u.ac.jp

Rotational Motion of Carbon Nanotube Induced by Rubbing with Carbon Nanotube

Yoshiteru Takagi[1,2], Takahisa Ohno[3] and Susumu Okada[1,2]

[1]*Center for Computational Sciences and Graduate School of Pure and Applied Science, University of Tsukuba, Tsukuba 305-8577, Japan*

[2]*CREST, Japan Science and Technology Agency, 4-1-8 Honcho, Kawaguchi, Saitama 332-0012, Japan*

[3]*Computational Materials Science Center, National Institute for Materials Science (NIMS), 1-2-1 Sengen, Tsukuba, Ibaraki 305-0047, Japan*

In this paper, we show the possibility that rotational motion of CNT is induced by rubbing with another CNT based on molecular dynamics simulation. We consider the system (Fig. 1) composed by a double wall CNT (DWCNT), in which outer CNT is shorter than inner one, and a single wall CNT (SWCNT) which is parpendicular to the DWCNT. We induce rotational motion in the inner CNT by controlling translational motion of the SWCNT. [1] In this structure, undulation of the potential energy resulting from the van der Waals interaction transmits kinetic energy from one CNT(A) to another CNT(B). The undulation comes from arrengement of carbom atoms in a CNT. Then, it is unnecessary to decolate CNTs with other materials, e.g. molecules or metal plates, in our system.

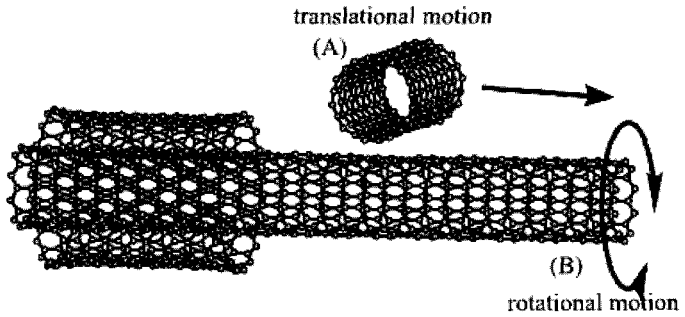

Fig. 1.Translational motion of CNT(A) induces rotational motion of CNT(B).

[1] Y. Takagi, T. Ohno and T. Uda, J. Chem. Phys. **128**,194704 (2008).

Corresponding Author: Yoshiteru Takagi

E-mail: ytakagi@comas.frsc.tsukuba.ac.jp

TEL: +81-29-853-5600(8233), FAX:+81-29-853-5924

Imaging of Conformational Changes of Triamide Molecules Covalently Bonded to a Carbon Nanohorn Surface

○Koji Harano[1], Masanori Koshino[2], Takatsugu Tanaka[1], Yoshiko Niimi[2], Yuki Nakamura[1], Hiroyuki Isobe[1,†], Eiichi Nakamura[1,2]

[1]*Department of Chemistry, The University of Tokyo, Hongo, Bunkyo-ku, Tokyo, 113-0033*
[2]*Nakamura Functional Carbon Cluster Project, ERATO, JST, Hongo, Bunkyo-ku, Tokyo, 113-0033*

Conformation of organic molecules exerts decisive effects on the function and activity of the molecules. However, there have been no experimental methods to study conformational changes of complex organic molecules on a single molecule basis in a time-resolved manner with near-atomic resolution. Here we present a new possibility for the conformational analysis and motion imaging of flexible organic molecules.[1] Thus, we put a biotinylated amide molecule of ca. 3 nm length on the exterior of aminated carbon nanohorns (**1**, Figure 1a), and captured near-atomic resolution TEM images of the time-dependent change of the conformation of the molecule (Figure 1b). The TEM images were compared iteratively with the simulated images that were generated from molecular models (Figures 1c and 1d). The level of the agreement of the actual and simulated TEM images was high enough to convince us that the 3D structure we proposed is one probable structure of the conformer out of > 10^8 conformational possibilities.

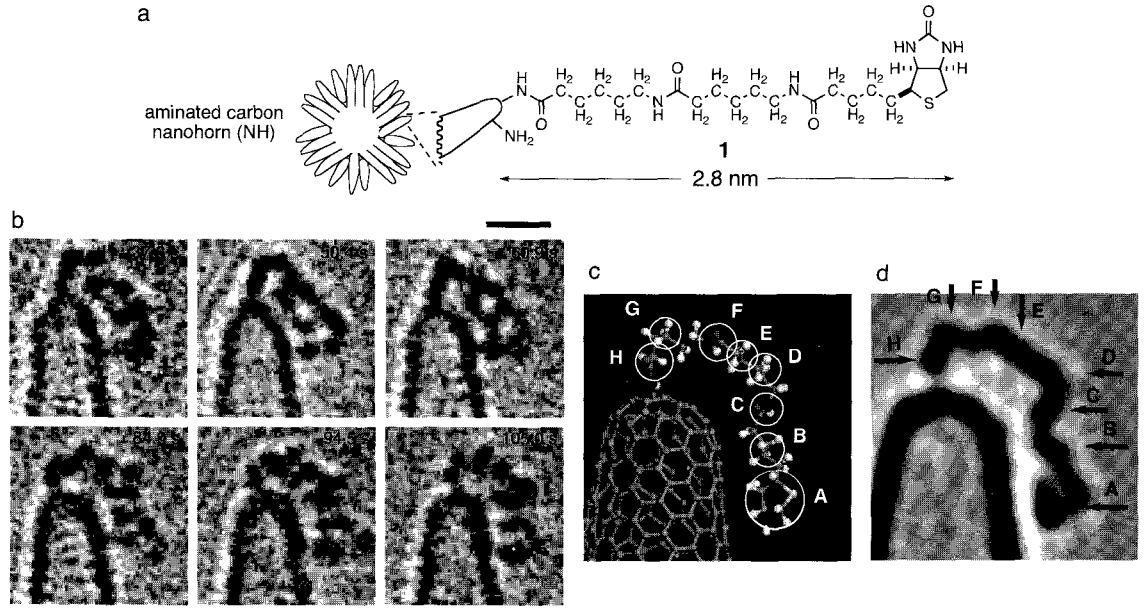

Figure 1. (a) Structure of triamide–NH conjugate **1**. (b) A series of TEM images of **1**. The figure captions refer to the time (seconds) after initiation of the observation, i.e., initiation of electron irradiation. Scale bar = 1 nm. (c,d) Molecular structure of **1** and its simulated image at 105.0 s in Figure 1a.

Acknowledgements: Works on electron microscopes were performed in collaboration with Nanotube Research Center, National Institute of Advanced Industrial Science and Technology (AIST).

†Present Address: *Department of Chemistry, Tohoku University, Japan*

[1] E. Nakamura, M. Koshino, T. Tanaka, Y. Niimi, K. Harano, Y. Nakamura, H. Isobe *J. Am. Chem. Soc.* **2008**, *130*, 7808-7809.

Corresponding Author: Eiichi Nakamura
E-mail: nakamura@chem.s.u-tokyo.ac.jp, **Tel:** +81-3-5841-4356, **Fax:** +81-3-5800-6889

Development of ultra-sensitive gas sensor utilizing fullerenes

○Morihiko Saida[1], Kenji Omote[1], Haruna Oizumi[1], Hiroyuki Sagami[1], Yuzo Mizobuchi[1], Yasuhiko Kasama[1], Kuniyoshi Yokoo[1], Shoichi Ono[1], Kazuaki Mizokami[2] and Takeo Furukawa[3]

[1]*Ideal Star Inc., Sendai 989-3204, Japan*
[2]*Nippon API Co., LTD., Yokohama 223-0066, Japan*
[3]*Graduate School of Faculty of Science, Tokyo University of Science, Tokyo 162-0826, Japan*

The oxygen gas sensor with sensitivity of parts-per-billion (ppb) order is desired due to management of semiconductor process gases like as nitrogen, argon and et al, because a presence of ppb levels of oxygen can adversely affect its device quality [1-3].

Since a fullerene crystal has large interstitial sites, gas molecules will be able to diffuse readily into its inside as shown in Fig. 1 [4,5]. Furthermore, it has been reported that the conductivity of fullerene thin films decreases drastically with oxygen adsorption[6-8]. Therefore, the fullerene is expected as a material of constructing sensitive oxygen sensors compared with a conventional solid type sensor which can detect only oxygen molecules adsorbing on its surface.

We have developed the oxygen sensor with ppb order sensitivity using a fullerene thin film as shown in Fig. 2. In this presentation, we will introduce the gas sensing properties of this fullerene sensor.

This work was supported by Tohoku Bureau of Economy, Trade and Industry.

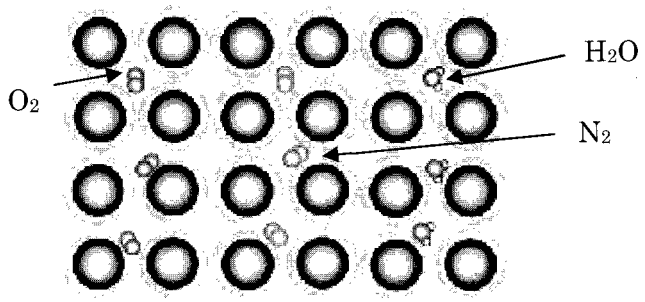

Fig.1. Relationship between the C_{60} crystal and gas molecules size.

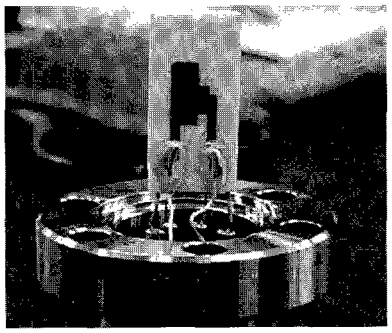

Fig.2. Fullerene gas sensor. (Size : 1 cm × 2 cm).

[1] K. Omote and K. Yokoo, *NEDO Research Report: The Investigation Regarding the Predominance in Regard to Industrial Utilization of Endohedral-Fullerens FY2006 result report*, **06002242-0-1**, 1-278 (2007).
[2] M. Katayama and S. Honda, OYO BUTURI, **76**, 1164 (2007).
[3] CETEC JAPAN 2007, Taiyo Yuden Co.,Ltd.
[4] R. A. Assink, J. E. Schirber, D. A. Loy, B. Morosin and G. A. Carlson, J. Mater. Res. **7**, 2136 (1992).
[5] P. Bernier, I. Luk'yanchuk, Z. Belahmer, M. Ribet and L. Firlej, Phys. Rev. B **53**, 7535 (1996).
[6] A. Tapponnier, I. Biaggio and P. Günter, Appl. Phys. Lett. **86**, 112114 (2005).
[7] T. Arai, Y. Murakami, H. Suematsu, K. Kikuchi, Y. Achiba, and I. Ikemoto, Solid State Commun. **84**, 827 (1992).
[8] B. Pevzner, A. F. Hebard and M. S. Dresselhaus, Phys. Rev. B **55**, 16439 (1997).

Corresponding Author : Morihiko Saida
TEL&FAX : +81-22-303-7336, +81-22-303-7339, E-mail : morihiko.saida@idealstar-net.com

Affect of the Substituent of C_{60}-derivatives on Electronic Structure: [6,6]-Phenyl-C_{61}-Butyric Acid Methyl Ester (PCBM)

○Kouki Akaike[1], Kaname Kanai[2], Hiroyuki Yoshida[3], Jun'ya Tsutsumi[3], Toshio Nishi[1], Naoki Sato[3], Yukio Ouchi[1] and Kazuhiko Seki[1]

[1]*Department of Chemistry, Graduate School of Science, Nagoya University, Nagoya 464-8602, Japan*
[2]*Research Center for Materials Science, Nagoya University, Nagoya 464-8602, Japan*
[3]*Institute for Chemical Research, Kyoto University, Kyoto 611-0011, Japan*

Recently, many fullerene (C_{60}) derivatives which have various substituents have been synthesized. [6,6]-phenyl-C_{61}-butyric acid methyl ester (PCBM) is one of them and often used for the *n*-type semiconductor in organic solar cells and field effect transistors. In these devices, the charge injection and extraction occur at organic/metal interfaces and their efficiency strongly depends on interfacial electronic structure. However, the electronic structure of PCBM has not been studied yet. In this study, we investigated the electronic structure of a PCBM molecule, thin film and interface with ultraviolet photoelectron spectroscopy (UPS), x-ray photoelectron spectroscopy (XPS), inverse photoemission spectroscopy (IPES) and density functional theory (DFT) calculations.

By analyzing the molecular orbital character, we found that the highest occupied molecular orbital (HOMO) and lowest unoccupied molecular orbital (LUMO) of PCBM are mainly composed of the π-orbital of the C_{60}-backbone. On the other hand, the UPS spectra in gas phase showed that the threshold ionization energy for PCBM is 7.17 eV, which is about 0.4 eV smaller than that for C_{60}. The threshold ionization energy and electron affinity are 0.5 - 0.6 eV smaller than those for C_{60}, which indicates that PCBM has a weaker electron acceptor nature than C_{60}. DFT calculations indicated that these trends can be due to the electron donation from the side chain to C_{60}-backbone [1].

We also investigated the interfacial electronic structure of PCBM/polycrystalline Ag substrate, which is a model for donor/cathode interface in organic solar cells. At C_{60}/Ag interfaces, the work function increases with the adsorption of C_{60} molecule on Ag substrates [2-4]. In contrast to C_{60}/Ag interfaces, the work function decreases by 0.12 eV at PCBM/Ag interface, which indicates that a PCBM molecule is charged positively. The XPS spectra of C1*s* and O1*s* showed that the charge transfer from the carbonyl oxygen atoms of the side chain to Ag substrate overcomes that from Ag substrate to the carbon atoms of the C_{60}-backbone, leading to the positive charge on a PCBM molecule. Moreover, the interfacial states were observed at PCBM/Ag interface. The IPES spectra revealed that the LUMO-derived peak is broadened at the interface, which indicates that the LUMO of PCBM contributes to the formation of the interfacial states. Therefore, the introduction of the substituent of C_{60}-derivatives affects the electronic properties of molecule and interfaces.

[1] Akaike *et al*, J. Appl. Phys. in press (2008).

[2] Veenstra *et al*, Appl. Phys. A **75**, 661 (2002).

[3] Purdie *et al*, Surf. Sci. **364**, 279 (1996).

[4] Hesper *et al*, Europhys. Lett. **40**, 177 (1997).

Corresponding Author: Kouki Akaike
E-mail: kakaike@mat.chem.nagoya-u.ac.jp Tel: 052-789-2945 Fax: 052-789-2944

Preparation of Fullerene (C_{60}) Nanosheets by Liquid-liquid Interfacial Precipitation Method

○M. Sathish, K. Miyazawa and T. Wakahara

Fullerene Engineering Group, Advanced Nano Materials Laboratory, National Institute for Materials Science, 1-1, Namiki, Tsukuba, Japan

Abstract:
In recent days, fullerene nanostructures with diverse morphologies like nanowhiskers, nanotubes, nanosheets, etc are under extensive investigation due to their potential application in nanodevice fabrication. They have good visible light absorption capacity and excellent electron transport properties with relatively high carrier mobility. Various methods have been reported for the preparation of fullerene nanostructures. Among them, liquid-liquid interfacial precipitation method has been extensively studied by Miyazawa *et al* for the preparation of fullerene nanowhiskers, nanotubes, nanosheets etc [1-3]. Here, we report the selective precipitation of fullerene nanosheets using the liquid-liquid interfacial precipitation method. Figure 1a and b, shows the SEM images of nanosheets prepared using benzene and toluene solvent system, respectively.

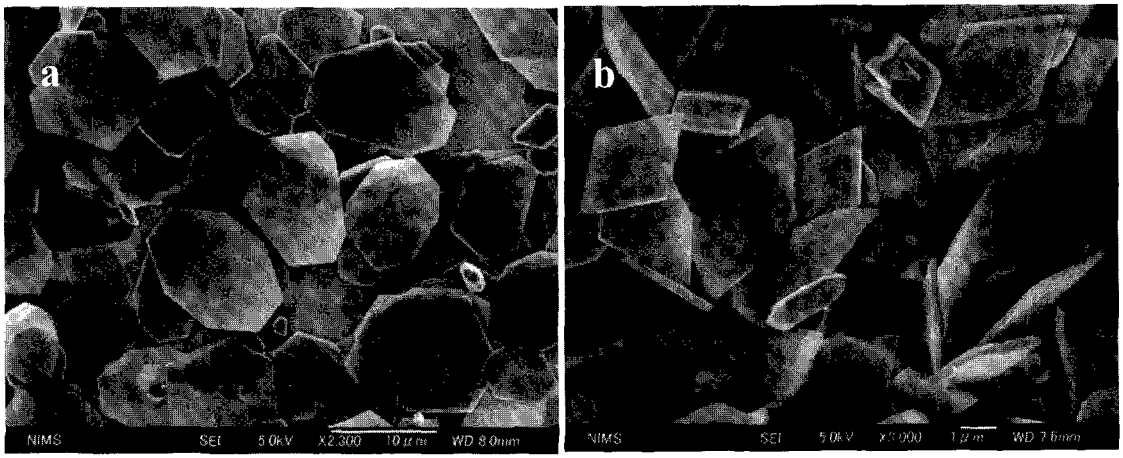

Figure 1. SEM images of nanosheets prepared in (a) benzene and (b) Toluene

By changing the solvent, the size (number of rings) of the nanosheets could be changed appropriately in a desired direction. The prepared nanosheets have been further characterized using XRD, TEM, Raman spectroscopy and TG- DTA. The XRD and TEM studies show that the nanosheets are very thin, porous, transparent and crystalline in nature. The preparation methodology and characterization results will be discussed in detail.

References:

1. K. Miyazawa, Y. Kuwasaki, A. Obayashi, and M. Kuwabara, J. Mater. Res. 17 (2002) 83.

2. M. Sathish and K. Miyazawa, J. Am. Chem. Soc, 129 (2007) 13816.

3. K. Miyazawa, J. Minato, T. Yoshii, M. Fujino and T. Suga, J. Mater. Res. 20 (2005) 688.

Corresponding Author: Marappan Sathish
E-mail: marappan.sathish@nims.go.jp
Tel & Fax : +81-29-860-4667

Visit to the Missing Fullerene World

○Hidefumi Nikawa,[1] Takashi Kikuchi,[1] Tomoya Yamada,[1] Hidenori Kuga,[1] Tsuyoshi Ito,[1] Slanina Zdenek,[1] Takeshi Akasaka,[1] Naomi Mizorogi,[2] and Shigeru Nagase[2]

[1]Center for Tsukuba Advanced Research Alliance, University of Tsukuba, Tsukuba, Ibaraki 305-8577, Japan [2]Department of Theoretical Molecular Science, Institute for Molecular Science, Okazaki, Aichi 444-8585, Japan

Fullerenes and endohedral metallofullerenes have attracted great interest due to their unique structures and properties.[1,2] Some of them could be extracted in common organic solvent, such as toluene.[3,4] The solubility of them is a primary factor contributing to the rapid advancement of fullerene chemistry.[5] Up to now, many soluble fullerenes and metallofullerenes have been extracted, separated, characterized, and functionalized. Meanwhile, many insoluble fullerenes and metallofullerenes, so-called *missing fullerenes*, have not yet been isolated though they are regularly observed in raw soot by mass spectrometry. In 1998, Alford and co-workers reported the extraction of insoluble fullerenes and indicated that they existed in raw soot and were the small band-gap.[6] Since then, missing fullerenes and metallofullerenes have attracted attention as new class of fullerene. However almost of them have not been isolated and characterized.

We have succeeded in the extraction and isolation of missing metallofullerenes, La@C_n (n = 72-82), as an endohedral metallofullerene derivative, La@$C_n(C_6H_3Cl_2)$. The structural determination for La@$C_{72}(C_6H_3Cl_2)$,[7] La@$C_{74}(C_6H_3Cl_2)$,[8] and La@$C_{80}(C_6H_3Cl_2)$ have been performed by spectroscopic and finally X-ray crystallographic analysis, and these properties are discussed on the basis of theoretical studies. As a result, it was found that the missing metallofullerenes (La@C_{72}, La@C_{74}, and La@C_{80}) have unique structure and a high radical character on the carbon cage. From the structural viewpoint, La@C_{72} has a non-IPR carbon cage and La@C_{80} possesses a novel C_{80} cage isomer, C_{2v}-C_{80}(80:3). These results indicate that there are still many insoluble and unknown endohedral metallofullerenes in raw soot and they could have an unexpected structure and properties.

This study would be an important stepping-stone to extraction and isolation of unknown fullerenes, not apply only to metallofullerenes. We expect that this study open a new fullerene science and enhance the possibilities for the application of fullerenes.

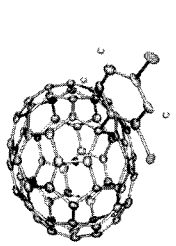

La@$C_{72}(C_6H_3Cl_2)$

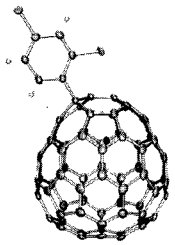

La@$C_{74}(C_6H_3Cl_2)$

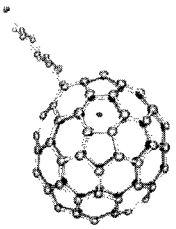

La@$C_{80}(C_6H_3Cl_2)$

[1] *Fullerenes: Chemistry, Physics, and Technology*; Kadish, K. M., Ruoff, R. S. Eds.; John Wiley & Sons, Inc.: New York, 2000. [2] *Endofullerenes: A new Family of Carbon Clusters*; Akasaka, T., Nagase, S., Eds.; Kluwer Academic Publisher: Dordrecht, 2002. [3] Kratschmer, W. et al. *Nature* **1990**, *347*, 354. [4] Chai, Y. et al. *J. Phys. Chem.* **1991**, *95*, 7564. [5] *Fullerenes: Chemistry and Reactions*; Hirsch, A., Brettreich, M.; Wiley-VCH Verlag GmbH &Co. KGaA: Weinheim, 2005. [6] Alford, J. M. et al. *Nature* **1998**, *393*, 668. [7] Wakahara, T. et al. *J. Am. Chem. Soc.* **2006**, *128*, 14228. [8] Nikawa, H. et al. *J. Am. Chem. Soc.* **2005**, *127*, 9684.

Corresponding Author: Takeshi Akasaka, **E-mail:** akasaka@tara.tsukuba.ac.jp, **Tel&Fax:** +81-29-853-6409

Design, Synthesis, and Testing of Fullerene-wheeled Nanocars

○Yasuhiro Shirai[1,2], Andrew J. Osgood[3], Jean-Francois Morin[1], Takashi Sasaki[1], Yuming Zhao[1], Jason M. Guerrero[1], Kevin F. Kelly[3] and James M. Tour[1]

[1]*Department of Chemistry, Smalley Institute for Nanoscale Science and Technology, Rice University, Houston, Texas 77005*
[2]*ICYS-MANA, National Institute for Materials Science, Tsukuba 305-0044, Japan*
[3]*Department of Electrical and Computer Engineering, Rice Quantum Institute, Rice University, Houston, Texas 77005*

Design, synthesis, and testing of new , fulle rene-wheeled single m olecular nanom achines, namely Nanocars, are presented (Fig. 1).[1] These nanovehicles are com posed of three basic components that include spherical fullerene wheels, freely rotating alkynyl axles, and a molecular chassis. The use of s pherical wheels based on C_{60} and freely rotating axles based on alkynes perm its directed nanoscale rolling of the mol ecular structure on g old surfaces.[2] Observed m otions of four -wheeled Nanocars and three-w heeled Nan ocars by STM provided d efinitive ev idence f or f ullerene-based wheel-like rolling m otion, not s tick-slip or sliding translation (Fig. 2). The st udies here underscore the ability to contro l dir ectionality of motion in molecular-sized nanostructures through precise molecular design and synthesis.

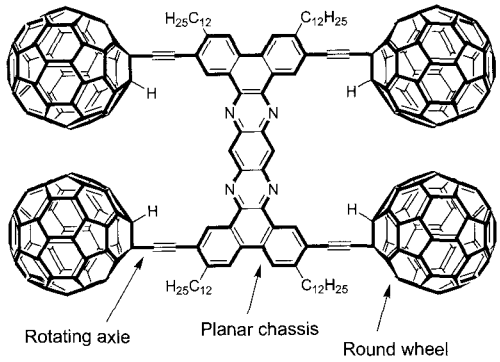

Fig. 1 Basic structure of nanovehicles.

A m otorized version o f the Nanocar was als o successfully synthesized.[3] However, it was found that th e presence of fulleren e-wheels can severely hinder photo-isom erization reactions, and the molecular motor in the Nanocar can not operate.[4] The m echanism of the d eactivation of m olecular motors by fullerene-wheels will be presented.

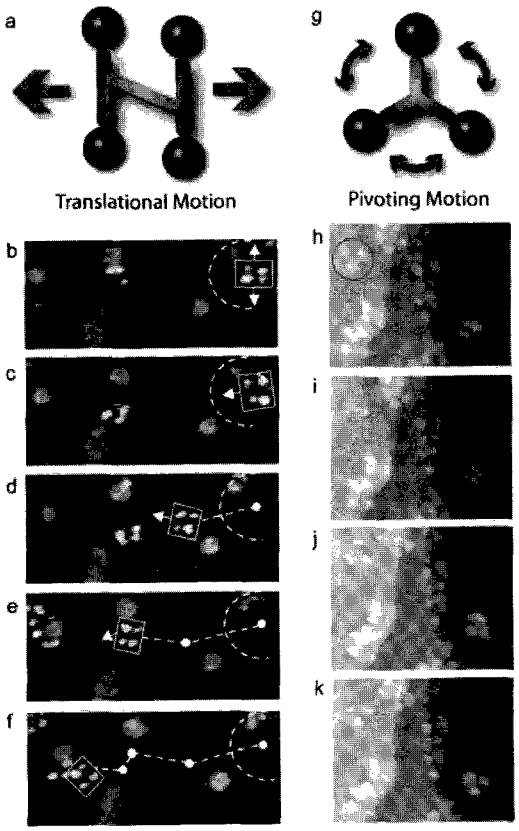

Fig. 2 Rolling motions of Nanocars.

[1] Y. Shirai, J. F. Morin, T. Sasaki, J. M. Guerrero and J. M. Tour, *Chem. Soc. Rev.*, **35**, 1043 (2006).
[2] Y. Shirai, A. J. Osgood, Y. M. Zhao, K. F. Kelly and J. M. Tour, *Nano Lett.*, **5**, 2330 (2005).
[3] J. F. Morin, Y. Shirai and J. M. Tour, *Org. Lett.*, **8**, 1713 (2007).
[4] Y. Shirai, T. Sasaki, J. M. Guerrero, B. C. Yu, P. Hodge and J. M. Tour, *ACS Nano*, **2**, 97 (2008).

Corresponding Author: James M. Tour
TEL: +1-713-348-6246, FAX: +1-713-348-6250,
E-mail: tour@rice.edu

Direct observation of nucleation and growth of carbon nanotubes from iron carbide nanoparticles

○Hideto Yoshida[1], Tetsuya Uchiyama[1], Hideo Kohno[1], Seiji Takeda[1], and Yoshikazu Homma[2]

[1]*Department of Physics, Graduate School of Science, Osaka University, 1-1 Machikaneyama, Toyonaka, Osaka 560-0043, Japan*

[2]Department of Physics, Tokyo University of Science, Shinjuku-ku, Tokyo 162-8601, Japan

Carbon Nanotubes (CNTs), one of the most important and promising materials for future nanotechnology, have been investigated over fifteen years. Nonetheless, the nucleation and growth process of CNTs has not been clarified at atomic level. For applying CNTs for not only pure science but actual industrial and technological applications, one crucially needs to understand the nucleation and growth of CNTs from nanoparticle catalysts in chemical vapor deposition (CVD) environment, which is now widely accepted as the best method for large scale production of CNTs. In order to elucidate the CVD growth mechanism of CNTs including the role of nanoparticle catalysts, we observe the nucleation and growth of single-walled CNTs (SWNTs) and multi-walled CNTs (MWNTs) in Fe catalyzed CVD by atomic-scale *in situ* environmental transmission electron microscopy (ETEM).

CNTs were grown in an ETEM by catalytic CVD with C_2H_2 gas on silicon substrate with surface oxide. Figure 1 shows the atomic-scale ETEM images of a growing MWNT. We have found that the MWNT grows from an iron carbide (Fe_3C) crystalline nanoparticle. Moreover, we have found that iron carbide nanoparticle catalysts fluctuate structurally in the CVD condition [1]. Based on *in situ* observations, we strongly suggest that carbon atoms migrate through the bulk of iron carbide nanoparticle catalysts. These finding may bring general understanding of catalyzed CVD growth of CNTs at atomic scale. In the symposium, we will discuss the structure of CNTs as well as that of nanoparticle catalysts in the CVD condition.

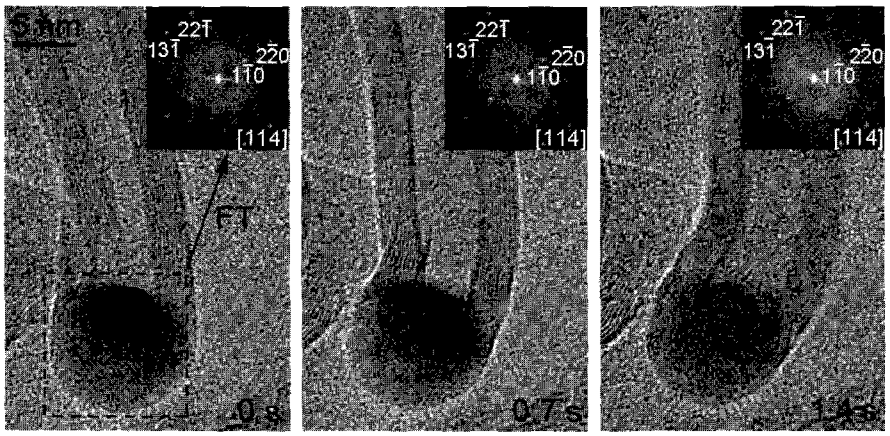

Fig. 1: *In situ* ETEM images showing a growing CNT from a Fe_3C nanoparticle catalyst.

[1] H. Yoshida, S. Takeda, T. Uchiyama, H. Kohno, and Y. Homma, Nano Lett. (2008) to be published.

Corresponding Author: Hideto Yoshida
E-mail: yoshida@tem.phys.sci.osaka-u.ac.jp
Tel: +81-6-6850-5753, Fax: +81-6-6850-5759

Simple Separation of Metallic and Semiconducting Carbon Nanotubes

○Takeshi Tanaka, Hehua Jin, Yasumitsu Miyata, Shunjiro Fujii, Hiroshi Suga, Yasuhisa Naitoh and Hiromichi Kataura

Nanotechnology Research Institute, National Institute of Advanced Industrial Science and Technology (AIST), 1-1-1 Higashi, Tsukuba, Ibaraki 305-8562, Japan

Single wall carbon nanotubes (SWCNTs) have attracted a great deal of attention towards versatile applications, especially in the field of electronics, such as field effect transistor (FET). However, as-produced SWCNTs always contain both the metallic and semiconducting phases, which is one of the most crucial problems preventing application of SWCNTs. At the last symposium, we reported a novel method for separation of metallic and semiconducting SWCNTs (MS separation) using agarose gel elctrophoresis[1].

In this study, we investigated detailed separation mechanism of the gel electrophoresis. It was found that the electric field was not always necessary for the MS separation with agarose gel. For example, the separation was achieved by just applying gravity to the agarose gel containing SWCNTs by centrifugation, where only metallic SWCNTs were squeezed out from the gel and semiconducting ones were retained in the gel debris. All the experimental results can be explained by a simple model based on the selective interaction between agarose gel and semiconducting SWCNTs (Fig. 1). We have successfully developed several new separation methods by applying this separation principle. Because the new separation methods are quite simple, quick, low cost and scalable, they should open the door for the industrial production of metallic and semiconducting SWCNTs and also accelerate the fundamental scientific research of SWCNT.

In this presentation, we will show details of the separation method and important parameters including typical characteristics of field effect transistors fabricated by using semiconducting SWCNTs obtained by the above methods.

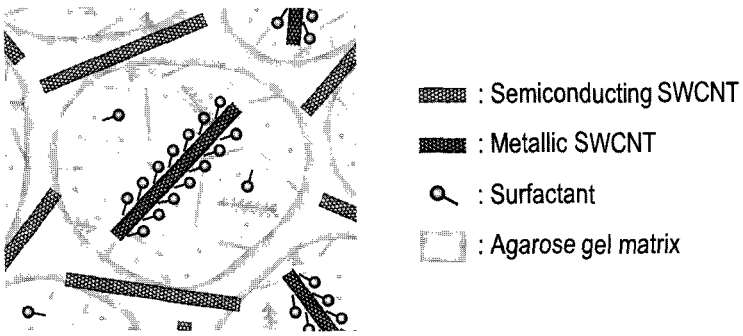

Fig. 1. The model of MS separation using agarose gel. Semiconducting SWCNTs specifically interact with agarose gel matrix, while metallic ones remains free state as surfactant micelles

Reference: [1] Tanaka et al., The 34th Fullerene-Nanotubes General Symposium, 2008, 3-6 (p47).

Corresponding Author: T. Tanaka, Tel: 029-861-2903, Fax: 029-861-2786, E-mail: tanaka-t@aist.go.jp

Ink-jet Printing of High-Performance SWNT Film Transistors

○Haruya Okimoto[1], Taishi Takenobu[1], Kazuhiro Yanagi[2,3], Yasumitsu Miyata[2], Hiromichi Kataura[2,3], Takeshi Asano[4], Yoshihiro Iwasa[1]

[1]*Institute for Materials Research (IMR), Tohoku University, Sendai 980-8577, Japan*
[2]*Nanotechnology Research Institute, AIST, Tsukuba, Ibaraki 305-8562, Japan,*
[3]*CREST/JST*
[4]*Brother Industries, Ltd., Nagoya 467-0855, Japan*

SWNT thin film transistors (TFTs) is a promising material for post-silicon electronics [1, 2]. In addition, Ink-jet printing is known to one of cost-effective ways to achieve patterns of various materials on both rigid and flexible substrates. Very recently, we applied ink-jet printing to the fabrication process of SWNT TFTs on their substrate [3]. Here we have reported the use of networks of SWNTs with high and moderated coverage for all of the conducting (i.e., source and drain electrodes) and semiconducting layers, respectively, since it is well known that the transport characteristics of SWNT films strongly depend on coverages (measured as number of tubes per unit area).

Purified SWNTs (laser-ablation method) were sonicated to disperse in DMF. After centrifugation, the supernatant was filtrated by 5 μm PTFE filter for removing the large residue. Figure 1 shows printed SWNT film transistors with different layers on Si/SiO_2 substrate. The both ends of each line are thick SWNT film area for electrode.

The transport characteristics of printed SWNT films have been perfectly controlled by coverageds, which was tuned by the number of printing as shown in figure 2. Importantly, high and moderated coverage revealed the conducting and semiconducting characteristics, respectively. As the result, we demonstrated the fabrication of all SWNT transistors using the conducting high-density SWNT film electrodes and the semiconducting low-density SWNT film. Using the optimized condition, we fabricated SWNT TFTs and obtained the carrier mobility of 2 cm^2/Vs and the on to off current ratio ~ 10^4, which is extremely higher than recent results of SWNT-TFT by ink-jet printing (mobility: ~ 0.07 cm^2/Vs and On/Off current ratio: ~ 100)[4].This study has been supported by Industrial Technology Research Grant Program in 2006 from New Energy and Industrial Technology Development Organization (NEDO) of Japan.

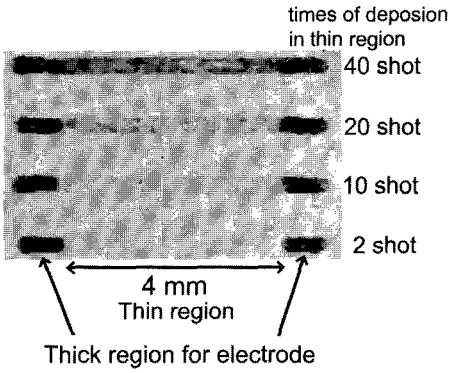

Fig.1 Optical micrograph of all SWNT TFTs on SiO_2.

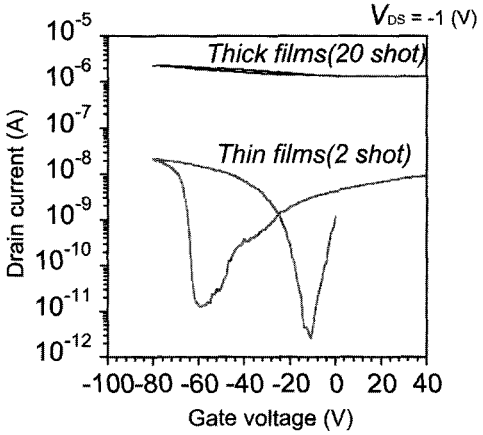

Fig.2 Transport characteristics of thick and thin SWNT film transistor

[1] M. Shiraishi *et al., Chem. Phys. Lett.*, **394**, 110 (2004).
[2] T. Takenobu *et al., Appl. Phys. Lett.*, **88**, 33511 (2006).
[3] T. Takenobu *et al.,* in preparation.[4] P. Beecher *et al., J. Appl. Phys.*, **102**, 043710(2007).

Corresponding Author: Haruya Okimoto
TEL: +81-22-215-2032, FAX: +81-22-215-2031, E-mail: haruya@imr.tohoku.ac.jp

Integrated Three-Dimensional Microelectromechanical Devices from Processable Carbon Nanotube Wafers

○Yuhei Hayamizu[1], Takeo Yamada[1], Kohei Mizuno[1], Robert C. Davis[2], Don N. Futaba[1], Motoo Yumura[1], Kenji Hata[1]

[1]*Nanotube Research Center, National Institute of Advanced Science and Technology (AIST), Tsukuba 305-8565, Japan*
[2]*Department of Physics & Astronomy, Brigham Young University, Provo, UT 84602, USA*

We describe the successful controlled self-assembly of carbon nanotubes (CNT) into closely packed and highly aligned 3-dimensional (3D) films that we denote as "CNT wafers" [1]. From CNT-wafers, we fabricated a wide range of complex 3D nanotube structures spanning from CNT islands on substrates, suspended sheets and beams linking single or multiple horizontal planes, and 3D cantilevers. These structures, each fabricated from thousands of nanotubes, are few microns in size and can be further integrated into functional 3D nanodevices. Every fabrication step is parallel and scalable, and thus massive nanodevices can be made simultaneously. Our approach opens up a new opportunity to fabricate rational nanodevices with unprecedented structural complexities and functionalities, and represents a giant step towards economical, scalable, and realistic nanodevice systems.

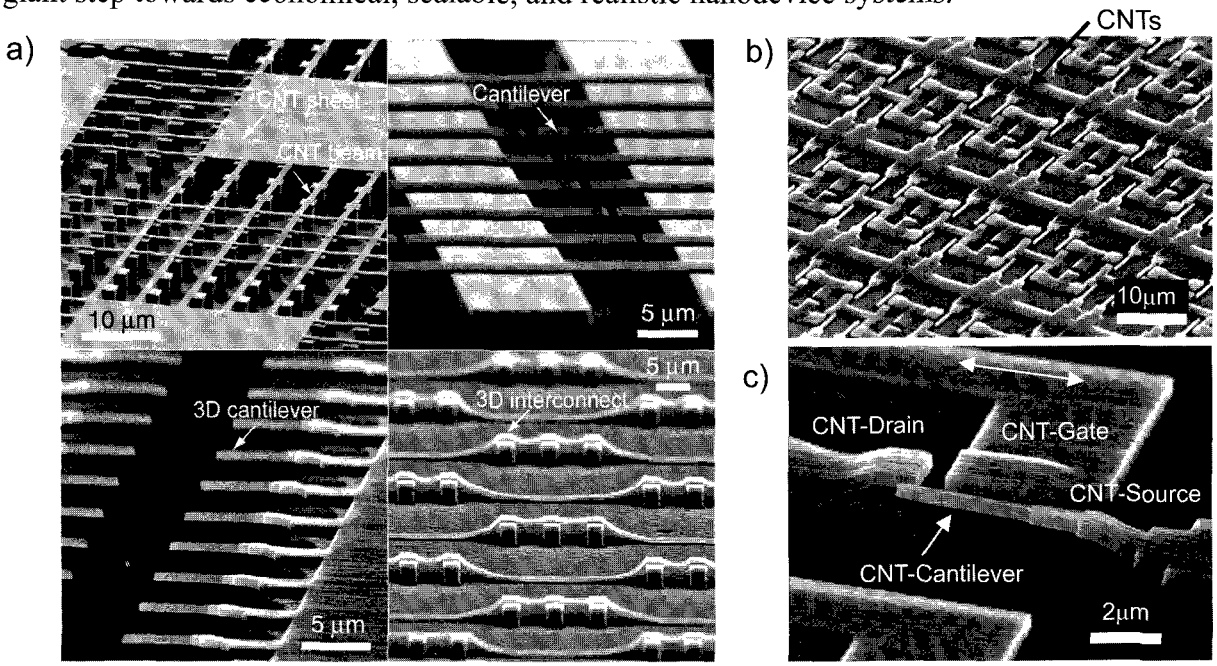

Fig. 1. Scanning electron microscope images of a) various shapes of CNT structures, b) integrated 3-dimensional CNT structures, and c) a CNT 3-terminal relay.

[1] Y. Hayamizu, T. Yamada, K. Mizuno, R. C. Davis, D. N. Futaba, M. Yumura, and K. Hata, Integration of three-dimensional microelectromechanical devices from carbon nanotube wafer, Nature Nanotechnology **3**, 289-294 (2008)

Corresponding Author: Kenji Hata
TEL: +81-29-861-4654, FAX: +81-29-861-4851, E-mail: kenji-hata@aist.go.jp

STM study on C_{70} close-packed layers

○Yohei Ohta[1], Ryoji Mitsuhashi[1], Yoshihiro Kubozono[1]

[1]*Research Laboratory for Surface Science (RLSS), Okayama University, Okayama 700-8530, Japan*

Scanning tunneling microscopy (STM) is a powerful technique for atomic and molecular scale imaging and modification of various types of surfaces. Recently, we succeeded in a removal, movement, and polymerization of C_{60} molecules by carrier injection from STM tip to C_{60} close-packed layer [1,2].

In this study, we have formed a C_{70} close-packed layer on Si(111) surface and tried to modify it. C_{70} was deposited on the well-defined Si(111) surface and heated at 100 ℃ to form a close-packed layer of C_{70} under 3×10^{-10} Torr for ~12 h. Figure 1 shows the C_{70} close-packed layer on the Si(111) surface. From this image, we have confirmed that the C_{70}-C_{70} intermolecular distance is 1.05 nm and the close-packed layer corresponds to the high-temperature hcp or fcc phase [3].

Moreover, we applied voltage pulse (2.8 V, 3 s) for the C_{70} surface from STM tip and observed a clear image for the removal of C_{70} molecule (Fig. 2). Thus, the application of voltage pulses caused a field-effect single-molecule evaporation, in the same manner as C_{60}. We currently investigate the threshold voltage and current for field-evaporation of C_{70} molecule. Furthermore, the field-effect nano-scale polymerization is also examined in the C_{70} close-packed layer.

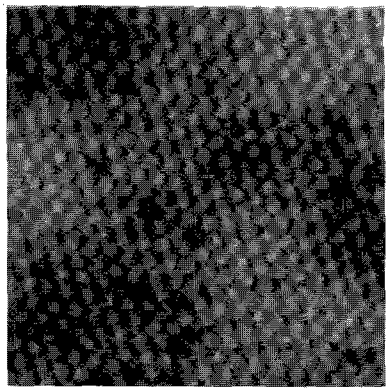

Fig.1 STM image of 20 nm × 20 nm C_{70} close-packed layer on the Si(111) surface at room temperature. The imaging condition was $V_s = 2.0$ V and $I = 0.2$ nA.

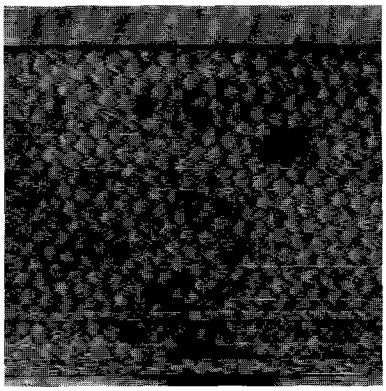

Fig. 2 STM image of 20 nm × 20 nm C_{70} close-packed layer after applied voltage pulse. The dark spot is assigned to the void of C_{70} molecule.

References:[1] S. Fujiki *et al.*, Chem. Phys. Lett. **420**, 82 (2006).
[2] R. Nouchi *et al.*, Phys. Rev. Lett. **97**, 196101(2006)
[3] G. B. Vaughan *et al.*, Science, **254**, 1350 (1991)

Corresponding Author: Yohei Ohta
E-mail: y-ota@cc.okayama-u.ac.jp
Tel: +81-86-251-7850, **Fax:** +81-86-251-7853

Electronic and optical properties of electron-beam-irradiated C_{60} films

○J. Onoe[1], T. Ito[2,3], S. Kimura[2,3], Y. Toda[4], S. Ryuzaki[1], K. Ohno[5], and T.A. Beu[6]

[1]*Research Laboratory for Nuclear Reactors and Department of Nuclear Engineering, Tokyo Institute of Technology, Tokyo 152-8550, Japan*
[2] *UVSOR Facility, Institute for Molecular Science, Aichi 444-8585, Japan*
[3]*School of Physical Sciences, The Graduate University for Advanced Studies (SOKENDAI), Aichi 444-8585, Japan*
[4]*Department of Applied Physics, Hokkaido University, Sapporo 060-8628, Japan*
[5]*Department of Physics, Yokohama National University, Yokohama 240-8501, Japan*
[6]*Faculty of Physics, University of "Babes-Bolyai", 3400 Cluj-Napoca, Romnia*

When a C_{60} film is irradiated by electron-beam (EB) with an incident energy of 3 kV, C_{60} molecules are polymerized to form a conducting peanut-shaped C_{60} polymer [1,2]. As far as our knowledge, this polymer is the first example of a negatively Gauss-curved π-electron conjugated system, though such kind of systems have been hypothetically proposed by Mackay so far. We recently performed *in situ* photoelectron spectroscopy of the peanut-shaped C_{60} polymer and found it to be metallic [3].

More recently, we have examined the carrier dynamics of this polymer using *ex situ* femtosecond-resolution pump-probe spectroscopy and found the energy gap formation associated with ordering fluctuation (the Peierls transition) below 50 K [4], which strongly suggests one-dimensional structure of the peanut-shaped C_{60} polymer. Furthermore, we have examined the temperature-dependence of its valence photoelectron spectra in the vicinity of the Fermi level and observed a Tomonaga-Luttinger behavior [5] in a similar manner to 1D metallic single wall carbon nanotube [6]. We will discuss the electronic and optical properties of the peanut-shaped C_{60} polymer, along with DFT calculations for several kinds of peanut-shaped C_{60} polymer candidates derived from the general Stone-Wales rearrangements [7,8].

[1] J. Onoe, T. Nakayama, M. Aono, and T. Hara, Appl. Phys. Lett. **82**, 595 (2003).
[2] J. Onoe, Y. Ochiai, T. Ito, S. Kimura, S. Ueda, Y. Noguchi, and K. Ohno, J. Phys. Conf. Ser. **61**, 899 (2007).
[3] J. Onoe, T. Ito, S. Kimura, K. Ohno, Y. Noguchi, and S. Ueda, Phys. Rev. B **75**, 233410 (2007).
[4] Y. Toda, S. Ryuzaki, and J. Onoe, Appl. Phys. Lett. **92**, 094102 (2008).
[5] T. Ito, J. Onoe, and S. Kimura, unpublished data.
[6] H. Ishii *et al.*, Nature **426**, 540 (2003).
[7] T. A. Beu and J. Onoe, Phys. Rev. B **72**, 155416 (2005); B **74**, 195426 (2006).
[8] S. Ueda, K. Ohno, Y. Noguchi, S. Ishii, and J. Onoe, J. Phys. Chem. B**110**, 22374 (2006).

Corresponding Author: J. Onoe
E-mail: jonoe@nr.titech.ac.jp
TEL & FAX: 03-5734-3073

Template Synthesis of Ordered Network Structure of Fullerene- or Nanotube-like Molecules

○Hirotomo Nishihara[1], Katsuaki Imai[1], Peng-Xiang Hou[1], Juan I. Paredes[2], Amelia Martínez-Alonso[2], Juan M.D. Tascón[2], and Takashi Kyotani[1]

[1]*Institute of Multidisciplinary Research for Advanced Materials, Tohoku University, Aba-ku, 2-1-1 Katahira, Sendai, Miyagi, 980-8577, Japan*
[2]*Instituto Nacional del Carbón, CSIC, Apartado 73, 33080 Oviedo, Spain*

Though nanocarbon networks constructed by fullerenes and carbon nanotubes have been theoretically predicted,[1] no one has succeeded in actually synthesizing such structure. Here we report a template-basis strategy to obtain fullerene or nanotube network structures (Fig. 1). Considering the size of zeolite pores (Fig. 1), it is theoretically possible to construct fullerene or nanotube network inside the zeolite pores if a carbon fraction in a carbon/zeolite composite reaches to 35~40 wt%. Moreover, the network should have the same ordered structure as nanopore network of zeolite (Fig. 1).

Using an acetylene CVD, large amount of carbon was introduced into zeolite pores. Then the carbon was liberated from the zeolite template with HF washing. Fig. 2 shows a TEM image and an XRD pattern of the obtained carbon. Lattice fringes in Fig. 2a and a sharp peak at $2\theta = 6.3°$ (the same position as zeolite (111) peak) in Fig. 2b are a direct evidence of the presence of ordered network structure shown in Fig. 1. In the composite, a fraction of carbon that was introduced zeolite pores was estimated to be 33 wt%, which is close to the necessary value (35~40 wt%) for fullerene or nanotube network structures. In order to introduce such large amount of carbon atoms into zeolite pore, graphene sheet must become spherical and/or tubular. Fig. 3a and 3b are two of the possible molecular models that accord to all the experimental results; network structures of fullerene-like (3a) or defective nanotube-like (3b) molecules. A steric hindrance imposed by zeolite is so strict that it is almost impossible to construct different types of structures other than the models shown in Fig. 3. The present method would be the only feasible pathway to synthesize ordered network structure of fullerene- or nanotube-like molecules.

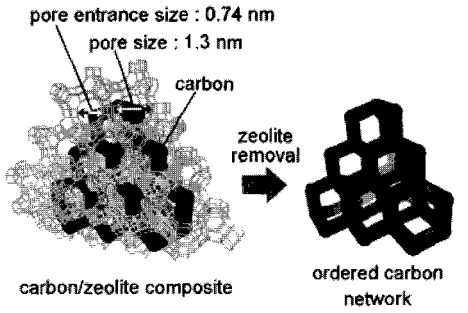

Fig. 1 Synthetic scheme of ordered carbon network.

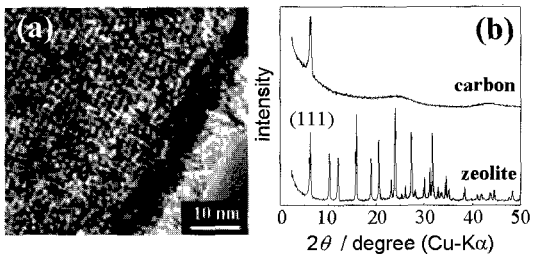

Fig. 2 TEM image (a) and XRD pattern (b) of the obtained carbon.

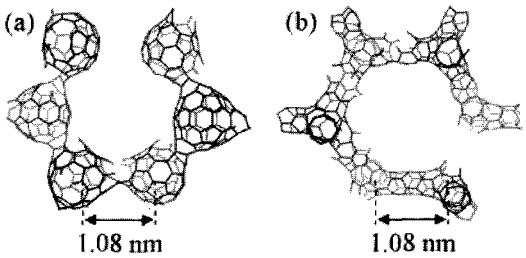

Fig. 3 Possible molecular models of the carbon; (a) fullerene-like network and (b) nanotube-like network. Each model was subjected to structure optimization by MOPAC.

[1]S. Saito, *Science*, **278**, 7 (2000).

Corresponding Author: Hirotomo Nishihara
TEL: +81-22-217-5627, FAX: +81-22-217-5627, E-mail: nisihara@tagen.tohoku.ac.jp

Diameter Control of Vertically Aligned SWNT Arrays from ACCVD

○ Rong Xiang, Zhengyi Zhang, Erik Einarsson, Jun Okawa,
Yoichi Murakami†, Shigeo Maruyama

Department of Mechanical Engineering, The University of Tokyo
†Department of Chemical System Engineering, The University of Tokyo

We present a detailed study on the diameter change and diameter control of vertically aligned single-walled carbon nanotube (SWNT) arrays from alcohol catalytic chemical vapor deposition (ACCVD). In the first part of this work, we compare three vertically aligned SWNT arrays that followed almost the same growth curve but grew for different CVD time. By subtracting the appropriate UV-Vis-NIR absorption spectra from each other, we obtained the localized absorption information, which clearly show that, quantitatively, the average diameter of SWNTs along a vertically aligned array is around 10-20% lager at the root than at the tip. This tendency is also consistent with Raman spectroscopy. Since our SWNTs grow via a root growth mechanism,[1] we propose two hypotheses to explain this diameter change: 1. smaller diameter SWNTs tend to grow slower or stop growing sooner, so that they detach from the substrate and remain in the upper portion of the film; 2. catalyst aggregation or ripening may occur during CVD at high temperature. The detailed mechanism is to be discussed in the presentation.

After the characterization of the diameter evolution of an aligned SWNT array, in the second part of work we present several strategies to control the diameters of these vertically aligned SWNTs. By changing the catalyst recipe, the average diameter of SWNT arrays from ACCVD can be tailored in a wider range than that in other processes shown previously.[2] Especially, small-diameter vertically aligned SWNT arrays (average diameter of 1.2 nm) were obtained. Also, we find the yield of SWNTs is nearly 100% even for larger diameters, which is unique to ACCVD.

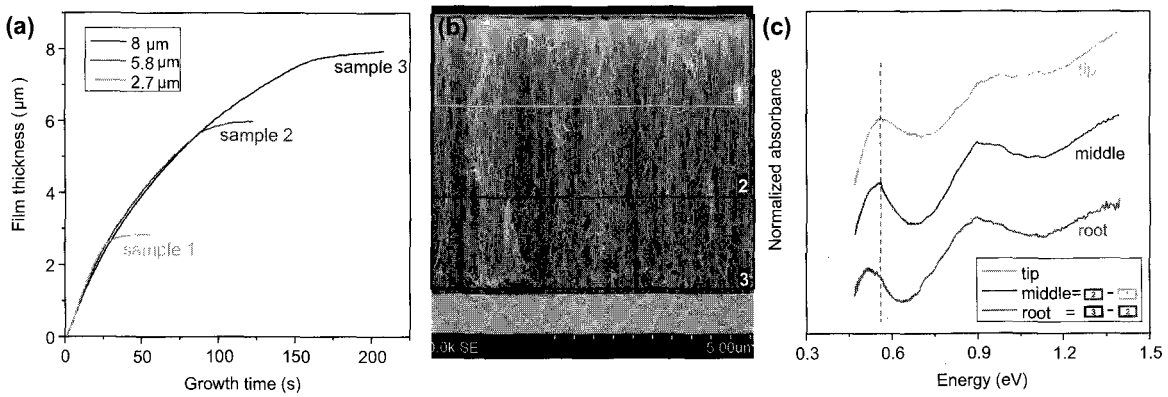

Figure 1: (a) Growth curves of three SWNT arrays grown to different thicknesses, with corresponding growth regions shown in (b). Absorbance spectra (c) showing the contribution from the top, middle, and root portions of a vertically aligned SWNT array reveal the diameter distribution is not uniform along the height of the array.

[1] R. Xiang, Z. Y. Zhang, K. Ogura, J. Okawa, E. Einarsson, et al., *Jpn. J. Appl. Phys.* **47** (2008) 1971.
[2] H. Sugime, S. Noda, S. Maruyama, Y. Yamaguchi, submitted to Carbon.

Correspondence author: Shigeo Maruyama, maruyama@photon.t.u-tokyo.ac.jp

Growth of Horizontally-Aligned Single-Walled Carbon Nanotubes on Surface Modified Silicon Substrate

○N. Yoshihara[1], H. Ago[*,1,2,3], K. Imamoto[1], M. Tsuji[1,2], T. Ikuta[4], K. Takahashi[4]
[1]*Graduate School of Engineering Sciences, Kyushu University, Fukuoka 816-8580, Japan*
[2]*Institute for Materials Chemistry and Engineering, Kyushu University, Japan*
[3]*PRESTO-JST, Japan*
[4]*Graduate School of Engineering, Kyushu University, Fukuoka 819-0395*

Recently, the horizontally-aligned growth of single-walled carbon nanotubes (SWNTs) along the atomic arrangements and/on the step-terrace structures have attracted a great interest in terms of electronic applications. The SWNT alignment was realized only on single crystalline substrates, such as sapphire (Al_2O_3) [1] and quartz (SiO_2) [2]. Si wafers, especially Si wafers with an amorphous SiO_2 insulating layer (denoted as SiO_2/Si), have widely been used for most electronic applications. It is therefore important to grow aligned SWNTs on SiO_2/Si substrates for electronics applications. In this study, we succeeded in growing horizontally aligned SWNTs along the radial steps on surface modified SiO_2/Si substrates.

A Si wafer with a 300 nm oxide layer was subjected to the plasma treatment to modify the surface. We optimized the plasma condition and, under a certain condition, obtained the radial steps on the SiO_2/Si substrate. The atomic force microscope (AFM) image of the radial steps is shown in Fig. 1. The mean step height was estimated to be 5.4 nm. For the growth of carbon nanotubes, the Fe-Mo binary metal catalyst was deposited on the plasma-treated SiO_2/Si substrate, followed by chemical vapor deposition (CVD) using CH_4 and H_2 gases at 900 °C.

Figure 2 shows the SEM images of nanotubes grown on the plasma-treated SiO_2/Si substrate. Interestingly, the nanotubes were found to orient parallel to the radial steps. Nanotube densities as high as 5 tubes/μm^{-1} were obtained. It is noted that randomly oriented nanotubes were also present on the surface where no radial steps were formed.

Though full control of the SWNTs alignment is still on the process, this is the first report of the aligned growth of SWNTs on Si wafers with an SiO_2 insulating layer. In the future, we aim to develop fully functional SWNTs-on-silicon device for electronic applications.

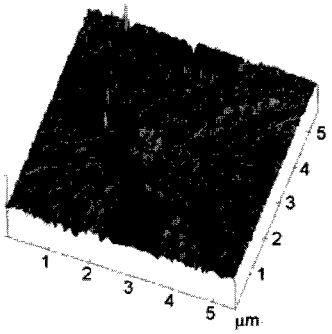

Fig. 1 AFM image of the radial steps formed on surface modified SiO_2/Si substrate. Height scale is 50 nm.

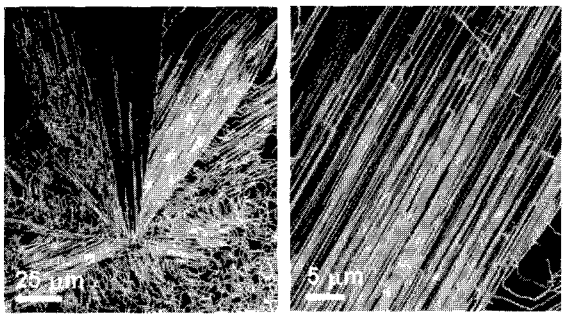

Fig. 2 SEM images of SWNTs aligned along the radial steps.

Reference
[1] H. Ago, K. Nakamura, K. Ikeda, N. Uehara, N. Ishigami, M. Tsuji., *Chem. Phys. Lett.*, **408**, 433 (2005).
[2] C. Kocabas, S. Hur, A. Gaur, M. A. Meitl, M. Shim, J. A. Rogers, *Small*, **1**, 1110 (2005).
Corresponding Author: Hiroki Ago (Tel&Fax: 092-583-7817, E-mail: ago@cm.kyushu-u.ac.jp)

5-nm-thick SWCNTs originated from catalyst particles with increasing diameters

Kei Hasegawa and Suguru Noda

Dept. of Chemical System Engineering, The University of Tokyo, Tokyo 113-8656, Japan

Carbon nanotubes (CNT s) have various pr operties depending on their structures including wall numbers, diameters, and chirality. Generally, CNT becomes single-walled and multi-walled when their diameters are about 1-2 nm and above 5 nm, respectively. This time, we report single-walled CNTs (SWCNTs) with diameters as large as 5 nm or above found in millimeter-tall forests rapidly grown by C_2H_4-CVD [1-3].

Catalysts of 0.5-nm-Fe / 15-nm-Al-Si-O were prepared by sputter-deposition on SiO_2/Si substrates. The growth condition was 8.0 kPa C_2H_4, 27 kPa H_2, 5.0 Pa H_2O, 67 kPa Ar at 1093 K [2, 3]. Vertically aligned SWCNT forest was grown up to 1 m illimeter in height. Figure 1 shows the Raman spectra of the cross-section of the SWCNT forest taken at their top, middle, and bottom. At the top of forest, which has SW CNTs grown at the beginning of their growth, strong G-band and RBM peaks were observed. At the bottom, which has SW CNTs grown at the end of t heir growth, these peak s m ostly disappeared. Figure 2 shows TEM i mages of SWCNTs. At the top of forest (a), SW CNTs were bundled and their diam eters were about 1 nm. At the bottom (c), on the other hand, they were isolated and their diam eters were 4-5 nm. Considering the f act that catalyst particles increase their di ameters during CVD possibly by Ostwald ripening, this change possibly m ade each SWCNTs to have an increasing d iameter correspondingly.

SWCNTs with lar ge dia meter will have dif ferent proper ties f rom those with narr ow diameter such as their s tability, narrower band gap, or lar ger inner vol ume. Control synthesi s of their diameter and analysis of properties is now ongoing to widen potential applications of SWCNTs.

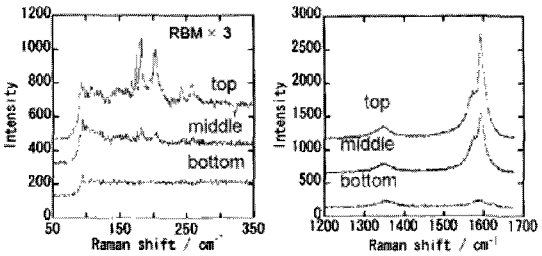

Fig. 1 Cross-section Ra man spectrum of SWCNTs, r ed: top surf ace of V A-SWCNT forest, blue: middle, green: bottom

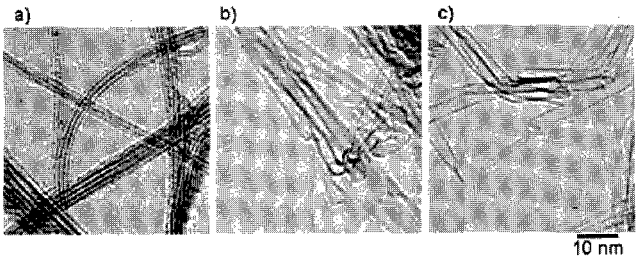

Fig. 2 TEM im ages, a) top su rface of VA-SWCNT forest, b) middle, c) bottom

[1] K. Hata, et al., *Science* **306**, 1362 (2004). [3] S. Noda, et al., *Jpn. J. Appl. Phys.* **46**, L399 (2 007). [4] K. Hasegawa et al., *J. Nanosci. Nanotechnol.*, in press.

Corresponding Author: Suguru Noda

TEL: +81-3-5841-7330, FAX: +81-3-5841-7332, E-mail: noda@chemsys.t.u-tokyo.ac.jp

Synthesis of Single-Walled Carbon Nanotubes from Defined Surface of Silicalite-1 Zeolite and their Photoluminescence Characterizations

○Yoichi Murakami[1], Takahiko Moteki[1], Watcharop Chaikittisilp[1], Yuhei Miyauchi[2], Suguru Noda[1], Tatsuya Okubo[1], Shigeo Maruyama[3]

[1]*Dept. of Chemical System Engineering, The University of Tokyo, Tokyo 113-8656, Japan*
[2]*Institute for Chemical Research, Kyoto University, Uji, Kyoto 611-0011, Japan*
[3]*Dept. of Mechanical Engineering, The University of Tokyo, Tokyo 113-8656, Japan*

Zeolites are microporous, crystalline aluminosilicates constructed from tetrahedral base units. We employed silicalite-1 (MFI-type) zeolite for supporting catalysts for the growth of single-walled carbon nanotubes (SWNTs). Cobalt was deposited on the *b*-surface (010 direction) where open periodic pores of 0.56 × 0.53 nm straight channels exist. The aim of the study is to engineer the chirality distribution of SWNTs by controlling the aggregation and/or morphology of the catalysts expecting their interactions with the crystalline surface.

Figure 1 shows typical FE-SEM images after the growth of SWNTs (CVD condition: 800 °C, 5 min, ethanol vapor = 0.4 kPa) where their intercalations between the top surfaces (*b*-surface) of the crystals are recognized. Such an intercalation of SWNTs allows us to use micro-photoluminescence spectroscopy to characterize the grown SWNTs *individually*. Figure 2 shows several PL spectra measured from those SWNTs. The effects of the SWNT growth conditions on the resultant chirality/diameter distributions are investigated.

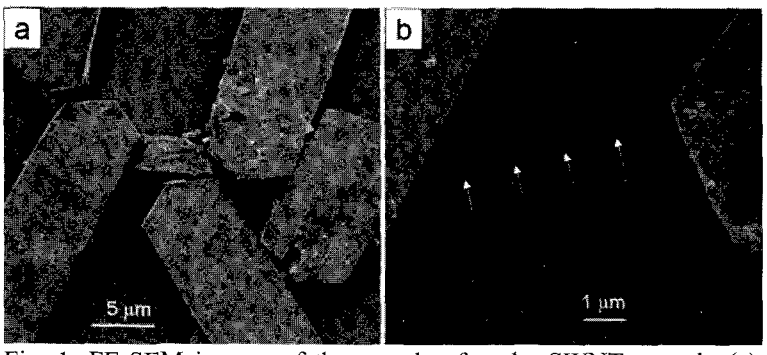

Fig. 1: FE-SEM images of the sample after the SWNT growth. (a) Silicalite-1 crystals on a quartz substrate. (b) Suspended SWNT between top surfaces of two silicalite-1 crystals (indicated by arrows).

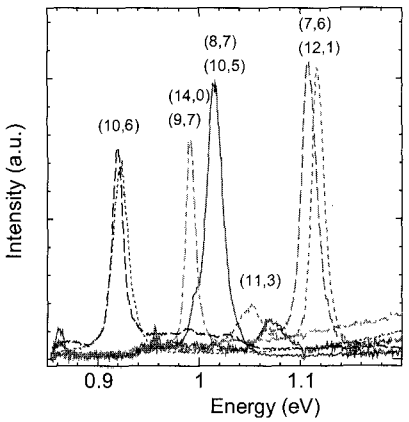

Fig. 2: PL spectra obtained from the sample. Excitation wavelength is 710 nm.

Corresponding Author: Shigeo Maruyama
TEL: +81-3-5841-6421, FAX: +81-3-5800-6983, Email: maruyama@photon.t.u-tokyo.ac.jp

Hard x-ray photoelectron spectroscopy analyses of novel carbon structure consisting of graphene multi-layers and aligned carbon nanotubes

○Daiyu Kondo[1], Shintaro Sato[1], Mizuhisa Nihei[1], Eiji Ikenaga[2], Masaaki Kobata[2], Jung Jin Kim[2], Keisuke Kobayashi[2] and Yuji Awano[1]

[1]*Nanotechnology Research Center, Fujitsu Laboratories Ltd., 10-1 Morinosato-Wakamiya, Atsugi 243-0197, Japan*
[2]*Japan Synchrotron Radiation Research Institute/Spring-8, 1-1-1 Kouto Sayo-cho Sayo-gun, Hyogo 679-5198, Japan*

We previously reported on novel carbon structure composed of graphene multi-layers and aligned multi-walled carbon nanotubes (MWNTs) [1]. This unique structure has graphene multi-layers spontaneously formed on the top of aligned MWNTs, which was obtained by chemical vapor deposition (CVD). The graphene layers are perpendicular to the aligned direction of MWNTs. While the obtained structure is clearly different from usual vertically-aligned MWNTs [2], its origin has not been completely understood yet. To elucidate roles of catalyst films in synthesizing the composite, we have investigated the electronic structures of the composite by using hard x-ray photoemission spectroscopy (PES). The PES measurements were performed at the BL47XU in the SPring-8.

The CVD process was performed in a low-pressure chamber. As the carbon source, a mixture of acetylene and argon gases was introduced into the CVD chamber. The substrate temperature was 510 °C. As a catalyst, a 2.6-nm cobalt film was used. Detailed conditions of the CVD process were shown elsewhere [1]. Figure 1 shows Co *2p* core level spectra of (a) the novel carbon composite structure and (b) the usual MWNTs grown from a 1-nm Co film measured by hard x-ray PES. The PES spectrum indicates that the Co catalyst after synthesizing the composite mainly consists of pure cobalt. On the other hand, the Co catalyst for the MWNTs was mainly oxidized. Taking into account the fact that the Co film was mostly oxidized before synthesis, this result means that the Co film of the composite was much more reduced during the growth, implying that high catalyst activity of the Co film is one of the origins of the composite structure. The details will be discussed in the presentation. The authors thank Dr. Naoki Yokoyama, Fellow of Fujitsu Laboratories Ltd. for his support and useful suggestions.

[1] D. Kondo *et al.*, APEX 1 (2008) 074073.
[2] S. Sato *et al.*, Chem. Phys. Lett. 402 (2005) 149.

Corresponding Author: Daiyu Kondo
E-mail: kondo.daiyu@jp.fujitsu.com
Tel&Fax: +81-46-250-8234&+81-46-250-8844

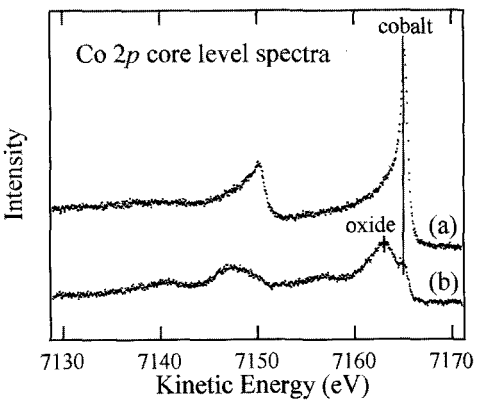

Figure 1 Co *2p* core level spectra of (a) the novel carbon structure and (b) usual MWNTs.

Megagauss Spectroscopy of Single-Walled Carbon Nanotubes

○Hiroyuki Yokoi[1], Mukhtar Effendi[1], Nobutsugu Minami[2], Eiji Kojima[3], Shojiro Takeyama[3],

[1]*Department of Materials Science and Technology, Kumamoto University, Kumamoto 860-8555, Japan*
[2]*Nanotechnology Research Institute, National Institute of Advanced Industrial Science and Technology, Tsukuba 305-8565, Japan*
[3]*Institute for Solid State Physics, University of Tokyo, Kashiwa, 277-8581, Japan*

Optical properties of single-walled carbon nanotubes (SWNTs) are governed largely by excitonic states because the exciton exists stably even at room temperature due to the one-dimensionality of their structures. It has been predicted theoretically that the excitonic state is split into singlet and triplet states due to valley mixing and exchange at K and K' points of the Brillouin zone because the electronic states are degenerate at the points [1]. Among these excitonic states, only the gerade state of the singlet states is optically active ("bright") and the others are optically inactive ("dark"). It has been one of the most important problems in the properties of SWNTs which state locates energetically lower between the singlet "bright" and "dark" excitonic states.

In order to approach this subject, we have conducted magneto-absorption measurements of aligned SWNT films in the visible light region at room temperature under ultra-short pulsed magnetic fields to 200 T using a single-turn coil system. We have succeeded to observe changing of absorption peaks originated from the second sub-band exciton in semiconducting SWNTs very clearly with increasing magnetic field in parallel to the alignment of SWNTs. The following changes are recognized for SWNTs with a chiral vector of (6, 5) or (7, 5): The absorption peak observed at 0 tesla shifts toward the *higher* energy side and a new one appears on the *lower* energy side for the (6, 5) SWNT while the former shifts toward the *lower* energy side and the latter appears on the *higher* energy side for the (7, 5) SWNT. No modification of absorption spectra has been detected by the application of magnetic fields perpendicular to the alignment of SWNTs up to 200 T, which suggests that the spectral changes mentioned above are attributed to the Aharonov-Bohm effect [2].
These experimental results prove that it is the "dark" excitonic state in (6, 5) SWNT and the "bright" one in (7, 5) SWNT that situates at the lower energy side in the case of the singlet splitting of the second sub-band excitonic state. This configuration is different from that reported in the other magneto-luminescence studies where the "dark" one situates at lower energies in all of the investigated SWNTs [3,4]. Further studies are required to resolve this contradiction.

[1] H. Ajiki and T. Ando, *J. Phys. Soc. Jpn*,, **65**, 505 (1996).
[2] T. Ando, *J. Phys. Soc. Jpn.*, **75**, 024707 (2006).
[3] I.B. Mortimer and R.J. Nicholas, *Phys. Rev. Lett.*, **98**, 027404 (2007).
[4] J. Shaver, J. Kono, O. Portugall, V. Krstic, G.L.J.A. Rikken, Y. Miyauchi, S. Maruyama, and V. Perebeinos, *Nano Lett.*, **7**, 1851 (2007).
Corresponding Author: Hiroyuki Yokoi
TEL.: +81-96-342-3727, FAX: +81-96-342-3710, E-mail: yokoihr@kumamoto-u.ac.jp

Meissner effect in thin films of boron-doped carbon nanotubes

N. Murata[1], ○J. Haruyama[1, 2, 5], J. Reppert[3], A. M. Rao[3], T. Koretsune[4], S. Saito[4]

[1]*School of Science and Engineering, Material Science course, Aoyama Gakuin University, 5-10-1 Fuchinobe, Sagamihara, Kanagawa 229-8558, Japan*

[2]*Institute for Solid State Physics, University of Tokyo, Kashiwanoha 5-1-5, Kashiwa, Chiba 277-8581, Japan*

[3]*Department of Physics and Astronomy, Center for Optical Materials Science and Engineering Technologies, Clemson University, Clemson, SC 29634, USA*

[4]*Department of Physics, Tokyo Institute of Technology, 2-12-1 Oh-okayama, Meguro-ku, Tokyo, 152-8551, Japan*

[5]*JST-CREST, 4-1-8 Hon-machi, Kawaguchi, Saitama 332-0012, Japan*

Abstract: Superconductivity in carbon nanotubes (CNTs) is attracting considerable attention [1-4]. However, its correlation with carrier doping has not been reported. Here, I show the Meissner effect found in thin films consisting of assembled boron-doped single-walled CNTs (*B*-SWNTs) [5]. The SWNTs are synthesized from Ni/Co catalyst including elementary boron by pulsed laser vaporization [6]. We find that only CNT films consisting of low boron concentration leads to evident Meissner effect with T_c = 12 K and also that a highly homogeneous ensemble of the CNTs is crucial for realizing the Meissner effect. Interestingly, the T_c value of 12K exactly agrees with that for an abrupt resistance drop in entirely end-bonded multi-walled CNTs [1]. The first-principles electronic-structure study strongly supports these results [4].

Homogeneously assembled *B*-CNTs, which can provide weakly interacted CNTs (quasi-1D property) so as to maintain both the 1D properties (e.g., contribution of a van Hove singularity and strong curvature in one SWNT) and the 3D property (e.g., Meissner shielding-current path across assembled SWNTs), are promising as a novel structure which is expected to open doors to the fields of carbon-based superconductivity and to obtain higher T_c.

References

[1]I.Takesue, J.Haruyama et al., **Phys.Rev.Lett.**96, 057001 (2006)

[2] N.Murata, J.Haruyama, M.Matsudaira, Y.Yagi, E.Einarsson, S.Chiashi, S.Maruyama, T.Sugai, N.Kishi, H.Shinohara, **Phys.Rev.B** 71, 081744 (2007)

[3]E.Perfetto and J.Gonzalez, **Phys.Rev.B** 74, 201403(R) (2006)

[4]T. Koretsune, S. Saito, *Phys. Rev. B* 77, 165417 (2008)

[5]N. Murata, J. Haruyama, J. Reppert, A. M. Rao, T. Koretsune, S. Saito, To be published on **Phys.Rev.Lett.** (July, 2008)

[6]K.McGuire, M.S.Dresselhaus, A.M.Rao et al., **Carbon** 43, 219 (2005)

Corresponding Author: Junji Haruyama

E-mail: J-haru@ee.aoyama.ac.jp

Tel&Fax: 042-759-6256 (Fax: 6524)

Structures and Phase behavior of quasi-one-dimensional water

○ Daisuke Takaiwa[1], Kenichiro Koga[1], and Hideki Tanaka[1]

[1] *Depertment of Chemistry, Faculty of Science, Okayama University. 3-1-1 Tushima-naka, Okayama 700-8530, Japan*

A material confined in extremely narrow space may exhibit properties that the bulk material never does. When water is confined in carbon nanotubes, quasi-one-dimensional solids called "ice nanotubes" form spontaneously at low temperature. Moreover the freezing transitions can be either continuous or discontinuous depending on pressure, which suggests an existence of liquid-solid critical point[1].

Molecular simulations and thermodynamic analysis are carried out to investigate water confined in quasi-one-dimensional space surrounded by hydrophobic wall(single walled carbon nanotube: SWNT). The structures of solid water under various thermodynamic conditions are classified in a systematic fasion[2,3,4].

Constant-temperature and constant-volume molecular simulations are carried out to examine novel structures of water at fixed densities corresponding to high pressure states. Several structures are found in this step and several other structures are deduced as possible phase(Fig.1, 2). Obtained structures of solid water can be classified into two net-like ices: one is square net sheet ice nanotubes and the other is hexagonal net sheet ice nanotubes. Furthermore, square net sheet ice nanotubes can be classified into two closely-packed forms of solid water: n-gonal ice nanotubes and n-helical ice nanotubes. The inner space of the ice nanotubes are either filled or unfilled with water molecules, depending on the tube diameter and pressure.

Constant-temperature and constant-pressure molecular simulations are carried out to make Pressure(P)—Temperature(T)— SWNT diameter(D) phase diagram of water(0.1 MPa $\leq$ P $\leq$ 6.0 GPa, 0 K $\leq$ T $\leq$ 450 K, 9 Å $\leq$ D $\leq$ 17 Å). The result at $P = 0.1$ MPa shows that the melting curve has many local maxima, each corresponding to highest melting point for each ice form(Fig. 3).

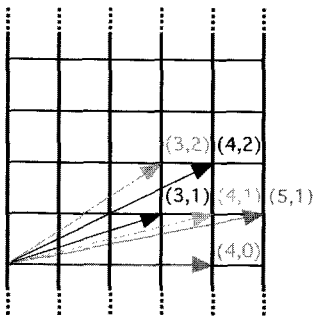

Fig. 1 Roll up vector (n, m)

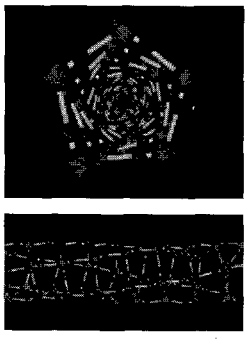

Fig. 2 Top and side views of (5, 1) **ice**

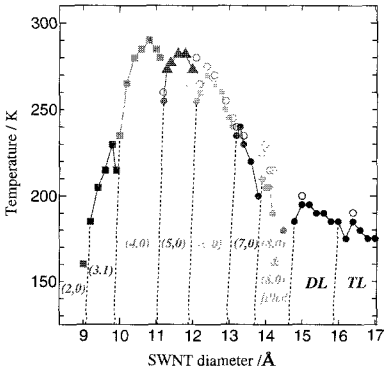

Fig. 3 TD**-phase diagram at 0.1 MPa**

[1] K. Koga, G.T. Gao, H. Tanaka, and X.C. Zeng, *Nature,* **412**, 802 (2001).
[2] D. Takaiwa, K. Koga, H. Tanaka, *Mol. Simulat.*, **33**, 127-132 (2007).
[3] D. Takaiwa, I. Hatano, K. Koga, H. Tanaka, *Proc. Natl. Acad. Sci. USA,* **105**, 39-43 (2008).
[4] D. Takaiwa, K. Koga, H. Tanaka, *in prepearation.*

Corresponding Author: Daisuke Takaiwa
E-mail: dns18303@cc.okayama-u.ac.jp

Fullerene Encapsulation Effects on Radial Breathing Mode Frequencies of Single-Walled Carbon Nanotubes

○Soon-Kil Joung[1], Toshiya Okazaki[1,2], Naoki Kishi[1], Takeshi Nakanishi[1], Susumu Okada[3], Shunji Bandow[4] and Sumio Iijima[1,4]

[1]*Research Center for Advanced Carbon Materials, AIST, Tsukuba 305-8565, Japan*
[2]*PRESTO, JST, 4-1-8 Honcho, Kawaguchi 332-0012, Japan*
[3]*Institute of Physics, Center for Computational Science, University of Tsukuba, Tsukuba 305-8571, Japan*
[4]*Department of Materials Science and Engineering, Meijo University, Nagoya 468-8502, Japan*

Single-walled carbon nanoubes (SWCNTs) encapsulating C_{60} (so-called "nanopeapods") have been expected as a new class of hybrid materials with novel physical properties. Resonance Raman scattering is an important tool for identification and probing the geometric and the electronic changes of SWCNTs upon molecular insertions. Because of the resonance process, the Raman intensity of SWCNTs strongly depends on the tube chirality and the excitation wavelength. Therefore two-dimensional resonant Raman mapping method by using many laser lines is appropriate for comprehensive characterizations.

Figure 1 shows the resonance Raman intensity map for radial breathing mode (RBM) obtained from C_{60} nanopeapods in SDBS micellar solution by using a tunable Ti-sapphire laser. In these excitation wavelengths (750-1040 nm), RBM signals of semiconducting SWCNTs with 1.25~1.41 nm in diameter are observed. The band gap modification of SWCNTs by C_{60} encapsulations [1] result in the resonance energy changes for each (*n, m*) tubes. The encapsulated C_{60} also affect the RBM frequencies. For smaller diameter tubes (1.25-1.28 nm), the RBM frequencies are shifted upward by 4-5 cm^{-1} upon C_{60} encapsulation whereas those of larger diameter tubes (1.35-1.41 nm) are down-shifted by 1-8 cm^{-1}. These frequency shifts can be explained by the steric hindrance of the encapsulated C_{60}, and the hybridization between the π-states of SWCNTs and C_{60}, respectively. Such a strong diameter dependence of the RBM frequency shifts is consistent with the theoretical predictions [2] and the previous photoluminescence excitation (PLE) results [1].

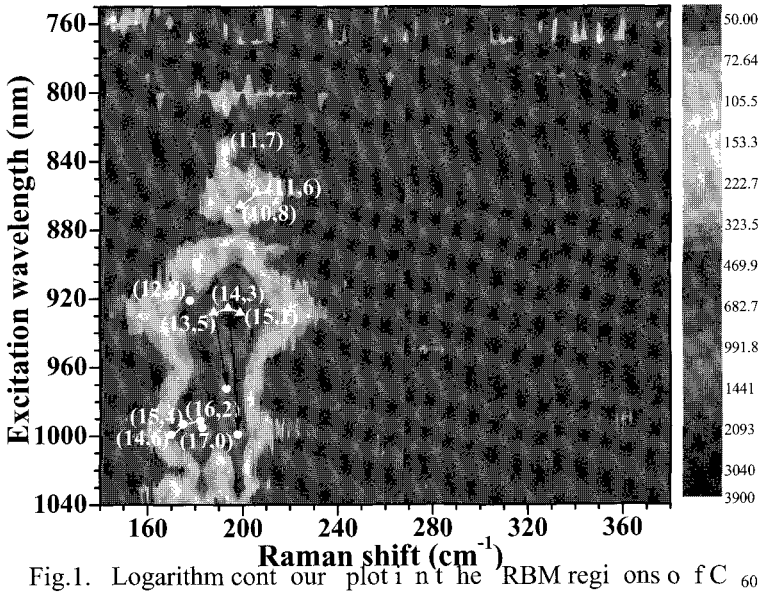

Fig.1. Logarithm contour plot in the RBM regions of C_{60} nanopeapod experimentally obtained; • peapod, ▲SWNTs.

[1] T. Okazaki *et al.*, ***J. Am. Chem. Soc.***, **130**, 4122 (2008). [2] S. Okada, ***Chem. Phys. Lett.***, **438**, 59 (2007).

Corresponding Author: Toshiya Okazaki **E-mail:** toshi.okazaki@aist.go.jp **Tel:** 029-861-4173, **Fax:** 029-861-6241

Fabrication and Characterization of Thin Metal Nanowires using Carbon Nanotube Template

○R. Kitaura[1], R. Nakanishi[1], T. Saito[2,3], T. Ohshima[2], H. Yoshikawa[1], K. Awaga[1] and H. Shinohara[1]

[1]*Department of Chemistry & Institute for Advanced Research, Nagoya University, Nagoya 464-8602, Japan*
[2]*Reseach Center for Advanced Carbon Materials, AIST, Tsukuba 305-8565, Japan*
[3]*PRESTO, Japan Science and Technology Agency, Kawaguchi 332-0012, Japan*

Substantial research efforts have been devoted to fabricate metallic or semiconducting nanowires because of their fundamental interest on optical, electrical and magnetic properties, which are qualitatively different from those at larger dimensions, as well as of versatile and promising applications towards nanoelectronic and nanospintronic devices[1]. To fabricate nanowire materials, chemically and thermally stable one-dimensional nanospace of carbon nanotubes (CNTs) can be used as an ideal nano-sized reaction-space. In this presentation, we have focused on high-yield fabrication of atomically thin metal nanowires using CNTs template and their structural characterization using high-resolution transmission electron microscope (HRTEM).

SWCNTs and DWCNTs were synthesized by chemical vapor deposition method and purified under high vacuum at high temperature to remove remaining metal catalysts and amorphous materials attached at outer surface of the CNTs. After opening fullerene end-caps, metal atoms have been introduced by a direct sublimation method. Figure 1 shows a HRTEM image of Eu@DWCNTs, for example. As clearly illustrated in the figure, Eu atoms align in a one-dimensional fashion with Eu-Eu distances of 4.6 Å, which is much larger than that of bulk crystal of Eu (4.0 Å). In this presentation, further structural analyses and electronic structure on the various metal nanowire encapsulated in CNTs are discussed.

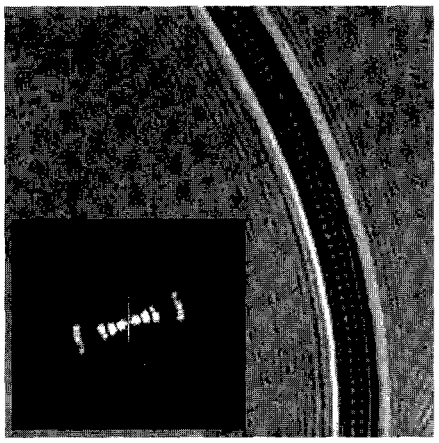

Figure 1. HRTEM image of Eu@DWCNTs (inset shows FFT image)

References

[1] C. M. Lieber *et. al.*, Acc. Chem. Res. 32, 5, 435-445 (1999)

Corresponding Author: Hisanori Shinohara

E-mail: noris@cc.nagoya-u.ac.jp

TEL: +81-52-789-2482, **FAX:** +81-52-747-6442

A Simple Formation of Carbon Nanotubes Filled Perfectly with Nanowires by Laser Vaporization

○Fumio Kokai, Tomoyuki Shimazu, Adachi Kazuma, Yutaka Takahashi, Akira Koshio

Graduate School of Engineering, Mie University
1577 Kurimamachiya, Tsu, Mie 514-8507

Carbon nanotubes (CNTs) filled with metals or their compounds have received extensive attention. So far, encapsulation of more than 40 metals were attempted using methods such as a chemical technique using capillary action, arc discharge, and plasma chemical vapor deposition. However, some of the CNTs were intermittently filled and the yields of the filled CNTs were usually low. We herein report a simple way to grow CNTs filled perfectly with nanowires of copper or silicon carbide using a laser vaporization technique. Unlike previous studies, all the grown CNTs contain Cu or SiC nanowires in their roots to tips and no empty CNT is present.

Laser vaporization of graphite mixed with Cu or Si was performed in the presence of Ar gas using a continuous-wave Nd:YAG laser (0.6 kW peak power) at room temperature. Depending on the Cu content and Ar gas pressure, the products showing different morphologies were obtained such as a single-wall carbon nanohorn aggregate hybridized with a carbon nanocapsule and a polyhedral graphite particle as observed previously [1]. In particular, at a high Ar gas pressure of 0.9 MPa, many Cu-filled CNTs (5–45 nm thick and 0.3–1 μm long) together with carbon nanocapsules were observed in the product (Fig. 1a). As seen in Fig. 1b, Cu wires, showing lattice fringes with a d-spacing of 0.21 nm corresponding to the (111) atomic plane, were covered with 1–5 graphitic layers. A selected area diffraction pattern showed spots corresponding to Cu (111) and Cu (200) reflections, indicating the formation of fcc crystalline nanowires. The formation of CNTs filled with SiC nanowires started from relatively low Ar pressure of 0.3 MPa. With increasing pressure, straight SiC-filled CNTs with 10–160 nm thick and 0.5–5.5 μm long were obtained. For the formation of these filled CNTs, high resident density of vaporized carbon and metal is thought to be essential like the growth of polyhedral graphite particles in a space confined by Ar gas [2]. From the TEM observation of the trace of a molten composite particle at the edge of a filled CNT, we believe the growth of a composite nanowire, which occurs from a molten particle with a specific metal-carbon composition, followed by phase separation plays a key role in the filled-CNT formation.

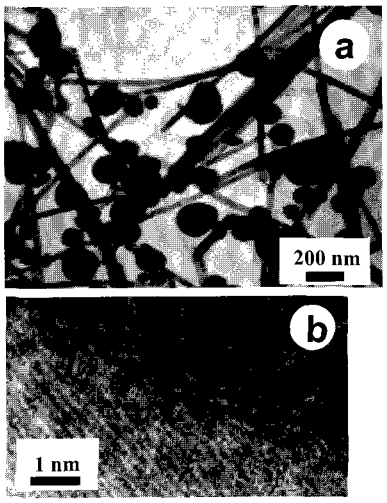

Fig. 1 TEM images of (a) the product produced by laser vaporization of graphite mixed with copper (20 at.%) at an Ar gas pressure of 0.9 MPa and (b) the outer region of a Cu-filled CNT.

References: (1) K. Kobayashi et al. Appl. Phys, A 89, 121 (2007); (2) F. Kokai et al. Carbon 42, 2515 (2004).
Corresponding Author: Fumio Kokai, **E-mail:** kokai@chem.mie-u.ac.jp, **Tel:** 059-231-9422, **Fax:** 059-231-9424

Formation of Si Fullerenes: A Molecular dynamics Study

○Kengo Nishio[1], Taisuke Ozaki[2], Tetsuya Morishita[1], and Masuhiro Mikami[1]

[1]*Research Institute for Computational Sciences (RICS), National Institute of Advanced Industrial Science and Technology (AIST), Central 2, Umezono 1-1-1, Tsukuba, Ibaraki 305-8568, Japan*

[2]*Research Center for Integrated Science (RCIS), Japan Advanced Institute of Science and Technology (JAIST), 1-1 Asahidai, Nomi, Ishikawa 923-1292 Japan*

Discovery of novel Si nanostructures would open up a new avenue for science and technology as the discovery of the carbon fullerene and carbon nanotube did. We have explored novel Si nanostructures by combining molecular dynamics (MD) simulations with the Tersoff potential and first-principles calculations[1-5]. Our MD simulations demonstrated [Fig. 1] a triple-shell Si fullerene $Si_{20}@Si_{80}@Si_{180}$, or an icosahedral Si nanodot, forms by freezing a droplet in vacuum[1], [Fig. 2] Si-fullerene-linked nanowires, such as Si_{16}- and Si_{20}-linked nanowires form by freezing liquid Si confined in carbon nanotubes[2], and [Fig. 3] a $Si_{20}@Si_{80}$-linked nanowire, or a polyicosahedral Si nanowire, forms by freezing liquid Si confined in a cylindrical pore[3,4].

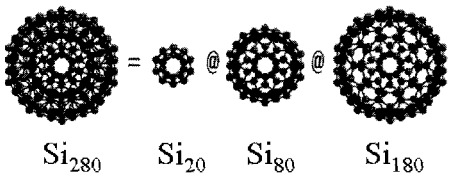

Fig. 1

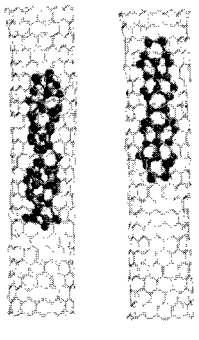

Fig. 2

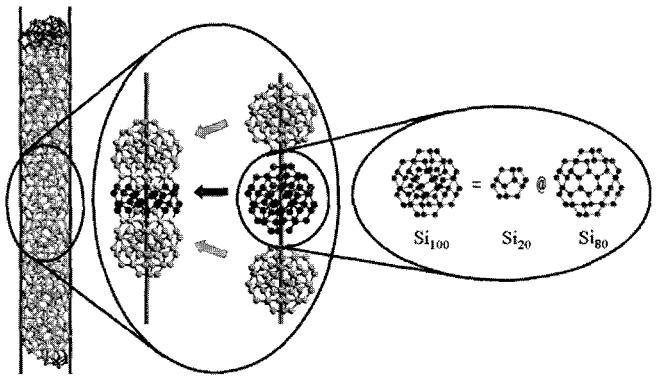

Fig. 3

[1] K. Nishio et. al. Phys. Rev. B **72**, 245312 (2005).

[2] K. Nishio et. al., Phys. Rev. B **77**, 2201401(R) (2008).

[3] K. Nishio et. al., J. Phys. Chem. **125**, 074712 (2006).

[4] K. Nishio et. al., Phys. Rev. B **77**, 075431 (2008).

Corresponding Author: Kengo Nishio

E-mail: k-nishio@aist.go.jp

Spin injection, spin coherence and robust spin polarization in graphene-based spin valves at room temperature

○M. Shiraishi [1,2], M. Ohishi [1], R. Nouchi [1], T. Nozaki [1], T. Shinjo [1,3] and Y. Suzuki [1]

[1] Graduate School of Engineering Science, Osaka University, Toyonaka, Japan
[2] JST-PRESTO, Kawaguchi, Japan, [3] IIAS, Kyoto, Japan

Molecular spintronics exploiting graphene-based materials attracts much attention because of its small spin-orbit coupling yielding good spin coherence and the success in injecting spins at room temperature (RT) [1-3]. Our group firstly reported the spin injection into graphene at room temperature [1] by fabricating a graphene thin film (GTF) spin valves and introducing a non-local 4-terminal method [4]. This success was achieved by avoiding a so-called conductance mismatch [5] between ferromagnets and molecules. In this presentation, we report on several important subjects of spin injection and spin transport in a GTF [6]; i) observation of spin injection signals by a local 2-terminal method, ii) observation of Hanle-type spin precession and estimation of spin transport properties in a GTF, iii) unprecedented robustness of spin polarization (P) of injected spins.

Figure 1 shows typical resistance hysteresis due to spin injection into GTF at room temperature. The magnetic field where the hysteresis appeared coincided very well, so it is concluded that a magnetoresistance (MR) effect at RT (MR ratio ~0.02%) was firstly observed in molecular spin valve with reliability by the local method. Spin coherent length and time at RT were estimated to be 1.6 μm and 120 ps from results on the Hanle-type spin precession, and they were comparable to those observed in a single layer graphene [2]. It is well-known that the MR ratio drastically decreases as a bias voltage increases in molecular spin valves (typically the MR ratio becomes a half at 5-10 mV) due to decrease of P. We found that the P in the GTF did not change until 500 mV and P was still 81% at 1.2 V. Such robustness is the best among all spintronics devices, which means obvious superiority of graphene-based spintronics.

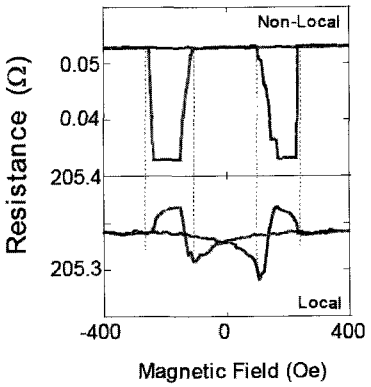

Fig. 1 Spin injection signals in non-local and local methods at RT.

References: [1] M. Ohishi, M. Shiraishi et al., JJAP46, L605 (2007). [2] N. Tombros et al., Nature 448, 571(2007). [3]S. Cho et al. APL 91, 123106 (2007). [4] F.J. Jedema et al., Nature 416, 713 (2002). [5] A. Fert et al., PRB64, 184420 (2001). [6] M. Shiraishi et al., Nature Nano. in submission.

Corresponding author: Masashi Shiraishi
E-mail: shiraishi@mp.es.osaka-u.ac.jp **Tel&Fax**: 06-6850-6426

MD Simulations for Mechanical Tearing of Graphene Sheets: Identification of Atomic Edge Configuration

○Takazumi Kawai[1], Susumu Okada[2,3], Yoshiyuki Miyamoto[1,3], and Hidefumi Hiura[1]

[1]*Nano Electronics Research Laboratories, NEC Corporation, 34 Miyukigaoka, Tsukuba 305-8501, Japan*
[2]*Institute of Physics and Center for Computational Science, University of Tsukuba, Tennodai, Tsukuba 305-8571, Japan*
[3]*CREST, Japan Science and Technology Agency, 4-1-8 Honcho, Kawaguchi, Saitama 332-0012, Japan*

Graphene attracts much attention due to its potential applications for nano-devices such as FET and device interconnection with higher mobility and robustness. For the thinner graphene the atomic structures at the edge could dramatically change the electronic properties of the device [1]. Thus the atomic structure of the graphene nano ribbons at the edge plays a very important role for various device applications. Recently, Li, et al succeeded mass production of graphene nano ribbons with width below 10 nm using chemomechanical breaking of the stably suspended graphene sheets [2]. They, however, have not been able to identify the atomic edge structures yet.

Here, we performed tight-binding molecular dynamics simulations for mechanical tearing of graphene sheets, which would correspond to the recent experimental conditions. When the graphene is torn along armchair direction, the atomically flat armchair edge appears. Meanwhile, the tearing along the zigzag direction results in a formation of zigzag edge for only an initial few steps. Then the initial zigzag edge structure is immediately followed by the armchair edge, and zigzag edge rarely appears again afterwards. We will explain the reason of selective formation of armchair edge for mechanical tearing of graphene sheets by local electronic structures at the tearing front.

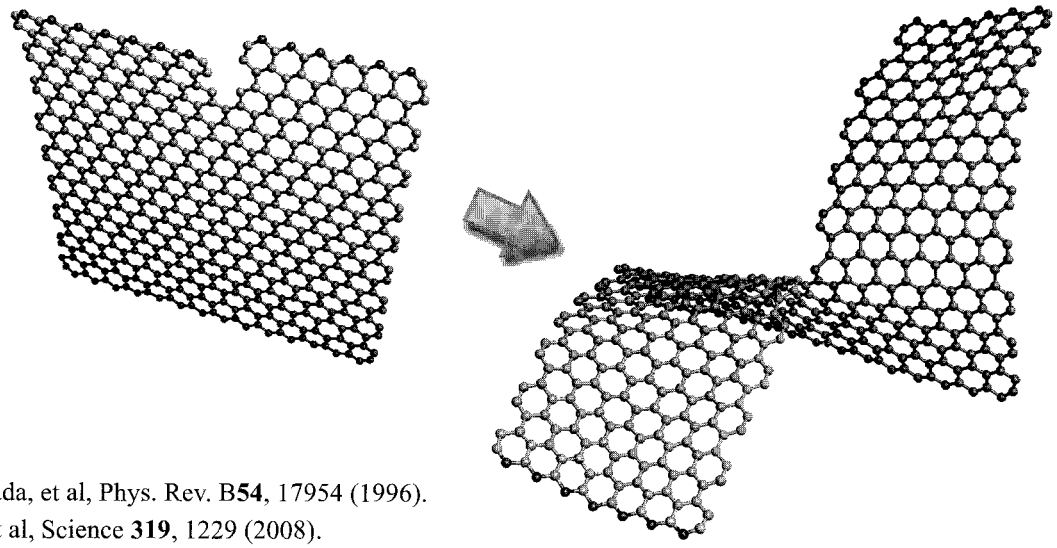

References

[1] K. Nakada, et al, Phys. Rev. B**54**, 17954 (1996).

[2] X. Li, et al, Science **319**, 1229 (2008).

Corresponding Author: Takazumi Kawai
E-mail: takazumi-kawai@mua.biglobe.ne.jp
Tel&Fax: 029-850-1554 (029-856-6136)

Synthesis, Photophysical Properties, and Ordered Supramolecular Structures of Liquid Crystalline Deca(organo)[60]Fullerenes

○ Chang-Zhi Li[1], Yutaka Matsuo[1], Eiichi Nakamura[1,2]

[1]*Nakamura Functional Carbon Cluster Project, ERATO, Japan Science and Technology Agency (JST), Hongo, Bunkyo-ku, Tokyo 113-0033, Japan*
[2]*Department of Chemistry, The University of Tokyo, Hongo, Bunkyo-ku, Tokyo 113-0033, Japan*

Fullerene liquid crystal (LC) materials with compact and orde r pa cking of fu llerene mo ieties a ttracted the interest of our g roup (columnar LC[1,2,3] a nd lamellar LC[4]), s ince the y a re pro mising s oft ma terials for organic electr onics application. Gener ally, s amples with c ovalent a ttachment of fu llerene mole cules to a mesomorphic pr omoter s uch as choles terols and dendrimers, d id no t result in the des ired pr operties in some cases, because of the bulky mesogenic group fail to yield well organization of fullerene moieties.

Buckyferrocene-caped deca(organo)[60]fullerene **1** (C_{12}) and **2** (C_{18}) (Figure 1a) obtained from three steps synthetic r oute. As shown in s ingle crystal structure of compound **1** (Figures 1b and 1c) , hoop -shaped π system is con structed, thr ough bottom and top detraction of 60 π el ectrons f or C_{60}. A tetr agonal cell unit consists of exceptionally large value of axes (a = b = 30. 6 Å, c = 68. 6 Å; α = β = γ = 90. 0 °). I n cr ystal packing, fulle rene moie ties tightly s tack toge ther to form a framework (F igure 1 d). C $_{12}$ alky l c hains suppose to be located in the inter vals of fullerene framework.

With furthe r inve stigation of pola rized optic al microscopy (POM), dif ferential s canning calor imetry (DSC) a nd p owder X -ray d iffraction (X RD), compounds **1** and **2** show thermally induced LC phase with a wide temperature range (Figure 2). Furthermore, these LC materials show luminescent and r edox active proprieties.

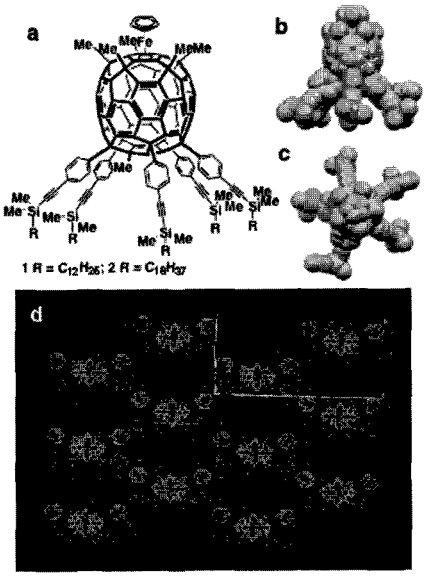

Figure 1 (a) Compound **1** a nd **2**; X-ray s tructure of **1**, (b) s ide vi ew and (c) t op vie w; (d) C rystal packing; C $_{12}$ ch ains ar e disordered and could not be located.

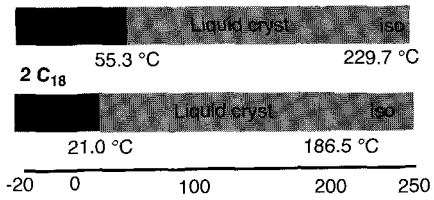

Figure 2 Phase transition behaviors.

[1] Sawamura, M. ; Kawai, K .; Ma tsuo, Y .; Kanie, K.; Kato, T .; N akamura, E. *Nature* **2002**, *419*, 702. [2] Matsuo, Y.; Muramatsu, A.; Hamasaki, R.; Mizoshita, N.; Kato, T.; Nakamura, E. *J. Am. Chem. Soc.* **2004**, *126*, 432. [3] Matsuo, Y.; Muramatsu, A.; Kamikawa, Y.; Kato, T.; Nakamura, E. *J. Am. Chem. Soc.* **2006**, *128*, 9586. [4] Zhong, Y-W.; Matsuo, Y.; Nakamura, E. *J. Am. Chem. Soc.* **2007**, *129*, 3052.

Corresponding Author: Yutaka Matsuo and Eiichi Nakamura
TEL/FAX: +81-3-5841-1476 E-mail: matsuo@chem.s.u-tokyo.ac.jp; nakamura@chem.s.u-tokyo.ac.jp

Radical Coupling Reaction of Paramagnetic Endohedral Metallofullerene La@C_{82}

○Yuta Takano,[1] Akinori Yomogida,[1] Hidefumi Nikawa,[1] Takatsugu Wakahara,[1] Takahiro Tsuchiya,[1] Midori O. Ishitsuka,[1] Yutaka Maeda,[2] Takeshi Akasaka,*[,1] Tatsuhisa Kato,[3] Zdenek Slanina,[1] Naomi Mizorogi,[4] and Shigeru Nagase[4]

[1]*Center for Tsukuba Advanced Research Alliance, University of Tsukuba, Tsukuba, Ibaraki 305-8577, Japan,*
[2]*Department of Chemistry, Tokyo Gakugei University, Koganei, Tokyo 184-8501, Japan,*
[3]*Department of Chemistry, Josai University, Sakado, Saitama 350-0295, Japan,*
[4]*Department of Theoretical and Computational Molecular Science, Institute for Molecular Science, Okazaki, Aichi 444-8585, Japan*

Endohedral metallofullerenes have attracted special attention because they engender new spherical molecules with unique electronic properties and structures that are unexpected for empty fullerenes.[1,2]

Recently, we have found that benzyl mono-adducts, La@$C_{82}(C_{2v})(CH_2C_6H_5)$ (**2a-2d**), are obtained by the radical coupling reaction in a toluene solution of La@$C_{82}(C_{2v})$. Thermolysis of 3-triphenylmethyl-5-oxazolidinone (**1**) may generate benzyl radical by hydrogen abstraction from toluene, which affords the radical coupling product with La@C_{82} (Scheme 1). The same mono-adducts are also obtained by photoirradiation of La@$C_{82}(C_{2v})$ in toluene in the absence of **1**. These reactions are applicable to other paramagnetic metallofullerenes, such as La@$C_{82}(C_s)$ and Ce@$C_{82}(C_{2v})$. Photoirradiation of La@$C_{82}(C_{2v})$ in 1,2-dichlorobenzene in the presence of α,α,2,4-tetrachlorotoluene (**4**) also affords the mono-adducts, La@$C_{82}(C_{2v})(CHClC_6H_3Cl_2)$ (**3a-3d**) (Scheme 2). These mono-adducts are fully characterized by spectroscopic analyses. Single-crystal X-ray structure analysis for **3d** reveals its unique structure. Theoretical calculation confirms that the cage carbons having high spin densities are selectively attacked by radical species to form the singly bonded mono-adducts linked by a carbon-carbon single bond.

Scheme 1.

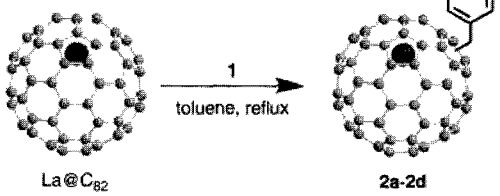

Scheme 2.

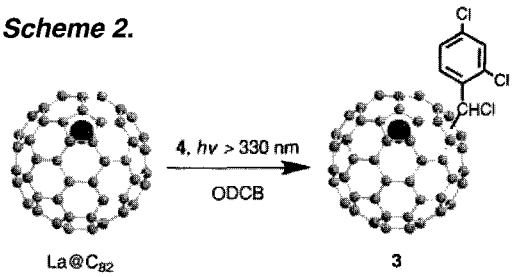

[1] *Endofullerenes: A New Family of Carbon Clusters*; Akasaka, T., Nagase, S., Eds.; Kluwer Academic Publisher: Dordrecht, 2002.

[2] Wilson, S.; Schuster, D.; Nuber, B.; Meier, M. S.; Maggini, M.; Prato, M.; Taylor, R. In *Fullerenes: Chemistry, Physics, and Technology*; Kadish, K. M., Ruoff, R. S., Eds. Wiley: New York, 2000; Chapter 3.3, pp 91-176.

Corresponding Author: Takeshi Akasaka
TEL & FAX: +81-29-853-6409, E-mail: akasaka@tara.tsukuba.ac.jp

ポスター発表
Poster Preview

1P – 1 ～ 1P – 52
2P – 1 ～ 2P – 52
3P – 1 ～ 3P – 50

Aziridination of C_{60} with Simple Amides and Catalytic Rearrangement of the Aziridinofullerenes to Azafulleroids

Ryoji Tsuruoka, ○Toshiki Nagamachi and Satoshi Minakata

Department of Applied Chemistry, Graduate School of Engineering, Osaka University, Suita, Osaka 565-0871, Japan

The development of a basic and facile method for the functionalization of C_{60} remains an important challenge because of recent demands for carbon nanomaterials. Recently, our group reported a new method for the ionic aziridination of C_{60} using chloramine-T (CT) as a readily available N_1 source, giving predominantly *N*-tosylated aziridinofullerene with high selectivity, and the unique rearrangement of the aziridinofullerene to azafulleroid using the combination of a catalytic amount of chloramines and MS4A. [1] The method, however, essentially requires the use of chloramine salts, some of which are not stable to be isolated.

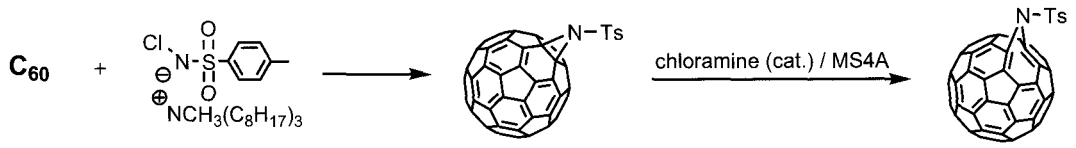

In order to expand the generality of the reaction, we report a new type of selective aziridination of C_{60} with a variety of simple amides, many of which are either commercially available or readily prepared from either corresponding acid, alcohols or amines. The method is based on the chlorination of amine derivatives followed by the reaction with C_{60} in the presence of a base.

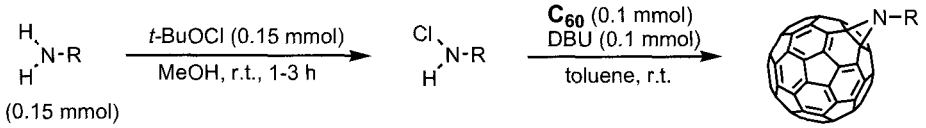

(0.15 mmol)

R = Cbz, Boc, $CONMe_2$, $POPh_3$, etc.

Moreover, catalytic rearrangement of the resulting aziridinofullerenes to azafulleroids by a chloramine salt and MS4A system was investigated. For example, an aziridinofullerene derived from a urea derivative was smoothly rearranged to the corresponding azafulleroid in good yield.

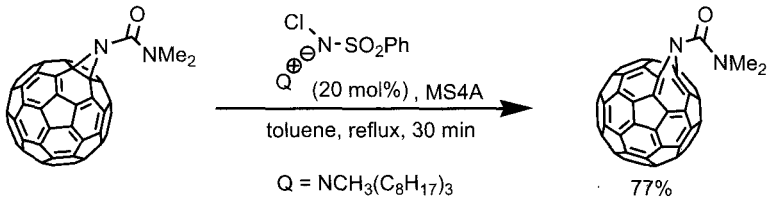

[1] S. Minakata, R. Tsuruoka, T. Nagamachi, M. Komatsu, *Chem. Commun.*, 323 (2008).

Corresponding Author: Satoshi Minakata
TEL: +81-6-6879-7403, FAX: +81-6-6879-7402, E-mail: minakata@chem.eng.osaka-u.ac.jp

Effects of various additives on reaction products of solid-state oxygenation of fullerene C_{60} via mechanochemical route

○Yuichi Ishiyama[1,2], Yusuke Tajima[2], Mamoru Senna[2,3], and Hiroto Watanabe[2,4]

[1]*Department of Applied Chemistry, Faculty of Science and Technology, Keio University, 3-14-1, Hiyoshi, Kohoku-ku, Yokohama, 223-8522, Japan*
[2]*Nano-Integration Materials Research Unit, RIKEN, 2-1, Hirosawa, Wako 351-0198, Japan*
[3]*Technofarm AXESZ Co. Ltd, 3-14-1, Chofu 182-0035, Japan*
[4]*Tokyo metropolitan Industrial technology Research Institute, 3-13-10, Nishigaoka, Kita-ku, Tokyo, 115-8586, Japan*

We recently reported fullerene oxygenation in a solid state under mechanical stressing [1]. Products contained fullerene oxides, $C_{60}O_n$, in the forms of epoxide and carbonyl, and of oxidative polymers of fullerene in a significant amount as well, presumably via [1,2].

In this study we examine the outcome of reactions by varying species and quantity of oxidant or antioxidant additives, in order to further elucidate the reaction mechanisms in an attempt to increase the yield of isolable epoxides.

Following additives were chosen: *m*-chloroperbenzoic acid (*m*-CPBA) as an oxidant, and 2,6-di-*tert*-butyl-*p*-cresol (BHT) or 2,6-di-*tert*-butyl-*p*-benzoquinone (BQ) as radical quenchers. After admixing with C_{60} powders, the mixture was mechanically activated by a single-ball vibration mill for 1 hour under oxygen atmosphere. We also carried out oxygenating fullerene via a conventional chemical route by using *m*-CPBA for comparison. The reaction products were separated from toluene-insoluble composition, and the soluble portions were subjected to the isomer assay by LC-APPI-MS.

It is generally recognized that preferential oxygenation on fullerene core occurs in the vicinity of the oxygen-bound benzenoid rings[3]. We observed the close similarity between the *m*-CPBA oxidation products via chemical and mechanochemical routes. In mechanochemical oxygenation, the addition of *m*-CPBA resulted in a significant increase in the toluene-soluble poly-epoxides, while suppressing fullerene polymerization. With BHT or BQ, both fullerene oxygenation and polymerization were inhibited efficiently.

Based on these experimental results, we further elucidate working mechanisms of mechanochemical oxygenation of fullerene, and discuss our scheme to increase the yield of non-polymerized epoxides.

[1]Watanabe, H., Matsui, E., Ishiyama, Y., Senna, M., *Tetrahedron Lett.*, **48**, 8132-8137, (2007)

[2]Watanabe, H., Ishiyama, Y., Tajima, Y., Senna, M., Abstracts of the 32nd Fullerene-Nanotubes General Symposium, p.120, (2007)

[3]Tajima, Y., Takeuchi, K., *J. Org. Chem.*, **67**, 1696-1698, (2002)

Corresponding Author : Yusuke Tajima

TEL: +81-48-467-9309, **Fax** : +81-48-462-4702, **E-mail** : tajima@riken.jp

Electrochemical Properties of Indolino[2',3':1,2][60]fullerenes

○Youhei Numata,[1] Jun-ichi Kawashima,[1,2] Yusuke Tajima[1,2]

[1]*Nano-Integration Material Research Unit, RIKEN, 2-1 Hirosawa 351-0198*
[2]*Graduate School of Science and Engineering, Saitama University, 255 Shimo-ohkubo 338-8570*

Previously, we developed regioselective substitutions of epoxide groups on fullerene cage to prepare functionalized fullerenes in good yield from $C_{60}O_n$ (n = 1, 2). [1,2] Applying this strategy, we synthesized indolino[2',3':1,2][60]fullerene derivatives (Figure 1) by reaction of $C_{60}O$ with aromatic amines in the presence of Lewis acid compound. [3]

We measured their electrochemical properties by cyclic voltammetry (CV) and differential pulse voltammetry (DPV). All indolino[60]fullerene derivatives demonstrated well-defined reversible redox waves. The first reduction potentials, E^1_{red} of indolino[60]fullerene derivatives were ranging from –1.090 to –1.189 V. This result indicates that we can vary their electrochemical properties by the change of the substituent. To elucidate the influence of the substituent on their E^1_{red} values, we plotted the E^1_{red} vs Hammett constant, σ_m of the substituent on the indoline moiety.

In Figure 2, the E^1_{red} vs σ_m plot is presented. This plot exhibited good linearity between the E^1_{red} and the σ_m. From this result, we expected that the electron-donating and withdrawing properties of substituents influenced their E^1_{red} values *via* the through bond interaction. Interestingly, 4'-MeO substituted derivatives demonstrated quite lower E^1_{red} values compared with other analogues (4',6'-di-MeO: –1.175 V, 4'-MeO-7'-Me: –1.189 V). We hypothesized that the MeO group on the 4'- position influenced the electronic structure of fullerene cage *via* the through space interaction. In the symposium, we will discuss about substituent effect of the indolino[60]fullerene derivatives on their electrochemical properties from both the experimental and theoretical aspects.

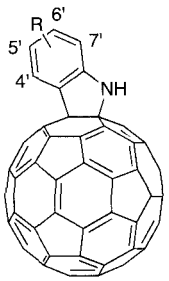

Figure 1. Chemical structure of indolino[60]fullerene

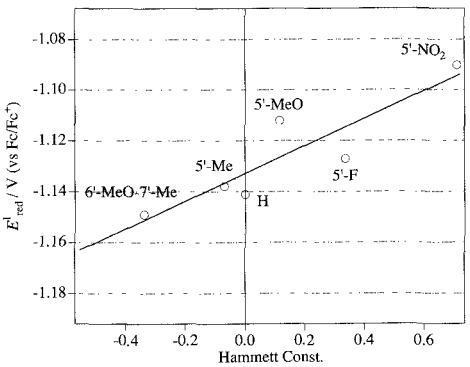

Figure 2. E^1_{red} vs σ_m of indolino[60]fullerenes

References:

[1] Y. Shigemitsu, M. Kaneko, Y. Tajima, K. Takeuchi, *Chem. Lett.* **2004**, *33*, 1604.

[2] Y. Tajima, T. Hara, T. Honma, S. Matsumoto, K. Takeuchi, *Org. Lett.* **2006**, *8*, 3202.

[3] J. Kawashima et al., *The 33rd Fullerene-Nanotubes General Symposium*, **2007** (Fukuoka), 2P-6.

Corresponding Author: Yusuke Tajima

E-mail: tajima@riken.jp

Tel: (+81)48-467-9309, **Fax:** (+81)48-462-4702

Formation of Benzo[*b*]furano[60]fullerene from [60]Fullerene Monoepoxide

○Junichi Kawashima[1,2], Youhei Numata[1], Yusuke Tajima[1,2]

[1]*Nano-Integration Materials Research Unit, RIKEN, Wako, 351-0198*
[2]*Department of Chemical Engineering, Saitama University, Saitama, 338-8570*

We previously reported various types of nucleophilic substitution of fullerene epoxide under acid condition [1-3]. Recently, we found that the reaction of $C_{60}O$ (**1**) with phenols in the presence of Montmorillonite K10 clay as conventional acid component, afforded benzo[*b*]furano[60]fullerene derivatives (**4**) with 1,2-dihydroxyfullerene (**2**) and 1-hydroxy-2-phenoxyfullerene (**3**). To investigate the mechanism of this reaction, we have examined the products formed by the reaction of **1** with phenols under varying acid components.

Reactions in the presence of boron trifluoride (Lewis acid) provided **4** as well, and *β*-phenoxyalcohols **3** was also formed during the initial stage of the reaction. Even in the presence of Amberlyst 15 (Brønsted acid), **4** was formed as main product, **2** and **3** were detected as initial products. Among these products, it was confirmed that the reaction of isolated **2** with phenol did not give **3** and **4** under any acid components. Consequently the formation of **4** is expected to proceed *via* cyclization of intermediate **3** in the same way as our previous report [3].

In general, the reactions of ordinary epoxide groups with phenols under acid condition result in the formation of *β*-phenoxyalcohols as final product [4]. To the best of our knowledge, there is no example of the formation of benzofuran moiety *via* cyclization of *β*-phenoxyalcohol. We will present the efficient formation of benzo[*b*]furano[60]fullerene and discuss about this unusual cyclization mechanism in detail.

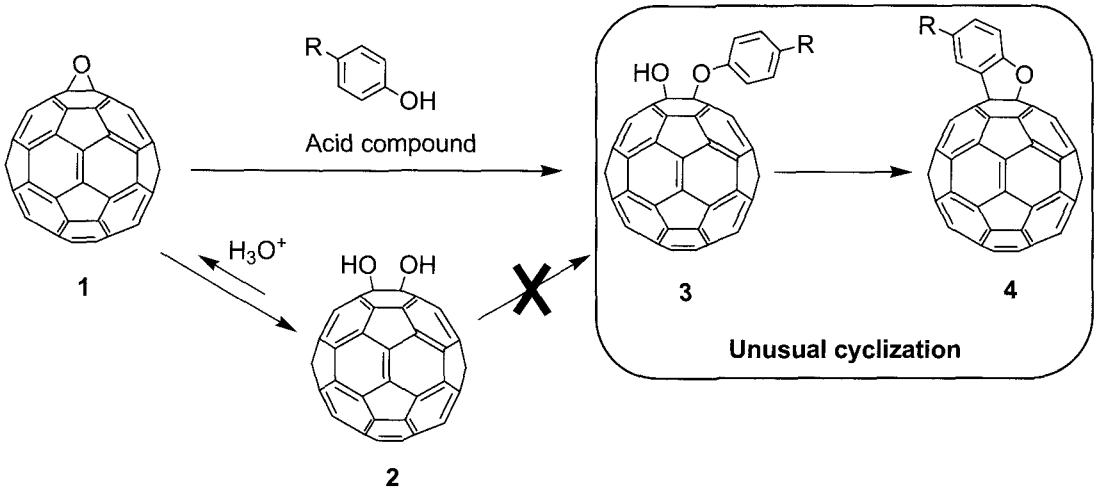

[1] Y. Shigemitsu, M. Kaneko, Y. Tajima, K. Takeuchi, *Chem. Lett.*, **2004**, *33*(12), 1604-1605.
[2] Y. Tajima, T. Hara, T. Honma, K. Takeuchi, *Org. Lett.*, **2006**, *8*(15), 3203-3205.
[3] J. Kawashima, T. Hara, T. Matsuura, Y. Numata, Y. Tajima, The 33rd F-NT General Symposium 2P-6 (2007).
[4] D. B. G. Williams, M. Lawton, *Org. Biomol. Chem.*, **2005**, *3*, 3269-3272.
Corresponding Author: Yusuke Tajima
TEL: +81-48-467-9309, FAX: +81-48-462-4702, E-mail: tajima@riken.jp

Electron Spin Properties for La@C_{82} in Solid Empty Fullerene Matrices

○Yasuhiro Ito[1], Jamie H. Warner[1], Mujtaba Zaka[1], Takayuki Aono[2], Noriko Izumi[2]
Haruya Okimoto[2], John J. L. Morton[1,3], Hisanori Shinohara[2] and G. Andrew D. Briggs[1]
[1]*Centered Department of Materials, Quantum Information Processing Interdisciplinary Research Collaboration, University of Oxford, Oxford, OX1 3PH, United Kingdom.*
[2]*Department of Chemistry and Institute for Advanced Research, Nagoya University, Furo-Cho, Chikusa-ku, Nagoya, 464-8602, Japan.*
[3]*Clarendon Laboratory, Department of Physics, University of Oxford, Oxford, OX1 3PU, United Kingdom.*

Mono-metallofullenes M@C_{82} have unique electronic and magnetic properties. The magnetic properties of La@C_{82} in solution have been investigated by electron spin resonance (ESR) and show a radical electron on the C_{82} cage identified by its hyperfine interaction with the nuclear spin I = 7/2 of ^{139}La.[1)] The magnetic properties of solid La@C_{82} have also been studied using ESR and SQUID.[2)] However, its hyperfine structure (hfs) has not be reported due to the presence of the exchange and spin-spin interaction between La@C_{82} molecules. Recently, ESR of La@C_{82} in dispersed in a solid C_{60} matrix was investigated and hfs was observed.[3)] However, the purity of La@C_{82} which was used in this report appears to be low since the ESR signature of solid La@C_{82} remains. This suggests that the interfullerene interaction between La@C_{82} and C_{60} has not been understood.

Here, we report the concentration dependences of the electron spin properties of La@C_{82} in solid empty fullerene matrices. The interfullerene interaction is controlled by changing the concentration of La@C_{82} or the molecular size of the empty fullerenes. Furthermore, we discuss the effects of empty fullerenes on the hfs of La@C_{82}.

Figure 1 shows the ESR spectra of La@C_{82} in solid C_{60} and C_{70} matrices. The concentration dependence of the hfs of La@C_{82} was very different in C_{60} and C_{70} matrices. The hfs for 0.5 % in C_{60} was almost same as that for 0.1 % in C_{70}, which indicates that C_{70} disperses La@C_{82} better than C_{60}. The hfs in C_{70} changed slightly from 1 % to 0.1 %. This suggests that La@C_{82} is not dispersed completely for 1 % in C_{70}. Furthermore, the linewidth of the hfs for 0.1 % in C_{60} was broader than that of 1 % in C_{70}, indicating rotational motion of C_{60} molecule affects the electron spin properties of La@C_{82}.

In the symposium, we will also discuss the ESR properties of La@C_{82} in higher empty fullerene matrices, and low temperature ESR measurements.

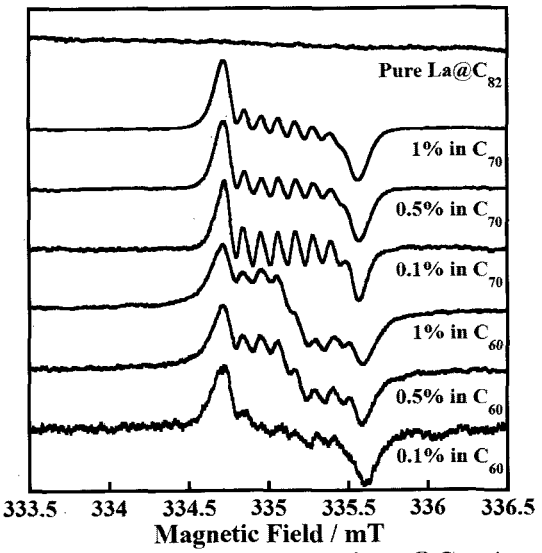

Figure 1 ESR spectra of La@C_{82} in solid C_{60} and C_{70} matrices at room temperature. Microwave frequency and power are 9.33 GHz and 0.2 mW, respectively.

References

1) R. D. Johnson, M. S. Devries, J. Salem, D. S. Bethune, C. S. Yannoni, *Nature* **355**, 239 (1992).
2) C. J. Nuttall, Y. Inada, K. Nagai and Y. Iwasa, *Phys. Rev.* B **62**, 8592 (2000).
3) P. Jakes, A. Gembus, K. P. Dinse and K. Hata, *J. Chem. Phys.* **128**, 52306 (2008).

Corresponding Author: Yasuhiro Ito
TEL: +44-1865-273790, **FAX**: +44-1865-273789, **E-mail**: yasuhiro.ito@materials.ox.ac.uk

1P-6

Ultraviolet Photoelectron Spectroscopy of $M_2@C_{80}$ (M=La, Ce, Lu, LuC)

○Takafumi Miyazaki[1], Yuusuke Aoki[1], Youji Tokumoto[1], Ryohei Sumii[2], Haruya Okimoto[3], Hisashi Umemoto[3], Masahiko Akachi[3], Yasuhiro Ito[3], Hisanori Shinohara[3], Shojun Hino[1]

[1] *Graduate School of Science & Technology, Ehime University*
[2] *Institute for Molecular Science*
[3] *Graduate School of Science, Nagoya University*

The valence band electronic structure of C_{80} endohedral fullerenes containing lanthanides was studied by ultraviolet photoelectron spectroscopy.

Figure 1 shows the ultraviolet photoelectron spectra (UPS) of $M_2@C_{80}$ (M=La, Ce, Lu, LuC) obtained by hν = 40eV irradiation. Their spectral onsets are 0.75 eV ($La_2@C_{80}$), 0.83 eV ($Ce_2@C_{80}$), 0.59 eV ($Lu_2@C_{80}$), 0.71 eV ($Lu_2C_2@C_{80}$), which are slightly smaller than that of empty C_{80}, (0.94 eV obtained with hν = 60eV irradiation, not shown in the figure). As for the upper valence band region (0 – 4 eV), the UPS can be classified into two categories; i) $La_2@C_{80}$ and $Ce_2@C_{80}$, ii) $Lu_2@C_{80}$ and $Lu_2C_2@C_{80}$, each group has the spectral similarity but there is few correspondence between the groups. This could be due to the difference in their symmetry: $Ce_2@C_{80}$ and $La_2@C_{80}$ have I_h cage structure, while $Lu_2@C_{80}$ and $Lu_2C_2@C_{80}$ have C_{2v} cage structure. Again this is another evidence that the cage structure dominates the electronic structure derived from π-electrons.

Two structures are observed at around 9.5 eV and 11.0 eV in the UPS of $Lu_2@C_{82}$ and $Lu_2C_2@C_{82}$, which are derived from Lu 4f electrons. Peak positions of these two peaks deviate slightly; those of $Lu_2@C_{82}$ are deeper than $Lu_2C_2@C_{82}$ by 0.1-0.2 eV. This difference may be attributed to the difference in the amounts of transferred electrons from entrapped atoms to the carbon atoms.

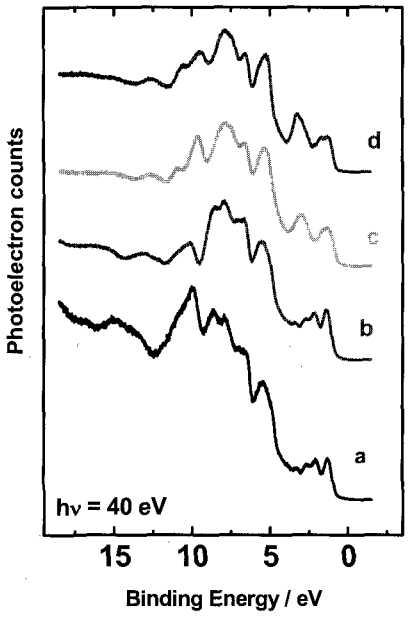

Figure 1 UPS of (a) $La_2@C_{80}$, (b) $Ce_2@C_{80}$, (c) $Lu_2@C_{80}$ and (d) $(LuC)_2@C_{80}$

Corresponding Author : S. Hino,
E-mail: hino@eng.ehime-u.ac.jp, phone: 089-927-9924

1P-7

Synthesis and Characterization of a Carbene Derivative of Sc_2C_{82}

○Hiroki Kurihara[1], Yuko Yamazaki[1], Midori O. Ishitsuka[1], Takahiro Tsuchiya[1], Takeshi Akasaka[1], Nomi Mizorogi[2] and Shigeru Nagase[2]

[1]*Center for Tsukuba Advanced Research Alliance, University of Tsukuba, Tsukuba, Ibaraki 305-8577, Japan*
[2]*Department of Theoretical and Computational Molecular Science, Institute for Molecular Science, Okazaki, Aichi 444-8585, Japan*

Endohedral metallofullerenes encapsulate one or more metal atoms inside a hollow fullerene cage.[1] These fullerenes have attracted special interest as new spherical molecules with unique properties that are not found in empty fullerenes.

Recently, we have found that the addi tion of ada mantylidene (Ad:) to La@C_{82} regioselectively proceeds to afford the mono-adducts.[2] The selectivity of the addition reaction is very important for further applications of endohedral metallofullerenes.

On the other hands, scandium metallofullerene attracts special interest as the high varie ty of fullerene size and encap sulated structures, Sc, Sc_2, Sc_2C_2, Sc_3C_2, Sc_3N and so on. Although Sc_2C_{82} is one of abundant metallofullerene, its structure isn't revealed because of the very low solubility precludes ^{13}C NMR measurement.[3]

In this context, we report here the synthesis and its characterization of Sc_2C_{82}(Ad) by means of spectroscopic analysis, redox property and theoretical calculation.

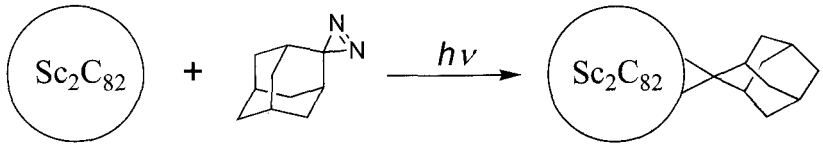

References

[1] Endofullerenes: A New Family of Carbon Clusters; *Akasaka, T., Nagase, S.; Eds.; Kluwer: Dordrecht,* ***2002.***

[2] Maeda, Y. *et al. J. Am. Chem. Soc.* **2004**, *126*, 6858.

[2] Wang, C. *et al. Chem. Phys. Lett.* **1999**, *300*, 379.

Corresponding author: Takeshi Akasaka
Tel & Fax: +81-298-53-6409
E-mail: akasaka@tara.tsukuba.ac.jp

Endohedral Metallofullerene Derivative: La@C_{82}($C_6H_3Cl_2$)

○Hidenori Kuga[1], Hidefumi Nikawa[1], Takahiro Tsuchiya[1], Midori O. Ishitsuka[1], Zdenek Slanina[1], Takeshi Akasaka[1]*, Naomi Mizorogi[2], Shigeru Nagase[2]

[1]*Center for Tsukuba Advanced Research Alliance, University of Tsukuba, Tsukuba, Ibaraki 305-8577, Japan,*
[2]*Department of Theoretical and Computational Molecular Science, Institute for Molecular Science, Okazaki, Aichi 444-8585, Japan*

Endohedral metallofullerenes have attracted special interest because of the unique structure and properties that are unexpected for empty fullerenes.[1,2] Since Smalley and co-workers reported in 1991 that lanthanum metallofullerenes were produced abundantly in the soot, but only La@C_{82} was extracted with toluene,[3] the chemistry of soluble endohedral metallofullerenes has started and up to now, many soluble endohedral metallofullerenes have been isolated and characterized.[1,2,4-8] On the contrary, insoluble endohedral metallofullerenes such as La@C_{60}, La@C_{70}, La@C_{72}, La@C_{74} and so forth have not yet been isolated, although they are regularly observed in the raw soot by mass spectrometry. Recently, we have reported the preparation and characterization of La@C_{72} and La@C_{74} derivatives, La@C_{72}($C_6H_3Cl_2$)[9] and La@C_{74}($C_6H_3Cl_2$).[10] In this context, we herein report the isolation and characterization of La@C_{82}($C_6H_3Cl_2$) .

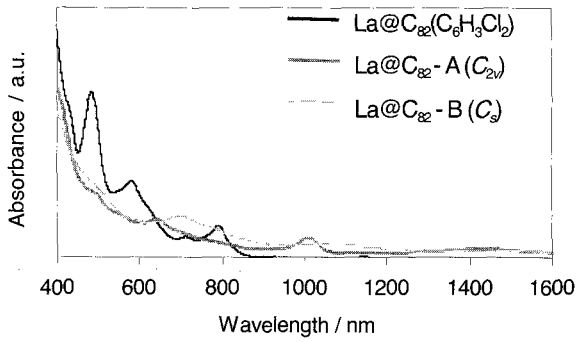

Figure.
Vis-NIR spectra of La@C_{82} derivative and tow La@C_{82} isomers.

References:

[1] *Endofullerenes: A New Family of Carbon Clusters*; Akasaka, T., Nagase, S., Eds.; Kluwer Academic Publisher: Dordrecht, The Netherlands, **2002**; pp 1. [2] Wilson, S.; Schuster, D.; Nuber, B.; Meier, M. S.; Maggini, M.; Prato, M.; Taylor, R. In *Fullerenes: Chemistry, Physics, and Technology*; Kadish, K. M., Ruoff, R. S., Eds.; Wiley: New York, **2000**; Chapter 3, pp 91. [3] Smalley, R. E. et al. *J. Phys. Chem.* **1991**, *95*, 7564. [4] Bethune, D. S. et al. *Nature* **1993**, *366*, 123. [5] Nagase, S.; Kobayashi, K.; Akasaka, T. *Bull. Chem. Soc. Jpn.* **1996**, *69*, 2131. [6] Nagase, S.; Kobayashi, K.; Akasaka, T. *J. Comput. Chem.* **1998**, *19*, 232. [7] Nagase, S.; Kobayashi, K.; Akasaka, T.; Wakahara, T. In *Fullerenes: Chemistry, Physics and Technology*; Kadish, K., Ruoff, R. S., Eds.; Wiley: New York, **2000**; Chapter 9, pp 395. [8] Akasaka, T. et al. *J. Am. Chem. Soc.* **2000**, *122*, 9316. [9] Wakahara, T. et al. *J. Am. Chem. Soc.* **2006**, *128*, 14228. [10] Nikawa, H. et al. *J. Am. Chem. Soc.* **2005**, *127*, 9684.

Corresponding Author: Takeshi Akasaka
Tel & Fax: +81-29-853-6409
E-mail: akasaka@tara.tsukuba.ac.jp

1P-9

Preparation and Characterization of A Carbene Derivative of $Sc@C_{82}$

○Makoto Hachiya[1], Yuko Yamazaki[1], Midori O. Ishitsuka[1], Takahiro Tsuchiya[1], Takeshi Akasaka*[,1], Naomi Mizorogi[2], Shigeru Nagase[2]

[1]*Center for Tsukuba Advanced Research Alliance, University of Tsukuba,* [2]*Department of Theoretical and Computational Molecular Science, Institute for Molecular Science*

Since the first success in the extraction of endohedral metallofullerenes in 1991, $M@C_{82}$ (M = Sc, Y, La and other lanthanide elements) has been most widely investigated as a prototype of mono-metallofullerenes [1]. For example, the structure and electronic property of $La@C_{82}$ have been revealed by theoretical calculations and various experimental methods such as ^{13}C NMR and X-ray powder diffraction studies and X-ray single-crystal structure analysis. Meanwhile, the structure of $Sc@C_{82}$ has been reported by X-ray powder diffraction study [2], however, its electronic property and chemical reactivity have not so far been clarified.

Because of the paramagnetic nature, it is difficult to determine the structure of $Sc@C_{82}$ by ^{13}C NMR measurement. We have developed a new method to determine the structures of a series of paramagnetic mono-metallofullerenes by ^{13}C NMR measurements in their anionic form [3]. Herein we report the structural determination of $Sc@C_{82}$ by using this method. Electronic property and chemical reactivity of $Sc@C_{82}$ were also investigated. We successfully synthesized adamantylidene derivative of $Sc@C_{82}$ for single crystal X-ray analysis, which was characterized by MALDI-TOF mass, vis-NIR absorption, CV and ^{13}C NMR measurement.

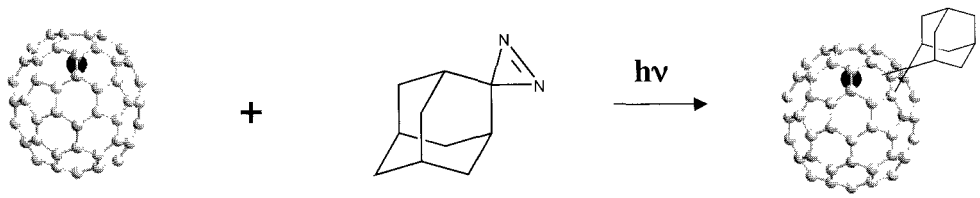

$Sc@C_{82}$ **adamantanediazirine** **$Sc@C_{82}$(Ad)**

References

[1] *Endofullerenes: A New Family of Carbon Clusters;* Akasaka, T., Nagase, S., Eds.; Kluwer: Dordrecht, 2002.

[2] Nishibori, E. et al. *Chem. Phys. Lett.* **1998**, *298*, 79.

[3] Akasaka, T. et al. *J. Am. Chem. Soc.* **2000**, *122*, 9316.

Corresponding Author: Takeshi Akasaka
TEL&FAX: +81-29-853-6409, E-mail: akasaka@tara.tsukuba.ac.jp

1P-10

Thermal reaction of $La_2@C_{80}$ with silacyclopropane

○ Mari Minowa[1], Michio Yamada[1], Masahiro Kako[2], Takahiro Tsuchiya[1], Midori O. Ishitsuka[1], Takeshi Akasaka[1]

[1]*Center for Tsukuba Advanced Research Alliance, University of Tsukuba, Tsukuba, Ibaraki 305-8577, Japan*
[2]*Department of Applied Physics and Chemistry, The University of Electro-Communications, Chofu, Tokyo 182-8585, Japan*

Since the discovery of endohedral metallofullerene $La@C_{82}$ in 1991,[1] many kinds of endohedral metallofullerenes have been prepared and isolated.[2] It is well known that endohedral metallofullerenes have relatively low redox potentials compared with hollow fullerenes, due to significant electron transfer from the encapsulated metal atom to the carbon cage.

The reaction of endohedral metallofullerenes with an electron-donating molecule has been studied with special interests because of the electronic properties of endohedral metallofullerenes. Meanwhile, it is known that organosilicon compounds including a Si—Si bond or an activated Si—C bond serve as good electron-donors. In this context, it can be expected that combination of organosilicon compounds and endohedral metallofullerenes form a new class of fullerene-organosilicon hybrid. However, the reaction of endohedral metallofullerenes with organosilicon compounds has been limited to bissilylation so far.[3]

Herein we report for the first time thermal reaction of $La_2@C_{80}$ with silacyclopropane.

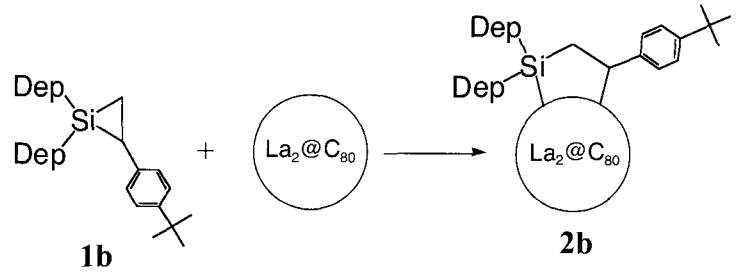

1b **2b**

Dep = 2,6-diethylphenyl

1) Chai, Y. et al. *J. Phys. Chem.* **1991**, *95*, 7564–7568.

2) *Endofullerenes: A New Family of Carbon Clusters*; Akasaka, T., Nagase, S., Eds.; Kluwer, Dordrecht, the Netherlands, 2002.

3) a) Akasaka, T. et al. *Nature* **1995**, *374*, 600–601, b) Yamada, M. et al. *J. Phys. Chem. B.*, **2005**, *109*, 6049–6051. c) Iiduka, Y. et al. *J. Am. Chem. Soc.*, **2005**, *127*, 9956–9957. d) Yamada, M. et al. *J. Am. Chem. Soc.*, **2005**, *127*, 14570–14571. e) Wakahara, T. et al. *J. Am. Chem. Soc.*, **2006**, *128*, 9919–9925. f) Wakahara, T. et al. *Chem. Commun.*, **2007**, 2680–2682.

Corresponding Author: Takeshi Akasaka
E-mail: akasaka@tara.tsukuba.ac.jp
Tel& Fax: +81-29-853-6409

Fabrication and characteristics of C_{60} thin film FETs with conducting polymer electrodes

Yumiko Kaji,[1] Naoko Kawasaki,[1] ○Yoshihiro Kubozono[1] and Akihiko Fujiwara[2]

[1]*Research Laboratory for Surface Science, Okayama University, Okayama 700-8530, Japan*
[2]*Japan Advanced Institute of Science and Technology, Ishikawa 923-1292, Japan*

Organic field-effect transistors (FETs) attract broad interest because of possible applications toward next-generation electronics since the organic FETs have many advantages such as mechanical flexibility, large-area coverage, low-cost/low-temperature process. Promising materials for active layers in organic FETs are C_{60} for *n*-channel operation and pentacene for *p*-channel operation, since these materials provide high filed-effect mobility, □, of ~1 $cm^2 V^{-1} s^{-1}$ [1,2]. Currently, regardless of an expectation to flexible FET, most of organic FETs are fabricated with metal electrodes such as Au and Pt. For a realization of complete mechanical flexibility, we require all plastic organic FETs.

In this study, we have fabricated C_{60} FETs with conducting polymer electrodes on Si/SiO_2 and poly(ethylene terephthalate) (PET)/Cytop™ substrates. Poly(3,4ethylenedioxythiophene):poly-(styrenesulfonate) (PEDOT:PSS) and doped polyaniline were used as conducting polymers and the source/drain electrodes were fabricated by an ink-jet printing technique on Si/SiO_2 and PET/Cytop™ substrates in bottom-contact structure; for PET substrate the conducting polymer was also used as gate electrode, while for Si substrate the heavily doped Si was used as gate electrode. The C_{60} thin film FETs with conducting polymers show *n*-channel enhancement-type characteristics with the high □ values of 0.2 - 0.3 $cm^2 V^{-1} s^{-1}$ and high on-off ratio of $> 10^6$. Typical output and transfer curves are shown in Fig. 1. These values are comparable to those in C_{60} FETs with Au electrodes [1,2], showing smooth carrier injections between conducting polymer electrodes and C_{60} thin films. Thus, it has been found that conducting polymer electrodes are available in a fabrication of flexible C_{60} FET exhibiting high-performance.

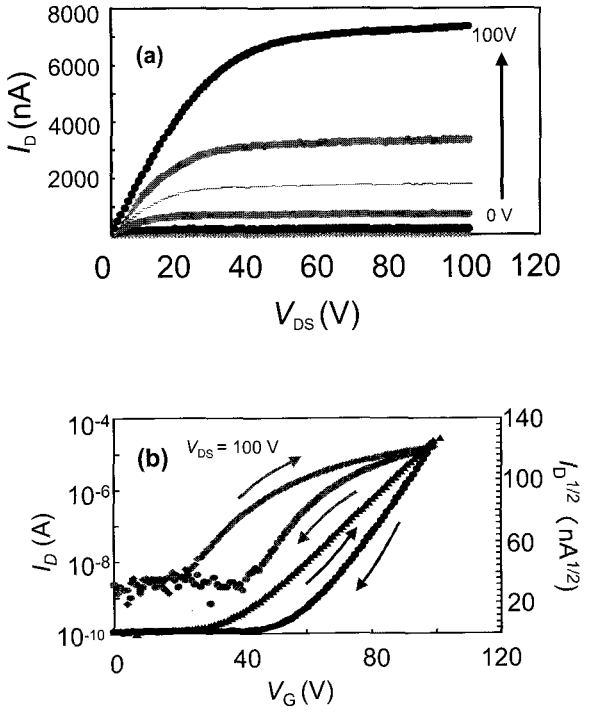

Fig. 1. (a) Output and (b) transfer curves of C_{60} FET with PEDOT:PSS electrodes on Si/SiO_2.

[1] S. Kobayashi *et al.*, Appl. Phys. Lett., 82, 4581 (2003).

[2] Y.-Y. Lin *et al.*, IEEE Electron Device Lett. 18, 606 (1997).

Corresponding Author: Yoshihiro Kubozono
E-mail: kubozono@cc.okayama-u.ac.jp
Tel&Fax: +81-86-251-7850/+81-86-251-7903

Vibrational Spectroscopy of an Electron-beam-irradiated C_{60} Film

○Toshiaki Nishii[1], Akito Takashima[2], Sou Ryuzaki[2], Toshihiro Kai[2], and Jun Onoe[2,3]

[1]*J-Power, Chigasaki, Kanagawa 253-0041, Japan*
[2]*Department of Nuclear Engineering, Tokyo Institute of Technology, Tokyo 152-8550, Japan*
[3]*Research Laboratory for Nuclear Reactors, Tokyo Institute of Technology, Tokyo 152-8550, Japan*

An electron-beam (EB) irradiated C_{60} film has been studied by means of *in situ* infrared (IR) and *ex situ* Raman spectroscopy. The time evolution of IR spectra (Fig. 1) shows that the peaks due to pristine C_{60} disappeared and a new intensive peak appeared around 1340 cm^{-1} after 25-h irradiation with the EB of 3 kV. According to the DFT calculations [1], only two C_{120} isomers, which are called P16 and P20 derived from the Stone-Wales rearrangements, have a corresponding peak at around 1340 cm^{-1}. On the other hand, Raman spectra of the same film after 25-h irradiation (Fig. 2) show that a broad peak at around 270 cm^{-1} appeared more intensively than the $A_g(1)$ peak of 493 cm^{-1} originating from the pristine C_{60} molecule [2]. The peak at around 270 cm^{-1} is slightly red-shifted compared to the $H_g(1)$ peak of pristine C_{60} molecules. This shift suggests vibrational softening by C_{60} polymerization. Recently, we have found the polymer to be a one-dimensional (1D) metallic C_{60} polymer by *in situ* high-resolution photoelectron spectroscopy [3], and to exhibit the Peierls transition at around 50 K, which is a typical phenomenon of 1D metal, by femtosecond-resolved pump-probe spectroscopy [4]. Assuming that the peak at around 270 cm^{-1} could be regarded as the radial breathing modes of single-walled carbon nanotubes, we estimated the average tube diameter of the present peanut-shaped C_{60} polymer to be about 0.9 nm.

[1] T. A. Beu and J. Onoe, *Phys. Rev. B*, **74**, 195426 (2006). [2] Z.-H. Dong, P. Zhou, J. M. Holden and P. C. Eklund, *Phys. Rev. B*, **48**, 2862 (1993). [3] T. Ito, J. Onoe, and S. Kimura, unpublished data. [4] Y. Toda, S. Ryuzaki, and J. Onoe, *Appl. Phys. Lett.*, **92**, 094102 (2008).

Corresponding Author: Jun Onoe TEL & FAX: +81-3-5734-3073, E-mail: jonoe@nr.titech.ac.jp

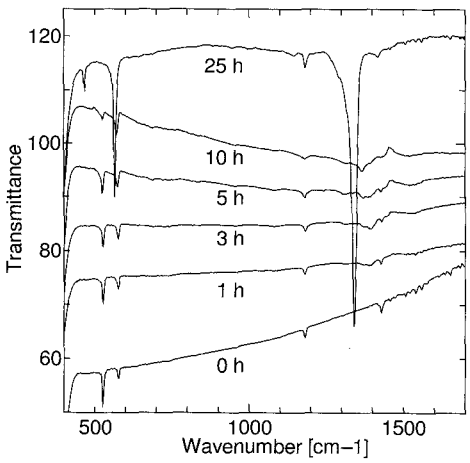

Fig. 1. *In situ* IR spectra of a C_{60} film with EB irradiation of 3 kV.

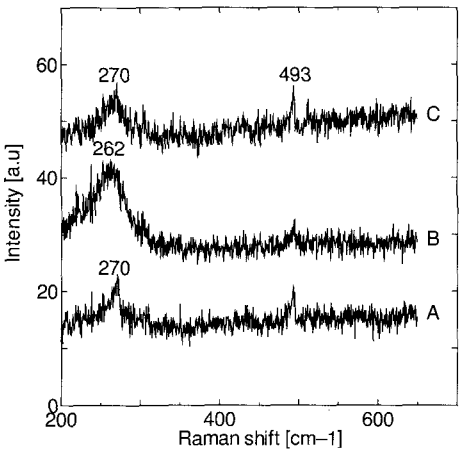

Fig. 2. Raman spectra of a C_{60} film measured at three arbitrary points after 25-h EB irradiation with an incident energy of 3 kV.

SEM Observation of Vertically-Aligned Fullerene Microtubes

○Sho Toita[1], Kun'ichi Miyazawa[2] and Masaru Tachibana[1]

[1]Yokohama City University, Yokohama, 236-0027,Japan
[2]National Institute for Materials Science, Tsukuba, 305-0044, Japan
E-mail:TOITA.sho@nims.go.jp

Since C_{60} fullerene works as an efficient electron acceptor and has relatively high electron mobility, C_{60}-based materials are expected as promising candidates in fields of organic electronics and solar cells [1]. It is known that C_{60} forms fiber-like single crystals (fullerene nanowhiskers: FNWs) [2] and tubular ones (fullerene nanotubes: FNTs) [3]. The other fullerene molecules such as C_{70}, fullerene derivatives and endohedral fullerenes can also form different kinds of FNWs and FNTs, which indicates that the FNWs and FNTs exhibit infinite new physical properties.

In order to use FNWs and FNTs for various applications, they should be arranged as desired structures. However, almost no approach has been performed up to now. Recently, Cha et al. succeeded to produce vertically-aligned fullerene microtubes (V-FMTs) on anodized alumina (AAO) membranes [4]. The whole area of substrates can be covered by the V-FMTs as shown in Figure 1. Their discovery opened the door to preparing designed architectures of fullerene nano and micro materials.

To control the structure and arrangement of V-FMTs, the growth mechanism of V-FMTs should be understood. The detailed mechanism, however, has been unknown. Hence, we performed scanning electron microscopy (SEM) observations in order to know the growth mechanism of V-FMTs prepared by using the method of ref.4. In the initial growth stage (growth time 60min), vertically-aligned thin fullerene micro non-tubular whiskers formed on the AAO substrates. The diameter and length of V-FMWs became increased with increasing the growth time. The tubular structures appeared at a growth time of around 90 min. At a growth time of 120min, vertically-aligned FMTs with hexagonal cross sections were obtained and their diameter and structure were maintained up to the final stage of growth time of 300 min. The average diameter and length of the V-FMTs were 30 μm and 300 μm, respectively.

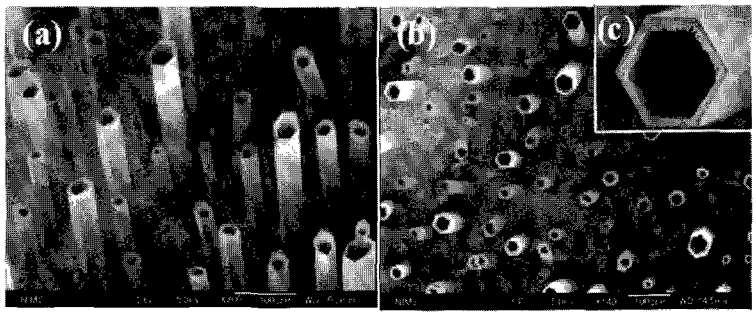

Figure 1 (a) Side and (b) plan views of V-FMTs (growth time 300min). (c) Cross section view of a V-FMT.

References:
1. P.S.Somani, S.P.Somani and M.Umeno, Appl. Phys. Lett. **91** (2007) 173503
2. K.Miyazawa, Y.Kuwasaki, A.Obayashi and M.Kuwabara, J. Mater. Res. **17** (2002) 83.
3. K.Miyazawa, J.Minato, T.Yoshii, M.Fujino and T.Suga, J.Mater.Res. **20**(2005)688.
4. S.I.Cha , K.Miyazawa and J.-D. Kim Chem. Mater. **20** (2008) 1667.

Corresponding Author: Kun'ichi Miyazawa
E-mail: MIYAZAWA.kunichi@nims.go.jp Tel: +81-29-860-4528 Fax: +81-29-860-4667

Atomistic observations of O_2 exposed C_{60} thin films

Masashi Shimura[1], Keisuke Kato[1], Morihiko Saida[2], Haruna Oizumi[2], Kenji Omote[2], Kuniyoshi Yokoo[2], Shigehiko Yamamoto[3], ○Masahiro Sasaki[1]

[1]*Institutet of Applied physics, University of Tsukuba, Tsukuba 305-8573, Japan*
[2]*Ideal star, Sendai 989-3204, Japan*
[3]*AIST, Tsukuba 305-8568, Japan*

It is known that the conductivity of C_{60} thin films is remarkably reduced upon exposed to O_2 ambient, which can be utilized for highly sensitive oxygen sensors. The mechanism of this phenomenon, however, has not been clarified yet. In this study, we have investigated atomistic features of the surface of C_{60} films exposed to oxygen by means of scanning tunneling microscopy (STM), where the local tunneling barrier height (LBH) imaging is adopted as well as the topographic imaging.

The C_{60} thin films grown on $MoS_2(0001)$ substrates are exposed to different amounts of O_2 ambient. The LBH imaging is realized by detecting the change in tunneling current pixel by pixel when the STM tip height is modulated during the constant current STM operation, usually used to obtain local work function images.

Figure 1 shows the STM and LBH images simultaneously measured from the C_{60} films exposed to 0.1 L (10^{15} Torr•s) of O_2 at room temperature. It is found that the dark areas in the LBH image are not localized at adsorption sites and expanded with increasing the O_2 exposure. The dark contrast in LBH in this image is attributed to the modification in the electronic and/or mechanical local properties of the C_{60} film surface, simply not to the lower work functions, since the macroscopic work function is not reduced upon O_2 exposure. Although the origin of the LBH contrast change has not been clarified at this moment, it can be concluded that oxygen easily diffuses in the bulk or the electronic properties modulated by oxygen exposure are delocalized similarly to that in the case of local work function of Cs adsorbed Pt(111) surface [1].

[1] A. Sinsarp et al., Jpn. J. Appl. Phys. 42 (2003) 4882.

Corresponding Author:
Masahiro Sasaki
e-mail: sasaki@bk.tsukuba.ac.jp
Tel: +81-29-853-5331
Fax: +81-29-853-5205

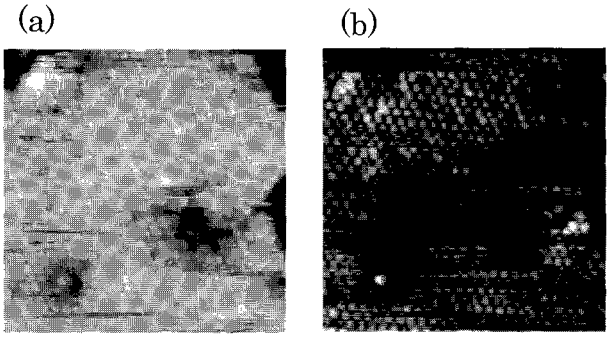

Fig.1 (a) STM and (b) LBH images of the C_{60} film exposed to 0.1 L of O_2. (V_S = −3.0 V, I_T = 0.3 nA, 21 nm × 21 nm)

Local work function of C_{60} monolayer on Cu(111) observed with scanning tunneling microscopy

○Keisuke Kato[1], Masashi Shimura[1], Morihiko Saida[2], Kenji Omote[2], Kuniyoshi Yokoo[2], Masahiro Sasaki[1]

[1]*institutet of Applied physics, University of Tsukuba, Tsukuba 305-8573, Japan*
[2]*Ideal star, Sendai 989-3204, Japan*

It is known that the electron transport in organic semiconductor devices is remarkably influenced by the level alignment at the interface between organic layer and metal electrode. However, the level alignment is not only determined by the work function of electrodes and the HOMO/LUMO levels of organic molecules, because the charge redistribution occurs at the interface. In order to predict the device performance, it is necessary to understand the mechanism of charge redistribution. In this research, we have studied the influence that molecular structure exerts on the local work function distribution by obtaining local barrier height (LBH) images, equivalent to local work function distributions, as well as topographic images with scanning tunneling microscopy (STM).

Experiments were carried out with STM housed in an ultrahigh-vacuum chamber. The LBH image is obtained at room temperature from the change in tunneling current due to the modulation of tip-sample distance during constant current STM imaging. Since the modulation frequency is much larger than that of feedback loop and the amplitude is small enough, The LBH measurement can be performed without disturbing STM measurement. A Cu(111) crystal was cleaned by repeated cycles of argon sputtering and annealing. Monolayer of C_{60} was deposited from a BN crucible in a preparation chamber. During C_{60} monolayer deposition, the crucible temperature was set at 870 K and the Cu(111) crystal was room temperature. The pressure was bellow 10^{-9} Torr even during the deposition.

The STM images reveal that there exist various molecular structures of C_{60} on the surface, which have been referred as p(4×4), p(2×2), linear wall maze and disordered maze by W.W. Pai et al.[1] The local work function distribution of C_{60} monolayer on Cu(111) is shown in Fig.1. The local work function of C_{60} monolayer depends on the structure. The most stable structure p(4×4) shows the LBH value of 3.5 eV and the others show lower values such as 2.8eV.

The absorption structure is determined by the rotation angle of the crystal axis between C_{60} and Cu substrate. The obtained results suggest that the work function is determined not only by the adsorption site respect to the Cu atom position but also the molecular structure.

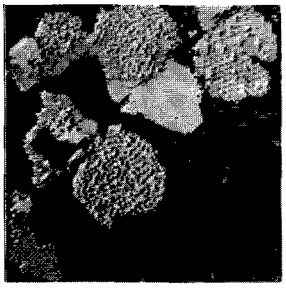

Fig.1 LBH image of the C_{60} monolayer on Cu(111)
I_t = 0.5 nA, Sample bias = -2.0 V,
Scan size = 1120 Å × 1120 Å,
Scan mode: Constant Current

[1]Woei Wu Pai, Ching-Ling Hsu, M. C. Lin, K. C. Lin, T. B. Tang, Phys. Rev. B **69** (2004) 125405.

1P-16

C_{60} crystal growth from organic solution for the field effect transistor

K. Kurihara, Y. Iio, R. Nokariya, F. Matsuyama, N. Iwata, and H. Yamamoto
College of Sicence and Technology, Nihon University,

7-24-1 Narashinodai, Funabashi, Chiba 274-8501, Japan

The aim of this study is to develop the easy and simple growth process for C_{60} single crystal applicable to superior channels of high speed and/or nano-scale field effect transistors (FETs). First of all, the C_{60} crystals were grown on substrates to figure out what kinds of shape and size of C_{60} crystals grew. The substrates were soaked in supersaturated solution with C_{60}, and the state was maintained until the solvent evaporated for approximately one week in refrigerator (12°C) or at room temperature (22°C). The test tube filled with solution was tilted with the angle between 0° and 90° from the ground. The used solvents were toluene, o-, m-, and p-xylene. Then, C_{60} crystals were grown as a channel on the electrodes deposited SiO_2/Si substrates by dipping into the solution with the drawing up speed of 1μm/s. The electrodes were deposited by sputtering or thermal evaporation method in advance.

Figures 1(a) and 1(b) show optical microscope (OM) images of the C_{60} crystal grown at 12°C and 22°C, respectively, with m-xylene solvent. The shape of the crystal was needle-like, meaning whisker, with the maximum size of 500 μm in length. We observed the Ag(2) mode at 1469 cm^{-1} in Raman spectrum. Larger amount of grown C_{60} whisker was obtained at 22°C. The C_{60} whisker was also obtained with toluene solvent grown at 12°C.

Figure 2 shows the OM image of the C_{60} whisker grown with toluene onto the substrate with sputtered Au electrodes. The C_{60} whiskers grew between the Au electrodes as well as on the electrodes. The size of the whiskers was approximately 1 μm in diameter and 50 μm in length. The typical electric conductivity of obtained C_{60} crystals was 639 S/m and very large comparing with that of pure C_{60}, 10^{-8}~10^{-14} *S/m.*

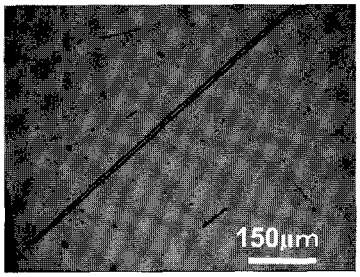

Figure 1(a) : The OM image of C_{60} whisker grown at 12 °C with m-xylene

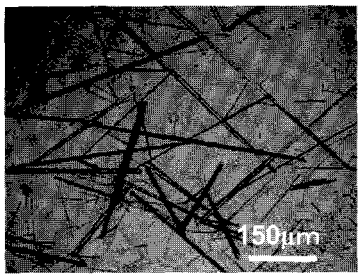

Figure 1(b) : The OM image of C_{60} whisker grown at 22 °C with m-xylene

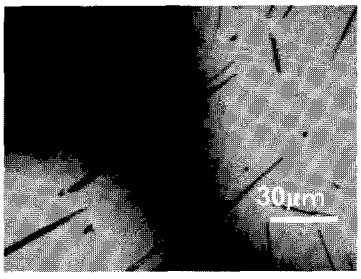

Figure 2 : The OM image of C_{60} whisker on Au sputtered substrate with toluene.

References

1. J. Yamaguchi et al. *Jap. Soc. Appl. Phys.* 44 (2005) 3757.
2. Rene Ceolin et al. *Chem. Phys. Lett.* 314 (1999) 21.
3. K. Miyazawa et al. *Sci. Tech. Adv. Mate.* 6 (2005) 388.

Extending the Polymerized C_{60} Size by Irradiating the Free Electron Laser during the Film Deposition

○Ryo Nokariya, Shinji Hachiya, Yasunari Iio, Nobuyuki Iwata and Hiroshi Yamamoto

Department of Electronics & Computer Science, College of Science & Technology, Nihon University, 7-24-1 Narashinodai, Funabashi-Shi, Chiba 274-8501 Japan

The aim of our study is to synthesize the three dimensional (3D) and amorphous C_{60} polymer in the meter scale. The polymer is expected to have three inconsistent characteristics; the hardness level higher than that of diamond, flexibility, and lightness. The used laser was free electron laser (FEL), which has the features of variable wavelength and sharp pulse width of several hundred fs. From the results of our previous works, the following are declared; i) the most efficient wavelength is 450 ~ 500 nm, ii) the pressure of approximately 7GPa is required for polymerization by FEL irradiation, iii) the size of polymerization is restricted to mm order, iv) the polymerized C_{60} film grew by FEL irradiation during growth, however less reproducibility, v) the polymer is obtained in a few hours. In order to extend the size of the polymer to meter scale, it is reasonable to investigate the polymerized film growth on the mm-order C_{60} polymer, which is prepared using an unique anvil with FEL irradiation in advance[1-4].

Figures 1 show a typical Raman spectrum around $Ag(2)$ mode of (a) as-compressed specimen at 7GPa, and of (b) film grown on C_{60} polymer with FEL. The 1469cm^{-1} peak is come from pure C_{60}, and lower than the peaks are come from polymerized C_{60}. After C_{60} film deposition as shown in Fig.1 (b), the peak intensity at 1469 cm^{-1} increased, however the peak position of the polymer downshifted, and the full width of half maximum of the peak was wider, demonstrated by the dotted lines. These results indicated that a part of the grown was polymerized.

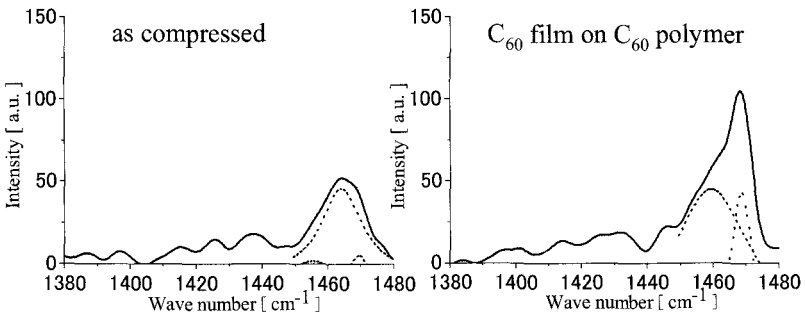

Figure 1. Raman spectrum of (a) as compressed C_{60} (b) C_{60} film on C_{60} polymer which was irradiated FEL. The dotted line shows Lorenz fitting.

References

[1] N. Iwata, Y. Iio, S. Ando, R. Nokariya, and H. Yamamoto, "Polymerization of Fullerene in Solution with Free Electron Laser Irradiation", Mater. Res. Soc. 2007 Fall Proc. 1057-II05-48.

[2] N. Iwata, S. Ando, R. Nokariya, and H. Yamamoto, "Synthesis of polymerized C_{60} bulk and film in three dimensions by irradiating a free electron laser", Jpn. J. Appl. Phys. **47** (2007) 1412-1415.

[3] S. Ando, R. Nokariya, R. Koyaizu, N. Iwata, and H. Yamamoto, "Synthesis of C_{60} Polymer by Free Electron Laser Irradiation with Hole-Doping Effect", Trans. Mate. Res. Jpn. **32** (2007) 1251-1254.

[4] The 31~34th Fullerene-Nanotubes General Symposium

TEM observation of fullerenes intratracheally instilled in the rat lung

○Kazuhiro Yamamoto[1], Miyabi Makino[1], Emiko Kobayashi[1],
Akira Ogami[2], Yasuo Morimoto[2]

1) National Institute of Advanced Industrial Science and Technology (AIST)
2) University of Occupational and Environmental Health

Abstract

Manufactured applications of nano carbon materials such as fullerenes and carbon nanotubes are reported in many fields recently. The toxicity of these nano carbon materials for the human is not clear, therefore, the toxicity test and risk assessment are very important. Transmission electron microscope (TEM) is powerful technique to study the nano materials. In the case of the observation for the biological cells, the cell specimens are usually stained with the heavy elements. However, it is difficult to observe the stained specimen of biological cells containing the nano-sized carbon materials, because the contrast from carbon is weak and below the background of the staining heavy elements. In this study, an energy-filtering TEM is applied to the observations of the rat lung tissue specimen after the intratracheal instillation of fullerenes solution.

The in-vivo test of fullerenes was performed using nine-week-old male Wister rats. The test solution was the fullerene nano particles in the water with 0.1g/l tween 80 dispersions. The fullerenes solutions of 0.1mg / 0.4ml or 0.2mg / 0.4ml content were intratracheally instilled into the rat lung. The lung tissues at one week, one month, and three months post-instillation were observed by energy-filtering TEM.

The some particles with the black contrast are observed at the cytoplasm in the low magnification zero-loss image of the alveolar macrophages at 1-week post-instillation. The lattice structure is observed in the high-resolution image of these particles, and it is clarified that these black particles observed in the alveolar macrophages are fullerenes according to the selected area electron diffraction analysis. The most of fullerenes particles are observed in the alveolar macrophages; however, some fullerenes are observed in the alveolar cells. Fullerenes still remains in the alveolar macrophages and the alveolar cells at 1 month or 3 months post-instillation.

This work was supported by NEDO Grant " Evaluating risks associated with manufactured nanomaterials ".

Corresponding Author: Kazuhiro Yamamoto

E-mail: k-yamamoto@aist.go.jp

Tel&Fax: 029-861-9414(Tel), 029-861-5301(Fax)

A Facile and Scalable Process for Size-Controllable Separation of Nanodiamond as Small as 4 nm in Size

○ Naoki Komatsu,[1] Yoichi Morita,[2] Tatsuya Takimoto,[1] Hiroshi Yamanaka,[3] Katsumi Kumekawa,[3] Shizuka Morino,[3] Shuji Aonuma,[2] Takahide Kimura[1]

[1] *Department of Chemistry, Shiga University of Medical Science, Seta, Otsu 520-2192*

[2] *Department of Materials Science, Osaka Electro-Communication University, Neyagawa, Osaka 572-8530*

[3] *Tomei Diamond Co. Ltd., 4-5-1 Jyoto, Oyama 323-0807*

Although centrifugation has been conventionally used for particle size sorting owing to its scalable and convenient nature, it has been attracting considerable attention for separating single-walled carbon nanotubes according to their length, diameter, electronic type and (*n*, *m*) structure. In this paper, we describe a facile and scalable method using ultracentrifugation to obtain bulk quantity of ND as small as 4 nm in size by separation of powdered ND prepared by static high-pressure high-temperature (HPHT) method [1]. The size was confirmed by particle size analysis and TEM (Figures 1 and 2). While the smallest size of ND (4 nm) we obtained is almost comparable to that of detonation nanodiamond (*d*-ND), the HPHT-ND possesses the following characteristics: very high crystallinity, little impurity and high controllability of the surface chemical structure. The median size of the separated ND is also tunable from 4 to 25 nm by controlling the conditions of the ultracentrifugation, its acceleration and duration, in this process (Figure 1). The wide spectrum of sizes in ND powder available by use of this facile and scalable process is highly expected to bring about significant progress in fundamental science and technological applications of NDs, especially in their biological and medicinal applications.

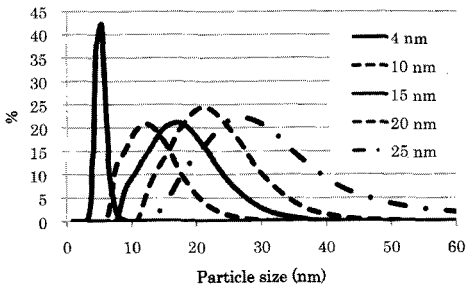

Figure 1. Particle size distribution of NDs with 4, 10, 15, 20 and 25 nm in size

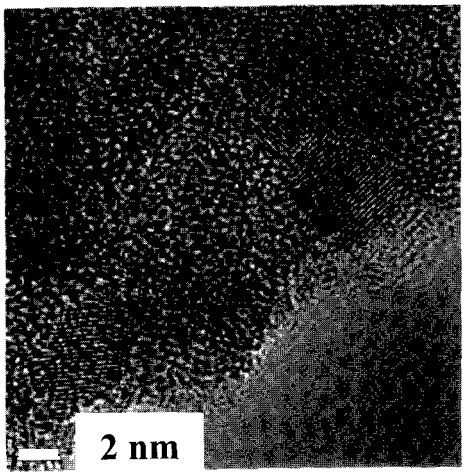

Figure 2. TEM image of ND with 4-5 nm in size

[1] Y. Morita, T. Takimoto, H. Yamanaka, K. Kumekawa, S. Morino, S. Aonuma, T. Kimura, and N. Komatsu, submitted for publication.

Corresponding Author: Naoki Komatsu

E-mail: nkomatsu@belle.shiga-med.ac.jp

Tel: +81-77-548-2102, **Fax:** +81-77-548-2405

1P-20

Synthesis and Magnetic Properties of Strontium Carbon Compound

○Satoshi Heguri, Nozomu Kimata, Mototada Kobayashi

Department of Material Science, Graduate School of Material Science
University of Hyogo, Ako, Hyogo 678-1297, Japan

In the past decade, rapid development of magnetoelectronics (also known as spintronics) intensified the research of ferromagnetic materials. We adopted nanocarbon materials for this purpose.

The peculiar magnetic behavior was reported in Europium graphite intercalation compound (GIC) EuC_6 [1]. Recently, superconductivity in CaC_6 was observed at surprisingly high critical temperature T_c = 11.5K. This attracted renewed interest in GIC family [2]. Kim et al. confirmed the superconductivity in SrC_6 at T_c = 1.65K and the absence of superconductivity in BaC_6 down to ~0.3K [3].

In this work, we report synthesis and magnetization of a novel ferromagnetic material based on carbon. Strontium carbon compound (SrC_x) was synthesized from pieces of highly oriented pyrolytic graphite (grade ZYA), powder graphite (99.9995%) or carbon powder (99%) and excess Sr metal (99.95%). They were sealed into quartz tube after evacuating and thermal treatment was performed in a furnace at 743~1373K for 10~520 hours.

Figure 1 shows the magnetization curves for SrC_x at 5K and 300K, respectively. These reveal that SrC_x has a ferromagnetic character. From the theoretical viewpoint, first-principles calculations predicted half-metallic ferromagnetism for SrC and BaC with rocksalt structure [4].

Details will be presented at the meeting.

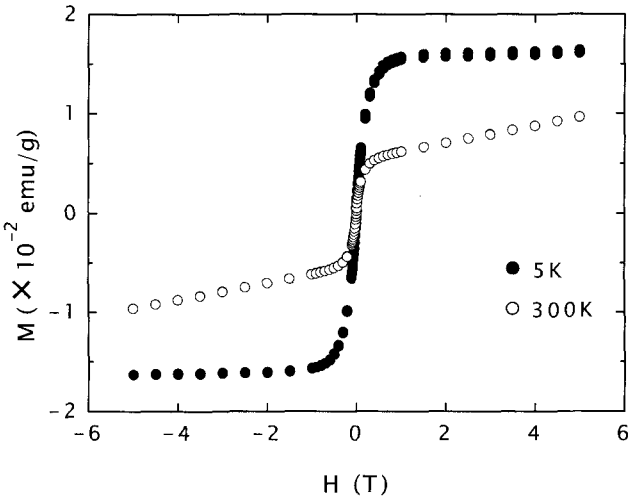

Fig.1. The magnetization curves for SrC_x at 5K and 300K, respectively.

References: [1] H. Suematsu et al., Solid State Commun. 40 (1981) 241.
[2] T. E. Weller et al., Nature Physics 1 (2005) 39.
[3] J. S. Kim et al., Phys. Rev. Lett. 99 (2007) 027001.
[4] G. Y. Gao et al., Appl. Phys. Lett. 91 (2007) 082512.

Corresponding Author: Satoshi Heguri
E-mail: rk07d004@stkt.u-hyogo.ac.jp
Tel&Fax: +81-791-58-0156/+81-791-58-0131

Global Spectral Analysis Method for Simulating Excitation-Emission Maps of Semiconducting Single-Walled Carbon Nanotubes

Author's name: Adam M. Gilmore ○

***Author's address & Affilication**: HORIBA JobinYvon Inc., 3880 Park Avenue, Edison, NJ 08820 USA*

Abstract: Recent research breakthroughs in the field of semiconducting single-walled carbon nanotubes (SWCNTs) have centered strongly around the acquisition and analysis of photoluminescence excitation-emission maps (EEMs). EEMs have been shown to provide both qualitative and quantitative information of SWCNT preparations including the helical distribution, diameter distribution, length distribution, bundling properties and intensity distribution. To date quantitative analysis of the three dimensional EEMs has relied heavily on manual estimations and 2-dimensional profiling to deal with overlapping peaks and other features in the EEM surface. The global analysis software and method described facilitates a rapid and statistically robust simulation of the 3D EEM surfaces in either wavelength or energy units to yield crucial coordinate and line-width information on all identified PL peaks. The model parameter initialization is facilitated by derivatization of the surface to identify all major peaks with adjustable amplitude discrimination. The program accepts EEM data in standard x-y-z columnar format in addition to matrix representation. An analytical form of the Voigt function is included to deconvolute the Lorentzian emission line shape from the Gaussian instrument response. The fitting functions can be fully constrained to ascertain physically realistic model parameterization using conserved themes for related data sets. Global linking/sharing of model spectral parameters is used to model excitation-emission peak coordinates relating the main energy levels (S3, S2 and S1) in addition to sidebands in the spectral emission. The model form can be adapted and constrained to yield information concerning anisotropic features, reabsorption phenomenon as well as energy transfer and quenching processes. The modeling routine also shows promise for adaptation to 3D surface simulations of Raman spectra of SWCNTs.

Corresponding Author: Adam M. Gilmore
E-mail: adam.gilmore@jobinyvon.com
Tel & Fax: Tel: 732-494-8660 x 135, Fax: 732-549-5157

Electric-field modulation in Carbon nanotubes

Yoshiyuki Miyamoto○

Nano Electronics Res. Labs. NEC, 34 Miyukigaoka, Tsukuba, 305-8501, Japan

Abstract: Optical property of carbon nanotube attracts lot of attention and alignment of nanotubes enabled us to monitor cross-excitation, which was not studied because of smaller oscillator strength and depolarization effect [1]. But recent experimental observations [2] suggested that the depolarization is not so strong as to completely suppress cross-excitation. An excitonic effect is considered to suppress depolarization effect [3] but localization of electron-hole pair in cross-polarization is weaker than those under parallel polarization [4], so theoretical understanding is still insufficient and a first-principles approach is necessary.

We studied cross-excitation of nanotubes by performing the time-dependent density functional simulation and monitored dielectric field inside the semiconducting (8,0) nanotube. The numerical scheme [5] was employed which does not include excitonic effect precisely.

Nevertheless, the depolarization effect was not so strong as to completely screen the electric field inside the carbon nanotube. When an applied electric field had a frequency corresponding to a wavelength of 800nm, the electric field (total field) inside nanotube remained with a modulated frequency as displayed in Fig. 1 (a). Furthermore, when the applied frequency was adjusted to a corresponding wavelength of 600 nm, which is closer to the E_{21} excitation energy, the field inside nanotube was even enhanced as shown in Fig. 1 (b).

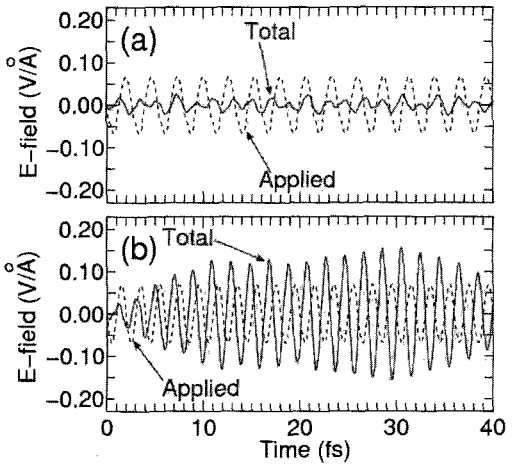

Fig.1 Time evolution of applied electric field (dotted line) and total field inside (solid line) nanotube. (a) is with wave length of 800 nm while (b) is with wavelength of 600nm.

The real-time dynamics of electrons (or frequency dependent dielectric function) is thus necessary to understand dynamical screening property of carbon nanotube. Furthermore, these results strongly suggest possibility of optical excitation of molecules encapsulated in nanotubes with modulated lights.

Acknowledgements-This work was done under collaboration with Prof. H. Zhang at Sichuan University. All calculations were performed by using the Earth Simulator.

References:

[1] H. Ajiki and T. Ando, Physica B, **201**, 349 (1994).

[2] See, for example, Y. Murakami, *et al.*, Phys. Rev. Lett. **94**, 087402 (2005)

[3] S. Uryu and T. Ando, Phys. Rev. B**76**, 115420 (2007).

[4] S. Kilina, S. Tretiak, Adv. Funct. Mater, **17**, 3405 (2007)

[5] Y. Miyamoto and H. Zhang, Phys. Rev. B**77**, 165123 (2008)

Corresponding Author: Yoshiyuki Miyamoto

E-mail: y-miyamoto@ce.jp.nec.com

Tel&Fax : +81-29-850-1586/+81-29-850-6136

Superconductivity in ensemble of boron-doped carbon nanotubes

○M. Matsudaira[1], J. Nakamura[1], N. Murata[1], J. Haruyama[1, 2, 5], J. Reppert[3], A. M. Rao[3], T. Koretsune[4], S. Saito[4], Y.Yagi[5]

[1]*School of Science and Engineering, Material Science course, Aoyama Gakuin University, 5-10-1 Fuchinobe, Sagamihara, Kanagawa 229-8558, Japan*

[2]*Institute for Solid State Physics, University of Tokyo, Kashiwanoha 5-1-5, Kashiwa, Chiba 277-8581, Japan*

[3]*Department of Physics and Astronomy, Center for Optical Materials Science and Engineering Technologies, Clemson University, Clemson, SC 29634, USA*

[4]*Department of Physics, Tokyo Institute of Technology, 2-12-1 Oh-okayama, Meguro-ku, Tokyo, 152-8551, Japan*

[5]*JST-CREST, 4-1-8 Hon-machi, Kawaguchi, Saitama 332-0012, Japan*

Abstract: Superconductivity in carbon nanotubes (CNTs) is attracting considerable attention [1-4]. However, its correlation with carrier doping has not been reported. Here, we report on the Meissner effect found in thin films consisting of assembled boron-doped single-walled CNTs (*B*-SWNTs) [5]. The SWNTs are synthesized from Ni/Co catalyst including elementary boron by pulsed laser vaporization [6]. We find that only CNT films consisting of low boron concentration leads to evident Meissner effect with T_c = 12 K and also that a highly homogeneous ensemble of the CNTs is crucial for realizing the Meissner effect. Interestingly, the Tc value of 12K exactly agrees with that in entirely end-bonded multi-walled CNTs [1]. The first-principles electronic-structure study of the *B*-SWNT strongly supports these results [4].

Homogeneously assembled *B*-CNTs, which can provide weakly interacted CNTs (quasi-1D property) so as to maintain both the 1D properties (e.g., contribution of a van Hove singularity and strong curvature in one SWNT) and the 3D property (e.g., Meissner shielding-current path across assembled SWNTs), are promising as a novel structure which is expected to open doors to the fields of carbon-based superconductivity.

References

[1]I.Takesue, J.Haruyama et al., **Phys.Rev.Lett.**96, 057001 (2006)

[2] N.Murata, J.Haruyama, M.Matsudaira, Y.Yagi, E.Einarsson, S.Chiashi, S.Maruyama, T.Sugai, N.Kishi, H.Shinohara, **Phys.Rev.B** 71, 081744 (2007)

[3]E.Perfetto and J.Gonzalez, **Phys.Rev.B** 74, 201403(R) (2006)

[4]T. Koretsune, S. Saito, *Phys. Rev. B* 77, 165417 (2008)

[5]N. Murata, J. Haruyama, J. Reppert, A. M. Rao, T. Koretsune, S. Saito, To be published on **Phys.Rev.Lett.** (July, 2008)

[6]K.McGuire, M.S.Dresselhaus, A.M.Rao et al., **Carbon** 43, 219 (2005)

Corresponding Author: Junji Haruyama

E-mail: J-haru@ee.aoyama.ac.jp

Tel&Fax: 042-759-6256 (Fax: 6524)

Interlayer nano p-n junctions formed in double-walled carbon nanotubes

○T.Shimizu[1], J.Haruyama[1,2,4], K.Nozawa[1], T.Sugai[3,4], H.Shinohara[3,4]

[1]*Aoyama Gakuin University, 5-10-1 Fuchinobe, Sagamihara, Kanagawa 229-8558, Japan*
[2]*Institute for Solid State Physics, University of Tokyo, Kashiwanoha 5-1-5, Kashiwa, Chiba 277-8581, Japan*
[3]*Nagoya University, Furo-cho, Chigusa, Nagoya 464-8602, Japan*
[4]*JST-CREST, 4-1-8 Hon-machi, Kawaguchi, Saitama 332-0012, Japan*

Abstract: Double-walled CNT s (DWNTs) that co mprise only two graphene layers have recently attracted considerab le attention due to their unique structures, synth esis, physics, and applications [1–7] . However, few researchers ha ve reported experim ental observations of electron transport in DWNT s [7]. We report the asymmetr ical ele ctric properties of current on both the so urce-drain and back-gate voltages (V_{BG}) dependence (asymmetric am bipolar behavior) found in field-effect transi stor (FET) using a double-walled carbon nanotube (D WNT) as a current channe l. We also find Coulomb oscillations with an anomalously large charging energy, observed only in a $+V_{BG}$ region. These results suggest the presence of p- and n-type sem iconducting behaviors of the outer and inner layers of the DWNT , resp ectively, and form ation of a corresponding interlayer nano p-n junction. The DWNT is an nealed in air atm osphere after synthesis and electro de contacts are form ed to d ifferent lay ers o n both end s. These allow formation of the nano p-n junction.

References

1. T.Sugai, H.Omote, S.Bandow, N.Tanaka and H.Shinohara, Jpn.J.Appl.Phys. 38, L477 (1999)
2. T.Sugai, H.Yoshida, T.Shimada, T.Okazaki and H.Shinohara, Nano Letters 3, 769 (2003)
3. A.Hashimoto, K.Suenaga et al., Phys. Rev. Lett. 94, 045504 (2005)
4. Z. Liu, K.Suenaga et al., Phys. Rev. Lett. 95, 187406 (2005)
5. R.Tamura, Y.Sawai and J.Haruyama, Phys. Rev. B 72, 045413 (2005)
6. S. Uryu and T. Ando, Phys. Stat. Sol. (B) 243, 3281 (2006)
7. T. Shimada, T. Sugai, T. Mizutani, H. Shinohara et al., Appl. Phys. Lett. 84, 2412 (2004)

Corresponding Author: Junji Haruyama
E-mail: J-haru@ee.aoyama.ac.jp
Tel&Fax: 042-759-6256 (Fax: 6524)

1P-25

Third-order nonlinear optical properties and phase relaxation time in semiconducting single-walled carbon nanotubes

M. Ichida[1,2], S. Saito[3], Y. Miyata[4], H. Kataura[4], and H. Ando[1,2]
[1]Graduate school of Nature Science, Konan University
[2]Quantum Nano-Technology Laboratory, Konan University
[3] National Institute for Information and Communications Technology
[4]Nanotechnology Research Institute, AIST

Third-order nonlinear optical susceptibility $\chi^{(3)}$ is an important parameter to govern the optical nonlinear properties. In general, the value of $\chi^{(3)}$ is determined by optical transition dipole moment, population and phase relaxation times (T_1 and T_2). In this study, we have measured $\chi^{(3)}$ and T_2 in isolated and bundled semiconducting single-walled carbon nanotubes (SWNTs) by Z-scan and two-beam degenerate four-wave mixing (DFWM) methods.

For isolated SWNTs sample, SWNTs were dispersed in D_2O with deoxycholic acid. For bundled sample, SWNTs with three different mean tube diameter were mixed and put onto a quartz substrate as a thin film. Figure1 shows the diameter dependence of figure of merit $\mathrm{Im}\chi^{(3)}/\alpha$. The absolute value increases with increasing tube diameter for both samples. Comparing the same diameter, $|\mathrm{Im}\chi^{(3)}/\alpha|$ measured in isolated sample is one order of magnitude larger than that in bundled thin film sample.

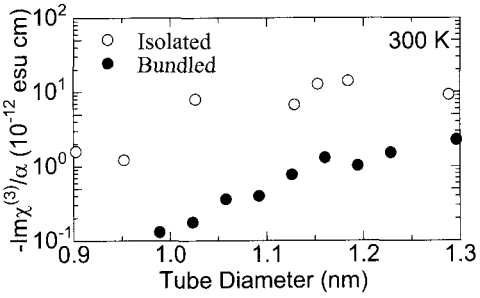

Fig.1: Im $\chi^{(3)}/\alpha$ as a function of tube diameter for isolated (open ircles) and bundled (closed circles) samples.

Figure 2 shows the time evolutions of DFWM signals in $\boldsymbol{k}_3$ ($=2\boldsymbol{k}_1-\boldsymbol{k}_2$) and $\boldsymbol{k}_4$ ($=2\boldsymbol{k}_2-\boldsymbol{k}_1$) directions, where $\boldsymbol{k}_1$ and $\boldsymbol{k}_2$ are the wave vectors of incident excitation beams. Both signals shift from $\tau_d=0$ because of T_2. From these time evolutions, we can obtain longer T_2 values of 90 fs for isolated sample than that of 20 fs for bundled sample. This result suggests that the T_2 is important factor to determine the enhancement of third-order optical nonlinearity in SWNTs.

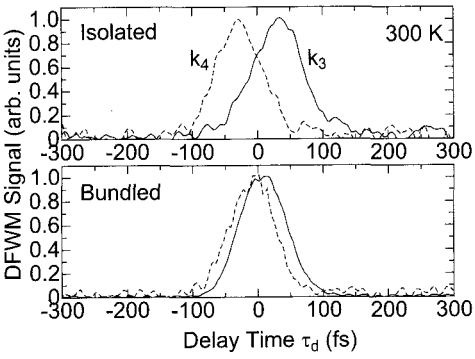

Fig.2: Time evolutions of DFWM signals in $\boldsymbol{k}_3$ and $\boldsymbol{k}_4$ directions for isolated and bundled samples.

Corresponding Author: Masao Ichida, E-mail: ichida@konan-u.ac.jp TEL&FAX: +81-78-435-2679

Li ion storage properties of organic molecules encapsulated single-walled carbon nanotubes

M. Hirose, S. Kawasaki, and Y. Iwai

Department of Materials Science & Engineering , Nagoya Institute of Technology, Japan

Single-walled carbon nanotubes (SWCNTs) are fascinating material, not only because of their unique structures, but also because of their extraordinary physical and chemical properties. Due to the ordered and huge nanospace of the SWCNT bundles consisting of not only inner space of the tube, but also the intertubular space in the bundle, the bundled SWCNTs have been expected to work as a new type gas and/or ion storage material. For example, the anode property of the SWCNTs for use in a Li ion secondary battery has been intensively investigated. In our previous paper [1], we reported that the reversible Li ion storage capacity of the SWCNTs increases by encapsulating C_{60}s in the tubes. However, the mechanism of the improvement has not been clarified yet. In order to elucidate the mechanism, we investigated the Li ion storage properties of the SWCNT samples in which several kinds of organic molecules are encapsulated.

Three kinds of organic molecules (9,10-dichloroanthracene, β-carotene, coronene) were doped into three kinds of SWCNTs having different diameter which were prepared by CVD, laser-ablation and arc-discharge methods. It was found that in the case of the CVD and lase-ablation tubes the reversible Li ion storage capacity of the SWCNTs significantly increased due to the encapsulation of the organic molecules while no significant encapsulation effect was observed for the capacity of the arc-discharge tube.

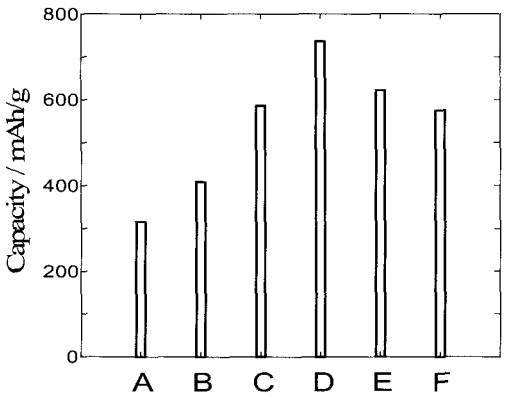

Fig. 1 Reversible Li ion storage capacities of the empty laser-SWCNT (A) and the peapods with dichloroanthracene (B), carotene (C), 7.3 wt% coronene (D), 13.7 wt% coronene (E), 23 wt% coronene (F).

[1] S. Kawasaki et al., *Mater. Res. Bull.*, in press.

Corresponding Author : Shinji Kawasaki Fax : +81-(52)-735-5221, E-mail : kawasaki.shinji@nitech.ac.jp

High-Performance Liquid Chromatographic Separation and Characterization of DNA-Wrapped Single-Wall Carbon Nanotubes

○Yuki Asada[1], Toshiki Sugai[1,2,*], Ryo Kitaura[1]
and Hisanori Shinohara[1,2]

[1]*Department of Chemistry, Nagoya University, Nagoya 464-8602, Japan*
[2]*Institute for Advanced Research, Nagoya University, Nagoya 464-8602, Japan*

DNA-wrapped SWNT s (DNA-SWNT s) have been known to exhibit unique characteristics in their structu res as well as the high so lubility in water [1]. Partial separations by chirality and length have been achieved by high perf ormance liquid chromatography (HPLC)[2]. We have recently reported the synthesis and characterization of isolated DNA-SWNT by using natural DNA from salmon sperm in aqu eous solutions[3]. Here, we report a detailed study on the SWNTs length separation by H PLC and their characterization by atomic force microscopy (AFM) and optical measurements.

DNA-SWNTs were separated by using size exclusion chrom atography (SEC) performed by using a Jasco corporation pum p with Sepax C NT (SEC 2000, 1000 and 300) columns. Fractions were collected at 1 m in intervals and characterized by AFM, UV-vis-NIR absorption, photoluminescence and Raman scattering to obtain information on the length dependence of SWNTs.

Figures 1 (a-c) are AFM im ages of DNA-SWNT s after the HPLC separation. The average length obtained is 353 ± 104 nm , 170 ± 26 nm and 77 ± 21 nm , for (a), (b) and (c) respectively. By using these chromatographed DNA-SWNTs, we have observed that optical properties vary sensitively dependingon the length of SWNTs separated.

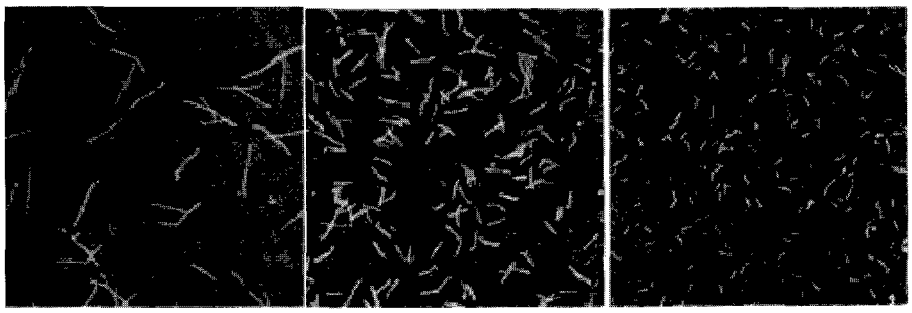

Figure 1 AFM images of HPLC separated DNA-SWNTs (Scale bar is 500 nm.)

* Present address: Department of Chemistry, Toho University

[1] M. Zheng, *et al.*, *Nat. Mater.* **2**, 338 (2003).; N. Nakashima, *et al.*, *Chem Lett.* **32**, 456 (2003).
[2] X. Huang, *et al.*, *Anal. Chem.* **77**, 6225 (2005).
[3] Y. Asada, *et al.*, *Nano.* **2**, 295 (2007).

Corresponding Author: Hisanori Shinohara
E-mail: noris@nagoya-u.jp, **TEL**: +81-52-789-2482, **FAX**: +81-52-747-6442

Roles of Conformational Restrictions of Carbene-derivatives in the Interactions with a Carbon Nanotube

○Takashi Yumura[1] and Miklos Kertesz[2]

[1]*Department of Chemistry and Materials Technology, Kyoto Institute of Technology, Matsugasaki, Sakyo-ku, Kyoto, 606-8585, Japan*

[2]*Department of Chemistry, Georgetown University, 37th and O streets NW Washington DC, 20057 1227, USA*

We have investigated double additions of a carbene-derivative into a nanotube for the purpose of constructing a strategy for site-specific functionalization. In the previous study, we employed density functional theory (DFT) calculations together with Clar valence bond (VB) representation, and found that the addition of the first CH_2 molecule into the outer surface of a nanotube does not affect Clar patterns of its pristine nanotube [1]. As a consequence it is expected that there should be no site-preference for the second outer CH_2 molecule after the first addition

The present study aims at gaining a clue to achieve site-selective outer additions by carbene derivatives. Since Diederich et al. [1] used diethylbutane-2,3-diyl bismalonate to functionalize C_{60} regioselectively, we focus on a bismalonate with a 2,3-butanediol tether as a possible candidate for selective bisfunctionalization of a nanotube, and have investigated by means of DFT PW91 calculations whether the bismalonate can achieve regioselective functionalization of the (10,10) nanotube. In order to elucidate roles of the bismalonate in the functionalization, the double CH_2 additions has been also analyzed. According to DFT calculations, conformational restrictions of the 2,3-butanediol tether should be responsible for site-preferences in the bismalonate addition into the nanotube.

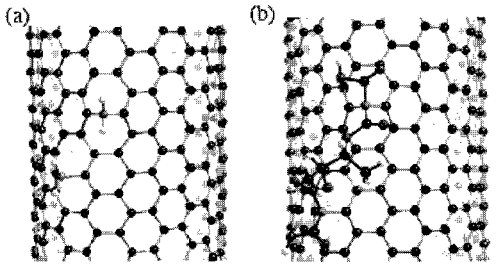

Figure 1 Optimized structures of functionalized (10,10) nanotubes

References:

[1] Yumura, T.; Kertesz, K. *Chem. Mater.* **2007**, *19*, 1028.

[2] Thilgen, C.; Diederich, F. *Chem. Rev.* **2006**, *106*, 5049.

Corresponding Author: Takashi Yumura

E-mail: yumura@chem.kit.ac.jp, Tel: +82-75-724-7571

Pressure-Induced Structural Phase Transition of Double-walled Carbon Nanotube and Electronic Structure of Carbon Nano-structured Materials

○Masahiro Sakurai and Susumu Saito

Department of Physics, Tokyo Institute of Technology
2-12-1 O-Okayama, Meguro, Tokyo 152-8551, Japan

Various carbon phases synthesized from fullerene using high-pressure and high-temperature technique are analyzed experimentally and theoretically. Although the high-pressure properties of carbon nanotube are of great interest, experimental details of pressure-induced structural transformation of carbon nanotube remain unclear because the carbon nanotube bundle with the uniform chirality has never been synthesized. Thus, we theoretically study pressure-induced structural phase transition of carbon nanotube using the constant-pressure molecular dynamics (MD) method combined with the transferable tight-binding model. In the MD method proposed by Wentzcovitch [1], volume and shape of the MD cell vary by the external pressure and the internal stress of the cell. Therefore, this method is suitable for the study of the pressure-induced structural phase transformation. Omata tight-binding model [2] we used is based on LDA energetics and reproduces well not only sp^2 and sp^3 covalent bonds but also sp^2 interlayer interaction.

As a result of the MD calculation for double-walled carbon nanotube bundles, double-walled nanotube is found to be more stable than single-walled nanotube under the external pressure. At 5 GPa, double-walled tube retains its initial geometry and the deformation of triangular lattice is found to be reversible. It is also found that sp^2-sp^3 hybrid structure and sp^3-rich anisotropic amorphous are obtained from (n,n)@(n+5,n+5) and (n,0)@(n+9,0) at the higher external pressure. The sp^2-sp^3 hybrid structure is composed of armchair or zigzag nanoribbons and sp^3-junctions. The sp^3-rich anisotropic amorphous phase is crystalline only in initial tube-axis. As a result of geometry optimization, these phases are considered to be energetically stable at room temperature and pressure. In addition, some of these phases are predicted to have a bulk modulus comparable with diamond. Double-walled nanotube composed of chiral tubes is also robust against the external pressure and transform into sp^3-rich amorphous with high density of about 6 $Å^3$/atom under the high pressure. We also report the electronic structure of the group of interesting nano-structured materials obtained by MD calculation using another tight-binding method which includes not only the transfer integrals but also the overlap integrals of the 2 *s* and 2 *p* orbital of a carbon atom and can reproduce well the LDA electronic structures [3].

References:

[1] R. M. Wentzcovitch, Phys. Rev. B **44**, 2358 (1991).

[2] Y. Omata, Y. Yamagami, K. Tadano, T. Miyake and S. Saito, Physica E **29**, 454 (2005).

[3] N. Hamada and S. Sawada, private communication; S. Okada and S. Saito, J. Phys. Soc. Jpn. **64**, 2100 (1995).

E-mail: sakurai@stat.phys.titech.ac.jp (M. Sakurai)

Polarized Raman Spectroscopy of Vertically Aligned Single-walled Carbon Nanotubes

○Zhengyi Zhang[1], Yoichi Murakami[2], Erik Einarsson[1],Yuhei Miyauchi[3], Shigeo Maruyama[1]

[1] *Department of Mechanical Engineering, the University of Tokyo*
[2] *Department of Chemical System Engineering, the University of Tokyo*
[3] *Institute for Chemical Research, Kyoto University*

We have prepared up to 30 μm thick vertically aligned single-walled carbon nanotube (VA-SWNT) films with high purity by the alcohol catalytic chemical vapor deposition (CVD) method[1][2]. In a previous polarized Raman spectroscopy study, we found anomalous anisotropic peaks such as at 180 cm^{-1} for the excitation by 488 nm laser and explained them as cross polarized excitation [3]. However, recent high resolution Raman spectrum shows that the strong 180 cm^{-1} is comprised by four fine sharp peaks which might be from isolated SWNTs. To clarify its origin, polarized Raman experiment is carried out using two configurations, where the orientation of the polarizer for inspecting the scattered light was parallel to (VV) and perpendicular to (VH) the polarization of the incident light. By changing the incident light orientation with respect to the VA-SWNT growth direction, two different polarization dependences were found for the radial breathing mode (RBM) peaks. The peaks at 160 and 203 cm^{-1} behave consistently with the parallel excitation, while peaks at 145, 181, 244, and 256 cm^{-1} exhibit the opposite behavior in the VV configuration. Although the selection rules for Raman scattering process allow cross-polarized excitation in RBM, 181cm^{-1} group peaks deviate much from the theoretical calculation assuming the orientation distribution by the order parameter obtained from absorption measurements[4]. Moreover, it is observed from high resolution SEM image that some isolated tubes distribute among the array which may correspond to the abnormal behaviors in CNTs.

[1] Y. Murakami *et al.*, *Chem. Phys. Lett.* **385** (2004) 298
[2] E. Einarsson *et al.*, *J. Phys. Chem. C* **111-48** (2007) 17861-17864
[3] Y. Murakami *et al*: *Phys. Rev. B* **71** (2005) 085403
[4] Y. Murakami *et al.*, *Phys, Rev. Lett.* **94** (2005) 087402

Corresponding author: Shigeo Maruyama E-mail: maruyama@photon.t.u-tokyo.ac.jp, Tel/Fax: +81-3-5800-6983

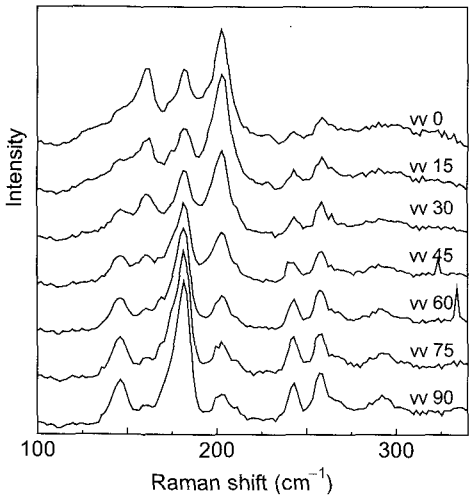

Fig. 1. Raman spectra of a VA-SWNT film in the VV configuration, and changing the incident polarization from 0° (along alignment direction) to 90° (perpendicular to the alignment direction).

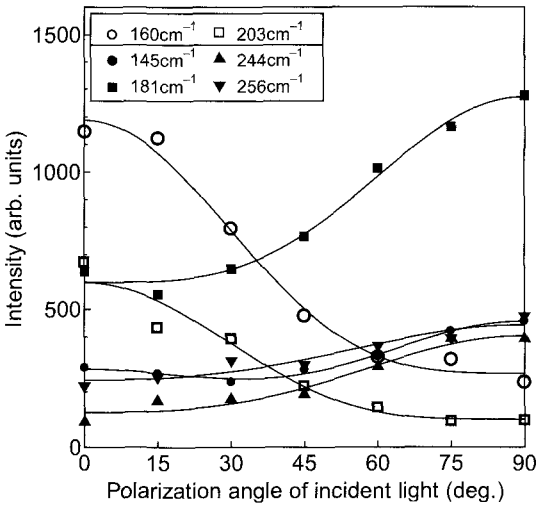

Fig. 2. RBM Peak intensity changes for incident light polarization from 0° to 90° with respect to the VA-SWNT growth direction (VV configuration).

1P-31

The effect of laser-induce defects on the Raman G band in metallic SWNTs

○Dongchul Kang[1], Kenichi Kato[1], Kenichi Kojima[1], Masaru Tachibana[1]

[1]*International College of Arts and Sciences, Yokohama City University, Kanagawa 236-0027, Japan*

Defects in SWNTs play a crucial role on the electronic, optical, and mechanical properties. Therefore, understanding the properties of defects is important for improving SWNT growth methods, tailoring their physical properties, and controlling the irradiation-induced damages.

Resonant Raman spectroscopy has been shown to be a powerful tool for characterizing the structural and electronic properties of SWNTs. In the Raman spectra of SWNTs, defect-induced phone mode (so-called D band) is observed at ~1350 cm^{-1}. The intensity of the D band can be enhanced with increasing the number of defects in the SWNT. Recently we reported that the D band intensity increase with the laser irradiation [1]. From the analysis in the D band intensity due to the thermal annealing, two relaxation processes for the laser-induced defects were revealed; one is the fast process with an activation energy of 0.4 eV and the other is the slow process with an activation energy of 0.7 eV [1]. It was suggested that these processes can correspond to vacancy-interstitial recombination and vacancy migration along the tube axis, respectively.

Moreover we found that the laser-induced defects influence not only D band but also G band observed at the range of 1540 ~1600 cm^{-1} associated with metallic SWNTs. The behavior of the G band due to laser-induced defects is of interest for more understanding the origin of G band associated with metallic SWNTs. In this paper, we report the behavior of G band associated with metallic SWNTs due to laser-induced defects.

[1] T.Uchida, M.Tachibana, and K.Kojima. J.Appl.Phys.101,084313(2007).

Corresponding Author: Masaru Tachibana
TEL: +81-45-787-2162, FAX: +81-45-787-2172, E-mail: tachiban@yokohama-cu.ac.jp

1D-Array of SWCNT Emitters Instantly Mounted in Micro-Cathodes

○Suguru Noda[1], Koji Furuichi[2], Yosuke Shiratori[1], Yoshiko Tsuji[1], and Hisashi Sugime[1]

[1]*Dept. of Chemical System Engineering, The University of Tokyo, Tokyo 113-8656, Japan*
[2]*DAINIPPON SCREEN MFG. CO., LTD, Tokyo 113-8656, Kyoto 602-8585, Japan*

Field emitters (FEs) are a candidate application of CNTs fully utilizing their unique characteristics such as geometrical sharpness and aspect ratio, electrical durability and conductivity, mechanical strength, and thermal and chemical stability. But their practical application to display devices suffers from the insufficient emission uniformity, short lifetime, and high operating voltage. The key solving these problems should be the control of the spacial distribution of vertically standing CNTs. We studied SWCNT emitters directly grown in line-shaped micro-cathodes, which is quite different from the screen printed MWCNT emitters around which dot-shaped micro-cathodes are constructed.

Figure 1 schematically shows the fabrication process and device structure of our SWCNT FEs. First, slit patterns are formed on the gate electrodes by lithography, and using this gate as mask, hemi-cylindrical trenches are formed in the insulating layer. Catalysts are sputter-deposited through the slits, forming micro-gradients on the cathode [1]. SWCNTs are then grown by chemical vapor deposition (CVD) and form different morphologies such as forests and grasses depending on catalyst thickness [1]. Under optimized catalyst and growth conditions, SWCNT bundles will stand beneath the slit spontaneously at a linear density > 10 /μm. By installing this line-shaped micro-cathodes at a 10 μm interval, emitter density > 10^8 /cm^2 should be possible. Emission current (typically~ 1 mA/cm^2) is distributed among emitters and the reduced current < 10 pA/emitter will realize long lifetime even for SWCNTs. Uniform emission and low operation voltage is expected for SWCNT emitters > 10^4 /pixel.

Figure 2 shows the structure and performance of our SWCNT FEs. SWCNTs were grown on p-type Si cathode by CVD from 30 Torr C_2H_5OH with Co/Al_2O_3 catalyst at 800 °C. Growth time was as small as 5 s owing to the growth enhancement of disordered Al_2O_3 layer [2, 3]. SWCNTs form "mountains" or "grasses" with their bundles standing beneath the slit. Uniform emission was achieved at a operation voltage as low as ~50 V.

Self-organized SWCNTs assisted by engineered catalysts fully show their excellent performance.

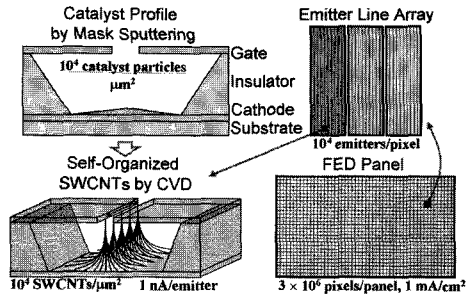

Fig. 1 Concept of our SWCNT FE array.

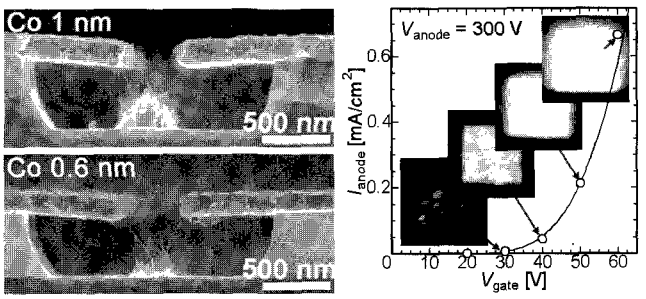

Fig. 2 Cross-sectional SEM and FE property of our SWCNT MFEs.

[1] S. Noda, et al., Carbon **44**, 1414 (2006).

[2] S. Noda, et al., Jpn. J. Appl. Phys. **46**, L399 (2007).

[3]Y. Shiratori, et al., Jpn. J. Appl. Phys. **47**, 4780 (2008).

Corresponding Author: Suguru Noda, Tel&Fax: +81-3-5841-7332, E-mail: noda@chemsys.t.u-tokyo.ac.jp

Semiconducting single wall carbon nanotubes network for field effect transistors devices

○Nicolas Izard[1], Said Kazaoui[1], Nobutsugu Minami[2]

[1]Nanotube Research Center, [2]Nanotechnology Research Institute
National Institute of Advance Industrial Science and Technology, Tsukuba, Japan

Novel materials for field effect transistors (FET) are highly demanded, and semiconducting single wall carbon nanotubes (s-SWNTs) are very promising. Several groups worldwide have demonstrated excellent transfer characteristics using individual s-SWNT. However, SWNTs networks and thin films still displays poor characteristics, mainly due to trace of metallic SWNT (m-SWNT). Recently, several approaches to extract s-SWNT were explored, using for example polymer wrapping[1] or density gradient ultra-centrifugation[2], but failed either by insufficient removal of m-SWNT or by trace of extracting material limiting FET's performances.

We will report on electronic properties of FET consisting of semiconductor-enriched single wall carbon nanotubes without detectable traces of metallic nanotubes and impurities. Nearly perfect removal of metallic nanotubes is confirmed by optical absorption, Raman and electrical measurements. This result was made possible in particular by ultracentrifugation (150,000g) of solutions prepared from SWNT powders using polyfluorene as an extracting agent in toluene. Such s-SWNTs processable solutions were applied to realize FET, embodying randomly or preferentially oriented nanotube networks prepared by spin coating or dielectrophoresis. Devices exhibit stable p-type semiconductor behavior in air with very promising characteristics: the on-off current ratio is 10^5, the on-current level is around 10 μA and the estimated field effect hole mobility is larger than 2 cm^2/vs [3].

[1] A. Nish, J.-Y. Hwang, J. Doig, R.J. Nicholas, *Nature Nanotech.*, **2**, 640 (2007).
[2] M.S. Arnold, A.A. Green, J.F. Hulvat, S.I. Stupp, M.C. Hersam, *Nature Nanotech.*, **1**, 60 (2006).
[3] N. Izard, S. Kazaoui. K. Hata, T. Okazaki, T. Saito, S. Iijima, N. Minami, *Appl. Phys. Lett.*, **92**, 243112 (2008).

Corresponding Author: Said Kazaoui
TEL: +81-29-861-4838, FAX: +81-29-861-4851, E-mail: s-kazaoui@aist.co.jp

Application for heat-release devices of carbon nanotube films made by surface decomposition of SiC

○Wataru Norimatsu[1,2], Chihiro Kawai[3], Michiko Kusunoki[1,2]

[1]*Japan Fine Ceramics Center, Nagoya 456-8587, Japan*
[2]*EcoTopia Science Institute, Nagoya University, Nagoya, 464-8603, Japan*
[3]*Sumitomo Electric Industries, Ltd., Hyogo, 664-0016, Japan*

Carbon nanotubes (CNTs) have the one-dimensional structure, resulting in the high thermal conductivity along the tube axis. Actually, complex materials containing CNTs dispersed in plastics or metals have been studied for applications such as the heat-release devices. We have developed the high-density and well-aligned CNT films connecting directly with the SiC substrate without metal-catalytic particles by surface decomposition of SiC [1]. CNTs obtained by this method have the elastic "buckling" nature of the tip of CNTs. Therefore, CNTs can intrude into microscopic dips on the surface of the materials to which CNTs are contacted, leading to decrease of the contact thermal resistance. In this study, we prepared the CNT films by the surface decomposition method and investigated their heat transfer characteristics.

CNT films were formed on the both sides of SiC substrates by annealing double-side polished SiC crystal at temperatures ranging from 1700 to 1900 °C in vacuum. Prepared CNT/SiC complex materials were sandwiched between the heat origin and the radiator as shown in the inset of Figure 1. Temperature difference ΔT between the heat origin and the radiator was measured. Dividing ΔT by the applied heat quantity Q leads to the thermal resistance of our materials.

Figure 1 shows the thermal resistance of CNT/SiC (SiC: single crystal or polycrystal produced by CVD method) samples referred to that of conventional grease. As shown in the figure, the thermal resistance of the samples with CNT films is much lower than that of the ones without CNTs, indicating the high-performance as thermal interface materials. This can be explained by the buckling effect of high-density CNTs which increased the contact area and reduced the thermal resistance at the interface, in addition to the high thermal conductivity of the CNTs. More experimental results of the comparison with other materials will be reported in the symposium.

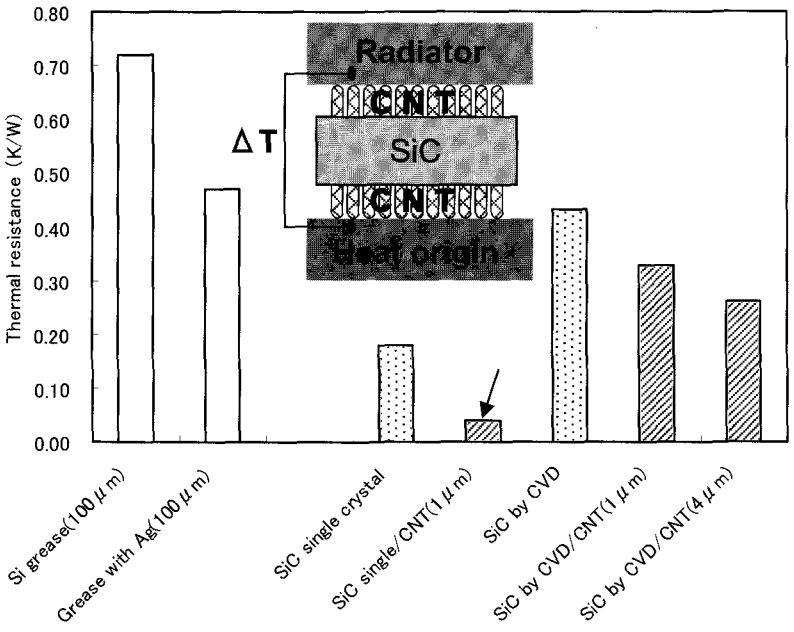

Figure 1 Thermal resistance of CNT/SiC complex materials.

[1] M. Kusunoki, et al., *Appl. Phys. Lett.* **77**, 531 (2000).

Corresponding Author: Wataru Norimatsu, TEL: +81-52-789-5859, E-mail: w_norimatsu@esi.nagoya-u.ac.jp

Fabrication and Transport Properties of Carbon Nanotube Transistors by Direct Growth Method

○Akihiko Fujiwara, Nobuhito Inami, Mohd Ambri Mohamed, Eiji Shikoh

School of Materials Science, Japan Advanced Institute of Science and Technology, Ishikawa 923-1292, Japan

Carbon nanotubes (CNTs) have attracted great attention as a next-generation material. For the application of CNTs to transparent and flexible semiconductor devices, studies on field-effect transistors (FETs) using randomly networked CNT films have been performed. In the fabrication process of FETs, the method for disposition of CNTs in the channel of FETs is one of the most important issues to be established. The direct growth method, where CNTs are directly grown from the electrodes and bridging the electrodes, is an ideal method. In spite of the advantages of the direct growth method, optimization of the fabrication process has not been established, and properties of FETs fabricated by this method are unexplored. In this study, we have fabricated CNT-FETs by direct growth technique for single-wall (SW) CNTs bridging the source and drain electrodes, and investigated their transport properties.

The FETs used in this study were of the back gate configuration type. The device structure and procedure are shown in Fig. 1. A Mo/Co layer was used both as the catalyst for CNT growth, and as the source and drain electrodes. The channel length L and the channel width W were designed to be 5 and 100 μm, respectively. The Mo layer (100 nm) was first deposited on the substrate at an angle of 8° to the normal by electron beam (EB) evaporation system, followed by EB deposition of the Co catalyst layer (nominal 1 nm) normal to the substrate. The angled deposition technique was employed to deposit a single layer of the Co catalyst on the side of Mo in order to enhance the growth of CNTs. CNTs were grown by fast-heating alcohol catalytic chemical vapor deposition (ACCVD) method with ethanol as the feed gas and Co as the catalyst [1, 2]. We found that carrier injection barrier heights of FETs in this study show smaller values (without any additional specific treatment after the device fabrication) than those of FETs fabricated by a conventional post-dispersion method [3].

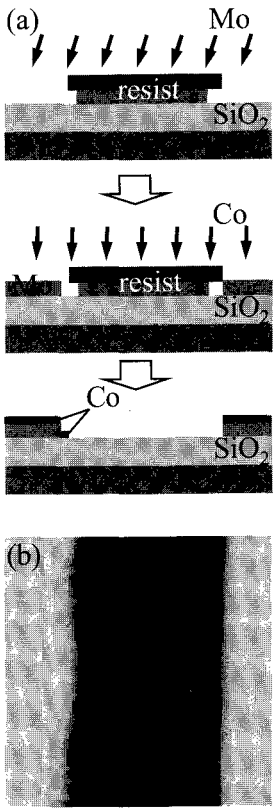

Fig. 1. (a) Schematic fabrication sequence. (b) AFM image of a CNT-FET: the size of this image is 7.5 x 7.5 μm^2.

[1] N. Inami, M. A. Mohamed, E. Shikoh, and A. Fujiwara, Sci. Technol. Adv. Mater. **8**, 292 (2007).

[2] M. A. Mohamed, N. Inami, E. Shikoh, Y. Yamamoto, H. Hori, and A. Fujiwara, Sci. Technol. Adv. Mater., to be published.

[3] N. Inami, M. A. Mohamed, E. Shikoh, and A. Fujiwara, Appl. Phys. Lett. **92**, 243115 (2008).

Corresponding Author: Akihiko Fujiwara

TEL: +81-761-51-1551, FAX: +81-761-51-1149, E-mail: fujiwara@jaist.ac.jp

Fabrication and characterization of field effect transistors by using high-purity semiconducting single-wall carbon nanotubes

○Shunjiro Fujii, Yasumitsu Miyata, Kazuhiro Yanagi, Takeshi Tanaka, Daisuke Nishide, Hiromichi Kataura

JST/CREST, Nanotechnology Research Institute, National Institute of Advanced Industrial Science and Technologies (AIST), Tsukuba, Ibaraki 305-8562, Japan

Single-wall carbon nanotube (SWCNT) is candidate material as a building block of the high-performance field effect transistor (FET), because of its superior transport properties. However, as-produced SWCNTs contain not only the semiconducting SWCNTs but also the metallic ones which highly degrade the performance and the reproducibility of SWCNT FET. One of the solutions of this problem is to use the separated high-purity semiconducting SWCNTs for the device fabrication. In this study, we fabricated SWCNT FETs by using semiconducting SWCNTs obtained by density-gradient ultracentrifugation (DGU) method [1,2] and then characterized them.

SWCNT FET was fabricated by dropping a semiconducting SWCNT dispersion in dimethylformamide (DMF) onto a SiO_2/Si substrate with the Au/Cr electrodes deposited in advance. AFM image of the channel showed the lengths of SWCNTs were 0.5～1 μm that is smaller than the channel length (2 μm).

Figure 1 shows a typical source-drain current (I_{sd}) vs gate voltage (V_g) characteristics. Most of FETs fabricated in this method show semiconducting behavior without electrical breakdown procedure, which is evidence of the high separation purity of DGU. Typical mobility and on/off ratio were 0.2 cm^2/Vs and 10^3, respectively, at this stage.

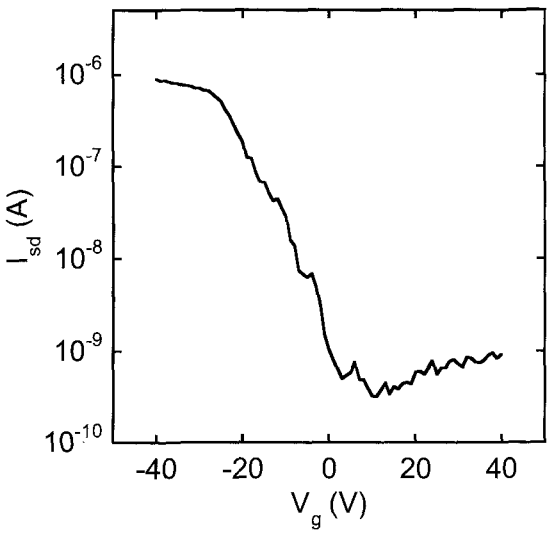

Fig. 1 Source-drain current (I_{sd}) vs gate voltage (V_g) characteristics (V_{sd} = 1 V).

References: [1] M. S. Arnold *et al.*, Nat. Nanotechnol. **1**, 60 (2006). [2] K. yanagi *et al.*, Appl. Phys. Exp. **1**, 034003 (2008).

Corresponding Author: Hiromichi Kataura
E-mail: h-kataura@aist.go.jp, **Tel:** +81-29-861-2551, **Fax:** +81-29-861-2786

1P-37

Light-driven Carbon Nanotube-Microdevice

○Eijiro Miyako, Hideya Nagata, Ken Hirano, Takahiro Hirotsu

Health Technology Research Center, National Institute of Advanced Industrial Science and Technology (AIST), 2217-14, Hayashi-cho, Takamatsu 761-0395, Japan

The development of high-performance CNT–polymer composites is progressed at a rapid rate for various applications. Efficiently and high-precision controlling the temperature of a reaction media on a micro- and nano-chip is a critical issue that will determine any future lab-on-a-chip applications. Recently, we have investigated about the photothermal effect of nanocarbons [single-walled carbon nanotube (SWNT) and single-walled carbon nanohorn][1–5]. In the present study, we show that a near-infrared (NIR) laser-induced poly(dimethylsiloxane) (PDMS) microchip encapsulating phospholipid (PL)–bovine serum albumin (BSA) functionalized SWNT (PL–BSA–SWNT) complex has a potential for the ultrarapid temperature control of a solution in a microspace (Figure). Our CNT microdevice allows not only ultrafast and high-precision temperature control in a microspace but also remote-controls of various bio-transformations, when triggered by NIR laser irradiation. Bio-transformations in the hot microspace will begin showing the conference.

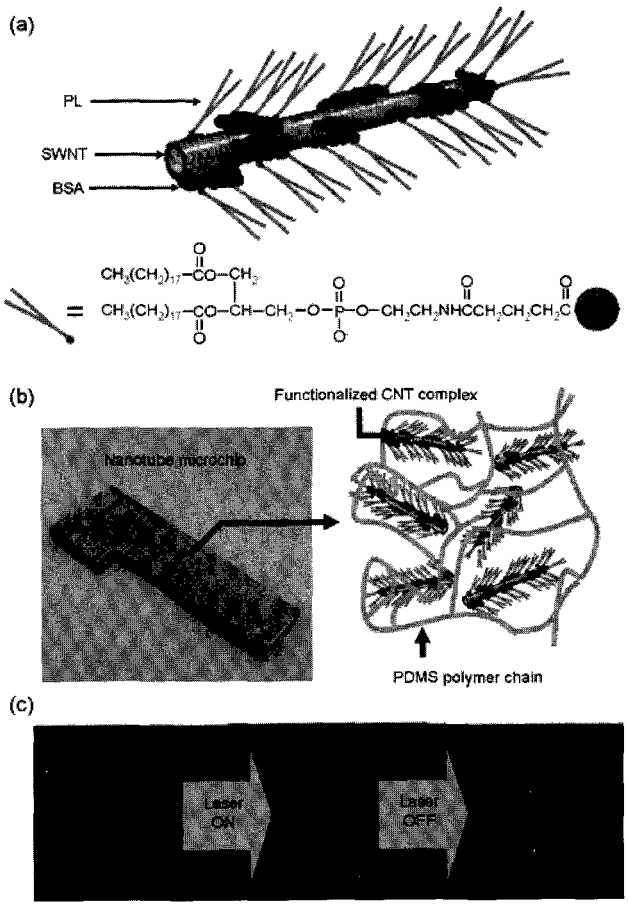

Figure. Ultrafast microthermal control by photoinduced CNT microchip. (a) Structure of functionalized CNT complex. (b) Photograph of CNT microchip. (c) A direct observation of ultrafast temperature change in a microspace.

References:

[1] E. Miyako *et al. Angew. Chem. Int. Ed.* **47**, 3610 (2008).

[2] E. Miyako *et al. Nanotechnology* **18**, 475103 (2007).

[3] E. Miyako *et al. Nanotechnology* **19**, 075106 (2008).

[4] E. Miyako *et al. Chem. Phys. Lett.* **456**, 220 (2008).

[5] E. Miyako *et al. Small* accepted (2008).

Corresponding Author: Eijiro Miyako

TEL: +81-87-869-3574, FAX: +81-87-869-3550, E-mail: e-miyako@aist.go.jp

Genomic DNA-Mediated Solubilization and Separation of Single Wall Carbon Nanotubes

Sang Nyon Kim,° Kristi M. Singh, Fahima Ounchen, James G. Grote and Rajesh R. Naik

Materials and Manufacturing Directorate

Air Force Research Laboratory

Wright Patterson AFB, OH 45433

By wrapping and/or groove-binding with SWCNTs via hydrophobic interactions, deoxyribonucleic acid (DNA) has been recognized as an efficient dispersion media that exfoliate and fractionate single wall carbon nanotubes (SWCNTs) according to their diameter and metallicity. $d(GT)_{20}$ DNA exhibited not only individual-level nanotube dispersion, but also effective SWCNT chirality separation when eluted from an anion exchange column at various salt concentrations.[1, 2] Here we present the use of sized genomic DNA as a cost-effective nucleic acid based method for SWCNT solubilization and separation. Using a salmon DNA (SaDNA), a byproduct of the fishing industry, we demonstrate that the SaDNA disperses SWCNTs on a comparable level to $d(GT)_n$ oligomer. The NIR, PLE emission and resonance Raman analysis from the SaDNA solubilized nanotube samples will be presented along with their chirality dependent separation results.

1. Zheng, M.; Jagota, A.; Strano, M. S.; Santos, A. P.; Barone, P.; Chou, S. G.; Diner, B. A.; Dresselhaus, M. S.; Mclean, R. S.; Onoa, G. B.; Samsonidze, G. G.; Semke, E. D.; Usrey, M.; Walls, D. J. *Science* 2003, 302, (5650), 1545-1548.
2. Zheng, M.; Semke, E. D. *J. Am. Chem. Soc.* 2007, 129, (19), 6084-6085.

Rajesh R. Naik

Rajesh.Naik@wpafb.af.mil

T) 1-937-255-9717

F) 1-937-255-9157

Acknowledgements: The authors thank AFOSR for the financial support. This research was performed while Dr. Kim held a National Research Council Research Associateship Award at AFRL.

An Experimental Investigation of Active Roles of sp^2 Carbon Precursors in SWCNT Growth

○B. Shukla [1], T. Saito [1,2], M. Yumura [1], S. Iijima [1]

[1] *Nanotube Research Center, AIST, Tsukuba 305-8565, Japan*
[2] *PRESTO, Japan Science and Technology Agency, Kawaguchi 332-0012, Japan*

Since, formation of single walled carbon nanotubes (SWCNTs) is a complex process, their growth mechanism and the assessment of the active CNT precursor are still challenging. Especially, about the growth mechanism of CNTs, only physical processes have been reported [1-5]. Although reaction mechanism of growth of CNT is important for quality and quantity control, it has not been clarified yet probably due to complexity of the process. The main purposes of this study are to explore the reaction mechanism of CNTs growth in CVD process and to investigate new and effective carbon sources that can produce high quality CNTs.

In this study we have tested the efficiency of some aromatic hydrocarbons with characteristic functional groups that is phenylacetylene, styrene, allylbenzene, toluene and ethylbenzene. Thermal, electronic and structural properties of produced SWCNTs, were characterized by TG-DTA, resonant Raman and optical absorption spectroscopies. As a result only styrene and allylbenzene could produce SWCNTs. These hydrocarbons differ in active carbon precursor species with different hybridizations produced from their thermal decompositions, such as sp species HCC• produced from phenylacetylene, sp^2 species C_2H_3• from styrene and allylbenzene and sp^3 species CH_3•/ CH_2CH_3• from toluene and ethylbenzene. To clarify the reason, why CNTs only produced from styrene and allylbenzene, all those hydrocarbons were tested with secondary carbon source C_2H_4 under same conditions during which SWCNTs were produced in all cases in different quantities. Raman analysis shows that SWCNTs produced from different hydrocarbons are differ in their diameters.

Production of SWCNTs from styrene and allylbenzene in both cases of with and without C_2H_4 and from other hydrocarbons only with C_2H_4, suggest that the most important gas phase CNT precursor should be C_2 species C_2H_3•/C_2H_4 having sp^2 hybridization. On this basis, it can be speculated that the network of sp^2 carbons in CNTs might be constructed by the active role of sp^2 carbons, C_2H_3•/C_2H_4. In this way the main originalities of this study are: (a) Investigation of new carbon sources (b) Investigation of active CNT precursor C_2H_3•/C_2H_4 (c) Starting of chemical reaction mechanism of growth of CNTs.

References

1. S.Huang, M. Woodson, R. Smalley, J. Liu , *Nano Lett.*, **2004**, 4,6,1025.

2. Y. Wang, M. J. Kim, H. Shan, c. Kittrell,. Fan, L.M. Ericson, W.Hwang, S. Arepalli, R.H.Hauge, R. E. Smalley, *Nano.Lett.*, **2005**,5,6,997.

3. W.H.Wang, Y.R.Peng, P.K. Chuang,, C.T.Kuo, *Diamond and Related Materials*,**2006**, 15, 1047

4. S. Inoue, Y. Kikuchi, *Chem.Phys. Lett.*,**2005**, 410, 209.

5. M. Grujicic, G. Cao, B. Gersten, *Appl. Surf. Sci.*, **2002**, 191, 223.

Corresponding Author: Takeshi Saito,
E-mail: takeshi-saito@aist.go.jp,
Tel/Fax: 029-861-4863/ 029-861-4413

Optical and (*n*, *m*) Enrichments of (7,5)-SWNTs through Extraction with Chiral Monoporphyrin

○Xiaobin Peng[1], Naoki Komatsu[1], Takahide Kimura[1], Atsuhiro Osuka[2]

[1] *Department of Chemistry, Shiga University of Medical Science, Otsu 520-2192, Japan*
[2] *Department of Chemistry, Graduate School of Science, Kyoto University, Sakyo-ku, Kyoto 606-8502, Japan*

Tetraarylporphyrin was reported to enrich semiconducting SWNTs through the selective complexation [1], and other tetra-substituted monoporphyrins also showed extraction ability for SWNTs. On the other hand, we have used gable-type diporphyrins for selective extraction of SWNTs [2,3]. In this study, we have employed 5,15-disubstituted chiral monoporphyrin to extract SWNTs and observed selectivity to the handedness and (*n*, *m*) structure of SWNTs.

As shown in Figure 1, the dominant and symmetrical CD peaks at 374 and 639 nm are assigned to E_{33} and E_{22} transitions of the (7,5)-SWNTs, indicating that the extracted SWNTs are optically active. Raman spectra of the as-received and extracted SWNTs (Figure 2) show clearly that semiconducting (7,5)-SWNTs (281 cm^{-1}) were enriched significantly, while specific metallic SWNTs corresponding to the band of 216 cm^{-1} largely decreased after the extraction. The solvent effects in the extraction ability of the monoporphyrin and the selectivity for SWNTs will be also discussed.

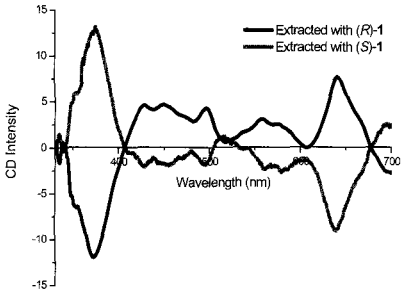

Fig. 1 CD spectra of D_2O/SDBS solutions of the SWNTs extracted with chiral monoporphyrin in methanol.

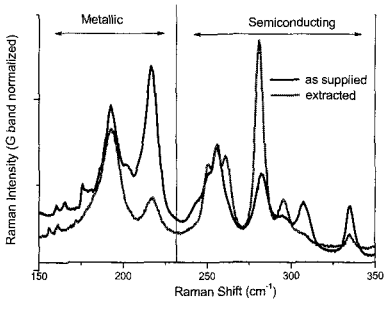

Fig. 2 Raman spectra (RBM) of as-received SWNTs and the ones extracted with monoporphyrin in methanol.

[1] Huaping Li, et al, *J. Am. Chem. Soc.* **2004**, 126, 1014
[2] X. Peng *et al.*, *Nature Nanotechnology*, **2007**, 2, 361
[3] X. Peng *et al.*, *J. Am. Chem. Soc.*, **2007**, 129, 15947

Corresponding Author: Xiaobin Peng
E-mail: xiaobin@belle.shiga-med.ac.jp, **Tel:** +81-77-548-2102, **Fax:** +81-77-548-2405

Synthesis of single-walled carbon nanotubes by arc plasma reactor with twelve-phase alternating current discharge

○Tsugio. Matsuura, Yukie. Kondo, Norio. Maki

Industrial Technology Center of Fukui Prefecture, Fukui 910-0102, Japan

Abstract

Several methods for synthesis of CNTs such as DC arc-discharge [1], laser ablation and thermal chemical vapor deposition (CVD) have been presented. The DC arc-discharge method can synthesize CNTs in highest quality than the other methods mentioned above. However, its yields are much lower. Up to date, CVD method is the mainstream of mass fabrication of CNTs [2]. In order to avoid the disadvantage of the DC arc-discharge method, the twelve-phase AC arc-discharge method has been developed [3]. In general, multiple-phase AC discharge plasma has unique features as follow [4, 5]; (a) no discharge break in spite of using very low frequency (in this case 60Hz) discharge, (b) rotation of discharge area depend on the frequency of the power source, (c) very low velocity and enriched uniform plasma production in wide space, almost 180mm in diameter, surrounded by multiple electrodes. Single-walled carbon nanotubes (SWCNT) are synthesized by using this new type of arc plasma reactor. The felt like SWCNTs shown in Fig.1 are observed in high yield on the wall inside of the reactor. SWCNTs obtained in high purity and high yields from the TEM image shown in Fig.2. The TEM image shown in Fig.3 has the inner diameter is about 1.5nm. The highest ratio of G-band (1580cm-1) and D-band (1360cm-1) measured by Raman spectrum is approximately 80. The catalyst was fed from the carbon electrodes containing 4.2%Atom-Ni and 1%Atom-Y respectively. The effects of gas pressure, kind of gas and total wattage of the reactor were investigated.

Fig.1 Felt like SWCNT

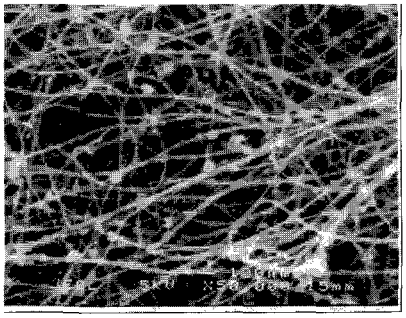

Fig.2 SEM image

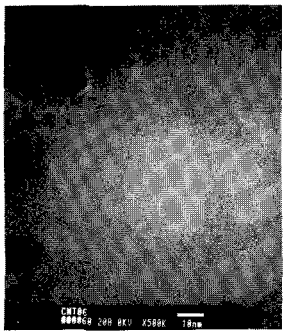

Fig.3 TEM image

References

[1] S. Iijima, Nature, 354, 56 (1991).

[2] K. Hata, et al, Science, Vol. 306, 19, Nov. (2004)

[3] T. Matsuura, et al, 17th Int. Sym. on Plasma Che. (2005)

[4] K. Matsumoto, et al, Proc. 6th International Coference on Reactive Plasma and 23rd Symposium on Plasma Processing (2006)

[5] T. Matsuura, et al, thin Soid Films, 515, 4240-4246 (2007)

Corresponding Author: Tsugio Matsuura

E-mail: Tsugio_Matsuura@fklab.fukui.fukui.jp

Tel: 0776-55-0664 Fax: 0776-55-0665

Effective Separation of Carbon Nanotubes and Metal Particles from Pristine Raw Soot by Ultracentrifugation

○D. Nishide, Y. Miyata, K. Yanagi, T. Tanaka, H. Kataura

JST/CREST, Nanotechnology Research Institute, National Institute of Advanced Industrial Science and Technologies (AIST), Tsukuba, Ibaraki 305-8562, Japan

Recently, the toxicities of soot containing carbon nanotubes (CNTs) have been reported by some groups [1,2]. According to their reports, it seems that such soot is hazardous to the living body under specific conditions. However, the detailed mechanism of the apparent toxicity is still unknown, because the samples used were not perfectly pure; *i.e.* the soot synthesized or purchased as "carbon nanotubes" certainly includes impurities, such as amorphous carbons and metal particles. For better understanding, it is important to prepare impurity-free CNTs and impurity particles separately from the original raw soot.

Here, we propose an effective method to separate metal particles from pristine CNTs using micelle-wrapping ultracentrifugation. By using ultracentrifugation, the impurities were preferentially dropped, resulting high-purity SWNTs were obtained as shown in Fig. 1 and 2. Moreover, the advantage of this method is that the impurity particles can be collected as residual soot in the ultracentrifugation process without any losses, while the impurity particles were more or less chemically modified or disappeared using previous purification protocols. In this presentation, detailed protocols of the present technique and spectroscopic/morphological properties of the obtained materials will be discussed.

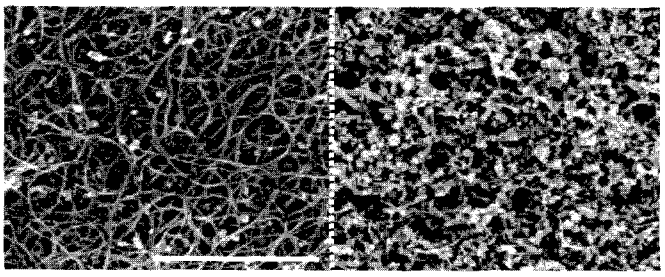

Fig. 1: SEM images of SWNTs (left) and residues (right) separated by the present process. Scale bar, 1μm.

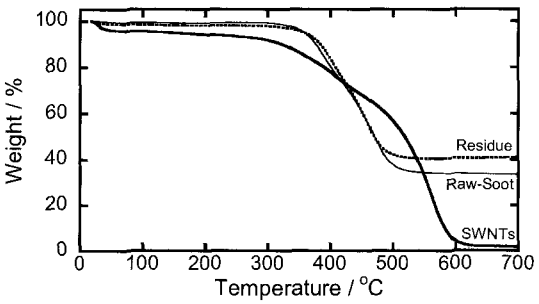

Fig. 2: TGA curves of the present materials

[1] A. Takagi *et al.*, *J. Toxicol. Sci.* **33** (2008) 105.

[2] C. A. Poland *et al.*, *Nature Nanotechnol.* **3** (2008) 423.

Corresponding Author: Hiromichi Kataura

E-mail: h-kataura@aist.go.jp

Tel:+81-29-861-2551 / **Fax:**+81-29-861-2786

Unidirectional Growth of Single-Walled Carbon Nanotubes

○Naoki Ishigami[1], Hiroki Ago[*,1,2,3], Tetsushi Nishi[1], Ken-ichi Ikeda[1], Masaharu Tsuji[1,2], Tatsuya Ikuta[4], and Koji Takahashi[4]

[1] *Graduate School of Engineering Sciences, Kyushu University, Fukuoka 816-8580, Japan*
[2] *Institute for Materials Chemistry and Engineering, Kyushu University*
[3] *PRESTO, Japan Science and Technology Agency, Saitama 332-0012, Japan*
[4] *Graduate School of Engineering, Kyushu University, Fukuoka 819-0395, Japan*

Horizontally-aligned single-walled carbon nanotubes (SWNTs) grown on single crystal sapphire (α-Al_2O_3) has attracted a great interest, because the SWNTs are oriented along a specific surface atomic arrangement of sapphire, due to anisotropic van der Waals interaction [1,2]. Recently, we found that the crystal plane affects not only the nanotube orientation but also the diameter and chirality, which can be developed to "epitaxial nanotube growth" [3].

It is known that the catalyst patterning offers the better alignment of longer SWNTs. Generally, the SWNTs grow from the catalyst pattern to both directions. Here, we report on the new growth mode, in which the SWNTs grow to only one side of the catalyst pattern, providing the unidirectional growth on sapphire. This unidirectional growth occurred irrespective of the gas-flow direction, and there was no change in the nanotube length (Figure 1). Our study suggests that the growth direction is determined in the early stage of nanotube growth, which signifying the strong influence of the sapphire surface. This unidirectional growth mode would contribute to the formation of advanced nanotube network for the future device applications.

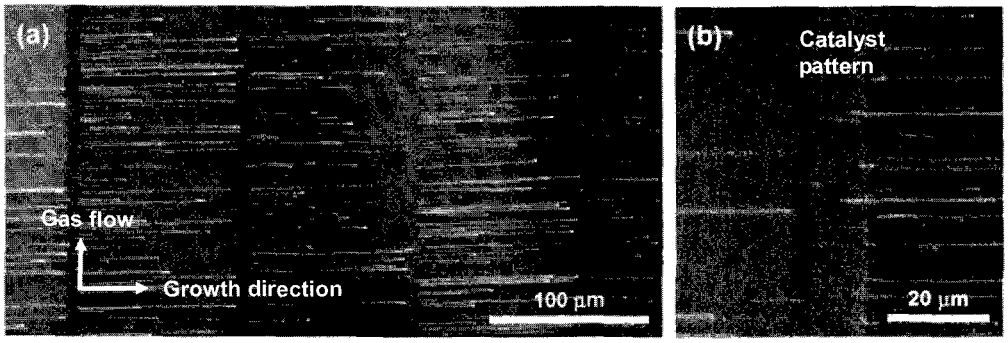

Figure 1 (a) Low- and (b) high-magnification SEM images of unidirectional aligned SWNTs on sapphire.

References: [1] H. Ago *et al.*, *Chem. Phys. Lett.*, **408**, 433 (2005). [2] S. Han *et al.*, *J. Am. Chem. Soc.*, **127**, 5294 (2005). [3] N. Ishigami *et al.*, *J. Am. Chem. Soc.* in press

Corresponding Author: Hiroki Ago (TEL&FAX: +81-92-583-7817, E-mail: ago@cm.kyushu-u.ac.jp)

Fabrication and Characterization of Telescope type Double walled Carbon Nanotubes

○Nobuyuki Fukui[1,2], Naoki Imazu[1], Keita Kobayashi[1], Hiromichi Yoshida[1], Shota Kuwahara[1], Toshiki Sugai[1*], Tomihiro Hashizume[2,3,4] and Hisanori Shinohara[1]

[1] *Dept. of Chem. & Inst. for Adv. Res., Nagoya Univ., Nagoya 464-8602, Japan*
[2] *WPI-AIMR, Tohoku Univ., Sendai 980-8577, Japan*
[3] *ARL, Hitachi Ltd. Hatoyama. 350-0395, Japan*
[4] *Dept. of Phys., Tokyo Institute of Technology, Tokyo 152-8522, Japan*

The Double Walled Carbon Nanotubes (DWNTs) which consist of only two layers, are good system for investigating interlayer interactions. Additionally, telescope type structure, which end of outmost tubes has been peeled off, helps us to use SPM measurements [1,2].

The telescope type Multi W alled Carbon Na notubes (T-MWNT) are comm on structure [3] and there have m any reports on preparation of T-MWNT by the electrical breakdown on device structure [4]. In contrast, Telescope type DWNT (T-DWNT) is very difficult to prepare and seldom reported.

This difficulty in prepar ation process of T -DWNT may ha ve origin in th eir stab ility of inne r tubes. Consider ing structural distortion of graphene sheets, smaller diam eter nanotube is unstable for their larger distortion. When a DWNT is exposed to high temperature, both inner and out er tube is dissociated at th e same time. To circumvent this situation, one of the answers is to introduce defect to outer tube. In this case, dissociation of outer tube is f ast and results in the residual single wall region, and may result in obtaining T-DWNT.

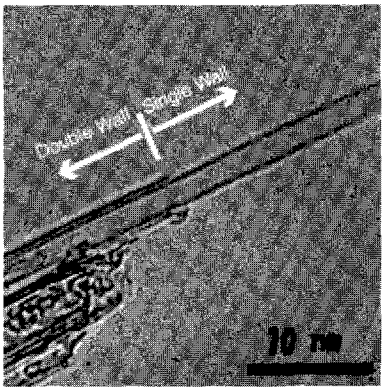

Fig. 1: HR-TEM image of T-DWNT

Here, we dem onstrate a new fabrication approach for obtaining T-DWNT by introduction of defects to outer tube. The hybrids of purified DWNT and Fe nano-particle are prepared by ultra-sonication in solve nt. After drying them , the sam ple was heated over 700 °C for a short time in ambient condition.

Figure 1 shows HR-TEM im age of obtained T -DWNT after removing Fe nano-particles by aci d. A part of outer tube is removed and clear single wall pa rt is observed. W e speculate that the heated Fe nano-particles, serving as catalyst, introd uce carbon defects on outer tube surface. The results support that the defective part of outer tube is easily oxidized and rem oved. In addition, DWNT which has partial single w all region w ere observed (F ig.2). This im age also supports selective oxidation and removal of defective outer tubes.

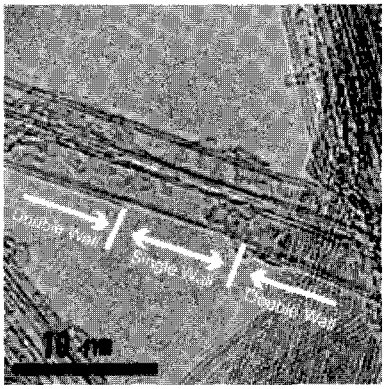

Fig.2: HR-TEM image of partial broken DWNT

[1]P. Ko walczyk *et.al.*, *Appl. Phys. A.*, **87**, 37 (2007) [2]N. Fuku i *et.al.*, T he abstract of the 33rd Fullerenes-Nanotube Symposium, Jul 11, 2007, Fukuoka, Japan [3]P. M. Ajayan *et.al.*, *Nature,* **362**, 522 (1993) [4] P. G. Collins *et.al.*, *Science*, **292**, 706 (2001)

***Present address**: Dept.of Chem., Toho Univ..*
Corresponding Author: Hisanori Shinohara
E-mail: noris@nagoya-u.ac.jp **Tel:** +81-52-789-2482 **Fax:** +81-52-747-6442

FT-IR Analysis in Alcohol Catalytic Chemical Vapor Deposition (2)

Tomohiro Shimazu[1], Yoshinobu Suzuki[1], Hisayoshi Oshima[1] and Shigeo Maruyama[2]
[1] *Research Laboratories, DENSO CORPORATION*
500-1 Minamiyama, Komenoki, Nisshin-shi, Aichi 470-0111, Japan
[2] *Depertment of Mechanical Engineering, The University of Tokyo*
7-3-1 Hongo, Bunkyo-ku, Tokyo 113-8656, Japan

Abstract:

Alcohol catalytic chemical vapor deposition (ACCVD) has become a popular CVD method for growth of high-purity single walled carbon nanotube (SWNT) films due to the low cost and easy handling of a non-hazardous CVD gas source [1]. Ethanol mainly decomposes into ethylene and water at CVD temperatures [2]. These thermally generated molecules could affect SWNT growth as is shown in ACCVD study [3]. We have investigated decomposed molecules behavior on the catalyst during ACCVD using Fourier Transfer infrared spectroscopy (FT-IR: Otsuka electronics IG-1000). FT-IR cell was inserted between a reactor tube and a vacuum pump (Fig.1). SWNT synthesis was performed using ethanol as a carbon source and Co/Mo bimetal as a catalyst. The behaviors of ethanol as a carbon source and ethylene, water, and carbon monoxide as the decomposed molecules on the catalyst have been reported by Shimazu *et.al*[4]. Water intensities show unusual behavior as is presented in Fig. 2. In the early stage of the reaction, water was generated by a catalytic reaction. After a few minutes, the behavior of water was changed from generation mode to consumption mode, which mode was continued during growth period. Finally, water was changed again to a generation mode.

We analyzed this behavior using three reaction models. (i) Generation of water at low active catalysts, (ii) Consumption of water by oxidation of amorphous carbons, and (iii) Generation of water by thermal decomposition of EtOH on the surface of SWNTs. Adjusting parameters of each mode to experimental data, the behavior of water is calculated as shown in Fig. 2. Good agreement was achieved and this result indicates validity of our reaction models.

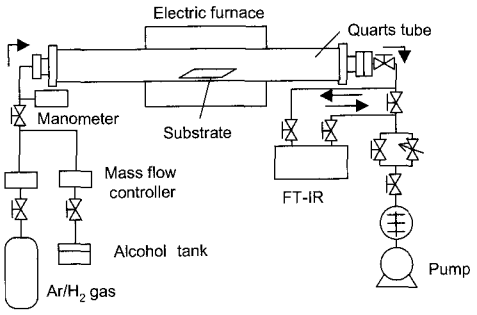

Fig.1 Schematic diagram of experimental apparatus for SWNT growth and ACCVD gas analysis.

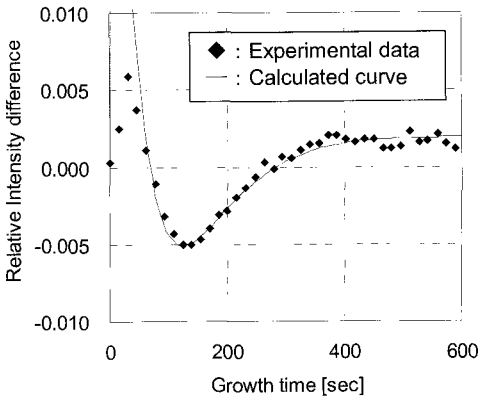

Fig. 2 Square points represent FT-IR water intensity difference measured with and without catalysts presence as function of growth time. The intensity is normalized by the intensity of ethanol at 2.7 kPa at RT. Solid line is the calculated data.

References:

[1] S. Maruyama *et al. Chem. Phys. Lett.*, **360**, 229 (2002)
[2] J. Herzler *et al. J. Phys. Chem.*, **101**, 5500 (1997)
[3] H. Oshima *et al. Jpn. J. Appl. Phys.*, **47**, 1982 (2008)
[4] T. Shimazu *et al. The 34th Fullerene-Nanotube General Symposium*, 2P-5 (2008)

Corresponding author: Hisayoshi Oshima
E-mail: hoosima@rlab.denso.co.jp
Tel.: +81-561-75-1860 **Fax.:** +81-561-75-1193

CNT growth on gas permeable substrates

Shinichi Mukainakano[1], Kenji Okeyui[1], Hisayoshi Oshima[1], and Shigeo Maruyama[2]

[1]*Research Laboratories, DENSO CORPORATION*
500-1 Minamiyama, Komenoki, Nisshin-shi, Aichi 470-0111, Japan
[2]*Depertment of Mechanical Engineering, The University of Tokyo*
7-3-1 Hongo, Bunkyo-ku, Tokyo 113-8656, Japan

Abstract

Different types of gas flow have been used for CNT growth. Usually the CNT are grown using gas flowing around the substrate. At such a condition the tubes can grow uniformly in CNT length in micrometers order. To grow CNT in higher orders the growth time can be extended. However, the length saturation at long time growth occurs. The reasons of saturation could be: catalyst degradation and/or lack of gas presence. On the other hand, when the length becomes in millimeter order the tube height profile becomes not uniform. [1] The reason of non-uniform height profile is that the gas can easily reach catalyst on the substrate on the side of the sample, while it is difficult to penetrate CNT forest in the substrate center. To eliminate these unwanted effects the new method called back supplied flow method is proposed. In this article we investigate possibility of CNT growth on gas permeable substrate using this new method

The CNT are grown using CVD method at atmosphere pressure in mixture of ethylene and argon gas with ratio of 1:1. The porous alumina sample with hole diameter of 0.2 μm, thickness of 100 μm and hole density of 50% of aluminum area is placed inside of the vertically positioned quartz tube. The 4 mm space between the quartz tube and substrate exists, thus the gas can flow over this slit and porous substrate. The temperature of 750°C is provided using IR heating system. The sample is coated by the iron catalyst using sputtering method. In the Fig.1 the CNT forest grown for 20 minutes on gas permeable alumina substrate is shown. The CNT are vertically aligned in the same direction as the gas flow over the permeable substrate. Advantage of the back supplied flow method consists of homogeneous gas distribution and supplying of fresh gas directly to the place of catalyst. Homogeneous gas distribution support same growth speed over the substrate area resulting in homogeneous CNT height profile. Fresh gas presence near the catalyst supports CNT growth for longer time and extends the growth time without length saturation.

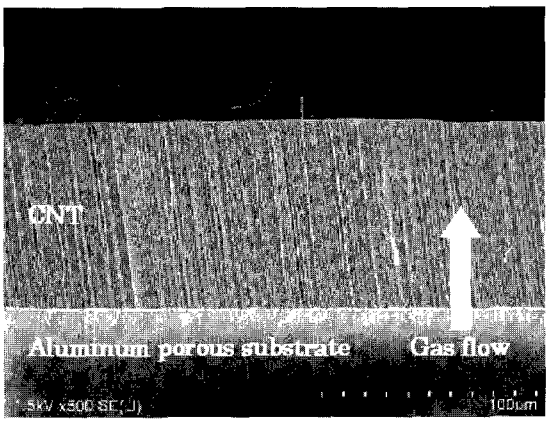

Fig1. SEM image taken in the middle of the substrate shows the CNT forest grown on the porous alumina .

In this work we verified possibility of CNT growth on gas permeable substrate using gas back supplied method.

References: [1] S. Noda, K. Hasegawa, H. Sugime, K. Kakehi, Z. Zhang, S. Maruyama and Y. Yamaguchi: Jap. J. Appl. Phys. **46**, 2007, pp L399-L401

Corresponding Author: Hisayoshi Oshima
E-mail: hoosima@rlab.denso.co.jp Tel.: +81-561-75-1860 Fax.: +81-561-75-1193

Super-Growth: Large Area Synthesis of SWNTs -Toward Industrial-scale Production-

○Satoshi Yasuda, Don N. Futaba,
Motoo Yumura, Sumio Iijima, and Kenji Hata

[1]*Nanotube Research Center, National Institute of Advanced Industrial Science and Technology (AIST), Tsukuba, 305-8576, Japan*

With the increasing utilization of vertically aligned carbon nanotube (CNT) forests, [1, 2] large area substrate-based synthesis of CNTs is widely being investigated for both application development and mass-production. However, while CNTs within the forests possess high-purity, vertical alignment, and millimeter-scale height and reports of highly efficient synthesis methods, such as "super-growth" [3, 4] show promise as a means for large scale production, intrinsic obstacles arise as a result of using substrates. Critical to large area growth is maintaining growth uniformity and high growth efficiency throughout the substrate area, both, of which, have direct consequence on the cost and potential application of forests. In order to overcome this obstacle, a well mixed feed gas uniformly supplied to substrate is key.

Here, we demonstrate the use of a new gas feeding system for the large area synthesis of super-growth SWNTs. In this study, using a prototype gas supply system, we examined the benefits in various aspects, from quality to scaled-up synthesis. Without the supply system, effects on the substrates downstream become obvious as the critical balance of gases changes as gas species are consumed by preceding samples. In contrast, with the gas shower, results show that yield, quality, uniformity, and catalyst lifetime can all be improved. This technique represents an important step in the scaling-up of forests synthesis toward industrial-scale production.

[1] D. N. Futaba, K. Hata, T. Yamada, T. Hiraoka, Y. Hayamizu, Y. Kakudate, O. Tanaike, H. Hatori, M. Yumura, and S. Iijima, *Nature Material* 2006, **5**, 987

[2] Y. Hayamizu, T. Yamada, K. Mizuno, R. C. Davis, D. N. Futaba, M. Yumura, and K. Hata, *Nature Nanotechnology.*2008, **3**, 289

[3] K. Hata, D. N. Futaba, K. Mizuno, T. Namai, M. Yumura, and S. Iijima, *Scinece* 2004, **306**, 1362

[4] D. N. Futaba, K. Hata, T. Yamada, K. Mizuno, M. Yumura, S. Iijima, *Phys. Rev. lett.* **2005**, *95*, 056104-1.

Corresponding Author: Kenji Hata

TEL: +81-29-861-4656 , FAX: +81-29-861-4851, E-mail: kenji-hata@aist.go.jp

1P-48

Title: Rotating fullerene chains in carbon nanopeapods

Author's name: Jamie H. Warner[1*], Yasuhiro Ito[1], Mujtaba Zaka[1], Ling Ge[1], Takao Akachi[2], Haruya Okimoto[2], Kyriakos Porfyrakis[1], Andrew A. R. Watt[1], Hisanori Shinohara[2], G. Andrew D. Briggs[1]

Author's address & Affilication:

[1]*Department of Materials, Quantum Information Processing Interdisciplinary Research Collaborationr, University of Oxford, Parks Rd, Oxford, OX1 3PH, United Kingdom.*

[2]*Department of Chemistry and Institute for Advanced Research, Nagoya University, Furo-Cho, Chikusa-ku, Nagoya, 464-8602, Japan.*

Abstract: The rotation of fullerene chains in SWNT peapods is studied using low-voltage high resolution transm ission electron m icroscopy. An isotropic fullerene chain structures (i.e C_{300}) are form ed in-situ in carbon nano-peapods via electron beam induced coalescence of individual fullerenes (i.e C_{60}). A low electron accelerating voltage of 80 kV is us ed to prevent damage to the SW NT. The larg e a symmetric C_{300} fulle rene stru cture e xhibits translational motion inside the SWNT and unique cork-screw like rota tion m otion. Another asymm etric fullerene chain containing mixed fullerene species is prepared by fusing smaller C_{60} fullerenes to a large r $Sc@C_{82}$ fullerene and this also exhibits co rk-screw rotational m otion. Chains of $Sc_3C_2@C_{80}$ in SWNT peapods adopt a zig-zag packi ng structure and the entire zig-zag chain rotates ins ide the SW NT to induce stru ctural m odifications to the SW NT diam eter and cross-sectional shape o f the SWNT. The expans ion and contraction of the diam eter of the SWNT is measured as 17%, demonstrating nano-actuation behaviour in carbon nano-peapods.

References: Times 10pt, Left

Corresponding Author: Jamie H. Warner
E-mail: Jamie.warner@materials.ox.ac.uk
Tel & Fax

Fabrication of Metal-Nanowire in Carbon Nanotube via Nano-Template Reaction Using Various Mono-, Di-, Tri-Metallofullerenes and Metal-Carbide Fullerenes Peapods

○ Naoki Imazu[1], Ryo Kitaura[1], Keita Kobayashi[1], Haruya Okimoto[1], Yasuhiro Ito[1], Takeshi Saito[2,3] and Hisanori Shinohara[1]

[1]*Department of Chemistry & Institute for Advanced Research, Nagoya University, Nagoya 464-8602, Japan*
[2]*Reseach Center for Advanced Carbon Materials, AIST, Tsukuba 305-8565, Japan*
[3]*PRESTO, Japan Science and Technology Agency, Kawaguchi 332-0012, Japan*

Single-wall carbon nanotubes (SWCNTs) have an ideal nanometer-scale and one-dimensional internal space where unique low-dimensional nanomaterials can be encapsulated and synthesized. Very recently, we have developed a nano-template reaction (NTR) technique to fabricate metal-nanowires by using SWCNTs and endohedral metallofullerenes[1]. In the NTR, one-dimensional arrays of $Gd@C_{82}$ inside SWNTs (i.e., peapods) were converted to Gd-nanowires encapsulated in double-wall carbon nanotubes (DWCNTs) by high-temperature heat treatment. The NTR can in principle be applied to a wide variety of endohedral metallofullerene peapods including various mono-, di-, tri-metallofullerenes and metal-carbide fullerenes peapods. For example, HRTEM image of Ce-nanowire@DWCNTs synthesized by the NTR using $(Ce@C_{82})$@SWCNTs is shown in figure 1. Dark spots aligned linearly inside the carbon nanotube correspond to Ce atoms, which are confirmed by EDX spectrum shown in figure 2. Moreover, alloy-nanowires can be synthesized using mixtures of different types of endohedral metallofullerenes.

We will report detailed structural study of some metal-nanowire in DWCNTs, which is based on HRTEM observation and image simulation of various metal-nanowires synthesized by the NTR.

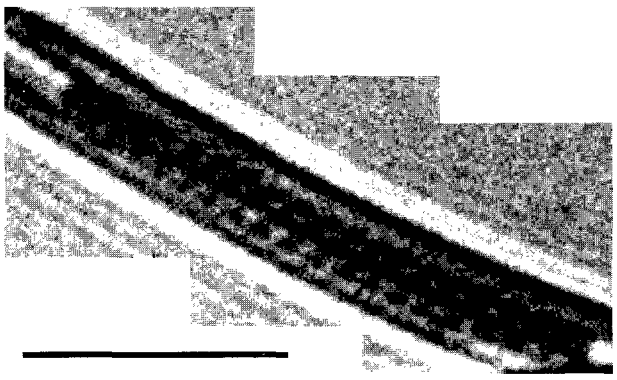

Figue.1 HRTEM image of Ce-nanowire@DWCNTs (Scale bar : 5 nm)

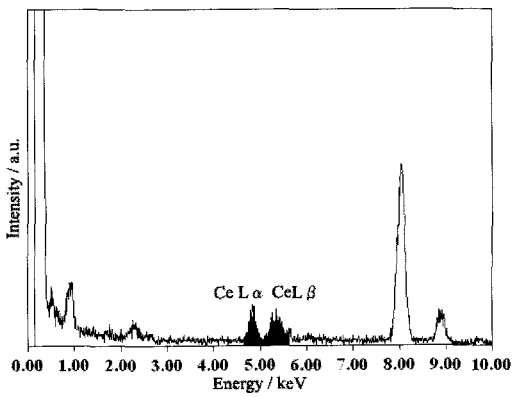

Figue.2 EDX spectrum obtained from Ce-nanowire@DWCNTs

References:[1] R. Kitaura, N. Imazu, K. Kobayashi and H. Shinohara., *Nano. Lett.* 8, 693(2008).

Corresponding Author: Hisanori Shinohara
TEL: +81-52-789-2482, FAX: +81-52-789-6442, E-mail: noris@nagoya-u.jp

1P-50

Motion of ssDNA inside the single-wall nanotube studied by electron microscopy

○ Masayuki Shoda, Yusei Maruyama[1], Shunji Bandow, Sumio Iijima

Department of Materials Science and Engineering, Meijo University, 1-501 Shiogamaguchi, Tenpaku, Nagoya 468-8502, Japan

[1] *Research Center for Micro/Nano Technology, Hosei University, Midorichou, Koganei, Tokyo 184-0003, Japan*

Electron m icroscopic stud y of single stranded DNA (ssDNA) in th e single wall carbon nanotube (SWNT) is int roduced. Insertion of ssDNA (a SIGMA, singl e stranded from calf thymus) was carried out by adding the open ended SWNTs (originally from a Meijo NanoCarbon) into aqueous solution of ssDNA. Observation of ssDNA in the SWNT was conducted by using a JEOL 2010F field emission electron microscope operated at 120 kV and the images were recorded by CCD cam era (Oly mpus Soft Im aging solu tions VELETA). Snap shots of ssDNA@SWNT are shown in the top line of Fig. 1. From these im ages, one can plainly find random m otion of stranded elem ent in the tube as illu strated in th e figure. These m otions, we consi der, were triggered by electron beam irradiation. As is well known, the back-bone of DNA is ne gatively charged, an d hence it is natural to consider th e wrapping of ssDNA@SWNT in the ionic surfactant will more or less m odify the m ovement of ssDNA. In the m iddle line of Fig.1, snap shots of a wrapped ssDNA@SW NT in anionic surfactant (SDBS) are in dicated. For anioni c surfactant, negatively char ged side or neutral si de chain will adhere to the nanotubes, so that the interaction between adhered surfactant and ssDNA i s somewhat repulsive. This m ay n ot suppre ss the motion of ssDNA, and thus one can identify the m ovement of ssDNA fro m the figure. In the bottom line of Fig. 1, we indicate a wrapped ssDNA@SWNT in cationic surfactant (benzalkonium chloride). In this case, the interaction will be attractive, so that the m ovement of ssDNA is suppressed. As expected, one can see som ewhat stabilized ssDNA in the figure.

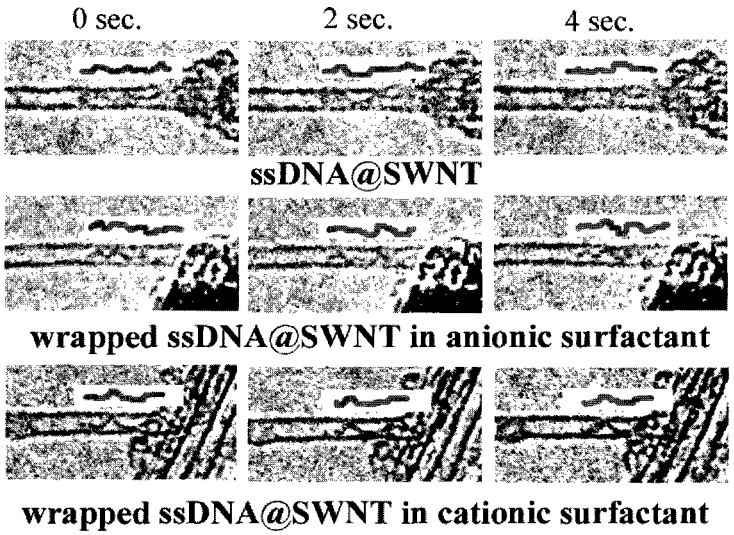

Fig. 1. Time traces of th e m otion of s sDNA ins ide th e S WNT. TEM images in the top line are taken for pristin e ssDNA inserted in SW NT (ssDNA@SWNT), and th e im ages in the m iddle li ne ar e for ssDNA@SWNT wrapped in anionic surfactant of SDBS. The bottom ones are for ssDNA@SWNT wrapp ed in cationic surfactant of benzalkonium chloride. Motions of ssDNA are illustrated in individual figures with thick solid lines.

Corresponding Author: Shunji Bandow,
E-mail: bandow@ccmfs.meijo-u.ac.jp, **Tel&Fax:** +81-52-834-4001.

1P-51

Phase behavior and fluid-wall interfacial tension of confined fluids

○Yoshinobu Hamada, Kenichiro Koga, and Hideki Tanaka

Department of Chemistry, Okayama University, Okayama 700-8530, Japan

When a fluid is confined in a nano pore, its properties are strongly affected by the pore size, shape, dimensionality, physical and chemical properties, etc. Structure and phase behavior of the fluid in such extreme confinement are qualitatively different from, and often much richer than, its bulk counterparts[1-3]. Our goal is to gain quantitative information on how each element that defines the pore is correlated with the phase behavior.

Components of the pressure tensor of a confined fluid are in general different from the equilibrium pressure of the bulk fluid, but how the pressure tensor is related with the bulk pressure has remained to be answered. Correlation between phase behaviors of a Lennard-Jones fluid in and out side a pore is examined for various thermodynamic conditions by grand canonical Monte Carlo simulations. A pressure tensor component of the confined fluid, a variable controllable in simulation but usually uncontrollable in experiment, is related with the pressure of a bulk homogeneous system in equilibrium with the confined system. It is found in the model systems that the component Px of the pressure tensor in the direction parallel to the slit-pore wall or to the axis of the cylindrical pore is linearly correlated with the equilibrium pressure P of the bulk fluid in a limited range of P, and the range becomes smaller with decreasing the pore size.

Effects of the pore dimensionality, size, and attractive potential on the correlations between thermodynamic properties of the confined and bulk systems are clarified. A fluid-wall interfacial tension defined as an excess grand potential is evaluated as a function of the pore size. It is found that the tension decreases linearly with the inverse of the pore diameter or width.

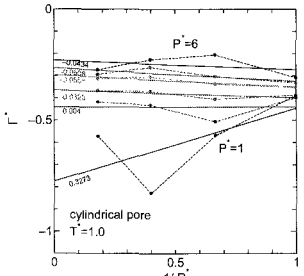

Fig. The amount of fluid adsorbed at the wall per unit area in cylindrical pore.

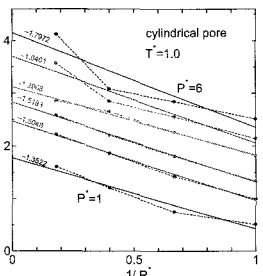

Fig The wall–fuid interfacial tension γ^* vs R^* in cylindrical pore.

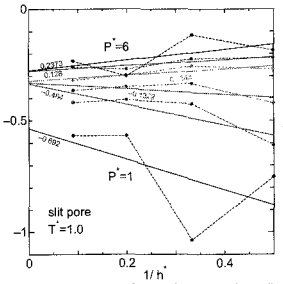

Fig. The amount of fluid adsorbed at the wall per unit area in slit pore.

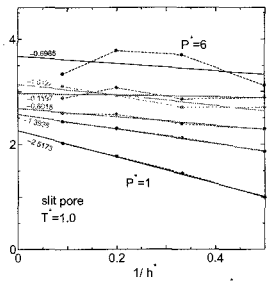

Fig The wall–fuid interfacial tension γ^* vs h^* in slit pore.

[1] L. D. Gelb and K. E. Gubbins and R. Radhakrishnan and M.Sliwinska-Bartkowiak, Rep. Prog. Phys., **62**, (1999).

[2] H. K. Christenson, J. Phys.: Condens. Matter., **13**, R95 (2001).

[3] K. Koga, G.T. Gao, H. Tanaka, and X.C. Zeng, Nature, **412**, 802 (2001)

Times 10pt, Left

Corresponding Author: Kenichiro Koga

E-mail koga@cc.okayama-u.ac.jp

Investigation of Electric and Mass Transport of a Copper Nano-Rod Encapsulated in a Carbon Nanotube

○Fumitaka Kimura[1], Koji Asaka[1], Hitoshi Nakahara[1], Fumio Kokai[2], Yahachi Saito[1]

[1]*Department of Quantum Engineering, Nagoya University, Nagoya 464-8603, Japan*
[2] *Department of Chemistry for Materials, Mie University, Tsu 514-8507, Japan*

For the application of copper filled carbon nanotubes (CNTs) as electronic devices, we investigated the structure and electric property of the individual nanotubes with a transmission electron microscope (TEM).

Copper filled CNTs were synthesized by the laser vaporization of graphite containing copper [1]. CNTs were dispersed on a copper plate of 30 μm thickness. A tungsten needle was made contact with an individual CNT protruding from the copper plate inside a TEM. Electric voltage was applied between the copper plate and the tungsten needle, and the structural change was observed with a TV camera. Electric current was recorded concurrently with TEM images.

Figure 1 shows TEM images of structural change of a CNT. In Figure 1, the dark region at the bottom is the copper plate, which was used as an anode. The diameter and the length of the CNT are 18 nm and 256 nm, respectively. The CNT encapsulates a copper nano-rod partially. Some copper particles adhered to the nanotube on the upper side of Figure 1. When the applied voltage was raised to 1.4 V, the current was increased to 10 μA (Fig.1(a)), corresponding to the current density of 4.0×10^6 A/cm^2, and at the same time the copper nano-rod started to move in the direction from the anode to the cathode along the inner wall of the CNT (Figs.1(b)-1(c)). The current density is comparable to that observed for electromigration of iron in CNTs [2]. After the shrinkage of the copper nano-rod, an empty CNT was left. The total resistance increased with the movement of the copper nano-rod. The total resistances at the states shown in Figs.1(a)-1(c) were 140, 155, and 179 kΩ, respectively. It indicates that the copper nano-rod contributes to the current transport.

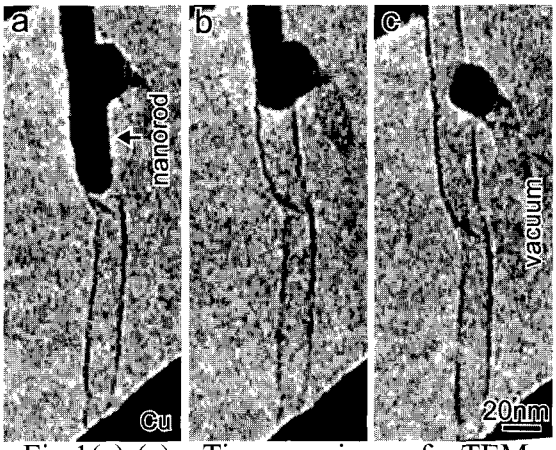

Fig.1(a)-(c) Time series of TEM images showing the flow of a copper nano-rod encapsulated in a carbon nanotube.

References:

[1] K. Adachi, A. Koshio, and F. Kokai, presented at the 38th Annual Meeting of Chemistry-Related Soc. In Chubu Area (2007), paper No, 2H19.

[2] K. Svensson, H. Olin, E. Olsson, Phys. Rev. Lett. 93, 145901(2004)

Corresponding Author: Fumitaka Kimura

E-mail: fumitaka@surf.nuqe.nagoya-u.ac.jp, **Tel&Fax:** +81-52-789-4659,+81-52-789-3703

Apoptosis Induction on HL-60 Cell by Cationic Fullerene Derivatives

○Sachiko Yokoo[1], Chiho Nishizawa[2], Kyoko Takahashi[1], Shigeo Nakamura[1], Tadahiko Mashino[1]

Department of Pharmaceutical Sciences, Faculty of Pharmacy, Keio University, Tokyo 105-8512, Japan
School of Pharmaceutical Sciences, Teikyo University, Sagamihara 229-0195, Japan

Recently, biological activities of fullerene derivatives related to the unique chemical properties attract a great deal of attention. We have synthesized many types of water-soluble fullerene derivatives and reported their biological effects.

We have already reported that cationic bis(*N*,*N*-dimethylpyrrolidinium)-derivative **NC$_1$2C$_0$** (Fig. 1) strongly inhibited *E. coli* growth and the mechanism is suggested to be respiratory chain inhibition [1]. **NC$_1$2C$_0$** also has an antiproliferative effect on human leukemic cell line (HL-60). This derivative also increased the DCF fluorescence intensity, the marker of intracellular oxidative stress. Pretreatment with α-tocopherol reduced **NC$_1$2C$_0$**-induced cell death and increase of DCF fluorescence intensity, respectively. These results suggest that **NC$_1$2C$_0$** increases intracellular reactive oxygen species level.

We also synthesized two series of cationic fullerene derivatives shown in Fig. 1. Alkyl chains are introduced at 2-position of pyrrolidinium ring of **NC$_1$2C$_0$** in **NC$_1$2C$_4$**, **NC$_1$2C$_6$** and **NC$_1$2C$_9$**, one methyl group on nitrogen is substituted by alkyl chain in **NC$_4$2C$_0$**, **NC$_7$2C$_0$** and **NC$_{10}$2C$_0$**, respectively. These derivatives also showed cytotoxicity on HL-60 cell, and the effectiveness was increased in the case of **NC$_7$2C$_0$** and **NC$_{10}$2C$_0$**. Apoptosis inducing activities evaluated by DNA fragmentation were higher when a longer alkyl chain was attached to **NC$_1$2C$_0$** at both positions (Fig. 2). The length of alkyl chain seems to affect the apoptosis induced by cationic fullerene derivatives.

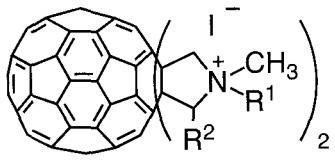

Compound	R^1	R^2
NC$_1$2C$_0$	CH_3	H
NC$_1$2C$_4$	CH_3	C_4H_9
NC$_1$2C$_6$	CH_3	C_6H_{13}
NC$_1$2C$_9$	CH_3	C_9H_{19}
NC$_4$2C$_0$	C_4H_9	H
NC$_7$2C$_0$	C_7H_{15}	H
NC$_{10}$2C$_0$	$C_{10}H_{21}$	H

Fig. 1 Cationic fullerene derivatives

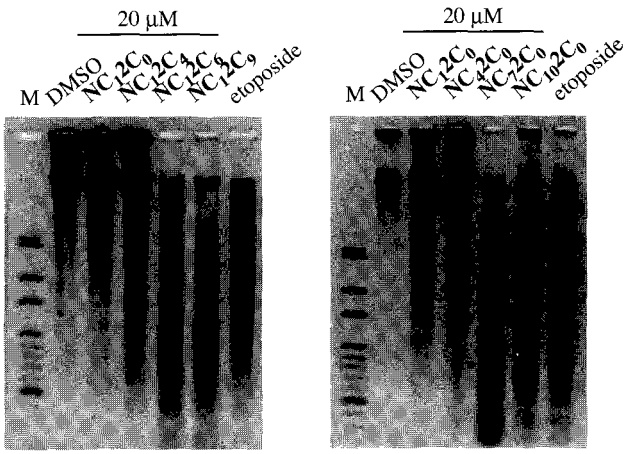

Fig. 2 DNA fragmentation by cationic fullerene derivatives

[1] T. Mashino, N. Usui, K. Okuda, T. Hirota, M. Mochizuki, *Bioorg. Med. Chem. Lett.* **11** (2003) 1433.

Corresponding Author: Tadahiko Mashino
E-mail: mashino-td@pha.keio.ac.jp
Tel: +81-3-5400-2694, **Fax:** +81-3-5400-2691

A Light-Emitting Cyclic Benzenoid as a Dendritic Core —Deca(carbazolylphenyl)[60]fullerene—

○Xiaoyong Zhang,[1] Yutaka Matsuo,[1] and Eiichi Nakamura[1,2]

[1]Nakamura Functional Carbon Cluster Project, ERATO, Japan Science and Technology Agency, 7-3-1 Hongo, Bunkyo-ku, Tokyo 113-0033, Japan, and [2]Department of Chemistry, The University of Tokyo, 7-3-1 Hongo, Bunkyo-ku, Tokyo 113-0033, Japan

The fullerene is one of the perfect choices for the core of dendrimers, since the fullerenes have three-dimensionally spherical structures and unique photophysical properties that can be controlled with modification of their large π-conjugated systems. We anticipate that the deca-adduct is a good candidate for the dendrimer cores. Because the deca-adducts possess three advantages: 1) unique photophysical properties due to its cyclic benzenoid structure: the highest fluorescence quantum yield (ϕ = 0.18)[1] among fullerene derivatives and long fluorescence lifetime. 2) unique three-dimensional structures with two concave space on theirs two ends, formed by each five aromatic units.[2] 3) ease of further modification of the molecules through the metal complexation in the concave cavity, and functionalization of the addends to obtain motifs for construction of supramolecular assembly.

Herein we report a dendritic deca(carbazolylphenyl)[60]fullerene bearing the cyclic π-system core. The carbazolylphenyl group was chosen as a dendron because the carbazole-based compounds have intense luminescence and electron-mobile ability, and serve as motifs for dendritic structures. The synthesis was performed as shown in Scheme 1. First, pentacarbazolylphenyl adduct (**1**) was synthesized in high yield (92%) from C_{60} by using a copper reagent, which was derived from a carbazolylphenyl Grignard reagent and $CuBr{\cdot}SMe_2$. Next, a further pentaaddition reaction was carried out from the penta-adduct **1** in the presence of pyridine[1] to obtain the dendritic deca-adduct (**2**, yield: 18%) with cyclic benzenoid structure. Unique photophysical properties of **2** including energy transfer and photoinduced charge transfer from carbazolyl antenna to the center π-system, high quantum yield, and so on will be reported. These details will be discussed at the meeting.

Scheme 1. Synthesis of deca-adduct.

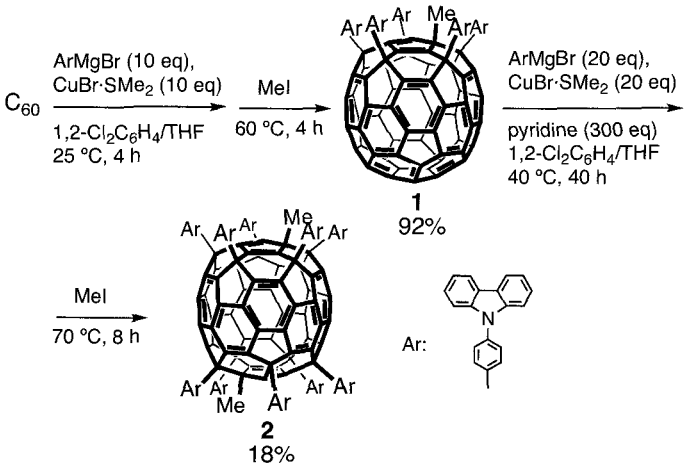

1) Matsuo, Y.; Tahara, K.; Morita, K.; Matsuo, K.; Nakamura, E. *Angew. Chem. Int. Ed.* **2007**, *46*, 2844.

2) Sawamura, M.; Kawai, K.; Matsuo, Y.; Kanie, K.; Kato, T.; Nakamura, E. *Nature*, **2002**, *419*, 702.

Corresponding Author: Yutaka Matsuo and Eiichi Nakamura

E-mail: matsuo@chem.s.u-tokyo.ac.jp; nakamura@chem.s.u-tokyo.ac.jp; Tel&Fax: (+81)-3-5841-1476

Electron Donor-Acceptor Interactions in Uniquely Shaped Double-Decker Buckyferrocenes

○Keiko Matsuo[1], Yutaka Matsuo[2], Dirk M. Guldi[3], and Eiichi Nakamura[1,2]

[1]*Department of Chemistry, The University of Tokyo, Hongo, Bunkyo-ku, Tokyo 113-0033, Japan*

[2]*Nakamura Functional Carbon Cluster Project, ERATO, Japan Science and Technology Agency, Hongo, Bunkyo-ku, Tokyo 113-0033, Japan*

[3]*Department of Chemistry and Pharmacy & Interdisciplinary Center for Molecular Materials, Friedrich-Alexander-Universität Erlangen-Nürnberg, Germany*

Donor-acceptor dyads capable of undergoing photoinduced energy or electron transfer are of current interest in areas of light-induced electron-transfer chemistry and solar-energy conversion. Fullerenes have been shown to be outstanding candidates for electron acceptors. As an electron donor, on the other hand, ferrocene and its derivatives have been integrated together with an electron-accepting fullerene in variable donor-acceptor conjugates. These compositions have been used to fine-tune the electronic coupling, orientation, and separation between donor and acceptor sites and the total reorganization energy. In our previous investigation[1] the results obtained during photophysical characterization of ferrocene/fullerene conjugates (i.e., mono-decker buckyferrocenes) were presented.

Herein, we take the uniquely shaped buckyferrocenes to the next level and report the physico-chemical properties of a novel series of conjugates, where now one fullerene shares two pentagons with two ferrocenes, $Fe_2(C_{60}Me_{10})Cp_2$ instead of just one pentagon. These conjugates are termed double-decker buckyferrocenes. In particular, we have focused on the characterization of two isomers of the double-decker buckyferrocenes conjugates, that is, a previously reported, highly symmetric D_{5d} and the newly synthesized, lower symmetric C_{2v} analog to fine-tune charge transfer and intervalence charge transfer transitions.

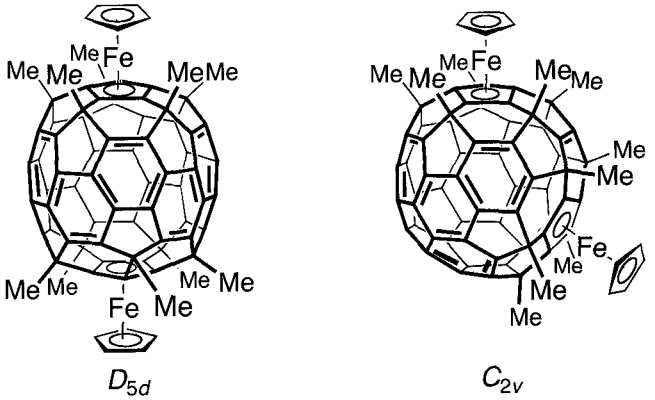

Figure 1. Structural formulas of the highly symmetric D_{5d} and lower symmetric C_{2v} $Fe_2(C_{60}Me_{10})Cp_2$.

[1] (a) D. M. Guldi, G. M. A. Rahman, R. Marczak, Y. Matsuo, M. Yamanaka, and E. Nakamura, *J. Am. Chem. Soc.* **2006**, *128*, 9420. (b) Y. Matsuo, K. Matsuo, T. Nanao, R. Marczak, S. S. Gayathri, D. M. Guldi, and E. Nakamura, *Chem. Asian J.* **2008**, *3*, 841.

Corresponding Author: Yutaka Matsuo and Eiichi Nakamura

TEL/FAX: +81-3-5841-1476; E-mail: matsuo@chem.s.u-tokyo.ac.jp; nakamura@chem.s.u-tokyo.ac.jp

Synthesis of Penta(organo)[60]fullerenes Methacrylates

○Hiromi Oyama, Yutaka Matsuo, and Eiichi Nakamura

Department of Chemistry, The University of Tokyo, Hongo, Bunkyo-ku, Tokyo 113-0033, Japan

Japan Science and Technology Agency, ERATO, Nakamura Functional Carbon Cluster Project, Hongo, Bunkyo-ku, Tokyo 113-0033, Japan

Regioselective multiple addition reactions to [60]fullerene are of great importance in fullerene chemistry. We have reported many functional materials using penta-addition reactions [1]. [60]Fullerene-containing polymers have been attracted interests because these polymers are expected to show unique electrochemical and physical properties [2]. Additionally, we anticipate that these polymers can be used to immobilize fullerene containing thin films that are recently emerging materials in organic photovoltaics and organic field effect transistor applications.

In the present study, [60]fullerene was first reacted with an organo-copper reagent that was prepared from *n*-BuC_6H_4MgBr and $CuBr{\cdot}SMe_2$. The penta-addition reaction was terminated with trimethylsilyl chloride, followed by deprotection of the trimethylsilyl group with aqueous HCl, to produce the compound **1** in good yield. Next, obtained alcohol **1** was treated with methyl methacroyl chloride in the presence of triethylamine in CH_2Cl_2 to afford ester **2** in moderate yield. The detail synthesis and properties will be discussed in the presentation.

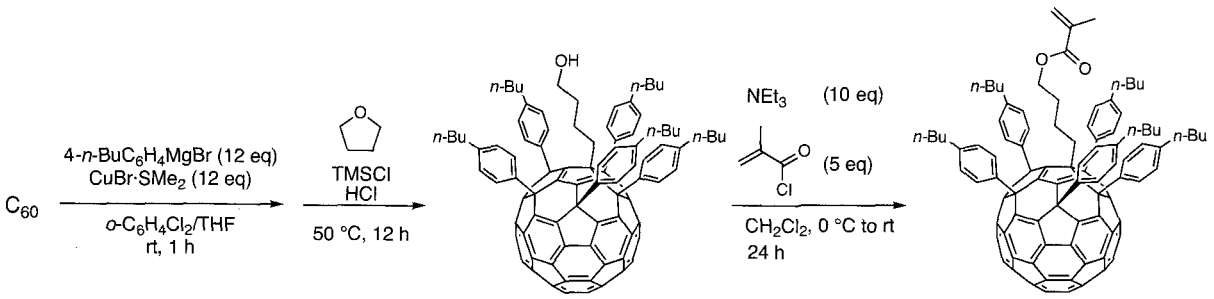

[1] (a) Y. Matsuo and E. Nakamura, *Chem. Rev.*, in press. (b) E. Nakamura and H. Isobe, *Acc. Chem. Res.*, **2003**, *36*, 807. (c) Y. Matsuo, A. Muramatsu, K. Tahara, M. Koide, and E. Nakamura, *Org. Synth.*, **2006**, *83*, 80.

[2] F. Giacalone and N. Martin, *Chem. Rev.*, **2006**, 106, 5136.

Corresponding Author: Yutaka Matsuo and Eiichi Nakamura

TEL/FAX: +81-3-5841-1476; E-mail: matsuo@chem.s.u-tokyo.ac.jp; nakamura@chem.s.u-tokyo.ac.jp

Enhanced Photoluminescence from Mono- and Di-Thulium Metallofullerenes

○Noriko Izumi[1], Masahiro Akachi[1], Yasuhiro Ito[1], Toshiya Okazaki[2], Ryo Kitaura[1], Toshiki Sugai[1,*] and Hisanori Shinohara[1]

[1]*Department of Chemistry & Institute for Advanced Reseach, Nagoya University, Nagoya 464-8602, Japan*

[2]*Research Center for Advanced Carbon Materials, National Institute of Advanced Industrial Science and Technology (AIST), Tsukuba 305-8565, Japan*

It is well known that the photoluminescence (PL) from thulium ion depends on its valence state such as 1,800 nm for Tm^{3+} ($^3F_4 \rightarrow {}^3H_6$ transition) and 1,200 nm for Tm^{2+} ($^2F_{5/2} \rightarrow {}^2F_{7/2}$ transition). However, it has been difficult to measure Tm^{2+} emission due to an electronic instability in various environments. Therefore, the investigation of photoluminescence properties on thulium metallofullerenes should be interesting since encapsulated metal atoms in fullerenes often exhibit unique valence states compared to those in the conventional bulk state[1].

It has been reported[2] that encapsulated thulium ions show trivalent states in $Tm_2@C_{82}$. In contrast, we have found, for the first time, that mono-thulium metallofulerenes such as $Tm@C_{88}$ are in divalent states. By using such Tm metallofullerenes, the PL property of Tm^{3+} can be compared with Tm^{2+} under a similar endohedral metallofullerene environment.

Here we report the first production, isolation and observation of some unique PL properties of series of Tm metallofullerenes: $Tm@C_{88}$(I, II, III), $Tm_2@C_{82}$(C_s(6), C_{2v}(9), C_{3v}(8)) and $(Tm_2C_2)@C_{82}$(C_s(6), C_{2v}(9), C_{3v}(8)). We propose a probable emission mechanism of Tm metallofullerenes in comparison with the reported Er^{3+} in $(Er_2C_2)@C_{82}$(C_{3v}(8))[3].

Figure1 shows the emission spectra of $Tm@C_{88}$(III) and $(Tm_2C_2)@C_{82}$(C_{3v}(8)) in CS_2 solution at room temperature. The excitation wavelengths of $Tm@C_{88}$(III) and $(Tm_2C_2)@C_{82}$(C_{3v}(8)) were 420 nm and 800 nm, respectively. The observed PL at 1,200 nm arises from the $^2F_{5/2} \rightarrow {}^2F_{7/2}$ transition of Tm^{2+} in $Tm@C_{88}$(III), whereas the 1,800 nm PL peak is due to the $^3F_4 \rightarrow {}^3H_6$ transition of Tm^{3+} in $(Tm_2C_2)@C_{82}$(C_{3v}(8)). These results can provide the first useful information on the PL mechanism of both Tm^{3+} and Tm^{2+} in almost the same fullerene environments.

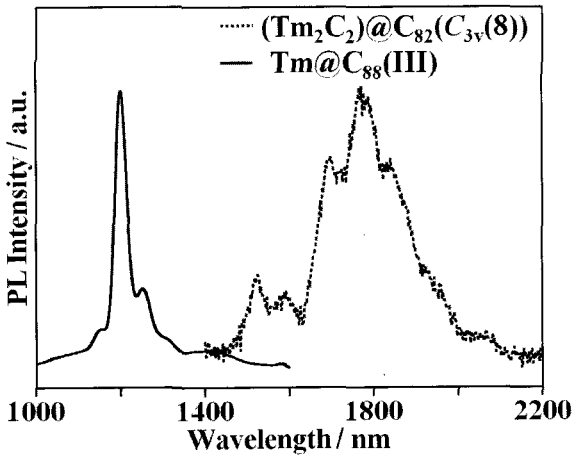

Figure 1
Emission spectra of $Tm@C_{88}$(III) and $(Tm_2C_2)@C_{82}$(C_{3v}(8))

*Present address: Dept. of Chemistry, Toho Univ.

[1] H. Shinohara, *Rep. Prog. Phys.*, **63**, 843 (2000).

[2] K. Kikuchi *et al.*, *Chem. Phys. Lett.*, **319**, 472 (2000).

[3] Y. Ito *et al.*, *ACS Nano*, **1**, 456 (2008).

Corresponding Author: Hisanori Shinohara

TEL: +81-52-789-2482, **FAX**: +81-52-747-6442, **E-mail**: noris@nagoya-u.jp

Bis-adduct of Non-IPR La@C_{72}

○ Tsuyoshi Ito[1], Hidefumi Nikawa[1], Takeshi Akasaka*[,1], Midori O. Ishitsuka[1], Takahiro Tsutiya[1], Zdenek Slanina[1,] Naomi Mizorogi[2], Shigeru Nagase[2]

[1]*Center for Tsukuba Advanced Research Alliance, University of Tsukuba, Tsukuba, Ibaraki 305-8577, Japan,*
[2]*Department of Theoretical and Computational Molecular Science, Institute for Molecular Science, Okazaki, Aichi 444-8585, Japan*

Abstract:

The chemical modification of endohedral metallofullerenes has attracted much attention, because the chemical properties of endohedral metallofullerenes are different from those of empty fullerenes due to an electron transfer from the encaged metal to fullerene cage.[1,2] Since the first exohedral adduct of La@C_{82} was reported in 1995,[3] the various kinds of endohedral metallofullerene derivatives have been successfully synthesized by several reactions, and some of these have been isolated and structurally characterized.[3,4] Most reported studies have been focused on the mono-adduct of endohedral metallofullerenes, while only a couple of papers are available for the bis-adduct of endohedral metallofullerenes[5,6]. The controlled synthesis of the bis-adducts of the endohedral metallofullerene may open a door to form the basis for the tailor-made design of a large variety of functionalized endohedral metallofullerene derivatives. Apparently, the investigation on the bis-adducts of endohedral metallofullerenes is a new hot topic in the fullerene chemistry. However, the bis-adduct of endohedral metallofullerenes with different substituents have not yet been reported. Recently, we have succeeded in the extraction, isolation and characterization of La@C_{72} as a derivative, La@C_{72}($C_6H_3Cl_2$)[7], which has a non-IPR cage. Non-IPR metallofullerene is one of the most interesting topics in the fullerene science. To the best of our knowledge, there is no report for the reactivity of non-IPR fullerene.

We herein report for the first time the synthesis and characterization of the bis-adduct of endohedral metallofullerene, La@C_{72}($C_6H_3Cl_2$)Ad. La@C_{72}($C_6H_3Cl_2$)Ad was prepared from the selective photochemical reaction of La@C_{72}($C_6H_3Cl_2$), with 2-adamantane-2,3-[3H]-diazirine. The reactivity of non-IPR metallofullerene derivative, La@C_{72}($C_6H_3Cl_2$), will be discussed on the basis of theoretical calculation.

References:

[1] *Endofullerenes: A New Family of Carbon Clusters;* Akasaka T. and Nagase S., Eds.; Kluwer: Dordrecht, The Netherlands, 2002

[2] Tsuchiya, T. et al. *J. Am. Chem. Soc.* **2006**, *126*, 6699-6703.

[3] Akasaka, T. et al. *Nature* **1995**, *374*, 600-601.

[4] Mikawa, M. et al. *Bioconjugate Chem.* **2001**, *12*, 510-514.

[5] Stevenson, S. et al. *J. Am. Chem. Soc.* **2005**, *127*, 12776-12777

[6] Cai, T. et al. *J. Am. Chem. Soc.* **2008**, *130*, 2136-2137.

[7] Wakahara, T. et al. *J. Am. Chem. Soc.* **2006**, *128*, 14228

Corresponding Author: Takeshi Akasaka
Tel&Fax: +81-29-853-6409
E-mail: akasaka@tara.tsukuba.ac.jp

Synthesis and Properties of Endohedral Metallofullerene Ligands

○ Yuya Yokosawa, Takahiro Tsuchiya, Takeshi Akasaka

Center for Tsukuba Advanced Research Alliance, University of Tsukuba, Tsukuba, Ibaraki 305-8577, Japan

Abstract: Studies on donor-acceptor dyads capable of undergoing photoinduced electron or energy transfer are of current interest to mimic the primary events of the photosynthetic reaction center and also to develop molecular electronic devices.[1,2] Toward constructing such dyads, fullerenes are particularly appealing as electron acceptors because of their three-dimensional structure, low reduction potential, and absorption spectra extending over most of the visible region. The preparation of various non-covalently linked donor-acceptor systems by coordination of fullerene derivatives bearing a pyridine unit to metal porphyrins have been reported.[2] On the other hand, endohedral metallofullerenes have lower reduction potentials and form more stable anions compared to the empty fullerenes, which is because of an intramolecular electron transfer from encapsulated metal(s) to the carbon cage.[3] Recently, we have found the complexation behavior of the paramagnetic endohedral metallofullerene La@C_{82} with the organic molecules by electron transfer between them.[4,5,6] The facile electron transfer is characteristic of endohedral metallofullerenes.

In this context, we synthesized the endohedral metallofullerene ligand, which has pyridine moiety as a ligand part to metal complexes.

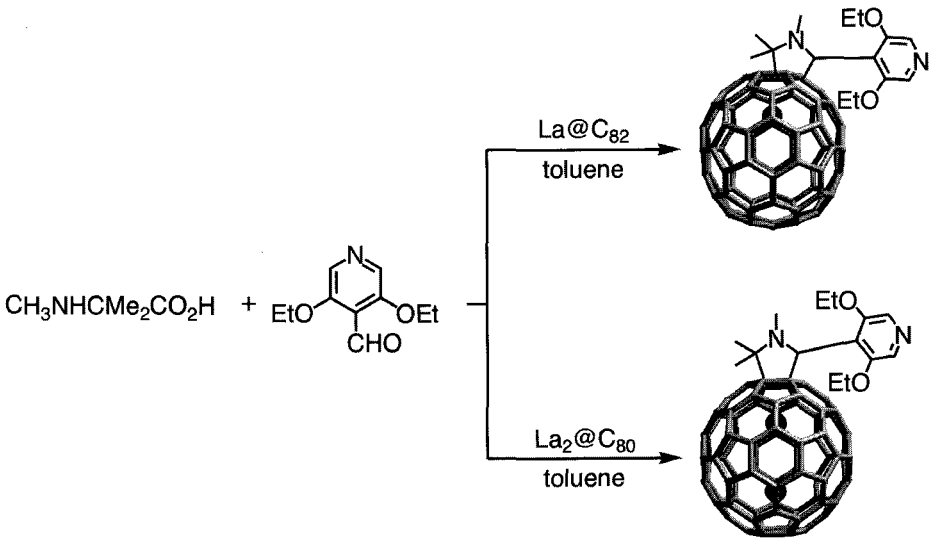

Reference:

(1) H. Imahori et al. *Eur. J. Org. Chem.* **1999**, 2445-2457.

(2) F. D'Souza et al. *J. Phy. Chem. B.* **2006**, *110*, 25240-25250

(3) T. Akasaka et al. *J. Am. Chem. Soc.* **2000**, *122*, 9316-9317

(4) T. Tsuchiya et al. *J. Am. Chem. Soc.* **2006**, *128*, 6699-6703

(5) T. Tsuchiya et al. *Chem. Commun.* **2006**, 3585-3587

(6) T. Tsuchiya et al. *J. Am. Chem. Soc.* **2006**, *128*, 14418-14419

Corresponding Author: Takeshi Akasaka

E-mail: akasaka@tara.tsukuba.ac.jp

Tel&Fax: +81-298-53-6409

Formation and Behavior of Supramolecular Complex based on Endhedral Metallofullerene

○ Ayumi Sato[1], Takahiro Tsuchiya[1], Takeshi Akasaka[1], Nazario Martin[2]

[1]*Center for Tsukuba Advanced Research Alliance, University of Tsukuba, Tsukuba, Ibaraki 305-8577, Japan*
[2]*Departmento de Quimica, Facultad de Quimica, Universidad Complutense, E-28040 Madrid, Spain*

Endofullerenes have attracted special interests with unique electronic properties and reactivities, which are not seen in empty fullerenes.[1] Among them, endohedral metallofullerenes are particularly interesting, because electron transfer from the encaged metal atom to the carbon cage takes place and this substantially alters electronic and magnetic properties and reactivities of fullerenes. The fact that endohedral metallofullerenes are more easily reduced than empty fullerenes is one of the most important factors to control their reactivities. On the other hand, the suplamolecular chemistry of *empty* fullerenes has been extensively investigated, and sophisticated host molecules for empty fullerenes have been synthesized. Recently, Martin and co-workers reported the complexation behavior of C_{60} with exTTF-diad and examined charge-transfer between C_{60} and exTTF-diad[2].Correspondingle, a suplamolecular systems based on endhedral metallofullerenes expected to exhibit predominant complexation and electron-transfer behavior[3]. In this context, we report here the complexation behavior of endohedral metallofullerenes La@C_{82} with exTTF-diad by electron-transfer in the ground state.

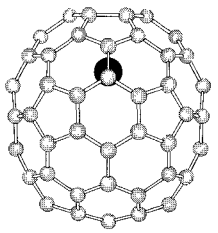

La@C_{82}

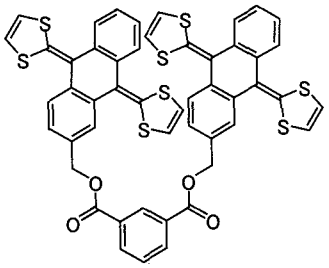

exTTF-diad

References:

[1] *Endofullerenes: A New Family of Carbon Clusters*; Akasaka, T.; Nagase, S., Eds.; Kluwer: Dordrecht, 2002.

[2] E. M. Perez, L. Sanchez, G. Fernandez, N. Martin *J. Am. Chem. Soc.* **2006**, *128*, 7172

[3] T. Tsuchiya, K. Sato, H. Kurihara, T. Wakahara, Y. Maeda, T. Akasaka, K. Ohkubo, S. Fukuzumi, T. Kato, S. Nagase *J. Am. Chem. Soc.* **2006**, *128*, 14418

Corresponding Author : Takeshi Akasaka
E-mail : akasaka@tara.tsukuba.ac.jp
Tel&Fax : +81-298-53-6409

Reversible and Regioselective Reaction of La@C_{82} with 1,2,3,4,5-Pentamethylcyclopentadiene

○ Satoru Sato,[1] Yutaka Maeda,[2] Koji Inada,[2] Michio Yamada,[1] Takahiro Tsuchiya,[1] Midori O. Ishitsuka,[1] Tadashi Hasegawa,[2] Takeshi Akasaka,*[,1] Tatsuhisa Kato,[3] Naomi Mizorogi,[4] Zdenek Slanina,[1] and Shigeru Nagase[4]

[1]Center for Tsukuba Advanced Research Alliance, University of Tsukuba, Tsukuba, Ibaraki 305-8577, Japan, [2]Department of Chemistry, Tokyo Gakugei University, Koganei, Tokyo 184-8501, Japan, [3]Department of Chemistry, Josai University, Sakado, Saitama 350-0295, Japan, [4]Department of Theoretical and Computational Molecular Science, Institute for Molecular Science, Okazaki, Aichi 444-8585,Japan

Endohedral fullerene is a new type of carbon cluster that contains one or more atoms inside the hollow fullerene cage. Especially, endohedral metallofullerenes have attracted special interest as the new spherical molecules because they have unique properties that are not seen in empty fullerenes.[1]

It is important to develop a reversible addition reaction of endohedral metallofullerenes, since reversible addition reaction is one of the useful methods for their separation[2] and template synthesis.[3] In this context, we reported the reversible and regioselective addition reaction of La@C_{82} with cyclopentadiene (Cp), in which the kinetic parameters for the retro–reaction of La@C_{82}(Cp) were determined.[4] This retro–reaction proceeds much faster than that of C_{60}(Cp). The fast retro–reaction has prevented detailed experimental characterization of derivative. Moreover, the reactivity between La@C_{82} and Cp was very low. Therefore, it is important to control the reactivity and the stability of adducts. In the reversible reaction, substituent effect is one of the important factors for controlling reactivity and stability of the adducts. It has been reported that an adduct of C_{60} with 1,2,3,4,5-pentamethylcyclopentadiene (Cp*) is more stable than C_{60}(Cp).[5]

Herein we demonstrate the reaction of La@C_{82} with Cp* to afford the mono–adduct. Cp* reacts much more readily with La@C_{82} than Cp does. The molecular structure of La@C_{82}(Cp*) is determined by the X-ray crystallographic analysis. In addition, the reaction mechanism of La@C_{82} with Cp* and the electronic properties of La@C_{82}(Cp*) are also discussed on the basis of theoretical calculation.

References:

[1] *Endofullerenes*: *A New Family of Carbon Clusters*; Akasaka, T., Nagase, S., Eds.; Kluwer Academic Publishers: Dordrecht, The Netherlands, 2002. [2] Nie, B. et al,. *J. Org. Chem. Soc.* **1996**, *61*, 1870. [3] Lamparth, I. et al,. *Angew. Chem., Int. Ed. Engl.* **1995**, *34*, 1607. [4] Maeda, Y. et al,. *J. Am. Chem. Soc.* **2005**, *127*, 12190. [5] Meidine, M. F. et al,. *J. Chem. Soc. Perkin Trans. 2*. **1994**. 1189.

Corresponding Author: Takeshi Akasaka
TEL & FAX: +81-29-853-6409, E-mail: akasaka@tara.tsukuba.ac.jp

2P-10

The external quantum efficiency of C_{60}/Zinc-porphyrin layered films

○Sou Ryuzaki[1], Toshihiro Kai[1], Toshiaki Nishii[2], and Jun Onoe[1,3]

[1]*Department of Nuclear Engineering, Tokyo Institute of Technology, Tokyo 152-8550, Japan*
[2]*Technology Development Center, Electric Power Development Co., Ltd. (J-Power), Kanagawa 253-0041, Japan*
[3]*Research Laboratory for Nuclear Reactors, Tokyo Institute of Technology, Tokyo 152-8550, Japan*

Organic thin-film photovoltaic (O-PV) cells consisting of electron- donor and acceptor molecules have been intensively investigated as a candidate for next-generation PV cells. However, their photo-energy conversion efficiency (η_E) is still low at most 6 % under a standard illumination condition (100 mW/cm^2, AM1.5). Metal porphyrin and C_{60} have often been used as an electron- donor and acceptor material, respectively. In particular, the interaction between octaethylporphyrins (OEPs) and C_{60} is strong. In addition, the η_E of a Schottkey-type PV cell using OEP [Al/H_2OEP/Ag] became lager by ten times than that using Pc [Al/MgPc/Ag].[1] This suggests that OEP is better than Pc as an electron-donor for fabrication of high-performance O-PV cells.

We recently examined the crystalliniy and molecular orientation of Zinc-octaethylporphyrin [Zn(OEP)] on SiO_2/Si and ITO substrates, because Zn(OEP) has a large absorbance in visible region and forms a multi-layered structure with C_{60}.[2] It was found that Zn(OEP) films with a thickness of more than 200 nm have two kinds of grains ("grain 1" with an interplane distance of d = 1.12 nm, "grain 2" with that of d = 1.24 nm). When the Zn(OEP) film is used for O-PV cells, a film thickness of less than 50 nm, which is comparable to the exciton diffusion length in the film, is suitable.[3] We also found that a 20 nm-thick Zn(OEP) film is amorphous, while a 40 nm-thick one has only "grain 1". In addition, the grain size (20 nm) was independent of film thickness and substrate temperature.

In the present study, we have fabricated two kinds of organic thin-film PV cells consisting of 20 nm or 40 nm-thick Zn(OEP) and 30 nm-thick C_{60} layered-structural films [ITO/Zn(OEP)/C_{60}/Al] and measured their external quantum efficiency (EQE). Both of them showed a spectral response corresponding to their individual photo-absorption spectra. The EQE of the cell using the 40 nm-thick Zn(OEP) film was obtained to be 13% at 400 nm, 6.6% at 545 nm, and 7.5% at 590 nm. These wavelength values correspond to the photo-absorption peaks of Zn(OEP). On the other hand, the EQE of the cell using the 20 nm-thick Zn(OEP) significantly increased to be 36% at 400 nm, 12% at 545 nm, and 14% at 590 nm. These results suggest that the grain boundaries inhibit the diffusion of excitons or free carriers for the former cell.

The present work has been financially supported by the collaboration research fund of J-Power.

[1] F. Kampas, M. Gouterman, *J. Phys. Chem.* 81. 690 (1977).
[2] S. Ryuzaki, T. Ishii, J. Onoe, *Jpn, J. Appl. Phys.* 46. 5363 (2007).
[3] P. Peumans, A. Yakimov, S. R. Forrest, Appl. Phys. Rev. 93. 3693 (2003)

Corresponding Author: Jun Onoe
E-mail: jonoe@nr.titech.ac.jp
Tel & Fax: +81-3-5734-3073,

Study of the Interaction between PMA-treated THP-1 Cells and FNWs

○Shin-ichi Nudejima[1], Kun'ichi Miyazawa[1],
Junko Okuda-Shimazaki[2] and Akiyoshi Taniguchi[2]

[1]*Fullerene Engineering Group, Advanced Nano Materials Laboratory, National Institute for Materials Science (NIMS), Tsukuba 305-0044, Japan*
[2]*Advanced Medical Material Group, Biomaterials Center, NIMS, Tsukuba 305-0044, Japan*

Because of their unique properties, nanomaterials possess enormous potentials of wide applications in various fields. But with release of industrial products of nanomaterials into environment, public concerns have raised their potential side effects. Carbon nanotubes (CNTs), one of the most promising nanomaterials, may be hazardous to health and environment owing to their needle-like morphology and strong mechanical properties like asbestos. Recent studies demonstrated that asbestos-like pathogenic behavior associated with CNTs indicates a structure-activity relationship based on length, to which asbestos and other pathogenic fibers conform [1].

Fullerene nanowhiskers (FNWs) are expected to have various application fields such as low-dimensional semiconductors, field emission tips, nanoprobes for microdevices, fiber-reinforced nanocomposites, composite elements for lubrication, and so on [2]. But FNWs are also needle-like crystals like asbestos. In this study, we investigate the interaction of FNWs with macrophages to evaluate toxicity of FNWs.

FNWs were prepared by the liquid-liquid interfacial precipitation method that uses an interface of a fullerene-concentrated toluene solution and isopropyl alcohol. The characterization was carried out by measuring FNWs' length and diameter using optical microscopy and scanning electron microscopy.

The human monocytic leukemia cell line THP-1 was cultured in RPMI 1640 medium supplemented with 10% heat inactivated FBS and penicillin/streptomycin. By the addition of phorbol 12-myristate 13-acetate (PMA), THP-1 cells were induced to differentiate to macrophage-like cells. PMA treated THP-1 cells were exposed to FNWs (mean diameter of about 660 nm; ranging from 300 nm to 1340 nm, mean length of about 6.0 μm; ranging from 1.1 μm to 17.0 μm).

Time-lapse microscopy observation was carried out to determine whether PMA treated THP-1 cells were capable of sensing and internalizing FNWs. Cells accumulated several FNWs in their intercellular spaces, and there was a possibility of phagocytosis of FNWs.

To reveal cells' capability of phagocytosis of FNWs, cells were fixed, stained with Hoeschst 33342 and rhodamine-phalloidin and observed by confocal laser scanning microscopy. We demonstrated that cells internalized FNWs by revealing FNWs in cells with differential interference contrast and confocal laser microscopy.

[1] C.A.Poland, R.Duffin, I.Kinloch, A.Maynard, W.A.H.Wallace, A.Seaton, V.Stone, S.Brown, W.Macnee and K.Donaldson, Nature Nanotechnology, ADVANCE ONLINE PUBLICATION 20 May 2008.
[2] K.Miyazawa, Y.Kuwasaki, A.Obayashi and M.Kuwabara, J.Mater.Res., **17 [1]**, 83 (2002).
Corresponding Author: Shin-ichi Nudejima
TEL: +81-29-851-3354 (EXT: 8463), FAX: +81+29-860-4667, E-mail: NUDEJIMA.Shinichi@nims.go.jp

First-principle calculations of the thorough electron states of one-dimensional peanut-shaped C_{60} polymers

○A. Takashima[1], T. Nishii[2], and J. Onoe[1,3]

[1] *Department of Nuclear Engineering, Tokyo Institute of Technology*
[2] *Technology Development Center, Electric Power Development Co., Ltd. (J-Power)*
[3] *Research Laboratory for Nuclear Reactors, Tokyo Institute of Technology*

When a C_{60} film is irradiated by electron-beam with an incident energy of 3 keV, C_{60} molecules are polymerized with each other to form a peanut-shaped C_{60} polymer that exhibits metallic *I-V* characteristics in air at room temperature [1]. As far as we know, this kind of polymer is the first example of π-electron conjugated systems with a negative Gauss curvature located in the waist region between adjacent C_{60} molecules [2]. Recently, we have found the polymer to be a one-dimensional (1D) metallic C_{60} polymer by *in situ* high-resolution photoelectron spectroscopy [3], and to exhibit the Peierls transition at around 50 K, which is a typical phenomenon of 1D metal, by femtosecond-resolved pump-probe spectroscopy [4].

To understand how the peanut-shape affects the π-electronic properties of the 1D metallic peanut-shaped C_{60} polymer, we first investigated the role of 7- and 8-membered rings located in the waist region for all the C_{120} stable isomers, which are a minimum unit of 1D polymer candidates, derived from the general Stone-Wales rearrangements [5], using the DV-Xα and Gaussian 2003 density-functional methods. DV-Xα calculations indicate that both 7- and 8-membered rings in the waist region of those C_{120} models constitute the HOMO (see Fig. 1), and that positive and negative effective charges tend to be localized at the 7- and 8-membered rings, respectively. We will discuss the details of the present results.

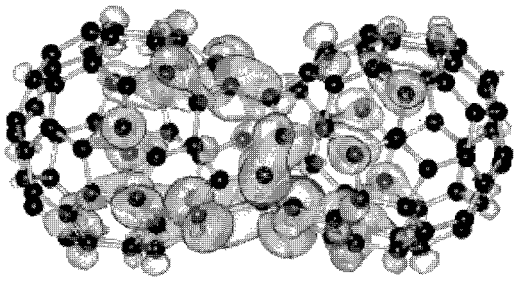

Fig.1 The HOMO of id07 stone-wales model constituted by the 7- and 8-membered ring in the waist region.

[1] J. Onoe et al., Appl. Phys. Lett. **82**, 595 (2003).
[2] J. Onoe, IEEJ Transactions on Electronics, Information and Systems **127**, 1324 (2004).
[3] T. Ito, J. Onoe, and S. Kimura, unpublished data.
[4] Y. Toda, S. Ryuzaki, and J. Onoe, Appl. Phys. Lett. **92**, 094102 (2008).
[5] H. Ueno et al., Fullerene Sci. Tecnol. **6**, 319 (1998).

Corresponding author: Prof. Jun Onoe
Tel/Fax: +81-3-5734-3073, E-mail: jonoe@nr.titech.ac.jp

First principles study of electron transport properties of Double-Decker Buckyferrocene

○Yoshihisa Ohshima

Cybernet Systems Co., Ltd.
FUJISOFT Bldg. 3 Kanda-neribeicho, Chiyoda-ku, Tokyo 101-0022, Japan

A double-decker buckyferrocene, $Fe_2(C_{60}Me_{10})Cp_2$ (see Figure 1), has been synthesized by Y. Matsuo, K. Tahara, and E. Nakamura as a functional molecule [1]. This kind of compound is expected to act as an active component for molecular devices. In this study, we analyzed the electron transport properties of a double-decker buckyferrocene. To reduce the computational cost of the calculation, the structure of $Fe_2(C_{60}Me_{10})Cp_2$ was simplified by replacing all of the $-CH_3$ residues to one hydrogen atom, so the practical molecular formula for calculations become $Fe_2(C_{60}H_{10})Cp_2$. The model used for calculations is shown in Figure 2. This system consists of two semi-infinite Au(111) electrodes and $Fe_2(C_{60}H_{10})Cp_2$ positioned between two electrodes

For all analyses of the electron transport properties, the nonequilibrium Green's function (NEGF) formalism combined with the density functional theory (DFT), implemented in the Atomistix ToolKit (ATK) program [2-3], was used. The main feature of ATK is to calculate electrical properties of nanostructures coupled to semi-infinite electrodes under a finite bias voltage. So, not only the transmission spectra but I-V character of our system was calculated by using ATK. In Figure 3, a transmission spectrum at bias voltage 0.5V is shown as an example. Moreover, through the calculations of MPSH (Molecular Projected Self-consistent Hamiltonian) eigenstates, we discussed relation between the channels for transmission and the molecular orbitals. Finally, we mentioned the difference of the transport properties between $Fe_2(C_{60}H_{10})Cp_2$ and C_{60} [4].

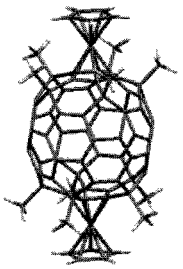

Fig. 1. Geometry of a double-decker bukyferrocene, $Fe_2(C_{60}Me_{10})Cp_2$.

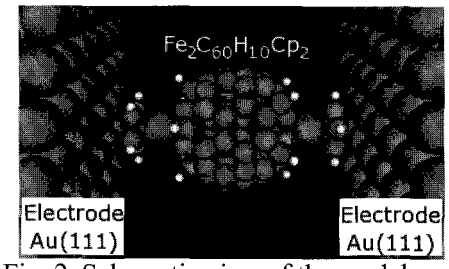

Fig. 2. Schematic view of the model used for transport calculations.

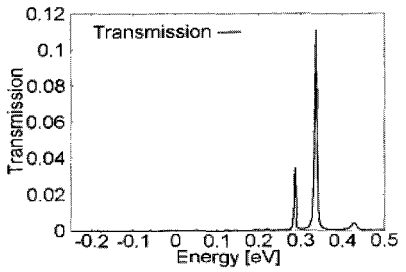

Fig. 3. Transmission spectrum at bias 0.5V

[1] Y. Matsuo, K. Tahara, and E. Nakamura, J. Am. Chem. Soc. **128**, 7154 (2006)

[2] M. Brandbyge, J.-L. Mozos, P. Ordejon, J. Taylor, and K. Stokbro, Phys. Rev. B **65**, 165401 (2002)

[3] http://www.cybernet.co.jp/nanotech/atomistix/, see also http://www.atomistix.com

[4] S. Usui, Y. Ohshima, S. Hirose, and T. Kitajima, 32nd Fullerene-Nanotubes General Symposium, 1P-36

Corresponding Author: Yoshihisa Ohshima

E-mail: yohshima@cybernet.co.jp

Tel: 03-5297-3246, Fax: 03-5297-3637

2P-14

Noncontact Thickness Monitor of Organic and Molecular Films

○Haruna Oizumi[1], Morihiko Saida[1], Hiroyuki Sagami[1], Kenji Omote[1], Yuzo Mizobuchi[1], Yasuhiko Kasama[1], Kuniyoshi Yokoo[1], Shoichi Ono[1] and Toshiyasu Tadokoro[2]

[1]*Ideal Star Inc., Sendai 989-3204, Japan*
[2]*Techno-Synergy, Inc., Hachioji 193-0832, Japan*

Organic semiconductors including molecular crystals like as fullerenes are expected to be applied to future thin film electronic devices such as an organic electro-luminescence panels, solar cells and et al. For these applications, it is important to control their film thicknesses with accuracy of a tenth nanometer or less. However, it is difficult to measure accurately the thickness of organic films without damage on their surfaces by using a normal contact method. We developed an optical system to measure a film thickness without contact on its surface and applied a system to C_{60} films. Reflection spectra of C_{60} films were measured first in the visible region (400~1000nm) and was compared with that expected from an optical model of the film based on the Kramers-Kronig relation up to a coincidence of both the spectra. Both the values of the film thickness and the optical constant agreed well with the thickness measured by the contact method (Fig.1) and that reported in the literature [1], respectively. The system is applicable to measure an optical constant and a film thickness of almost all of organic materials and their multi layers without damage on their surfaces.

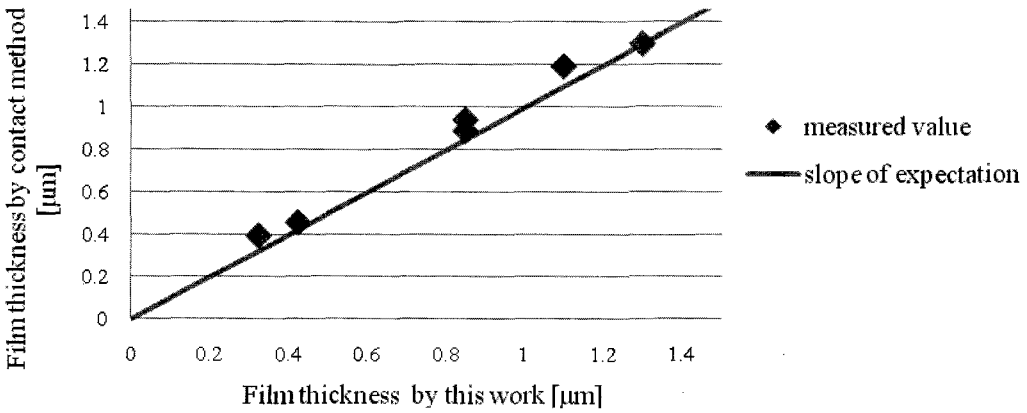

Fig.1 Correlation of C_{60} film thickness measured by this work and a contact method.

[1]A. Richten and J. Sturm, Appl. Phys. A **61**, 163 (1995)

Corresponding Author : Haruna Oizumi
TEL : +81-22-303-7336, Fax : +81-22-303-7339, E-mail : haruna.oizumi@idealstar-net.com

High Temperature Heat-treatment of C_{60} Nanotubes

○Ryoei Kato[1], Kun'ichi Miyazawa[1], Toshiyuki Nishimura[1] and Zheng-ming Wang[2]

[1]*National institute for Materials Science, Tsukuba, Ibaraki, 305-0044, Japan*
[2]*Energy Technology Research Institute, AIST, Tsukuba, Ibaraki 305-8569, Japan*

Single crystalline nanowhiskers consisting of C_{60} molecules with a high aspect ratio of length to diameter, typically a diameter of sub-micrometer and a length of more than 100 μm were synthesized[1]. Furthermore, tubular C_{60} nanowhiskers, i.e., C_{60} nanotubes were fabricated by the same method as the C_{60} nanowhiskers[2].

In this study, C_{60} nanotubes were heat-treated at various temperatures up to 3000 °C. The structural characteristics of the C_{60} nanotubes heat-treated at each temperature are examined using transmission electron microscopy (TEM).

The C_{60} nanotubes were synthesized by the liquid-liquid interfacial precipitation method, using pyridine for the solvent of C_{60} powder and isopropyl alcohol as nucleator. The pyridine solution saturated with C_{60} was exposed to UV light for 1 day before the preparation of C_{60} nanotubes. The prepared C_{60} nanotubes were heated for 60 min at 900 °C in an evacuated fused silica tube set in a muffle furnace. The C_{60} nanotubes heated at 900 °C were collected from the silica tube and further heated at 2000 °C, 2500 °C and 3000 °C, respectively, for one hour in Ar atmosphere. The microstructure of samples was examined using a high-resolution transmission electron microscope (HRTEM, JEM-4010, JEOL) and a transmission electron microscope with in-column energy filter (Zeiss LEO922).

Figure 1(a) shows a low magnification image of a typical sample which was heated at 3000 °C. The heated nanotube retained the tubular morphology. Figure 1(b) shows a high-resolution image of the surface of the tube shown in Fig. 1(a). By the high-temperature heat treatment, the C_{60} nanotubes turned to glassy carbon composed of randomly oriented ribbons with graphitic layers with an interlayer spacing which is close to that of the (002) planes of graphite.

Although the structure of C_{60} nanotubes turned to glassy carbon by the high-temperature heat treatment, the C_{60} nanotubes retained their original tubular morphology.

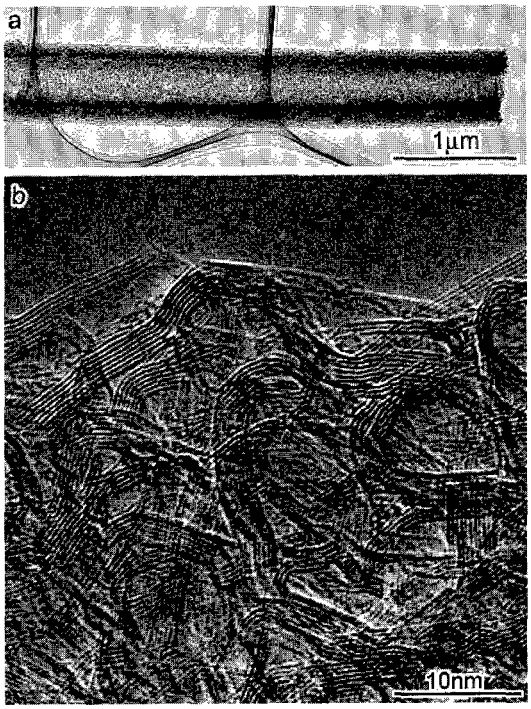

Fig. 1. (a) Low-magnification image of a heated C_{60} nanotube at 3000 °C. (b) High-resolution image of the surface of the C_{60} nanotube of (a).

[1] K. Miyazawa, A. Obayashi, and M. Kuwabara, *J. Am. Ceram. Soc.*, **84**, 3037 (2001)
[2] J. Minato and K. Miyazawa, *Diam. Relat. Mater.*, **15**, 1151 (2006)
Corresponding Author: Kun'ichi Miyazawa
TEL: +81-029-860-4528, FAX: +81-029-860-4667, E-mail: MIYAZAWA.Kunichi@nims.go.jp

The simplest cyclic-carbon-chain growth by atomic-carbon-insertion reactions

○ Teruhiko Ogata, Yutaka Shibi and Yoshio Tatamitani

Department of Chemistry, Shizuoka University, Shizuoka 422-8529, Japan

The atomic-carbon-insertion reaction (ACIR) is simple and efficient, wherein the atomic-carbon, :C, jumps into CC bond without cleaving the overall structure and with no side-product[1]. The linear-carbon-chain growth by ACIR is reported in this symposium separately. In this presentation, we report the cyclic-carbon-chain growth mechanism by ACIR and its interpretation of the unsolved mystery of the Exxon Group's Spectrum [2a].

According to the ACIR, linear-carbon-chain molecules are lengthened by the stepwise mono-carbon insertions. The structure of small C_n ions was revealed by using ion chromatography to be linear for C_4 to C_9 and a monocyclic isomer starting with C_{10} [3]. Ab initio MO calculations found that the clusters exhibit local minima at n = 10, 14, and 18. As the continuation of linear carbon chain growth, a cyclic-carbon-chain is considered to be grown by the ACIR as shown in Figure 1.

On other hand, in the fragmentation of large carbon clusters, preferential evaporations of strong C_n ion signals at n = 10, 14, 18, and 22 are observed [2b,4], which is reminiscent of the Hűckel rule $4n$+2 for aromaticity. These stable fragments ions may be involved in the further ACIR as the case below.

Mystery of the Exxon Group's Spectrum

Cox and co-workers observed famous bimodal mass spectrum in carbon clusters and found, in the range of 9 to 30, a periodic alteration in the ion signal amplitude every four atoms, with maxima at n = 11,15,19,23, and 27 and minima at n = 13,17,21,25, and 29, instead of maxima at n = 10,14,18,22, and 26 [2a]. They are interpreted by the two-step reactions consist of a soot formation followed by the soot fragmentation and ACIR as follows:

$$C_{10\,(14,18,22,26\ldots)} \xrightarrow{:C} C_{11\,(15,19,23,27\ldots)} \xrightarrow{:C} C_{12\,(16,20,24,28\ldots)} \xrightarrow{:C} C_{13\,(17,21,25,29\ldots)}$$

The ACIR also concerns many carbon processes such as the formation/growth of fullerene and soot [1].

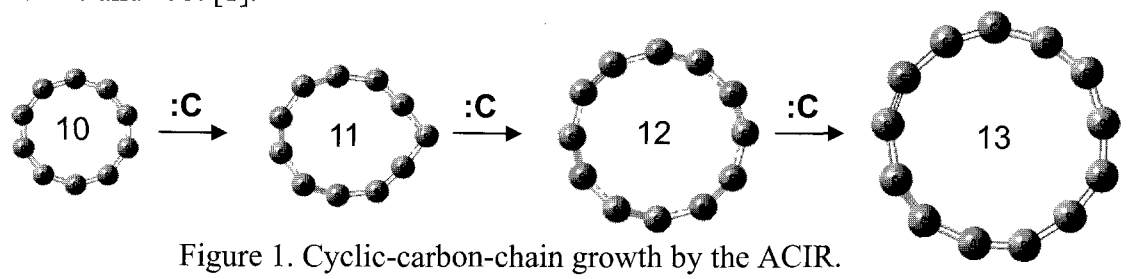

Figure 1. Cyclic-carbon-chain growth by the ACIR.

References:

[1] (a) T. Ogata, et al., *F&NT Symposium*, 33th, 3P-28 (2008); (b) *ibid.* 34th, 2-5 (2008); (c) T. Ogata, et al., *Proceedings of Carbon Conference*, B083 (2007); (d) *ibid.* 16Cam06 (2008).

[2] Cox and co-workers, (a) *JCP*, 81, 3322 (1984); (b) *JCP*. **88**, 1588 (1988).

[3] Achiba & co-workers, (a) *JCP*, **106**, 9954(1997); (b) *J.* **107**, 8927(1997).

[4] M. Pellarin, et al., *JCP*, 117, 3088 (2002).

Corresponding Author: Teruhiko Ogata, **Tel&Fax:** +81-54-238-5105, **E-mail:** sctogat@ipc.shizuoka.ac.jp

Thermal conductivity characterization of vertically-aligned single-walled carbon nanotube films by three-omega method

○Kei Ishikawa[1], Saburo Tanaka[2], Koji Miyazaki[2], Junichiro Shiomi[1], Shigeo Maruyama[1]*

[1] *Department of Mechanical Engineering, The University of Tokyo, Tokyo 113-8656, Japan*
[2] *Department of Biological Functions and Engineering, Kyushu Institute of Technology, 2-4 Hibikino, Wakamatsu-ku, Kitakyushu-city, Fukuoka 808-0196*

Single-walled carbon nanotubes are expected to have high thermal conductivity. Detailed heat conduction characteristics of SWNTs have been widely investigated numerically [1][2]. Individual SWNTs have been measured to be around 3000 W/mK [3][4]. Thermal properties of vertically-alinged single-walled carbon nanotubes (VASWNTs) [5] have been experimentally investigated by laser flash method [6] and by thermoreflectance method [7], however the property is far from being fully exploited.

In this work, thermal properties of VASWNTs have been measured by utilizing 3-omega method, which is commonly used for thin-film thermal conductivity measurements [8][9]. The obtained film thermal resistance Rth = 3 ~ 18 $\times 10^{-5}$ m^2K/W is in fairly good agreement compared with the previous work [7]. Substituting the film thickness and neglecting the thermal resistance at the boundary, the film thermal conductivity value is determined to be 0.55 W/mK.

Thermal conductivity of the independent SWNTs can be deduced by dividing the thermal conductivity value by the fraction ratio of the VASWNT film. Using the fraction ratio 1.6%, the thermal conductivity of the equivalent independent SWNT is 36 W/mK. This value is quite low compared to that of experimentally measured independent SWNTs values. The reason for the low thermal conductivity will be discussed.

[1] Maruyama, S., Igarashi, Y., Taniguchi, Y., and Shiomi, J., *J. Therm. Sci. Tech.*, **1**, 138 (2006).
[2] Shiomi, J., and Maruyama, S., *Japan. J. Appl. Phys.*, **47**, 2005, (2008).
[3] Pop, E., Mann, D., Wang Q., Goodson, K. E., and Dai, H., *Nano Lett.*, **6**, 96 (2006).
[4] Yu, C., Shi, L., Yao, Z., Li, D., and Majumdar, A., *Nano Lett.*, **5**, 1842 (2005).
[5] Murakami, Y., Chiashi, S., Miyauchi, Y., Hu, M., Ogura, M., Okubo, T., and Maruyama, S., *Chem. Phys. Lett.*, **385**, 298 (2004).
[6] Akoshima M., Hata, K., Futaba, D., Baba, T., Kato, H., Yumura, M., *26th Japan Symp. Thermophys. Prop.*, 32 (2005).
[7] Panzer, M. A., Zhang, G., Mann, D., Hu, X., Pop, E., Dai, H., and Goodson, K. E., *J. Heat Trans.*, **130**, 052401-1 (2008).
[8] Cahill, D. G., *Rev. Sci. Instrum.*, **61**, 802 (1990).
[9] Borca-Tasciuc, T., Kumar, A. R., and Chen G., *Rev. Sci. Instrum.*, **72**, 2139 (2001).

Corresponding Author: Shigeo Maruyama
Tel&Fax: +81-3-5800-6983, E-mail: maruyama@photon.t.u-tokyo.ac.jp

Electronic Structure and Energetics of Semiconducting Nanotubes adsorbed on SiO_2 (0001) Surfaces

Susumu Okada

Center for Computational Sciences and Graduate School of Pure & Applied Sciences, University of Tsukuba, Tsukuba 305-8577

CREST, Japan Science and Technology Agency, 4-1-8 Honcho, Kawaguchi, Saitama 332-0012

Carbon nanotubes have been keeping a premier position with their various interesting electronic properties which sensitively depend on the tiny differences of the atomic arrangements. The peculiar electronic property opens a possibility of fabricating superior nanometer scale electronic devices which consist presumably of hybrids of nanotubes and conventional materials. Indeed, it has been demonstrated that the individual semiconducting nanotubes can work as field-effect transistors in which nanotubes form contacts with various metal and semiconductor surfaces. Although the experiments give many interesting properties which depend on the contact material species, fundamental properties of the interface are rarely addressed before.

In the preset work, we perform the first-principle total-energy calculations to clarify the energetics and electronic structures of the interfaces between semiconducting nanotubes and SiO2(α-quartz). We find that the small but substantial interaction between the CNT and SiO_2 results in the tiny modulation of the electron states of the CNT: The calculated E_{11} and E_{22} gaps of CNT adsorbed on SiO_2 decreases by 50 meV and increases by 181 meV than those of the isolated CNT, respectively. It is expected that the modulation affects absorption/emission properties of CNT.

Corresponding Author: Susumu Okada
E-mail: sokada@comas.frsc.tsukuba.ac.jp
Tel/Fax: 029-853-5921/029-853-5924

Determination of the absorption coefficient of semiconducting single-wall carbon nanotubes selectively dispersed with polyfluorene

○Yoshisuke Futami[1], Said Kazaoui[2], Nobutsugu Minami[1]

[1]*Nanotechnology Research Institute, AIST Central 5, Tsukuba, 305-8565, Japan*
[2]*Nanotube Research Center, AIST Central 5, Tsukuba 305-8565, Japan*

Absorption coefficients of single-wall carbon nanotubes (SWNT) have not been determined yet despite the fundamental importance for their characterization. The reason lies in the difficulty in extracting a sufficient quantity of high purity SWNTs and in measuring its weight. Another difficulty is that SWNT's absorption spectra have been obscured by many poorly resolved peaks and the large background signal. Recently, it is shown that the use of polyfluorene (PFO) as a dispersant dissolved in toluene results in the selective isolation and extraction of semiconducting SWNTs (s-SWNTs) [1, 2]. Remarkably, the UV-Vis-NIR absorption spectrum of s-SWNTs thus obtained is simple, sharp, well-resolved, and freed from the large background. On the basis of these unprecedented advantages and by devising an effective extraction method, we succeeded in determining an averaged absorption coefficient of s-SWNTs.

Two-step ultracentrifugation was employed to efficiently extract s-SWNTs: first the supernatant was collected and then this supernatant was re-centrifuged for the precipitate to be collected. We found that the ratio PFO/SWNT, which was originally huge, can be greatly reduced by these procedures, facilitating the weighing of SWNTs. Figure 1 shows the absorption spectrum of the final precipitate re-dissolved in toluene, where the reduced absorbance of PFO can be used to estimate its concentration after appropriate calibration, enabling the accurate determination of the weight of SWNTs.

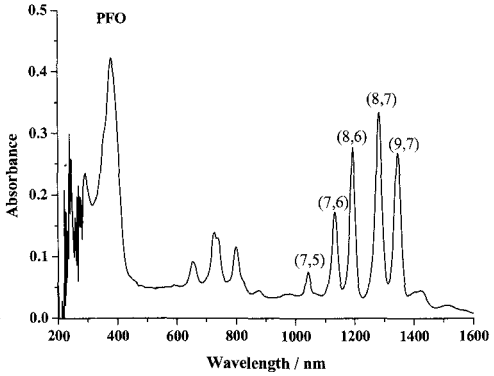

Figure 1 UV-Vis-NIR absorption spectrum of an s-SWNT and PFO mixture in toluene. The 1000-1500 nm and the 600-900 nm peaks derive from the first and the second bandgap of s-SWNTs, and the peak at 380 nm from PFO.

[1] Nish et al., Nature Nanotechnology 2, 640 (2007). [2] Chen et al., Nano Lett. 7, 3013 (2007).

Corresponding Author: Nobutsugu Minami
TEL: +81-29-861-9385, FAX: +81-29-861-6309, E-mail: n.minami@aist.go.jp

Heat-Induced Charge Transfer from Sapphire to Aligned Carbon Nanotubes

○Hiroki Ago,[*,1,2,3] Izumi Tanaka,[2] Masaharu Tsuji,[1,2] Ken-ichi Ikeda,[2] and Seigi Mizuno[2]

[1]*Institute for Materials Chemistry and Engineering, Kyushu University, Fukuoka 816-8580,*
[2]*Graduate School of Engineering Sciences, Kyushu University, Fukuoka 816-8580*
[3]*PRESTO-JST*

The growth of single-walled carbon nanotubes (SWNTs) on single crystal substrates, such as sapphire and quartz, has attracted a current interest, because these substrates offer high density aligned SWNTs, realizing high device productivity and high current operation. The growth mechanism as well as SWNT–sapphire interaction is also interesting, because the aligned growth has a potential to control the nanotube structure based on "epitaxial nanotube growth" [1,2].

It was reported that the heat treatment of powdered SWNTs or double-walled carbon nanotubes (DWNTs) in vacuum induces the coalescence of nanotubes, giving large-diameter nanotubes [3,4]. This indicates that the heat treatment strongly influences the properties of nanotubes. In the case of the horizontally-aligned SWNTs on sapphire, the SWNTs are mostly isolated and the full length of the nanotube adheres to the sapphire surface. Therefore, it is interesting to study effects of the heat treatment of the aligned SWNTs in relation to the interaction with the underlying substrate surface.

Here, we studied the effect of heat treatment of the aligned SWNTs in high vacuum. As shown in Fig. 1, the heat treatment at 800 and 1000 °C shifted the G-band to higher frequencies. At 1200 °C, in spite of the high vacuum condition, the most of aligned SWNTs were oxidized. The Auger measurements suggested that the preferential desorption of oxygen from sapphire occurred at high temperature. We concluded that the blueshift of the G-band is originated in the transfer of positive charges from the sapphire surface to the SWNTs. We think that this is the first demonstration of the hole-doping from a substrate to SWNTs without applying dopant molecules and an electric field [5].

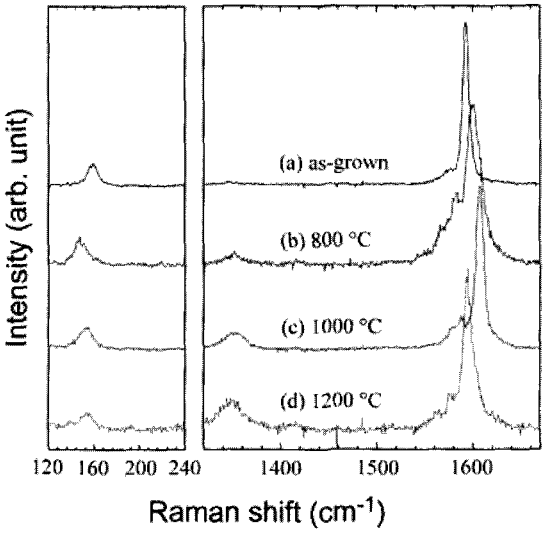

Fig. 1. Typical Raman spectra of the as-grown and heat treated SWNTs.

References [1] N. Ishigami *et al.*, *J. Am. Chem. Soc.*, in press., [2] N. Ishigami *et al.*, Abstract of this Symposium, [3] M. Yudasaka *et al.*, *NanoLett.*, **1**, 487 (2001)., [4] M. Endo *et al.*, *Small*, **2**, 1031, (2006). [5] H. Ago *et al.*, submitted.

Corresponding Author: Hiroki Ago (TEL&FAX: +81-92-583-7817, E-mail: ago@cm.kyushu-u.ac.jp)

Geometries, Electronic Properties and Energetics of Single-Walled Armchair Carbon Nantotubes

○Koichiro Kato and Susumu Saito

Department of Physics, Tokyo Institute of Technology,
2-12-1 Oh-okayama, Meguro-ku, Tokyo 152-8551, Japan

Ever since the discovery of carbon nanotubes (CNTs), many experimental and theoretical works have been devoted to them. According to the study using the tight-binding approximation, their electronic structures sensitively depend on their diameter and chirality and they are classified into three types [1]. As for the thick nanotubes, these classifications agree with the results of the density functional calculations. On the other hand, it has been pointed out from the first-principle electronic-structure calculations with structural relaxation for zigzag nanotubes that above classifications may not apply to the small-diameter nanotubes [2-4]. While several thin zigzag CNTs are predicted to be semiconductors in the tight-binding study, they are metallic in the density functional theory. The origin of this difference is explained by the following two reasons. First, large π - σ hybridization effects can occur in small nanotubes which drastically change the energy of the lowest lying conduction band states [2]. This effect can be taken into account even in the tight-binding method if not only π but also σ states are incorporated. Secondly, the effect of nearly free electron (NFE) state is found to be sizable due to a relative large interspace of carbon nanotube [3]. The NFE states can be represented in the tight-binding approximation. As for the geometry of zigzag nanotubes, there should be two kinds of bonds which can have different lengths, one is longer than that of graphene and the other is shorter. These differences become significantly larger with their diameters [3,4]. Therefore, structural optimization using the density functional theory play an important role in predicting their electronic and optical properties. Importantly, there are serious differences between the first-principles results and the tight-binding results for thin nanotubes.

We study the geometries, electronic properties and energetics of isolated single-walled armchair nanotubes in the framework of the density functional theory. Because of the unique electronic structure of armchair nanotubes, their first-principles studies have scarcely been reported. We adopt the very dense *k-point mesh* to obtain the highly converged results and study the armchair nanotubes in the range from (3,3) to (15,15) with the complete geometry optimization. It is found that their structural parameters and their electronic properties strongly depend on their diameter. Importantly, the Fermi wave vector and Fermi velocity of (15,15) are higher by about 30% than those of (3,3). It is also found that NFE states play an important role in the electronic properties of thin nanotubes. We discuss the geometries and the energetics of armchair nanotubes in comparison with zigag and chiral nanotubes.

[1] N. Hamada, S. Sawada and A. Oshiyama, *Phys. Rev. Lett.*, **68**, 1579 (1992).

[2] X. Blasé, L. X. Benedict, E. L. Shirley and S. G. Louie, *Phys. Rev. Lett.*, **72**, 1878 (1994)

[3] K. Kanamitsu and S. Saito, *J. Phys. Soc. Jpn.*, **71**, 483 (2002)

[4] O. Gülseren, T. Yildirim and S. Ciraci, *Phys. Rev. B*, **63**, 153405 (2002)

E-mail : kato@stat.phys.titech.ac.jp (K. Kato)

Diameter Dependence on Absorption Coefficients of Single-Wall Carbon Nanotubes

○Shota Kuwahara, Yuki Asada, Toshiki Sugai*, Hisanori Shinohara

Department of Chemistry & Institute for Advanced Research, Nagoya University, Nagoya 464-8602, Japan

To evaluate the number of carbon nanotubes (CNTs) in unit volume, we have developed a new spray technique coupled with atomic force microscopy (AFM) [1]. With this technique, the molar absorbance coefficient of single-walled carbon nanotubes was evaluated and found to be ca. 2-3 x 10^7 L mol^{-1} cm^{-1} at 280 nm.

Recent progress has been reported on the correlation between electric properties of CNTs and their absorption in the UV region using the separated samples through density gradient ultracentrifugation (DGU), and the shape and the intensity of UV absorption was changed by the metallic (M-) or semiconductor (S-) single-walled carbon nanotubes (SWNTs) [2]. In this study, we estimate the absorption coefficient of M- and S- SWNTs, and discuss the correlation between electric properties of CNTs and their absorption in the UV region normalized by the number of SWNTs

By using the reported protocol of separation of SWNTs through DGU [3], M- and S-SWNTs have been prepared. Three different types of SWNTs were used: HiPco (Carbon Nanotechnologies Inc.; average diameter d_t: ~1.0 nm), CoMoCAT (Southwest Nanotechnologies; d_t: ~0.8 nm) and laser-vaporization (LV; d_t: ~1.4 nm). To evaluate the number of SWNTs, iodixanol, sodium cholate and deoxycholate sodium salts were removed by dialysis in 1 wt% aqueous SDS. After dialysis, the obtained samples were used for measuring absorption spectra, and sprayed onto SiO_2 substrates for AFM evaluation.

Figure 1 shows absorption spectra of sorted LV samples. As seen in the visible region, M- and S- SWNTs were well separated. The red shift of peaks of M-SWNTs was observed in UV region. The absorbance coefficient, which was considered the difference, can be extended to other synthetic types and diameter distributions, and leads to standardize CNT's evaluation.

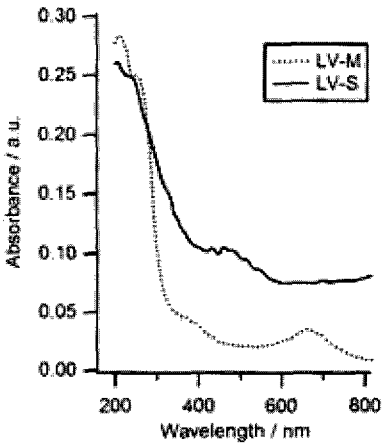

Figure 1: Comparison of the absorbance of LV metallic and semiconductor SWNTs in SDS solution.

Reference:

[1] S. Kuwahara, et al., the 32nd Fullerene-Nanotubes General Symposium

[2] Y. Miyata, et al., *J. Phys. Chem. C* (2008).

[3] K. Yanagi, et al., *Appl. Phys. Express* (2008).

*Present address: Dept. of Chemistry, Toho Univ.
Corresponding Author: Hisanori Shinohara
E-mail: noris@cc.nagoya-u.ac.jp
TEL: +81-52-789-3660, FAX: +81-52-747-6442

2P-23

Interference Effects on Conductance between Two STM Probes in Carbon Nanotubes

○ Takeshi Nakanishi[1] and Tsuneya Ando[2]

[1]*Nanotube Research Center, AIST 1–1–1 Higashi, Tsukuba 305-8565, Japan*
[2]*Department of Physics, Tokyo Institute of Technology 2–12–1 Ookayama, Meguro-ku, Tokyo 152-8551, Japan*

The scanning-tunneling-microscopy (STM) is a powerful technique for directly viewing electronic wave functions at the atomic level. Quite recently multi-probe STM was developed. In this paper the conductance image between two STM probes is calculated in armchair and zigzag carbon nanotubes within a tight-binding model and a realistic model for STM probes [1]. We show that a Kekulé-type pattern usually appears due to interference of states at K and K' points except in special cases.

In order to deal rigorously with the infinite nanotube, we solve numerically a scattering problem in a finite nanotube connected at both ends to semi-infinite nanotubes. The STM probes have been modeled with sp Slater-Koster hopping terms. The conductance is given by Landauer's formula and transmission probabilities between these two STM probes are numerically calculated by the use of recursive Green's function technique.

In the calculation, a left STM probe is fixed at several points and a right probe is continuously swept over the wide region. The Kekulé-type pattern peak usually appears in the calculated conductance, as shown in figure. It disappears in special cases where an electron is injected into a single propagating state classified by the parity in the effective-mass scheme.

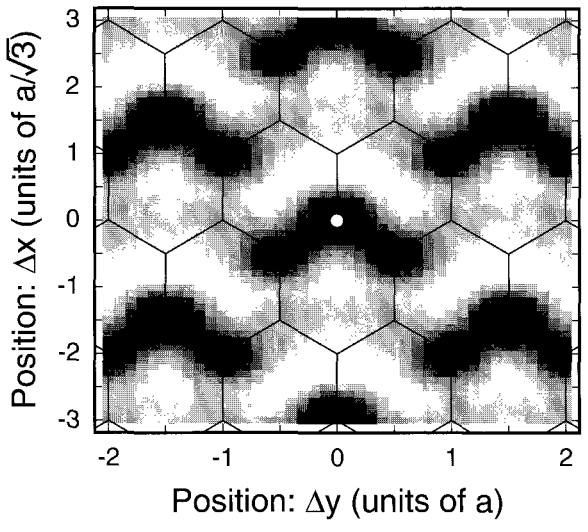

Figure: Calculated conductance for armchair nanotubes as a function of right STM tip position. The left STM tip is fixed above a position denoted by a open circle, but its actual position is at $(0, -45)a$ in the coordinate system and therefore is quite far from the right tip. The conductance is shown by the density in the maximum $9.9 \times 10^{-10} e^2/\pi\hbar$ as plot range.

[1] T. Nakanishi and T. Ando, J. Phys. Soc. Jpn. 77 (2008) 024703.

Corresponding Author: Takeshi Nakanishi
TEL: +81-298-61-9277, FAX: +81-298-61-2662, E-mail: t.nakanishi@aist.go.jp

Electronic-Structure Modifications of Collapsed Single-Walled Carbon Nanotubes: The Case of Armchair Tubes

Masayuki Hasegawa[1] and Kazume Nishidate[2]

[1] *Department of Materials Science and Engineering, Iwate University, Morioka 020-8551, Japan*

[2] *Department of Electric and Electronic Engineering, Iwate University, Morioka 020-8551, Japan*

Recently, radial deformation of carbon nanotubes has attracted increasing attention because of its unusual effects on the mechanical and electronic properties [1], which is expected to pave the way to a new technological application. In this report we elucidate electronic structure modification by radial deformation of single-walled carbon nanotubes (SWNTs). The radial deformation of individual SWNTs presumed under hydrostatic was predicted using the method developed in the previous work [2]. We have applied this method to the zigzag ($3i \pm 1$, 0) SWNTs, where i is an integer, and found a universal band-gap modulation by radial deformation [3]. For these tubes the band-gap closure occurs at $R_{\mathrm{min}} \approx$ 0.24 nm irrespective of tube size, where R_{min} is an averaged minimum curvature radius along the circumference of a deformed cross section perpendicular to the axis. This electronic-structure transformation occurs in the elastic regime for small tubes with diameters less than 2.5 nm [2], suggesting a possible application such as a nano-mechanical switch. Very recently, the electronic-structure of a large collapsed tube, identified as an armchair (21, 21) SWNT, has been probed by scanning tunneling microscopy (STM) by Giusca *et al* [4]. They observed in this experiment that the flat region shows a metallic nature with a finite density of states at the Fermi level, while the gap opening occurs in the edge region at either side of the flattened tube, indicative of a semiconducting nature. These observations are in marked contrast to the implications found for zigzag SWNTs, which show the reversed natures of the flat and edge regions. We also performed electronic structure calculations for the collapsed armchair (21, 21) SWNTs to clarify the experimental observations and the details of these investigations will be discussed.

[1] O. Gulseren *et al.*, Phys. Rev. B **65**, 155410 (2002).

[2] M. Hasegawa and K. Nishidate, Phys. Rev. B **74**, 115401 (2006).

[3] K. Nishidate and M. Hasegawa, unpublished.

[4] C. E. Giusca, Y. Tison, and S. R. P. Silva, Phys. Rev. B **76**, 035429 (2007).

Corresponding Author: Masayuki Hasegawa

TEL: +81-19-621-6360, FAX: +81-19-621-6365, E-mail: hasegawa@iwate-u.ac.jp

2P-25

Annealing effect on mechanical properties of carbon nanocoils

○Shun Sato[1], Yoshiaki Araki[1], Ryo Kanada[1], Yoshikazu Nakayama[2] and Seiji Akita[1]

[1]*Department of Physics and Electronics, Graduate School of Engineering, Osaka Prefecture University,1-1 Gakuen-cho, Naka-ku, Sakai, Osaka 599-8531, Japan.*
[2]*Department of Mechanical Engineering, Graduate School of Engineering, Osaka University, 2-1 Yamadaoka, Suita, Osaka 565-0871, Japan*

Carbon nanocoils (CNC)[1,2], having the 3D helical structures and unique mechanical properties, are expected to be one of components for the nano-electro-mechanical system (NEMS), such as nano-springs, resonant elements, or novel reinforcement in high-strain composites. However the mechanical properties of the CNCs are still unclear. In this study, we have investigated the annealing effect on the mechanical properties of CNC.

Nanocoils examined were synthesized by catalytic chemical vapor deposition (CVD) method. Cantilevered CNCs were vibrated mechanically using a piezo device in a scanning electron microscope (SEM) at room temperature to measure the resonant frequency and Q factor, where the cantilevered CNC was vibrated laterally. The resonant frequency and Q factor for pristine sample was measured followed by the samples annealed at 1000 °C for 30 min in He. The shear modulus of CNC was evaluated from the resonant frequency by using the continuum model.

Figure 1(a) shows one of resonant curves for pristine CNCs. In this case, the resonant frequency and Q factor are 700 kHz and 16.5, respectively. The shear moduli for all pristine CNCs evaluated were in the range of 10-50 GPa. As shown in Fig. 1(a), there are several dips on the resonant curve and the vibration mode was changed at the dip such as the precession. The Q factors for pristine CNC are less than 50, which is much smaller than that for CVD grown carbon nanotubes. This low Q factor may come from structural defects on CNCs or supporting point loss. From the transmission electron microscopy, the pristine CNC has many structural defects such as cup stack structures. After the annealing at 1000 °C, both of the resonant frequency and Q factor are much improved as shown in Fig. 1(b). The resonant frequency is 3 times higher than that for the pristine CNC, which corresponds to 9 times higher shear modulus. Furthermore, the improvement of Q factor indicates the recovery of the defect and/or tightening the supporting point of the CNC cantilever. Thus, the mechanical properties of CNC can be changed by the annealing treatment.

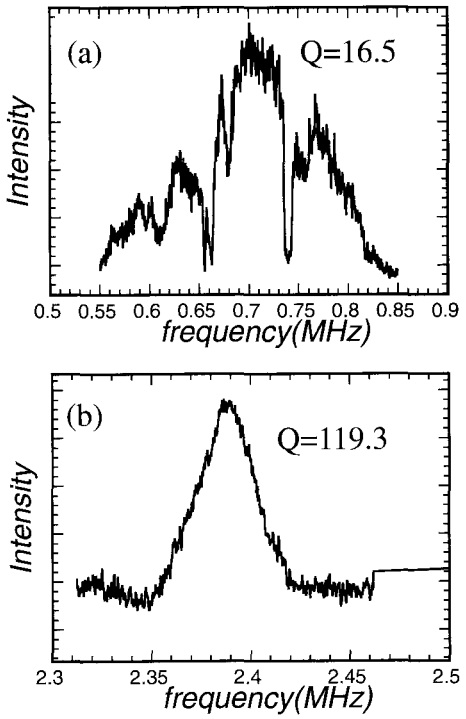

Fig.1 Frequency response curve of (a) pristine CNC and (b) CNC after annealing at 1000 °C for 30min in He.

Referances:

[1] M. Zhang, Y. Nakayama, and L. Pan: Jpn. J. Appl. Phys. **39**, L1242(2000). [2] X. Chen *et al.*: Nano Lett. **3**, 1299 (2003).

E-mail:akita@pe.osakafu-u.ac.jp

Tel&Fax:+81-72-254-9261

High Temperature Infrared Optical Spectroscopy of Single-Walled Carbon Nanotubes

○ Mukhtar Effendi, Hiroyuki Yokoi, Noritaka Kuroda

Department of Materials Science and Technology, Kumamoto University, Kumamoto 860-8555, Japan

The transport properties of single-walled carbon nanotubes (SWNTs) above room temperature are studied in this work. Shiraishi et al. examined experimental results on the temperature dependence of electrical resistance of SWNT mats below room temperature and proposed a quasi-one dimensional (quasi-1D) metal model to explain the conduction mechanism of SWNTs. On the other hand, almost no theoretical or experimental research on electric resistivity of SWNTs above room temperature is known to be conducted. This research aims to measure the reflectivity of SWNT mats in the infrared region, which has an advantage of evading the influence of electrode contact during the measurement of resistivity of SWNT mats sample, and to clarify the high temperature conduction mechanism of SWNTs. Purified SWNT (HiPco) mats were used as received from Carbon Nanotechnology Inc. The Fourier transform infrared micro-spectrometer was employed for measurements of the reflectivity spectra in the infrared region between 0.08 eV and 0.8 eV under Ar gas flow at temperatures between 330 K and 840 K. Temperature dependence of the transmission of ZnSe optical window of the cryostat was corrected. Figure 1 shows infrared reflectivity spectra of the SWNT mats obtained at several temperatures. These spectra have the typical appearance of the metallic reflectivity. Examination within the framework of the Drude-Lorentz model was performed to work out the electric resistivity for each reflectivity spectrum. It was found that the resistivity of SWNTs in the temperature range from 330 K to 690 K increases superlinearly and can be explained by the quasi-1D metal model very well. However, the resistivity in the temperature above 690 K which exhibited the tendency of saturation deviated from the quasi-1D metal model (Fig.2). This behavior could be attributed to the thermal excitation of free carriers in the semiconducting SWNTs included in the SWNT mats.

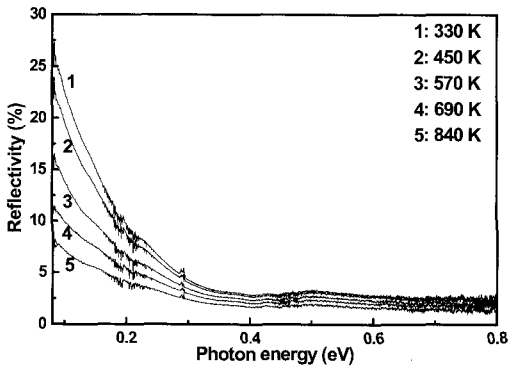

Fig. 1. Infrared reflectivity spectra of an SWNT mat at various temperatures.

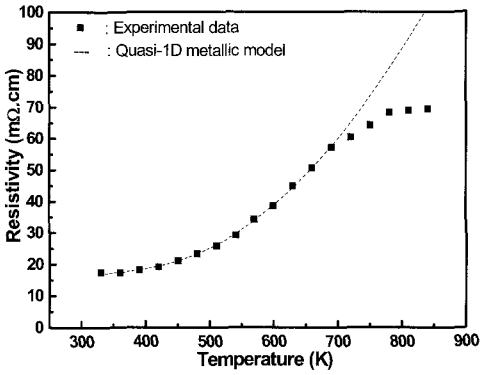

Fig. 2. Temperature dependence of electric resistivity of an SWNT mat.

[1] M. Shiraishi, et al., Synth. Met. 128 (2002) 235.

Corresponding author.: Hiroyuki Yokoi
TEL.: +81-96-342-3727, FAX: +81-96-342-3710, E-mail: yokoihr@kumamoto-u.ac.jp

Fabrication of Carbon Nanotube Atomic Force Microscope Tip by Using Ionic Liquid and Its Characterization

○ Yuya Kamizono[1], Chien-Chao Chiu[2], Masamichi Yoshimura[2], Kazuyuki Ueda[2], Yuki Asada[1], Shota Kuwahara[1], Ryo Kitaura[1], Toshiki Sugai[1,*] and Hisanori Shinohara[1]

[1]*Department of Chemistry & Institute for Advanced Research, Nagoya University, Nagoya 464-8602, Japan*
[2]*Nano High-Tech Research Center, Toyota Technological Institute, 2-12-1 Hisakata, Tempaku, Nagoya 468-8511, Japan*

Carbon Nanotube (CNT) is suited for atomic force microscope (AFM) tip because of its high aspect ratio and stiffness. Although the application of CNT to the AFM tip has been so far reported [1,2], the fabrication through manual attachment under scanning electron microscope (SEM) requires high skill and long processing time. Here, we propose a new method using an ionic liquid gel including CNTs to shorten the processing time. We demonstrate that the CNT-AFM tips fabricated in the present method are superior in the spatial resolution to commercial silicon tips.

The gel was prepared by grinding HiPco DWNT in 1-Ethyl-3-methylimidazolium Tetrafluoroborate followed by centrifuging. Immersing commercial silicon tips into the gel and extracting them from the gel in the SEM chamber CNT-AFM tips were reproducibly fabricated. Figure 1 shows a CNT-AFM tip successfully fabricated. CNT-AFM tips were used for AFM measurements of DNA wrapped SWNT on mica, silicon surface, etc.

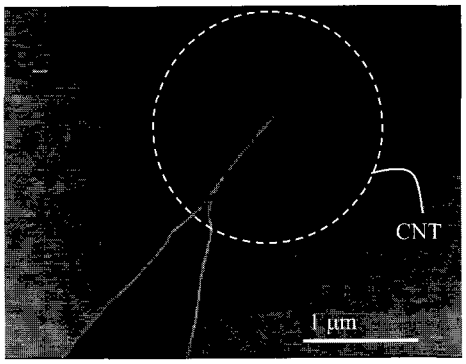

Figure 1 SEM image of fabricated CNT-AFM tip

Figure 2 is typical AFM image of a DNA wrapped SWNT taken by the CNT-AFM tip. Analysis of section heights clearly shows that wrapped DNA helical pitch is around 18 nm. The results indicate that the CNT-AFM tips are sharper in the radius than commercial silicon tips. It is also found that the lifetime of CNT-AFM tips are much longer than that of commercial silicon tips.

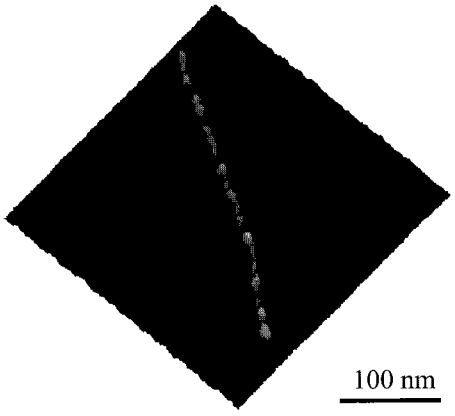

Figure 2 AFM image of DNA wrapped SWNT

*Present address: Dept. of Chemistry, Toho Univ.

References:
[1] S. Kuwahara *et al., Chem. Phys. Lett.* **429**, 581 (2006).
[2] S. Akita *et al., J. Phys. D: Appl. Phys.* **33**, 2673 (2000).

Corresponding Author: Hisanori Shinohara
E-mail: noris@nagoya-u.jp
Tel: +81-52-789-2482, **Fax:** +81-52-747-6442

Optimization of gas sensing characteristics using networked SWNTs

○Isao Sasaki and Nobutsugu Minami

Nanotechnology Research Institute, National Institute of Advanced Industrial Science and Technology (AIST), 1-1-1 Higashi, Tsukuba, Ibaraki 305-8565 Japan

The purpose of this presentation is to study the effects of the preparation conditions on the perform ance of single-wall carbon nanotube (SW NT) gas sensors. In our previous study, SWNT bundles were dispersed in aque ous solutions of hydroxypropylcellulose (HPC) [1]. The spin-cast SWNTs/HPC composite was annealed at 350 °C under vacuum to remove the HPC. Then, the networked SWNT s were u sed f or con ductometric NO_2 gas sensing sensitive down to 25 ppb [1].

In this study, the properties of SWNTs were systematically modified by varying the annealing temperature between 350 °C to 550 °C to compare the sensing characteristics of graphitic S WNTs with those of therm ally degraded (def ective) SWNT s. The sensing performance is evaluated through three essentia l sensing characteristics: sensitivity to NO_2, humidity interfering effect, and sensor stability, all tested at room temperature. The modified SWNT properties were monitored by Raman spectroscopy and AFM.

The results suggest that the sensor annealed at 400 °C maintains the properties of graphitic S WNTs and shows the highest NO_2 sensitivity (Fig. 1), negligible hum idity interfering effect (the sensitivity ratio is close to unity) (Fig. 2), and high sensor stability. In contrast, higher annealing tem peratures lead to structural degradation and thus lower the sensing perform ance. W e propose that the ex cellent physical and ch emical properties of graphitic SWNTs are suitable for gas sensing applications.

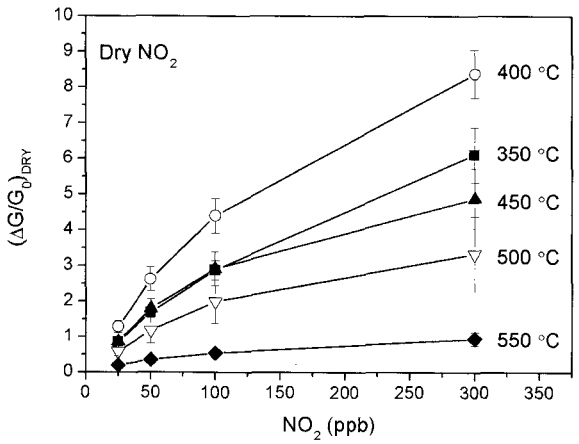

Fig. 1. R oom te mperature calibration curves of SWNTs-based sens ors i n dry ai r an nealed at various tem peratures. T he error bars re present the standard deviation (n = 4).

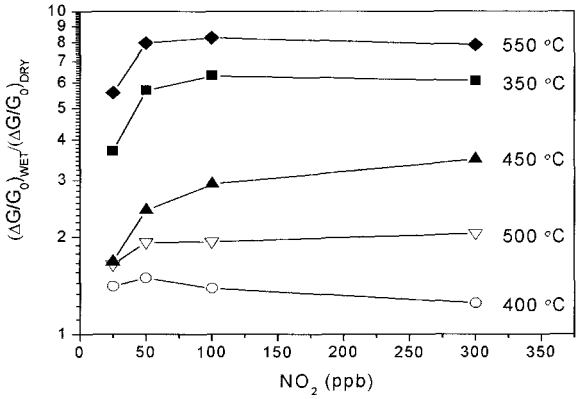

Fig. 2. Humidity interfering effect expressed by the sensitivity ratio, $(\Delta G/G_0)_{WET}/(\Delta G/G_0)_{DRY}$. Note that an i deal se nsor without an y interferi ng e ffects of water vapor should have the sensitivity ratio = 1 for any concentration.

[1] A. Karthigeyan, N. Minami and K. Iakoubovskii, Jpn. J. Appl. Phys., **47**(9), in press.

Corresponding Author: Nobutsugu Minami,
E-mail: n.minami@aist.go.jp, Tel&Fax: +81-29-861-9385/+81-29-861-6309

Contractile activity measurement of rat's digestive organ by CNT-based force transducer

○Takamichi Hirata[1], Takatsugu Yanaka[2], Satoshi Sakahara[2], Kanako Koike[2], Chihiro Tsutsui[2], Takafumi Sakai[2], Masahiro Akiya[1]

[1]*Department of Biomedical Engineering, Musashi Institute of Technology, Tokyo 158-8557, Japan*
[2]*Division of Life Science, Graduate School of Science and Engineering, Saitama University, Saitama 338-8570, Japan*

We are currently carry ing out research on the developm ent of bio-nanosensors using nanocarbon m aterials, such as fullerenes and carbon nanotubes (CNT s), with the aim of investigating applic ations f or these new sensor -type devices in the field of biom edical engineering [1,2]. In this study, we are fabricated a force transducer designed to be i mplanted into a living body by using the vari ation in the resistance attributable to the m echanical deformation of CNT. We are attach ed the force transducer to the rat s tomach to ev aluate its characteristics (particularly, the relationship between stom ach contractions and the change in resistance evoked by an *in vivo* injection of acetylcholine in rats).

CNT-based force tran sducer is a structu re that poly[ethylene glycol] (PEG)-grafted multi-walled carbon nanotubes (PEG-MWCNTs) are dispersed and applied to the comb-like Au-electrode formed on the poly[dim ethylsiloxane] (PDMS) sheet as s hown in Fig.1(a). W e are inves tigated the relationsh ip b etween s tomach contraction s and the variation in the resistance that originates in mechanical distortion or electric contact between PEG-MWCNTs bundles when a chemical compound (acetylcholine) that induces muscle contractions injected into the veins of the rat [Fig.1(b)].

In the case of physiological salin e injection, it is showed no ef fect on the change in the resistance [Fig.2(a)], but acety lcholine is cause d a resistan ce change attributab le to stom ach contractions [Fig.2(b)]. When the acetylcholin e concentration is varied, the change in the resistance is proportional to logΔR as shown in Fig.2(c). Here, ΔR is defined as $\Delta R = R_{max} - R_0$ (R_0: initial resistance, R_{max}: maximum resistance). In additio n, since a big resistance variation is shown, a clear observation is possible even by a slight, continuous stom ach contraction. Moreover, since the relaxation tim e of the stom ach contractions alm ost matched the in-blood duration tim e of the acetylcholine, fine m ovement is dem onstrated to be detectable.

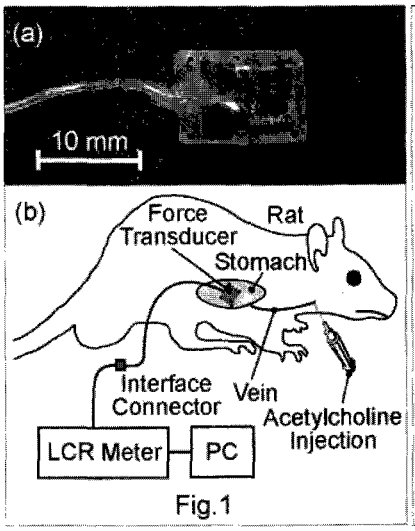

Fig.1

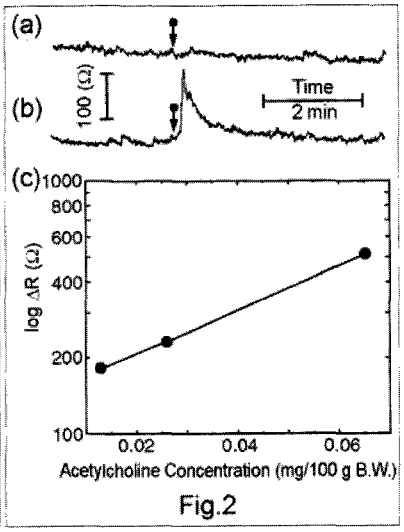

Fig.2

References

[1] T. H irata *et al.*, Ap pl. Phys. Lett. **90**, 233106 (2 007). [2] T. Hirata *et al.*, Jpn. J. A ppl. Phys. **47**, 2067 (2008).

Corresponding Author
E-mail:
hirata@bme.musashi-tech.ac.jp
Tel&Fax: +81-3-5707-2183 (D.I)

2P-30

Bio-Hazardous Effects of Carbon Nanotubes under Microwave Radiation

○Hirokazu Horiguchi and Masahito Sano

Department of Polymer Science and Engineering, Yamagata University 992-8510, Japan

Carbon nanotubes (CNT s) are heated very ef ficiently by m icrowave radiation. Temperatures of CNTs may reach over 100 °C w ithin seconds by irradiating with microwave at a few tens watts (W) power. Such a high ef ficiency of heating has led us to consider possible hazardous effects of CNTs, since we are constantly irradiated by microwave radiation in every day life. For instance, a mobile pho ne communicates using nearly 1 W microwave power with a base station which radiates abou t 30 W . Most IC tip s in elec tronic devices operate at m icrowave frequencies. Recently , CNT s are actively s tudied for m edical applications such as DDS, cell scaffolds and artificial joints. Other than those cases that CNTs are intentionally incorp orated into bodies, they can be inhaled accide ntally during ordinary handling. Thus, it is of great importance to know what level of microwave radiation af fects living bodies with CNTs inside.

We have reported that, a re d blood cell protein, hem oglobin (Hb) adsorbs specifically on CNTs [1]. When m icrowave was irradiated on Hb/CNT system, 5 W for 25 sec irradiation clearly affected some of the proteins while the Hb without CNT s had no dam age under the same irradiation. However, Hb is not heat stab le and can be denatured easily by warm water. The above result m ay be overestimated since so me Hb might have been denatured by heated water rather than CNTs directly. To see the effect of CNT m ore clearly, a m itochondrial protein, cytochrome-c (Cyt-c) was inv estigated. Cyt-c is stable against heat and has a reversible folding/unfolding transiti on at 67 °C . As shown in the figure, it takes about 8W irradiation to affect Cyt-c/CNT, which is higher than the case of Hb/CNT but th eir dif ference is sm all. The detailed stu dies on f erroCyt-c an d f erriCyt-c using UV -Vis adsorption, circular dichroism, and reson ance Ram an spectrosco pies indicate that, whereas ferroCyt-c is denatured directly by CNTs under m icrowave, some ferriCyt-c is first reduced by CNTs before denaturation.

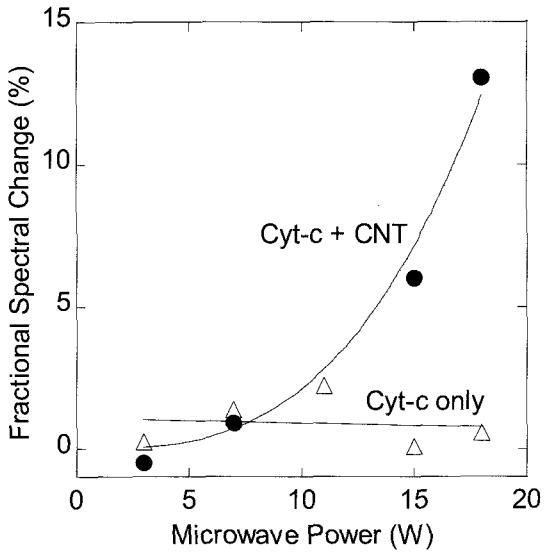

[1] K. Kato, M. Sano, *Chem. Lett.* **35**, 1062-1063 (2006).

Corresponding Author: Masahito Sano
E-mail: mass@yz.yamagata-u.ac.jp
Tel&Fax: +81-238-26-3072

2P-31

Field Effect Chromatography for Separating Chiral Carbon Nanotubes

○ Yuki Orinouchi[1], Akara Hashimoto[2], Yasushi Suzuki[2],
Yasuyuki Watanabe[2] and Masahito Sano[1]

[1]*Department of Polymer Science and Engineering, Yamagata University 992-8510, Japan*
[2]*Shimadzu Corporation, Kyoto 604-8511, Japan*

Importance of separatin g carbon nanotubes (C NTs) accord ing to their chirality has led many researchers to develop various techni ques, including chemical adsorption, chemical reactions, electrophoresis, diel ectrophoresis, and centrifuga tion. Because all techniques require solutions of well-dispersed CNTs, some kinds of surfactants or polymers are added to stabilize CNT dispersions. Although these techniques are useful for separating chrality, the rem aining stabilizing agents ham per applying the chr ality-controlled CNT s to applications such as electron ic devices. Also, better separation of ten m eans less quan tity. Som e techniques yield so little CNT s that are not enough for practical applications. W e are interested in developing chrom atography techniques that (1) involve no addi tives, (2) yield practical am ounts although separation may not be comple te, and (3) requires no special skills to ope rate. In th is way, the chrality-concentrated CNTs may be used for ap plications th at a re no t s o sensitive to chra lity o r m ay be sent out for other separation processes for better chirality control.

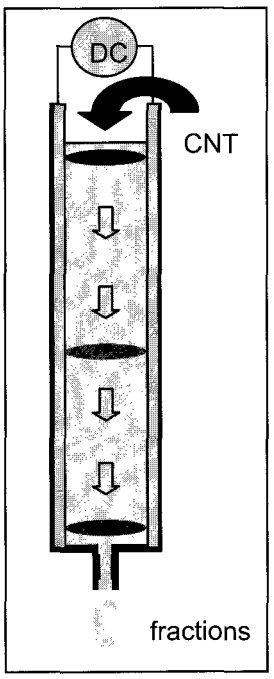

In chrom atography system s, CNT dispersions are injected into a column supporting a solven t flow which carries CNT s to another end of the colu mn. Separation takes p lace while C NTs are flowing downstream. We can obtain the separated CNT s by sim ply collecting the solu tion com ing out of the co lumn. In field-ef fect chromatography. dc electric field is applied perpendicular to the flow direction. We have designed the column so that the flow has non-uniform velocity distribution ac ross the electrodes. Then, CNT s that exh ibit dif ferent electrop horetic movem ents experience dif ferent flow velocity . C onsequently, collecting the fractions that have came out of the column at different tim e contain CNT s that h ave dif ferent electrophoretic properties.

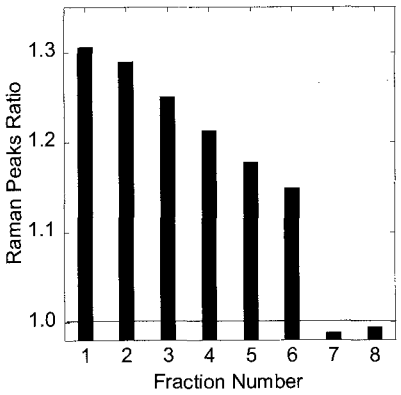

We will re port th e ef fects of app lied vo ltage, column length, flow velocity , and solvents on separation efficiencies. W e have f ound that stability of CNT dispersion (without any additives) is the m ain factor that determines an optimum condition for better separation.

Corresponding Author: Masahito Sano
E-mail: mass@yz.yamagata-u.ac.jp
Tel&Fax: +81-238-26-3072

2P-32

Ideal interfacial structure constructed by the two-step assembly of Polybenzimidazole with Multi-walled Carbon Nanotubes and Pt nanoparticles for fuel cell catalyst

○Minoru Okamoto, Tsuyohiko Fujigaya, Naotoshi Nakashima

Department of Applied Chemistry, Graduate School of Engineering
Kyushu University, Fukuoka, Japan

Abstract: Polybenzimidazole (PBI: **Fig. 1**) is expected to the use for electrolyte membrane of Polymer Electrolyte Fuel Cell (PEFC) under dry condition and seen as an alternative to Nafion®. The electrode catalyst of the PEFC is usually composed of Pt, Electrolyte and Carbon support. Carbon Nanotubes (CNTs) was emerged as a better carbon support material than Carbon Black. We recently reported the PBI is adsorbed to CNTs and acts as the solubilizer [1]. This finding enables to hybrid Pt, PBI and CNTs for PBI-base electrode catalyst.

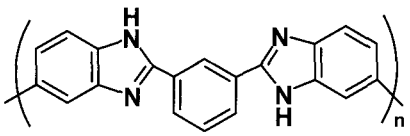

Fig. 1 Polybenzimidazole (PBI).

Pt supporting on MWNT/PBI composites was carried out by the polyol approach. **Fig.2** shows the TEM and SEM images of electrode catalyst composites (MWNT/PBI/Pt). Pt catalysts were supported on MWNT/PBI.

TGA analysis of MWNT/PBI/Pt revealed that 60 wt% of Pt was supported on MWNT/PBI. This value was larger than MWNT/Pt (40 wt%). This result and IR measurement indicate that PBI acts as an anchor of Pt ion and the volume of Pt was increased.

In addition this, the Electrochemically Active Surface Area (ECSA) of MWNT/PBI/Pt was also better than that of MWNT/Pt. Pt catalyst was well-dispersed on MWNT/PBI and form ideal interface (**Fig.3**).

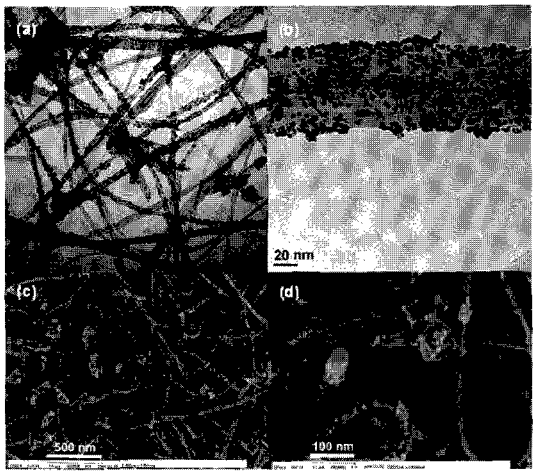

Fig. 2 (a),(b) TEM and (c), (d) SEM images of MWNT/PBI/Pt composites.

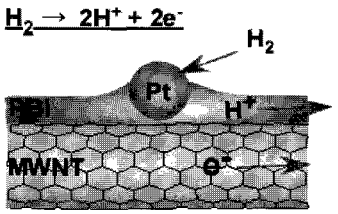

Fig. 3 The ideal interface of electrode catalyst.

References: [1] M. Okamoto, T. Nakashima, N. Nakashima, *Adv. Funct. Mater.* **2008**, 18, 1776-1782.

Corresponding Author: Naotoshi Nakashima
E-mail: nakashima-tcm@mail.cstm.kyushu-u.ac.jp
Tel&Fax: +81-92-802-2840

Electron Optical Evaluation of a Carbon Nanotube Field Emitter for Electron Microscopes

○Y.Kusano, K.Asaka, H. Nakahara, and Y. Saito

Dept. of Quantum Eng., Nagoya University, Furo-cho, Nagoya 464-8603

Carbon nanotubes (CNTs) are one of ideal materials for field emission (FE) electron sources, because of its small tip radius, high aspect ratio, robustness, low cost, etc. We have developed a test system of FE electron gun to evaluate and compare a CNT FE tip with a tungsten one.

CNTs used in this experiment are multiwalled nanotubes (MWNTs) produced by catalyst free arc discharge method. Average diameter of MWNTs is about 15 nm. A MWNT is attached to a tip of a chemically etched tungsten wire using electrophoresis (Fig. 1). A single crystalline tungsten (W) tip used for comparative experiments is a commercial FE tip for a SEM (S-800; Hitachi). The test FE electron gun system is composed of an emitter, an einzel lens, a phosphors screen, and a micrometer driven knife edge. The emitter, the extractor and the anode are designed compatible to the SEM described above. Base pressure of the apparatus is about 10^{-8} Pa.

Fig. 2 shows I-V characteristics (applied voltage between the emitter and the extractor versus emission current) of a CNT and a W emitters. According to the Fowler-Nordheim (F-N) equation, the slope and the intercept of the figure depends on a voltage-to-field conversion factor β, an emission area A, and a work function φ of an electron emitter. Using reported values of φ for CNT (4.6 eV) and W (4.35 eV), β and A values for the CNT and the W emitters are obtained as; $\beta = 4.4\times10^{5}$ and 2.7×10^{4} [cm^{-1}], and $A = 3.0\times10^{-12}$ and 3.7×10^{-9} [cm^{2}] respectively. Assuming that the area A corresponds to a hemisphere of a tip, the tip radii for respective emitters are calculated as 6.9 nm for the CNT and 240 nm for the W, which are consistent with the SEM measurements of those emitter tips.

Brightness B of each emitter are also measured by knife edge method with acceleration voltage at 5 kV under convergence condition using the einzel lens. The measured B values of the CNT and the W emitters are 3.8 and 0.14 A/$cm^2\cdot$sr, respectively. Both I-V characteristic and brightness results show that even a thick MWCNT of ~15 nm diameter has much higher performance than a conventional single crystalline tungsten emitter.

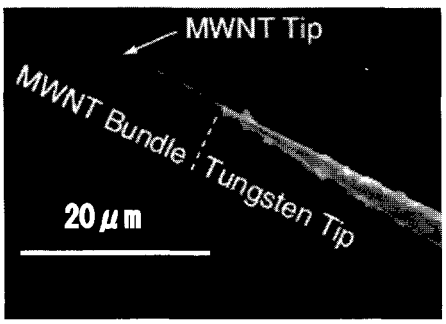

Figure 1: SEM image of an MWNT emitter

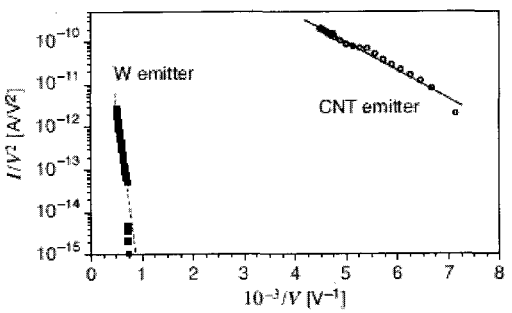

Figure 2: F-N plots for the MWNT and the tungsten emitters

Corresponding Author: Yoshikazu Kusano

E-mail: yoshikazu@surf.nuqe.nagoya-u.ac.jp Tel:+81-52-789-3714 , Fax:+81-52-789-3703

The Attempt of Chirality Control of Semiconducting Single-Walled Carbon Nanotubes by the Free Electron Laser Irradiation

○ Daisuke Ishizuka[1], Keijiro Sakai[2],
Katsumi Uchida[2], Nobuyuki Iwata[1], Hirofumi Yajima[2] and Hiroshi Yamamoto[1]

[1] *Department of Electronics & Computer Science, College of Science & Technology, Nihon University, 7-24-1 Narashinodai, Funabashi, Chiba 274-8501, Japan*
[2] *Department of Applied Chemistry, Faculty of Science, Tokyo University of Science, 12-1 Funagawara-cho, Ichigaya, Shinjyuku-ku, Tokyo 162-0826, Japan*

We attempt to control the chirality of single-walled nanotube (SWNT) using free electron laser (FEL) irradiation during growth. In particular, semiconducting SWNTs are expected for application of field effect transistor. It is expected that the irradiation excites the corresponding SWNT, and the SWNT with the specific chirality is promoted to grow. The quartz substrates, which were annealed for five min at 500°C, were dipped in methanol dissolving Co and Mo Catalysts. The dipping speed was 600μm/s. The dipped substrate was annealed for five min at 400°C. The CNTs were grown using alcohol catalytic chemical vapor deposition (ACCVD) method with ethanol. For the chirality control, the FEL was *in-situ* irradiated during the ACCVD. In the SWNTs grown without FEL, the peak of radial breathing modes (RBM) was observed. From one of the peak centers, the diameter of the SWNTs was estimated at 1.1 nm, but the electric property is probably metallic because of the Raman measurement carried out with only 532 nm excitation laser. From the simulation by Strano, the irradiation of FEL with the wave length of 1300 ~ 1500 nm was expected to be effective to promote the synthesis of semiconducting SWNTs with the diameter of 1.1 nm[1-2]. With the 1300nm FEL irradiation, any RMB peaks did not appear. Nevertheless it was a promising result, because resonance Raman effects just did not occur. It is anticipated that the RBM peaks should appear with around 800 nm excitation laser. The obtained results revealed the possibility of chirality control by FEL irradiation. If expected SWNTs grew up, the obtained chirality might be (n, m) = (9, 7) or (13, 2). The properties of other SWNTs which were grown under FEL irradiation as changing wavelength will be appeared.

References

[1] M. S. Strano, J. Am. Chem Soc. 125 (2003) 16148
[2] H. Kataura et al. Synthetic Metals 103 (1999) 2555

Selective Separation Methods for Metallic and Semiconducting Single-walled Carbon Nanotube in Aqueous Solution with High-fluence Pulsed OPO Laser

○Isamu Tajima, Katsumi Uchida, Tadahiro Ishii, and Hirofumi Yajima*

Department of Applied Chemistry, Faculty of Science, Tokyo University of Science
12-1 Funagawara-machi, Shinjyuku-ku, Tokyo 162-0826, Japan

Selective separations of metallic (m) and semiconducting (s) single-walled carbon nanotubes (SWNTs) have been requested for practical and advanced applications. We have proposed a new selective separation method with pulsed optical parametric oscillator (OPO) laser, choosing adequate excitation wavelength for the resonance absorption of the SWNTs solution.

A nanosecond OPO pulsed laser operating at 10 Hz with pulse energy of 20 mJ was focused into 10 mm quarts cell filled with 2 mL SWNTs dispersion (suspended in sodium dodecylsulfate (SDS) solution). The laser irradiation was made by tunably selecting excitation-wavelength in the region of M11 and S22 bands. Therein, as the irradiation wavelengths in the M11 region, the three wavelengths (485, 510, 533nm) across chiral peak of 510nm including either side one for the peak were selected. On the other hand, as the irradiations wavelengths in the S22 region, the three wavelengths (690, 730, 768nm) across chiral peak of 730nm including either side one of the peak were selected. Then, the effects of laser irradiation on the optical properties of the individually dispersed SWNTs in the SDS solutions were investigated by UV-vis-NIR absorption, NIR photoluminescence and resonance Raman scattering spectroscopies and dynamic light scattering measurements.

As a result, the efficiencies of the laser irradiation at either side wavelength (485 or 533 nm in M11 region and 690 or 768 nm in S22 region) for the chiral peak (510nm in M11 region and 730nm in S22 region) were greater than that at the main chiral peak. Additionally, the laser irradiation in M11 region decreased overall spectral intensity derived from m- and s-SWNTs. On the other hand, the 730 and 768 nm irradiation in S22 region gave rise to the concentration of the m-SWNTs components.

Two species of contributions for energy migration processes, that is, photo-relaxation and thermal-relaxation are multiply involved in the energy conversion for the SWNTs exited with the laser irradiation. In the S22 irradiation, the photo-relaxation (photoluminescence) process is predominated for the resonance excitation of a chiral SWNT, whereas the thermal-relaxation process is predominated for the excitation at the wavelengths deviated from the chiral peak, accompanied by the collapse of SWNTs due to huge temperature rise. On the other hand, the collapse of SWNTs induced by the M11 irradiation is concerned with the thermal-relaxation process through the plasmon absorption, regardless of excitation wavelengths.

***Corresponding Author:** Hirofumi Yajima
TEL: +81-3-5228-8705, FAX: +81-3-5261-4631, E-mail: yajima@rs.kagu.tus.ac.jp

Enhancement of Carbon Nanotube Growth at Low Temperature using Al_2O_x Buffer Layer in Alcohol Gas Source Method

○Takahiro Maruyama, Kuninori Sato, Tomoyuki Shiraiwa, and Shigeya Naritsuka

Department of Materials Science & Engineering, Meijo University, Nagoya 468-8502, Japan

Recently, we have been developing a gas source method in an ultra-high vacuum (UHV) chamber for carbon nanotube (CNT) growth [1]. This growth technique enables CNT growth in a high vacuum, which is useful for investigation of the growth mechanism and can reduce the growth temperature below 400°C. In spite of these advantages, the yields of CNTs grown by the gas source method have been insufficient. In this study, we utilized an Al_2O_x layer in CNT growth to attain a yield enhancement.

Co/Al_2O_x catalysts were formed on SiO_2(100 nm)/Si substrates and Mo TEM grids. The nominal thickness of the Al was varied from 0 to 60 nm, whereas the Co thickness was set to a constant 0.1 nm. Subsequently, CNT growth was carried out by the gas source technique using ethanol. The supply of ethanol gas was controlled by monitoring the ambient pressure.

When the growth was carried out at 700 °C under 10^{-1} Pa of ethanol, web-like CNTs were directly grown on the SiO_2/Si substrates, as shown in Fig. 1(a). The CNT density was enhanced by inserting the Al_2O_x layer between Co and the substrates. As the thickness of the Al layer increased, the density of CNTs increased and reached a maximum at an Al thickness of 30 nm (Fig. 1(b)), and vertically aligned CNTs were also observed in some areas. TEM observation showed that Co catalyst formed nanosized particles which were suitable for CNT growth, although some diffusion of catalyst into the Al_2O_x layers were seen. We also attempted to utilize the buffer layer for the growth at 400 °C. The density was increased by inserting the Al_2O_x layers in CNT growth at 400 °C under 10^{-4} Pa of ethanol, whereas it was quite low without the buffer layer (Figs. 1(c) and (d)). From these results, we concluded that the Al_2O_x buffer layers were effective to enhance CNT growth even at low temperature.

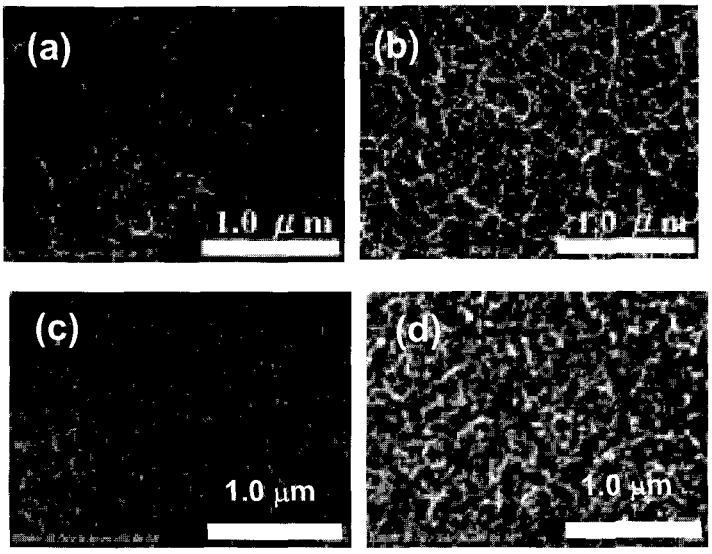

Fig. 1 SEM images of CNTs grown on SiO_2/Si at (a), (b) 700°C under 10^{-1} Pa of ethanol and (c), (d) 400°C under 10^{-4} Pa. The CNT growth was carried out without (a) (c) and with (b) (d)Al_2O_x buffer layers, respectively.

References: [1] K. Tanioku, T. Maruyama and S. Naritsuka, Diamond Relat. Mater. 17 (2008) 589.

Corresponding Author: Takahiro Maruyama
E-mail: takamaru@ccmfs.meijo-u.ac.jp
Tel: +81-52-838-2386, **Fax**: +81-52-832-1172

Separation of metallic and semiconducting single-wall carbon nanotubes by using sucrose as a gradient medium

○Kazuhiro Yanagi[1], Toshie Iitsuka[1], Shunjiro Fujii[1], Hiromich Kataura[1,2]

[1]*Nanotechnology Research Institute, National Institute of Advanced Industrial Science and Technology (AIST), 305-8562 Tsukuba, Japan,* [2]*JST-CREST*

Abstract: Single-wall carbon nanotubes (S WCNTs) exhibit m etallic and sem iconducting characteristics depending on their chirality . Various production techniqu es of SWCNT s have been propos ed, however, the p roduced sam ples ar e in a m ixed state of the m etallic and th e semiconducting nanotubes. Separation of the two types of nanotubes is crucial for their device applications, thus a lot of separation technique s have been proposed to solve this problem .[1] Density gradient ultracentr ifugation (DGU), which was firs tly proposed by Arnold et al., [2] is one of the m ost suitable techniques to obt ain high-purity m etallic and sem iconducting nanotubes. Since their work, various DGU techniques concerni ng purification, length and chirality selections of SWCNT s have been proposed. [3] Rem arkably, in a ll the prev ious DGU separations of SWCNT s, iodixa nol was used as a gradient medium. Separation with other gradient m edium such as sucrose, which is the most popular m edium in DGU, has not been reported yet. It is well-known that the am ount and the types of surfactants significantly influence separation capability . However , influe nce of the gradient medium on s eparation capability h as not been understood well. If iod ixanol is th e only gradient m edium that can separate m etallic and sem iconducting nanotubes, specific interactions between iodixanol and SWCNTs must be taken into co nsideration to understand the separation mechanisms in DGU. For the detailed understanding of physical backgrounds of metal-semiconductor separations in DGU, it is im portant to verify whether it is possible to separate the m etallic and the semiconducting types by using other gradient medi um than iodixanol. In this study, we tried to separate m etallic and sem iconducting n anotubes by using sucrose as a gradient m edium (sucrose-DGU). Such clar ification is a lso of im portance to im prove the cost of separation, since i odixanol is an expensive reagent. As shown in Fig. 1, we found that it is possible to enrich m etallic an d sem iconducting nanotubes through sucrose-DGU b y tuning the concentrations and the types of surfactan ts and tem perature du ring DGU.

This study was supported by industrial technology research grant program from New Energy and Industrial Technology Development Or ganization (NEDO) of Japan.

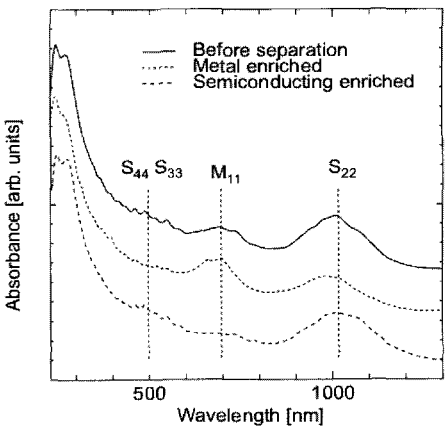

FIG 1: Optical absorption spectra of initial SW CNT, m etallic SWCNT enriched, and semiconducting SW CNT enriched so lutions ob tained by sucrose-DGU.

References: [1] a revi ew pa per by M.C. Hersam, Nat. Nanotechnology, **3** (2008) 387 . [2] Arnold et al., Nat. Nanotechnology, **1** (2006) 60. [3] Yanagi et al., Appl. Phys. Express, **1** (2008) 034003. Fagan et al., Adv. Mater., **20** (2008) 1609. Green and Hersam, Nano Lett., **8** (2008) 1363.

Corresponding Author: K. Y., E-mail: k-yanagi@aist.go.jp
Tel&Fax: 029-861-3132 & 2786

Liquid-phase Synthesis of Highly Aligned Carbon Nanotubes with Heat-treated Stainless Steel Substrates

○Kiyofumi Yamagiwa, Yoshihiro Yamaguchi, Tomoka Kikitsu, Shunsuke Yamashita, Tsuneharu Takeuchi, Morihiro Saito and Jun Kuwano

Department of Industrial Chemistry, Faculty of Engineering, Tokyo University of Science, 12-1 Ichigayafunagawara-machi, Shinjuku-ku, Tokyo 162-0826, Japan

Ando *et al.* have recently reported the liquid-phase synthesis of highly aligned carbon nanotube arrays (HA-CNTAs) on Si substrates [1,2]. Our group has also developed one-step liquid-phase synthesis of HA-CNTAs with a stainless steel substrate and homogeneously alcoholic solution of metallocene catalysts [3,4].

In this study, we have developed a novel low cost and simpler process for the liquid-phase synthesis of HA-CNTAs with heat-treated stainless steel substrates. This method requires no catalysts besides the stainless steel substrate.

We used commercially available stainless steels (SUS304, 5×25×0.1 mm^3) as the substrate: [A] as-supplied, [B] heat-treated at 500°C for 25 min in air prior to the synthesis. The substrate was resistance-heated at 800°C for 15 min in an alcohol (200 ml) by applying an alternate current. Straight-chain primary alcohols (methanol, ethanol, and 1-butanol) were used as a carbon source.

Multi-walled CNTs (MWCNTs) were grown lying irregularly on the substrate [A] from all the alcohols. On the other hand, HA-CNTAs (multi-walled) were grown from ethanol and 1-butanol on the substrate [B] (Fig. 1). MWCNTs were not aligned on the substrate [B] from methanol, but the yields of CNTs were large compared with the case of the substrate [A]. Metallic nanoparticles containing Fe, Cr, and Ni were often observed in the insides of the tips of HA-CNTAs under TEM.

The SEM observation revealed that the substrate [B] (before the CNT synthesis) had concave and convex surface due to coarsening of grains (~100 nm). We presumed that those grains functioned as catalysts of the CNT growth.

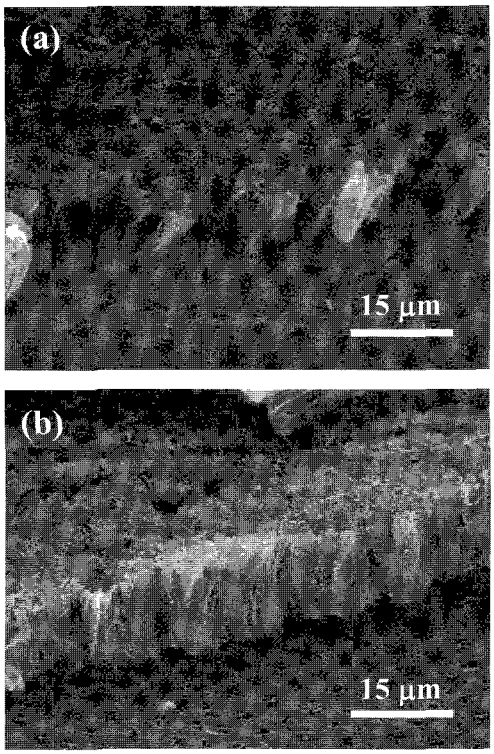

Fig. 1. SEM images of HA-CNTAs prepared from (a) ethanol and (b) 1-butanol.

[1] Y. F. Zhang, M. N. Gamo, C. Y. Xiao and T. Ando, *Physica B*, **323**, 293 (2002).

[2] Y. F. Zhang, M. N. Gamo, C. Y. Xiao and T. Ando, *Jpn. J. Appl. Phys.*, **41**, L408 (2002).

[3] K. Yamagiwa *et al.*, *Key Eng. Mater.*, **350**, 19 (2007).

[4] M. Mikami *et al.*, *Key Eng. Mater.*, **350**, 23 (2007).

Corresponding Author: Jun Kuwano

TEL/FAX: +81-3-5228-8314, E-mail: kuwano@ci.kagu.tus.ac.jp

2P-39

Temperature dependence in the diameter distributions of SWNTs revealed by optical absorption measurements in solution

○T. Nakayama, A. Inoue, K. Yokoi, Y. Tsuruoka, T. Kodama and Y. Achiba

Department of Chemistry, Tokyo Metropolitan University, Hachioji, Tokyo 192-0397, Japan

Controlling chiral distribution of single walled carbon nanotubes must be one of the most important key technologies for realizing potential application of SWNTs to nano-eletcronic devices. However, the knowledge of controlling the growth process to produce the SWNTs with particular chirality has been very limited so far. In the present paper, we will demonstrate *quantitative* experimental evidence concerning how furnace temperature of a laser vaporization method does work on the diameter and chiral distributions of SWNTs by measuring optical absorption spectra in organic solution.

The sample of SWNTs used in the present work was prepared by laser vaporization-furnace method in connection with systematical change of the furnace temperature from 900℃ to 1250℃ in the rare gas atmosphere. Ni/Co was used as a catalyst. The prepared SWNTs soot and PFO (*poly-9, 9-di-n-octyl-fluorenyl-2, 7-diyl*) [1] were mixed in toluene followed by homogenization and sonication. After 1-hour water-bath and 5 min tip sonication, the mixture solution was centrifugation f or 30 min. using a desktop centrifuge (5000-10000g).

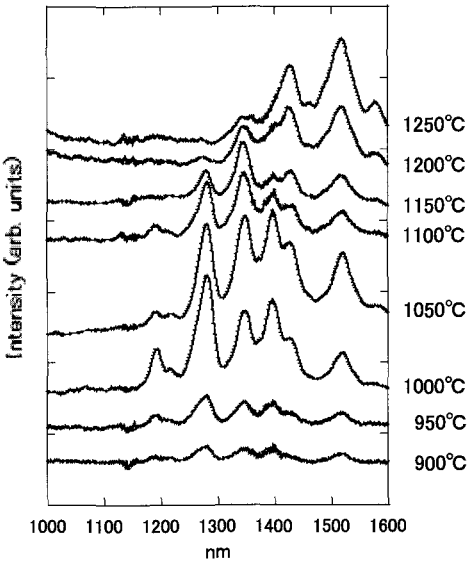

Fig. 1 Absorption spectral chang e in the E_{11} energy range of se miconducting SWNTs by changing pr eparation temperature from 900℃ t o 1250℃.

Figure 1 shows absorption spectral change in the E_{11} energy range of semiconducting SWNTs by changing preparation temperature from 900℃ to 1250℃. It was found that at around 1000-1050℃、the yield of particular tubes such as (8,7) and (9,7) increases very much, whereas at the higher temperature, the tubes with the lower chiral angle such as (10,6) or (12,5) increases. The more detailed results will be discussed in the symposium.

[1] A. Nish, et al., *nature nanotechnology.* **2**, 290 (2007)

Corresponding Author: Yohji Achiba
Tel: 042-677-2534, E-mail: achiba-yohji@tmu.ac.jp

Optical properties of SWNTs with very small diameter

ON.Takamizu[1],Y.Ohnishi[1],K.Urata[1],S.Suzuki[2],H.Nagasawa[3],and Y.Achiba[1]

[1]*Department of Chemistry, Tokyo Metropolitan University, Tokyo 192-0397,Japan*
[2]*Department of Physics, Kyoto Sangyo University, Kyoto 603-8555, Japan*
[3]*Nitta Haas Inc. ,Tokyo 104-0061, Japan,*

So far we have reported the synthesis of SWNTs with small diameter and narrow diameter distribution by using platinum metal particle as a catalyst and porous glass (PG) as a support material [1,2]. Since the analyses of SWNTs by TEM, Raman and photoluminescence spectroscopy were not enough to deduce *quantitatively* the relative yield of each SWNT with different chiral induces, in the present paper, we measured optical absorption spectra of the SWNTs by which the relative yield could be more easily and precisely determined.

The sample of SWNTs was synthesized by alcohol CVD method using ethanol as carbon source. For the purpose of obtaining the SWNTs with the diameter as small as possible, in the present work, the ambient temperature and inner pressure of ethanol were kept at 800℃ and 0.07 torr, respectively. The as-grown sample of SWNTs were characterized by Raman by 488nm and 633 nm excitation, and then dispersed in SDBS/H_2O solution to measure optical absorption and PL.

In Figs.1 (a) and (b), Raman and absorption spectra are shown to compare the relative intensity of SWNTs with different chirality. Since the numbers of SWNTs with different chiral induces are very limited for the prepared sample, each absorption bands obtained were easily able to be assigned as shown in Fig.2. From this figure, it is seen that the most abundant SWNTs are (5,4) and (6,4) tubes. More detailed results will be shown in the symposium.

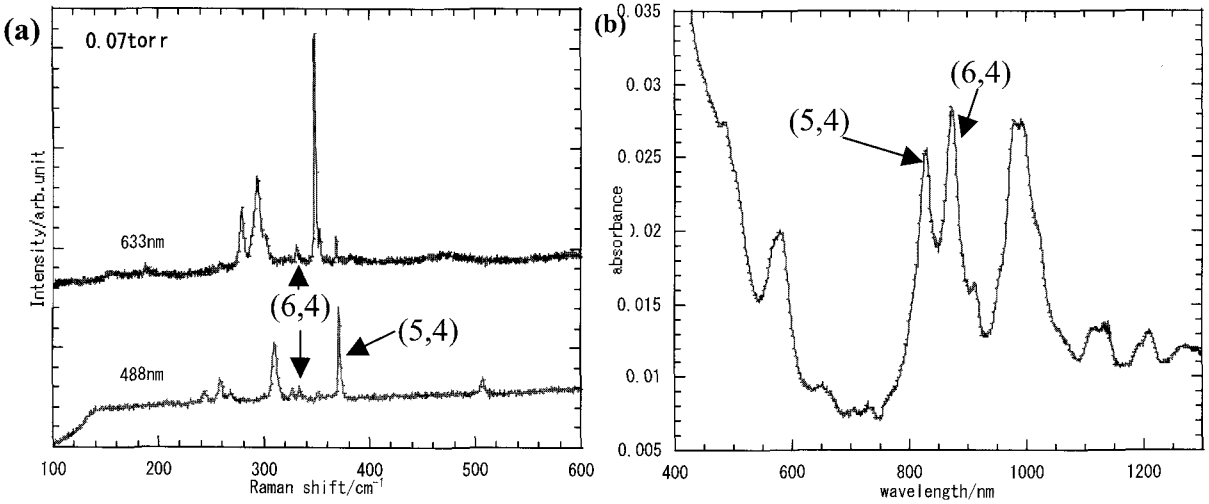

Fig.1(a):Raman spectrum at 488nm and 633nm of SWNTs synthesized at 800℃ .
(b):Optical absorption spectrum of SWNTs in SDBS/H_2O solution.

References:[1] Y. Aoki et al., Chem. Lett., **562**, 34(2005)
[2] K. Urata et al., The 34th Fullerene-Nanotubes General Symposium, 2P-9 (2008).

Corresponding Author: Yohji Achiba

E-mail: achiba-yohji@c.metro-u.ac.jp, **TEL**:042-677-2534

Precursors in Co catalyzed CVD for vertically aligned SWCNT

○Hisashi Sugime and Suguru Noda

Dept. of Chemical System Engineering, The University of Tokyo, Tokyo, 113-8656, Japan

In direct growth of SWCNTs on substrates by CVD methods, several groups have succeeded in growing vertically aligned SWCNTs under different conditions. Ethanol is an effective carbon feedstock for the growth of VA-SWCNTs when Co-Mo catalyst is used [1,2]. However, the precursors which directly grow SWCNTs are not clear because ethanol easily decomposes at high temperature.

In this study we used our "cold-gas CVD" apparatus consisted of preheating zone, cooling zone, and growth zone. At the growth zone, a ribbon shaped substrate is resistively heated and the gas was kept at low temperature while passing over the substrate. We can independently control the gas phase reaction and catalyst reaction by changing the temperatures of preheating and reaction zones. This time, we used Co/Al_2O_3 catalyst, which can grow SWCNTs faster than Co-Mo, and gradient thickness profile is formed in Co layer by applying a combinatorial method [2].

When the ethanol pressure was 1.2 Torr and substrate temperature was 800 °C, vertically aligned SWCNTs effectively grew only when the temperature of preheating zone was higher than 900 °C. In the CHEMKIN [3] simulation, ethanol decomposes in the gas phase rapidly in a few seconds and the partial pressures of H_2, C_2H_2, C_2H_4 depend on the gas temperature whereas those of CH_4, CO, H_2O do not depend on it. Among these species C_2H_2 is known to be highly active, so we carried out CNT growth by applying C_2H_2 with low pressure estimated from CHEMKIN simulation. Figure (a) and (b) show the SEM images of CNT forest grown from C_2H_5OH with gas preheating at 1000 °C and Fig. (c) and (d) show that grown from C_2H_2 without gas preheating. The temperature of substrate was 800°C in both cases. Figure (e) shows the Raman spectra taken from top of CNT forests shown in Fig. (a) and (c). Vertically aligned SWCNTs with high G/D ratio grew from C_2H_2 without preheating implying that C_2H_2 is the direct precursor for rapid growth of vertically aligned SWCNTs.

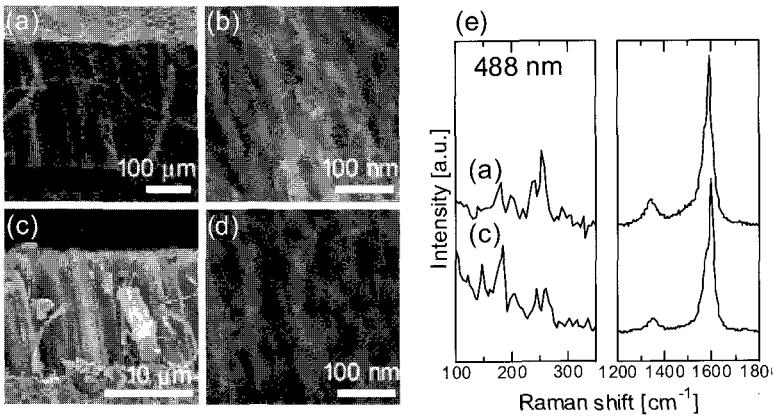

Fig. SEM images and Raman spectra of CNT forest grown using C_2H_5OH (a and b) and C_2H_2 (c and d). (b) and (d) are the magnified images of (a) and (c), respectively. Raman spectra were taken from top of (a) and (c).

[1] Y. Murakami, et al., Chem. Phys. Lett. **385**, 298 (2004). [2] S. Noda, et al., Carbon **44**, 1414 (2006). [3] Marinov NM. Int. J. Chem. Kinetics. **31**, 183 (1999).

Corresponding Author: Suguru Noda TEL/FAX: +81-3-5841-7330/7332, E-mail: noda@chemsys.t.u-tokyo.ac.jp

Controlling the wall number of carbon nanotubes by changing the carrier gases

○Daisuke Yokoyama[1], Takayuki Iwasaki[1], Kentaro Ishimaru[1], Masatomo Iizuka[1], Shintaro Sato[2], Mizuhisa Nihei[2], Yuji Awano[2] and Hiroshi Kawarada[1]

[1]*School of Science and Engineering, Waseda university, Tokyo 169-8555, Japan*
[2]*MIRAI-Selete, Atsugi 243-0197, Japan*

In plasma CVD, the balance of carbon and hydrogen radicals was crucial for carbon nanotube (CNT) growth [1]. In this study, we focus on the effect of the hydrogen on the growth of multi-walled CNTs (MWNTs) by remote plasma CVD.

The Co particles with a mean diameter of 3.8 nm were used as catalysts and MWNTs growth was carried out at a substrate temperature of 390°C [2] in different atmospheres of H_2/CH_4 and He/CH_4. Figure 1 shows TEM images of MWNTs grown at different atmospheres. MWNT grown at He/CH_4 was covered with amorphous carbon and the outer diameter (mean. 10 nm) was larger than that of H_2/CH_4 (mean. 7 nm). Figure 2 indicates that MWNTs grown at He/CH_4 has larger number of walls compared to H_2/CH_4 growth. However, the Co particles annealed at 390°C in He/CH_4 atmosphere were smaller than those of H_2/CH_4. Therefore, it is speculated that the hydrogen removes partially carbon precursors for growing MWNTs at the nucleus formation stage and contributes to forming the MWNTs with the small diameter. The wall number of MWNTs could be controlled by the ratio of H_2 during catalytic CVD growth.

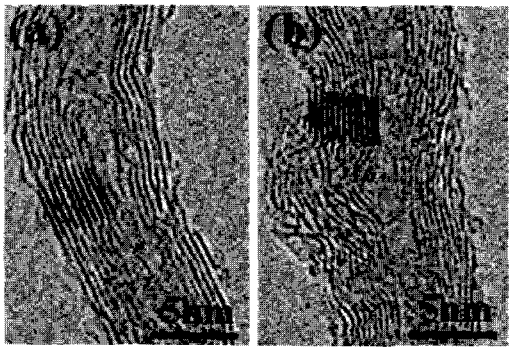

Fig. 1 TEM images of MWNTs grown at (a) H_2/CH_4 and (b) He/CH_4 atmospheres

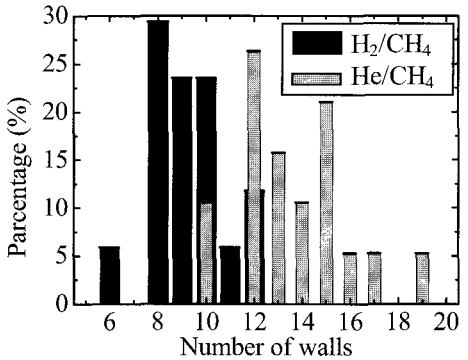

Fig. 2 Distribution of wall number of MWNTs grown at different atmospheres

Acknowledgements: This work was completed as part of the MIRAI Project supported by NEDO.

[1] G Zhang, et al. Proc. Natl. Acad. Sci. U.S.A. 102, 16141 (2005).

[2] D. Yokoyama, et al., Appl. Phys. Lett. 91, 263101 (2007).

Corresponding Author: H. Kawarada E-mail : kawarada@waseda.jp Tel&Fax : +81-3-5286-3391

Correlations between gas pressure and diameter distribution of single-walled carbon nanotubes in diffusion plasma CVD

○S. Kuroda, T. Kato, T. Kaneko, and R. Hatakeyama

Department of Electronic Engineering, Tohoku University, Sendai 980-8579, Japan

Single-walled carbon nanotubes (SWNTs) are nano carbon materials consisting of a single graphene sheet. Since they have great and unique electrical properties, a carbon nanotube field effect transistor (CNT-FET) is expected to be a critical component of next-generation nano electronic devices. In order to realize the practical use of the CNT-FET, however, it is an inevitable issue to precisely control SWNT structures such as tube diameter, length, chirality, alignment, and so on. Based on this back ground, we investigate effects of gas pressures over a wide range on the structures of SWNTs with diffusion plasma CVD which has been developed by ourselves [1]. The mixture of methane and hydrogen gas is used as a carbon source and the pressure range is varied from 20 Pa to 800 Pa. The SWNTs production is carried out on a Fe 0.3 nm /Al_2O_3 20 nm /Ag substrate that is heated and set underneath a lower discharge-electrode called an anode. The chirality distribution of as-grown SWNTs is analyzed with photoluminescence (PL) spectroscopy [2]. Figure 1 illustrates the photoluminescence-excitation (PLE) map of SWNTs produced by the diffusion plasma CVD method as a function of gas pressure. The results show that the small diameter SWNTs tend to decrease with an increase in the pressure during the plasma irradiation. This fact indicates that the amount of precursor plays an important role in the diameter distribution of SWNTs and it might be possible to control the chirality or diameter distribution of SWNTs by precisely adjusting the plasma parameters.

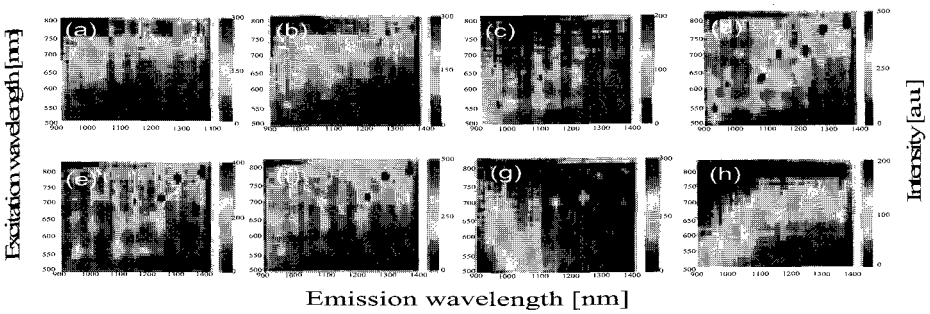

Fig. 1: PLE map of as-grown SWNTs. (a) 20 Pa , (b) 30 Pa, (c) 60 Pa, (d) 100 Pa, (e) 300 Pa, (f) 550 Pa, (g) 650 Pa, (h) 800 Pa.

[1]T. Kato and R. Hatakeyama, *Appl. Phys. Lett.* **92**, 031502 (2008).

[2]T. Kato and R. Hatakeyama, *J. Am. Chem. Soc.* **130**, 8101 (2008).

Corresponding Author: S. Kuroda
TEL: +81-22-795-7046, FAX: +81-22-263-9225, E-mail: kuroda@plasma.ecei.tohoku.ac.jp

Growth of Helical Carbon Nanofiber by Catalytic Chemical Vapor Deposition Using Co/Sn Catalyst

○Y. Shinohara[1], M. Yokota[1], Y. Suda[1], S. Oke[1], H. Takikawa[1],
Y. Fujimura[2], T. Yamaura[2], S. Itoh[2], K. Miura[3], M. Morioki[4]

[1]*Department of Electrical and Electronic Engineering, Toyohashi University of Technology.*
[2]*Research and Development Center, Futaba Corporation.*
[3]*Fuji Research Laboratory, Tokai Carbon Co., Ltd.*
[4]*Fundamental Research Department, Toho Gas Co., Ltd.*

Fe, Ni, and Co are used as a catalyst for carbon nanofiber (CNF) and carbon nanotube (CNT) growth. So far, we have grown helical shaped CNF (HCNF) from Fe/Sn or Ni/Sn catalyst [1]. HCNF is classified into two types, carbon nanocoil (CNC) which has a coil shape and carbon nanotwist (CNTw) which has a twist shape. CNC is grown from Fe/Sn catalyst at 800 °C and CNTw from Ni/Sn catalyst at 550 °C. In this study, we investigated nanocarbon growth from Co/Sn as a catalyst. HCNF is grown by catalytic CVD using acetylene as source gas and nitrogen as dilution gas. Figures 1 and 2 show the SEM images of synthesized CNFs. At 550 °C, thin and tortuous CNFs were grown. At 800 °C, thick and tortuous CNFs were grown and small quantities of CNCs, CNTws and long CNFs were observed.

This work has been partly supported by the Outstanding Research Project of the Research Center for Future Technology, Toyohashi University of Technology; the Research Project of the Research Center for Future Vehicle, Toyohashi University of Technology; the Research Project of the Venture Business Laboratory, Toyohashi University of Technology; Global COE Program "Frontiers of Intelligent Sensing" from the Japanese Ministry of Education, Culture, Sports, Science and Technology (MEXT); The Japan Society for the Promotion of Science (JSPS), Core University Programs (JSPS-KOSEF program in the field of "R&D of Advanced Semiconductors."); and Grant-in-Aid for Scientific Research.

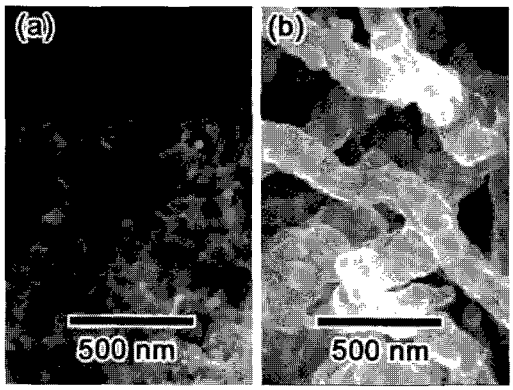

Fig. 1. SEM image of CNFs : (a) grown at 550 °C and (b) at 800 °C

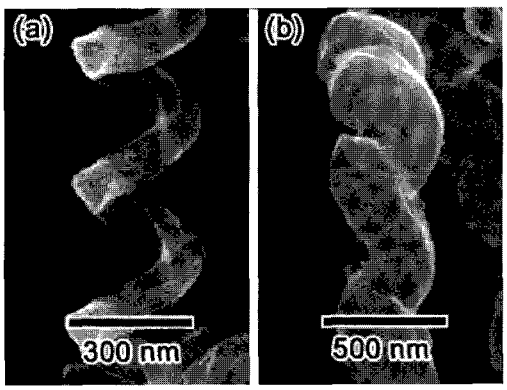

Fig. 2. SEM image of HCNF grown at 800 °C : (a) CNCs and (b) CNTws.

References:

[1] Guochun Xu, et al.: Jpn. J. Appl. Phys. 44 (2005) pp. 1569-1576

Corresponding Author: Yoshiyuki Suda
E-mail: suda@eee.tut.ac.jp, **Tel:** +81-532-44-6726

Diameter-Dependent Band Gap Modification of Single-Walled Carbon Nanotubes by Encapsulated Fullerenes

○Toshiya Okazaki[1,2,3], Shingo Okubo[1], Naoki Kishi[1], Takeshi Nakanishi[1], Susumu Okada[4] and Sumio Iijima[1]

[1]*Nanotube Research Center, AIST, Tsukuba 305-8565, Japan*
[2]*PRESTO, JST, Kawaguchi 332-0012, Japan*
[3]*Department of Chemistry, University of Tsukuba, Tsukuba 305-8577, Japan*
[4]*Institute of Physics and Center for Computational Sciences, University of Tsukuba, Tsukuba 305-8577, Japan, and CREST, JST, Kawaguchi 332-0012, Japan*

Recently, optical band gap modifications of SWCNTs by encapsulated C_{60} were reported by using photoluminescence excitation (PLE) spectroscopy.[1] One of the important factors for the band gap modification is found to be a diameter of SWCNTs because the interaction between the host SWCNTs and the guest C_{60} is sensitive to the interwall distance. For further characterization of the tube-fullerene interactions, however, various kinds of nanopeapods are needed to investigate. Especially, SWCNTs having larger diameters should be examined to elucidate the detailed mechanisms of the band gap change. The SWCNTs produced by the arc discharging method are suited for this purpose because the diameter of arc-SWCNTs (d_t = ~1.3-1.5 nm) is normally larger than those of SWCNTs by the laser-oven method.

In this study, optical band gap shifts of arc-SWCNTs encapsulated C_{60} are investigated by the PLE spectroscopy. The results reveal that the induced band gap shifts strongly depend on the tube diameter and the "$2n + m$" family-type. For C_{60} nanopeapods with smaller diameter (d_t < ~1.32 nm), the steric hindrance of the encapsulated C_{60} is responsible to the shifts. For larger diameter regime (d_t > ~1.32 nm), hybridization between π state of C_{60} and NFE state of SWCNTs causes similar effects to the radial compression on SWCNTs, resulting in the "$2n + m$" family-type dependent band gap modifications.

[1] T. Okazaki, S. Okubo, T. Nakanishi, S.-K. Joung, T. Saito, M. Otani, S. Okada, S. Bandow and S. Iijima, *J. Am. Chem. Soc.*, **130**, 4122 (2008).

Corresponding Author: Toshiya Okazaki
E-mail: toshi.okazaki@aist.go.jp **Tel:** +81-29-861-4173 **Fax:** +81-29-861-6241

Fusion Process of C_{60} fullerenes in Carbon-Nanotube Peapod

○Yuichiro Yamagami and Susumu Saito

Department of Physics, Tokyo Institute of Technology
2-12-1 Oh-okayama, Meguro-ku, Tokyo 152-8551

It is well known that, when C_{60}-peapod is heated, inner C_{60} fullerenes coalesce and turn into a finite-length single-walled nanotube inside the outer carbon nanotube (CNT) [1]. This structural phase transformation has attracted a lot of attention, and many theoretical studies have been performed so far [2,3]. However, the detail of its atomic process has not been revealed yet. In addition to the essential complexity of the process, the technical issue of the molecular dynamics (MD) simulation for this process remains to be solved. When C_{60} fullerenes with a certain length l are all converted to CNT, the length of the converted tube is generally shorter than l. On the other hand, the outer CNT should remain unchanged during the phase transformation process. Therefore, it is impossible to simulate this process in the usual MD calculation. In order to overcome this difficulty, in the present work, we replace the outer tube with the potential with a diameter of the (10,10) nanotube. Moreover, we adopt the variable-cell MD method to simulate perfectly the fusion process involving the system-length change. We perform two kinds of simulations: (1) high temperature and (2) high temperature and high pressure simulations. In the simulation (1), we give an initial temperature ranged from 1500 to 3000 K. On the other hand, in the simulation (2), we vary the external pressure from 0.01 to 10 GPa and give an initial temperature of 3000 K.

It is found that high temperature induces coalescence subsequent to polymerization. In the present work, two types of coalesced structures are obtained (Fig. 1 (a) and (b)). In (a), seven-membered rings appear at the part of the joint, while eight-membered rings also appear in (b). In addition, it is found that the external pressure gives an interesting effect on the transition path. Although the transition to (a) is dominant under zero pressure, the transition to (b) becomes dominant under moderate pressure (0.1 to 5 GPa). Furthermore, under high pressure, C_{60} fullerenes directly coalesce without undergoing polymerization, and immediately turns into a defective nanotube. Interestingly, in some cases, the transition from a defective tube to a perfect tube is observed.

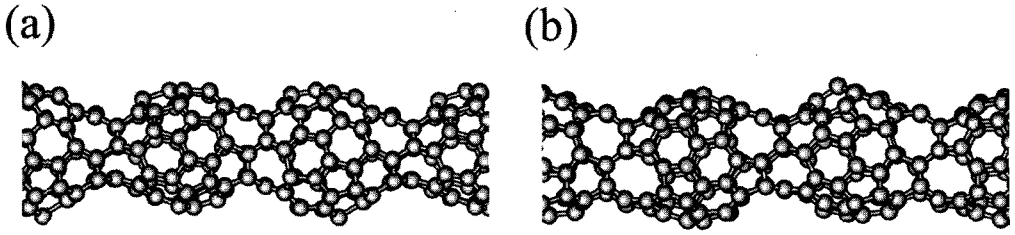

Figure 1. Coalesced structures obtained in the simulations of (a) 2100 K and (b) 2200 K.

[1] S. Bandow, M. Takizawa, K. Hirahara, M. Yudasaka, and S. Iijima, *Chem. Phys. Lett.* **337**, 48 (2001).
[2] E. Hernández, V. Meunier, B. W. Smith, R. Rurali, H. Terrones, M. B. Nardelli, M. Terrones, D. E. Luzzi, and J.-C. Charlier, *Nano Lett.* **3**, 1037 (2003).
[3] Y. Omata, Y. Yamagami, K. Tadano, T. Miyake, and S. Saito, *Physica E* **29**, 454 (2005).

Corresponding Author: Yuichiro Yamagami
TEL: 03-5734-2386, FAX: 03-5734-2739, E-mail: yamagami@stat.phys.titech.ac.jp

Fabrication and Property Evaluation of Calcium Encapsulated Single-Walled Carbon Nanotubes

○T. Shimizu, T. Kato, W. Oohara*, and R. Hatakeyama

Department of Electronic Engineering, Tohoku University, Sendai 980-8579, Japan
** Graduate School of Science and Engineering, Yamaguchi University, Yamaguchi 755-8611, Japan*

Carbon nanotubes (CNTs) with nanometer-order diameter and millimeter-order length attract a great deal of attentions aiming for their novel applications such as next-generation nanoelectronic devices. Accommodation of various dopant atoms, molecules, and compounds is available for modifying the intrinsic electronic and optical properties of single-walled carbon nanotubes (SWNTs). According to our past research, alkali-metal- and halogen-encapsulated SWNTs have been known to exhibit n-type and p-type transport properties under the field effect transistor (FET) configuration[1-2]. If alkaline-earth metal atoms which form doubly-charged positive ions are encapsulated in SWNTs, it is supposed that the n-type transport property can drastically be enhanced. Based on these backgrounds, an alkaline-earth plasma consisting of calcium (Ca) positive ions is utilized as an ion source, and it is attempted to encapsulate them in the hollow space of SWNTs. Electronic-transport characterization of Ca encapsulated SWNTs under the FET configuration is also precisely investigated.

Figure 1 represents the drain current (I_{DS}) -gate voltage (V_G) characteristics of Ca ion encapsulated SWNTs measured with drain-source voltage (V_{DS}) of 1 V in vacuum. The drastic transition of Ca encapsulated SWNTs from p- to n-type transport properties is observed by increasing the Ca ion irradiation time, and the unipolar n-type behavior is realized by the long time Ca irradiation. These results indicate that Ca atoms work as an electron donor and the electronic structure of SWNTs can effectively be modified by the Ca irradiation.

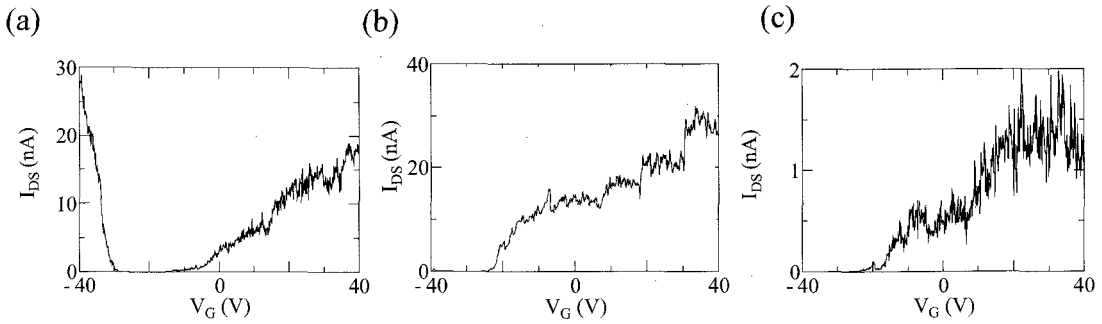

Fig. 1. I_{DS}-V_G characteristics of SWNTs measured at V_{DS} = 1 V by varying Ca ion irradiation time. (a) 30 min, (b) 1 h, (c) 4 h, respectively.

[1] T. Izumida, R. Hatakeyama, Y. Neo, H. Miura, K. Omote, and Y. kasama, Appl. Phys. Lett. **89**, 093121 (2006).

[2] J. Shishido, T. Kato, W. Oohara, R. Hatakeyama, and K. Tohji, Jpn. J. Appl. Phys. **47**, 2044 (2008).

Corresponding Author: T. Shimizu
TEL:+81-22-795-7046, FAX:+81-22-263-9225, E-mail: shimizu@plasma.ecei.tohoku.ac.jp

Nano Scale Separation of the Different Cage Size Empty Fullerene by Nanopeapod Synthesis

○Teguh Endah Saraswati[1], Naoki Imazu[1], and Hisanori Shinohara[1,2]

[1]*Department of Chemistry, Nagoya University, Nagoya 464-8602, Japan*
[2]*Institute for Advanced Research, Nagoya University, and CREST/JST*

Here we report the separation of fullerene in the nano scale. C_{60} in I_h isomer and C_{84} in mixture of D_2 and D_{2d} major isomer have been isolated by the multistage high performance liquid chromatography (HPLC) method using 5PYE and 5PBB column. Mass Spectroscopy spectra and UV/Vis/NIR absorption spectra were taken to confirm their symmetry. The mixture of C_{60} and C_{84} was successful encapsulated inside carbon nanotubes by vapor phase reaction method already reported [1]. Both of those fullerenes performed nanopeapod in high yield. The cage size of the fullerenes inside the carbon nanotubes can be distinguished well each other. Each of those fullerenes performed the packing arrangement inside the tube with the same cage size fullerene in the suitable diameter. It shows that the fullerene tends to group together and form a homogeneous nanopeapod which is strongly related to the tube diameter and the size of fullerene. Their imaging has been studied by using JEOL JEM-2100F electron microscopy at an acceleration voltage of 80 kV. Based on these studies, the fullerene behaviors inside the carbon nanotubes are discussed.

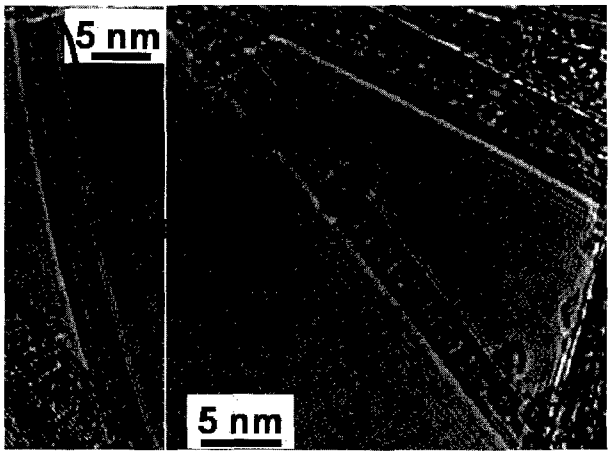

Fig. 1. The encapsulation of the mixture of C_{60} and C_{84} fullerene inside the multi-wall carbon nanotubes. The images performed well separation between them. The images were taken on the same sample.

References :

[1] Ning, G.; Kishi,N.; Okimoto, H.; Shiraishi, M.; Kato, Y.; Kitaura, R.; Sugai, T.; Aoyagi, S.; Nishibori, E.; Sakata, M.,; Shinohara, H. *Chem. Phys. Lett.* **2007**, 441, 94

Corresponding Author : Hisanori Shinohara

E-mail : noris@cc.nagoya-u.ac.jp, **Tel :** +81-52-789-2482, **Fax :** +81-52-789-1169

Supporting RuO_2 on Arc-Soot by Colloidal Method using Ultrasonic Sonication for Electrode Material of Supercapacitors

○H. Uruno[1], M. Yamamoto[1], Y. Izumi[1], S. Oke[1], Y. Suda[1], H. Takikawa[1], S. Itoh[2], T. Yamaura[2], K. Miura[3], T. Okawa[4], N. Aoyagi[4]

[1] *Department of Electrical and Electronic Engineering, Toyohashi University of Technology*
[2]*Futaba Corporation,* [3]*Tokai Carbon Co., Ltd.,* [4]*Daiken Chemical Co., Ltd.*

Ruthenium (Ru)-supported carbon materials for supercapacitors have been researched and several supporting method have been tested. We have supported Ru on arc-soot (AS) by using polyol synthesis method [1]. However, Ru-supported AS (Ru-AS) prepared by the method could have only 4 wt% of Ru on it. In this study, we tried colloidal method [2] using ultrasonic sonication (US) to increase Ru loading on AS.

RuO_2-supported AS (RuO_2-AS) was prepared by mixing NH_4HCO_3 in an aqueous $RuCl_3 \cdot xH_2O$ solution and adding AS into the solution, treating the solution with ultrasonic sonication for 60 minutes and Ru was oxidized. The amount of Ru supported was measured to be 24 wt%. Fig. 1 shows cyclic voltammograms of AS and RuO_2-AS electrodes. Specific capacitance of the RuO_2-AS electrode prepared by colloidal method using US was 170 F/g, 69% higher than specific capacitance of the RuO_2-AS electrode prepared by polyol synthesis method of 101 F/g.

This work has been partly supported by the Outstanding Research Project of the Research Center for Future Technology, Toyohashi University of Technology (TUT); the Research Project of the Research Center for Future Vehicle, TUT; the Research Project of the Venture Business Laboratory, TUT; Global COE program "Frontiers of Intelligent Sensing" from the Ministry of Education, Culture, Sports, Science and Technology (MEXT); Grant-in-aid for scientific research from the MEXT; The Japan Society for the Promotion of Science (JSPS), Core University Programs (JSPS-KOSEF program in the field of "R&D of Advanced Semiconductor" and JSPS-CAS program in the field of "Plasma and Nuclear Fusion").

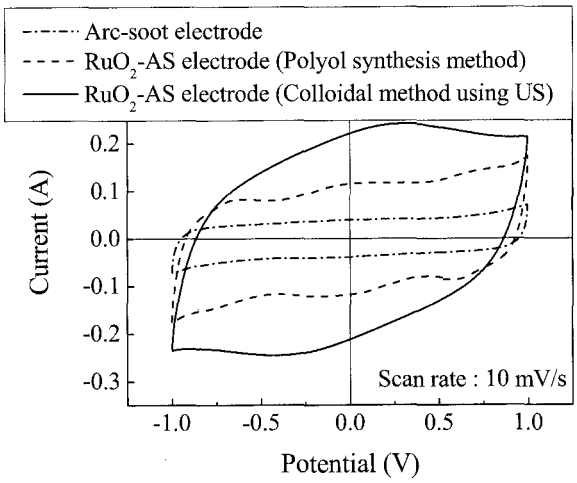

Fig. 1. Cyclic voltammograms of AS and RuO_2-AS electrodes in 1 M H_2SO_4 electrolyte.

[1] W. Li *et al.*: *Carbon*, **42**, 436 (2004)
[2] H. Kim, B.N. Popov: *J. Power Sources*, **104**, 52 (2002)

Corresponding author: Shinichiro Oke
Tel: +81-532-6728, fax: +81-532-6757, e-mail: oke@eee.tut.ac.jp

Effect of Polyethylene Glycol-Peptide Conjugates on Dispersing Carbon Nanohorns and Their Accumulation in Lung

○Sachiko Matsumura[1], Shigeo Sato[2], Masako Yudasaka[3], Akihiro Tomida[2], Takashi Tsuruo[2], Sumio Iijima[4], Kiyotaka Shiba[1]

[1] Cancer Institute, JFCR, Tokyo 135-8550, Japan
[2] Cancer Chemotherapy Center, JFCR, Tokyo 135-8550, Japan
[3] Nanotube Research Center, AIST, Tsukuba, Ibaraki 305-8565, Japan
[4] Meijo University, Nagoya, Aichi 468-8502, Japan

The potentials of single-walled carbon nanohorns (SWNHs) as a drug carrier are being revealed by their ability of loading and releasing drugs [1] and low toxicity [2]. To apply and evaluate SWNHs in this context, well-dispersed SWNHs are strongly preferable. On the other hand, it is known that the surface characters of particulate nanocarrier have great influence on the fate when administered into a body [3]. Therefore, nanoparticles are often modified with polyethylene glycol (PEG) to coat the surfaces to improve their dispersibility and biocompatibility. We previously reported that the conjugate of nanohorn-binding peptide (NHBP-1) and a linear PEG chain bound onto the surfaces of oxSWNHs (oxidized SWNHs) and dispersed them in aqueous solutions [4]. Based on this, we improved the dispersibility of oxSWNHs in a high concentration aqueous solution of salts toward their *in vivo* application.

We synthesized the conjugates consisting of different PEG structure and several NHBP-1. The conjugate of comb-shaped PEG and NHBP-1 showed a higher ability to disperse oxSWNHs in phosphate-buffered saline (PBS) than that of linear PEG and NHBP-1. The dispersibility became even higher by using the PEG having more NHBP-1 units. The dispersion of oxSWNHs modified with the conjugate of comb-shaped PEG and two or three NHBP-1 units was stable in PBS and the particle size did not vary for at least 48 hours. It was suggested that this conjugate had stronger affinity for oxSWNHs and avoided their self-agglomeration.

In addition to the *in vitro* studies, we injected oxSWNHs into tail vein of mice and evaluated the effect of modification with PEG-NHBP conjugates on their accumulation. Since the lung capillary is the first one that the oxSWNHs injected into tail vein pass through, the accumulation in lung should be avoided. We found that the accumulation of agglomerated oxSWNHs in lung remarkably decreased by modifying with comb-shaped PEG having two or three NHBP-1 units, and that the large part of oxSWNHs accumulated in liver and spleen. These results indicated that the modification of oxSWNHs with PEG-NHBP potentially improved the biocompatibility of oxSWNHs.

References:

[1] T. Murakami et al. *Mol. Pharm.* **1**, 399 (2004), K. Ajima et al. *Mol. Pharm.* **2**, 475 (2005)

[2] J. Miyawaki et al. *ACS Nano* **2**, 213 (2008)

[3] A. Vonarbourg et al. *Biomaterials* **27**, 4356 (2006)

[4] S. Matsumura et al. *Mol. Pharm.* **4**, 723 (2007)

Corresponding Author: Kiyotaka Shiba, **E-mail:** kshiba@jfcr.or.jp

Tel: +81-3-3570-0489, **Fax:** +81-3-3570-0461

2P-51

Anticancer Effect of Cisplatin Incorporated Inside Single-Walled Carbon Nanohorns

Kumiko Ajima*[1], Tatsuya Murakami[2], Yoshikazu Mizoguchi[2], Kunihiro Tsuchida[2], Toshinari Ichihashi[3], Sumio Iijima[1,3,4,5], ○Masako Yudasaka[1,3,5]

[1]*SORST-JST, Tsukuba, Ibaraki 305-8501.*

[2]*Fujita Health University, Toyoake, Aichi 470-1192.*

[3]*NEC 34 Miyukigaoka, Tsukuba, Ibaraki 305-8501.*

[4]*Meijo University, 1-501 Shiogamaguchi, Tempaku-ku, Nagoya 468-8502.*

[5]*AIST, Central 5, 1-1-1 Higashi, Tsukuba, 305-8565, Japan.*

We have been studying incorporation of cisplatin (CDDP), an anticancer drug, inside single-wall carbon nanohorns with holes opened (SWNHox), and its release from SWNHox. The results have shown that the preparation of CDDP@SWNHox is easy, and the release of CDDP takes hours and days [1]. The released CDDP has found to have higher anticancer-effect than the intact CDDP, which has been confirmed through *in vitro* tests [2]. In this report, we show that the similar effect was also found *in vivo*.

CDDP@SWNHox used in this study was prepared by the nano-precipitation method: SWNHox was well dispersed in an aqueous solution of CDDP, and the water was evaporated in a flowing N_2 gas at room temperature. The CDDP quantity in the obtained CDDP@SWNHox was about 50% in weight. The released test in physiological solutions showed that most of the incorporated CDDP was released in about 3 days.

The anticancer effect of CDDP@SWNHox was compared with CDDP in vitro using human lung cancer cells (H460). The CDDP dose necessary to kill about 50% of the H460 cells decreased to 1/2~1/4 by incorporating CDDP inside SWNHox.

In *in vivo* tests using nude mice, H40 cells were subcutaneously transplanted in the mice (Day 0). On day 11 and 15, saline, SWNHox, CDDP, and CDDP@SWNHox were intratumorally injected. The relative tumor sizes increased with days. On days 20-25, the average tumor size for the CDDP@SWNHox injected mice became about 1/2~2/3 of that for the intact-CDDP injected mice. The reason why the CDDP anticancer effect was enhanced by the incorporation inside SWNHox will be discussed in the presentation.

References : [1] K. Ajima, et al. *Mol. Pharm.* **2**, 475 (2005). [2] K. Ajima, et al. DDS 学会 2-C-25, 2007.

Corresponding Author: M. Yudasaka (yudasaka@aist.go.jp, TEL: 029-861-4818).

*Current address: Shinshu University School of Medicine.

Thermal Hole closing of Single-Wall Carbon Nanohorns Influenced by Functional Groups at Hole Edges.

○Michiko Irie[3], Jing Fan[1], Sumio Iijima[1,2,3], Jin Miyawaki[1], Ryota Yuge[2], Takazumi Kawai[3], and Masako Yudasaka[1,3]

1) SORST/JST, NEC Corporation, 34 Miyukigaoka, Tsukuba 305-8501, Japan
2) NEC Corporation, 34 Miyukigaoka, Tsukuba 305-8501, Japan
3) AIST, Central 5-2, 1-1-1 Higashi, Tsukuba, 468-8502, Japan

Our previous experimental results and theoretical calculations indicated that the holes at the tips of single-wall carbon nanohor ns (SWNH) could be closed by the heat treatment (HT) at1200°C in Ar atm osphere [1]. W e also f ound that the hole closing exhibited the close-open-close evolution during the heating when the hole sizes w ere about 0.7 nm [2]. When the hole sizes were smaller or larger, the close-open-close evolution did not appear, that is, the holes were closed and never re-ope ned. The m echanism of these chang es were investigated precisely. And it was inferred that the close-open-close phenomenon was induced by the oxygenated functional groups located at the edges of holes [2]. This idea was experimentally investigated by changing the functional groups at the h ole edges, which is shown in this report.

To open the holes, SWNHs were oxidized in aqueous solution of H_2O_2 at 100°C for about 5 hours, followed by washing with water and dr ying under the vacuum (SWNHhpox). It was confirmed that SWNHhpox had more oxygenated groups such as –COOH than SWNHox that was prepared by the slow com bustion in ai r [3, 4]. T o close the holes of SWNHhpox, SWNHhpox was heat-treated in Ar at various temperatures for 3 hours or at 1200°C for 0~ 3 h. The hole closing was confirmed by measuring xylene-adsorption quantity using TGA [5].

The xylene adsorption quantitie s of SWNHhpox decreased afte r HT in Ar at various temperatures for 3 h or after HT at 1200°C for various periods. It is interesting that the xylene adsorption decrease after 3 h HT treatment was similar with that of SWNHox (Ttarget: 500°C). On the other hand, the decrease of xylene adsorption quantity of SW NHhpox caused by HT for various periods was different. We consider from these results that the long-period (3 h) HT was not m uch influenced by the functional groups located at the hole e dges, suggesting that the hole sizes were similar to that of SWNHox (Ttarget:500°C). On the other hand, however, the transient closing process was inf luenced by the oxygenated groups existing at hole edges. Probably, the increased num ber of the oxygenated groups enhanced hole closing process, which is in good agreement with the idea previously reported.

References:
[1] J. Miyawaki et al. *J. Phys. Chem. C* **111** (2007) 1553. [2] J. Fan et al. *J. Phys. Chem. C* **112** (2008) 8600.
[3] J. Fan al. *J. Phys. Chem. B* **110** (2006) 1587. [4] M. Zhang, et al, *ACSNano*, **1** (2007)265
[5] M. Yudasaka et al. *J. Phys. Chem. B* **109** (2005) 3809.

Corresponding Author: Yudasaka Masako E-mail: m- yudasaka@aist.go.jp T el:029-861-4818

Organic Photovoltaic Devices of Penta(organo)[60]fullerenes and Their Iron and Ruthenium Complexes

○Yutaka Matsuo, Takaaki Niinomi, Masahiko Hashiguchi, Yoshiharu Sato, and Eiichi Nakamura

Nakamura Functional Carbon Cluster Project, ERATO, Japan Science and Technology Agency, Hongo, Bunkyo-ku, Tokyo 113-0033, Japan

Organic photovoltaics (OPV) have been intensively studied in particular for the past 5 years, because of potential low-cost production, low-weight, and flexible cells. So far, light-absorbing electron donor (i.e., phthalocyanines and polythiophenes) and electron-accepting fullerene derivatives have been often employed in such photovoltaic cells. Interpenetrating structures of donor and acceptor materials, so-called bulk heterojunction (BHJ), has proven to be an efficient way for large area charge separation with ultrafast charge transfer (~40 fs).

Although methanofullerenes such as [6,6]-phenyl C61-butyric acid methyl ester (PCBM) currently lead the way in contributing to the most efficient BHJ cells, there are little attempt with other fullerene derivatives. Any family of structures containing the fullerene core theoretically has the capability of acting as an acceptor in photovoltaic devices. In the search for alternative and improved acceptor materials, recent organic/inorganic functionalization methodologies on the fullerenes offer an abundance of derivatives that cause interesting changes to the physical and electronic properties of the fullerene.[1] Herein we report performance of the OPV devices assembled with the multifunctionalized fullerenes and their transition metal complexes. High open circuit voltage (*V*oc) and effect of organized structures will be discussed.

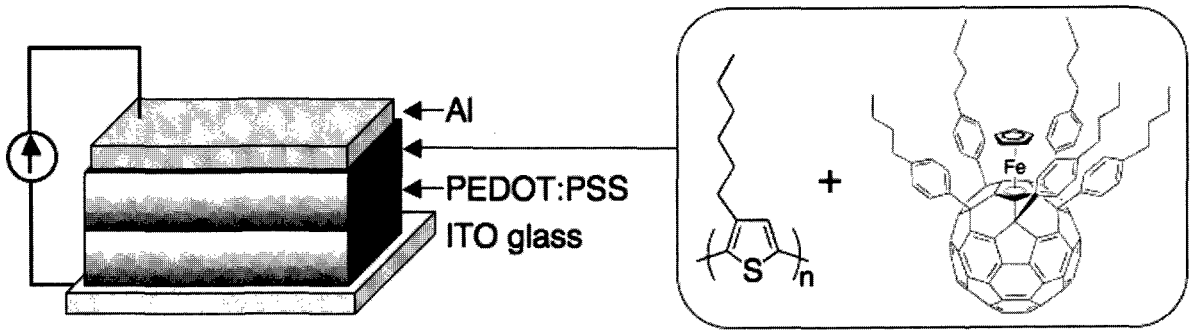

[1] (a) Y. Matsuo and E. Nakamura, *Chem. Rev.*, in press. (b) E. Nakamura and H. Isobe, *Acc. Chem. Res.* **2003**, *36*, 807. (c) Y. Matsuo, A. Muramatsu, K. Tahara, M. Koide, and E. Nakamura, *Org. Synth.* **2006**, *83*, 80.

Corresponding Author: Yutaka Matsuo and Eiichi Nakamura
TEL/FAX: +81-3-5841-1476; E-mail: matsuo@chem.s.u-tokyo.ac.jp; nakamura@chem.s.u-tokyo.ac.jp

Fullerenes C_{32} and $X@C_{32}^{n-}$ (X= He, Ne and Ar; n= 0, 2)

Weiwei Wang and Xiang Zhao*

Department of Chemistry and Institute for Chemical Physics, Xi'an Jiaotong University, Xi'an 710049, P. R. China

On the basis of density functional theory, the relative stabilities of ten lower energy C_{32} fullerene isomers together with the neutral and bivalent stabilities of two most stable isomers encapsulated with inert gas atom are investigated by the generalized gradient approximation (GGA) functional of PW91. Further geometry optimizations and vibrational analyses, at the B3LYP/6-31G(d) and PBE1PBE/6-31G(d) levels of theory, are carried out on the two most stable C_{32} isomers and their bivalent states. As a result, the most stable isomer of C_{32} fullerenes is id51 with two four-membered rings in the structure is validated, and the second stable isomer is id1 behaved as a classical fullerene.

Since there is the reaction like $X@C_{32} \rightarrow X + C_{32}$, a formula is defined as follows, $\triangle E = E(X@C_{32}) - E(X) - E(C_{32})$. The inert gas He, Ne and Ar are included in this study. The above expression has shown the reactivity of the $X@C_{32}$ structure in the arc discharge process. The results have revealed that all reactions studied are exothermic reactions. As the inert gas atom number inserted into fullerenes becomes bigger, $\triangle E$ raises. That may be because the bulk becomes large as long as atom ordinal increases, therefore results in energy hoisting when inert gas atom encapsulated into fullerene cages. It should also be noticed that the reaction energy for id51 is smaller than one for id1. In another words, id51 holds a smaller energy difference between the empty cage C_{32} and $X@C_{32}$ than id1 case.

The relative energetics of C_{32}^{2-} for id1 and id51, and also the $\triangle E$ of reaction as $X@C_{32}^{2-} \rightarrow X + C_{32}^{2-}$ (X= He, Ne, Ar) have been considered as well. Results have shown that inserting the inert gas into id51 at bivalence will hold more energetic stability. It should also been noticed that two four-membered rings in id51 behaves much more reactive at the di-anion state C_{32}^{2-}. This may show some interesting characteristics in their derivatives, such as fullerene hydrogenation.

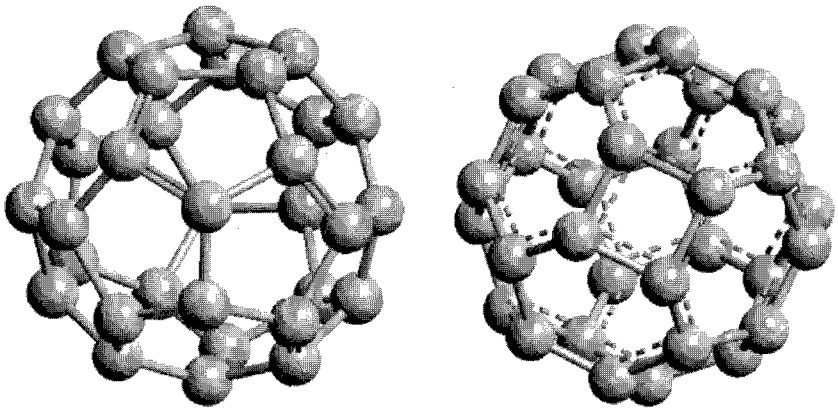

Id1 id51

[*] Email: xzhao@mail.xjtu.edu.cn Fax: +86-29-82668559

Syntheses and Electrochemical Properties of Di-ruthenium [70]Fullerene Complexes

○Takeshi Fujita[1], Yutaka Matsuo[2], Eiichi Nakamura[1,2]

[1]*Department of Chemistry, The University of Tokyo, Hongo, Bunkyo-ku, Tokyo 113-0033, Japan*

[2]*Nakamura Functional Carbon Cluster Project, ERATO, Japan Science and Technology Agency (JST), Hongo, Bunkyo-ku, Tokyo 113-0033, Japan*

Electronic communication between metal atom centers of multi-metal complexes through π-electron conjugated linkers is one of the most attractive subject in the fields of inorganic and materials chemistry. Fullerenes have large spherical π-systems and multi-metal coordination sites, and a di-iron complex of [60]fullerene exhibited the electronic interaction between two metals.[1] Herein we report on syntheses of di-ruthenium [70]fullerene complexes and their electrochemistry.

Hexaaryl adducts of [70]fullerene $C_{70}Ar_6H_2$ (**1a-d**), which has two indene parts for metal coordination, were directly synthesized from [70]fullerene by the reaction with arylcopper reagents derived from aryl Grignard reagents and $CuBr{\cdot}SMe_2$ in the presence of pyridine.[2] Repetitive deprotonation and complexation of hexaadducts **1** gave di-ruthenium complexes $Ru_2C_{70}Ar_6(C_5R_5)_2$ (**2a-c**) In cyclic voltammogram of di-ruthenium [70]fullerene complexes **2**, two reversible one-electron oxidation waves were observed, which demonstrates electronic communication exists between two ruthenium atoms. Di-ruthenium complexes **2** underwent further functionalization and electronic interactions in the products were also evaluated.

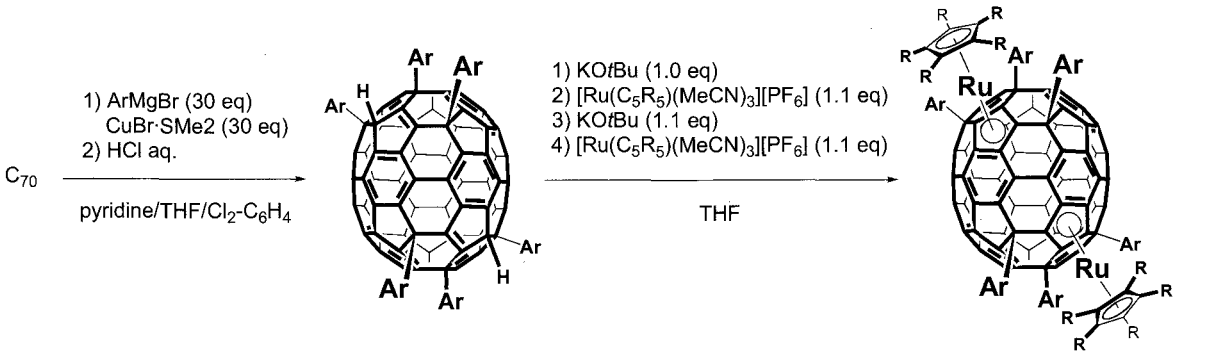

1a: Ar = C_6H_5
1b: Ar = C_6H_4-(*tert*-C_4H_9)-*p*
1c: Ar = C_6H_4-CH_3-*p*
1d: Ar = C_6H_4-OCH_3-*p*

2a: R = H, Ar = C_6H_4-CH_3-*p*
2b: R = H, Ar = C_6H_4-(*tert*-C_4H_9)-*p*
2c: R = CH_3, Ar = C_6H_4-(*tert*-C_4H_9)-*p*

1) Matsuo, Y.; Tahara, K.; Nakamura, E. *J. Am. Chem. Soc.* **2006**, *128*, 7154.

2) Matsuo, Y.; Tahara, K.; Morita, K.; Matsuo, K.; Nakamura, E. *Angew. Chem. Int. Ed.* **2007**, *46*, 2844.

Corresponding Author: Yutaka Matsuo and Eiichi Nakamura

E-mail: matsuo@chem.s.u-tokyo.ac.jp; nakamura@chem.s.u-tokyo.ac.jp; Tel&Fax: (+81)-3-5841-1476

Well-Defined Metal Catalysts for Fullerene Functionalization

○Susumu Mori, Masakazu Nambo, and Kenichiro Itami

Department of Chemistry, Graduate School of Science, Nagoya University, and PRESTO, JST, Nagoya 464-8602, Japan

The chemical modification of fullerenes has proven to be a promising approach for the preparation of new nanocarbon-based materials, providing the opportunity to tune the properties of these interesting materials. In order to explore new directions in metal-catalysis and nanocarbon chemistry, we recently initiated a program aimed at developing new functionalization chemistry of nanocarbons using transition metal catalysts.

As our initial foray into the area of nanocarbon chemistry, we developed a new organoboron-based functionalization of C_{60} catalyzed by Rh complexes.[1,2] This reaction enables the introduction of various organic fragments and a hydrogen atom on the fullerene surface in a highly regioselective and mono-addition selective manner. We also developed the highly reactive yet bench-stable Pd catalyst for the organoboron-based hydroarylation of C_{60}.[3]

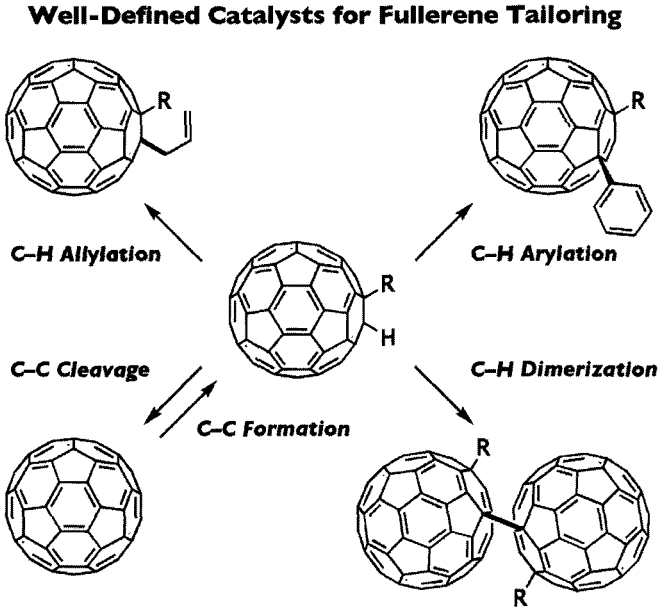

A notable feature of the resultant organo(hydro)fullerenes (R–C_{60}–H) is that they possess an acidic C–H bond reflecting the highly conjugated fullerene backbone. We have recently established that Pd catalysts enable a number of C–H bond transformations of organo(hydro)fullerenes by taking advantage of these highly acidic C–H bonds.[4] The C–H bond allylation reaction can be a versatile and general method to functionalize fullerenes. Although the C–H bond arylation reaction is still in its infancy, the two new reactions found while investigating the arylation reaction are intriguing. The C–H bond dimerization reaction might contribute in the generation of new fullerene-assembled materials that are otherwise difficult to make. The C–C bond-cleaving reaction may find use in the "deprotection" of fullerenes, assuming an alkynyl(hydro)fullerene as a "masked" soluble fullerene. The present finding of multidextrous palladium catalysis in transforming organo(hydro)fullerenes not only highlights the potential of transition metal catalysis for fullerene functionalization, but also unlocks opportunities for markedly different strategies in nanocarbon synthesis.

References: (1) M. Nambo, R. Noyori, K. Itami, *J. Am. Chem. Soc.* **2007**, *129*, 8080. (2) M. Nambo, K. Itami, *McGraw-Hill Yearbook of Science & Technology*, in press. (3) S. Mori, M. Nambo, L.-C. Chi, J. Bouffard, K. Itami, to be submitted. (4) M. Nambo, K. Itami, submitted.

Corresponding Author: Kenichiro Itami

E-mail: itami@chem.nagoya-u.ac.jp

Tel&Fax: 052-788-6098

Systematic X-Ray Diffraction Studies on Crystal Structure of Mono-metallofullerene M@C_{82} (C_{2v})

○Takayuki Aono[1], Eiji Nishibori[2], Ryo Kitaura[1], Shinobu Aoyagi[2], Masaki Takata[3], Makoto Sakata[2], Hiroshi Sawa[2] and Hisanori Shinohara[1,4]

[1]*Department of Chemistry, Nagoya University, Nagoya 464-8602, Japan*

[2] *Department of Applied Physics, Nagoya University, Nagoya 464-8603, Japan*

[3]*RIKEN SPring-8 Center, 1-1-1 Kouto, Sayo-cho, Sayo-gun, Hyogo 679-5148, Japan*

[4]*Institute for Advanced Research, Nagoya University, Nagoya 464-8602, Japan*

The endohedral metallofullerenes, M@C_{82} (C_{2v}), have attracted interests due to their unique structural and electronic properties [1]. It is known that M@C_{82} is one of the most abundant metallofullerenes so far synthesized and structurally characterized. The M@C_{82} (C_{2v}) has been widely used for applications such as MRI contrast agents and FET devices. Although the molecule structures of M@C_{82} (C_{2v}) metallofullerenes might be similar with each other, many of molecular structures for M@C_{82} (C_{2v}) have not yet been determined experimentally except for several examples [2]. We have been carried out systematic structural studies of M@C_{82} (C_{2v}) by using synchrotron X-ray powder diffraction (SXRD) at SPring-8. Powder diffraction at SPring-8 enable us to measure high quality powder data from a small amount of powder sample. In this study, we report the powder structural studies of series of M@C_{82} (C_{2v}) at low temperature.

The soot containing M@C_{82} (C_{2v}) (M=La, Ce, Sm, Yb, Lu) were synthesized by the DC arc-discharge method. The M@C_{82} (C_{2v}) metallofullerenes were purified by high-performance liquid chromatography (HPLC). Powder samples were crystallized from toluene solvent. The XRD patterns were collected at SPring-8 BL02B2 beamline. Temperature of the sample was controlled by a N_2 gas flow low temperature device.

The SXRD peak positions of metallofullerenes M@C_{82} (C_{2v}) (M=La, Ce, Sm, Yb, Lu) are almost identical, indicating a mutually similar structure at room temperature. The remarkable peak split around 2θ=6° is observed in the powder data of Sm@C_{82} below 160K (cf. Fig. 1). A similar peak split is also found in powder diffraction data of Yb@C_{82}. In the cases of powder data for M@C_{82} (M=La, Ce, Lu), such split has never been observed from 90K to 300K. The electronic state of Sm and Yb in M@C_{82} (C_{2v}) are +2 and La, Ce and Lu are +3 from absorption spectrum. A novel structural phase transition relating to valence states of encapsulated metal atoms are observed from SXRD at SPring-8. Detailed structural analysis is now in progress.

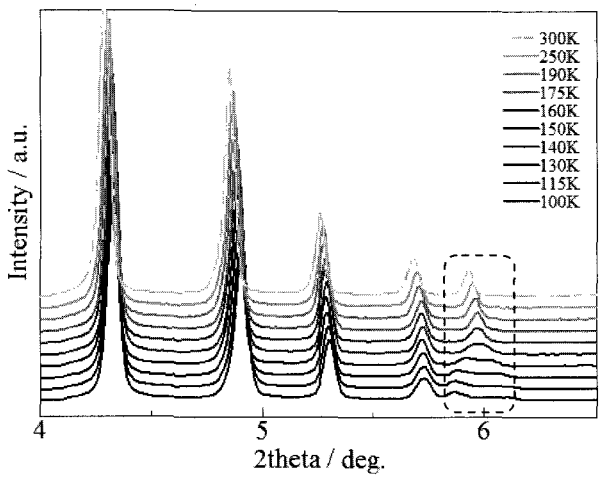

Fig.1 The X-ray powder diffraction pattern change of Sm@C_{82} on cooling process. The peak around 2θ=6° was splitted by cooling

[1] H. Shinohara, ***Rep. Prog. Phys.***, 63, 843 (2000)

[2] E. Nishibori *et al.*, ***Chem. Phys. Lett.*** 330, 497 (2000)

[3] R. Kitaura *et al.*, *33th Fullerene-Nanotube General Symposium*, **1P-14** (2007)

Corresponding Author: Hisanori Shinohara **E-mail:** noris@nagoya-u.jp

Tel: +81-52-789-2482 **Fax:** +81-52-747-6442

Characterization of N@C_{60} / C_{60} Nano-whisker by ESR

○Tatsuhisa Kato[1], Ryouichi Osada[1], Tohru Edamatsu[1], Michael Scheloske[2], Wolfgang Harneit[2], Takatsugu Wakahara[3], Kunich Miyazawa[3]

[1]*Department of Chemistry, Josai University, Keyakidai 1-1, Sakado Saitama 350-0295, Japan*
[2]*Institute of Experimental Physics, Free University Berlin, Arnimallee 14, D-14195 Berlin, Germany*
[3]*Fullerene Engineering Group, Advanced Nano Materials Laboratory, National Institute for Materials Science, 1-1 Namiki, Tsukuba, Ibaraki 305-0044, Japan*

C_{60} nano-whisker containing N@C_{60} (N@C_{60}/C_{60} NW) was prepared by the crystal growth at the interface between toluene and isopropyl alcohol solutions [1]. N@C_{60}/C_{60} NW exhibited an ESR spectrum[2] of N@C_{60} at 273K, as shown in Fig. 1. The ESR spectrum of material N@C_{60}/C_{60} powder showed a typical powder pattern of a quartet spin below Tc=258K [2], as shown in the left figure of Fig. 2. Comparing the spectrum, N@C_{60}/C_{60} NW exhibited more enhanced broadening of ESR lines with decrease of temperature, as shown in the right figure of Fig.2. The enhanced broadening at low temperature reflects that the local symmetry at the nitrogen site in N@C_{60}/C_{60} NW becomes lower than in C_{60} powder. ESR spectrum of N@C_{60}/C_{60} NW would give a good indicator of polymerization with neighboring C_{60} by [2+2] cyclo-addition [3].

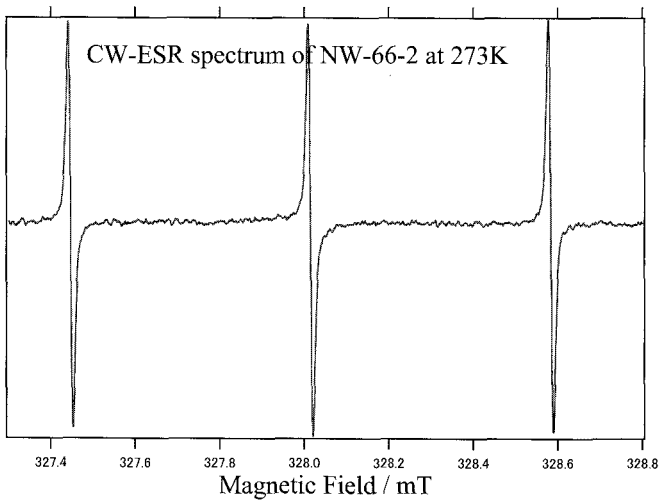

Fig. 1

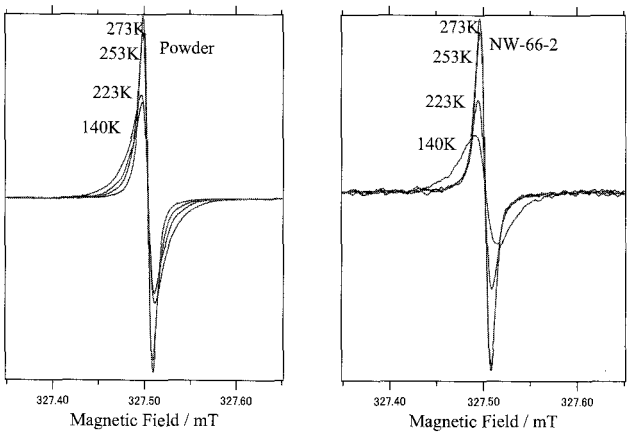

Fig. 2

[1] K. Miyazawa, Y. Kawasaki, A. Obayashi, and M. Kuwabara, *J. Maet. Res.*, **17**, 83-88 (2002).

[2] N. Weiden, H. Kaess, and K. –P. Dinse, *J. Phys. Chem. B*, **103**, 9826-9830 (1999).

[3] B. Goedde, M. Waiblinger, P. Jakes, N. Weiden, K. –P. Dinse, and A. Weidinger, *Chem. Phys. Lett.*, **334**, 12-17 (2001).

Corresponding Author: Tatsuhisa Kato
TEL: +81-49-271-7295, FAX: +81-49-271-7985, E-mail: rik@josai.ac.jp

Ion Implantation System for Production of Endohedral Fullerenes

○Tatsuya Katabuchi[1], Hitoshi Fukuda[1], Jun Hasegawa[1], Yoshiyuki Oguri[1] and Satoshi Watanabe[2]

[1]*Research Laboratory for Nuclear Reactors, Tokyo Institute of Technology, 2-12-1 O-okayama, Meguro, Tokyo 152-8550, Japan*
[2]*Quantum Beam Science Directorate, Japan Atomic Energy Agency, Takasaki, Gunma 370-1292, Japan*

An ion implantation system has been developed to produce endohedral fullerenes. Our future goal is medical application using endohedral fullerenes incorporating radioactive nuclei. Requirement to produce radioactive endohedral fullerenes is efficient technique to incorporate a microscopic amount of radioactive material into fullerenes. Ion implantation is more feasible than other methods such as laser vaporisation [1], standard arc discharge [2] and high pressure [3] methods because ion implantation requires less material. A significant concern in ion implantation is low endohedral fullerene production rate, previously reported for implanting ^{133}Xe ions into fullerene films at bombarding energies of 30 to 38 keV [4]-[6]. We concluded that destruction process of fullerenes by successive ion implantaion lowers endohedral fullerene production rate [7]. Thus, our ion implantation system is designed to enable ion implantation at energies as low as several hundred eV, thereby suppressing fullerene destruction process.

The ion implantation system has been built and tested. This system ionizes supplied gas by cold cathode Penning gauge (PIG) discharge. A typical Ar ion beam intensity of 3 μA was obtained. We have successfully implanted Ar ions into C_{60} fullerene film at a bombarding energy of 500 eV for 12 hours. Particle-induced X-ray emission analysis on the implanted fullerene samples to measure the production rate of endohedral fullerenes is underway.

[1] Y. Chai, T. Guo, C. M. Jin, R. Haufler, L. P. F. Chibante, J. Fure, L. Wang, M. Alford, R. E. Smalley, J. Phys. Chem. **95**, 7564 (1991)

[2] D. S. Bethune, R. D. Johnson, J. R. Salem, M. S. D. Vries, C. S. Yanonni, Nature, **366**, 123 (1993)

[3] M. Saunders, H. A. Jimenez-Vazquez, R. J. Cross, S. Mroczkowski, M. L. Gross, D. E. Giblin, R. J. Poreda, J. Am. Chem. Soc. **116**, 2193 (1994); R. Tellgmann, N. Krawez, S. -H. Lin, I. V. Hertel, E. E. B. Campbell, Nature, **382**, 407 (1996)

[4] S. Watanabe, N. S. Ishioka, T. Sekine, A. Osa, M. Koizumi, H. Shimomura, K. Yoshikawa, H. Muramatsu, J. Rad. Nucl. Chem. **255**, 495 (2003)

[5] S. Watanabe, N. S. Ishioka, H. Shimomura, H. Muramatsu, T. Sekine, Nucl. Instr. Meth. B**206**, 399 (2003)

[6] S. Watanabe, T. Katabuchi, N. S. Ishioka, S. Matsuhashi, H. Muramatsu, Proceedings of the Asia-Pacific Symposium on Radiochemistry-05, Beijing, CHINA, October 17--21, 2005

[7] T. Katabuchi, Bull. Res. Lab. Nucl. Reactor **31**, 42 (2007)

Corresponding Author: Tatsuya Katabuchi
TEL: +81-3-5734-3378, FAX:03-5734-2959, E-mail: buchi@nr.titech.ac.jp

Production and ESR detection of N@C_{60}

○Tomonari Wakabayashi[1,2] and Takayoshi Kuroda[1,2,3]

[1]*Department of Chemistry, School of Science and Engineering, Kinki University*
[2]*Research Center for Quantum Computing, Kinki University and MEXT*
[3]*Joint Research Center (JRC), Kinki University*

The endohedral N@C_{60} exhibits unusual property that the nitrogen atom in the carbon cage preserves its atom-like energy levels [1]. The twelve levels resulting from the electron spin S=3/2 and the nuclear spin I=1 of ^{14}N constitute a system for quantum computation (QC) and quantum information processing (QIP) [2]. Using ^{15}N of I=1/2, spins were manipulated to realize pseudoentanglement [3]. Much effort has been devoted to obtain a pure material [4-7]. However, issues remain to be improved. 1) The yield is too low, as the fraction N@C_{60}/C_{60} being ~10^{-4} or less. 2) The separation of N@C_{60} requires elaborating operations of HPLC. 3) The spin manipulation is performed by pulse operations both in the mw and rf [8]. A new protocol for manipulating qubits to perform QC and QIP are welcome to be proposed.

We report ESR detection of N@C_{60} for our ion-bombarded C_{60} sample. The N_2 gas at ~2.7 Pa was excited to discharge in an rf coil supplied by 500 W power at 13.56 MHz. The cationic species were extracted through an aperture of 2 cm in diameter and accelerated toward the surface of a water-cooled electrode to which dc voltage of −80 V was applied. The C_{60} molecules were sublimed from a crucible and deposited on the inner surface of the cylindrical electrode where the molecules were bombarded with the cations. Typical ion current under operation was ~11 mA. The deposited materials were collected in air, sonicated with a small volume of CS_2. The ESR spectra were recorded on JEOL JES-PX1050 spectrometer.

Figure 1 shows a typical X-band ESR spectrum of ^{14}N@C_{60}/C_{60} mixture suspended in CS_2 at room temperature. The remarkably sharp, three lines are the ESR transitions (ΔM_S=+1, ΔM_I=0) for M_I=+1, 0, −1 from the low field, respectively. Even with a narrow modulation frequency of 0.5 μT, we could not observe further splitting, as reported for purified ^{14}N@C_{60} in CS_2 [9]. The purity and homogeneity as well as removal of other paramagnetic species are crucial to access the individual transition.

References

1) T. Almeida-Murphy et al. PRL 77 (1996) 1075.
2) W. Harneit, PRA 65 (2002) 032322.
3) M. Mehling et al. PRL 93 (2004) 206603.
4) T. Suetsuna et al. Chem. Eur. J. 8 (2002) 5080.
5) P. Jakes et al. PCCP 5 (2003) 4080.
6) H. Nikawa et al. FNTSympo34 (2008) 2P35.
7) S. Nishigaki et al. FNTSympo34 (2008) 2P36.
8) J. J. L. Morton, Nature Physics 2 (2006) 40.
9) J. J. L. Morton, JCP 122 (2005) 174504.

Corresponding Author: Tomonari Wakabayashi
E-mail: wakaba@chem.kindai.ac.jp
Tel. 06-6730-5880 (Ex.4101)
Fax. 06-6723-2721

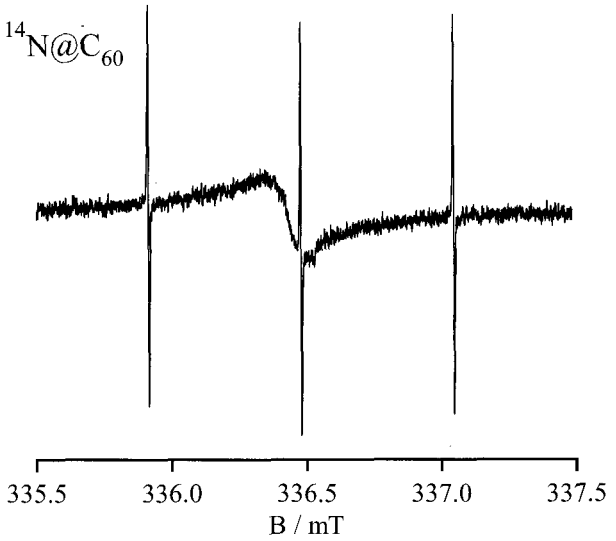

Fig. 1. X-band ESR spectrum of ^{14}N@C_{60}/C_{60} in CS_2 at R.T.

Bis-carbene derivatives of a non-IPR metallofullerene: $La_2@C_{72}$

Xing Lu,[†] Hidefumi Nikawa,[†] Midori O. Ishitsuka,[†] Takahiro Tsuchiya,[†] Yutaka Maeda,[‡] Takeshi Akasaka,[*,†] Zdenek Slanina,[†] Naomi Mizorogi,[§] and Shigeru Nagase[*,§]

[†]Center for Tsukuba Advanced Research Alliance, University of Tsukuba, Tsukuba, Ibaraki 305-8577, Japan, email: akasaka@tara.tsukuba.ac.jp,

[‡]Department of Chemistry, Tokyo Gakugei University, Tokyo 184-8501, Japan,

[§]Department of Theoretical and Computational Molecular Science, Institute for Molecular Science, Okazaki 444-8585, Japan.

Abstract: $La_2@C_{72}$ reacts readily with 2-adamantane-2,3-[3H]-diazirine (**1**) to generate both mono- and bis-adducts.[1], Previous experimental and theoretical results of mono-adduct isomers confirmed that $La_2@C_{72}$ has a D_2-symmetric non-IPR cage with two pairs of fused-pentagons, and more importantly, it was for the first time disclosed that the [5,5]-junction carbons are stabilized by the encaged carbons.[1] As two fused-pentagon pairs are available in $La_2@C_{72}$, the reactivity of both is certainly of high interest, and the results are reported here. Bis-carbene adducts, $La_2@C_{72}Ad_2$ were obtained and structurally characterized, which show that the two Ad groups tend to attach to the two fused-pentagon regions, forming candy-like fullerenes. The results show that the two fused-pentagon regions are much more reactive than other sites of $La_2@C_{72}$. As the Ad group has an electron-donating ability to $La_2@C_{72}$, it is possible to concisely control the electrochemical properties of $La_2@C_{72}$.

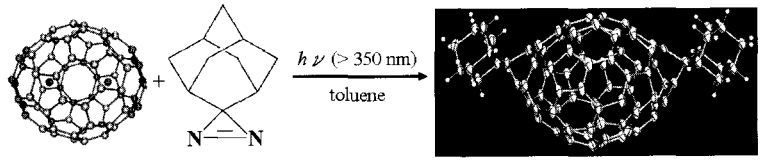

$La_2@C_{72}$ (#10611) **1** Candy-like fullerene: $La_2@C_{72}Ad_2$

References

[1]. X. Lu, H. Nikawa, T. Nakahodo, T. Tsuchiya, M. O. Ishitsuka, Y. Maeda, T. Akasaka, M. Toki, H. Sawa, Z. Slanina, N. Mizorogi, S. Nagase, *J. Am. Chem. Soc.* **2008**, *130*, 9129-9136.

3P-10

ESR spectra of superconducting sodium fulleride $Na_{8.2}C_{60}$

○Nozomu Kimata, Satoshi Heguri, and Mototada Kobayashi

Department of Material Science, Graduate School of Material Science, University of Hyogo, Ako, Hyogo 678-1297, Japan

The structure and physical properties of sodium fullerides Na_xC_{60} are interesting because they are different from those of other alkali-doped C_{60}. Since the Na^+ ion has a small ionic radius, Na_xC_{60} with large x value can be expected to be synthesized. Yildirim *et al.* reported the synthesis of $Na_{9.7}C_{60}$ with a face-centered cubic (fcc) structure and suggested the Na-saturated phase to be $Na_{11}C_{60}$[1]. We reported magnetic properties for superconducting $Na_{8.2}C_{60}$ at the last symposium[2]. Here we report the structure and the ESR spectra of superconducting $Na_{8.2}C_{60}$ together with those of other sodium fullerides $Na_xC_{60}(x>6)$.

Sodium-doped fullerides were prepared from sublimed C_{60} powder with 99.95% purity (MTR Ltd.) and sodium metal. The mixture of degassed C_{60} and sodium metal was encapsulated in a stainless steel tube and sealed in a Pyrex glass tube after evacuating. Thermal treatments were carried out in a furnace. The sample with nominal composition $Na_{8.2}C_{60}$ is found to be superconducting at 14K with a shielding fraction of 0.5%.

The X-ray powder diffraction profile for $Na_{8.2}C_{60}$ at room temperature using MoK_α radiation is shown in Fig. 1. The profile can be assigned to a hexagonal lattice with lattice parameters of a=1.013nm and c=1.656 nm, respectively. We performed ESR measurement at X-band between 5 and 295K. Figure 2 shows the temperature dependence of ESR spectra for $Na_{8.2}C_{60}$. The g factor and ΔH_{pp}(ESR peak-to-peak linewidth) at room temperature were g=2.0001 and ΔH_{pp}=2.48G, respectively. Details will be discussed at the meeting.

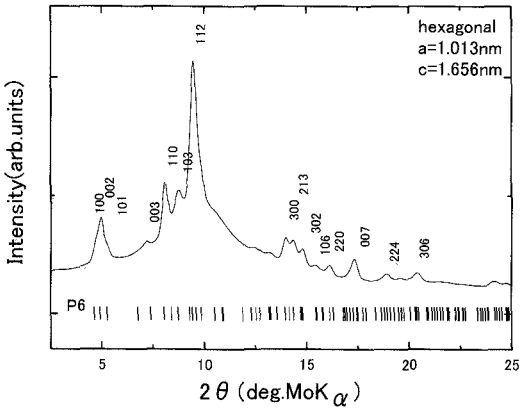

Fig.1. X-ray powder diffraction profile for $Na_{8.2}C_{60}$.

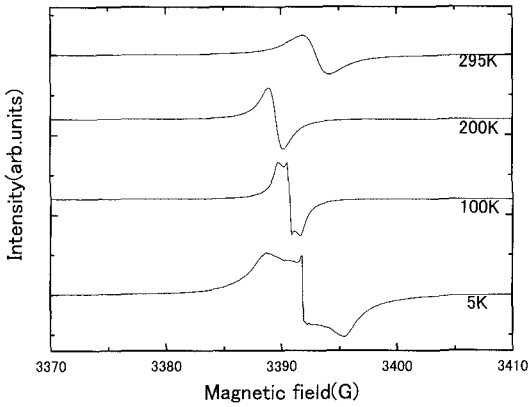

Fig.2. Temperature dependence of ESR spectra for $Na_{8.2}C_{60}$.

[1] T.Yildirim, O.Zhou, J.E.Fischer, N.Bykovetz, R.A.Strongin, M.A.Cichy, A.B.Smith III, C.L.Lin and R.Jelinek, *Nature*, **360**, 568(1992).

[2] K. Nozomu, S. Heguri, M. Kobayashi, The 34th Fullerene-Nanotubes General Symposium, 3P-50 (2008).

Corresponding Author: Nozomu Kimata

TEL: +81-791-58-0156, FAX:+81-791-58-0132, E-mail: ri07v005@stkt.u-hyogo.ac.jp

3P-11

Electric phase transitions of $Eu_{2.75}C_{60}$ and $Sm_{2.75}C_{60}$

○Takashi Kambe, Yusuke Yamanari, Noako Kawasaki, Yohei Ohta, Kumiko Imai, and Yoshihiro Kubozono,

Graduate of Natural Science and Technology, Okayama University, Okayama 700-8530, Japan

Lanthanide metal doped C_{60} materials supply very interesting electric phase, such as metallic phase, ferromagnetic phase and superconducting phase. Among them, $Sm_{2.75}C_{60}$ shows a negative thermal expansion at low temperatures, which is associated with a temperature induced valence transition of Sm atom [1]. This is attributable to the large deference of ionic radius between Sm^{2+} (0.114nm) and Sm^{3+} (0.096nm). Below 30K, the valence state of Sm atom is changed from a mixed valence state to 2+. $Eu_{2.75}C_{60}$ and $Yb_{2.75}C_{60}$ also show the negative thermal expansion due to the valence transition. Thus, the valence transition is characteristics of lanthanide metal doped C_{60} materials.

In this study, we have investigated the electric and magnetic properties of $Eu_{2.75}C_{60}$ and $Sm_{2.75}C_{60}$. The figures show the temperature dependence of magnetic susceptibility and ESR intensity, and g-factor in $Eu_{2.75}C_{60}$. Both the magnetic susceptibility and ESR parameters show a drastic change around 70~80K. This transition temperature is consistent with the onset temperature of negative thermal expansion, i.e., valence transition temperature T_v (=90K) [2]. We will discuss the change of ESR and magnetic susceptibility on the basis of the valence transition of Eu and Sm atoms.

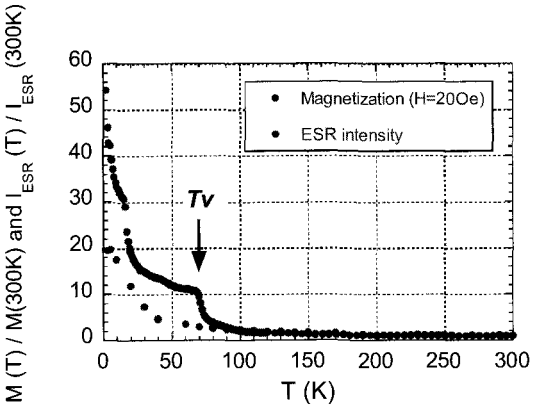

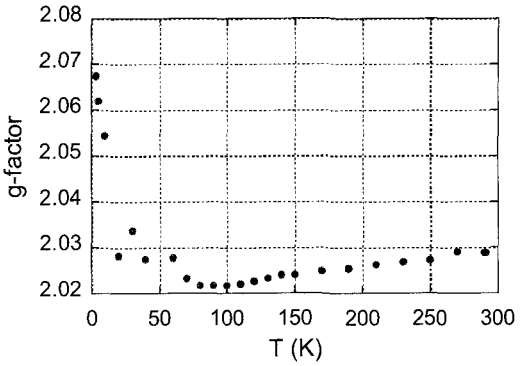

[1] J. Arvanitidis, *et al.*, Nature 425, 599 (2003).

[2] K. Prassides, *etal.*, Phil.Trans.R.Soc.A,366,151 (2008).

Corresponding Author; Takashi Kambe

E-mail; kambe@science.okayama-u.ac.jp

Tel&Fax; +81-86-251-7829/+81-86-251-7830

Structure and Electronic Properties of $Na_xH_yC_{60}$ Ternary Compounds

○Hironori Ogata[1] and Hideyuki Oonami[2]

[1]*Department of Chemical Science and Tchnology, Hosei University, Tokyo 184-8584, Japan*

[2]*Research Center for Micro-Nano Technology, Hosei University, Tokyo 184-0003, Japan*

Since the discovery of superconductivity in $Na_xX_yC_{60}$(X=N: T_c=12K, X=H: T_c=15K), there has been many interests in the structure and the electronic states of the Na-X-C_{60} ternary systems. It has been suggested that nitrogen or hydrogen in the systems contribute not only to a spacer which suppress the structural instability but also to the electronic states near the Fermi level.

In the present work, we report the structure and electronic properties of stable phase in $Na_xH_yC_{60}$ compounds for x=1 to 4 investigated by powder X-ray diffraction, magnetic susceptibility and solid state NMR measurements.

[1] K.Imaeda *et al.*, SSC87(1993)375.
[2]K.Imaeda *et al*, SSC99(1996)479.

Corresponding Author: Hironori Ogata, E-mail: hogata@hosei.ac.jp
Tel&Fax: 042-387-6229

3P-13

Electronic Structure of Cs_3C_{60}

Susumu Saito

Department of Physics, Tokyo Institute of Technology
2-12-1 Oh-okayama, Meguro-ku, Tokyo 152-8551

The outermost *s* orbital of an alkali atom, especially the K or heavier alkali atom generally has a large radius, and the electron trapped in this orbital gives rise to a small ionization potential of the atom. In the case of Cs, its atomic radius is as large as 3.34 Å, more than half of the radius of the fullerene C_{60} which is the atom-like building block of the novel crystalline and nanocrystalline materials [1]. Therefore, alkali-doped C_{60} crystalline materials are considered as interesting compounds between atom-like building blocks and real atoms with considerable amount of electron transfer from alkali *s* states to the C_{60} lowest-unoccupied state (t_{1u} state) [2]. Among them, the face-centered-cubic (fcc) A_3C_{60} (A=K, Rb, or combination of Na, K, Rb, and Cs) has attracted considerable attention due to the high-transition temperature (T_c) superconductivity observed in these compounds [3,4]. So far, the highest-T_c fcc A_3C_{60} known to date is Cs_2RbC_{60} with the T_c of 33 K [5]. However, from the total-energy study of various Cs_3C_{60} phases in the framework of the density functional theory, it was predicted that the fcc Cs_3C_{60} phase, the potential higher-T_c phase, could be produced and should be stable once it were formed [6]. Actually the production of the fcc Cs_3C_{60} phase was reported this year together with the A15 Cs_3C_{60} phase [7]. In this presentation I will report the electronic structure of the fcc Cs_3C_{60} phase and compare it with the other fcc A_3C_{60} compounds.

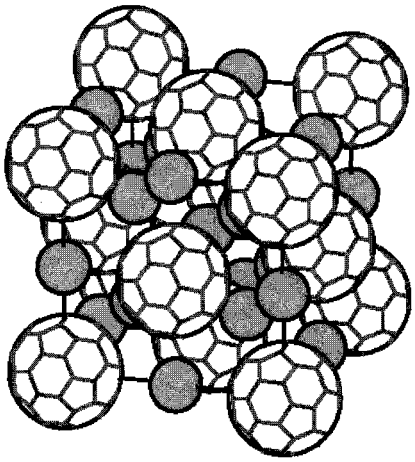

fcc Cs_3C_{60} [6]

References:

1. S. Saito, Mat. Res. Soc. 1990 Fall Meeting Proc. Vol.206, p.115.
2. S. Saito and A. Oshiyama, Phys. Rev. Lett. **66**, 2637 (1991).
3. R. C. Haddon, A. F. Hebard, M. J. Rosseinsky *et al.*, Nature **350**, 320 (1991).
4. S. Saito and A. Oshiyama, Phys. Rev. B **44**, 11536 (1991).
5. K. Tanigaki, T.W. Ebbesen, S. Saito, J. Mizuki, J.S. Tsai, Y. Kubo, and S. Kuroshima, Nature **352**, 222 (1991).
6. S. Saito, K. Umemoto, S. G. Louie, and M. L. Cohen, Solid State Commun. **130**, 335 (2004).
7. A. Ganin, Y. Takabayashi, Y. Z. Khimyak, S. Margadonna, A. Tamai, M. J. Rosseinsky, and K. Prassides, Nature Materials **7**, 367 (2008).

E-mail saito@stat.phys.titech.ac.jp
Fax 03-5734-2739

Pressure dependence of T_c in Cs_3C_{60}

○Takumi Takano[1], Nao Takeshita[2], AlexeyY. Ganin[3], Yasuhiro Takabayashi[4], Matthew J. Rosseinsky[3], Kosmas Prassides[4], Hidenori Takagi[5], Yasunori Tokura[6], Yoshihiro Iwasa[1,7]

[1]*Institute for Materials Research, Tohoku University, Sendai 980-8577, Japan*
[2]*National Institute of Advanced Industrial Science and Technology, Tsukuba 305-8562, Japan*
[3]*Department of Chemistry, University of Liverpool, Liverpool L69 7ZD, UK*
[4]*Department of Chemistry, University of Durham, Durham DH1 3LE, UK*
[5]*Graduate School of Frontier Sciences, University of Tokyo, Kashiwa, Chiba 277-8581, Japan*
[6]*Department of Applied Physics, University of Tokyo, Bunkyo-ku, Tokyo 113-8656, Japan*
[7]*CREST, Japan Science and Technology Corporation, Kawaguchi 332-0012, Japan*

The discovery of superconductivity in alkali-metal (A) intercalated A_xC_{60} has led to a broad class of superconductors of composition A_3C_{60} with superconducting critical temperature, T_c, up to 33 K in $RbCs_3C_{60}$ at ambient pressure [1]. The transition temperature T_c of superconducting A_3C_{60} compounds can be scaled with the size of the unit cell (i.e., interfullerene spacing), and T_c values of A_3C_{60} both at ambient and at high pressure is consistent with T_c being modulated by the density of states at the Fermi level, $N(\varepsilon_F)$. As the interfullerene spacing increases, the overlap between the molecular orbital of C_{60} decreases; this leads to a reduced band width, and, for a fixed band filling, to an increased density of states. Therefore, Cs_3C_{60} is a key material in the superconducting family, because Cs^+ is the largest alkali-ion. However, superconductivity in Cs_3C_{60} compounds have not identified owing to extremely small shielding fractions and low crystallinity despite the tremendous efforts made so far by many researchers.

Recently, A. Y. Ganin *et al.* succeeded in the synthesis of Cs_3C_{60} with high quality, demonstrating bulk superconductivity at 38 K with high pressure condition up to 12 kbar [2], which is the highest T_c value of any molecular materials. In this presentation, we report the pressure dependence of T_c of Cs_3C_{60} up to 25 kbar by using a conventional clamp-type pressure cell made of NiCrAl non-magnetic alloy.

The pressure dependence of T_c in Cs_3C_{60} below 12 kbar is in well agreement with the previous study; Mott-insulator-to-superconductor transition occurred at around 5 kbar, having maximum T_c ~38 K at 7 kbar. On the other hand, the value of T_c is continuously decreased in higher pressure region above 12 kbar, and almost completely disappeared at around 20 kbar, indicating that superconductor-to-non-superconductor transition is induced by applying the high pressure.

[1] K. Tanigaki *et al.*, *Nature* **352**, 222 (1991).
[2] A. Y. Ganin *et al.*, *Nature Materials*, **7**, 367 (2008).
Corresponding Author: Takumi Takano
TEL: +81-22-215-2032, FAX: +81-22-215-2031, E-mail: takano@imr.tohoku.ac.jp

Precise Structural Study of a Single Crystal $H_2@C_{60}$ Using Synchrotron X-ray diffraction

○Makoto Toki[1], Hiroshi Sawa[2], Yusuke Wakabayashi[1], Eiji Nishibori[2], Yasujiro Murata[3], Koichi Komatsu[3], Hidefumi Nikawa[4], Takeshi Akasaka[4], Katsumi Tanigaki[5]

[1]*Photon Factory, High Energy Accelerator Research Organization (KEK), Oho, Tsukuba, Ibaraki 305-0801, Japan*
[2]*Depertment of Applied Physics, , Nagoya University, Nagoya 464-8602, Japan*
[3]*ICR, Kyoto University, Uji, Kyoto 611-0011, Japan*
[4]*TARA, Univ. of Tsukuba, Tsukuba, Ibaraki 305-8577, Japan*
[5]*Tohoku University , Aoba, sendai 6-3, Japan*

Single crystal structure analyses of C_{60} and $H_2@C_{60}$ under 50K were made with the weissenberg camera installed to BL-1A, the Photon Factory.

Various types of endohedral fullerene complexes have been synthesized in order to study the properties and the applications of them as nano-materials. We have focused on the structural properties of gas incorporated fullerenes such as $H_2@C_{60}$ and $Ar@C_{60}$. Our previous synchrotron powder diffraction data[1] allows us to study not only the occupancy of the gas molecule, but also the effect of the incorporated gas species on the orientational ordering of the C_{60} cage and thermal expansion coefficient as a function of temperature. However, the error on the estimated H_2 occupancy was not satisfactorily small. This error is inevitable for powder diffraction, in which a numbers of peaks are superimposed.

In order to make more precise analysis, we conducted single crystal structure analyses on C_{60} and $H_2@C_{60}$. Such analysis has, even on empty C_{60}, never made yet because of the two difficulties below: (a) twin structure due to the orientational ordering transition at 260K, and (b) coexistence of two types of ratchet rotational mode, so called five- and six-membered ring coordination. We established the way to get through these difficulties and succeeded in making not only structure analysis but electron density analysis. The result shows the occupancy of H_2 is 1.95±0.02. This small error in the occupancy implies the quality of our result is high enough to discuss subtle change in electron density.

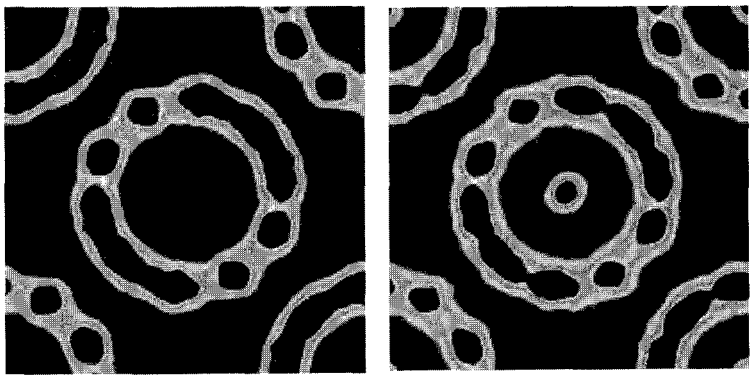

Electron density maps of C_{60} (left) and $H_2@C_{60}$ (right) in the range of 0-1 e/Å^3

[1]K.Yakigaya et,al., New Journal of chemistry, **2007**,31,973

Corresponding Author: Makoto Toki
TEL: 029-864-5299, E-mail: toki@post.kek.jp

The simplest linear-carbon-chain growth by atomic-carbon-insertion reactions.

○Teruhiko Ogata and Yoshio Tatamitani

Department of Chemistry, Shizuoka University, Shizuoka 422-8529, Japan

The atomic-carbon-insertion reaction (ACIR) is simple and efficient, wherein the atomic-carbon, :C, or its precursors, :CCO and C_3O_2, jump into the CC bond without cleaving the overall structure, and hence do not produce a side-product, as summarized in Scheme 1 [1,2].

The formation mechanism of linear-carbon-chain molecules, C_nO (n = 2 - 9), synthesized in the discharge of C_3O_2 has been investigated based on the detailed analyses of former FTMW spectroscopic data [2]. The relative abundances of the C_nO products determined from their rotational spectrum intensities agree with those for the C_nO^+ ions. The active chemicals in the reaction system include :C and :CCO only, and the observed products exclusively consist of C_nO, leading to the formation mechanism of the atomic-carbon-insertion reaction.

Scheme 1. Linear-carbon-chain growths by various atomic-carbon-insertion reactions.

a) Potolysis of C_3O_2

$$O{=}C{=}C{=}C{=}O \xrightarrow{h\nu} :C{=}C{=}O + CO \xrightarrow{h\nu} :C + 2CO \quad (1)$$

$$C{=}C + :C{=}C{=}O \xrightarrow{h\nu} \triangleright C{=}C{=}O \xrightarrow[-CO]{h\nu} \triangleright C: \longrightarrow C{=}C{=}C \quad (2)$$

b) Ion + C_3O_2 reactions

$$C_nO^+ + C_3O_2 \longrightarrow C_{n+3}O_3^+ \xrightarrow[-2CO]{} C_{n+1}O^+ \ (n = 1\text{-}6) \quad (3)$$

$$C_nO_2^+ + C_3O_2 \longrightarrow C_{n+3}O_4^+ \xrightarrow[-2CO]{} C_{n+1}O_2^+ \ (n = 1\text{-}18) \quad (4)$$

$$C_nH_6^+ + C_3O_2 \longrightarrow C_{n+3}H_6O_2^+ \xrightarrow[-2CO]{} C_{n+1}H_6^+ \ (n = 1\text{-}4) \quad (5)$$

c) Discharge of C_3O_2

$$n\,C_3O_2 \longrightarrow C + CO + C_2O + C_3O + C_4O + C_5O + C_6O + C_7O + C_8O + C_9O \quad (6)$$

The following is the reaction mechanisms for the formation of C_nO molecules, as we suggested in a previous paper [2a]. That is, for singlet C_nO molecule **1**, a carbon atom is inserted into the acetylene-type C≡C bond to form cyclopropenylidene **2**. The carbene-carbon in the three-member ring further attacks the C=C bond, and then finally reaches the cummulene-type triplet molecule **3**. On the other hand, a carbon atom is inserted into the C=C double bond for the triplet C_nO molecule **3**, and then via **4** and **5**, reaches the acetylene-type singlet molecule **6**. Then the processes in Scheme 2 are repeated.

This formation mechanism is simple and efficient, and is applicable not only to other linear-carbon-chains but also to a wide-range of carbon processes, in particular, to ultra low temperature or poor combustion conditions [3].

Scheme 2. The reaction mechanisms for the formation of C_nO molecules by the proposed atomic-carbon-insertion reactions.

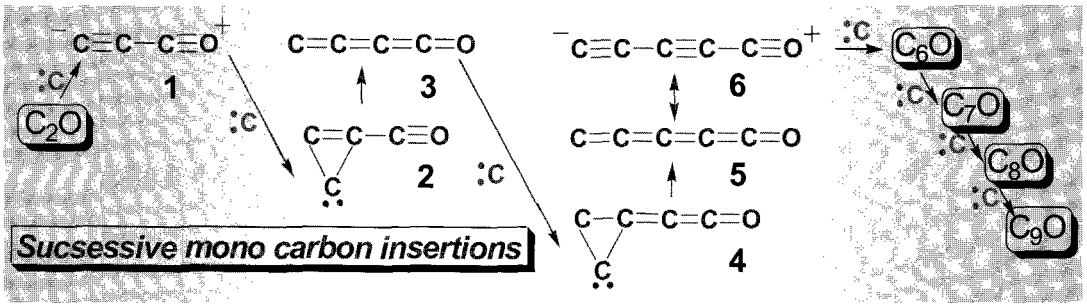

References:

[1] (a) K. D. Bayes, *JACS*, 84, 4077 (1962); (b) S. M. Schildcrout, et. al. *JACS*, , 92, 251 (1970); (c) O.Bortolini, et al., *Int. J. Mass Spectrom.*, 190/19, 171 (1999).
[2] (a) T. Ogata, et al., *JACS*, 117, 3593 (1995); (b) Y. Ohshima, et al., *JCP*, 102, 1493 (1995).
[3] (a) T. Ogata, et al., *F&NT Symposium*, 33th, 3P-28 (2008); (b) *ibid.* 34th, 2-5 (2008); (c) T. Ogata, et al., *Proceedings of Carbon Conference*, B083 (2007); (d) *ibid.* 16Cam06 (2008).

Corresponding Author: Teruhiko Ogata, **Tel&Fax:** +81-54-238-5105, **E-mail:** sctogat@ipc.shizuoka.ac.jp

Effect of dopant combinations on the single-walled carbon nanotube pn junction features

○T. Kato, J. Shishido, W. Oohara, R. Hatakeyama, and K. Tohji*

Department of Electronic Engineering, Tohoku University, Sendai 980-8579, Japan
** Graduate School of Environmental Studies, Tohoku University, Sendai 980-8579, Japan*

The hetero junction structure of sem iconducting materials has widely been investigated due to their prominent potential abilities and is regarded as an inevitable building block to construct high perform ance electric circuits. Single-walled carbon nanotubes (SWNTs) are the carbon-based nano-m aterial including superior electrical characteristics and attracting a gr eat dea l of atten tion as a potential candidate for post-silicon stage in semiconducting device fields. Since the pristine SWNTs exhibit the monotonic p-type characters, it is the critical ar gument how to realize the SW NT-based hetero junction aim ing for industrial applications su ch as flexible el ectrical circuits, high frequency devices , and solar cells. W e report on th e succes sful fabrication of ultimate one-dimensional hetero junction wires based on SW NT field effect transistors (FETs). The hete ro jun ction stru cture of Cs/I (Cs/I@) and Cs/C $_{60}$ (Cs/C_{60}@) were formed inside the SWNT s with the advanced plasm a ion irradia tion process [1]. The Cs/I@SWNTs were found to show clear hum p current features through the p-n junction barrier, which is known as a tunneling di ode, whereas the asymm etry Coulom b dot features depending on the carrier t ype were also realized in Cs/C $_{60}$@SWNTs. T hese phenomena can be explained by the dif ference of the depletion layer form ed between p and n junction area. The required condition to achieve the one dimensional p-n junction diode obtained through the com parative studies of dopant pares shows the critical and fundamental viewpoints for the future in dustrial applications of SWNT nano electronics.

Reference:

[1] G.-H. Je ong, A. A. Fa rajian, R. Hat akeyama, T. Hirata, T. Yaguchi, K. Tohji, H. Mizuseki, a nd Y. Kawazoe, Phys. Rev. B, **68**, 075410 (2003).

Corresponding Author T. K ato

E-mail: kato12@ ecei.tohoku.ac.jp

Tel&Fax: +81-22-795-7046 / +81-22-263-9225

Polarized photoluminescence excitation spectroscopy of DNA-wrapped single-walled carbon nanotubes

○Erik Einarsson[1], Yoichi Murakami[2], Ming Zheng[3], Slava V. Rotkin[4,5], Yuhei Miyauchi[6], Shigeo Maruyama[1]

[1]*Dept. of Mechanical Engineering, The University of Tokyo, Tokyo 113-8656, Japan*
[2] *Dept. of Chemical System Engineering, The University of Tokyo, Tokyo 113-8656, Japan*
[3]*DuPont Central Research & Development, Wilmington, DE 19880, USA*
[4]*Dept. of Physics, Lehigh University, Bethlehem, PA 18015, USA*
[5]*Center for Adv. Materials & Nanotechnology, Lehigh University, Bethlehem, PA 18015, USA*
[6]*Institute for Chemical Research, Kyoto University, Uji, Kyoto 611-0011, Japan*

Polarized photoluminescence excitation (PLE) spectra were obtained from single-walled carbon nanotubes (SWNTs) by the L-format [1] method. The SWNTs were wrapped by single-stranded DNA (ssDNA) [2] and dispersed in D_2O. Wrapping by ssDNA has been predicted [3] to break the symmetry of the SWNTs due to the induced helical Coulomb potential. We investigate this predicted symmetry breaking by decomposing the PLE spectra into parallel and perpendicular components, and by comparing to SWNTs wrapped by polymers such as polyfluorene.

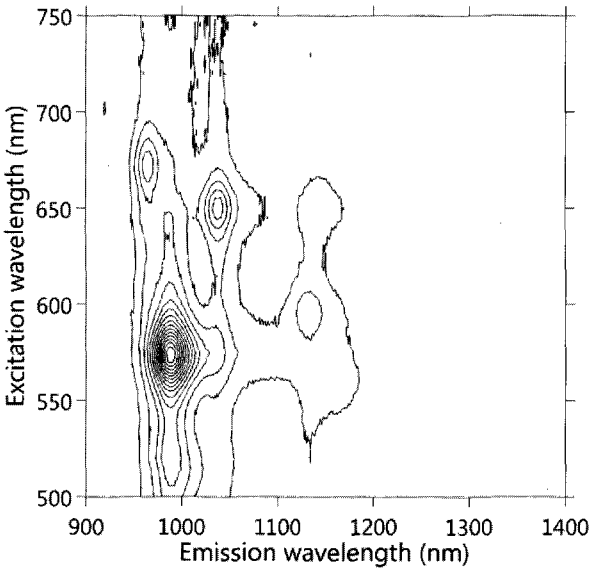

Fig. 1: Total-intensity PLE map of DNA-wrapped SWNTs.

[1] Y. Miyauchi, M. Oba, S. Maruyama, *Phys. Rev. B* **74** (2006) 205440.
[2] M. Zheng, A. Jagota, M.S. Strano, A.P. Santos, P. Barone, S.G. Chou, B.A. Diner, M.S. Dresselhaus, R.S. McLean, G.B. Onoa, Ge.G. Samsonidze, E.D. Semke, M. Usrey, D.J. Walls, *Science* **302** (2003) 1545.
[3] S.E. Snyder and S.V. Rotkin, *Small* **4**-9 (2008) in press: *arXiv*:0803.3802v1, cond-mat (2008).

Corresponding Author: Shigeo Maruyama
TEL: +81-3-5841-6421, FAX: +81-3-5800-6983, Email: maruyama@photon.t.u-tokyo.ac.jp

Reduction of SWNT heat conduction by surrounding materials

○Junichiro Shiomi* and Shigeo Maruyama

[1]*Department of Mechanical Engineering, The University of Tokyo*
7-3-1 Hongo, Bunkyo-ku, Tokyo 113-8656, Japan

Characterization of thermal properties of single-walled carbon nanotubes (SWNTs) is a key issue for their prospective electrical and thermal device applications. The importance of probing SWNT heat conduction has attracted many recent researches in ideal environment, which have revealed remarkable heat conduction properties at low and high temperatures [1-4]. The heat conduction exhibits complex diffusive-ballistic feature for realistic nanotube-length in many applications even at room temperature. As a consequence, unique steady and unsteady heat conduction characteristics manifests [5-9], which is particularly evident in the length effect of the thermal conductivity or conductance [5,6,9]. The possibility and trend of heat conduction divergence with respect to the tube length have been discussed in relation with the scattering dynamics of long wave phonons and the effect of low-dimensional confinement [9].

While these properties encourage the device applications of SWNTs, their sensitivities to the surrounding environment become a key issue in practice. The question is how much of the ballistic heat conduction is preserved in a practical environment. In a system with significant contribution from ballistic heat transport, the intrinsic phonon distribution function and thus effective heat conduction is expected to depend strongly on the mode-dependent scattering dynamics at the interfaces [10]. In this study, the sensitivity of the diffusive-ballistic nature of the SWNT heat conduction to the environment has been investigated by modeling molecular dynamics (MD) of an SWNT surrounded by simple fluid. Non-equilibrium and equilibrium MD simulations suggest that the heat conduction suffers significantly from the presence of the surrounding material. The surrounding fluid was found to selectively attenuate the transport of long range phonons, the main heat carriers of an SWNT.

[1]. C. Yu *et.al.*, *Nano Lett.* **5**, 1842 (2005).

[2]. E. Pop *et.al.*, *Nano Lett.* **6**, 96 (2006).

[3]. J. Hone *et.al.*, *Appl. Phys. A* **74**, 339 (2002).

[4]. T. Yamamoto, *et.al.* , *Phys. Rev. Lett.* **92**, 075502 (2004).

[5]. S. Maruyama, *Micro. Therm. Eng.* **7**, 41 (2003).

[6]. N. Mingo and D. A. Broido, *Nano Lett.* **5**, 1221 (2005).

[7]. J. Shiomi and S. Maruyama, *Phys. Rev. B*, **73**, 205420 (2006).

[8]. J. Shiomi and S. Maruyama, *Phys. Rev. B.* **74**, 155401 (2006).

[9]. J. Shiomi and S. Maruyama, *Jpn. J. Appl. Phys.* **47**, 2005 (2008).

[10]. F. Carlborg, *et.al.* (submitted).

E-mail: shiomi@photon.t.u-tokyo.ac.jp.

Recovering and Redispersion of Composite of Single-Walled Carbon Nanotubes and Dispersing Agent

○Ayumu Sakai, Katsumi Uchida, Tadahiro Ishii, and Hirofumi Yajima

Department of Applied Chemistry, Faculty of Science, Tokyo University of Science
12-1 Funagawara-machi, Shinjyuku-ku, Tokyo 162-0826, Japan

We have investig ated the dispers ion state of dispersed SWNT s in water using various dispersing agents such as polysaccharid es and surfactants. The disp ersion s tate of the dispersed SW NTs was dependent on pH of the aqueous solution. Using carboxymethylcellulose (CMC) as a dispersing ag ent, SWNTs were well dispersed under the pH condition except extrem ely high or low pH, however , at extrem ely high or low pH, the aggregation of SWNT s was appear ed. By returning from extreme high or low pH t o neutral pH of the SW NTs s olution, the aggrega tion was disappeared, and the SWNT s were redispersed. On the other hand, in the case of sodium dodecylsulfate (SDS), the dispersion state of SWNT s changed responsiv e to pH, sim ilarly to CMC. However , the redispersion of SWNTs by the pH-returning was not occurred. This re sult indica ted that the SW NTs dispersion m echanism by using CMC was dif ferent fro m SDS, that is, SDS for med a micelle-like structure com posed of inner co re of SWNT s, on the other hand, CMC wrapped SWNTs. Thus, it' s considered that CM C-wrapped SWNT s cannot for m strong bundle structure in the aggregation state. In view of the relationship between the SWNTs aggregation state and th e disp ersing agent, we have di scussed about the redispersion of the SW NTs recovered as a powder . The dispersed SW NTs solution was prepared by using a dispersing agent. Next, by lyophilization of the solution, the SWNT s powder, that is, the composite of SWNTs and the dispersing agent, was obtained. Th e redispersion state of the powder in water was analyzed. The res ults showed that the SWNT s powder including CMC was well redispersed in water at pH 7, and the aggreg ation of SWNT s was disappeared. On the othe r hand, the SWNT s powder includ ing SDS was not well redisper sed. At present, we have prepared th e SWNT s powder in cluding synthesized polym er such as polystyrene and discussed about the redispersion state of the powder in organic solvent.

Corresponding Author : Hirofumi Yajima
E-mail : yajima@rs.kagu.tus.ac.jp
Tel : +81-3-3260-4272 (ext.5760) , **Fax** : +81-3-5261-4631

Boron-doped MWNTs synthesized by hot-filament CVD

○ Satoshi Ishii, Tohru Watanabe, Shunsuke Tsuda, Takahide Yamaguchi, Yoshihiko Takano

National Institute for Materials Science, 1-2-1, Sengen, Tsukuba, Ibaraki 305-0047, Japan

Boron-doped multiwalled carbon nanotubes (MWNTs) have been synthesized by a hot-filament chemical vapor deposition (CVD) method. A methanol solution of boric acid was used as a source material. In the boron-doped MWNTs previously synthesized by a thermal CVD method, the electrical resistivity has been reduced by increasing a boron concentration in the source solution up to 2.0 atm % (Fig. 1 (a)) [1]. In order to decrease the resistivity further, more effective doping method has been needed. Hot-filament CVD is expected to dope a larger amount of boron because induced plasma can decompose the vaporized source solution more effectively. The hot-filament CVD process was performed inside a flask filled with the source solution. The MWNTs were grown on a surface of Si substrate precoated with metal catalysts. A tungsten filament was placed less than 1 mm above the surface of Si substrate. During the MWNTs growth, to induce the plasma, the tungsten filament was heated by applying the current. For the produced MWNTs, the electrical resistivity of an individual MWNTs was measured with four electrodes which were fabricated by electron beam lithography. The ρ/ρ_{RT} of MWNTs synthesized by the hot-filament CVD method showed nonlinear temperature dependences (Fig.1 (b)), while those of MWNTs synthesized by the thermal CVD method showed linear dependences. We will discuss about the differences of conduction mechanism and doping effects depending on the synthesis methods.

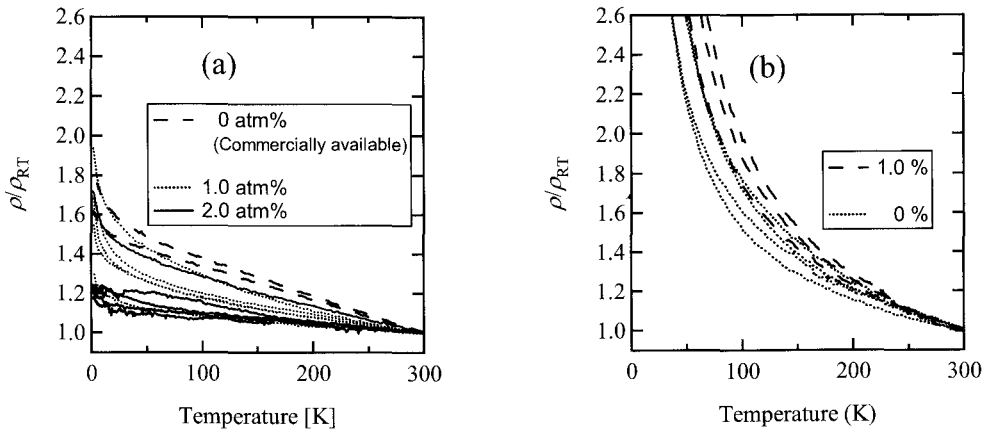

Fig. 1 Temperature dependence of normalized resistivity ρ/ρ_{RT} in the MWNTs synthesized from (a) thermal CVD method and (b) hot-filament CVD.

Reference: [1] S. Ishii *et al.*, Appl. Phys. Lett. **92**, 202116 (2008).

Corresponding Author: Satoshi Ishii
E-mail: ISHII.Satoshi@nims.go.jp
Tel: +81-29-859-2644, **Fax:** +81-29-859-2601

Sheet resistance of metallic single-wall carbon nanotube thin films

○Yasumitsu Miyata[1], Kazuhiro Yanagi[1,2], Yutaka Maniwa[2,3], Hiromichi Kataura[1,2]

[1]*Nanotechnology Research Institute, AIST, 1-1-1 Higashi, Tsukuba 305-8562, Japan*
[2]*JST-CREST, Kawaguchi 330-0012, Japan*
[3]*Department of Physics, Tokyo Metropolitan University, 1-1 Minami-Osawa, Hachioji, Tokyo 192-0397, Japan*

Single wall carbon nanotube (SW CNT) thin films are one of the candidates for a next-generation flexible and transparent electrode. In the practical use of the transparent electrode, the stability of sheet resistance is one of the most important issues in maintaining its function. It is well known that the conductivity of semiconducting SWCNTs is sensitive to carrier doping due to their huge density of state (DOS) at the edges of valence and conduction band. On the other hand, the metallic SWCNTs should have stable resistance against chemical doping because the metallic SWCNTs have a constant DOS near the Fermi level and the degree of the Fermi level shift upon chemical doping is less sensitive than for the semiconducting SWCNT due to the finite DOS.

In this work, we investigated the stability of the sheet resistance of the metallic SWCNT film and the mixture of metallic and semiconducting SW CNT film as a reference.[1] For the film preparation, the metallic SWCNTs were separated using the density gradient centrifugation method reported by Arnold et al.[2] When the films were exposed to air after high vacuum annealing, the metallic SW CNT film showed the stability of the sheet resistance within 10%, while the reference SWCNT film showed a 50% decrease in the resistance. For the chemical doping of sulfuric acid (H_2SO_4), the metallic SWCNTs showed only a 30% reduction in sheet resistance although the resistance of the reference SW CNTs decreased to 1/6. Because the SWCNTs used for both thin films were the same except for the concentration of semiconductors, the extreme stability in the sheet resistance of the metallic SW CNT thin film was apparently caused by the lack of semiconductors. The Fermi level shift of H_2SO_4-doped metallic SWCNTs was evaluated to be 0.7 eV using optical absorption and Raman spectroscopy. Because the shift was smaller than the M1 vHS energy (1.0 eV), the stability of the sheet resistance can be explained by the unchanged DOS against the Fermi level shift within the linear bands of metallic SWCNTs. The high stability in the sheet resistance of the metallic SWCNTs due to the constant DOS is the great advantage for the conductive film application.

References:
[1] Y. Miyata et al., J. Phys. Chem. C 112 (2008) 3591.
[2] M.S. Arnold et al., Nat. Nanotechnol. 1 (2006) 60.
Corresponding Author: Hiromichi Kataura,
E-mail: h-kataura@aist.go.jp,
Tel: +81-29-861-2551, **Fax:** +81-29-861-2786

3P-23

Electric Double Layer Transistor of Graphene

J. T. Ye[1], H. Shimotani[1], M. F. Craciun[2], A. F. Murpurgo[2], and Y. Iwasa[1]

[1]Institute for Materials Research, Tohoku University, Sendai 980-8577, Japan
[2]Kavli Institute of Nanoscience, Delft University of Technology, Lorentzweg 1, 2628CJ Delft, The Netherlands

Combination of graphene and electrochemical transistors method provides the largest tunable carrier density on graphene at a much lower gate voltage compared with the conventional back gate configuration [1]. Charge accumulation on graphene by the electronic double layer manipulates its electronic properties into a new regime. Wider tunable range of carrier density provides a possible way for the realization of novel transport phenomena like superconductivity. On the application point of view, electrochemical method is important for various kind of sensing and integration of soft material with microelectronics.

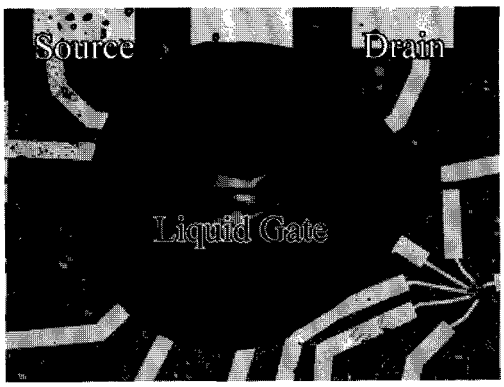

Fig.1 Gaphene-based EDLT Devices.

Graphene-based EDLT devices are fabricated on the top of SiO_2/Si substrate with the ionic liquid as the liquid gate media (Fig. 1). Charges are accumulated by the capacitor of the electronic double layer formed on the surface of the graphene. Transfer curves for the device shows typical bipolar behavior of graphene (Fig. 2). Due to the large capacitance of the electronic-double layer, the charge density is one order of magnitude larger than the maximum using SiO_2 back gating at an operating voltage about two orders of magnitude smaller [1].

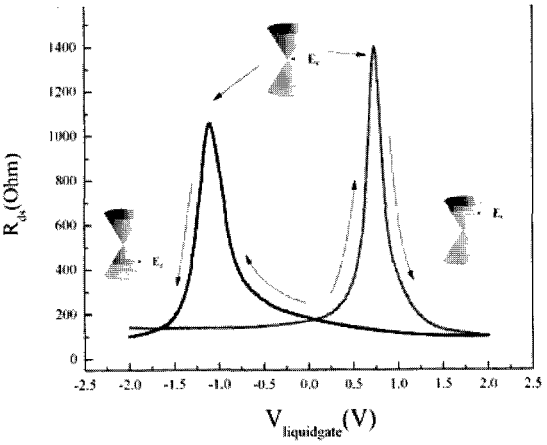

Fig. 2 Transfer curve of graphene EDLT device

[1] K. S. Novoselov, A. K. Geim, etal, Science 306, 666 (2004).

Corresponding Author: Jianting Ye
E-mail: yejianting@imr.tohoku.ac.jp
Tel&Fax: 022-215-2032 & 022-215-2031

Electronic structures of impurity doped carbon nanotubes

○Takashi Koretsune and Susumu Saito

Department of Physics, Tokyo Institute of Technology
2-12-1 Oh-okayama, Meguro-ku, Tokyo 152-8551

Carbon nanotubes are considered to be attractive materials for nanoscale electronic device in the next generations. To control the transport properties of semiconducting nanotubes, substitutional impurities such as boron or nitrogen will play an important role. So far, we have clarified the effect of boron doping in the carbon nanotubes and the ionization energy of impurity states[1]. In the experiment, however, the carbon nanotubes often behaves as a p-type semiconductor. Thus, to control the semiconducting behavior, it is important to discuss the donor impurity as nitrogen. Here, we study nitrogen-doped carbon nanotubes using the density functional theory.

In this study, we take (10,0) carbon nanotubes as a typical semiconductor tube and consider a nitrogen as a substitutional impurity. We first obtain the optimized structure and discuss the stability of substitutional nitrogen impurity. Then, we calculate the doping rate dependence of the gap of nitrogen-doped carbon nanotubes as shown in Fig. 1. From this data, we extrapolate the gap to the low nitrogen-density limit and estimate the depth of the impurity level. We will also discuss the difference between the substitutional doping of nitrogen or boron and the interstitial doping.

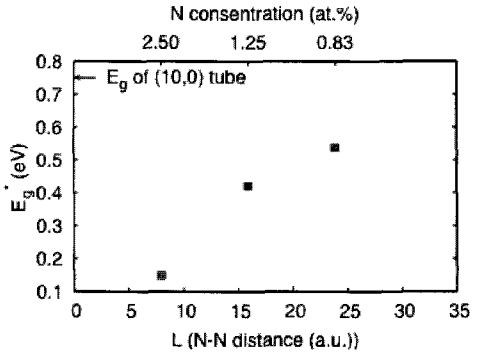

Fig 1 Gap of nitrogen-doped carbon nanotubes.

References:

[1] T. Koretsune and S. Saito, Phys. Rev. B77 165417 (2008).

Corresponding Author: Takashi Koretsune
E-mail: koretune@stat.phys.titech.ac.jp
Tel: 03-5734-2387

Decrease in Weight of Carbon Nanocoil by Acid Treatment and Its Dependence on Temperature and Time

○M. Yokota[1], Y. Shinohara[1], Y. Suda[1], S. Oke[1], H. Takikawa[1], Y. Fujimura[2]
T. Yamaura[2], S. Itoh[2], K. Miura[3], M. Morioki[4]

[1] *Department of Electrical and Electronic Engineering, Toyohashi University of Technology*
[2] *Research and Development Center, Futaba Corporation.*
3 Fuji Research Laboratory, Tokai Carbon Co., Ltd.
4 Fundamental Research Department, Toho Gas Co., Ltd.

Carbon nanocoil (CNC) is a material of carbon fiber with helical shape. CNCs are synthesized by chemical vapor deposition on a substrate using a composite catalyst, Fe-Sn. The composite catalyst-loaded substrate was placed in the center of a quartz-made reaction tube. The reaction temperature, the gas flow rates of nitrogen as a dilution gas and acetylene as a source gas, and the reaction time were 700 °C, 1000 sccm , 150 sccm , and 10 min, respectively. CNCs grown were treated in hydrogen peroxide 30% solution under reflux for purification. In this study, we examined the dependences of CNC weight on treatment temperature and time. As shown in Fig. 1 (a), weight of CNC was decreased significantly at higher than 80°C and split as well as flattened CNCs appeared simultaneously. But the weight loss became constant of about 40% over 140 °C. Fig. 1 (b) shows the change of weight by treatment time at 100 °C and 140 °C. The higher the treatment temperature the lower the weight of carbon.

This work has been partly supported by the Outstanding Research Project of the Research Center for Future Technology, Toyohashi University of Technology (TUT); the Research Project of the Venture Business Laboratory, and Global COE Program "Frontiers of Intelligent Sensing" from the Ministry of Education, Culture, Sports, Science and Technology (MEXT); and The Japan Society for the Promotion of Science (JSPS), Core University Programs (JSPS-KOSEF program in the field of "R&D of Advanced Semiconductor"; JSPS-CAS program in the field of "Plasma and Nuclear Fusion"); and Grant-in-Aid for Scientific Research from the MEXT.

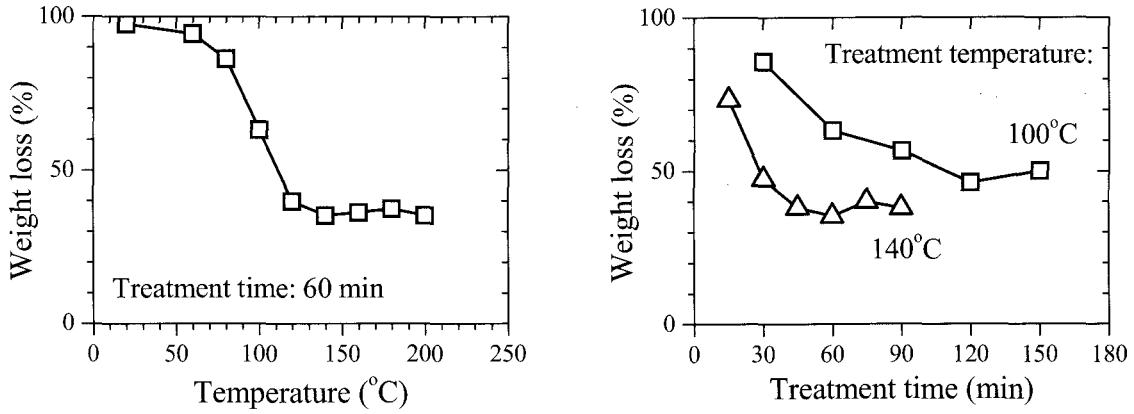

Fig. 1 Weight loss of CNC in acid treatment as a function of (a) temperature and (b) time.

Corresponding Author: Yoshiyuki Suda
E-mail: suda@eee.tut.ac.jp, Tel: +81-532-44-6726

Tissue response of multi-walled carbon nanotube blocks cross-linked by de-fluorination against subcutaneous tissue of rats *in vivo*

○Yoshinori Sato[1], Atsuro Yokoyama[2], Takao Kasai[2], Shinji Hashiguchi[3], Kenichi Motomiya[1], Balachandran Jeyadevan[1], Kazuyuki Tohji[1]

[1] *Graduate School of Environmental Studies, Tohoku University, Sendai, 980-8579, Japan.*
[2] *Graduate School of Dental Medicine, Hokkaido University, Sapporo, 060-8586 Japan.*
[3] *Stella Chemifa Co., 1-41, Rinkai-cho, Izumiotsu, Osaka, 595-0075, Japan.*

Recently, basic biomedical research concerning drug delivery and the use of scaffolds and catheters has been carried out using a new type of carbon allotrope comprising carbon nanotubes (CNTs). We have investigated the use of alternative artificial hard tissue materials comprising CNT composites. As CNTs possess low density, high mechanical strength and protein adsorption properties, artificial hard tissue alternative materials comprising CNTs can potentially be utilized as porous and strong 3-dimensional materials composed of 1-dimensional CNTs that offer advantages in comparison with the use of traditional C/C materials. We have produced large-sized binder-free multi-walled carbon nanotube (MWCNT) blocks from fluorinated MWCNTs using thermal heating and a compression method *in vacuo* (the blocks are referred to as "de-F-MWCNT blocks") [1]. This technique resulted in the formation of covalent MWCNT networks generated by the introduction of sp^3-hybridized carbon atoms that cross-link between nanotubes following de-fluorination. The resulting CNT blocks are lighter than graphite, can be machined and polished, possess average bending strengths of 102.2 MPa and a bending modulus of 15.4 GPa, and can potentially be employed for use as alternative artificial hard tissue materials.

Here, we report on the tissue response in subcutaneous tissue and evaluate the biocompatibility of binder-free de-F-MWCNT blocks using rats *in vivo*. MWCNT/resin blocks carbonized with 50wt% phenol resin were examined, with poly(methyl methacrylate) (PMMA) and Ni being used as a negative and positive controls, respectively.

[1] Y. Sato *et al*, *ACS Nano* **2008**, *2*, 348.

Corresponding Author: Yoshinori Sato
E-mail: hige@bucky1.kankyo.tohoku.ac.jp
Tel&Fax: +81-22-795-3868

Thermal diffusivity of single walled carbon nanotubes/UV-curable resin nanocomposites

○Takahiro Fukumaru, Tsuyohiko Fujigaya, and Naotoshi Nakashima

Department of Applied Chemistry, Graduate School of Engineering, Kyushu University, 744 Motooka, Nishi-ku, Fukuoka 819-0395, Japan

The exceptional thermal and mechanical properties and the very large aspect ratio of single walled carbon nanotubes (SWNTs) make them promising filler materials for polymer composites. We reported composites of SWNTs and UV-curable monomer (**1**) by in situ photo-polymerization and the composite films indicated extremely high electrical conductivity and low percolation threshold compared to other SWNT/polymer composites and nice 2D patterns of composites by using nanoimprint lithography[1]. In this presentation, we report : 1) the fabrication of SWNT/polymer composites by in situ photo polymerization using UV-curable monomer (**1** and **2**), and 2) the thermal diffusivity of the composites.

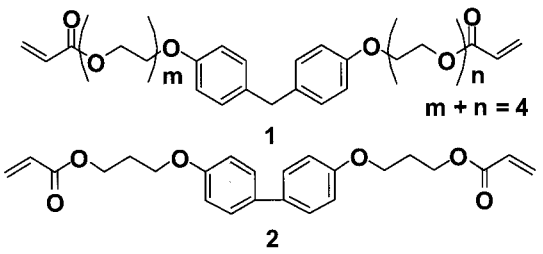

Fig. 1 Chemical structure of monomer **1** and **2**.

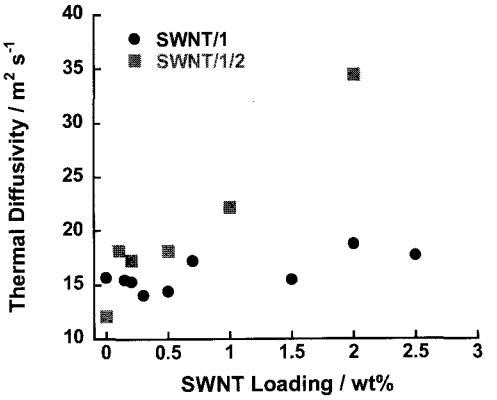

Fig. 2 Plots of thermal diffusivity as a function of SWNT loading for SWNT/**1** (filled circle) and SWNT/**1**/**2** (filled square).

Plots of the thermal diffusivity of SWNT/**1** composites as a function of SWNT loading are shown in figure 2. Even if SWNTs increased in the composites, there were few changes of the thermal diffusivity of the composites. To improve the thermal diffusivity of the composites, UV-curable monomer (**2**) with a mesogenic unit was introduced into the UV-curable monomer (**1**). The mesogenic unit is expected to form π-stack structure which works as phonon path in the composites. In comparison with the SWNT/**1** composites, thermal diffusivity of the SWNT/**1**/**2** composites increased with increasing of SWNTs introduction. We have found that the addition of the mesogenic unit improved the thermal diffusivity of the composites.

[1] Tsuyohiko Fujigaya, Shinsuke Haraguchi, Takahiro Fukumaru and Naotoshi Nakashima, *Adv. Mater.* **2008,** *20*, 2151–2155.

Corresponding Author: Naotoshi Nakashima
TEL: +81-92-802-2840, FAX: +81-92-802-2842, E-mail: nakashima-tcm@mail.cstm.kyushu-u.ac.jp

3P-28

Characterization of growth process of VA-SWNT films and their applications for Dye-Sensitized Solar Cell

○Jun Okawa, Junichiro Shiomi and Shigeo Maruyama

Department of Mechanical Engineering, The University of Tokyo
7-3-1 Hongo, Bunkyo-ku, Tokyo 113-8656, Japan

Towards the application of SWNTs, clarification of their growth mechanism and control of their diameter, alignments and chirality is important. For these purposes, we firstly investigated the growth process of vertically aligned SWNTs (VA-SWNTs). We have monitored the growth of VA-SWNT films using optical absorbance technique [1] and obtained the growth curves of these films. Variation of growth profiles was observed when the flow rate of ethanol during the ACCVD [2] was controlled precisely (Fig. 1). Furthermore, careful consideration was given for these outcomes by comparing with the results of CHEMKIN simulations and FT-IR gas analysis.

Secondly, as an example of the applications, we attempted to use VA-SWNT films as counter electrodes (CEs) for dye-sensitized solar cells (DSCs). Although platinum has been popularly adopted as a catalyst on CEs, it is rare and expensive. Hence, there is a strong demand for new materials for CEs. By detachment technique of SWNT films from substrates [3], the film was transferred on a transparent conductive oxide (TCO) substrate to form a CE. Figure 2 shows the I-V characteristics of DSCs using Pt and SWNT films. Even though the fill factor of the cell with SWNT was smaller than that with Pt, the similar short circuit current (Isc) and open ciruit voltage (Voc) was obtained. Smaller fill factor may be caused by the contact resistance between the SWNT film and TCO. Although this problem needs to be solved, current result indicates SWNT films can be useful as a material of CEs.

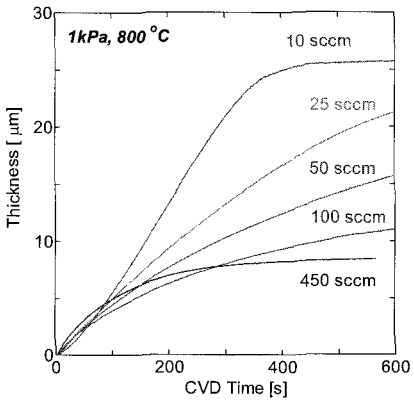

Fig. 1 Growth curve of VA-SWNT for different flow rates.

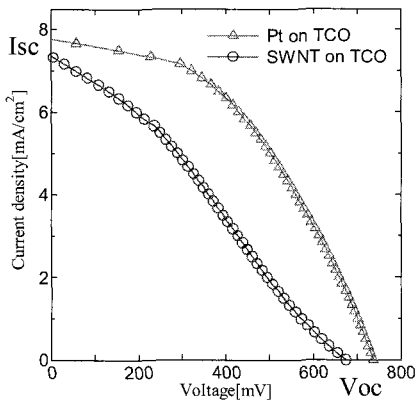

Fig. 2 I-V characteristics of DSCs with Pt and SWNT CEs.

[1] S. Maruyama *et.al., Chem. Phys. Lett.***403** (2005) 320

[2] S. Maruyama *et.al., Chem. Phys. Lett.***360** (2002) 229

[3] Y. Murakami and S. Maruyama, ,*Chem. Phys. Lett.***422** (2006) 575

Corresponding Author: Shigeo Maruyama

Tel/Fax: +81-3-5800-6983

E-mail: maruyama@photon.t.u-tokyo.ac.jp

A Stable Electroactive Monolayer Composed of Soluble Single-Walled Carbon Nanotubes on ITO

○ Qiguan Wang[1], Hiroshi Moriyama[1,2]

1.*Research Center for Materials with Integrated Properties;* 2. *Department of Chemistry, Toho University, Miyama 2-2-1, Funabashi, 274-8510, Japan*

Functionalized single-walled carbon nanotubes (SWNT) has drawn much attention for the potential application in the field of nanodevices. Recently, significantly soluble SWNT with dispersed particle size (< 3 nm) was obtained in a 1:1 H_2SO_4/ HNO_3 (v/v) mixed solution using microwave radiation under high pressure [1], However, from the viewpoint of process safety and instrumental simplicity, another method, such as the formation of these soluble SWNTs at ambient conditions, is required. In this presentation, we will demonstrate that a similar soluble SWNT has been safely obtained via a two-step process assisted by microwave radiation, which has been used to fabricate an electrochemical stable layer (SAM–ITO) self-assembled on 3-aminopropyltrimethoxysilane modified ITO, as shown in Scheme 1.

Cyclic voltammetry (CV) measurements with the SAM–ITO as the working electrode in acidic aqueous systems showed unexpected oxidation signals due to redox reactions involving the defects and sidewalls of soluble functionalized SWNTs. Interestingly, after introducing a conductive oligomer of tetramer aniline onto the residual carboxyl groups on the surface of the SWNTs, the CV data showed a single reversible redox couple, which indicated a more stable state (Figure 1). This stable super-thin SWNT layer would show a wealth of applications in nanocomposite architectures.

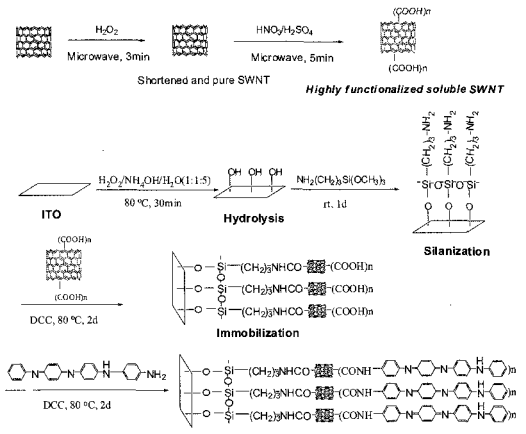

Scheme 1. Preparation route to attaching a functionalized SWNT layer on to ITO end-capped by a tetramer aniline group.

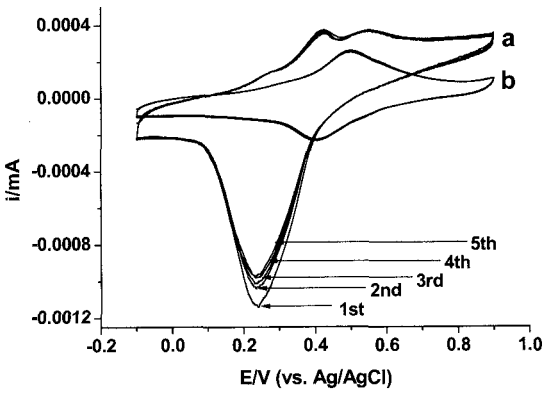

Figure 1. CV traces of: (a) SWNT SAM–ITO and (b) SWNT SAM–ITO end-capped by tetramer aniline groups in an aqueous 1.0 M H_2SO_4 solution. Scan rate = 0.05 V/s.

References:

[1] Y. B. Wang, Z. Iqbal, S. Mitra, *J. Am. Chem. Soc.* **128**, 95-99 (2006).

Corresponding Author: Hiroshi Moriyama
E-mail: moriyama@chem.sci.toho-u.ac.jp **Tel:** 047-472-1211, **Fax:** 047-476-9449

Effective Chemical Functionalization of SWNT with microwave oven

ONozomi Kuroki, Mariko Kondo, Toshiki Sugai, Hiroshi Moriyama*

Department of Chemistry, Toho University, Miyama 2-2-1, Funabashi, 274-8510 Japan

Considerable efforts have been performed to functionalize SWNT to be soluble and to produced materials between metal particles.[1-3] There are varieties of the functionalization methods such as DNA wrapping, attachment of π conjugate materials and oxidation. The oxidation is especially important, since various functional groups can be introduced to the ends of SWNT keeping their unique electronic states unchanged with strong covalent bonds. The oxidation, so far, takes long treatment time like reflux in HNO_3 for days. In this study, we have succeeded to oxidize SWNT using a microwave oven with H_2O_2 and HNO_3 effectively and easily.

The oxidation was performed with a microwave oven (NE-710G) for cooking. 20 mg of HiPco-SWNT (PO276:CNI) and 20 ml of H_2O_2 (30%) or 20 ml of conc-HNO_3 were mixed in a glass bottle, to which the microwave was irradiated for 0-180sec (H_2O_2) and for 0-2h (HNO_3), respectively. The oxidized products were characterized by IR and Raman measurements, and their weight loss during the irradiation.

Figure 1 shows IR spectra of the products with salient peaks at 3400 cm^{-1} and 1650 cm^{-1} revealing that hydroxyl groups (OH) were mainly introduced with H_2O_2, whereas HNO_3 functionalizes SWNT with carboxylic groups (COOH) in a short period. These effective functionalizations were also supported by the sample weight dependence on the treatment time. Within several minutes, 80% of the sample were burned. This weight loss in minutes with the microwave corresponds to that in days with the reflux. Furthermore, Raman spectra of these products show intense RBM and G-band, which prove that SWNT was not destructed. These characterizations reveal that we have produced functionalization SWNT effectively with microwave. The products show much higher dispersibility in DMF than pristine SWNT.

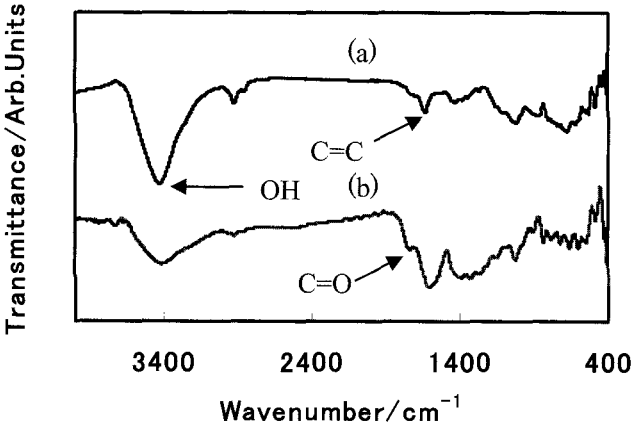

Fig. 1. (a) IR spectra of oxidation of SWNT with H_2O_2 under irradiation microwave at 250 W for 60 sec and (b)with HNO_3 at 350 W for 2 hours.

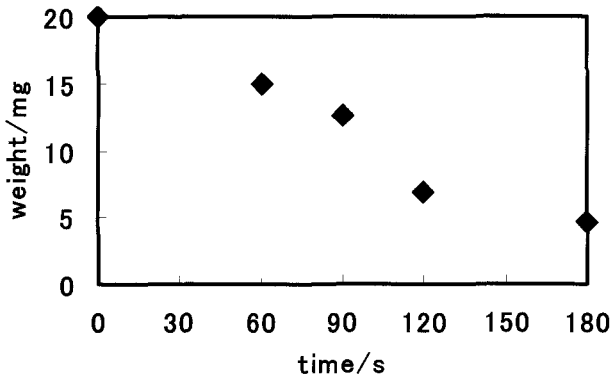

Fig. 2. Relation between irradiation time and weight reduction through treatments at 250 W with H_2O_2 for 0-180sec.

Acnowledgements: Raman observations were supported by Prof. Katsuhide Terada (Faculty of Pharmaceutical Science, Toho University).

1) K. Fu and Y. -P. Sun, *J. Nanosci. Nanotech.* **2003**, *3*, 351-364.
2) S. Banerjee, T. H. Benny, S. S. Wong, *Adv. Mater.* **2005**, *17*, 17-19.
3) Y. Wang, Z. Iqbal, and S. Mitra, *J. Am. Chem. Soc.* **2006**, *128*, 95-99.

Corresponding Author: Hiroshi Moriyama e-mail: moriyama@chem.sci.toho-u.ac.jp
Tel: 047-472-1211, Fax: 047-476-9449

3P-31

Single Wall Carbon Nanohorn for Controlled Release

O Xu Jianxun,[1] Yudasaka Masako,[2] Iijima Sumio[1,2]

[1] *Meijo University, 1-501 Shiogamaguchi, Tenpaku-ku, Nagoya 468-8502, Japan*
[2]*Nanotube Research Center, AIST, Tsukuba, 305-8565, Japan*

Thanks to its abundant nanospaces and high surface area, Single Wall Carbon Nanohorn (SWNH) possesses som e prom ising applications for st orage and transpo rtations, including m ethane storage, drug delivery, am ong others. To construc t a "sm art" carrier system, the release of the cargoes in a controllable m anner is of special importance. Thus, so me efforts have been m ade to probing the interactions between SW NH and various loadings , esp ecially some m edical molecules, and the possible con trolled releas e ab ility of SW NH, as discussed briefly in the following text.

Vancomycin (VCM), an antibio tic with the illu strated struc ture in Fig. 1, was found to interact with oxidized SWNH (SWNHox) strongly, m aybe through the pi-pi stacking and hydrophobic interactions. This strong interaction resulted in the slow release of VCM from SWNHox. Around 18% loaded VCM was released into the PBS a queous phase after 10 days, even though VCM itself can be dissolved in water very fast (Fig. 2).[1] Besides VCM, the releases of Dex amethasone (DEX) and C $_{60}$ from SW NHox were also investigated. [2,3] I t is in teresting th at c isplatin incorporated inside SWNHox, a small chem otherapeutant h aving high water so lubility without benzenoid structures, w as also released in a sl ower rate in aqueous so lutions co mpared with naked cisplatin. To get a better control of various drug molecules is a key issue for drug delivery application of SWNH, which will be discussed in the presentation.

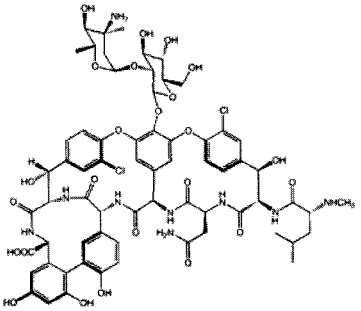

Figure 1. Scheme of 2D structure of vancomycin (VCM).

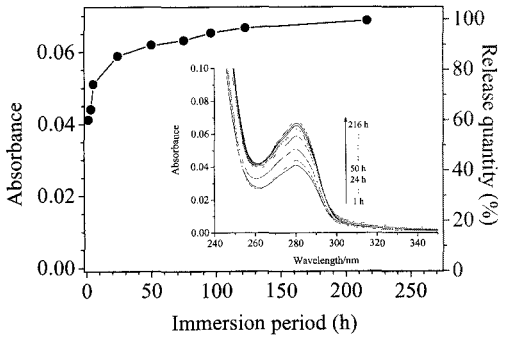

Figure 2. The release profile of Phospholipid-poly(ethylene glycol) m odified VCM-SW NHox in PBS solution. The inset is the according UV absorption spectra of the release solutions.

References:
1. J. Xu,* M. Yudasaka,* S. Kouraba, M. Sekido, Y. Yamamoto and S. Iijima Chem. Phys. Lett. Accepted.
2. T. murakami, K. Ajima, J. Miyawaki, M. Yudasaka, S. Iijima, K. Shiba Mol. Pharm. 2004, 1, 399.
3. R. Yuge et al. J. Phys. Chem. B 2005, 109, 17861.

Corresponding Author: Xu Jianxun, Yudasaka Masako; **E-mail:** jianxun-xu@aist.go.jp, m-yudasaka@aist.go.jp; **Tel/Fax:** 029-861-6290

Comparative Study of Carbon and BN Nanographenes: Ground Electronic States and Energy gap Engineering

Xingfa Gao,[1,o] Zhongfang Chen[2] and Shigeru Nagase[1]

[1]*Department of Theoretical and Computational Molecular Science, Institute for Molecular Science, Myodaiji, Okazaki 444-8585, Japan*
[2]*Department of Physics, Applied Physics, and Astronomy, Rensselaer Polytechnic Institute, Troy, NY 12180, USA*

Since its first experimental discovery in 2004,[1] graphene, an atomic monolayer of carbon atoms arranged in a honeycomb lattice, has rapidly risen as one of the hottest stars in material science. The chemistry of graphene has just begun;[2] however, it has shown promising abilities in conquering the bottleneck problems in graphene preparation, purification and functionalization. As another ultra-thin material, the synthesis of single layer boron nitride (BN) has also been achieved.[3]

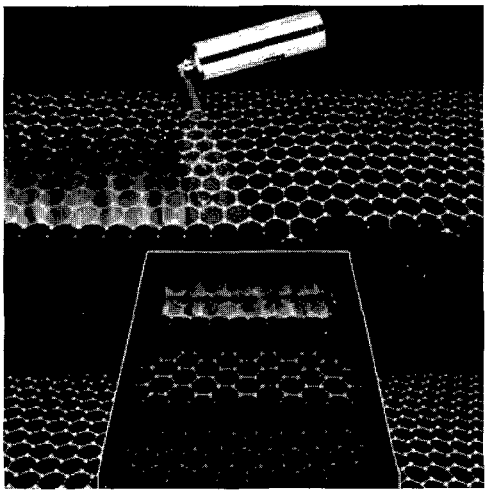

Because of the increasing interest in graphene and graphene-like materials, it becomes important to grasp their ground electronic state, chemical reactivity and the subsequent electronic consequences from the bottom to top. In this talk, our recent results[4] on the titled topic will be presented.

The relationship between stabilities and shape confirmations of carbon and boron nitride nanographenes were studied using the B3LYP/6-31G* method. The HOMO-LUMO energy gaps of rectangular-shaped carbon nanographenes (CNGs) decrease as the graphene sizes increase, with a direct inverse dependence on the length of zigzag edge. In contrast, the energy gaps of BN nanographenes (BNNGs) have a weak dependence with size. CNGs with long zigzag edges are less favorable energetically than their structural isomers with long armchair edges, while BNNGs have the opposite preference. Chemical reactions that change the long zigzag edge into armchair type can efficiently stabilize the kinetically unstable CNGs and modify their energy gaps.

References

1. Novoselov, K. S.; Geim, A. K.; Morozov, S. V.; Jiang, D.; Zhang, Y.; Dubonos, S. V.; Grigorieva, I. V.; Firsov, A. A. *Science* **2004**, *306*, 666-669.

2. Ruoff, R. *Nat. Nanotechnol.* **2008**, *3*, 10-11.

3. Novoselov, K. S.; Jiang, D.; Schedin, F.; Booth, T. J.; Khotkevich, V. V.; Morozov, S. V.; Geim, A. K. *Proc. Natl. Acad. Sci. USA* **2005**, *102*, 10451-10453.

4. Gao, X. F.; Zhou Z.; Zhao, Y. L.; Nagase, S.; Zhang, S. B.; Chen, Z. F.; *J. Phys. Chem. C* , in press.

Corresponding Author: Xingfa Gao
E-mail: gao@ims.ac.jp
Tel: 0564-55-7222

Effect of hydrogen gas on single-walled carbon nanotubes growth over gold catalyst using chemical vapor deposition method

○ Z. Ghorannevis, T. Kato, T. Kaneko, and R. Hatakeyama

Department of Electronic Engineering, Tohoku University, Sendai 980-8579, Japan

Single-walled carbon nanotubes (SWNTs) are attracting much interest due to their unique electronic, mechanical properties and the potential applications in various fields [1]. In this paper we have investigated the effect of hydrogen gas on the growth of carbon nanotubes (CNTs) using thermal (TCVD) and plasma chemical vapor deposition (PCVD) methods over nonmagnetic gold catalyst [2,3]. Measurements of Raman spectra show that increasing hydrogen flow rate decreases SWNT density in the case of using gold, while hydrogen can work well in case of iron. This indicates that reactive hydrogen species are generally unfavorable to SWNT nucleation and growth over Au catalyst. Figure1 gives the plot of G band intensity of Raman spectra (I_G) in terms of hydrogen flow rate. It is found that increasing the hydrogen flow rate is accompanied by the I_G decrease, which can be explained by difference of the catalytic activity between Au and Fe. Since materials such as Au have week interaction with carbon atoms, compared with Fe, the nucleation of SWNTs on Au surface is strongly suppressed due to their etching effect.

In case of PCVD, on the other hand, poorly crystallized CNTs are observed while using gold as a catalyst, which is considered to originate from plasma- assisted decomposition. Specifically, since any H_2 leads to hydrogen reactants, concentration of hydrogen reactants is much more in comparison with TCVD.

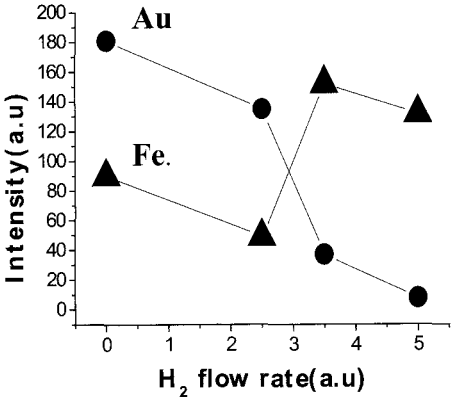

Fig. 1: Effect of hydrogen flow rate on the growth of SWNTs from Au and Fe catalysts.

References:

[1] R. Saito, G. Dresslhaus, and M. S. Dresselhaus, physical properties of carbon nanotubes, Imperical college Press, London (1998).

[2] T. Homma, H. Suzuki, and Y. Kobayashi, Nano Lett. **6**, 2642 (2006).

[3] T. Kato, G. Jeong, T. Hirata, R. Hatakeyama, K.Tohji, and K. Motomiya, Chem. Phys. Lett. **381**, 422 (2003).

Corresponding Author:

E-mail: zohreh@plasma.ecei.tohoku.ac.jp **Tel & Fax:** 022-795 7046 , 022-263 9225

Chirality Separation for Single-walled Carbon Nanotube with Density Gradient Electrophoresis

Yoshiya Kaminosono, Katsumi Uchida, Tadahiro Ishii, and Hirofumi Yajima*

Department of Applied Chemistry, Faculty of Science, Tokyo University of Science
12-1 Funagawara-machi, Shinjyuku-ku, Tokyo 162-0826, Japan

Chirality separations for single-walled carbon nanotubes (SWNTs) have attracted a great deal of attraction for their practical and advanced applications. In view of the relationship between the chirality and diameter, we have attempted the development of a new chirality separation method with density gradient electrophoresis (DGE). In the present study, the individually dispersed HiPco SWNTs in SDS solutions was prepared by ultrasonication treatment for 60 min in an ice bath at about 20 W power, following ultracentrifugation treatment at 163,000 g for 60 min. The density gradient (1.05-1.22) was prepared by adding 50% sucrose to TBE buffer. Resonance Raman measurements revealed that thin SWNTs with either metallic (m) or semiconducting (s) characters was concentrated in the high density region, whereas thick SWNTs with either s-SWNTs characters were concentrated in the low density region. The DGE method is expected to be promising for the chirality separations. At present, more DGE study for probing the dominant factors involved in the chirality separation is in progress.

Corresponding Author: Hirofumi Yajima

TEL: +81-3-3260-4272(ext.5760), FAX: +81-3-5261-4631, E-mail: yajima@rs.kagu.tus.ac.jp

Carbon nanotube growth with (Fe,Co)Pt catalysts by a chemical vapor deposition method

○ Takuya Sonomura, Nobuyuki Iwata, and Hiroshi Yamamoto

Department of Electronics & Computer Science, College of Science & Technology, Nihon University, 7-24-1 Narashinodai, Funabashi, Chiba 274-8501, Japan

For spintronics using single-walled carbon nanotubes (SWNTs), we carried out a thermal chemical vapor deposition (TCVD) with the catalysts, which should have high spontaneous magnetization, and the grains of which is required not to coalesce at the high temperature where SWNT can grow. It is expected that the (Fe, Co)Pt catalysts are the candidates, because the magnetization is still high even though it includes Pt, coalescence is prevented due to the inclusion of Pt, and the structure is almost same to fcc. In this study we will report the carbon nanotube (CNT) growth by TCVD with (Fe, Co)Pt catalysts.

The quartz substrate was ultrasonically cleaned. The cleaned quartz substrates were soaked and drawn up with 6μm/s to deposit Co/Fe/Pt, Co/Pt or Fe/Pt catalysts. The substrate annealed at 450°C in air for 5 min. The TCVD was carried out for 5 min on the annealed substrate at 800°C and 100 kPa with Ar : H_2 : C_2H_4 = 200 : 10 : 20 ccm. The grown CNTs were evaluated by SEM, optical microscope and Raman scattering excited with second harmonic of YAG laser, 532 nm.

Figure 1 shows SEM image after TCVD with CoFePt catalyst. The length and the diameter of grown CNTs was approximately 10 μm and 20 nm, respectively. The CNTs grew randomly in all over the substrate. Figure 2 shows Raman spectrum with CoFePt catalyst. The peak of radial breathing modes (RBM) did not appear. The G/D ratio was approximately 1.05. The grown CNTs were not SWNTs but multi-walled CNT. The results with other catalysts and the reason why the SWNT did not grew will be also discussed.

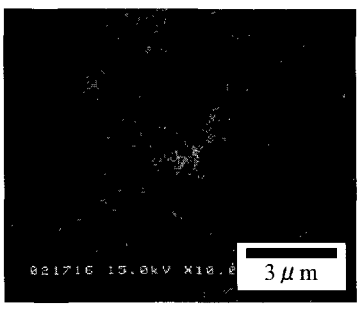

Fig.1 SEM image with CoFePt catalyst

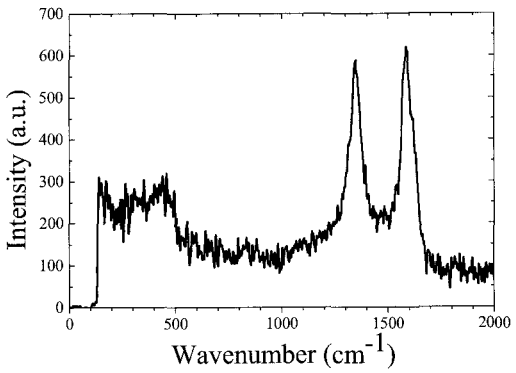

Fig.2 Raman spectrum

Analyses of Source Gas Consumption during Carbon Nanotube Growth using In-situ FTIR Measurements and Numerical Simulations

○Shintaro Sato, Tatsuhiro Nozue, Akio Kawabata, Tomo Murakami, Daiyu Kondo, Mizuhisa Nihei, Yuji Awano

MIRAI-Selete (Semiconductor Leading Edge Technologies, Inc.)
10-1 Morinosato-Wakamiya, Atsugi 243-0197, Japan

The Carbon nanotube (CNT) is a promising candidate for an interconnect material in future LSI. We have actually been trying to use a bundle of multi-walled carbon nanotubes (MWNTs) for vertical wiring (via) in LSI. We previously reported on the fabrication of CNT vias with a diameter of 160nm having a resistance as low as that of W plugs [1].

We are trying to understand the growth mechanism of CNTs to further increase the site-density of MWNTs in a via hole. As part of such efforts, in this work, we analyzed the consumption of the source gas during low-temperature growth using an FTIR analyzer, which was attached to the exhaust line of a low-pressure chemical vapor deposition (CVD) chamber.

The MWNTs were synthesized on a substrate at 450 °C at 6 kPa by thermal CVD using a mixture of C_2H_2 and Ar. Nickel particles with a diameter of 4 nm were used as a catalyst. The growth rates of MWNTs were estimated using scanning electron microscopy for various partial pressures of C_2H_2. It was found that the initial growth rate increased linearly with the partial pressure up to a certain partial pressure (supply-limited condition), but became almost constant beyond that (reaction-limited condition). In-situ FTIR measurements performed at the same time showed that, under a supply-limited condition, the C_2H_2 consumption was almost constant during growth. On the other hand, we observed a rapid increase and a subsequent decrease in the C_2H_2 consumption under a reaction-limited condition (Figure 1), corresponding to rapid deactivation of catalyst particles. Numerical simulations for a flow and C_2H_2 concentrations in the CVD chamber were also performed to obtain information concerning reactions of C_2H_2 on the substrate. The details of the analyses will be given in the presentation.

This work was completed as part of the MIRAI Project supported by NEDO.

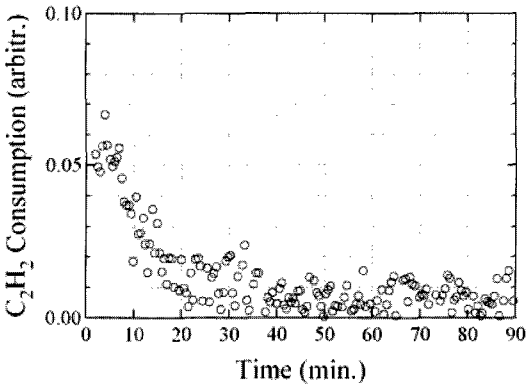

Figure 1. Acetylene consumption with time under a reaction-limited condition.

References

[1] A. Kawabata et al, Proc. IEEE Int. Interconnect Technol. Conf. 2008, p.237 (2008)

Corresponding Author: Shintaro Sato
TEL: +81-46-248-3280, FAX: +81-46-248-3285
E-mail: sato.shintaro@selete.co.jp

Growth Control of Single-Walled Carbon Nanotubes by High Vacuum CVD Method

○Yohei Yamamoto, Hiroto Okabe, and Shigeo Maruyama

Department of Mechanical Engineering, The University of Tokyo, Tokyo 113-8656, Japan

Single-walled carbon nanotubes are one of the attractive materials for nanodevices because of their small diameter (~1 nm), high mechanical strength, high thermal conductivity, and structure-dependent electrical conduction property. Currently the alcohol catalytic chemical vapor deposition (ACCVD) method [1] is widely used to synthesize SWNTs because it can control the position and orientation to some extent. Shiokawa *et al.* [2] have reported that SWNTs can be grown at low temperature for nanodevices by performing CCVD at low pressure (less than 0.1 Pa). The advanced generation method based on the SWNT growth mechanism is necessary for the achievement of device applications in the future.

In this work, our main purpose is the clarification of the growth mechanism of SWNTs by controlling the synthesis reaction in the environment of a high vacuum. We developed an experimental apparatus to control the atmosphere gas accurately while performing ACCVD (Fig. 1), and successfully synthesized SWNTs at various temperatures and pressures. Analysis by resonant Raman spectroscopy (Fig. 2), scanning electron microscopy and atomic force microscopy indicates that SWNTs synthesized under high vacuum have higher purity than the one synthesized with the standard CVD apparatus. Moreover, the results suggest that the flow rate of the ethanol influences the diameter of SWNTs.

[1] S. Maruyama, R. Kojima, Y. Miyauchi, S. Chiashi, M. Kohno, *Chem. Phys. Lett.* **360** (2002) 229.

[2] T. Shiokawa, P. H. Zhang, M. Suzuki, K. Ishibashi, *Jpn. J. Appl. Phys.* **45** (2006) L605.

Corresponding Author: Shigeo Maruyama

TEL: +81-3-5841-6421, FAX: +81-3-5841-6408, E-mail: maruyama@photon.t.u-tokyo.ac.jp

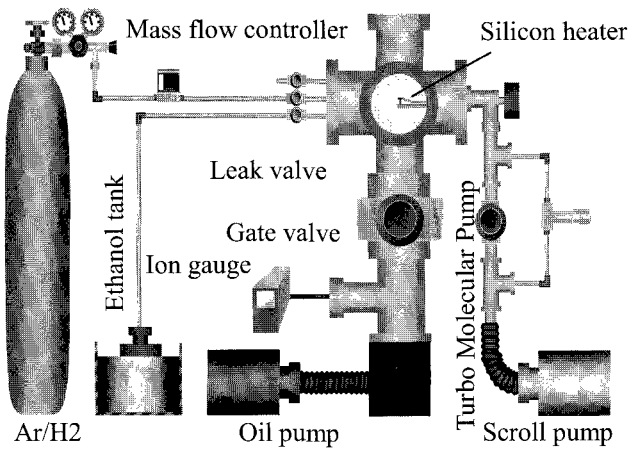

Fig. 1: HV-CVD experimental apparatus

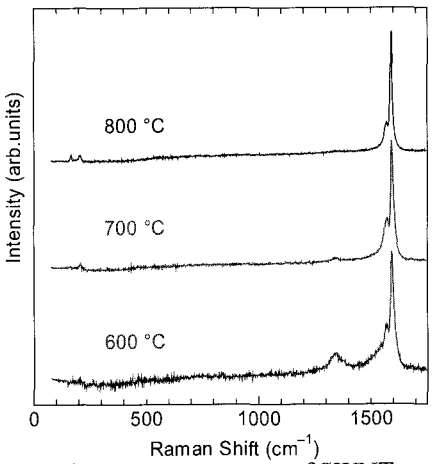

Fig.2: Raman spectra of SWNTs

Evaluation of the ratio of metallic to semiconducting single-wall carbon nanotubes by optical measurement

○Yasumitsu Miyata[1], Kazuhiro Yanagi[1,2], Yutaka Maniwa[2,3], Hiromichi Kataura[1,2]

[1]*Nanotechnology Research Institute, AIST, 1-1-1 Higashi, Tsukuba 305-8562, Japan*
[2]*JST-CREST, Kawaguchi 330-0012, Japan*
[3]*Department of Physics, Tokyo Metropolitan University, 1-1 Minami-Osawa, Hachioji, Tokyo 192-0397, Japan*

In this work, we have investigated th e metal-to-semiconductor ratio for SW CNTs produced by laser ablation using optical ab sorption spectroscopy.[1] To evaluate the ratio, the pristine SW CNTs were s eparated into metals and se miconductors using the density gradient centrifugation m ethod.[2] Th e optical absorption spectra of m etallic and semiconducting SWCNT films were measured from the near-infrared to ultraviolet and norm alized for the corresponding film thickness (Fig. 1). Then, the absorption spectrum of the pristin e SW CNTs was repr oduced using the weighted sum of the spectra of the m etallic and sem iconducting SW CNTs. This sim ple superposition analysis revealed the pristine SWCNTs consist of 27 ± 3% m etallic SWCNTs and 73 ± 3% semiconducting SWCNTs. This result suggest s that there is little chirality selection in the laser ablation m ethod. Furthermore, it was found the integral intensity of the M_{11} band of metallic SWCNT s was 1.2 tim es lar ger than that of the S_{22} band of semiconducting SW CNTs for a diameter distribution of 1.1~1.3 n m from the o scillator fitting of the spectra. From this result, the ratio of metallic S WCNTs, R_{Metal}, can b e expressed as

$$R_{Metal} = \frac{1}{1+1.2\frac{I_{S22}}{I_{M11}}} ,$$

where I_{M11} (I_{S22}) is the integ ral intensity for the M_{11} (S_{22}) band of a SWCNT s ample. This equation allows us to estim ate the metal-to-semiconductor ratio of various S WCNT samples without the separation.

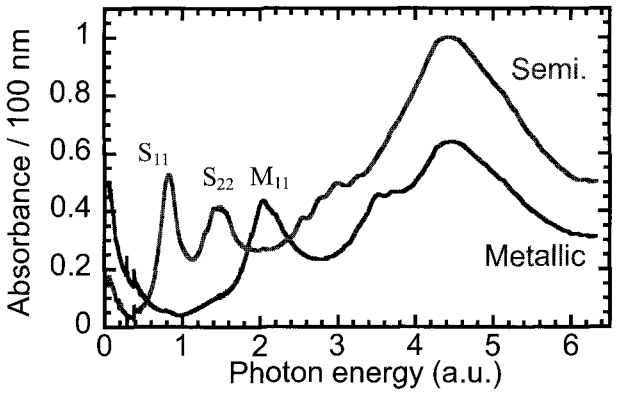

Fig. 1. Optical abso rption spectra of the thin films of m etallic and sem iconducting SWCNTs. The spectra were normalized by the film thickness.

References:
[1] Y. Miyata et al., J. Phys. Chem. C, accepted.
[2] M.S. Arnold et al., Nat. Nanotechnol. 1 (2006) 60.
Corresponding Author: Hiromichi Kataura,
E-mail: h-kataura@aist.go.jp,
Tel: +81-29-861-2551, **Fax:** +81-29-861-2786

Dispersion of single-walled carbon nanotubes made by using arc-burning technique in nitrogen atmosphere

○Takashi Mizusawa[1], Shinzo Suzuki[1], Yohji Achiba[2]

[1]*Department of Physics, Kyoto Sangyo University, Kamigamo-Motoyama, Kita-ku, Kyoto 603-8555, Japan*

[2]*Department of Chemistry, Tokyo Metropolitan University, Hachioji, Tokyo 192-0397, Japan*

Abstract: In the last symposium, we have shown that single-wall carbon nanotubes (SWNTs) made by using arc-burning technique in n itrogen atm osphere could be successfully mono-dispersed in the sodium chlorate (S C) solution, and the photolum inescence m apping indicated th at th e diameter di stribution of them was found to be re latively nar row (alm ost comparable to those made by laser-furnace technique [1-3].

These few years, a lot of che mical substances were used for the m ono-dispersion of SWNTs m ade by CVD techniqu e (e.g. HiPCO na notube). However, it has been still under question whether those chem ical substances co uld also be used for the m ono-dispersion of SWNTs made by arc-burning technique, ex cept for a few cases , such as sodium carboxymethyl cellulose (Na-CMC) solution [4].

In this presentation, several kinds of chemical substances are inves tigated for the dispersion of SW NTs m ade by using arc-burning technique in n itrogen atmosphere. The figure shows the case of Na-CMC solution, indicating that Na-CMC solution has the ability of dispersion for these SWNTs.

This work was partly supported by the funds of Ni ppon Sheet Glass Foundation for Material Science and Engineering (NSG Foundation).

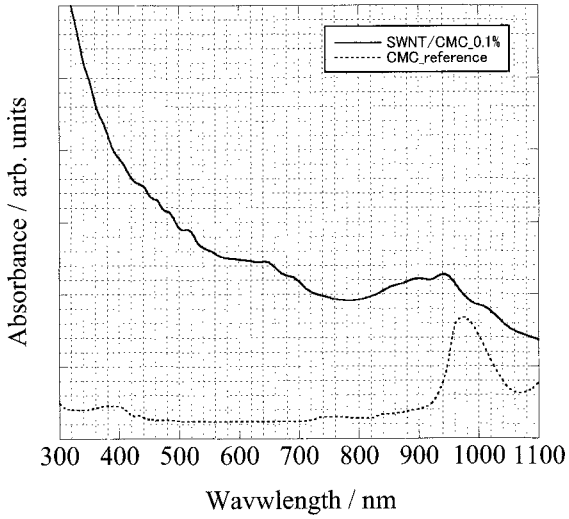

References:

[1] T. Mizusawa et al., The 34th Fullerene-Nanotube symposium proceeding, (2008).

[2] S. Suzuki et al., *Eur. Phys. J. D*, **43**, 143-146(2007).

[3] T. Okazaki et al., *Chem. Phys. Lett.*, **420**, 286(2006).

[4] N. Minami et al., *Appl. Phys. Lett.*, **88**, 093123(2006).

Corresponding Author: Shinzo Suzuki

E-mail: suzukish@cc.kyoto-su.ac.jp

Tel: 075-705-1945 Fax: 075-705-1640

Synthesis of Single-Walled Carbon Nanotube by using Rapid Temperature Alteration Alcohol CCVD Method

Mao Shoji[1] and Hironori Ogata[2]
[1]*Department of Materials Chemistry, Hosei University, Tokyo 184-8584, Japan*
[2]*Department of Chemical Science and Tchnology, Hosei University, Tokyo 184-8584, Japan*

Alcohol catalytic chemical vapor deposition (ACCVD) method has been known as one of the synthesis method of single-walled carbon nanotubes (SWNTs). However, it has been reported that diameter distribution of the SWNTs synthesized by this method is larger than other methods such as arc discharge method or laser ablation method. It is assumed to be due to the mismatch between optimum temperature condition of catalytic activity and that of growth of SWNTs with a small diameter distribution by the ordinary ACCVD method. The establishment of the method of controlling the diameter of the SWNTs is an important challenge in ACCVD method.

In this study, we developed the rapid temperature alteration alcohol CCVD method to control the temperature condition of catalytic activity and that of growth of SWNTs with a small diameter distribution independently and to serach their optimization conditions for diameter control in ACCVD method. Figure 1 shows the SWNTs growth temperature dependence of Raman spectra of SWNTs obtained by the rapid temperature alteration alcohol CCVD method.

In this presentation, we will report the detailed relationship between the synthesis condition and the structure of SWNTs.

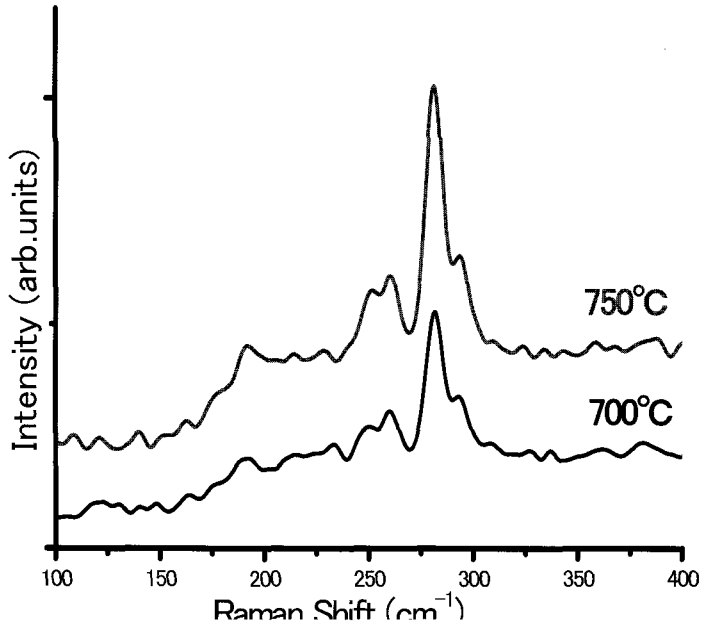

References:
1.S. Maruyama, R. Kojima, Y. Miyauchi, S. Chiashi and M. Kohno, *Chem. Phys. Lett.*, (2002), 360-3-4, 229-234

Corresponding Author: hogata@hosei.ac.jp
TEL:042-386-6229, FAX042-387-6229: , E-mail: hogata@hosei.ac.jp

Reaction Temperatures Dependence of SWCNT Diameters in e-DIPS Process

○Takeshi Saito[1,2], Bikau Shukla[1], Toshiya. Okazaki[1,2], Motoo Yumura[1] and Sumio Iijima[1]

[1] *Nanotube Research Center, AIST, Tsukuba 305-8565, Japan*
[2] *PRESTO, Japan Science and Technology Agency, Kawaguchi 332-0012, Japan*

By the recent progress in the chemical vapor deposition (CVD) synthesis of single-walled carbon nanotubes (SWCNTs), the diameter- and chirality-control of SWCNTs have been realized in the production of selected types of SWCNTs with relatively narrower diameters [1, 2]. Especially in the alcohol CVD (ACCVD) method, it has been reported that the reaction temperature strongly affects the chirality distribution in produced SWCNTs, probably due to its effect in the nucleation of catalyst nanoparticles. Most recently, to achieve the goal of this diameter-controlled large-scale synthesis of SWCNTs, we have developed a novel gas phase CVD growth technique called enhanced direct injection pyrolytic synthesis (e-DIPS) method [3]. The e-DIPS method needs two kinds of hydrocarbons as carbon sources and we have reported [3] that the control of these carbon sources can tune the mean diameter of produced SWCNTs to any point in the range of ca. 1 nm to 2 nm. However, the effect of reaction temperatures on the quality and productivity of SWCNTs in the e-DIPS process has not been investigated yet.

In this study, we have investigated the reaction temperatures dependence in the properties of SWCNTs produced by e-DIPS method by using resonant Raman, optical absorption, and photoluminescence spectroscopies. Contrary to the case of ACCVD, it was found that decreasing the reaction temperature gradually increases the diameter of produced SWCNTs. This result suggests that the key factor for controlling the diameter in e-DIPS is not nucleation process of catalysts like in ACCVD, but supply of carbon precursor. Details of this dependence will be discussed in the presentation.

Reference

[1] B. Kitiyanan, W. E. Alvarez, J. H. Harwell, D. E. Resasco, *Chem. Phys. Lett.*, 317(2000)497.
[2] Y. Miyauchi, S. Chiashi, Y. Murakami, Y. Hayashida, and S. Maruyama, *Chem. Phys. Lett.*, 387(2004)198.
[3] T. Saito, S. Ohshima, T. Okazaki, S. Ohmori, M. Yumura and S. Iijima, *Journal of Nanoscience and Nanotechnology*, in press.

Corresponding Author: Takeshi Saito
E-mail: takeshi-saito@aist.go.jp
Tel / Fax: 029-861-4863 / 029-861-4413

Growth of Single-Wall Carbon Nanotube within the Pores of Meso -, and Micro-Porous Materials by Catalyst-Supported Chemical Vapor Deposition

○Keita Kobayashi[1], Ryo Kitaura[1], Yoko Kumai[3], Yasutomo Goto[3], Shinji Inagaki[3] and Hisanori Shinohara[1, 2]

[1]*Department of Chemistry, Nagoya University, Nagoya 464-8602, Japan*
[2]*Institute for Advanced Research, Nagoya University, Nagoya 464-8602, Japan*
[3]*Toyota Central R&D Labs., Inc., Nagakute, Aichi 480-1192, Japan*

Since the successful growth of single-wall carbon nanotubes (SWNTs) by catalyst-supported chemical vapor deposition (CCVD) using porous catalyst supporters such as mesoporous materials [1] and zeolite [2], the CCVD method has been extensively investigated due to its potential for a large-scale synthesis of SWNTs. In CCVD, preparation of size-controlled metal catalyst nanoparticles is essential to realize diameter-controlled growth of SWNTs. Hence, the diameter of SWNTs depends on the size of catalyst nanoparticles employed. Meso- and micro-porous materials, such as FSM-16 and zeolite, respectively, have ideal channels with a narrow size distribution. These provide suitable nanometer sized ordered space to prepare regulated nanometer sized metal catalyst nanoparticles. However, metal nanoparticles prepared using meso- and micro-porous materials usually possess a broad size distribution because of the formation of aggregates on the outer surface during CCVD processes. Therefore, it is important to reduce formation of metal aggregates on the surface of meso- and micro-porous materials for a diameter-controlled growth of SWNTs by CCVD.

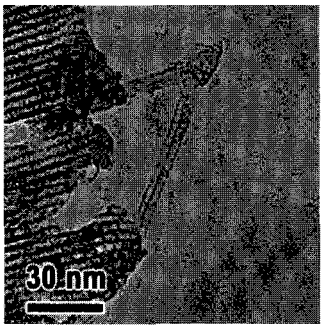

Figure TEM image of SWNTs SWNTs evolving from the channels of

In a previous study, we have reported synthesis of SWNTs by CCVD using size-ordered metal nanoparticles which are supported in channels of FSM-16 [3, 4] and surface-treated zeolites [5]. Here, we report the growth of diameter-controlled SWNTs by CCVD using size-controlled metal catalysts supported within pore of FSM-16 and zeolite, and discuss the pore size dependence of the diameter distributions of obtained SWNTs.

References: [1] P. Ramesh et al., *J. Phys. Chem. B*, **110**, 130 (2006).
[2] N. Kishi et al., *J. Phys. Chem. B*, **110**, 24816 (2006).
[3] K. Kobayashi et al., *Chem. Phys. Lett.*, **458**, 346 (2008).
[4] K. Kobayashi et al., *in preparation*.
[5] K. Kobayashi et al., *Abstract The 34th Fullerene-Nanotube General Symposium*, 162 (2008).

Corresponding Author: Hisanori Shinohara
E-mail: noris@nagoya-u.jp **Tel&Fax**: 052-789-3660 / 052-789-6442

Nucleation of an SWNT from a catalytic metal cluster inside a carbon nanotube

○Yoshifumi Izu, Junichiro Shiomi and Shigeo Maruyama

Department of Mechanical Engineering, The University of Tokyo
7-3-1 Hongo, Bunkyo-ku, Tokyo 113-8656, Japan

Molecular encapsulation in the hollow space of a carbon nanotube has attracted interests with various applications. Experiments have been reported on formation of DWNT from C_{60} fullerenes peapods [1] and ferrocene filled SWNT [2, 3]. The reports demonstrate that the growth mechanism of the inner tube depends on filler precursor.

In this work, we have performed MD simulations of the nucleation process of an SWNT from a catalytic metal cluster inside an SWNT template to gain understanding in the growth mechanism. The same potential models as in the previous work [4] were used. By supplying carbon atoms to a Ni cluster with dissolved carbon atoms placed inside a rigid carbon nanotube, the nucleation process of the inner SWNT was observed (Fig. 1). Simulations were performed for various metal-cluster sizes and outer tube diameters, which resulted in minor differences in the carbon density distribution function of the inner tube (Fig. 2). Additional simulations without van der Waals interaction between inner and outer nanotube resulted in slight decrease of the interlayer distance. The interlayer distances were clearly smaller than the equilibrium distance of carbon atoms. The results suggest that the interlayer distance is determined by the layered distance of metal intercalated graphite.

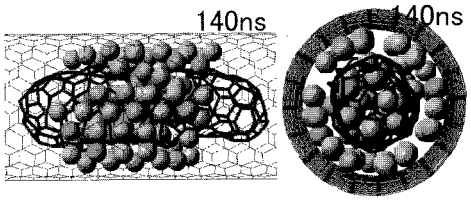

Fig. 1 Nucleation of the inner SWNT from a catalytic metal cluster inside carbon nanotube

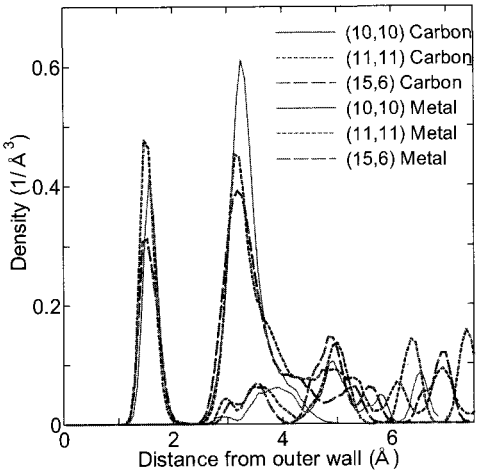

Fig. 2 Density distribution functions of carbon atoms in the inner tube and metal atoms

[1] S. Bandow, etal Phys. Chem. Lett., 337 (2001) 48.

[2] L. Guan, etal., Carbon., 43 (2005) 2780.

[3] H. Shiozawa, etal., Adv. Mater., 20 (2008) 1443.

[4] Y. Shibuta and S. Maruyama, Chem. Phys. Lett., 382 (2003) 381.

Corresponding author: Shigeo Maruyama E-mail: maruyama@photon.t.u-tokyo.ac.jp, Tel/Fax: +81-3-5800-6983

^{13}C NMR Study of C_{60}-Peapods

○Kazuyuki Matsuda[1], Yutaka Maniwa[1,3], and Hiromichi Kataura[2,3]

[1] *Faculty of Science, Tokyo Metropolitan University, 1-1 Minami-osawa, Hachioji, Tokyo 192-0397, Japan*
[2] *Nanotechnology Research Institute, National Institute of Advanced Industrial Science and Technology (AIST), Central 4, Higashi 1-1-1, Tsukuba, 305-8562, Japan*
[3] *CREST, Japan Science and Technology Corporation*

Single-walled carbon nanotubes (SWNTs) filled with fullerenes (e.g., C_{60}), so-called "peapods", have attracted considerable attention due to their peculiar electronic and structural properties. In particular, because the C_{60} linear arrays inside SWNTs with typical diameters of around 13.5 Å may be treated as an ideal one-dimensional (1D) crystal, a C_{60}-ordered structure should not be achieved at finite temperature.

In order to study rotational dynamics of C_{60} molecules composing 1D linear array inside SWNTs, we have performed ^{13}C NMR measurements in a temperature range from 4.2 to 300 K. The temperature dependence of the NMR line shape and spin-lattice relaxation time (T_1) indicate that the encapsulated C_{60} molecules exhibit a quasi-free-rotation with correlation times of 5–10 ps at 300 K. With decreasing temperature, the large amplitude molecular rotation continues to 30 K with an activation energy of 467 K. It is suggested that the C_{60} linear array does not undergo an orientational phase transition, which is associated with its 1D nature. Furthermore, no evidence for the polymerization of C_{60} molecules is found from the ^{13}C NMR line shape analysis.

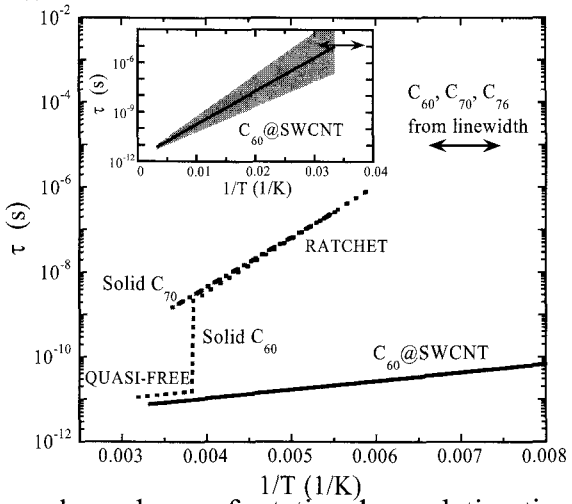

Fig.1. Temperature dependence of rotational correlation time for C_{60} encapsulated inside SWNTs. In the figure, values for quasi-free-rotational phase and ratchet phase in the C_{60} bulk crystals (dotted line) and for the ratchet phase below 280 K in the C_{70} bulk crystals (dash-dotted line) are also displayed for comparison.

[1] K. Matsuda, Y. Maniwa, and H. Kataura, Phys. Rev. B 77, 075421 (2008).

Corresponding Author: Kazuyuki Matsuda
E-mail: matsuda@phys.metro-u.ac.jp, TEL: +81-426-77-2498, FAX +81-426-77-2483

Phase transition of water inside SWCNTs

Haruka Kyakuno[1], Fuminori Mikami[1], Toshimi Imaizumi[1], ○Kazuyuki Matsuda[1], Takeshi Saito[2], Satoshi Ohshima[2], Motoo Yumura[2], Sumio Iijima[2], Yasumitsu Miyata[3], Hiromichi Kataura[3,4], and Yutaka Maniwa[1,4]

[1] *Faculty of Science, Tokyo Metropolitan University, 1-1 Minami-osawa, Hachioji, Tokyo 192-0397, Japan*
[2] *Research Center for Advanced Carbon Materials, National Institute of Advanced Industrial Science and Technology (AIST), Tsukuba 305-8565, Japan*
[3] *Nanotechnology Research Institute, National Institute of Advanced Industrial Science and Technology (AIST), Central 4, Higashi 1-1-1, Tsukuba, Ibaraki 305-8562, Japan*
[4] *JST, CREST, Kawaguchi, 332-0012, Japan*

In the macroscopic world, liquid water cannot enter the extremely narrow pores of hydrophobic materials. However, both computational and experimental investigations have shown that hydrophobic single-wall carbon nanotubes (SWCNTs) with diameters below 1.44 nm can encapsulate water even at ambient conditions. This water arranges in tubule structures so-called ice nanotubes (ice NTs) at low temperatures, and shows quite an unusual dependence of the melting (freezing) temperature T_m on the SWCNT–diameter (D) compared to the macroscopic water.[1] This fact strongly suggests the presence of a crossover from microscopic (atomic) to macroscopic water inside SWCNTs. Here, we report experimental observations of the crossover phenomena in SWCNTs. It is found that the crossover takes place around D_c = 1.4-1.5 nm and is essentially related to the changes in water from single to multi-shell structures formed inside SWCNTs.

[1] Y. Maniwa, H. Kataura, M. Abe, A. Udaka, S. Suzuki, Y. Achiba, H. Kira, K. Matsuda, H. Kadowaki, and Y. Okabe, Chem. Phys. Lett. **401**, 534-538 (2005).

Corresponding Author: Kazuyuki Matsuda
E-mail: matsuda@phys.metro-u.ac.jp, TEL: +81-426-77-2498, FAX +81-426-77-2483

3P-46

Molecular dynamics simulations for temperature dependence of molecular-linear-motor inside nanotube

Y. Ueno[1], H. Somada[1,2], K. Hirahara[2], Y. Nakayama[2], and S. Akita[1]
[1]*Department of Physics and Electronics, Osaka Prefecture University, 1-1 Gakuen-cho, Naka-ku, Sakai, Osaka 599-8531, Japan*
[2]*Department of Mechanical Engineering, Graduate School of Engineering, Osaka University, 2-1 Yamadaoka, Suita, Osaka 565-0871, Japan*

The phenomenon that a nano-capsule (NC) inside a carbon nanotube (CNT) moved along the outer CNT and was trapped at the end of the outer CNT has been observed under the transmission electron microscopy.[1] We have investigated the transfer phenomenon by using molecular dynamics (MD) simulation in terms of the end-cap effect on the NC trapping.

To investigate the NC size dependence, we examined two models with different size; one model is that an inner NC is (5, 5) with the length of 1.5 nm and free to move in an outer CNT with a chirality of (10, 10) and another model is that an inner NC and an outer CNT are (12, 0) and (22, 0), respectively. For both cases, one end of the outer CNT was fixed and another end was free, where we arranged fixed cap-NCs for both ends of the outer CNT as shown in Fig.1. We performed MD simulations to analyze the linear motor phenomena and the effect of the interlayer vdW interactions on the trapping phenomenon, where an empirical potential field of a Brenner-type potential and a Lennard-Jones type potential were used for an intra-nanotube interaction and an inter-nanotube vdW interaction, respectively.

To evaluate the vdW energy between the NC and the cap, the initial temperature and the NC velocity were set to be 1 K to eliminate thermal effects and 1 nm/ps, respectively. To investigate the trap and release phenomena, the temperatures were varied from 300 to 3000 K, where the NC was initially set at the trapped position and the released time was measured for each temperature. When the NC position is closer to the cap, the vdW energies for both models become minimum of 60 and 450 meV, respectively. This indicates that the NC is subjected to the vdW force between the NC and the cap. Thus, the NC should be trapped at the equilibrium position at low temperature. For both models, the temperature dependences of the escape time behave as the activation type as shown in Fig. 2 and the activation energies for the escape time are very close to the dip of the vdW energies for the equilibrium position of the NC. Thus, as mentioned above, this trap and release events of the NC originate from the vdW interaction between the NC and the cap.

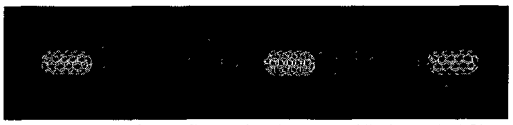

Fig. 1 Model for MD calculation; (5,5)-(10,10).

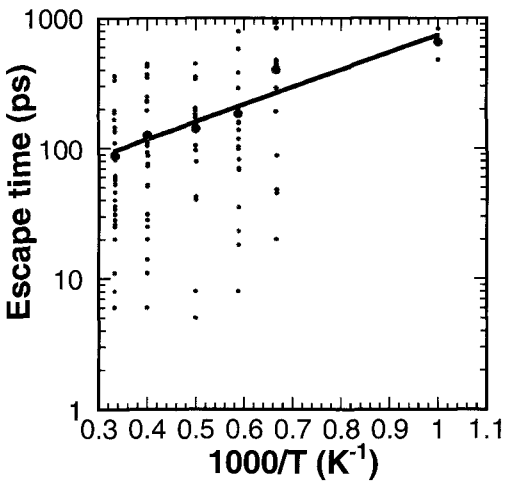

Fig. 2 Temperature dependence of escape time; (12,0)-(22, 0).

The escape time at the room temperature can be estimated to be 1.1 ms from the activation energy and the pre-factor for the time constant in the model of (12, 0)/(22, 0). This time constant is about 2 orders of magnitude smaller than the time constant observed in the experiment [1]. This discrepancy may come from the structural distortion at high temperature and the chirality dependence. Further study is needed to understand the discrepancy.

Reference [1] H. Somada, K. Hirahara, et al. submitted.

E-mail:akita@pe.osakafu-u.ac.jp
Tel&Fax:+81-72-254-9261

Synthesis, Characterization, and Magnetic properties of Europium-Nanowires Fully Encapsulated into Single Wall Carbon Nanotubes.

○ R. Nakanishi[1], R. Kitaura[1], T. Saito[2,3], T. Ohshima[2], H. Yoshikawa[1], K. Awaga[1] and H. Shinohara[1]

[1]*Department of Chemistry & Institute for Advanced Research, Nagoya University, Nagoya 464-8602, Japan*

[2]*Reseach Center for Advanced Carbon Materials, AIST, Tsukuba 305-8565, Japan*

[3]*PRESTO, Japan Science and Technology Agency, Kawaguchi 332-0012, Japan*

The chemically and thermally stable one-dimensional (1D) nano space of single-wall carbon nanotubes (SWCNTs) have narrow diameter (typically 1~2 nm), which can be used as a nano-sized reaction vessel to fabricate novel low-dimensional nanomaterials such as nanowires and nanoclusters. Fabrications of low-dimensional nanomaterials using SWCNTs are emerging on metal complexes, metal salts and molecules but still very few on metal nanowires, where we can expect interesting transport and magnetic properties arising from quantum effects. In this presentation, we have focused on a synthesis of metal nanowires using SWCNTs as a nano-sized reaction vessel.

Cap-opened SWCNTs and Eu were sealed in Pyrex glass under 10^{-4} Pa, and heated at 873 *K* for several days. After removing process of Eu atoms attached at outer surface of SWNTs, HRTEM observations were performed. Figure 1 shows a HRTEM image of Eu@SWCNTs. Structural analyses, which are based on simulated annealing calculations and HRTEM image simulations, have revealed that the structure of the Eu nanowire dose not correspond to 1D section of bulk bcc crystals but to that of hcp packing structure (Fig. 2). In this presentation, further structural analyses and magnetization behavior of Eu nanowires encapsulated in SWCNTs are discussed.

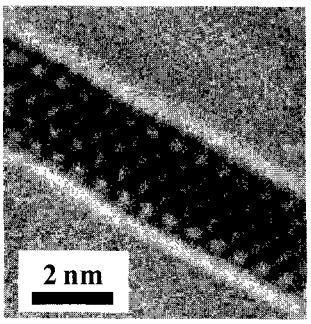

Figure. 1 HRTEM image of Eu@SWCNTs.

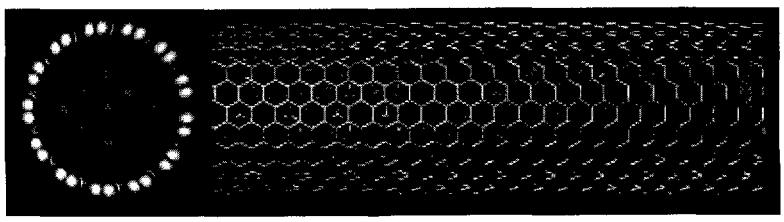

Figure. 2 Proposed structure model of Eu@SWCNTs: pink balls represents encapsulated Eu atoms.

Corresponding Author: Hisanori Shinohara

E-mail: noris@cc.nagoya-u.ac.jp

Tel: (+81) 52-789-2482, **Fax:** (+81) 52-747-6442

Encapsulation of Linear-Polyynes inside Thin Double-Wall Carbon Nanotubes

○Chen Zhao, Daisuke Nishide[1], Ryo Kitaura and Hisanori Shinohara

Department of Chemistry & Institute for Advanced Research, Nagoya University, Nagoya 464-8603, Japan

We have recently reported that various linear-polyyne molecules, $C_{2n}H_2$ (n=4-6), can be encapsulated inside single-wall carbon nanotubes (SWNTs) and that spectroscopic properties of the polyynes strongly depend on a diameter of SWNTs together with the length of polyynes[1].

In this work, we report that the polyyne molecules are well encapsulated inside double-wall carbon nanotubes (DWNTs). Since DWNTs used in this works possess narrow inner-diameter (d_{inner} = ~0.7 nm), the polyynes are preferentially encapsulated and strongly stabilized inside such DWNTs. Raman spectra of both $C_{10}H_2$@DWNTs and $C_{10}H_2$@SWNTs are shown in Fig. 1, which shows that vibrational frequency of $C_{10}H_2$ varies depending on the kind of carbon nanotubes, i.e., DWNTs and SWNTs. Moreover, by using high-resolution transmission electron microscopy (HRTEM), we have successfully observed polyyne molecules encapsulated inside DWNTs as shown in Fig. 2. This is the first direct TEM imaging of linear-polyynes molecules entrapped in DWNTs. In this presentation, further spectroscopic and structural analyses of the polyynes@DWNTs are discussed.

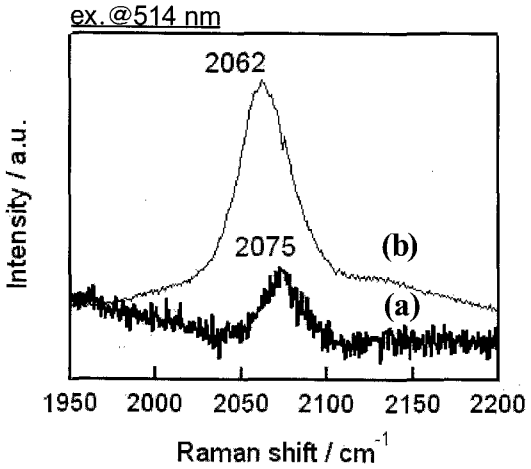

Fig. 1: Raman spectra of $C_{10}H_2$ inside DWNTs and SWNTs (a) $C_{10}H_2$@DWNT and (b) $C_{10}H_2$@SWNT

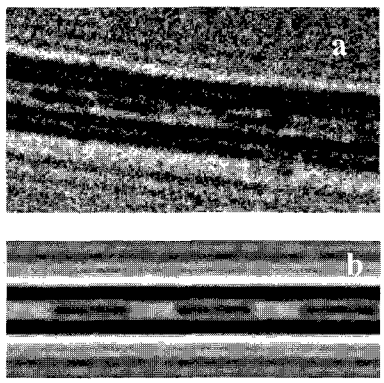

Fig. 2: HRTEM image of $C_{10}H_2$@DWNT: (a) observed and (b) simulated

References

[1] D. Nishide *et al.*, *J. Phys. Chem. C* **111** (2007) 5178.

1. Present Address: Nanotechnology Research Institute, AIST, Tsukuba, Ibaraki 305-8562, Japan

Corresponding Author: Hisanori Shinohara,

E-mail: noris@cc.nagoya-u.ac.jp

TEL: +81-52-789-2482, **FAX:** +81-52-747-6442

Fabrication and Characterization of Room Temperature Ionic Liquids inside SWNTs

Shimou Chen, Chen Zhao, Keita Kobayashi, Naoki Imazu, Ryo Kitaura, Hisanori Shinohara

Department of Chemistry and Institute for Advanced Research, Nagoya University,Nagoya, 464-8602, Japan

Room te mperature ionic liquids (ILs) have received m uch attention during the past decade due to its im portance in a broad range o f applications.[1] The m ain difference between ILs and s imple m olten s alts are that ILs a re co mposed of bulky, asym metrical ions that can only loosely fit together . Carbon nanotubes (CNT s) are a type of desirable m aterial to encapsulate variou s ty pes of m olecules and to form quasi-1D arrays. The ef fect of nanometer-sized confinem ent on m olecular pack ing, orientation, transl ational and rotational motions, and reactivity has been investigated by a number of researchers.[2]

What will happen when ILs is conf ined in the narrow hollo w interior of CNTs? In our past work, [3] we report the transition of ionic liquid [bm im][PF_6] from t he liqu id state to a high-melting-point crystal when confined in multi-wall carbon nanotubes. Here, we report the synthesis and characterization of single-wall CNTs (SWNTs) encapsulating some ionic liquid.

A zinc contained quaternary amm onium based ionic liquid [Me $_3NC_2H_4OH]^+[ZnCl_3]^-$ (named as $ChZnCl_3$ for simplicity) was chosen to achieve better reso lution for TEM imaging. We have found that the ionic liquid in SW NTs shows a tubular structure and that the tubular structure can be prolonged by a nnealing at h igh tem perature. The typical TEM images were shown in F igure 1, where ChZnCl $_3$ filled SW NTs is ref er to as Ch $ZnCl_3$@SWNTs. The Raman spectra of SWNTs and $ChZnCl_3$@SWNTs are presented in Figure 2.

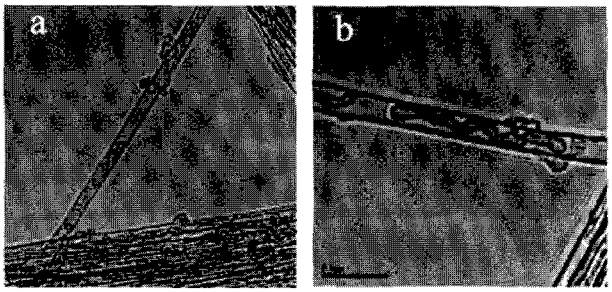

Figure 1. T ypical HR TEM i mage of C $hZnCl_3$@SWNTs (a) and $ChZnCl_3$@SWNTs hold at 300℃ for 6h (b)

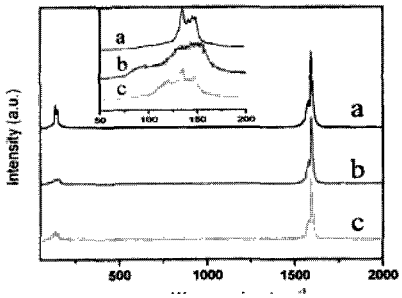

Figure 2. Ram an spect ra o f S WNTs (a); $ChZnCl_3$@SWNTs (b); and ChZnCl3@SWNTs hold at 300℃ fo r 6h (c)

References

(1) Welton, T. Chem. Rev.1999, 99, 2071.

(2) Khlobystov, A. N.; Britz, D. A., Briggs, G. A. D. Acc. Chem. Res. 2005, 38, 901.

(3) Chen, S.; Wu, G.; Sha, M.; Huang, S. J. Am. Chem. Soc. 2007, 129, 2416

Corresponding Author: Hisanori Shinohara

E-mail: noris@nagoya-u.jp

Tel: +81-52-789-2482

Anomalous Transfer Characteristics of Graphene Field-Effect Transistors with Co Contacts

○Ryo Nouchi[1], Masashi Shiraishi[2,3] and Yoshishige Suzuki[2]

[1]*WPI-Advanced Institute for Materials Research, Tohoku University, Sendai 980-8577, Japan*
[2]*Division of Materials Physics, Graduate School of Engineering Science, Osaka University, Machikaneyama-cho 1-3, Toyonaka 560-8531, Japan*
[3]*PRESTO, JST, 4-1-8 Honcho, Kawaguchi 332-0012, Saitama, Japan*

Graphene, one-atomic carbon sheet with a honeycomb structure, have been attracting incredible attention for its unique physical properties such as a massless Dirac fermion system [1]. This material shows an extraordinary high carrier mobility of higher than 200,000 $cm^2 V^{-1} s^{-1}$ [2], and is considered to be a major candidate for a future high-speed transistor material. In addition, graphene has shown its ability to transport charge carriers with spin conservation even at room temperature [3-5], and is regarded as a pivotal material in the emerging field of molecular spintronics. In this presentation, we report on the effect of metal contacts to transfer (I_D-V_G) characteristics of graphene field-effect transistors (FETs).

Graphene layers were formed onto a highly-doped Si substrate with a 300-nm-thick thermal oxide layer on top of it by a conventional mechanical exfoliation. The starting graphite crystal was Super Graphite® (Kaneka) [6]. Metal electrodes were fabricated onto the graphene layers by lithographic techniques.

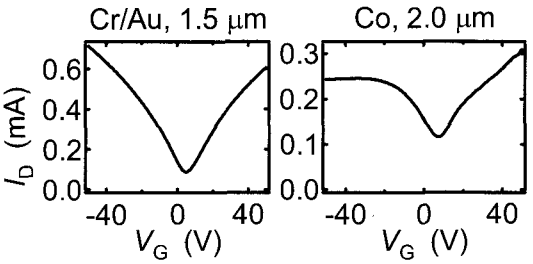

Right figure shows two-terminal transfer characteristics of graphene FETs with Cr/Au and Co contacts with channel lengths of 1.5 and 2.0 μm, respectively. Cr/Au is an ordinary metallic material for electronic devices, and Co is a popular material for spin-electronic devices as a source of a spin-polarized current. Although the graphene FET with Cr/Au contacts shows conventional transfer characteristics widely reported before, one with Co contacts displays anomalous distorted characteristics. The distortion was disappeared when the channel length became longer than roughly 3 μm, indicating that it is a contact-induced effect. Possible mechanism will be discussed based on a contact-induced band alteration of the graphene channel [7].

[1] A. K. Geim and K. S. Novoselov, Nature Mater. **6**, 183 (2007).
[2] K. I. Bolotin, K. J. Sikes, Z. Jiang, G. Fundenberg, J. Hone, P. Kim and H. L. Stormer, Solid State Commun. **146**, 351 (2008).
[3] M. Ohishi, M. Shiraishi, R. Nouchi, T. Nozaki, T. Shinjo and Y. Suzuki, Jpn. J. Appl. Phys. **46**, L605 (2007).
[4] N. Tombros, C. Jozsa, M. Popinciuc, H. T. Jonkman and B. J. van Wees, Nature (London) **448**, 571 (2007).
[5] S. Cho, Y.-F. Chen and M. S. Fuhrer, Appl. Phys. Lett. **91**, 123105 (2007).
[6] M. Murakami, N. Nishiki, K. Nakamura, J. Ehara, H. Okada, T. Kouzaki, K. Watanabe, T. Hoshi, and S. Yoshimura, Carbon **30**, 255 (1992).
[7] G. Giovannetti, P. A. Khomyakov, G. Brocks, V. M. Karpan, J. van den Brink, and P. J. Kelly, Phys. Rev. Lett. **101**, 026803 (2008).

Corresponding Author: Ryo Nouchi
TEL: +81-22-795-6468, FAX: +81-22-795-6470, E-mail: nouchi@sspns.phys.tohoku.ac.jp

発表索引
Author Index

Author Index

~A~

Achiba, Yohji 3S-1,2P-39,2P-40,3P-39
Adachi, Kazuma 3-8
Ago, Hiroki 1P-43,2P-20
Akachi, Masahiro 2P-5
Akachi, Takao 1P-48
Akaike, Kouki 1-14
Akasaka, Takeshi 1-3,2-1,3-13,1P-7,1P-8, 1P-9,1P-10,2P-6,2P-7, 2P-8,2P-9,3P-9,3P-15
Akita, Seiji 2P-25,3P-46
Akiya, Masahiro 2P-29
Ando, H. 1P-25
Ando, Tsuneya 2P-23
Aoki, Yuusuke 1P-6
Aono, Takayuki 1P-5,3P-5
Aonuma, Shuji 1P-19
Aoyagi, Shinobu 3P-5
Aoyagi, Y. 3S-2
Araki, Yoshiaki 2P-25
Asada, Yuki 1P-27,2P-22,2P-27
Asaka, Kouji 1P-52,2-33
Asano, Takeshi 2-5
Awaga, K. 3-7,3P-47
Awano, Yuji 3-2,2P-42,3P-36
Ayumi, Sato 2P-8

~B~

Bandow, Shunji 3-6,1P-50
Beu, T.A. 2-8
Briggs, G. Andrew D. 1P-5,1P-48

~C~

Chaikittisilp, Watcharop 3-1
Chen, Shimou 3P-49
Chen, Zhongfang 3P-32
Chiashi, Shohei 1-7
Chiu, Chien-Chao 2P-27
Craciun, M. F. 3P-23

~D~

Davis, Robert C. 2-6
Dresselhaus, G. 1-8
Dresselhaus, M.S. 1-8

~E~

Edamatsu, Tohru 3P-6
Effendi, Mukhtar 3-3,2P-26
Einarsson, Erik 2-10,1P-30,3P-18
Endo, Morinobu 1S-1

~F~

Fan, Jing 2P-52
Farhat, H. 1-8
Fujigaya, Tsuyohiko 1-2,2P-32,3P-27
Fujii, Shunjiro 1P-36,2-4,2P-37
Fujimura, Youhei 2P-44,3P-25
Fujita, Takeshi 3P-3
Fujiwara, Akihiko 1P-11,1P-35,
Fukuda, Hitoshi 3P-7
Fukui, Nobuyuki 1P-44
Fukumaru, Takahiro 3P-27
Furuichi, Koji 1P-32
Furukawa, Takeo 1-13
Futaba, Don N. 2-6,1P-47
Futami, Yoshisuke 2P-19

~G~

Ganin, A. Y. 3P-14
Gao, Xingfa 3P-32
Ge, Ling 1P-48
Ghorannevis, Z. 3P-33
Gilmore, Adam M. 1P-21
Goto, H. 3S-2
Goto, Yasutomo 3P-42
Grote, James G. 1P-38
Guerrero, Jason M. 2-2
Guldi, Dirk M. 2P-3

~H~

Hachiya, Makoto 1P-9
Hachiya, Shinji 1P-17
Hamada, Yoshinobu 1P-51
Harano, Koji 1-12
Harneit, Wolfgang 3P-6
Haruyama, J. 3-4,1P-23,1P-24
Hasegawa, Jun 3P-7
Hasegawa, Kei 2-12

Hasegawa, Masayuki 2P-24
Hasegawa, Tadashi 2P-9
Hashiguchi, Masahiko 3P-1
Hashiguchi, Shinji 3P-26
Hashimoto, Akara 2P-31
Hashizume, Tomihiro 1P-44
Hata, Kenji 2-6,1P-47
Hatakeyama, R. 1-9,2P-43,2P-47,3P-17, 3P-33
Hayamizu, Yuhei 2-6
Hayashi, T. 1S-1
Heguri, Satoshi 1P-20,3P-10
Hirahara, Kaori 1-1,3P-46
Hirano, Ken 1P-37
Hirata, Takamichi 2P-29
Hirori, Hideki 1-6
Hirose, M. 1P-26
Hirotsu, Takahiro 1P-37
Hiura, Hidefumi 3-11
Homma, Yoshikazu 1-7,2-3
Horiguchi, Hirokazu 2P-30
Hou, Peng-Xiang 2-9

～I～

Ichida, M. 1P-25
Iijima, Sumio 1-4,3-6,1P-39,1P-47,1P-50, 2P-45,2P-50,2P-51,2P-52, 3P-31,3P-41,3P-45
Iio, Yasunari 1P-17
Iitsuka, Toshie 2P-37
Iizuka, Masatomo 2P-42
Ikeda, Ken-ichi 1P-43,2P-20
Ikenaga, Eiji 3-2
Ikuta, Tatsuya 1P-43
Imahori, Hiroshi 1-10
Imai, Katsuaki 2-9
Imai, Kumiko 3P-11
Imaizumi, Toshimi 3P-45
Imamoto, Kenta 2-11
Imazu, Naoki 1P44,1P-49,2P-48,3P-49
Inada, Koji 2P-9
Inagaki, Shinji 3P-42
Inami, N. 1P-35
Inoue, Akihito 2P-39
Irie, Michiko 2P-52
Ishigami, Naoki 1P-43
Ishiguro, Masafumi 1-7
Ishii, Satoshi 3P-21
Ishii, Tadahiro 2P-35,3P-20,3P-34
Ishikawa, Kei 2P-17
Ishimaru, Kentaro 2P-42
Ishitsuka, Midori O. 3-13,1P-7,1P-8,1P-9, 1P-10,2P-6,2P-9,3P-9
Ishiyama, Yuichi 1P-2
Ishizuka, Daisuke 2P-34
Isobe, Hiroyuki 1-12
Itami, Kenichiro 3P-4
Ito, T. 2-8
Ito, Tsuyoshi 2-1,2P-6
Ito, Yasuhiro 1P-5,1P-6,1P-48,1P-49, 2P-5
Itoh, S. 2P-44,2P-49,3P-25
Iwai, Y. 1P-26
Iwasa, Y. 3P-23
Iwasa, Yoshihiro 2-5,3P-14
Iwasaki, Takayuki 2P-42
Iwata, Nobuyuki 1P-17,2P-34,3P-35
Izard, Nicolas 1P-33
Izu, Yoshifumi 3P-43
Izumi, Noriko 1P-5,2P-5
Izumi, Y. 2P-49

～J～

J. T., Ye 3P-23
Jeyadevan, Balachandran 3P-26
Jianxun, Xu 3P-31
Jin, Hehua 2-4
Joung, Soon-Kil 3-6

～K～

Kai, Toshihiro 1P-12,2P-10
Kaji, Yumiko 1P-11
Kako, Masahiro 1P-10
Kambe, Takashi 3P-11
Kaminosono, Yoshiya 3P-34
Kamizono, Yuya 2P-27
Kanada, Ryo 2P-25
Kanai, Kaname 1-14
Kanda, A. 3S-2
Kaneko, Toshiro 1-9,2P-43,3P-33
Kanemitsu, Yoshihiko 1-6

Kang, Dongchul 1P-31
Kasai, Takao 3P-26
Kasama, Yasuhiko 1-13,2P-14
Katabuchi, Tatsuya 3P-7
Kataura, Hiromichi 2-4,2-5,1P-25,1P-36,1P-42, 2P-37,3P-22,3P-38,3P-44, 3P-45
Kato, Keisuke 1P-14,1P-15
Kato, Koichiro 2P-21
Kato, Ryoei 2P-15
Kato, Tatsuhisa 3-13,2P-9,3P-6
Kato, Toshiaki 2P-43,2P-47,3P-17,3P-33
Kawabata, Akio 3P-36
Kawai, Chihiro 1P-34
Kawai, Takazumi 3-11,2P-52
Kawarada, Hiroshi 2P-42
Kawasaki, Naoko 1P-11,3P-11
Kawasaki, S. 1P-26
Kawashima, Jun-ichi 1P-3,1P-4
Kazaoui, Said 1P-33,2P-19
Kertesz, Miklos 1P-28
Kikitsu, Tomoka 2P-38
Kikuchi, Takashi 2-1
Kim, Jung Jin 3-2
Kim, Sang Nyon 1P-38
Kim, Y.A. 1S-1
Kimata, Nozomu 1P-20,3P-10
Kimura, Fumitaka 1P-52
Kimura, S. 2-8
Kimura, Takahide 1P-19,1P-40
Kishi, Naoki 3-6,2P-45
Kishimoto, Shigeru 1S-2
Kitaura, Ryo 3-7,1P-27,1P-49,2P-5, 2P-27,3P-5,3P-42,3P-47, 3P-48,3P-49
Kobata, Masaaki 3-2
Kobayashi, Emiko 1P-18
Kobayashi, Keisuke 3-2
Kobayashi, Keita 1P-44,1P-49,3P-42,3P-49
Kobayashi, Mototada 1P-20,3P-10
Kodama, Takeshi 2P-39
Koga, Kenichiro 3-5,1P-51
Kohno, Hideo 2-3
Koike, Kanako 2P-29
Kojima, Eiji 3-3
Kokai, Fumio 3-8,1P-52
Komatsu, Koichi 3P-15
Komatsu, Naoki 1P-19,1P-40
Komatsu, Naoya 1-3
Kondo, Daiyu 3-2,3P-36
Kondo, Mariko 3P-30
Kondo, Yukie 1P-41
Kong, J. 1-8
Koretsune, Takashi 3-4,1P-23,3P-24
Koshino, Masanori 1-12
Koshio, Akira 3－8
Koyama, S. 1S-1
Kubozono, Yoshihiro 2-7,1P-11,3P-11
Kuga, Hidenori 2-1,1P-8
Kumai, Yoko 3P-42
Kumashiro, Ryotaro 1-3
Kumekawa, Katsumi 1P-19
Kurihara, Hiroki 1P-7
Kurihara, Kouhei 1P-16
Kuroda, Noritaka 2P-26
Kuroda, Shunsuke 2P-43
Kuroda, Takayoshi 3P-8
Kuroki, Nozomi 3P-30
Kusano, Yoshikazu 2P-33
Kusunoki, Michiko 1P-34
Kuwahara, Shota 1-5,1P-44,2P-22,2P-27
Kuwano, Jun 2P-38
Kyakuno, Haruka 3P-45
Kyotani, Takashi 2-9

～L～

Li, Chang-Zhi 3-12
Li, Yongfeng 1-9
Liu, Huaping 1-7
Lu, Xing 3P-9

～M～

Maeda, Yutaka 1-3,3-13,2P-9,3P-9
Maki, Norio. 1P-41
Makino, Miyabi 1P-18
Maniwa, Yutaka 3P-22,3P-38,3P-44,3P-45
Martinez-Alonso, Amelia 2-9
Maruyama, Hiroyuki 1-1

Maruyama, Shigeo 2-10,3-1,1P-30,1P-45, 1P-46,2P-17,3P-18,3P-19, 3P-28,3P-37,3P-43
Maruyama, Takahiro 2P-36
Maruyama, Yusei 1P-50
Mashino, Tadahiko 2P-1
Matano, Yoshihiro 1-10
Matsuda, Kazunari 1-6
Matsuda, Kazuyuki 3P-44,3P-45
Matsudaira, M. 1P-23
Matsumura, Sachiko 2P-50
Matsuo, Keiko 2P-3
Matsuo, Yutaka 3-12,2P-2,2P-3,2P-4,3P-1, 3P-3
Matsuura, Tsugio 1P-41
Matsuyama, Humihiko 1P-16
Mikami, Fuminori 3P-45
Mikami, Masuhiro 3-9
Minakata, Satoshi 1P-1
Minami, Nobutsugu 3-3,1P-33,2P-19,2P-28
Minowa, Mari 1P-10
Miura, K. 2P-44,2P-49,3P-25
Miyako, Eijiro 1P-37
Miyamoto, Yoshiyuki 3-11,1P-22
Miyata, Yasumitsu 2-4,2-5,1P-25,1P-36,1P-42, 3P-22,3P-38,3P-45
Miyauchi, Yuhei 1-6,3-1,1P-30,3P-18
Miyawaki, Jin 2P-52
Miyazaki, H. 3S-2
Miyazaki, Koji 2P-17
Miyazaki, Takafumi 1P-6
Miyazawa, Kun'ichi 1-15,1P-13,2P-11,2P-15, 3P-6
Mizobuchi, Yuzo 1-13,2P-14
Mizokami, Kazuaki 1-13
Mizorogi, Naomi 2-1,3-13,1P-7,1P-8,1P-9, 2P-6,2P-9,3P-9
Mizuno, Kohei 2-6
Mizuno, Seigi 2P-20
Mizusawa, Takashi 3P-39
Mizutani, Takashi 1S-2
Mohamed, Mohd Ambri 1P-35
Mori, Susumu 3P-4
Morimoto, Tatsuro 1-2
Morimoto, Yasuo 1P-18
Morin, Jean-Francois 2-2
Morino, Shizuka 1P-19
Morioki, Masakatsu 2P-44,3P-25
Morishita, Tetsuya 3-9
Morita, Yoichi 1P-19
Moriyama, Hiroshi 3P-29,3P-30
Morton, John J. L. 1P-5
Moteki, Takahiko 3-1
Motomiya, Kenichi 3P-26
Mukainakano, Shinichi 1P-46
Murakami, Tomo 3P-36
Murakami, Yoichi 2-10,3-1,1P-30,3P-18
Muramatu, H. 1S-1
Murata, N. 3-4,1P-23
Murata, Yasujiro 3P-15
Murpurgo, A. F. 3P-23

～N～

Nagamachi, Toshiki 1P-1
Nagasawa, H. 2P-40
Nagase, Shigeru 2-1,3-13,1P-7,1P-8,1P-9, 2P-6,2P-9,3P-9,3P-32
Nagata, Hideya 1P-37
Naik, Rajesh R. 1P-38
Naitoh, Yasuhisa 2-4
Nakahara, Hitoshi 1P-52
Nakamura, Eiichi 1P-12,3-12,2P-2,2P-3, 2P-4,3P-1,3P-3,
Nakamura, J. 1P-23
Nakamura, Shigeo 2P-1
Nakamura, Yuki 1-12
Nakanishi, R. 3-7,3P-47
Nakanishi, Takeshi 3-6,2P-23,2P-45
Nakashima, Naotoshi 1-2,2P-32,3P-27
Nakayama, Takashi 2P-39
Nakayama, Yoshikazu 1-1,2P-25,3P-46
Nambo, Masakazu 3P-4
Naritsuka, Shigeya 2P-36
Nihei, Mizuhisa 3-2,2P-42,3P-36
Niidome, Yasuro 1-2
Niimi, Yoshiko 1-12
Niinomi, Takaaki 3P-1
Nikawa, Hidefumi 2-1,3-13,1P-8,2P-6,3P-9, 3P-15
Nishi, Tetsushi 1P-43
Nishi, Toshio 1-14

Nishibori, Eiji 3P-5,3P-15
Nishidate, Kazume 2P-24
Nishide, Daisuke 1P-36,1P-42,3P-48
Nishihara, Hirotomo 2-9
Nishii, Toshiaki 1P-12,2P-10,2P-12
Nishimura, Toshiyuki 2P-15
Nishio, Kengo 3-9
Nishizawa, Chiho 2P-1
Noda, Suguru 2-12,3-1,1P-32,2P-41
Nokariya, Ryo 1P-17
Norimatsu, Wataru 1P-34
Nouchi, Ryo 3-10,3P-50
Nozaki, T. 3-10
Nozawa, K. 1P-24
Nozue, Tatsuhiro 3P-36
Nudejima, Shin-ichi 2P-11
Numata, Youhei 1P-3,1P-4
～O～
Odaka, S. 3S-2
Ogami, Akira 1P-18
Ogata, Hironori 3P-12,3P-40
Ogata, Teruhiko 2P-16,3P-16
Oguri, Yoshiyuki 3P-7
Ohishi, M. 3-10
Ohmori, Shigekazu 1-4
Ohnishi, Y. 2P-40
Ohno, K. 2-8
Ohno, Takahisa 1-11
Ohno, Yutaka 1S-2
Ohshima, Satoshi 3P-45
Ohshima, Yoshihisa 2P-13
Ohta, Yohei 2-7,3P-11
Oizumi, Haruna 1-13,1P-14,2P-14
Okabe, Hiroto 3P-37
Okada, Susumu 1-11,3-6,3-11,2P-18,2P-45
Okamoto, Minoru 2P-32
Okawa, Jun 2-10,3P-28
Okawa, T. 2P-49
Okazaki, Toshiya 3-6,2P-5,2P-45,3P-41
Oke, Shinichiro 2P-44,2P-49,3P-25
Okeyui, Kenji 1P-46
Okimoto, Haruya 2-5,1P-5,1P-6,1P-48,1P49
Okubo, Shingo 2P-45
Okubo, Tatsuya 3-1
Okuda-Shimazaki, Junko 2P-11
Omote, Kenji 1-13,1P-14,1P-15,2P-14
Ono, Shoichi 1-13,2P-14
Onoe, Jun 1P-12,2P-10
Oohara, Wataru 2P-47,3P-17
Oonami, Hideyuki 3P-12
Ootuka, Y. 3S-2
Orinouchi, Yuki 2P-31
Osada, Ryouichi 3P-6
Osgood, Andrew J. 2-2
Oshima, Hisayoshi 1P-45,1P-46
Osuka, Atsuhiro 1P-40
Ouchi, Yukio 1-14
Ounchen, Fahima 1P-38
Oyama, Hiromi 2P-4
Ozaki, Taisuke 3-9
～P～
Paredes, Juan I. 2-9
Peng, Xiaobin 1P-40
Porfyrakis, Kyriakos 1P-48
Prassides, Kosmas 3P-14
～R～
Rao, A. M. 3-4,1P-23
Reppert, J. 3-4,1P-23
Rosseinsky, Matthew J. 2S-1,3P-14
Rotkin, Slava V. 3P-18
Ryuzaki, Sou 2-8,1P-12,2P-10
～S～
Sagami, Hiroyuki 1-13,2P14
Saida, Morihiko 1-13,1P-14,1P-15,2P-14
Saito, Morihiro 2P-38
Saito, R. 1-8
Saito, S. 1P-25
Saito, Susumu 3-4,1P-23,1P-29,2P-21, 2P-46,3P-13,3P-24
Saito, Takeshi 1-4,3-7,1P-39,1P-49,3P-41, 3P-45,3P-47
Saito, Yahachi 1P-52,2P-33
Sakahara, Satoshi 2P-29
Sakai, Ayumu 3P-20
Sakai, Keijiro 2P-34

Sakai, Takafumi 2P-29
Sakata, Makoto 3P-5
Sakurai, Masahiro 1P-29
Sano, Masahito 2P-30,2P-31
Saraswati, Teguh Endah 2P-48
Sasaki, Isao 2P-28
Sasaki, K. 1-8
Sasaki, Takashi 2-2
Sathish, M. 1-15
Sato, Kuninori 2P-36
Sato, Naoki 1-14
Sato, Satoru 2P-9
Sato, Shigeo 2P-50
Sato, Shintaro 3-2,2P-42,3P-36
Sato, Shun 2P-25
Sato, T. 3S-2
Sato, Yoshiharu 3P-1
Sato, Yoshinori 3P-26
Sawa, Hiroshi 3P-5,3P-15
Scheloske, Michael 3P-6
Seki, Kazuhiko 1-14
Senga, Ryosuke 1-1
Senna, Mamoru 1P-2
Shiba, Kiyotaka 2P-50
Shibi, Yutaka 2P-16
Shikoh, E. 1P-35
Shimazu, Tomohiro 1P-45
Shimazu, Tomoyuki 3-8
Shimizu, Tetsuhiro 1P24,2P-47
Shimotani, H. 3P-23
Shimura, Masashi 1P-14,1P,15
Shinjo, T. 3-10
Shinohara, Hisanori 1-5,3-7,1P-5,1P-6,1P-24, 1P-27,1P-44,1P-48,1P-49, 2P-5,2P-22,2P-27,2P-48, 3P-5,3P-42,3P-47,3P-48, 3P-49
Shinohara, Yuichiro 2P-44,3P-25
Shiomi, Junichiro 2P-17,3P-19,3P-28,3P-43
Shirai, Yasuhiro 2-2
Shiraishi, Masashi 3-10,3P-50
Shiraiwa, Tomoyuki 2P-36
Shiratori, Yosuke 1P-32
Shishido, J. 3-P17
Shoda, Masayuki 1P-50
Shoji, Mao 3P-40
Shukla, Bikau 1-4,1P-39,3P-41
Singh, Kristi M. 1P-38
Slanina, Zdenek 3-13,1P-8,2P-6,2P-9,3P-9
Somada, H. 3P-46
Sonomura, Takuya 3P-35
Suda, Yoshiyuki 2P-44,2P-49,3P-25
Suga, Hiroshi 2-4
Sugai, Toshiki 1-5,1P-24,1P-27,1P-44, 2P-5,2P-22,2P-27,3P-30
Sugime, Hisashi 1P-32,2P-41
Sumii, Ryohei 1P-6
Sumiya, Hitoshi 2S-2
Suzuki, Shinzo 2P-40,3P-39
Suzuki, Yasushi 2P-31
Suzuki, Yoshinobu 1P-45
Suzuki, Yoshishige 3-10,3P-50

～T～

Tachibana, Masaru 1P-13,1P-31
Tadokoro, Toshiyasu 2P-14
Tajima, Isamu 2P-35
Tajima, Yusuke 1P-3,1P-4
Takabayashi, Y. 3P-14
Takagi, H. 3P-14
Takagi, Yoshiteru 1-11
Takahashi, Koji 1P-43
Takahashi, Kyoko 2P-1
Takahashi, Yutaka 3-8
Takaiwa, Daisuke 3-5
Takamizu, N. 2P-40
Takano, T. 3P-14
Takano, Yoshihiko 3P-21
Takano, Yuta 3-13
Takashima, Akito 1P-12
Takeda, Seiji 2-3
Takenobu, Taishi 2-5
Takeshita, N. 3P-14
Takeuchi, K. 1S-1
Takeuchi, Tsuneharu 2P-38
Takeyama, Shojiro 3-3
Takikawa, Hirofumi 2P-44,2P-49,3P-25
Takimoto, Tatsuya 1P-19

Tanaka, Hideki 3-5,1P-51
Tanaka, Izumi 2P-20
Tanaka, Masaki 3P-5
Tanaka, S. 3S-2
Tanaka, Saburo 2P-17
Tanaka, Takatsugu 1-12
Tanaka, Takeshi 2-4,1-12,2-4,1P-36,1P-42
Tanigaki, Katsumi 1-3,3P-15
Taniguchi, Akiyoshi 2P-11
Tascon, Juan M. D. 2-9
Tatamitani, Yoshio 2P-16,3P-16
Tezuka, Noriyasu 1-10
Toda, Y. 2-8
Tohji, Kazuyuki 3P-17,3P-26
Toita, Sho 1P-13
Toki, Makoto 3P-15
Tokumoto, Youji 1P-6
Tokura, Y. 3P-14
Tomida, Akihiro 2P-50
Tour, James M. 2-2
Tsuchiya, Takahiro 3-13,1P-7,1P-8,1P-9, 1P-10,2P-62P-7,2P-8,2P-9, 3P-9
Tsuda, Shunsuke 3P-21
Tsuji, Masaharu 1P-43,2P-20
Tsuji, Yoshiko 1P-32
Tsukagoshi, Kazuhito 3S-2
Tsuruo, Takashi 2P-50
Tsuruoka, Ryouji 1P-1,2P-39
Tsuruoka, Yasuhiro 2P-39
Tsutsui, Chihiro 2P-29
Tsutsumi, Jun'ya 1-14

～U～

Uchida, Katsumi 2P-34,2P-35,3P-20,3P-34
Uchiyama, Tetsuya 2-3
Ueda, Kazuyuki 2P-27
Ueno, Y. 3P-46
Umeyama, Tomokazu 1-10
Urata, K. 2P-40
Uruno, H. 2P-49

～W～

Wakabayashi, Tomonari 3P-8
Wakabayashi, Yusuke 3P-15
Wakahara, T. 1-15
Wakahara, Takatsugu 3-13,3P-6
Wang, Qiguan 3P-29
Wang, Weiwei 3P-2
Wang, Zheng-ming 2P-15
Warner, Jamie H. 1P-5,1P-48
Watanabe, Hiroto 1P-2
Watanabe, Satoshi 3P-7
Watanabe, Tohru 3P-21
Watanabe, Yasuyuki 2P-31
Watt, Andrew A. R. 1P-48

～X～

Xiang, Rong 2-10

～Y～

Yagi, Y. 1P-23
Yajima, Hirofumi 2P-34,2P-35,3P-20,3P-34
Yamada, Michio 1P-10,2P-9
Yamada, Takeo 2-6
Yamada, Tomoya 2-1
Yamada, Michio 1P-10
Yamagami, Yuichiro 2P-46
Yamagiwa, Kiyofumi 2P-38
Yamaguchi, Takahide 3P-21
Yamaguchi, Yoshihiro 2P-38
Yamamoto, Hiroshi 1P-16,1P-17,2P-34,3P-35
Yamamoto, Kazuhiro 1P-18
Yamamoto, M. 2P-49
Yamamoto, Shigehiko 1P-14
Yamamoto, Yohei 3P-37
Yamanaka, Hiroshi 1P-19
Yamanari, Yusuke 3P-11
Yamashita, Shunsuke 2P-38
Yamaura, Tatsuo 2P-44,2P-49,3P-25
Yamazaki, Yuko 1P-7,1P-9
Yanagi, Kazuhiro 2-5,1P-36,2P-37,3P-22, 3P-38
Yanaka, Takatsugu 2P-29
Yasuda, Satoshi 1P-47
Yokoi, Hiroyuki 3-3,2P-26
Yokoi, Kazuma 2P-39
Yokoo, Kuniyoshi 1-13,1P-14,1P-15,2P-14
Yokoo, Sachiko 2P-1
Yokosawa, Yuya 2P-7

Yokota, Masashi 2P-44,3P-25
Yokoyama, Atsuro 3P-26
Yokoyama, Daisuke 2P-42
Yomogida, Akinori 3-13
Yoshida, Hideto 2-3
Yoshida, Hiromichi 1P-44
Yoshida, Hiroyuki 1-14
Yoshihara, Naoki 2-11
Yoshikawa, H. 3-7,3P-47
Yoshimura, Masamichi 2P-27
Yudasaka, Masako 2P-50,2P-51,2P-52,3P-31
Yuge, Ryota 2P-52
Yumura, M. 1P-39
Yumura, Motoo 1-4,2-6,1P-47,3P-41,3P-45
Yumura, Takashi 1P-28
～Z～
Zaka, Mujtaba 1P-5,1P-48
Zdenek, Slanina 2-1
Zhang, Xiaoyong 2P-2
Zhang, Zhengyi 2-10,1P-30
Zhao, Chen 3P-48,3P-49
Zhao, Xiang 3P-2
Zhao, Yuming 2-2
Zheng, Ming 3P-18

複写される方へ

フラーレン・ナノチューブ学会は、有限責任中間法人　学術著作権協会（学著協）に複写に関する権利委託をしていますので、本誌に掲載された著作物を複写したい方は、学著協より許諾を受けて複写して下さい。

但し、社団法人日本複写権センター（学著協より複写に関する権利を再委託）と包括複写許諾契約を締結されている企業の社員による社内利用目的の複写はその必要はありません。（※社外頒布用の複写は許諾が必要です。）

権利委託先：有限会社中間法人　学術著作権協会
〒107-0052　東京都港区赤坂 9-6-41　乃木坂ビル 3 階
電話：03-3475-5618　　FAX：03-3475-5619　　E-Mail：info@jaacc.jp

注意：複写以外の許諾（著作物転載・翻訳等）は、学著会では扱っていませんので、直接、フラーレン・ナノチューブ学会へご連絡下さい。

Notice for Photocopying

If you wish to photocopy any work of this publication, you have to get permission from the following organization to which licensing of copyright clearance is delegated by the copyright owner.

＜All users except those in USA＞
Japan Academic Association for Copyright Clearance, Inc. (JAACC)
6-41 Akasaka 9-chome, Minato-ku, Tokyo 107-0052 Japan
TEL：81-3-3475-5618
FAX：81-3-3475-5619　　E-Mail：info@jaacc.jp

＜Users e in USA＞
Copyright Clearance Center, Inc.
222 Rosewood Drive, Danvers, MA 01923 USA
Phone：1-978-750-8400　　FAX：1-978-646-8600

2008 年 8 月 27 日発行

第３５回記念フラーレン・ナノチューブ総合シンポジウム
講演要旨集

＜フラーレン・ナノチューブ学会＞
〒464-8602　愛知県名古屋市千種区不老町
名古屋大学大学院理学研究科　物質理学専攻
篠原研究室内
Tel：052-789-5948
Fax：052-747-6442
E-mail：fullerene@nano.chem.nagoya-u.ac.jp
URL：http://fullerene-jp.org
印刷　/　製本　株式会社トービ

nacalai tesque
The quality for certainty.

金属内包フラーレン用ＨＰＬＣカラム

COSMOSIL® Buckyprep-M

今まで分離できなかった
金属内包フラーレンが分離可能！！

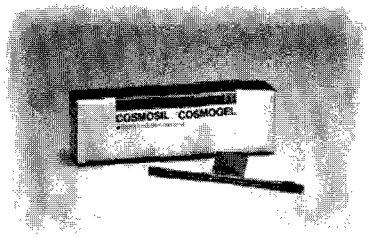

■分析例

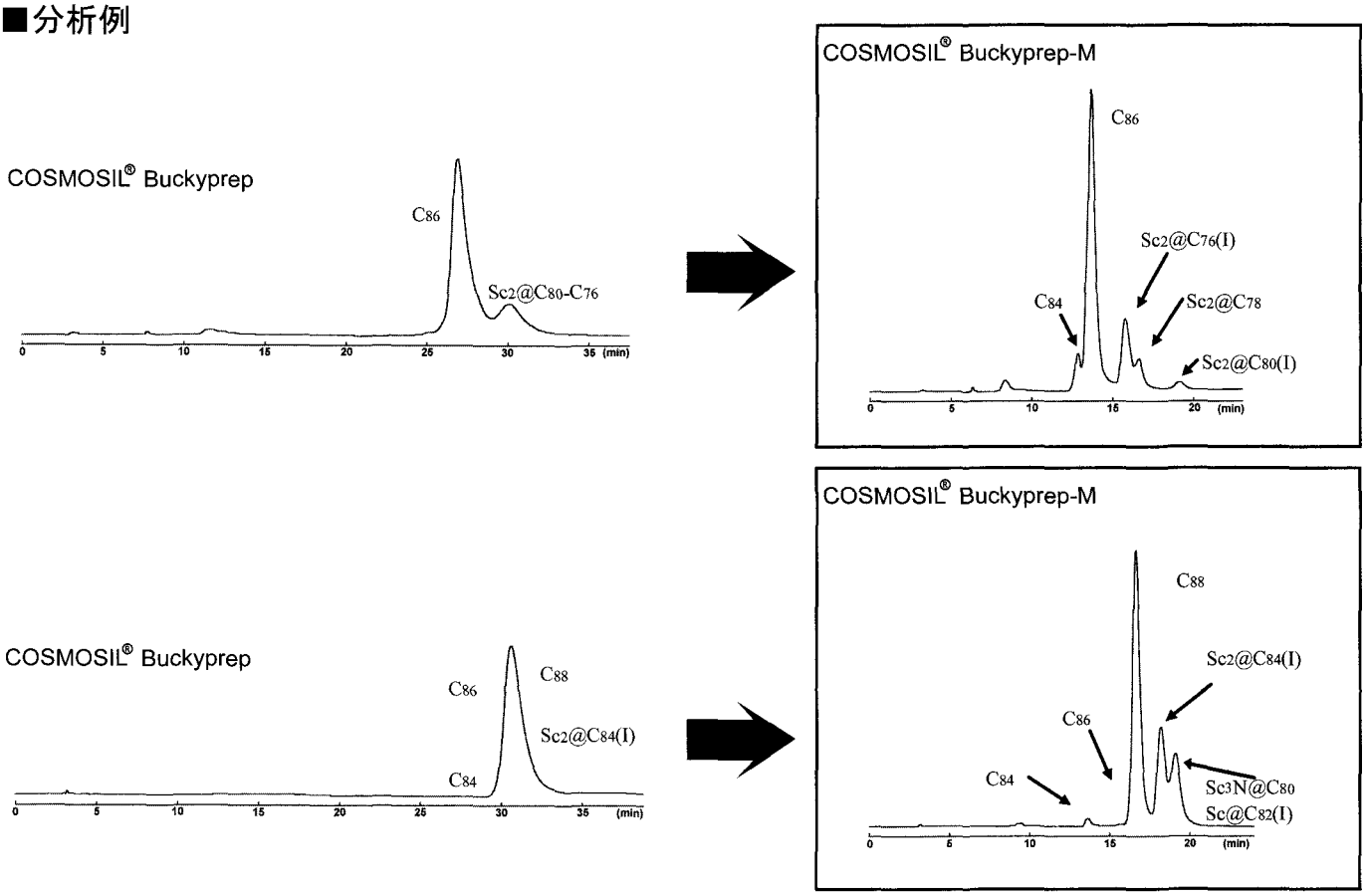

分析条件
カラムサイズ：4.6mmI.D.×250mm, 移動相：トルエン, 流速：1.0ml/min, 温度：30℃, 検出：UV312

資料提供：名古屋大学　大学院理学研究科物質理学専攻　篠原 久典教授

■その他COSMOSIL® フラーレン関連カラム

フラーレン分離のスタンダードカラム	⟶	COSMOSIL® Buckyprep
C_{60}, C_{70}等の大量分取に	⟶	COSMOSIL® PBB

詳しい情報はWeb siteをご覧下さい。

ナカライテスク株式会社
〒604-0855　京都市中京区二条通烏丸西入東玉屋町498

価格・納期のご照会　フリーダイヤル　0120-489-552
製品に関するご照会　TEL：075-211-2703　FAX：075-211-2673
Web site :http://www.nacalai.co.jp

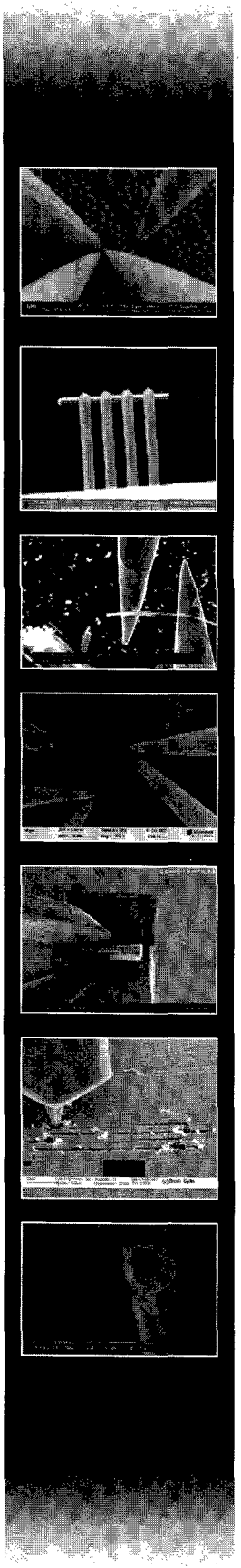

kleindiek
nanotechnik

for Electron microscope

Micromanipulator Substage

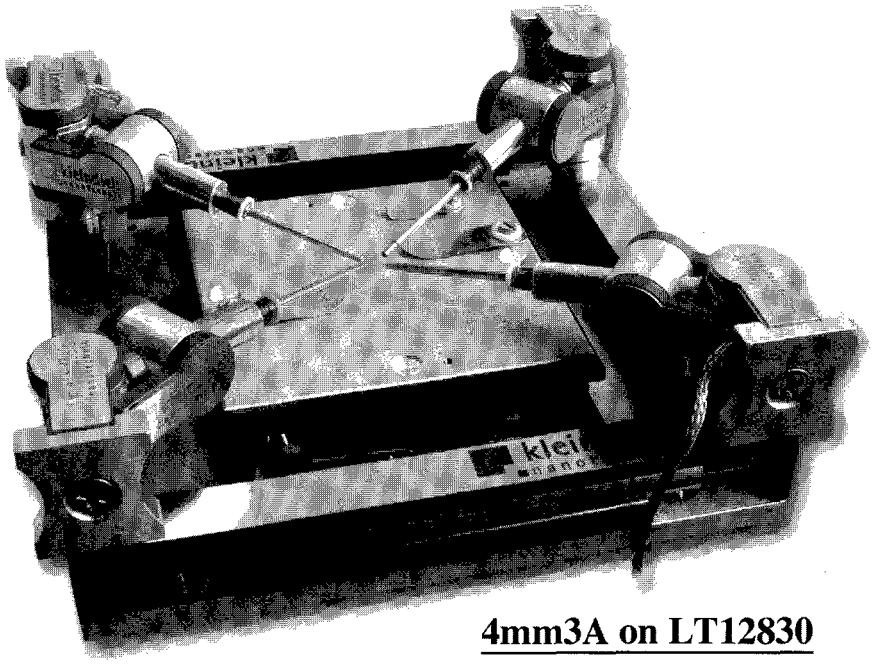

4mm3A on LT12830

Semiconductor/R&D

- Electrical probing
- Failure analysis
- IC test&repair
- TEM samplepreparation
- eBeam lithography
- Cell counting

Material science

- Manipulation
- Electrical&Mechanical characterization
- Microinjection in ESEM
- Force measurement
- Nanoindentation
- STEM
- Scanning probe microscopy

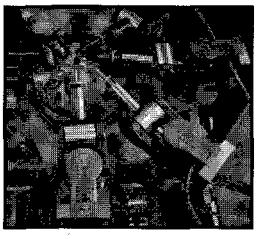

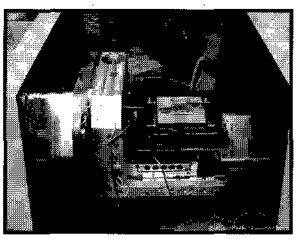

ADS 株式会社 アド・サイエンス

〒273-0005 千葉県船橋市本町2-2-7サンテックビル TEL:047-434-2090 FAX:047-434-2097 http:// www.ads-img.co.jp

CaHC

ライフサイエンスサポート企業へ。

株式会社「カーク」は、『創造と努力』『誠実と感謝』を企業理念とし、
科学・医学・産業の研究・開発の発展に寄与するため
試薬をはじめ、工業薬品、検査薬、分析機器の販売を通して顧客に貢献しています。
特に、バイオサイエンス・ライフサイエンスの分野において、
オンリーワン、ナンバーワンとしての存在を目指しています。

For Customer

株式会社 カーク

〒460-0002 名古屋市中区丸の内 3-8-5
Tel 052-971-6533(代)
http://www.cahc.co.jp

愛知東営業所 0564-66-1580
岐阜営業所 058-268-8151
浜松営業所 053-431-6801
三重営業所 059-236-2531

BRUKER

Bruker Daltonics

MALDI-TOF/TOF-MS, MALDI-TOF-MS Ion Trap MS^n, ESI-TOF/MS, ESI-Qq TOF/MS

Flex シリーズに autoflexIII、ultraflexIII が新登場。ラインナップが autoflexIII TOF、autoflexIII TOF/TOF、ultraflexIII TOF、ultraflexIII TOF/TOF、microflexIIITOF になりました。
特許 LIFT 技術により、極微量サンプルから超高速・超高感度で卓越した MS/MS データを得ることが可能です。

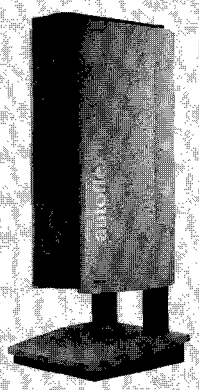

autoflex III TOF/TOF

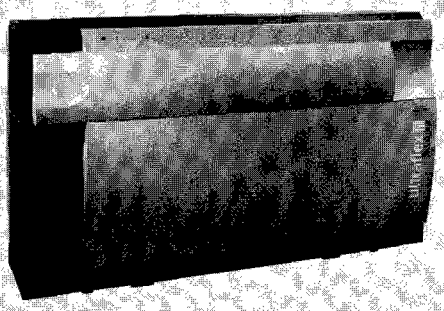

ultraflex III TOF/TOF

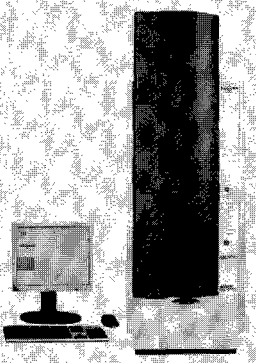

microflex TOF

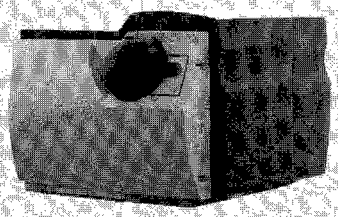

HCT*ultra*
Ion Trap MS^n 電子転移解離 ETD システム

micrOTOF 新型 *focus*
新型高性能卓上型 ESI-TOF/MS

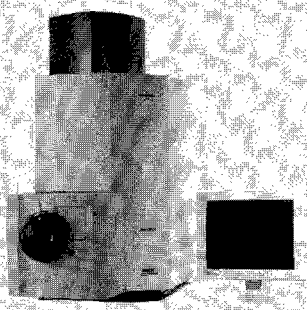

micrOTOF-Q
新型高性能卓上型 ESI-Qq TOF/MS

ブルカー・ダルトニクス株式会社

■ 営業本部・テクニカルサポートセンター
〒 221-0022
横浜市神奈川区守屋町 3-9
A 棟 6F
TEL：045-440-0471
FAX：045-440-0472

■ 大阪営業所
〒 532-0004
大阪市淀川区西宮原 1-8-29
テラサキ第 2 ビル 2F
TEL：06-6396-8211
FAX：06-6396-1118

■ 本社
〒 305-0051
茨城県つくば市二の宮 3-21-5
TEL：029-852-3510
FAX：029-852-6729

think forward

MS Solutions

リサイクル分取HPLCはJAIのLC-9000シリーズ!

Recycling Preparative HPLC

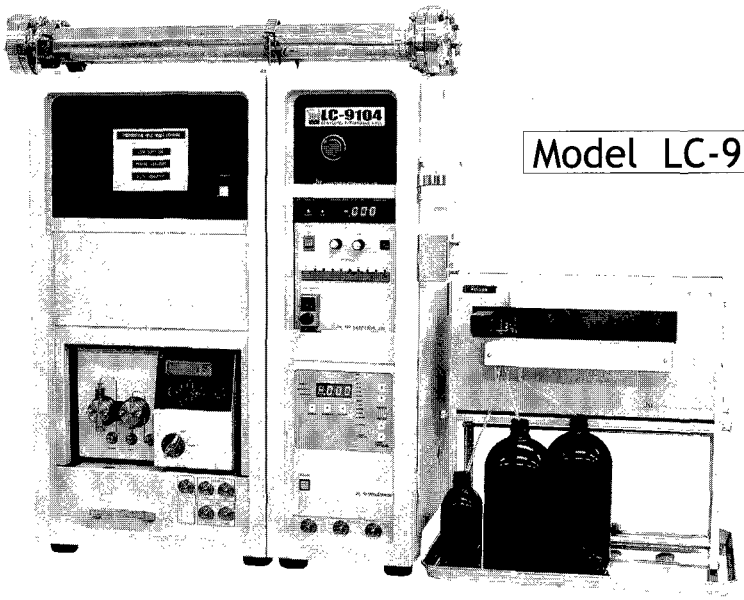

Model LC-9104

◆LC-9104　大量分取モデル
専用のGPCカラム(40 φ×600 mm)を装着すれば、試料処理量は、LC-9101型の約4倍。試料注入から分取まで自動化されています。また、ODS・シリカカラムなど、大量分取用カラムの性能を最大限に引き出す装置設計がなされています。

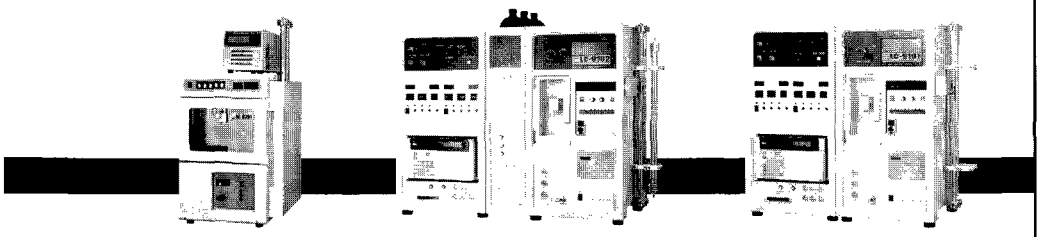

◆ LC-9201/LC-9204
コンパクトモデル
分離分取に定評のあるLC-9101型の高い性能を受継ぎながら、サイズをコンパクトにし、省スペース化と低価格化を実現しました。

◆ LC-9102/9103
グラジエントモデル
グラジエントとリサイクルがワンタッチで切替えられます。

◆ LC-9101
標準モデル
専用のGPCカラム(20 φ×600 mm)を装着すれば、分離能を落とすことなく、常時300 mgを注入することができます。

高分子分析の未来と取り組む!

分取LCに関する新連携認定企業

JAI 日本分析工業株式会社

ISO9001／14001取得

URL:http//www.jai.co.jp/　E-mail:sales-1@jai.co.jp

□本社・工場:〒190-1213 東京都西多摩郡瑞穂町武蔵208 TEL 042-557-2331 FAX 042-557-1892
□大阪営業所:〒532-0002 大阪市淀川区東三国5-13-8-303 TEL 06-6393-8511 FAX 06-6393-8525
□名古屋営業所:〒465-0025 愛知県名古屋市名東区上社3-609-3D TEL 052-709-5400 FAX 052-709-5403

Nanomaterials

ALDRICH Chemistry

好評発売中！

直線配列多層カーボンナノチューブ（MWCNT）

Hy-Energy LLCのK. Gross博士のご提案による、高品質カーボンナノチューブアレイが発売になりました！

- シリコン基板と銅基板の製品ございます。
- ガス吸着センサー基板[1]ほか、各種センサー基板、触媒[2]、電池、コンデンサーなど幅広い材料の研究開発に独自のプラットフォームを提供できます[3]。

Carbon nanotube array, multi-walled, vertically aligned, on silicon wafer substrate
687804-1EA ¥180,000

Carbon nanotube array, multi-walled, vertically aligned, on copper substrate
687812-1EA ¥180,000

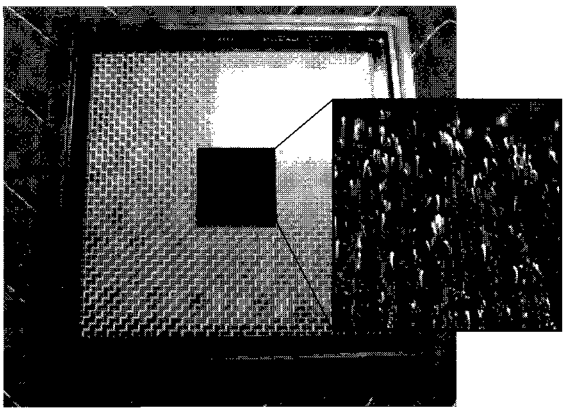

半導体グレードのパッケージに納められたCNTアレイ（黒い正方形）。挿入写真は、垂直配列したMWCNTのSEM画像。

特徴：

- MWCNTとして99.9%
- CNTの直径は100 nm ± 10 nm
- CNTの長さは30 µm ± 3 µm
- アレイの密度～2 x 10^9 MWCNT/cm^2
- アレイの寸法は1平方cm
- プラズマ励起CVD（PECVD）により成長
- ニッケル触媒チップが劣化しない状態で成長
- クリーンルーム内で梱包、半導体グレードのパッケージで保存および出荷

参考文献：

(1) Collins, P.G., Bradley, K. Ishigami, M. Zettl, A., *Science*, **2000**, 287, 1801. (2) Bonard, J. M., Stockli, T., Maier, F., De Herr, W. A., Chatelain, A., Ugarte, D., Salvetat, J. P., Forro, L., *Physical Review Letters*, **1998**, 81, 1441. (3) Frackowiak, E., Gautier, S., Gaucher, H., Bonnamy, S., Beguin, F., *Carbon*, **1999**, 37, 61

Material Matters™

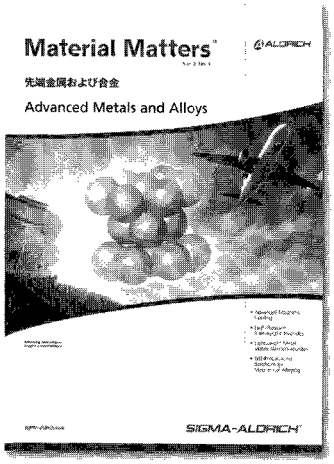

第一線の研究者による、テクニカルレビュー、アプリケーションノートを紹介したニュースレターです！

日本語版既刊：

Vol.1 No.1 高分子材料
Vol.1 No.2 分子自己組織化
Vol.1 No.3 セラミックおよびハイブリッド材料の堆積／成長

NEW

Vol.2 No.1 ナノ材料の応用最前線（08年2月発行）
Vol.2 No.2 水素貯蔵材料（08年2月発行）
Vol.2 No.3 有機エレクトロニクス（08年3月発行）
Vol.2 No.4 先端金属およびアロイ（08年5月発行）
Vol.3 No.1 3次元ナノおよびマイクロ構造（08年5月発行）

以下続刊

日本語版のご請求および登録は、日本語サイトから！

材料関連の詳細情報は、*sigma-aldrich.com/matsci*（*US*サイト）および*sigma-aldrich.com/japan*（日本サイト）をご覧ください！

SIGMA-ALDRICH®

シグマ アルドリッチ ジャパン株式会社

〒140-0002東京都品川区東品川2-2-24
天王洲セントラルタワー4階

■製品に関するお問い合わせは、弊社テクニカルサポートへ
TEL：03-5796-7330 FAX：03-5796-7335
E-mail：sialjpts@sial.com

■在庫照会・ご注文方法に関するお問い合わせは、弊社カスタマーサービスへ
TEL：03-5796-7320 FAX：03-5796-7325
E-mail：sialjpcs@sial.com

http://www.sigma-aldrich.com/japan

Access to your success

SHIMADZU

Best for Our Customers

～すべてはお客様のために～

を合言葉にナノテク新材料における最高のソリューションを提供します。

①微量測定 ②純　度 ③直　径 ④観　察 ⑤カイラリティ ⑥凝集分散

① 熱分解生成物・発生ガスの分析
ガスクロマトグラフ質量分析計
GCMS-QP2010 Plus

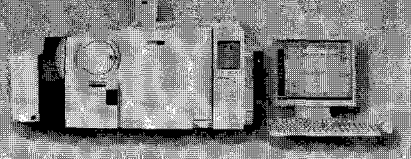

① 微量CNTの純度・熱特性評価
① CNTの結晶性と耐熱性の評価
ミクロ熱重量測定装置
TGA-50

TG/DTA同時測定装置
DTG-60/60H

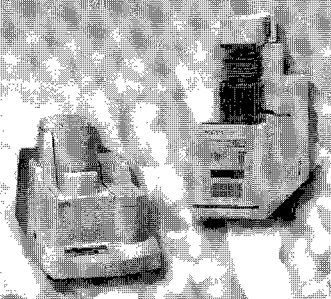

①② CNTの紫外可視近赤外吸収スペクトル測定
紫外可視近赤外分光光度計
SolidSpec-3700

紫外可視近赤外分光光度計
UV-3600

② CNTの密度測定
乾式自動密度計
アキュピック1330

② 触媒元素の測定
ツインシーケンシャル形ICP発光分析装置
ICPS-8100

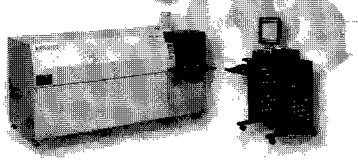

②③ 直径測定
②③ 結晶性と耐熱性の評価
ラマン分光光度計
Holo-Probe モニタリングシステム

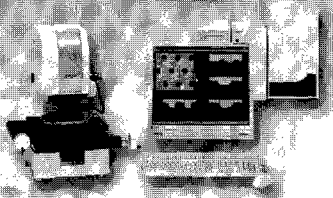

③④ あらゆるナノテク材料を観察・測定
ナノサーチ顕微鏡
SFT-3500

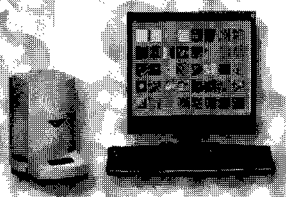

③④ 直径測定
③④ 精製前後の観察
③④ CNTとポリマーコンポジット試料の観察
走査型プローブ顕微鏡
SPM-9600

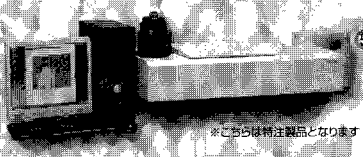

⑤ SWNTの近赤外PL 3次元分布測定
近赤外フォトルミネッセンス測定システム
NIR-PL System
※こちらは特注製品となります

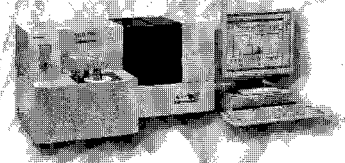

⑥ 分散・凝集過程評価
ナノ粒子径分布測定装置
SALD-7100

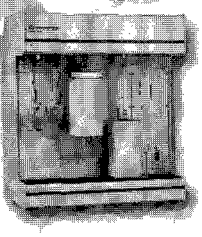

⑥ 比表面積と吸着特性
マイクロメリティックス
高速比表面積/細孔分布測定装置
アサップ2020シリーズ

nanotech
SHIMADZU

Total solutions for the future of nanotechnology

株式会社島津製作所

分析計測事業部　マーケティング部　セールスプロモーションG
〒604-8511 京都市中京区西ノ京桑原町1
TEL075-823-1468 FAX075-823-1380 http://www.shimadzu.co.jp

米国・MTR社 フラーレン価格表(税抜)

株式会社マツボー
東京都港区虎ノ門3-8-21
電話 03-5472-1723
FAX 03-5472-1720
email: fulen@matsubo.co.jp

1. フラーレン混合物 *(C60:50-60%, C70:35-45%*)

5g未満	¥17,000/g
5g以上	¥6,800/g
25g以上	¥4,100/g
100g以上	¥2,800/g

*(C60:50-60%, C70:35-45%、07/01現在)
混合割合は変更となる場合がございます。

2. フラーレンC60	>99%販売中止になりました	>99.5%	>99.8%	>99.98%	Sublimed
5g未満	~~¥7,600/g~~	¥9,100/g	¥10,100/g	¥14,000/g	¥29,000/g
5g以上	~~¥6,400/g~~	¥7,900/g	¥ 9,900/g	¥13,000/g	¥29,000/g
10g以上	~~¥5,400/g~~	¥6,500/g	¥ 8,800/g	¥11,300/g	¥26,000/g
50g以上	~~¥4,900/g~~	¥6,000/g	¥ 7,800/g	¥ 9,800/g	¥23,000/g
100g以上	~~¥4,200/g~~	¥4,900/g	¥ 7,000/g	¥ 8,500/g	¥19,000/g

3. フラーレンC70	>98%	>99%	>99.5%	Sublimed
0.25g	¥13,000/0.25g	¥19,800/0.25g	¥30,000/0.25g	¥48,000/0.25g
1g以上	¥12,000/0.25g	¥19,000/0.25g	¥29,000/0.25g	¥47,000/0.25g
2g以上	¥12,000/0.25g	¥18,000/0.25g	¥28,000/0.25g	¥46,000/0.25g
5g以上	¥12,000/0.25g	¥17,000/0.25g	¥28,000/0.25g	¥42,000/0.25g
10g以上	¥11,300/0.25g	¥16,000/0.25g		

4. SWナノチューブ(20-40%) クローズドエンド

1g以下	¥23,000/g
5g以下	¥23,000/g
10g未満	¥22,000/g
10g以上	¥20,000/g
25g以下	¥18,000/g
50g以下	¥16,000/g

5. SWナノチューブ(50%-70%) クローズドエンド

5g以下	¥50,000/g
25g以下	¥47,500/g
50g未満	¥44,000/g
50g以上	¥42,000/g

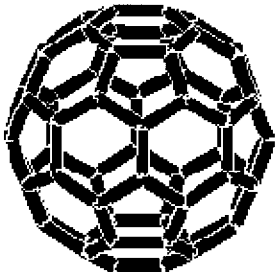

6. SWナノチューブ(70～80%)

50～60%がオープンエンド	~~90,000/0.1g~~

現在販売中止中です

7. MWナノチューブ(20～40%)クローズドエンド

1g以下	~~¥8,400/g~~
5g以下	~~¥8,000/g~~
10g以下	~~¥7,200/g~~
25g以下	~~¥6,600/g~~
50g以下	~~¥6,000/g~~

現在販売中止中です

8. MWナノチューブ(95%)クローズドエンド

5g未満	¥72,000/g
5g以上	¥68,000/g

9. MWナノチューブ(70～80%) 現在販売中止中です

50～60%がオープンエンド	~~¥72,000/g~~

10. MWナノチューブ(85～90%)

95%以上がオープンエンド	¥88,000/g

*純度はHPLCにより測定されています。
*Minimum Orderは￥10,000. -です。

UNISOKU
SCIENTIFIC INSTRUMENTS

電子顕微鏡・光学顕微鏡下での多探針・ナノ/マイクロプロービングシステムのラインナップがますます充実しました 最先端表面分析ツールとして最適です

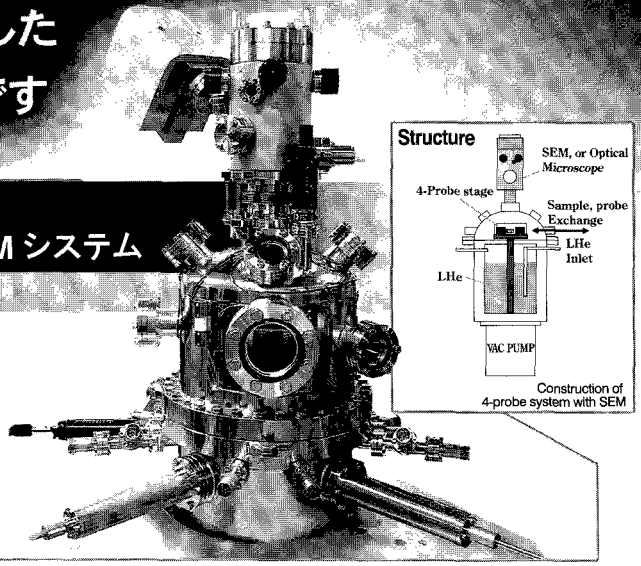

4プローブ＋ FE-SEM・超高真空・極低温条件でのSPMシステム

USM-1400-4P

- ◆ ロードロック室・処理室・観測室の3室構成、SPMコントローラ、FE-SEM、真空ポンプを含んだフルシステムです
- ◆ 各プローブの機能は用途に応じて選択できます（3軸ナノプロービング、STM、AFM、KFM・・・・）
- ◆ 液体ヘリウム冷却により10K以下での測定が可能です FE-SEMの分解能は20nm程度です（2008年3月現在）

新製品 大気型4プローブ表面測定システム

UP2000-4P

大気中における「ミクロンオーダー」から「ナノオーダー」の各種表面電気測定やマニュピレーションを可能にするシステムです

- ◆ 光学顕微鏡でサンプル表面を観察しながら4つのプローブの各々独立なXYZ-3軸操作がPCとリモコンにより簡単に
- ◆ サンプルステージ側も独立したXY移動が可能なので煩雑なサンプル位置調整が不要
- ◆ PC画面上に表示されたサンプル表面を見ながら、直観的で容易なマニュピレーション操作が可能

市販の電子顕微鏡に後付け可能な4プローブ表面電気特性測定システム

UMP1000-4P

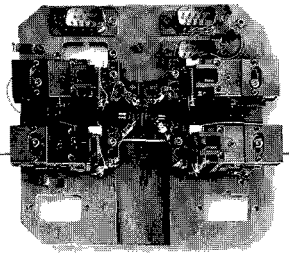

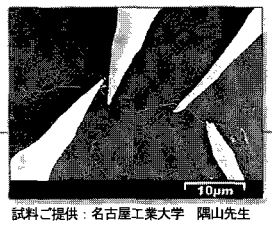

試料ご提供：名古屋工業大学　隅山先生

- ◆ 各プローブが独立したアクチュエーターとしてナノオーダーでXYZ3軸共制御可能
- ◆ SEM測定上の任意の位置での試料表面電気特性測定をはじめナノマニュピレーション等応用した用途にも使用できます

上記システムをベースに特注のニーズ（大気中プロービング、プローブ数指定・・）にもお応えいたします。お気軽にご相談ください。

プローブのラインナップも充実しております

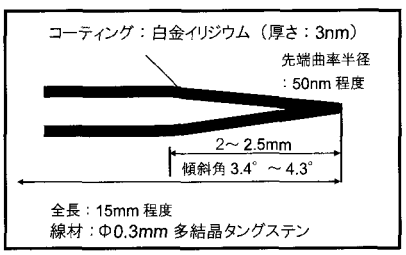

図：ナノプロービング用白金イリジウムコートナノプローブ UP-100P

- ◆ **ナノプロービング用白金イリジウムコートナノプローブ UP-100P**
  0.3mm dia 10本1組で販売
  - ■ タングステン線材へ白金イリジウムをコーティングすることによりサンプルとソフトな接触が実現
  - ■ 傾斜角が小さいので4プローブ以上の多探針プロービングにおいても隣の針と接触しません
- ◆ **STM用白金イリジウム探針（機械研磨）**
  0.5mm dia 10本1組で販売
- ◆ **STM用タングステン探針（電解研磨）**
  0.3mm dia 10本1組で販売
- ◆ **ナノプロービング用タングステン探針（電解研磨）**
  0.3mm dia 10本1組で販売

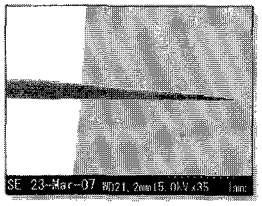

株式会社 ユニソク
〒573-0131 大阪府枚方市春日野2丁目4番3号
TEL(072)858-6456㈹ FAX(072)859-5655
E-mail:info@unisoku.co.jp
http://www.unisoku.co.jp

Photal
OTSUKA ELECTRONICS

濃厚溶液から希薄溶液まで幅広い濃度範囲に対応

ゼータ電位・粒径測定システム

ZETA-POTENTIAL & PARTICLE SIZE ANALYZER

ELSZ series

ゼータ電位	-200～200mV
粒径測定	0.6nm～7μm
濃度範囲	0.001%～40%※

※ Latex 116/262nm：0.001%～10%タウロコール酸：～40%

■カーボンナノチューブのゼータ電位

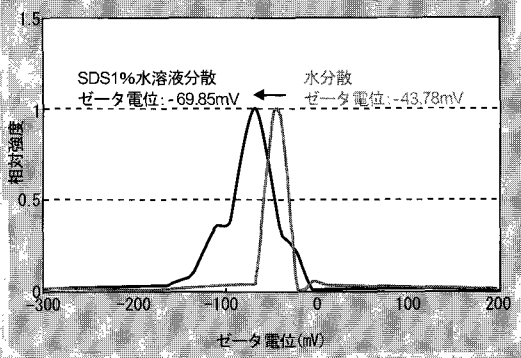

■カーボンナノチューブの粒径分布

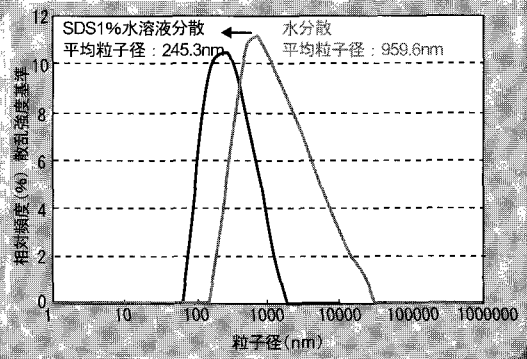

- 希薄溶液に加え濃厚溶液でのゼータ電位測定が可能。
- 取り扱いが簡単な電気泳動セルにより操作性が向上。
- 電気浸透流を実測することで信頼性の高いゼータ電位測定が可能。
- 粒径範囲(0.6nm～7μm),濃度範囲(0.001%～40%)に対応。
- 従来のリニアスケール相関計に加えLogスケール相関計を搭載。ナノ粒子の高精度な解析や、濃厚系サンプルの解析など多様な用途に対応。

第20回 散乱研究会 開催のご案内

2008年12月4日(水)

日本薬学会館 長井記念ホール(東京・渋谷)　　詳細は後日 WEB上に掲載します。

TÜV SÜD ISO 9001

大塚電子株式会社はテュフズードジャパンより、ISO9001の認証を取得しています。

大塚電子株式会社

ホームページ　http://www.photal.co.jp/

●本　社　〒573-1132 大阪府枚方市招提田近3丁目26-3　TEL. (072)855-8564　FAX. (072)850-9159

●東京支店　〒192-0082 東京都八王子市東町1-6 橋完LKビル4F　TEL. (042)644-4951　FAX. (042)644-4961

SOGO 株式会社　十 合

物質の状態は、固体と液体を除くと「ガス」です。
ガスは入れ物と配管がなければ、使うことができません。
また、「都市ガス」や「プロパンガス」だけが「ガス」ではありません。

現代社会の最先端を行く研究分野の中で、分析装置、レーザー設備、半導体設備、燃料電池、触媒設備で「ガス」を使用しないものはほとんどありません。

お客様から要求されるガスの純度、安全管理、供給管理は年々高度化してきています。

私どもの会社は、工業用や医療用、研究用に使用されるガス、および関連機器の販売商社でしたが、それだけでは、お客様のニーズを満足させることはできません。 そこで、先端研究設備で要求される仕様を十分満たす「ガス供給設備」の設計施工を手がけてまいりました。

これからも、常に知識技術の向上に努め、新世紀を生き抜ける企業を目指し、なおかつお客様の成功に貢献していきたいと考えています。

今後とも、末永いお付き合いのほど、よろしくお願い申し上げます。

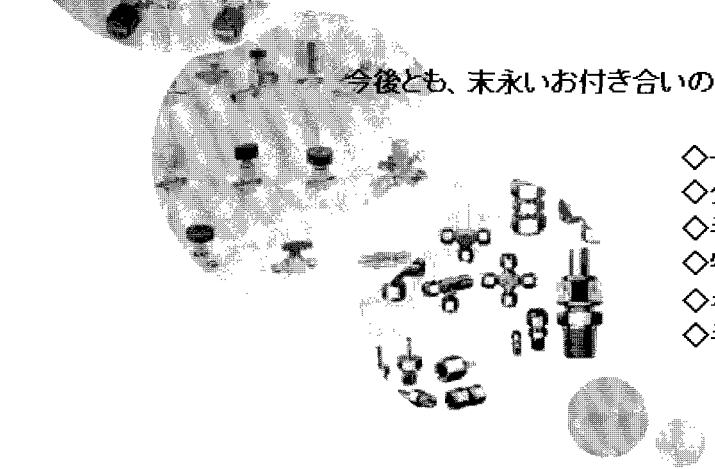

◇一般高圧ガス
◇分析用標準ガス
◇半導体製造用ガス
◇特殊配管用弁類及び継手
◇各種ガス供給システムの設計施工
◇半導体製造ガス供給システムの設計施工

株式会社　十　合　　**お客様第一主義に徹します**

本　社　〒464-0075　名古屋市千種区内山一丁目24番9号（第2ダイワビル 3F）
TEL （052）741－0288　FAX （052）731－6617
営業所　〒470－0213　西加茂郡三好町大字打越字三本松30－30
TEL （0561）32－0621　FAX （0561）32－0623
Eメールは、sogomail@sogo-inc.jpまでお願いします。

atomistix 第一原理量子輸送計算プログラム

Atomistix ToolKit & Virtual NanoLab

サイバネットシステム株式会社ではAtomistix社製品を利用して下記の研究発表を行っています。ナノチューブ、グラフェンやシリコン材料などナノスケールデバイスの電気伝導特性計算のプロフェッショナルとして委託計算・共同研究などのご相談に応じます。 お問合せ先：atomistix-info@cybernet.co.jp

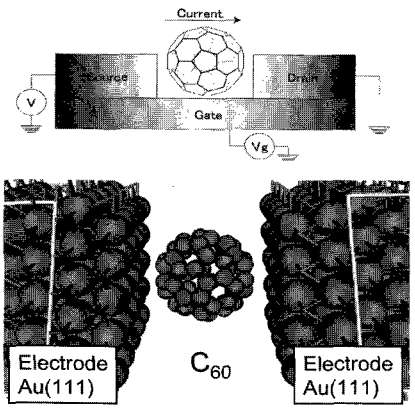

● 第32回フラーレン・ナノチューブ学会での研究発表

サイバネットシステムはAtomistix社製品を利用してフラーレン単分子デバイスの電気伝導特性に関する理論計算の発表を行いました。本研究では、金電極上におけるC_{60}の配置の変化や、電極とC60の距離変化に伴うIV特性を計算し、これらの変化がC_{60}のデバイス応用を果たす上で重要な要因となることを示唆しました。

■発表資料：
http://www.cybernet.co.jp/nanotech/atomistix/download/dl/070215_fn_poster.pdf

● 第34回フラーレン・ナノチューブ学会での研究発表

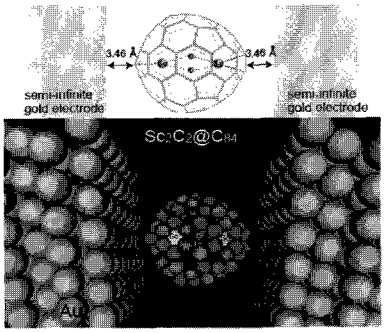

続く第34回学会では「内包されたSc_2C_2部位を導線構造としたSc_2C_2 @C_{84}の電気伝導特性。第一原理計算による解析」と題し、注目を集める金属内包フラーレンの電気伝導特性を、Atomistix ToolKit を用いて解析しました。本研究では、C_{84}に内包されたC_2の回転の影響を受けて、劇的に変化する電気特性を報告すると共に、この系の分子インバーターへの適応可能性について議論しています。

■発表資料：
http://www.cybernet.co.jp/nanotech/atomistix/download/dl/080304_fn_poster.pdf

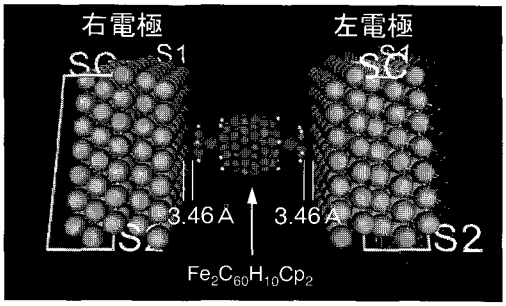

● 第35回フラーレン・ナノチューブ学会での研究発表

本学会では、ERATO 中村活性炭素クラスタープロジェクトにて研究が進められている double-decker buckyferrocene のデバイス応用の可能性について、Atomistix ToolKit を用いた理論計算に基づき考察します。詳細は発表にて。

■ 引用論文：
Y. Matsuo, K. Tahara, and E. Nakamura, J. Am. Chem. Soc. 128, 7154 (2006)

上記発表資料は本会議サイバネットシステム社ブースにて配布しております。お気軽にお立ち寄り下さい。

CYBERNET つくる情熱を、支える情熱。

カーボンナノチューブの生成に
試験研究用　真空熱処理装置

均温熱処理装置　GFA430VN

卓上サイズで、均一な温度分布を広く得られる高性能な電気炉です。

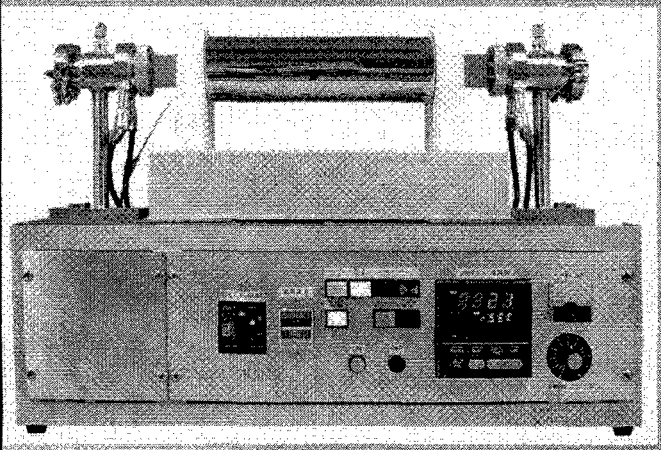

《 仕様 》

- ○ 最高到達温度　1000℃
- ○ 最大昇温速度　1000℃まで30分
- ○ 均温体積　約φ36×200mm
- ○ 最高到達真空度　5×10^{-4}Pa
- ○ 所要電力　AC200V15A

炉芯管両端に、NW40と1/4スエジロックのフランジが付いており、各種雰囲気に対応可能です。

赤外線導入加熱装置　GVL298

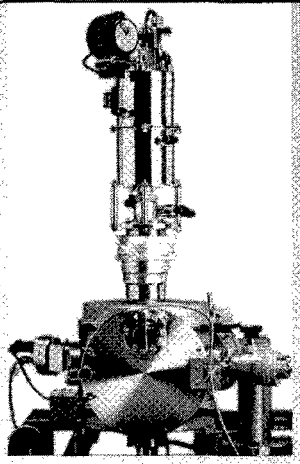

真空中試料をクリーン加熱、急速加熱ができる装置です。
既存装置の、ICF70フランジに取付可能です。

《 仕様 》

- ○ 最高到達温度　1500℃
- ○ 最大昇温速度　150℃/秒
- ○ 所要電力　100V 20A

株式会社　サーモ理工

〒181－0013　東京都三鷹市下連雀8－7－3　三鷹ハイテクセンター
TEL ： 0422 － 76 － 2511　　FAX ： 0422 － 76 － 2514

他にも多数製品がございます。詳しくはWEBでご覧ください。

サーモ理工　検索

CNTコートディッシュ

@ Meijo Arc

●Meijo Arc（名城ナノカーボン製CNT）をポリスチレンディッシュに特殊薄層コート
●低血清培地において効果的な細胞培養ディッシュを実現

CNTコートディッシュの写真

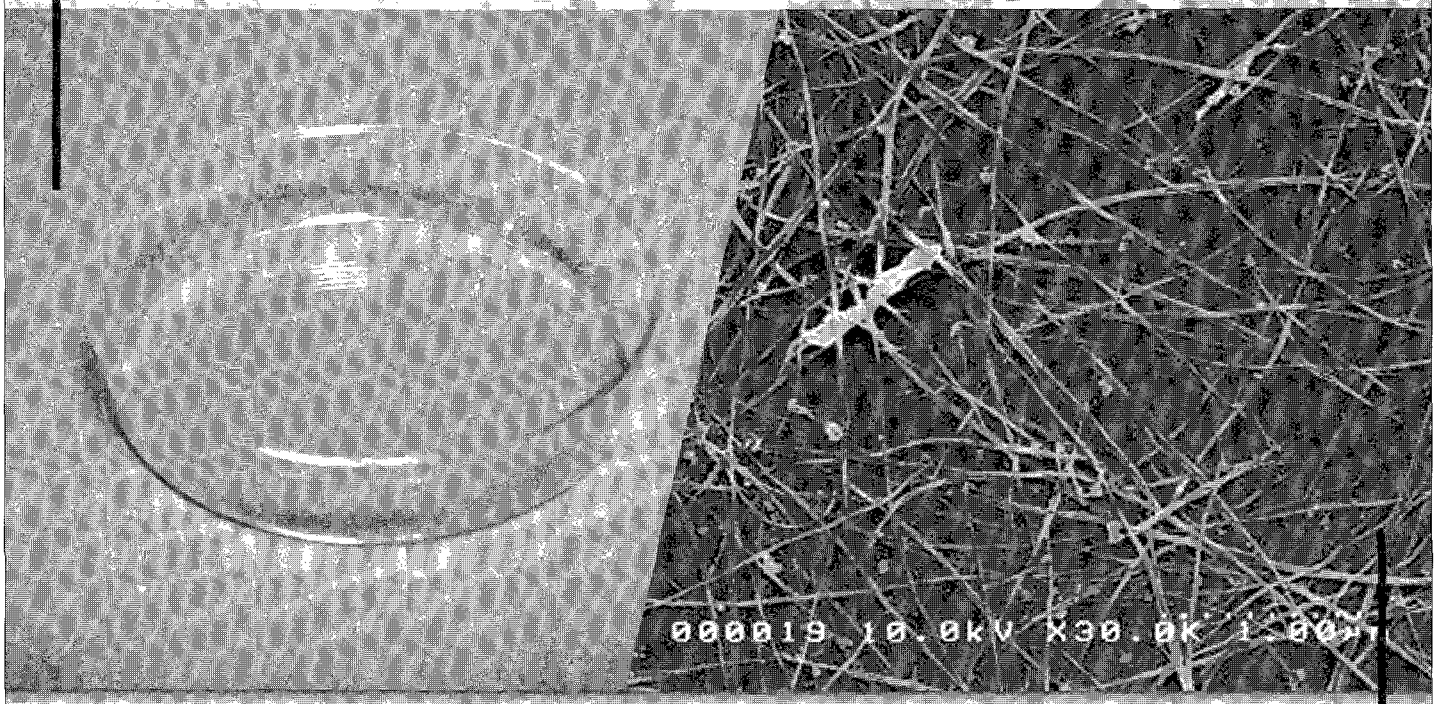

ディッシュ表面のSEM写真×3万倍

＊「CNTコートディッシュ@Meijo　Arc」は
北海道大学大学院歯学研究科　生体理工学教室亘理文夫教授、赤坂司助教、
口腔機能補綴学教室　横山敦郎教授グループと共同開発いたしました。

＊「Meijo Arc」とは（株）名城ナノカーボン製高品質CNTです。

〒460-0002　愛知県名古屋市中区
丸の内3-4-10 大津橋ビル4F
HP：http://www.meijo-nano.com

meijo nano carbon
株式会社 名城ナノカーボン

TEL:052-971-2408
FAX:052-955-3257
✉:hashimo@ccmfs.meijo-u.ac.jp

季刊 ナノテク読本 広告企画のご案内

ナノテクノロジーを活用した製品は日進月歩で開発が進み、続々と市場に登場しています。さらに、これからのナノテク実用化を目指した各分野の研究開発も着実な進歩を見せており、産業界や自治体からの期待は高まる一方です。

08年初頭より、半導体産業新聞は「週刊ナノテク」と統合し、各方面からの大きな期待を背負うナノテクノロジーを精力的に追いかけていますが、今回、「週刊ナノテク」の魂を継承し、当社がこれまで培ってきたナノテクの取材ノウハウをフル活用した新媒体として、『季刊 ナノテク読本』を企画いたしました。この媒体は、エレクトロニクス、エネルギー、環境、ライフサイエンスなど様々な分野で芽吹いているナノテクノロジーの現在を、豊富な取材データをもとに俯瞰し、その将来像を展望することを主眼においています。また、ナノテクノロジーに関連性の深い国内展示会・学会ともタイアップし、その見どころをご紹介していきます。年4回の発行を予定しております。

2008年発刊スケジュール

Vol.1：2008年 2月 8日 発行
「nano tech 2008」「FC EXPO / PV EXPO」特集号

Vol.2：2008年 6月 6日 発行
「国際バイオEXPO」「マイクロマシン/MEMS展」特集号

Vol.3：2008年 8月下旬 発行予定
「2008分析展」特集号

Vol.4：2008年11月下旬 発行予定
「セミコン・ジャパン 2008」特集号

媒体概要

○媒　体　名：季刊 ナノテク読本
○価　　格：2,100円(本体:2,000円)
○発行予定部数：15,000部
○体裁・頁数：A4変形判、オフセット印刷、平綴じ、70ページ
○特　　典：各展示会にて会場無料配布

広告料金

スペース	普通版
4色1ページ	¥350,000(税込：¥367,500)
2色1ページ	¥250,000(税込：¥262,500)
1色1ページ	¥200,000(税込：¥210,000)
2色1/2ページ	¥150,000(税込：¥157,500)
1色1/2ページ	¥120,000(税込：¥126,000)
1色1/3ページ	¥80,000(税込：¥84,000)

広告原稿サイズ(天地mm×左右mm)

スペース	普通版	断切版
1　ペ　ー　ジ	255×180	280×208
ヨコ1/2ページ	118×172	――
ヨコ1/3ページ	80×172	――

株式会社 産業タイムズ社 広告部　〒101-0032 東京都千代田区岩本町1-10-5 TMMビル3F　TEL：03-5835-5892
E-Mail：ad@sangyo-times.co.jp　FAX：03-5835-5492

東京都千代田区岩本町1-10-5
TMMビル3F　〒101-0032
TEL:03-5835-5892/FAX:03-5835-5492

産業タイムズ社の出版案内

詳細カタログ呈
Fax.での注文も承ります。定価は税・送料込み。

好評発売中! **半導体工場ハンドブック2008**
グローバリゼーションに突入した次世代ラインの全貌
A4変形判・145頁・定価4,200円(本体4,000円)

2008年7月下旬発刊予定 **アジア半導体/液晶ハンドブック2008-2009**
台湾・韓国・中国・東南アジアのメーカー別プロフィール・設備投資を一覧
A4変形判・約110頁・定価4,200円(本体4,000円)

好評発売中! **半導体産業会社録2008年度版**
日本で唯一の半導体産業ダイレクトリ "最新・大改訂版"
A4変形判・552頁・定価15,750円(本体15,000円)

好評発売中! **液晶・PDP・ELメーカー計画総覧2008年度版**
大画面／極薄／有機EL化競争が始まった薄型テレビへ搭載されるFPD
B5判・391頁・定価14,700円(本体14,000円)

2008年9月上旬発刊予定 **半導体産業計画総覧2008-2009年度版**
A4変形判・約550頁

好評発売中! **プリント回路メーカー総覧2008年度版**
部品内蔵基板市場が本格立ち上り
B5判・294頁・定価16,800円(本体16,000円)

2008年9月下旬発刊予定 **太陽電池産業総覧2008-2009**
"本物"の成長が見えてきた太陽光発電有力企業70社の事業戦略と展望
B5判・約240頁

好評発売中! **燃料電池産業総覧2008**
主要100社の最新事業計画と、大学・研究機関の研究開発動向を網羅
B5判・303頁・定価18,900円(本体18,000円)

好評発売中! **ナノテク産業総覧**
ナノテクキーカンパニー700社収録
キーパーソン300人網羅
A4変形判・540頁・定価25,200円(本体24,000円)

波長可変チタンサファイアレーザー

3900S

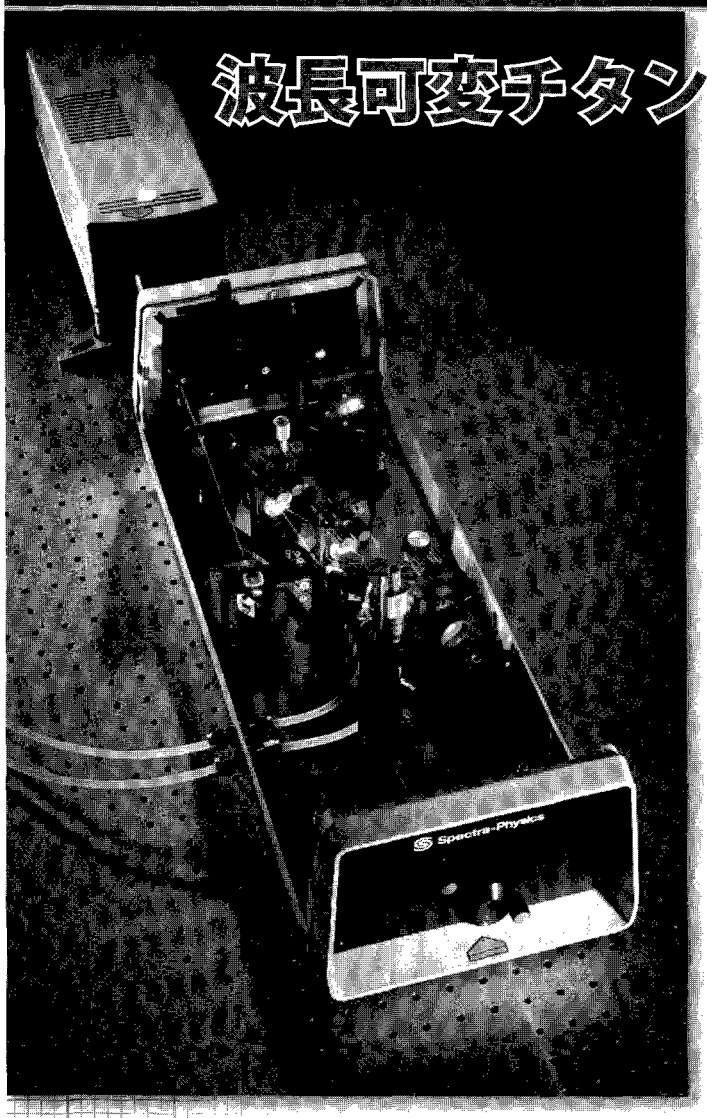

- 優れた操作性とメンテナンス性、高い変換効率を実現
- 高い安定性を実現し、675～1100nmの超広帯域発振が可能
- フラーレン・ナノチューブの分光用光源として最適

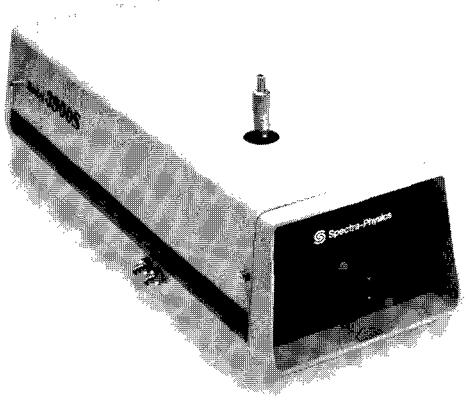

【主な仕様】

平均入力	：	5Wおよび10W
発振波長域	：	700-1000nm(5W励起)/675-1100nm(10W励起)
線幅	：	40GHz以下(1GHz以下のオプション有り)
ノイズ	：	1%以下
安定性	：	3%以下
空間モード	：	TEM_{00}

Spectra-Physics
A Division of Newport Corporation

スペクトラ・フィジックス株式会社
本　社　〒153-0061 東京都目黒区中目黒4-6-1 大和中目黒ビル　TEL(03)3794-5511 FAX(03)3794-5510
大阪支社　〒550-0005 大阪府大阪市西区西本町3-1-43 西本町ソーラービル　TEL(06)4390-6770 FAX(06)4390-2760

MAKE LIGHT | MANAGE LIGHT | MEASURE LIGHT

製品情報・お問い合わせは　http://www.spectra-physics.jp

収差補正（Cs）レンズで
世界最高性能の電子顕微鏡

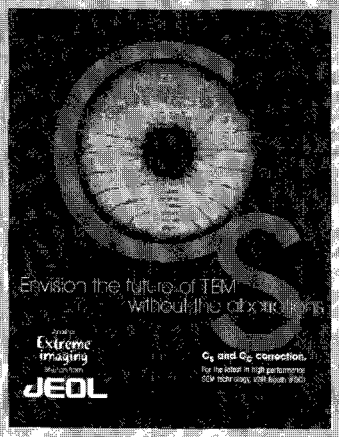

JEM-2100F
フィールドエミッション電子顕微鏡

次世代超高性能電子顕微鏡

レンズの球面収差を補正することにより、分解能を飛躍的に向上させた次世代超高性能収差補正装置（球面収差補正形電子レンズ）を、電子光学技術で高い技術を誇るドイツのCEOS社との共同開発により完成させ、最新のTEMに導入しました。

主な特長

照射系（コンデンサ）レンズの収差補正により、非常に細い電子ビームが形成され、走査透過電子顕微鏡（STEM）の分解能や元素分析などを行う際の空間分解能が飛躍的に向上

対物レンズの収差補正により、点分解能が0.12nmまで向上し、フリンジが解消され、高精度での微小結晶界面などの特定が可能

お問い合せは、電子光学機器営業本部（EO販促グループ） ☎042(528)3353

JEOL
Serving Advanced Technology

日本電子株式会社 http://www.jeol.co.jp/
本社・昭島製作所 〒196-8558 東京都昭島市武蔵野３－１－２ ☎(042)543-1111
営業統括本部 〒190-0012 東京都立川市曙町2－8－3 新鈴春ビル3F ☎(042)528-3381
札幌 (011) 726-9680・仙台 (022) 222-3324・筑波 (029) 856-3220・東京 (042) 528-3211・横浜 (045) 474-2181
名古屋 (052) 581-1406・大阪 (06) 6304-3941・広島 (082) 221-2500・福岡 (092) 411-2381

ISO 9001 & 14001 REGISTERED FIRM
JEOL ISO 9001 & ISO 14001 認証取得

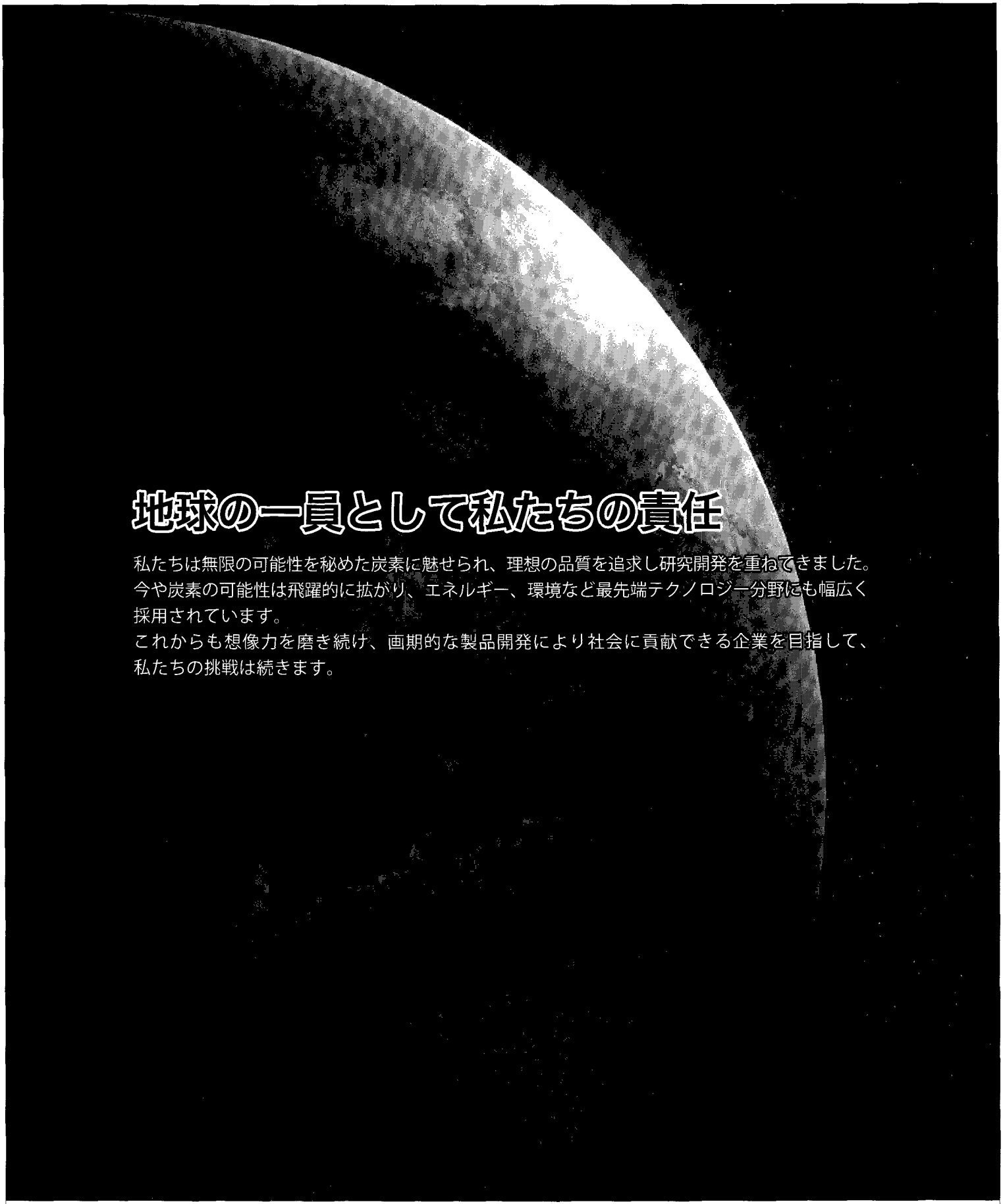

地球の一員として私たちの責任

私たちは無限の可能性を秘めた炭素に魅せられ、理想の品質を追求し研究開発を重ねてきました。
今や炭素の可能性は飛躍的に拡がり、エネルギー、環境など最先端テクノロジー分野にも幅広く採用されています。
これからも想像力を磨き続け、画期的な製品開発により社会に貢献できる企業を目指して、私たちの挑戦は続きます。

TOYO TANSO
Inspiration for Innovation

東洋炭素株式会社
本社　〒530-0001 大阪市北区梅田3-3-10 梅田ダイビル10F　Tel 06-6451-2114　Fax 06-6451-2186　www.toyotanso.co.jp

住友商事のカーボンナノチューブ

Produced by Unidym, Inc.（旧Carbon Nanotechnologies Inc.）

住友商事はUnidym社の日本・アジア地域での総代理店として、学術研究用途から事業化・応用開発用途まで、各種用途に適した製品のご提供に加え、共同開発の推進や事業化支援プロジェクトの実施など、カーボンナノチューブの応用製品開発を総合的に支援しています。

● HiPco® 単層カーボンナノチューブ

直径約1nmの単層カーボンナノチューブです。基礎研究や高機能用途向けに、触媒残留率の異なる下記3製品をご提供しております。

製品名	触媒残留率
HiPco® As Produced （未精製品）	< 35 wt%
HiPco® Purified （精製品）	< 15 wt%
HiPco® Super Pure （超高純度品）	< 5 wt%

＊ Bucky Plus™（フッ化カーボンナノチューブ）など、修飾品についてもご相談ください。

■ 単層カーボンナノチューブ TEM像 ■

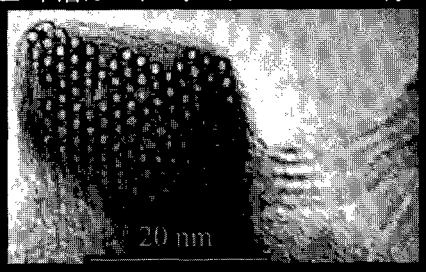

● Unidym ™ ESDシリーズ

Unidym社独自の製法で製造された、用途別産業応用向けカーボンナノチューブです。量産性に優れ、導電性付与/複合材（EMI, ESD, Anti-Static）、ディスプレイ光源、燃料電池の電極用途などに、安定した製品供給が可能です。詳細につきましては、下記連絡先までお問合せください。

■ 二層カーボンナノチューブ TEM像 ■

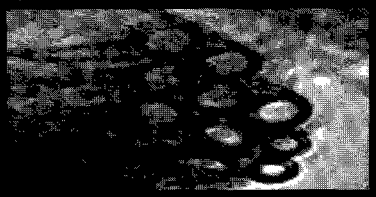

● 二層カーボンナノチューブ

Unidym社独自の製法で製造された、直径約2nmの二層カーボンナノチューブです。

● CNT水性塗料　帯電防止~制電コーティング

CNT水性塗料をコーティングすることにより、透明性を維持しながら帯電防止～制電機能を付与

⇒　各種機能性フィルムへの応用

上記製品群を中心に、研究用から量産対応品、共同開発によるカスタマイズ対応など、用途に応じたカーボンナノチューブの開発を進めています。弊社までお気軽にお問合せ下さい。

本件に関するお問合せ先:
住友商事株式会社
エレクトロニクス・マテリアル第二事業部 (担当:河本)
E-mail : nano@sumitomocorp.co.jp
TEL : 03-5166-4546　FAX :03-5166-6234
住所 : 〒104-8610 東京都中央区晴海1-8-11
URL : www.sumitomocorp.co.jp/section/joho/nanotube.shtml

マルチコアには
インテル® コンパイラー

インテル® コンパイラーはシミュレーション、解析用プログラムを高速化することで研究の効率化を支援します。

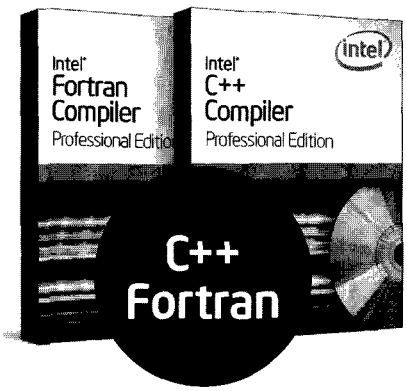

- ☑ **最新のマルチコア向けに並列化 / 高速化**
- ☑ **並列化のコストを大幅に削減**
- ☑ **短期間で学べる技術セミナーも充実**

Windows/Linux/Mac OS

- **サイエンス・テクノロジー分野の研究、開発に最適！**
- **研究機関、企業での実績多数！**

お客様の声

「私の研究では 10 万元程度の連立1次方程式を数万回繰り返し解く作業に帰着させます。インテルのコンパイラーを用いれば、gcc に比べて格段に実行時間が減らせますので、大変役に立っています。」

国立大学 工学部 情報工学科 殿

画像パターンマッチング処理にてインテル® コンパイラーを使用した場合、評価アルゴリズムの速度が約 30% 向上しました。

大手 宇宙情報システム開発会社 殿

インテル独自の「最適化」と「自動並列化」機能により、最新のマルチコア・プロセッサー上で高速化を実現します。

インテル® コンパイラーのパフォーマンス優位性

インテル® Core™2 Duo プロセッサーにおける Spec2006 整数ベンチマーク（値が高いほど高性能）

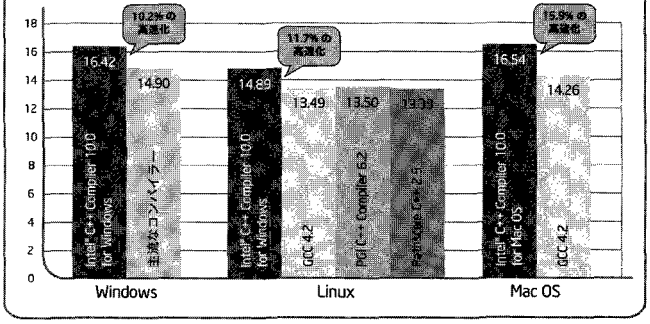

設定情報：SPEC2006 ベンチマークの詳細は、www.spec.org/cpu2006/ をご覧ください。
- Compilers:
  Windows*: Intel® C++ Compiler 10.0 for Windows, Microsoft® Visual C++® 8.1
  Linux*: Intel® C++ Compiler 10.0 for Linux, PGI C++ Compiler 6.2, GCC 4.2, Pathscale C++ 2.5
  Mac OS*: Intel® C++ Compiler 10.0 for Mac OS, GCC 4.2
- Hardware & OS: Windows: Intel® Core™ 2 Duo Processor, 2.4GHz, 2GB, 4096KB, Operating System: Windows 2003_64 SP1, 0
  Linux: Intel® Core™ 2 Duo Processor, 2.4GHz, 2GB, 4096KB, Operating System: RHEL4_64 WS UP03, kernel 2.6.9-34.ELhjl.4smp, glibc glibc-2.3.4-2.19
  Mac OS: Intel® Core™ 2 Duo Processor, 2x3.0GHz, 4GB, 4096KB, Operating System: MacOS 10.4.8, kernel 8.8.1, glibc 0

30 日間無料体験版でお試しください！

製品の詳細に関するお問い合わせ先

XLSOFT エクセルソフト株式会社
www.xlsoft.com/intel/
TEL: 03-5440-7875 FAX: 03-5440-7876 E-mail: intel@xlsoft.com

ご購入に関するお問い合わせ先

インテル® ソフトウェア開発製品 販売代理店
以下の web サイトをご覧ください
http://www.xlsoft.com/jp/products/intel/purchase.html

インテル、Intel は、アメリカ合衆国および他の国における Intel Corporation またはその子会社の商標または登録商標です。* その他の社名、製品名などは一般に各社の表示、商標または登録商標です。© 2008 Intel Corporation. 無断での引用、転載を禁じます。

自社国内開発・自社国内生産・企業向け組み込みシステムメーカ

Made in Japan
Designed in Japan

Interface®

新製品
Intel Atom プロセッサ 搭載

省エネコンピュータ

SFC-A016　今秋発売開始！

●より小さく

160(W)×109(D)×22(H) mm
約700g

●より安く

●より堅牢に

瞬停，電源強制切断でも壊れない（ソフトウェアRAID，専用ドライバにより実現）
オンボードSolidStateDisk：4GB×2（RAID構成のため実質4GB）
オンボードメモリ：1GB（メモリソケットなし）
単一DC電源入力（ワイドレンジ 7V~27V）
環境にやさしい，環境に強い（省エネ，低電力，耐振動，耐衝撃，耐ノイズ）
FANレス，密閉ケース入り，無音
USBターゲット機能でUSBホストと通信
一般的なコンピュータ（USBホスト）とUSBケーブルで接続

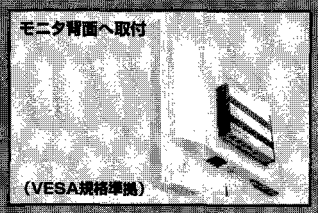

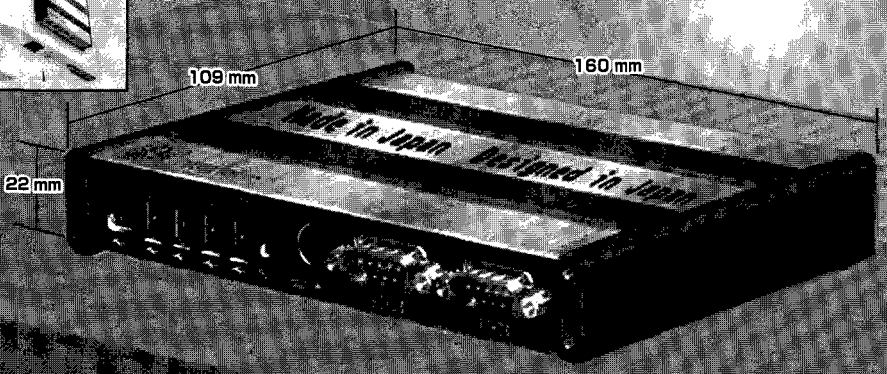

○仕様一覧

仕様については変更する場合があります。詳細は Web site まで。

項目		仕様
型式		SFC-A016
価格		オープンプライス
外形寸法		160（W）×109（D）×22（H）mm 突起含まず
外形寸法	CPU	intel® Centrino® Atom™ Processor Z530（FSB533Mhz）
外形寸法	動作クロック	1.6GHz
チップセット		Intel US15W（Poulsbo）
BIOS		Phoenix製 オリジナルBIOS
メモリ（オンボード）		1GB（DDR2SDRAM DDR2-533）メモリソケットなし
ビデオ	コントローラ	Intel US15W内蔵
ビデオ	Video RAM	メインメモリと共用
ビデオ	Video BIOS	64KB
記憶装置（オンボード）		SSD 4GB×2（ソフトウェアRAID構成のため実質4GB）
OS		別売：Web site上で選択 Windows XP Embedded， Interface Linux System，Interface DOS System
カレンダ時計		大容量（10年程度保持）電池搭載 BR-1/2AA（松下電器）
入力電源仕様		DC+12V~DC+24V（+10%/-0%）
消費電力		7W（Min）
重量		約700g

項目		仕様
インタフェース	グラフィックス	1：DVI-D（HDMIコネクタ使用） 2：LCD IF（24ビットLVDS） 26ピンハーフピッチコネクタ（10226-2210PE）X1
インタフェース	USB	USB Rev.2.0準拠 × 5 シリーズAコネクタX4 / miniABコネクタX1
インタフェース	LAN	1000BASE-T（RJ-45コネクタ）×2
インタフェース	シリアルポート	RS-232C（9ピンD-sub）×2
インタフェース	キーボード/マウス	PS/2互換 6ピン丸型ミニDIN X1（スプリッタ接続時マウス使用可）
LED		電源LED / ディスクアクセスLED
ハードウェアモニタ		CPU温度 / ボード温度 / 電源電圧
ウォッチドッグタイマ		ソフトウェアプログラマブル（1~255秒）
ウォッチドッグタイマ		リセットまたは割り込み通知のいずれかを選択可能
耐環境性	耐振動性	~5.0G
耐環境性	耐衝撃性	~10G
耐環境性	使用条件	0℃~50℃　10%~90%（結露なきこと）
耐環境性	耐ノイズ性	静電気→接触:±6kV，気中:±8kV，放射電磁界 10V/m， 伝導→10V/m，サージ→2kV（線間1kV）， FTB→信号:1kV，電源:2kV
耐環境性	規格	CEマーキング対応，RoHS指令対応

新製品
Intel Core 2 Duo プロセッサ搭載

3UサイズCompactPCI

スロットインFAシステム

CEZ-C02CD22
今秋発売開始！

すべて前面よりスロットイン！

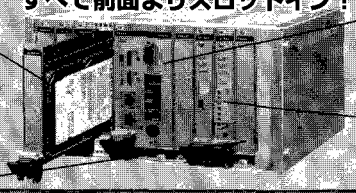

スロットインHDDモジュール
SATA，2枚使用でRAID構成
OS Windows XP Professional
Windows XP Embedded
Interface Linux System
Interface DOS System

スロットインバッテリモジュール

CPUモジュール
CPU：Intel Core 2 Duo，メモリ：最大2GB，USB：5，
LAN：1GB×2，シリアル：1，ビデオ：デジタル出力×2，PS/2×1

スロットイン電源モジュール
絶縁 AC100V/200V，DC100V/110V，DC+48V，DC+24V
非絶縁 DC+24V，DC+12V
ATX 100W出力モジュール

Interface®
Vision&Freedom
株式会社 インタフェース

Web siteよりオンラインでカスタマイズできます！
見積もり・出荷日確認・発注も簡単にできます！

FAコンピュータ製品のCPU、メインメモリ、デバイス（HDD/CF）容量、オプションを簡単にカスタマイズ！
オンラインでご希望の製品の見積もり・出荷日確認・発注が簡単に行えます。

www.interface.co.jp

~カスタマーサポートセンター~
フリーダイヤル
TEL :0120-447213
FAX :0120-458257
URL :www.interface.co.jp
E-mail: support@interface.co.jp

製品の仕様、デザイン、価格については、予告なく変更する場合がありますので、ご了承ください。本広告に記載した会社名、製品名は、それぞれの商標または登録商標です。

1/1,000,000,000メートルの世界。
そこが、東レのフィールド。

物質を原子レベルの大きさで正確にコントロールする技術。東レは
ナノテクを使い、様々な分野で新しい価値を生み出しています。

未来を変える先端材料を創る。
それが、東レのナノテク。

'TORAY'
Innovation by Chemistry

東レ株式会社/〒103-8666 東京都中央区日本橋室町2丁目1番1号 TEL:(03)3245-5181(宣伝室) URL:http://www.toray.co.jp

Nano & Bio

――フロンティア出版のナノテクノロジー・ナノマテリアルシリーズ――

自己組織化ナノマテリアル
ーフロントランナー85人が語るナノテクノロジーの新潮流ー
企　画：理化学研究所　フロンティア研究システム
　　時空間機能材料研究グループ
監　修：国武豊喜（北九州市立大学／理化学研究所）
編集幹事：下村政嗣（北海道大学／理化学研究所）
　　山口智彦（産業技術総合研究所）
■体裁／B5判・392頁　■価格／57,750円（税込）

有機・無機・金属ナノチューブ
ー非カーボンナノチューブ系の最新技術と応用展開ー
編　集：清水敏美（産業技術総合研究所）
　　木島　剛（宮崎大学）
■体裁／B5判・330頁　■価格／57,750円（税込）

ナノ粒子の創製と応用展開
編　集：米澤　徹（東京大学）
■体裁／B5判・322頁　■価格／57,750円（税込）

ナノコンポジットマテリアル
ー金属・セラミック・ポリマー3大物質のナノコンポジットー
編　集：井上明久（東北大学）
■体裁／B5判・363頁　■価格／52,500円（税込）

ナノオプティクス・ナノフォトニクスのすべて
ーナノ光技術の基礎から実用までー
監　修：河田　聡（大阪大学／理化学研究所）
編　集：梅田倫弘（東京農工大学）
　　川田善正（静岡大学）
　　羽根一博（東北大学）
■体裁／B5判・352頁　■価格／57,750円（税込）

MEMS/NEMSの最先端技術と応用展開
編　集：前田龍太郎（産業技術総合研究所）
　　澤田廉士（九州大学）
　　青柳桂一（マイクロマシンセンター）
■体裁／B5判・285頁　■価格／52,500円（税込）

ナノインプリントの基礎と技術開発・応用展開
ーナノインプリントの基盤技術と最新の技術展開ー
編　集：平井義彦（大阪府立大学）
■体裁／B5判・281頁　■価格／52,500円（税込）

ナノバイオエンジニアリングマテリアル
ーバイオインターフェイス・ナノバイオプロセッシング
　・バイオコンジュゲーション・バイオマトリックスー
監　修：石原一彦（東京大学）
■体裁／B5判・350頁　■価格／52,500円（税込）

フロンティア出版
〒110-0012 東京都台東区竜泉1-21-18　TEL：03-6802-1640　FAX：03-6802-1641　E-mail：info@frontier-books.com
http://www.frontier-books.com

株式会社　マシナックス

代表取締役　佐野隆治

〒454-0856　名古屋市中川区小碓通 2-6

ＴＥＬ　052-654-5021㈹　　ＦＡＸ 052-654-5125

HP　　http://www.mashinax.jp/

メール　mashinax@sf.starcat.ne.jp

okamura

BREZZA

ヒュームフード［ブレッツァ］シリーズ

人間工学を取り入れた最新型のヒュームフード。
研究者の安全性はもちろん、機能性と快適性をご提案します。

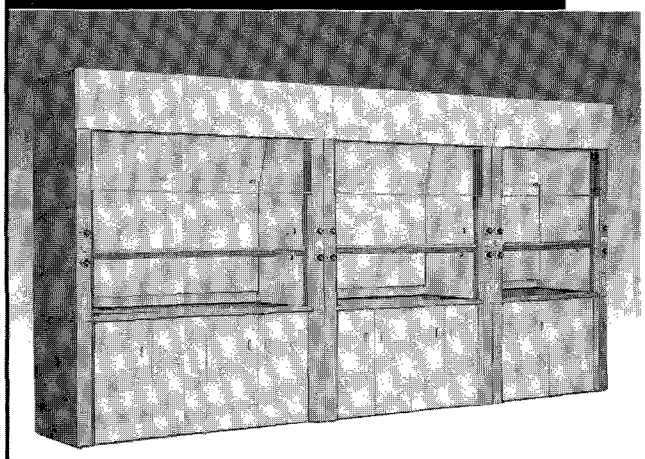

見やすい“大型の観察扉（ガラス）”

観察扉（ガラス）の占める割合を増やすことで、フードの内部が見やすくなりました。

使いやすい“大型のフード内サイズ”

作業面から邪魔なカランを取り除くことで、フードの内部がより一層広くなりました。

環境にやさしい“エコロジー設計”

塗装は耐薬性に優れ有機溶剤を使わない専用の粉体塗装を施しています。メンテナンスを考慮した分別設計はもちろんのこと、耐震設計まで考慮しています。

オカムラの研究施設用家具

オカムラは、先進性とフレキシビリティを備えた設備機器の提供や、研究目的・人員に対応したスペースプランニングなど、研究者にとって快適な研究環境をご提案します。

LABO-AS series

オールスチール実験台［AS］シリーズ

オールスチールで設計された新しい形の実験台。
研究目的に合わせて変化する実験・研究環境を柔軟にサポートします。

※棚板1段（1800W）当たり、最大150Kgの積載が可能です。

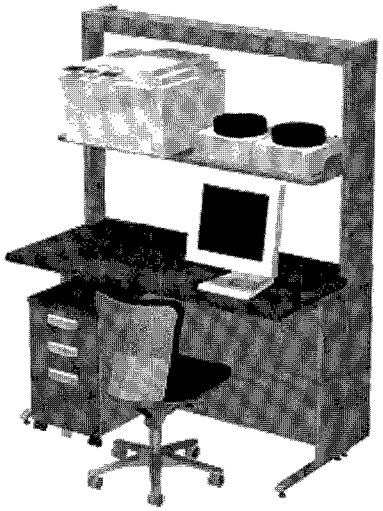

（イメージ）

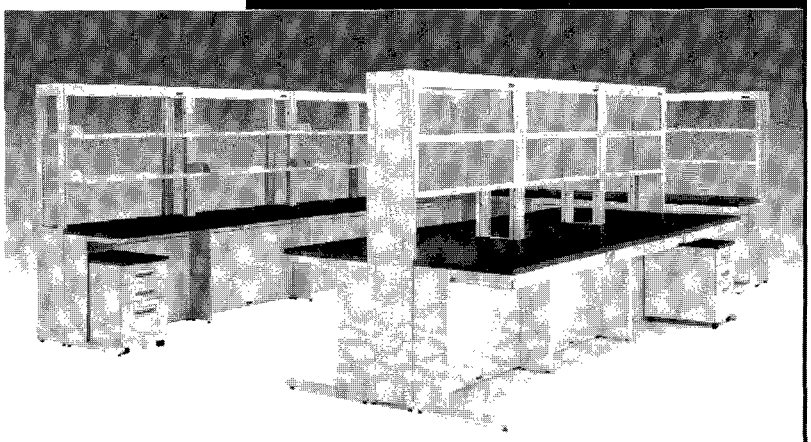

棚が使える“機能性”

作業面に載せていた計測機器を棚に設置することで、作業面を確保できます。また、機器のサイズに合わせて棚板高さを調整できます。

組替え自由な“拡張性”

研究の目的にあわせてレイアウト変更が簡単にできます。

［名古屋支店］
〒450-6020 名古屋市中村区名駅1-1-4 JRセントラルタワーズ20階 TEL:052(551)3180 FAX:052(551)3185

お問い合わせは［お客様サービスセンター］へ… フリーダイヤル 0120-81-9060 月曜～金曜（祝日を除く）9:00～18:00
○オカムラの最新情報をご覧下さい。［ホームページアドレス］ http://www.okamura.co.jp/

よい品は結局おトクです

オカムラ

株式会社 岡村製作所

SPM systems and actuators for in situ TEM

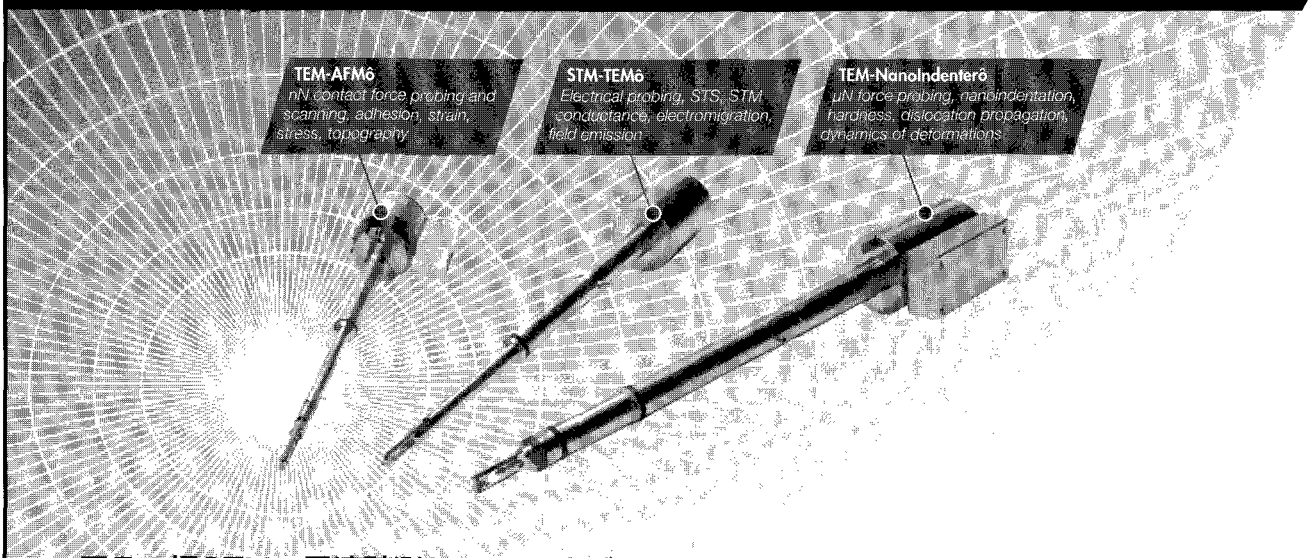

■その場STM、電流計測用TEMホルダー

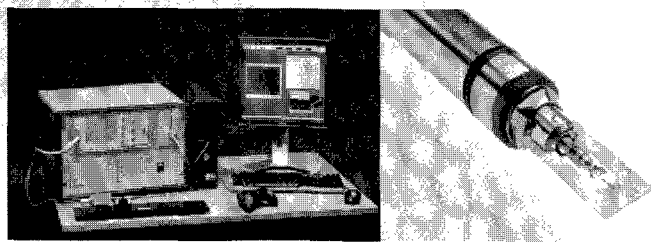

STM-TEMシステムは透過型電子顕微(TEM)と走査トンネル顕微鏡(STM)の両方を組み合わせたシステムであり、試料の完全キャラクタリゼーションを一度に行うことが出来ます。このシステムは、STMを搭載したTEMホルダー、制御コントローラー、PCとナノファクトリー独自のソフトウエアで構成されています。STMプローブスキャナーには、3D位置調整メカニズム(特許)が搭載されており、正確なプロービング位置調整から粗動位置及び方位調整に至るピコメーターからミリメーターまでの広範囲の動作をカバーしています。

STM-TEMシステムは非常に広範な用途に利用することができます。例えば、ナノ構造体の局所的な電気特性をサブナノの精度で計測できます。代表的な使用法としては、STM観察、STS接触電動などです。TEMと併用することにより、プローブの形状だけでなく、トンネルの接合点やプローブ／試料間の相互作用に関する非常に重要な情報を得ることが出来ます。TEMの様々な分析手法と併用することで、その場計測法に新しい展開が期待できます。

■アプリケーション：STM-TEMイメージング

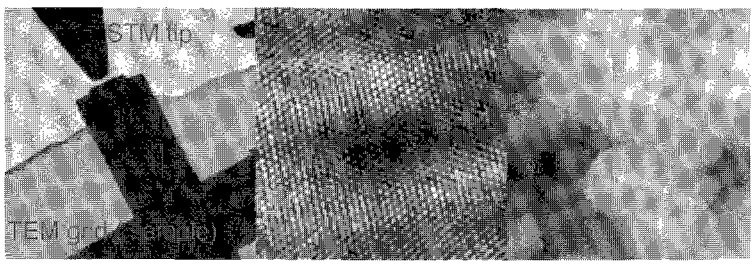

（左）TEMグリッド試料に対して位置調整したSTMチップのTEM像。
(中央）金のSTMチップを高分解能TEM観察した像。
（右）TEM内で同じ金のSTMチップを用いて観察したSTM像。

nanoFACTORY™
INSTRUMENTS www.nanofactory.com

Corporate Headquarters:
Nanofactory Instruments AB
Chalmers Science Park
412 88 Gteborg, Sweden
Phone: +46-31-719 07 20
Fax: +46-31-16 59 85

US Office:
Nanofactory Instruments Inc.
Suite 126, 3400 Waterview Parkway
Richardson, TX 75080, USA
Phone: +1-972-437-6552
Fax: +1-972-437-6949

ナノファクトリーインストルメンツ・ジャパン株式会社
〒106-0032 東京都港区六本木 1-10-3-901
スウェーデン大使館内
練馬事務所 〒178-0063 東京都練馬区東大泉 3-61-11
直通電話/FAX: 03-5387-3585
携帯電話: 090-1439-1329
E-mail: yasuji.miyamori@nanofactory.com
URL: www.nanofactory.com

溶液中の粒子のナノレベル微細化・分散に

BRANSON 超音波ホモジナイザー

ホーン先端部の振幅の安定性を、より高めた Advance タイプ になりました。

近年のナノテクノロジーの発展及び粉体関連技術の向上により、より微細な粒子に対する乳化分散処理の要望が増えてまいりました。
超音波ホモジナイザーを使用し、均質な乳化分散処理を行い、安定させることにより製品の機能は向上します。
ブランソン社では 20kHz 機と、40kHz 機の 2 タイプを用意しております。
1 次粒子の凝集力にも拠りますが、20kHz 機では 100nm 程度までの分散力があります。40kHz 機は、さらに細かいレベルで分散ができる可能性があります。

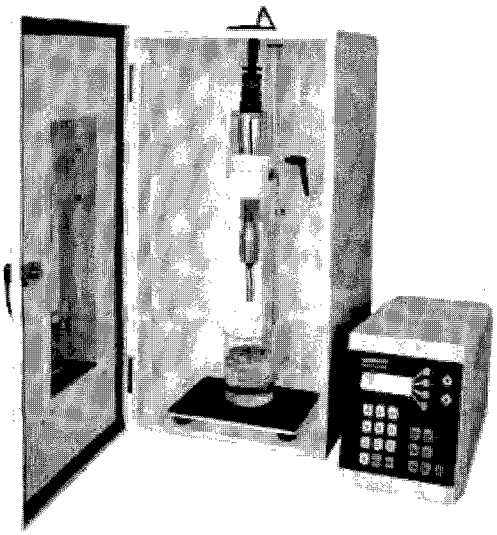

20KHz 超音波ホモジナイザー
BRANSON SONIFIER シリーズ

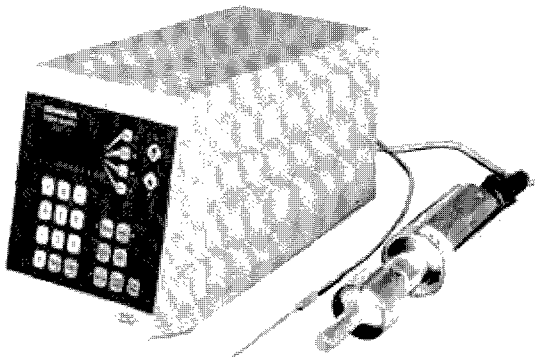

高周波 40KHz 超音波ホモジナイザー
BRANSON SLPe シリーズ

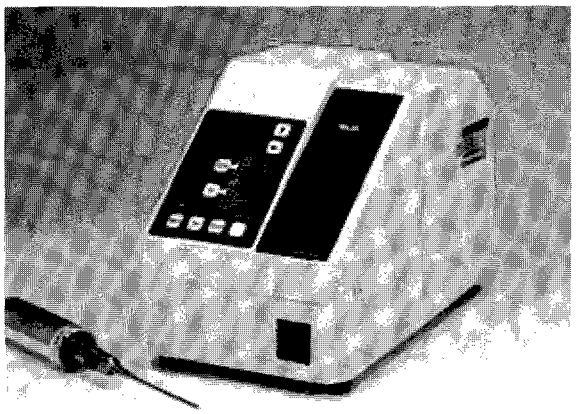

ブランソン社の製品は、ホーン先端部の振幅の安定性が高く、強力なキャビテーションが得られ、効率良く、再現性の高い分散処理が行えます。

主なアプリケーション

分散

カーボンナノチューブ　有機顔料　無機顔料　セラミック　セメント　感光体　記録材料
磁性粉　粉末冶金　酸化鉄　金属酸化物　シリカ　アルミナ　カーボンブラック
ポリマー　ラテックス　製紙　ファンデーション
研磨剤　電池　フィラー　光触媒　触媒　ワクチン　体外診断薬　歯磨き粉　シャンプー
半導体　電子基盤　液晶　貴金属　金属　宝石　タイヤ　発酵菌類　その他

乳化

エマルジョン製剤　農薬　トナー　ラテックス　界面活性剤　クリーム　乳液　クリーム　等

株式会社 セントラル科学貿易
本社：111-0052 東京都台東区柳橋 1-8-1
Tel 03-5820-1500 Fax 03-5820-1515
URL http://www.cscjp.co.jp/

大阪支店：Tel 06-6325-3171 Fax 06-6325-5180
福岡営業所：Tel 092-482-4000 Fax 092-482-3797
札幌出張所：Tel 011-764-3611 Fax 011-764-3612

フロンティアカーボン(株)の フラーレンおよびフラーレン誘導体 サンプル一覧

銘柄		分子構造	純度(HPLC面積%、代表値)	取扱数量
nanom purple フラーレンC60	ST	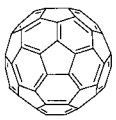	99	10g以上
	TL		99.5	5g以上
	SU		99.5/昇華精製品	2g以上
	SUH		99.9/昇華精製品	1g以上
nanom orange フラーレンC70	ST		97	1g以上
	SU		98/昇華精製品	0.5g以上
nanom mix 混合フラーレン	ST	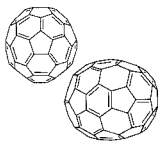	C60、C70、その他高次フラーレンの混合物 ST-FはSTの微粒化品	50g以上

銘柄	分子構造	純度(HPLC面積%、代表値)	取扱数量
nanom spectra E100 PCBM (phenyl C61-butyric acid methyl ester)	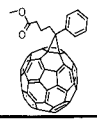	99	1g以上
nanom spectra E200 PCBNB (phenyl C61-butyric acid n-butyl ester)	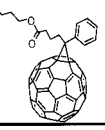	99	1g以上
nanom spectra E210 PCBIB (phenyl C61-butyric acid i-butyl ester)	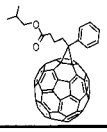	99	1g以上
nanom spectra E110 C70PCBM (phenyl C71-butyric acid methyl ester)	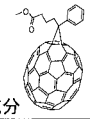 主成分	99（異性体トータル） 位置異性体の混合物	0.5g以上

銘柄	分子構造	内容	取扱数量
nanom spectra D100 水酸化フラーレン	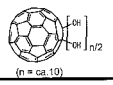	$C_{60}OH_n$ n=10を主成分とする混合物	2g以上
nanom spectra B100 酸化フラーレン	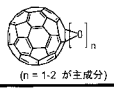	$C_{60}O_n$ n=1および2を主成分とする混合物	2g以上
nanom spectra A100 水素化フラーレン	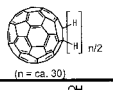	$C60H_n$ n=30を主成分とする混合物	2g以上
nanom spectra G100	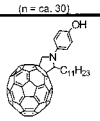	純度(HPLC面積%, 代表値) 99	1g以上

銘柄、取扱数量等は予告無く変更する場合がございます。予めご了承下さい。

2008年7月1日現在

当社製品は、下記2社から購入いただけます。詳細は直接お問い合わせください。

・関東化学株式会社　試薬事業本部
〒103-0023 東京都中央区日本橋本町3-11-5 TEL:03-3663-7631 FAX:03-3667-8277
http://www.kanto.co.jp E-mail:reag-info@gms.kanto.co.jp
・第一実業株式会社　新事業推進室 【担当:鎰広(カギヒロ)】
〒102-0084 東京都千代田区二番町11-19 TEL:03-5214-8579 FAX:03-5214-8501

＜本資料に関するお問い合わせ先＞
フロンティアカーボン株式会社 営業販売センター【担当:梶原】
〒806-0004 福岡県北九州市八幡西区黒崎城石1-1 （移転いたしました）
TEL:093-643-4400 FAX:093-643-4401 http://www.f-carbon.com
※弊社へのお問い合わせはHPよりお願いいたします。

Frontier Carbon Corporation

ISO9001 JQA-0298
ISO14001 JQA-E-80039
IMS
HORIBAは統合マネジメントシステム(IMS)を運用しています
OHSAS18001 JQA-OH0004
ISO13485 JQA-MD0011

ハイテクの一歩先に、いつも。

HORIBA

Explore the future

CNTの測定にはデファクトスタンダードのLabRamHR−800が最適

～RBM／フォトルミネッセンスを同一スポットで測定～

顕微レーザラマン分光測定装置 LabRamシリーズ

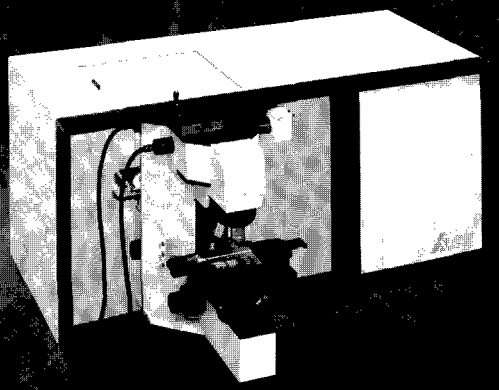

・244nm～1064nmのレーザによる測定が可能
・焦点距離800nmの分光器により高分解能測定を実現

SWCNTの近赤外領域の蛍光測定を大幅にスピードアップ

～ ナノテクリサーチに ～

近赤外対応蛍光分光測定装置 SPEX NanoLogシリーズ

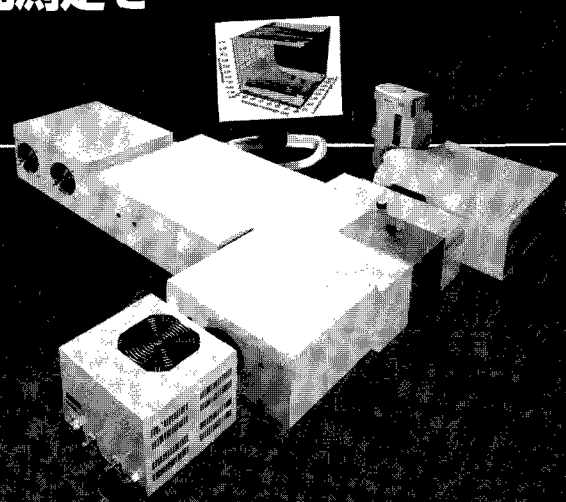

・InGaAsアレイ検出器による高感度測定
・高速・高分解能マトリックスマッピング
・モジュールユニットだからアプリケーションに応じた各種NIR検出器の組み合わせも可能

HORIBA JOBIN YVON

株式会社堀場製作所

科学システム営業部 03-3861-8234

本社 〒601-8510 京都市南区吉祥院宮の東町2 TEL(075)313-8121
●仙台(022)308-7890 ●つくば(0298)56-0521 ●東京(03)3861-8231
●横浜(045)451-2091 ●名古屋(052)936-5781 ●大阪(06)6390-8011
●広島(082)288-4433 ●愛媛(0897)34-8143 ●福岡(092)472-5041

製品の詳しい情報は
http://www.horiba.co.jp/

http://www.horiba.co.jp e-mail:info@horiba.co.jp

AFMシステムの価格革命
破格の価格で提供可能

簡易型 AFM『Eddy』520万円、研究用 AFM『Spotty』640万円

ドイツ Anfatec 社との業務提携により今までには成し得なかった価格で AFM システムのご提供が可能になりました。
簡易型 AFM『Eddy』は安価ながら分解能 5nm と高水準な機能を保持しております。
測定モードはコンタクトモード、ダイナミックモード、LFM(水平力顕微鏡) が標準装備されており他の測定モードの追加も可能です。また、簡易型『Eddy』には 3 種類 (計 15 個) の測定サンプル 4 種類 (計 130 個) のカンチレバーが付属しており、マニュアル、ソフトウェアもわかり易く作成されていますので、初心者でも簡単に使用することが可能です。メーカー指導の 2 日間のトレーニングも標準セットに含まれています。
研究用『Spotty』には、更に FMM(フォースモジュレーション)、MFM(磁気力顕微鏡) を搭載しており他の測定モード (EFM、KPFM、SCM、CAFM) の追加も可能です。

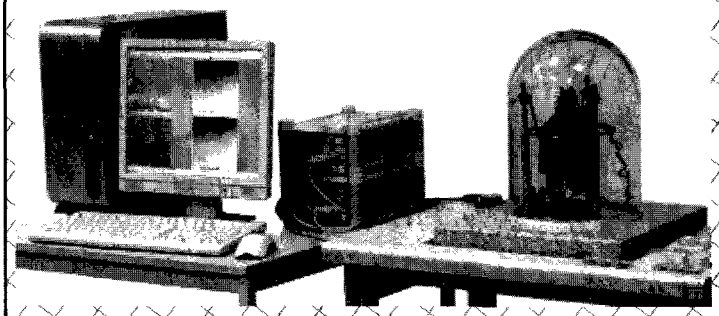

特徴・仕様

簡易型『Eddy』

分解能	**5nm(X,Y)、0.4nm(Z)**
スキャン可能範囲	**30μm**
最大サンプルサイズ	**4×4cm**
手動測定可能範囲	**5×5mm**

コンタクトモード、ダイナミックモード、LFM
CCD カメラ内蔵
オートアプローチ機能

簡易型『Eddy』は以下に当てはまる方々におすすめです

- 初めて AFM を使用する方
- AFM を教育機材として使用したい方
- 手軽に使用出来る AFM がほしい方
- いままでの AFM が高価なので導入出来なかった方

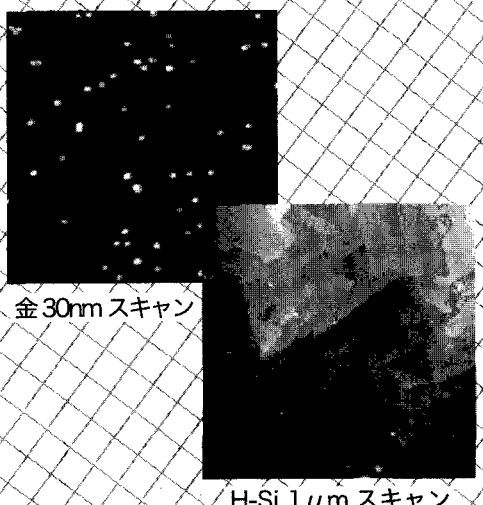

金 30nm スキャン

H-Si 1μm スキャン

簡易型『Eddy』の標準セット

3 種類 15 個のサンプル
4 種類 130 個のカンチレバー
2 日間のトレーニング
パソコン 1 台
(※除振台、保護ガラスは付属しておりません)

Anfatec

Anfatec 社はこの他にも、高性能 AFM、STM、SPM コントローラ、ロックインアンプなども取扱っております。
詳細はこちらの弊社ホームページをご覧下さい。

http://www.scilab.co.jp/

次世代技術知識集団
SCIENCE LABORATORIES
株式会社 サイエンス ラボラトリーズ
〒270-0021 千葉県松戸市小金原 7-10-25
TEL:047-309-8311 FAX:047-309-8310
MAIL:sales@scilab.co.jp WEB:scilab.co.jp

進化する売れ筋ナノテク材料

弊社取扱いナノテク材料群

フラーレン材料群

【60】【70】【84】PCBMフラーレン
bis【60】PCBMフラーレン
高次フラーレン(C76,C78,C84)
水溶性フラーレン
C60(OH)$_6$, C60(OH)$_{22\text{-}26}$,C60(OH)$_{24}$,
C60(OH)$_{18\text{-}22}$(O$^-$K$^+$)$_4$フラーノール
アミノ酪酸フラーレン誘導体
アミノカプロン酸フラーレン
ビスマロン酸エチルフラーレン
C13安定同位体置換フラーレン
Gd@C82金属内包フラーレン
La@C82金属内包フラーレン
Anti-HIVフラーレン
C60F$_{36}$,C60F$_{48}$,C60Br$_{24}$フラーレン

カーボンナノチューブ

高純度多層カーボンナノチューブ
高純度単層カーボンナノチューブ
水溶性ナノチューブ
SWNT-COOH,SWNT-NH$_2$,SWNT-PEG,SWNT-SH
MWNT-COOH,MWNT-NH$_2$,MWNT-PEG,MWNT-SH
大口径カーボンナノチューブ
2層構造カーボンナノチューブ
カーボンナノチューブ・フィルム【Cu,Si,Ni,Graphite】
カーボンナノチューブ・カソード【Cu,Si】

金ナノ微粒子

金ナノ微粒子,0.01%金,2～50nm
Dextranコート,0.01%金,10～50nm
PEGコート,0.01%金,10～50nm
Biotinラベル,0.01%金,5～50nm
Streptavidinラベル,0.01%金,5～50nm
その他銀ナノ微粒子

希少価値金属(レアメタル)

ニッケル,コバルト,フェロクロム,フェロマンガン,フェロバナジューム,亜鉛,チタン,スズ,アンチモン,タングステン

電気鋳造精密メッシュ

金,銅,ニッケル,透過率(36～98%),標準サイズ279×279mm

ナノ微粒子群

1.元素材料
Au,Ag,Al,Cu,Fe,In,Mo,Ni,Si,Ti,W,Zn

2.非酸化物ナノ化合物
BN,GaP,InP,SiC,TaN,TiC,TiN,WC,WC/Co

3.酸化物
Al$_2$O$_3$,Al$_2$(OH)$_3$,B$_2$O$_3$,BaCO$_3$,BaFe$_{12}$O$_{19}$,BaSO$_4$,BaTiO$_3$,Bi$_2$O$_3$,CeO$_2$,CoFe$_2$O$_4$,Co$_{0.5}$Zn$_{0.5}$Fe$_2$O$_4$
CoO,Co$_3$O$_4$,CrO$_3$,Cr$_2$O$_3$,CuO,Dy$_2$O$_3$,Er$_2$O$_3$,Eu$_2$O$_3$,Fe$_2$O$_3$,Fe$_3$O$_4$,Gd$_2$O$_3$,HfO$_2$,In$_2$O$_3$,In(OH)$_3$
In$_2$O$_3$:SnO$_2$,Li$_4$Ti$_5$O$_{12}$,MgAl$_2$O$_4$,MgO,Mg(OH)$_2$,Mn$_2$O$_3$,MoO$_3$,Nd$_2$O$_3$,NiFe$_2$O$_4$,Ni$_{0.5}$Zn$_{0.5}$Fe$_2$O$_4$
NiO,Ni$_2$O$_3$,Pr$_6$O$_{11}$,Sb$_2$O$_3$,SiO$_2$Sm$_2$O$_3$,SnO$_2$,SrAl$_{12}$O$_{19}$,SrCO$_3$,SrFe$_{12}$O$_{19}$,SrTiO$_3$,Tb$_4$O$_7$,TiO$_2$
VO,V$_2$O$_3$,V$_2$O$_5$,WO$_3$,Y$_{2.98}$Ce$_{0.02}$AlO$_{12}$,Y$_3$Al$_5$O$_{12}$,Y$_2$O$_3$,ZnFe$_2$O$_4$,ZnO,ZrO$_2$,ZrO$_2$+,MgB$_2$

詳しいお問合せはこちら **http://atr-atr.co.jp**

株式会社ATR
〒270-0021 千葉県松戸市小金原 7-10-25
TEL：047-394-2112　FAX：047-394-2100
Mail：sales@atr-atr.co.jp
Advanced Technology Research